NOVA SCHOOL OF SCIENCE & TECHNOLOGY
universidade de aveiro
U.PORTO
DEPARTAMENT OF CHEMISTRY

# NEW MONO- AND HETERO-BRANCHED SENSITIZERS FOR DSSC

GABRIELA RODRIGUES MALTA

Master in Bioorganic Chemistry

DOCTORATE IN SUSTAINABLE CHEMISTRY

NOVA University Lisbon

September, 2024





DEPARTAMENT OF CHEMISTRY

# NEW MONO- AND HETERO-BRANCHED SENSITIZERS FOR DSSC

**GABRIELA RODRIGUES MALTA**

Master in Bioorganic Chemistry

**Adviser:** Paula Cristina de Sério Branco
*Associate Professor with Habilitation,* NOVA School of Science and Technology, *NOVA University of Lisbon*

**Co-advisers:** António Jorge Dias Parola
*Full Professor,* NOVA School of Science and Technology, *NOVA University of Lisbon*

**Examination Committee:**

**Chair:** Eurico José da Silva Cabrita,
Full Professor, NOVA School of Science and Technology, NOVA University of Lisbon

**Rapporteurs:** Augusto Costa Tomé,
Associate Professor with Habilitation, Universidade de Aveiro

Artur Jorge Carneiro Moro,
Researcher, NOVA School of Science and Technology, NOVA University of Lisbon

**Adviser:** Paula Cristina de Sério Branco,
Associate Professor with Habilitation, NOVA School of Science and Technology, NOVA University of Lisbon

**Members:** Maria Paula Alves Robalo,
Coordinator Professor with Habilitation, ISEL-Instituto Superior de Engenharia de Lisboa

Jaime Alfredo da Silva Coelho,
Assistant Researcher, University of Lisbon

Eurico José da Silva Cabrita,
Full Professor, NOVA School of Science and Technology, NOVA University of Lisbon

# ACKNOWLEDGMENTS

First and foremost, I would like to express my deepest gratitude to my supervisor, Prof. Paula Branco, and my co-supervisor, Prof. A. Jorge Parola, for accepting me into their laboratories as a PhD student. Their guidance, expertise, support and patience have been fundamental to the completion of this thesis.

I want to acknowledge "Fundação para a Ciência e a Tecnologia" for the PhD grant (SFRH/BD/145324/2019) along with the Doctoral Program in Sustainable Chemistry. I also want to acknowledge the Associate Laboratory for Green Chemistry–LAQV, financed by national funds from FCT/MCTES (UIDB/50006/2020 and UIDP/50006/2020) and the network of Nuclear Magnetic Resonance of the chemistry department of FCT-UNL (Financed by FCT/MCTES RECI/BBB-BQB/0230/2012 and RECI/BBB-BEP/0124/2012). FCT is also acknowledged for funding the project PTDC/QUI-QOR/7450/2020 "Organic Redox Mediators for Energy Conversion".

I want to express my gratitude to Dr. Ana Teresa Lopes from the NMR service for her availability, professionalism and patience. I would also like to acknowledge Dr. Luz Fernandes for the MS processing.

I would like to thank Hugo Cruz for his help with the cyclic voltammetry measurements, as well as Tiago Mateus and Ivan Santos for their support with the IPCE measurements.

A special thanks goes to Ana Lúcia Pinto for her enthusiasm and joy in teaching me how to assemble the DSSC devices.

To my senior lab companions Rafael Rippel, Sofia Santos, João Macara, Ricardo Chagas and Diogo Poeira, thank you for always being there to help me whenever I needed it. I would also like to extend my gratitude to my fellow lab colleagues Rita Reis, João Sarrato, Margarida Martins, Flávia Leitão, Luís Pinheiro, Joana Ferreira, Diana Gago, Joana Pereira, Beatriz Dedeiras, Bruna Guerreiro, Catarina Caldeira, Stéphanie Leal, Micael Paulino and Catarina Cipriano, whose companionship, support, and friendship have made this PhD journey even more rewarding.

I want to express my gratitude to my friends, especially Maria Beatriz and Edgar. To my parents, brother and grandma, thank you for supporting me throughout this journey and for

the values you have instilled in me over the years. Lastly, I would like to thank Henrique, my light at the end of the day, for his encouragement, affection, patience and for always holding my hand during these four years.

# Abstract

The development and use of renewable energies represent one of the principal approaches regarding the important struggle against climate change. Given the existent renewable energies, nowadays solar light possesses a great potential to generate energy. The development around solar energy generation has received great attention throughout the last couple of decades. Considering existent solar cells, dye sensitized solar cells (DSSCs) are a promising alternative to traditional silicon-based solar cells. The development of dye sensitizers that allow the obtention of superior photovoltaic efficiencies is of utmost importance. The use of organic dyes in DSSCs are an interesting alternative to the traditionally employed ruthenium-based dyes. The development of these organic molecules uses a design containing donor, π-bridge and acceptor units.

A set of dyes that can be applied in DSSCs has been developed. These possess as central cores coumarins, acenaphthenes, acenaphthylenes, and thieno[3,4-*b*]thiophenes. Considering the employed nuclei, the efficiency of DSSC devices through variation of the π-bridges and donor groups was studied. Different structural designs were used, namely the linear, di-branched, and the dianchoring designs.

This work involved the synthesis of all the chromophores, and their photophysical and electrochemical characterization. Additionally, it involved theoretical calculations (DFT and TD-DFT). The DSSC devices were built from scratch and, subsequently, the photovoltaic performance of the final chromophores was tested by measuring the *I*-*V* curves.

**Keywords**: dye sensitized solar cells, organic dyes, coumarin, acenaphthylene, thieno[3,4-*b*]thiophene

# RESUMO

A utilização e desenvolvimento de energias renováveis representam uma das principais abordagens relativamente ao importante combate às alterações climáticas. Tendo em conta as energias renováveis existentes, atualmente a energia gerada a partir da luz solar é considerada como tendo um dos maiores potenciais para gerar energia. O desenvolvimento em torno da energia solar tem sido alvo de grande atenção ao longo das últimas décadas. De entre as células solares existentes, as células solares sensibilizadas por corante (DSSCs) apresentam-se como sendo uma alternativa promissora às tradicionais células solares à base de silício. O desenvolvimento de corantes sensibilizadores que permitam a obtenção de eficiências fotovoltaicas superiores em dispositivos de DSSCs é de extrema importância. Os corantes orgânicos aplicados em DSSCs são uma alternativa aos de ruténio habitualmente utilizados. O desenvolvimento destas moléculas orgânicas envolve um design contendo unidades doadoras, pontes-π e unidades aceitadoras.

Um conjunto de corantes que pode ser aplicado em DSSCs foi desenvolvido. Estes corantes apresentam como núcleos centrais cumarinas, acenaftenos, acenaftilenos e tieno[3,4-*b*]tiofenos. Atendendo aos vários núcleos utilizados, estudou-se o efeito da variação das pontes-π e grupos doador na eficiência em dispositivos de DSSCs. Diferentes designs estruturais foram aplicados, nomeadamente o linear, o dirramificado e o diancorado.

Este trabalho envolveu a síntese de todos os corantes e a sua caracterização fotofísica e eletroquímica. Envolveu também cálculos teóricos (DFT e TD-DFT). Os dispositivos de DSSC foram construídos de raiz e a performance fotovoltaica dos cromóforos foi testada através da medição das curvas *I-V*.

**Palavras chave:** células solares sensibilizadas por corante, corantes orgânicos, cumarina, acenaftileno, tieno[3,4-*b*]tiofeno

# CONTENTS


1 INTRODUCTION ..... 33

1.1 Context and motivation ..... 34

1.2 History ..... 36

1.3 Dye-sensitized solar cells (DSSCs) ..... 37

1.3.1 DSSC structure ..... 38

1.3.2 DSSC operational process ..... 40

1.3.3 Solar spectrum ..... 42

1.3.4 Solar cell parameters ..... 42

1.4 Dyes for DSSCs ..... 45

1.4.1 Ruthenium dyes ..... 46

1.4.2 Natural sensitizers ..... 46

1.4.3 Organic metal-free dyes ..... 47

2 COUMARIN DERIVATIVES AS PHOTOSENSITIZERS ..... 55

2.1 General overview ..... 56

2.2 Results and discussion ..... 65

2.2.1 Synthetic methodology ..... 65

2.2.2 Absorption and Fluorescence ..... 73

2.2.3 Photovoltaic performance ..... 74

2.3 Conclusion ..... 77

2.4 Experimental section ..... 78

2.4.1 Synthesis of 5,7-dimethoxycoumarin-based dyes ..... 80
2.4.2 Synthesis of 6,7-dimethoxycoumarin derivatives ..... 84
3 ACENAPHTHENE DERIVATIVES AS PHOTOSENSITIZERS ..... 91
3.1 General overview ..... 92
3.1.1 Bis(arylimino)acenaphthenes ..... 92
3.1.2 7*H*-acenaphtho[1,2-*d*]imidazoles ..... 93
3.1.3 Acenaphthylene ..... 94
3.2 Results and discussion ..... 99
3.2.1 Synthetic methodology ..... 99
3.2.2 Photophysical and photovoltaic studies ..... 117
3.2.3 Electrochemical characterization ..... 126
3.2.4 Theoretical Calculations ..... 127
3.3 Conclusion ..... 130
3.4 Experimental section ..... 131
3.4.1 Synthetic procedure for the preparation of bis(phenylimino)acenaphthene derivatives ..... 132
3.4.2 Synthesis of 7H-acenaphtho[1,2-d]imidazole derivatives ..... 140
3.4.3 Shynthesis of diethynylacenaphthylene derivatives ..... 144
4 OLIGOTHIOPHENES DERIVATIVES AS PHOTOSENSITIZERS ..... 157
4.1 General overview ..... 158
4.1.1 The π-spacer ..... 158
4.1.2 The donors ..... 163
4.2 Results and discussion ..... 164
4.2.1 Synthetic methodology ..... 165
4.2.1 Photophysical and photovoltaic studies ..... 174
4.3 Conclusion ..... 176
4.4 Experimental section ..... 177

GENERAL CONCLUSIONS ..... 193

WORK DISSEMINATION ..... 195

BIBLIOGRAPHY ..... 197

# LIST OF FIGURES

Figure 1. Sustainable development goals [4] .....35
Figure 2. Architecture of a typical DSSC. .....39
Figure 3. Operation principles of a DSSC containing an iodine electrolyte with $I^-/I_3^-$ redox couple. 1. Dye photoexcitation; 2. Injection of excited electron into the CB of $TiO_2$; 3. Electron transport via external circuit; 4. Regeneration of the electrolyte; 5. Regeneration of the oxidized dye; 6. Recombination; 7. Dark current; 8. Electron's decay from the excited to the fundamental state. .....41
Figure 4. Reference spectra AM0 and AM1.5G (ASTM G173-03).[49] .....42
Figure 5. Typical photocurrent-voltage (*I-V*) curve for a DSSC. .....43
Figure 6. Number of research articles per year using the keywords: "Dye sensitized solar cell" or "DSSC" (blue / left bar); "Dye sensitized solar cell" or "DSSC" and "Organic dye" (purple / right bar) (data source: ISI Web of Knowledge) .....45
Figure 7. Structures of ruthenium-based dyes N-719, N-3, and N-749. .....46
Figure 8. Chemical structures of natural sensitizers. .....47
Figure 9. Mono-branched D–π–A architecture of an organic dye sensitizer. Schematic representation of the ICT from the donor to the acceptor and electron injection into the $TiO_2$ nanoparticles. .....48
Figure 10. Schematic representation of multi-branched and multi-anchoring design of organic DSSC dyes .....49
Figure 11. Chemical structures of di-branched di-anchoring sensitizers and respective unidimensional analogues. .....50
Figure 12. Structures that can be used as donors, π-bridges, acceptors, and substituents alkyl chains in DSSC chromophores. .....52
Figure 13. Binding modes of carboxylic acids with metal oxide surface. .....52

Figure 14. Chemical structures of the highly efficient dyes R6 and ZL003. ..... 53
Figure 15. Chemical structures of the highly efficient sensitizers SL9 and SL10 ..... 54
Figure 16. Chemical structure of coumarin. ..... 56
Figure 17. Different synthetic methods for the preparation of coumarins. ..... 57
Figure 18. ICT effect in 7-dimethylaminocoumarin via absorption and emission of light.[98] ..... 58
Figure 19. Chemical structures of 7-diethylaminocoumarin dyes for DSSC application. ..... 59
Figure 20. Chemical structures of coumarin dyes containing diphenylamine, difluorenylamine and triarylamine as additional donor groups. ..... 62
Figure 21. Chemical structures dyes based on NKX coumarins and 6,7-dihydroxycoumarins. 64
Figure 22. Structures of the synthesized and studied coumarin chromophores in this work. ..65
Figure 23. Catalytic cycles of Pd and Cu in Sonogashira coupling.[138,140] ..... 68
Figure 24. $^1$H NMR (400 MHz) spectra of **2.11a-b** and **2.19c-d** final dyes (**2.11a** ($CDCl_3$); **2.11b** (DMF-$d_7$); **2.19c** (DMSO-$d_6$); **2.19d** (DMF-$d_7$)). ..... 73
Figure 25. Normalized absorption and fluorescence emission spectra for compounds **2.11b** and **2.19b-e** in acetonitrile solution and in the solid state (adsorbed in $TiO_2$ films) at 293K. ..... 74
Figure 26. A- *I–V* curves of the test cells based on the synthesized coumarin dyes under 100 mW.cm$^{-2}$ under simulated AM 1.5 illumination; B- Structures of the tested coumarin chromophores; C- structure of the 6,7-dihydroxycoumarin based dye already reported In the literature[79] ..... 75
Figure 27. *I–V* curves of the test cells based on the synthesized coumarin dye **2.19c** containing $I^-/I_3^-$ electrolyte and EL-HPE® (GreatCell Solar) electrolyte, under 100 mW.cm$^{-2}$ under simulated AM 1.5 illumination. ..... 77
Figure 28. Cu(I) Ar-BIAN complexes applied in DSSCs as sensitizers. ..... 92
Figure 29. Reaction scheme for the synthesis of Ar-BIAN derivatives. ..... 93
Figure 30. Debus-Radziszewski reaction for the synthesis of 2,4,5-trisubstituted imidazole and 1,2,4,5-tetrasubstituted imidazole. ..... 93
Figure 31. Reactional scheme for the preparation of imidazole derivatives with a fused phenanthrene core embedded in the structure. ..... 94
Figure 32. Chemical structures of dyes bearing bistriphenylamine fluoranthenes and acenaphthopyrazines cores. ..... 95
Figure 33. Chemical structures of some PAHs-based dyes used in DSSCs ..... 97
Figure 34. Structure of the target Ar-BIAN-based dye (**3.5**) ..... 99
Figure 35. Structure of the final diethynylacenaphthylene dyes **3.37a-d**. ..... 111
Figure 36. $^1$H NMR spectra of the final chromophores 3.37a-d in DMSO-$d_6$ at 400 Hz. ..... 114

Figure 37. Structure of a diethynylacenaphthylene dye containing an acenaphthylene core with an electron donating group (EDG) in position 5. ..... 115
Figure 38. Structure of chromophore **3.23**..... 117
Figure 39. Normalized absorption (solid) and fluorescence emission (dotted; $\lambda_{exc}$=390 nm) of compound **3.23** in methanol at room temperature. ..... 118
Figure 40. *I–V* curves of the test cells based on the synthesized dye **3.23** and reference N-719 under 100 mW.cm$^{-2}$ simulated AM 1.5 illumination (best performing cell). ..... 119
Figure 41. Normalized absorption (dotted) and fluorescence emission (solid; $\lambda_{exc}$(**3.37a**)= 364 nm and 486 nm; $\lambda_{exc}$(**3.37b**)=351 nm; $\lambda_{exc}$(**3.37c**)=402 nm and 507 nm; $\lambda_{exc}$ (**3.37d**)= 407 nm and 521 nm spectra of chromophores **3.37a-d** in DMF solution at room temperature (compounds excited at two different $\lambda_{exc}$ have identical emission spectra). ..... 120
Figure 42. *I–V* curves of the test cells based on the synthesized acenaphthylene dyes and reference N-719 under 100 mW.cm$^{-2}$ simulated AM 1.5 illumination (best performing cell, [CDCA] = 0 mM)..... 121
Figure 43. *I–V* curves of the test cells based on the synthesized acenaphthylene dyes (**3.37a-d**) under 100 mW.cm$^{-2}$ simulated AM 1.5 illumination (best performing cell, [CDCA] = 0 mM, 10 mM and 50 mM). ..... 123
Figure 44. *I–V* curves of the test cells based on the synthesized dye 3.37a using the electrolyte composed by LiI and $I_2$ and the commercial electrolyte EL-HPE (GreatCell Solar) under 100 mW.cm$^{-2}$ simulated AM 1.5 illumination (best performing cell, [CDCA] = 0 mM). ..... 124
Figure 45. IPCE spectra for the DSSCs based on dyes **3.37a-d** (best performing cell, [CDCA] = 0 mM)..... 125
Figure 46. Schematic representation of the HOMO and LUMO energy levels of each chromophore vs. the CB of $TiO_2$ and $I^-/I_3^-$ redox potentials. ..... 126
Figure 47. Optimized structures and frontier molecular orbitals (MO) of the HOMO and LUMO calculated with DFT on a B3LYP/6-311G(d,p) level of the dyes. The theoretical optical band gaps (Eg) are also included. ..... 130
Figure 48. Possible isomeric forms of thienothiophenes. ..... 158
Figure 49. Chemical structures of dyes containing fused thiophenes and arylamines for DSSC application..... 160
Figure 50. Chemical structures of dyes containing thienothiophenes for DSSC application. 162
Figure 51. Chemical structure of phenothiazine and phenoxazine. ..... 164
Figure 52. Chemical structure of carbazole. ..... 164

Figure 53. Delineated chromophores with a D-π-$(A)_2$ architecture containing a thieno[3, 4-*b*]thiophene in their π-bridge. 165
Figure 54. Chemical structure of π-spacer. 165
Figure 55. Suzuki-Miyaura cross-coupling reaction. 167
Figure 56. Catalytic cycle of Pd in Suzuki-Miyaura coupling. 168
Figure 57. Chemical structures of donors 10-(2-ethylhexyl)-10*H*-phenothiazine and 9-phenyl-9*H*-carbazole. 170
Figure 58. *I–V* curves of the test cells based on the synthesized thieno[3,4-*b*]thiophene based dyes and reference N-719 under 100 $mW.cm^{-2}$ simulated AM 1.5 illumination (best performing cell). 175
Figure 59. IPCE spectra for the DSSCs based on dyes **4.23a-d** (best performing cell). 176

# LIST OF SCHEMES

Scheme 1. Synthesis of 5,7-dihydroxycoumarin (**2.2**). ..... 66
Scheme 2. Synthesis of 5,7-diethylcarbonatecoumarin (**2.3**) and 3-bromo-5,7-diethylcarbonatecoumarin (**2.4**). ..... 67
Scheme 3. Synthesis of 3-bromo-5,7-dihydroxycoumarin and 3-bromo-5,7-dimethoxycoumarin. ..... 67
Scheme 4. Copper co-catalyzed Sonogashira reaction. ..... 67
Scheme 5. Synthesis of compounds **2.7** and **2.8** via Sonogashira coupling. ..... 69
Scheme 6. Preparation of the intermediate compound (**2.9**) and synthesis of compound **2.10** by introduction of the 2,2′-bithiophene π-bridge. ..... 70
Scheme 7. Synthesis of the final 5,7-dimethoxycoumarin chromophores **2.11a** and **2.11b**. ..... 70
Scheme 8. Synthesis of 6,7-dimethoxycoumarin (**2.13**) and 3-bromo-6,7-dimethoxycoumarin (**2.14**). ..... 71
Scheme 9. Synthesis of 3-ethynyl-6,7-dimethoxycoumarin (**2.16**) ..... 71
Scheme 10. Introduction of the π-bridges thiophene (**2.17c**) and benzotriazole (**2.17d**) in 3-ethynyl-6,7-dimethoxycoumarin via Sonogashira coupling to obtain compounds **2.18c** and **2.18d** respectively. ..... 72
Scheme 11. Synthesis of the 6,7-dimethoxycoumarin final chromophores 2.19c and 2.19d. ..... 72
Scheme 12. Synthetic route for the preparation of Ar-BIAN 3.5 starting with 4-aminobenzoic acid (**3.2**). ..... 100
Scheme 13. Synthetic route for the preparation of Ar-BIAN **3.5** using 4-(1,3-dioxolan-2-yl)aniline (**3.8**). ..... 101

Scheme 14. Synthetic route for the preparation of Ar-BIAN 3.5 using (4-aminophenyl)methanol (**3.11**)..... 102
Scheme 15. Synthetic route for the preparation of Ar-BIAN **3.5** using 3-(4-aminophenyl)-2-cyanoacrylic acid (**3.15**). ..... 104
Scheme 16. Synthetic route for the preparation of Ar-BIAN **3.5** using ethyl-3-(4-aminophenyl)-2-cyanoacrylate (**3.17**)..... 105
Scheme 17. Reaction scheme for the synthesis of an Ar-BIAN imidazolium chloride derivative (**3.20**)..... 105
Scheme 18. Reactional scheme for the synthesis of 7H-acenaphtho[1,2-d]imidazol-8-yl derivative (**3.23**). ..... 107
Scheme 19. Reactional scheme for the synthesis of an 7*H*-acenaphtho[1,2-d]imidazol-8-yl derivative with a thiophene moiety (**3.25**). ..... 107
Scheme 20. Attempted synthesis of 7*H*-acenaphtho[1,2-d]imidazole derivatives containing different substituents on the pyrrolic nitrogen (**3.27**). ..... 108
Scheme 21. Alternative approaches for the synthesis of 3.27. ..... 109
Scheme 22. Synthesis of 1,2-dibromoacenaphthylene (**3.32**)..... 111
Scheme 23. Synthesis of acenaphthenedialdehydes **3.35a-d**. Reactional conditions: a) **3.32** (1 eq.) $Pd(PPh_3)_4$ (0.30 eq.), $PPh_3$ (0.12 eq.), CuI (0.24 eq.), 4-ethynylbenzaldehyde (3.0 eq.), DIPA (3 eq.), dry dioxane, 40°C in a degassed Schlenk tube; b) **3.32** (1 eq.), $Pd(PPh_3)_4$ (0.30 eq.), $PPh_3$ (0.12 eq.), CuI (0.24 eq.), ethynyltrimethylsilane (3.0 eq.), DIPA (3 eq.), dry dioxane, 40°C in a sealed tube; c) **3.34** (1 eq.), $K_2CO_3$ (2 eq.), Dioxane/MeOH (1:1 v/v), RT; d) $Pd(PPh_3)_4$ (0.20 eq.), $PPh_3$ (0.12 eq.), CuI (0.24 eq.), bromoaryl aldehydes (**3.36b-d**) (2.2 eq.), DIPA (2.0 eq.), dry dioxane, 40°C in a degassed Schlenk tube. ..... 112
Scheme 24. A. Synthetic procedure for the preparation of 7-bromo-2-(2-ethylhexyl)-2*H*-benzo[d][1,2,3]triazole-4-carbaldehyde (**3.36c**). B. Synthetic procedure for the preparation of 5-bromothieno[3,2-*b*]thiophene-2-carbaldehyde (**3.36d**)..... 113
Scheme 25. Synthesis of the final chromophores **3.37a-d**..... 113
Scheme 26. A- Synthetic procedure for the synthesis of 1,2-dibromoacenaphthylene substituted with a triarylamine on position 5. B - Synthetic procedure for the synthesis of 1,2-dibromoacenaphthylene substituted with a diethylamine on position 5. Reactional conditions: a) Compound **3.38** (1 eq.), $Pd(PPh_3)_4$ (8 mol%), aq. solution $K_2CO_3$ 2.5 M (4.0 eq.), $C_{18}H_{14}B(OH)_2N$ (1.0 eq.), THF reflux (Suzuki coupling). b) Compound **3.41**, diethylamine aq. (excess), $CuSO_4 \cdot 5H_2O$ (0.05 eq.), DMF. c) Compound **3.42** (1eq.), diethylamine (3 eq.), $Pd_2(dba)_3$ (4 mol%),

Xantphos (4 mol %), $Cs_2CO_3$ (3 eq.), toluene 80°C. d) Compound **3.38**, diethylamine (6 eq.), $Pd_2(dba)_3$ (8 mol%), Xantphos (8 mol %), $Cs_2CO_3$ (3 eq.), toluene 80°C. ..... 116
Scheme 27. Synthetic route for the preparation of 7-bromo-2-(2-ethylhexyl)-2H-benzo[d][1,2,3]triazole-4-carbaldehyde (**3.36c**) using as starting material 1,2,3-benzotriazole. ..... 146
Scheme 28 Synthetic pathway for the preparation of 5-bromothieno[3,2-*b*]tiophene-2-carbaldehyde (3.36d) using as starting material 2,5-dibromothieno[3,2-*b*]thiophene. ..... 148
Scheme 29. Synthetic pathway for *the synthesis of aldehydes (**3.33b-d**)*..... 149
Scheme 30. Synthesis of compounds **4.4a** and **4.4b** starting from 3,4-dibromothiophene (**4.1**) ..... 166
Scheme 31. Possible pathways to achieve compounds **4.5a** and **4.5b**. ..... 167
Scheme 32. Suzuki coupling to obtain **4.5a** and **4.5b** and bromination reaction to obtain **4.6**. ..... 169
Scheme 33. Synthesis of boronic ester **4.9**. ..... 169
Scheme 34. Miyaura borylation reaction for the preparation of compound **4.11**. ..... 170
Scheme 35. Derivatization of phenothiazine. ..... 171
Scheme 36. Derivatization of carbazole. ..... 172
Scheme 37. Synthesis of compounds **21a-d** via Sonogashira coupling. ..... 173
Scheme 38. Synthesis of the final chromophores **4.23a-d**..... 174

# LIST OF TABLES

Table 1. Spectroscopic and photovoltaic parameters of di-branched di-anchoring sensitizers and respective unidimensional analogues. 50
Table 2. Spectroscopic and photovoltaic parameters of highly efficient sensitizers R6, ZL003, SL9, SL10 54
Table 3. Spectroscopic and photovoltaic parameters of 7-diethylaminocoumarin sensitizers applied in DSSCs in the last decade. 60
Table 4. Spectroscopic and photovoltaic parameters of coumarin sensitizers containing diphenylamine, difluorenylamine and triarylamine as additional donors applied in DSSCs in the last decade. 63
Table 5. Spectroscopic and photovoltaic parameters of dyes based on NKX coumarins and 6,7-dihydroxycoumarins in the last decade. 64
Table 6. Spectroscopic data (absorption and fluorescence emission maxima, molar extinction coefficients, ε, and Stokes shift, $\Delta_{SS}$) for compounds **2.11b** and **2.19b-e** in acetonitrile solution and absorbed in $TiO_2$ films at 293 K. 74
Table 7. Performance values of the test cells based on the synthesized dyes and reference dye N719 under 100 $mW.cm^{-2}$ AM 1.5 illumination. The results presented correspond to the average values of at least two cells per dye, each cell measured 5 times. The prepared anodes were soaked for 16 h in an $CH_2Cl_2$/MeOH/$H_2O$ 65:20:2 (% v/v) solution of the dye (0.5 mM), at room temperature in the dark. Electrolyte composition: 0.8 M LiI and 0.05 M $I_2$ in an acetonitrile/valeronitrile (85:15, % v/v) 76
Table 8. Spectroscopic and photovoltaic parameters of bistriphenylamine fluoranthenes and acenaphthopyrazines based dyes applied in DSSCs. 95
Table 9. Spectroscopic and photovoltaic parameters of PAHs-based dyes applied in DSSCs. 98
Table 10. Different conditions for the reduction of (4-nitrophenyl)methanol (**3.11**) 103

Table 11. Assays carried out to obtain compound **3.27** and conversion ratio of anilines (**3.26**) into acetamides (**3.28**)..... 108
Table 12. Different methods for the synthesis of compound **3.27** without using $CH_3COOH$, recovery of aniline (**3.26b**), conversion rate of the starting materials into compounds **3.29** and **3.30**..... 109
Table 13. Performance values of the test cells based on the synthesized dyes and reference dye N-719 under 100 $mW.cm^{-2}$ AM 1.5 illumination. The results presented correspond to the average values of at least two cells per dye, each cell measured 5 times. The prepared anodes were soaked for 16 h in ethanol solution of the dye (0.5 mM), at room temperature in the dark. Electrolyte composition: 0.8 M LiI and 0.05 M $I_2$ in an acetonitrile/valeronitrile (85:15, % v/v). ..... 119
Table 14. Spectroscopic data for the synthesized compounds (**3.37a-d**) in DMF solution at room temperature (absorption ($\lambda_{abs}$) and emission($\lambda_{em}$) maxima, molar extinction coefficients (ε) and Stokes shift (ΔSS)). ..... 120
Table 15. Performance values of the test cells based on the synthesized dyes and reference dye N-719 under 100 $mW.cm^{-2}$ AM 1.5 illumination. The results presented correspond to the average values of at least two cells per dye, each cell measured 5 times. Different concentrations of CDCA were applied (0 mM, 10 mM and 50 mM). The prepared anodes were soaked for 16 h in an CH2Cl2/MeOH/H2O 65:35:5 (%v/v) solution of the dye (0.5 mM), at room temperature in the dark. Electrolyte composition: 0.8 M LiI and 0.05 M I2 in an acetonitrile/valeronitrile (85:15, % v/v)..... 122
Table 16. Performance values of the test cells based on the dye **3.37a** under 100 $mW.cm^{-2}$ AM 1.5 illumination. The results presented correspond to the average values of at least two cells per dye, each cell measured 5 times. The prepared anodes were soaked for 16 h in an $CH_2Cl_2$/MeOH/$H_2O$ 65:35:5 (%v/v) solution of the dye (0.5 mM), at room temperature in the dark. Electrolytes composition: 0.8 M LiI and 0.05 M $I_2$ in an acetonitrile/valeronitrile (85:15, % v/v); commercial electrolyte EL-HPE(GreatCell Solar) - 1-butyl-3-methylimidazolium iodide, 4-tert-butylpyridin (TBP), and guanidinium thiocyanate (GuSCN)..... 124
Table 17. Electrochemical properties obtained from cyclic voltammetry measurements in dimethylformamide (DMF) solution with a dye (**3.37a-d**) concentration of $1.5X10^{-4}$ M and 0.1 M $TBAPF_6$ at scan rates of 50, 100, 250, 500 mV $s^{-1}$. ..... 127
Table 18. Computed absorption properties (predicted vertical excitation energies and associated orbitals transitions major contributions together with oscillator strengths, f, and dipole moments) for the chromophores 3.37a-d obtained by TD-DFT at the CAM-B3LYP/6-

311G(d,p) level (using the Polarizable Continuum Model, PCM, to take into account the solvent effects of N,N-dimethylformamide) after ground-state geometry optimization using the same functional and basis set..... 129
Table 19. Spectroscopic and photovoltaic parameters of sensitizers applied in DSSCs containing fused thiophenes and arylamines..... 160
Table 20. Spectroscopic and photovoltaic parameters of sensitizers applied in DSSCs thienothiophenes. ..... 162
Table 21. Performance values of the test cells based on the dyes **4.23a-d** under 100 mW.cm$^{-2}$ AM 1.5 illumination. The results presented correspond to the average values of at least two cells per dye, each cell measured 5 times. The prepared anodes were soaked for 16 h in an $CH_2Cl_2$/MeOH/$H_2O$ 65:35:5 (%v/v) solution of the dye (0.5 mM), at room temperature in the dark. Electrolyte composition: 0.8 M LiI and 0.05 M $I_2$ in an acetonitrile/valeronitrile (85:15, % v/v). ..... 175

# Abbreviations

| | |
|---|---|
| A | Acceptor/Anchoring group |
| AM | Air mass |
| AM1.5G | Air Mass 1.5 Global |
| aq. | Aqueous |
| Ar | Aromatic ring |
| Ar-BIAN | Bis(arylimino)acenaphthene |
| ATR | Attenuated Total Reflectance |
| BPHA | 4,7-Bis(4-hexylthiophen-2-yl)benzo[c] [1,2,5] thiadiazole |
| CB | Conduction band |
| CDCA | Chenodeoxycholic acid |
| CE | Counter electrode |
| CIGS | Copper indium gallium selenide |
| D | Donor group |
| DBTP | Di(1-benzothieno)[3,2-*b*:2′,3′-*d*]pyrrole |
| DDQ | 2,3-Dichloro-5,6-dicyano-1,4-benzoquinone |
| DFT | Density functional theory |
| DSSC | Dye sensitized solar cell |
| $e^-/h^+$ | Electron-hole |
| EDG | Electron donating group |
| $E_g$ | Optical band gap |
| eq. | Equivalent |
| EQE | External Quantum Efficiency |
| FF | Fill factor |
| FTO | Fluorine doped tin oxide |
| GHG | Greenhouse gas |
| GuSCN | Guanidinium thiocyanate |
| HOMO | Highest occupied molecular orbital |

| | |
|---|---|
| HRMS | High Resolution Mass Spectrometry |
| ICT | Intramolecular charge transfer |
| IL | Ionic Liquid |
| IPCE | Incident photon to current efficiency |
| IR | Infrared Spectroscopy |
| *I-V* (curves) | Current-Voltage (curves) |
| *J* | Coupling constant |
| $J_{sc}$ | short-circuit current |
| LC-ESI-MS | Liquid Chromatography Electrospray Ionization Mass Spectrometry |
| LHE | Light-harvesting efficiency |
| LUMO | Lowest unoccupied molecular orbital |
| MLCT | Metal-to-ligand charge transfer |
| N-3 | Cis-bis(isothiocyanato)bis(2,2′-bipyridyl-4,4′-dicarboxylato)ruthenium(II) |
| N-719 | Di-tetrabutylammonium cis-bis(isothiocyanato)bis(2,2′-bipyridyl-4,4′-di-carboxylato)ruthenium(II) |
| N-749 | Tris(N,N,N-tributyl-1-butanaminium)[[2,2″6′,2″-terpyridine]-4,4′,4″-tri-carboxylato(3-)-N1,N1′,N1″]tris(thiocyanato-N)hydrogen ruthenate |
| NBS | *N*-Bromosuccinimide |
| NIR | Near infrared |
| NMR | Nuclear Magnetic Resonance |
| OFET | Organic field-effect transistor |
| OPV | Organic photovoltaic cell |
| PAH | Polycyclic aromatic hydrocarbon |
| PCE, η | Photoconversion efficiency |
| Pin | Incident solar energy |
| PLC | Preparative-layer chromatography |
| Pmax | Maximum photoelectric output power |
| POZ | Phenoxazine |
| PTZ | Phenothiazine |
| Ref. | Reference |
| RT | Retention time |
| S | Sensitizer |
| S* | Sensitizer in the excited state |
| $S^+$ | Oxidized sensitizer |

| | |
|---|---|
| SDG | Sustainable development goal |
| TBA | Tetrabutylammonium |
| TBAF | Tetrabutylammonium fluoride |
| $TBAPF_6$ | Tetrabutylammonium hexafluorophosphate |
| TBP | 1-butyl-3-methylimidazolium iodide, 4-butylpyridin |
| TBP | 4-butylpyridine |
| TCE | Translucent conductive electrode |
| TCO | Transparent conductive oxide |
| TD-DFT | Time-Dependent Density Functional Theory |
| TLC | Thin-layer chromatography |
| VB | Valence band |
| $V_{oc}$ | Open-circuit voltage |
| $\varepsilon$ | Molar extinction coefficient |
| $\eta_{inj}$ | Electron injection efficiency |
| $\lambda_{max}$ | Absorption maximum wavelength |
| $\pi$ | $\pi$-bridge |
| $\delta$ | Chemical shift |
| $\eta_{coll}$ | Charge collection efficiency |

# 1

# INTRODUCTION

## 1.1 Context and motivation

Fossil fuel consumption has increased dramatically in the last decades as a result of global population growth and industrialization. This contributes to the constant increment of concentrations of greenhouse gases (GHGs) in the atmosphere, and thus causing aggravation of environmental pollution, global warming, and health problems. Besides that, these resources are finite and will be depleted within a few years at current use levels. In response to this, most of the countries with high harmful greenhouse gas emissions are committed to achieve carbon neutrality by 2050.[1,2]

The climate change concern and the production of sustainable energy are also included in the 17 Sustainable Development Goals (SDGs) for 2030 founded by the United Nations. These goals are a common strategy for world peace and prosperity, and the following are considered to be the most representative regarding this area: 7- Ensure access to affordable, reliable, sustainable and modern energy for all; 11- Make cities and human settlements inclusive, safe, resilient and sustainable; 13 - Take urgent action to combat climate change and its impacts (**Figure 1**).[3]

In light of this, it becomes imperative to invest in the development of renewable energies such as solar energy, hydropower and wind power. These have a minimal negative impact on the environment and will help to achieve carbon neutrality.[2]


Figure 1. Sustainable development goals [4] [a]

The sun the most powerful source of energy for the planet. The total amount of solar radiation that reaches the Earth's surface each year is equivalent to 7500 times the world's energy consumption.[5] As such, this source of renewable energy has great potential to contribute significantly to the global energy demand issue. Unfortunately, there is a gap between its potential and its use due to the high costs and low energy conversion capacity of light-harvesting devices. The development of technologies capable of efficient energy conversion and great stability is, thus, required. [6-8]

The composition of the first and second-generation solar cells includes mainly silicon.[9] The energy efficiency percentage of these conventional classical solar cells ranges from 16% to 22%. Due to this low conversion efficiency, a higher number of panels/cells must be used in order to generate a suitable amount of power output. Some of these cells are composed of pure silicon crystals, which increases their price.[10] In addition, the scarcity, the rising cost of raw materials and their inherent toxicity are all concerning factors, which become more relevant with the rise in the device's manufactoring.[11] A third generation of photovoltaic cells emerged as an alternative to classical photovoltaic cells. They use low-cost abundant materials, and are easily fabricated and produced on a large scale. Specifically, dye-sensitized solar cells (DSSCs) which were mainly developed through the work of Gratzël[12] represent a very suitable substitute

[a] The content of this publication has not been approved by the United Nations and does not reflect the views of the United Nations or its officials or Member States

for traditional silicon solar cells.[13] Ruthenium complexes are the most often applied dyes in these devices.[14] However, ruthenium is not an accessible metal,[15] and the photovoltaic performance of DSSCs must be upgraded to compete with the traditional silicon ones. As a result, the research for efficient totally organic dyes was considered a viable alternative.

This doctoral thesis' primary goal is to synthesize new push-pull organic molecules that can be an alternative to the ruthenium dyes applied in DSSCs. Taking into account the state of the art for dye sensitisers, this project aims to go further and, through molecular tailoring, propose the synthesis of new promising molecules. The dyes were obtained through the functionalization of different main cores, namely: coumarins, acenaphthenes acenaphthylenes and thieno[3,4-*b*]thiophenes. The final compounds were characterized by $^{1}$H NMR, $^{13}$C NMR and HRMS. The photophysical and electrochemical characterization was performed for the final sensitizers, as well as the theoretical calculations (DFT and TD-DFT). The DSSC devices were built from scratch and, subsequently, the photovoltaic performance of the final chromophores was tested by measuring the *I-V* curves and photocurrent action spectrum (IPCE).

## 1.2 History

It was a long time ago that Becquerel observed that voltage was generated under sunlight when two platinum electrodes were submerged in an electrolyte containing metal halide salts. This observation led him to discover the photovoltaic effect in 1839. In the photovoltaic effect, when light strikes a semiconductor material, electron-hole ($e^-/h^+$) pairs are generated. This leads to an electrical potential difference in the junction between the two semiconductors (n- and p-type[b]), which drives current across a circuit. This process of converting light energy into electrical energy has become the base of solar energy harvesting devices. [16-18]

An investigation group at Bell Labs created the first silicon solar cell in 1954.[19] Three years later it was patented as a monocrystalline silicon cell with a p-n junction that achieved a promising efficiency.[20] Since then, this technology has been incorporated into small daily objects, homes, and more complex structures, such as satellites. The development of this photovoltaic technology followed the necessity to replace the energy derived from fossil fuels. Four distinct

[b] n-type semiconductors are doped semiconductors in which the main charge carrier is an electron, whereas p-type semiconductors are semiconductors in which the dominant charge carrier is a hole.

generations of photovoltaic solar cells have emerged. The first one concerns the aforementioned silicon solar cells, using a wafer-based design composed of layers of crystalline silicon or gallium arsenide (GaAs). They have become the leading commercial cells, due to their promising effectiveness and robustness. The second generation consists of thin film cells and it uses cheaper materials than the first one, namely amorphous silicon, gallium selenide ($Ga_2Se_3$), copper indium gallium selenide ($CuIn_{1-x}Ga_xSe_2$ with $0 \leq x \leq 1$; usually abbreviated as CIGS), and cadmium telluride (CdTe). [9,21] The third generation has been developed as a substitute to the conventional inorganic p–n junction solar cells. They are easy to manufacture and can be produced on a large scale and use abundant and inexpensive materials. Some examples are organic photovoltaics, perovskites solar cells, quantum dots solar cells and dye-sensitized solar cells. The fourth generation, also known as "nano photovoltaics", applies new materials to this field such as graphene or carbon nanotubes that can be included in DSSCs and polymers/organic photovoltaic cells. [22]

## 1.3 Dye-sensitized solar cells (DSSCs)

Beyond the aforementioned photovoltaic cells, dye-sensitized solar cells (DSSCs) represent a very promising alternative to conventional silicon cells.[13] DSSCs were first reported in the 1870s, when Vogel discovered a silver halide gelatin that exhibited activity under UV light. Later, by applying dyes with this silver halide gelatin emulsion, it was possible to observe activity under visible light. This photosensitization phenomenon was corroborated by Moser in 1887, with this device achieving a voltage of around 0.04 V.[17,23,24] In the same year, Hertz found that photons can eject electrons from a solid conductor surface to generate energy. After several decades, the field continued to expand with the sensitization of ZnO with cyanines (Hishiki, 1965)[25] and rose Bengal (Tributsch, 1968) being reported.[26] In 1977, $TiO_2$ was employed as an alternative semiconductor to ZnO by Spitler and Calvin.[27] In 1991 Brian O'Regan and Michael Grätzel described a promising photovoltaic cell with ruthenium-based dyes adsorbed on colloidal $TiO_2$ films.[12]

The work of Grätzel's group was the beginning of a new era on DSSC research. These devices are regarded as one of the most promising substitutes for conventional silicon solar cells and have generated considerable interest, due to their lower cell fabrication costs when compared to silicon cells, flexible molecular design of the sensitizers, transparency, relatively high energy

conversion efficiencies, and ability to operate under diffuse light.[28-30] These cells separate the function of light absorption from charge carrier transport and use dye molecules that absorb photons, converting them into electric charge. This separation of functions allows the use of materials with lower purity, which makes these devices a low-cost option. The DSSC operational process is a biomimetization of photosynthesis, in which the dye functions as an electron transfer sensitizer similar to chlorophyll present in plants.[12,31,32]

### 1.3.1 DSSC structure

Since Grätzel's work[12], the structure of the DSSCs generally hasn´t changed much and contains a photoelectrode (anode), a counter electrode (cathode), and an electrolyte (redox mediator) (Figure 2).

The photoelectrode comprises a dye adsorbed to a porous semiconductor layer, which is deposited on glass containing a translucent conductive electrode (TCE). Due to its thermal and physical resistance, chemical stability, electrical conductivity, ample availability, and optical transparency, the fluorine doped tin oxide (FTO) is the conductive electrode of choice.[33] Since Gratzel's primordial work, nanocrystalline $TiO_2$ is the most employed semiconductor metal oxide, and the use of these nanoparticles ensures a larger surface area for dye adsorption than flat $TiO_2$ films. Regarding the existent polymorphs of $TiO_2$, anatase (tetragonal) is the preferred one to be applied in DSSCs due to its superior efficiency, photocatalysis, and stability. Contrasting with other polymorphs, anatase is an indirect band gap semiconductor, which means that excited electrons are unable to go directly from the conduction band (CB) to the valence band (VB), leading to longer photoexcited electron lifetimes.[10,34-36] Usually the dye sensitizer anchors to the $TiO_2$ through carboxylic acid or cyanoacrylic acid anchoring groups. This adsorption typically occurs by submerging the anode containing a $TiO_2$ layer in a dye solution. The solvent used, the adsorption time, the dye concentration and the pH of the solution will influence this dye sensitization process. In the last decades, the search of dyes for more efficient DSSCs has been extensive. This topic is detailed in section 1.4.

The electrolyte regenerates the dye continuously and transports the inner charge carrier between the anode and cathode. In their constitution they have a solvent (e.g. acetonitrile) and a redox mediator, generally the redox couple $I^-/I_3^-$.[37,38] Despite its excellent performance, the $I^-/I_3^-$ pair has certain drawbacks due to its corrosive nature and the significant thermodynamic loss during the dye renewal process. Alternatively, electrolytes based on Co(II)/Co(III)[39] and

Cu(I)/Cu(II)[40] have been successfully employed. Ionic liquids (ILs), which possess exceptional thermal stability, almost negligible vapor pressure, and non-flammability properties, have also been applied as electrolytes in DSSCs and represent a suitable option for the aforementioned liquid electrolytes.[41] To increase the performance of the DSSC, additives can be added to the electrolyte, such as 1-butyl-3-methylimidazolium iodide, 4-butylpyridine (TBP), and guanidinium thiocyanate (GuSCN) present in EL-HPE High Performance Electrolyte®.

The counter electrode comprises a transparent conductive oxide (TCO) glass covered with a catalyst (e.g platinum or carbon), capable to receive electrons from the external circuit and then reduce the redox couple ($I_3^-$ to $I^-$).[38]

Despite the advancements in these devices, their efficiencies remain lower than other competing technologies. As such, to improve their photovoltaic performance all the key components of these cells must be refined. This includes the photoanode, dye sensitizer, electrolyte, cathode, and also the architecture of the cell itself.[42]

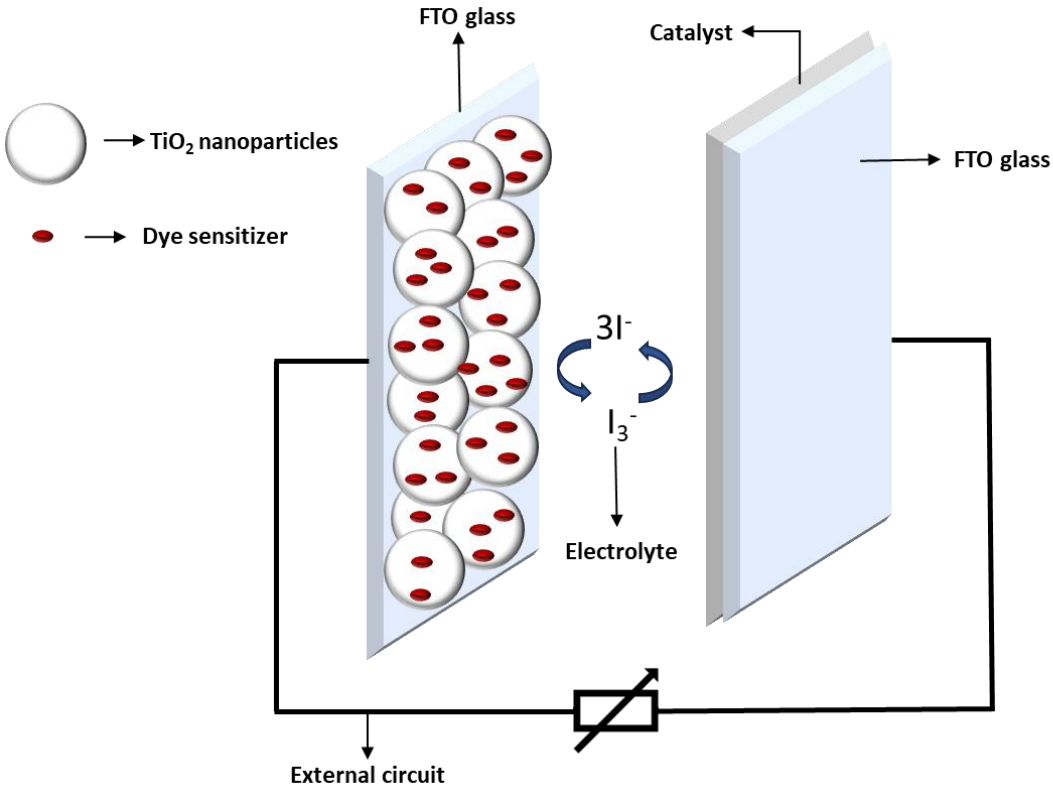


Figure 2. Architecture of a typical DSSC.

### 1.3.2 DSSC operational process

In a DSSC's operational process (**Figure 3**), the dye sensitizer absorbs visible light, resulting in photoexcitation from the HOMO to the LUMO of the molecule (1, Equation 1). Then, the excited electron is injected into the CB of the $TiO_2$ layer (2, Equation 2), and the dye is oxidized. The injected electron is transported through the $TiO_2$ nanoparticles to achieve the FTO glass. Subsequentially, the electron passes to the counter electrode via an external circuit (3). The circuit is completed when the electrolyte is regenerated at the counter electrode (CE) (4, Equation 4) (the $I_3^-$ ion is reduced to $I^-$). The oxidized dye is regenerated by electron donation from the iodide ion present in the electrolyte (5, Equation 3) and, as a result, the $I^-$ ion is oxidized to $I_3^-$.[43-45]

Unwanted processes may occur during the operational DSSC process, thus negatively affecting the cell performance. Recombination and dark current are two examples of what may occur during cell operation. Recombination happens when the injected electrons in the CB of $TiO_2$ recombine with the oxidized dye (6, Equation 5). They can also recombine with the redox couple in the $TiO_2$ surface, the process commonly called as dark current (7, Equation 6). Another undesired event is the electron's direct decay from the excited to the ground state (8, Equation 7).[43,46]

The dye's chemical composition (functional groups capable of inter and intramolecular interactions, polarity, presence or absence of long alkyl chains) will have an impact on its intrinsic capacity to interact with another molecule. If a clustering of molecules is formed (dye aggregation), this may affect the homogeneous distribution of the dye in the metal oxide surface or inhibit the $TiO_2$---dye interaction and, as a consequence, efficient electron injection will cease to exist.[47]

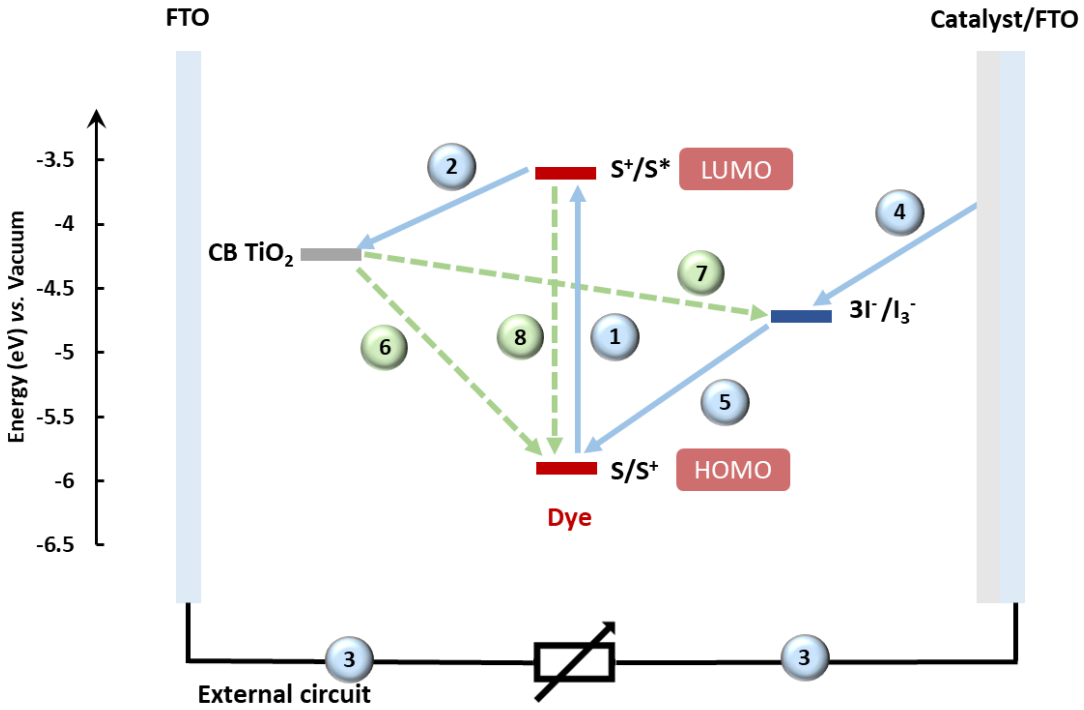


Figure 3. Operation principles of a DSSC containing an iodine electrolyte with $I^-/I_3^-$ redox couple. 1. Dye photoexcitation; 2. Injection of excited electron into the CB of $TiO_2$; 3. Electron transport via external circuit; 4. Regeneration of the electrolyte; 5. Regeneration of the oxidized dye; 6. Recombination; 7. Dark current; 8. Electron's decay from the excited to the fundamental state.

| | | |
|---|---|---|
| Dye excitation | $S\ [TiO_2] + h\nu \rightarrow S^*\ [TiO_2]$ | (1) |
| Electron Injection / Dye oxidation | $S^*\ [TiO_2] \rightarrow S^+\ [TiO_2] + e^-\ [TiO_2]$ | (2) |
| Dye regeneration / Redox mediator oxidation | $2S^+\ [TiO_2] + 3I^- \rightarrow 2S\ [TiO_2] + I_3^-$ | (3) |
| Redox mediator regeneration | $I_3^- + 2e^-\ [CE] \rightarrow 3I^-$ | (4) |
| Recombination | $e^-\ [TiO_2] + S^+\ [TiO_2] \rightarrow S\ [TiO_2]$ | (5) |
| Dark current | $2e^-\ [TiO_2] + I_3^- \rightarrow 3I^-$ | (6) |
| Direct decay to the fundamental state | $S^*\ [TiO_2] \rightarrow S\ [TiO_2]$ | (7) |

### 1.3.3 Solar spectrum

The solar spectrum extends from 280 to 4000 nm. Part of this spectrum is filtered after passing through the planet's atmosphere. Given this, the solar spectrum in space differs from the spectrum that reaches the planet's surface. The passage through the atmosphere determines the total amount of irradiation at the Earth's surface, which is determined by a coefficient denoted air mass (AM). Although the irradiation at the surface varies with the time of the year, a standardized spectrum for energy conversion applications is required. The solar irradiance measured outside the atmosphere is represented by the reference spectrum AM0, and it is used for testing solar cells in space. The spectrum that characterizes the radiation reaching at the planet's surface after passing through 1.5 times a standard air mass, with the sun at 48.2°, is denominated Air Mass 1.5 Global (AM1.5G). This is the standard spectrum to measure the photovoltaic performance of terrestrial solar cells and it has a power intensity of 1000 W $m^{-2}$ (**Figure 4**).[13,48]

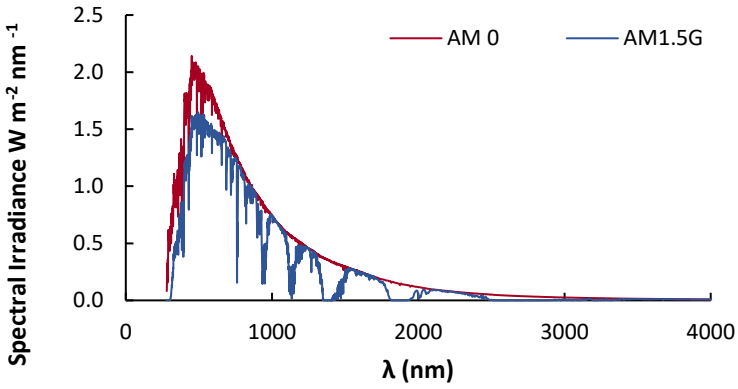


Figure 4. Reference spectra AM0 and AM1.5G (ASTM G173-03).[49]

### 1.3.4 Solar cell parameters

#### 1.3.4.1 Photocurrent-voltage curves

To evaluate a DSSC efficiency, the cell is irradiated by a simulator calibrated against a reference spectrum, in the terrestrial conditions under simulated AM1.5G conditions. Voltage is

applied across the cell and the current flowing through it is measured, allowing for the obtention of the photocurrent-voltage curves (*I-V* curves) (**Figure 5**). These curves represent the relationship between the current and the voltage across its terminals at a given irradiance, temperature, and different external circuit loads.

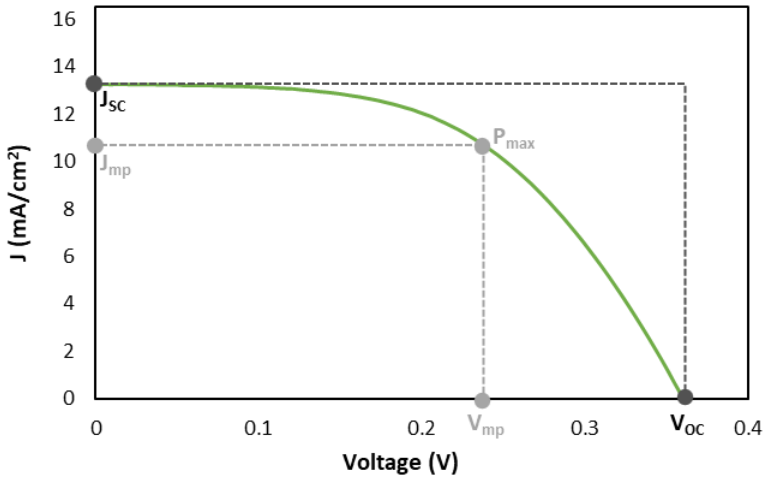


Figure 5. Typical photocurrent-voltage (*I-V*) curve for a DSSC.

The photoconversion efficiency (PCE, η) of a DSSC can be determined by the ratio between the maximum photoelectric output power ($P_{max}$) and the incident solar energy ($P_{in}$). $P_{max}$ is equal to the product of the current and voltage values where the output energy is maximal ($J_{mp}$ and $V_{mp}$ respectively).[50] (Equation 8)

$$\eta = P_{max}/P_{in} = (J_{mp} \times V_{mp})/P_{in} \quad (8)$$

In an *I-V* curve (Figure 5), the short-circuit current ($J_{sc}$) represents the current flow when the voltage is 0 V, and the open-circuit voltage ($V_{oc}$) represents the voltage difference across the cell when the current is 0 A. These two values correspond respectively to the greatest current and voltage that can be obtained from the solar cell.[51]

The fill factor (FF), whose values range from 0 and 1, determines the amount of electrical and electrochemical losses occurring when the DSSC is operating. It can be determined by the following equation 9 and indicates the amount of the rectangular area for $J_{sc}$ x $V_{oc}$ is filled by the $J_{mp}$ x $V_{mp}$ rectangle area (black and grey dashed rectangles respectively).[31,43]

$$FF = (J_{mp} \times V_{mp})/(J_{sc} \times V_{oc}) \quad (9)$$

Thus, the relationship between overall PCE (η), $V_{oc}$, $J_{sc}$, and FF of a DSSC is given by equation 10.

$$\eta = P_{max}/P_{in} = (J_{sc} \times V_{oc} \times FF)/P_{in} \quad (10)$$

The chosen sensitizer has a massive impact on the cell efficiency. Each parameter $J_{sc}$, $V_{oc}$ and FF must be considered individually, to better understand why a dye has a considerably higher or lower PCE in a DSSC device.

The short-circuit current ($J_{sc}$) is mainly affected by the molar extinction coefficient, the spectral range of the dye and, also, electron injection efficiency. The open circuit-voltage ($V_{oc}$) concerns the difference between the energy level of the redox couple and the quasi-Fermi level of the semiconductor. It is given by the following equation 11, in which $E_{CB}$ is the level of CB $TiO_2$, n is the number of electrons on $TiO_2$, $N_{CB}$ is the effective density of states, $E_{redox}$ is the HOMO energy level of the redox couple and q is the unit charge. To improve the $V_{oc}$ value, it is necessary to increase the $E_{CB}$ or decrease the $E_{redox}$.[46,52]

$$V_{oc} = \frac{E_{CB}}{q} + \frac{kT}{q}\ln\left(\frac{n}{N_{CB}}\right) - \frac{E_{redox}}{q} \quad (11)$$

#### 1.3.4.2 Incident photon to current conversion efficiency

The incident photon to current conversion efficiency (IPCE) is the ratio between the generated electrons and the incident photons as a function of λ. In short circuit conditions, the IPCE is given by equation 12, where $J_{sc}$ (λ) is the $J_{sc}$ produced under monochromatic illumination and Φλ is the incident monochromatic photon flux.[16,53]

$$IPCE = 1240 \times \frac{J_{sc}(\lambda)}{\lambda \times \Phi_{\lambda}} \quad (12)$$

IPCE can also be defined as the product of electron injection efficiency from the dye's excited state ($\eta_{inj}$), light-harvesting efficiency (LHE), and charge collection efficiency ($\eta_{coll}$) (Equation 13).

$$IPCE = \eta_{inj} \times LHE\ (\lambda) \times \eta_{coll} \quad (13)$$

LHE can be obtained through the absorbance of the dye on the $TiO_2$ (a), as described on the following equation 14.[54]

$$LHE = 1 - 10^{a} \quad (14)$$

## 1.4 Dyes for DSSCs

The development of new efficient dyes for DSSCs devices has been a case of study for the past few decades. Research on DSSCs reached its pinnacle in 2014, but it remains a topic of scientific interest to this day (**Figure 6**). They can be divided into several classes, such as ruthenium-based dyes, natural sensitizers, and organic metal-free dyes.[55]

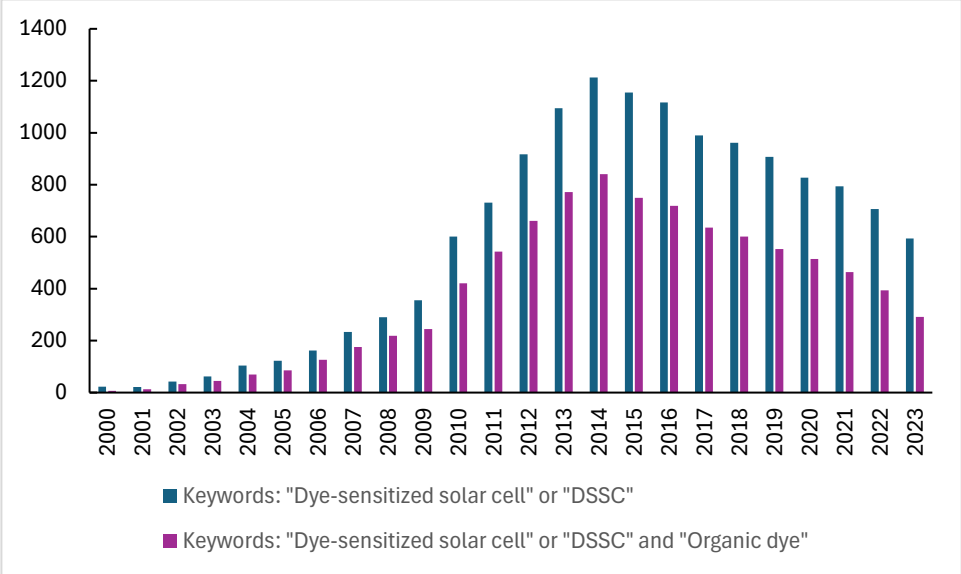


Figure 6. Number of research articles per year using the keywords: "Dye sensitized solar cell" or "DSSC" (blue / left bar); "Dye sensitized solar cell" or "DSSC" and "Organic dye" (purple / right bar) (data source: ISI Web of Knowledge)

### 1.4.1 Ruthenium dyes

Since Gratzel's work in 1991[12] ruthenium-based dyes have been the preferred sensitizers for several years. These sensitizers consist of a central ruthenium metal ion, which is linked to ancillary ligands (e.g. bipyridines or terpyridines), and anchoring groups like (e.g. carboxylic acid). They have long-term chemical stability and superior quantum yield of electron injection into the CB of $TiO_2$. Moreover, the metal-to-ligand charge transfer (MLCT) process is responsible for a large absorption range (from visible to NIR).[14,50] The most representative ruthenium(II)–polypyridyl complexes include N-719, N-3, and N-749 (black dye), which have achieved DSSCs efficiencies of 11.2 %, 10.0 %, and 11.1% respectively (**Figure 7**).[56] These polypyridyl complexes contain carboxylate groups, which decreases the energy of the π* orbital.[57] Despite the high efficiencies, inferior molar extinction coefficients, complicated purification steps and the existence of dye aggregation represent drawbacks in this family of compounds.[14] Besides that, ruthenium is an expensive metal and is not earth-abundant and its price increased drastically in the last decade, which compromises the use of these complexes on a large scale.[15,58]

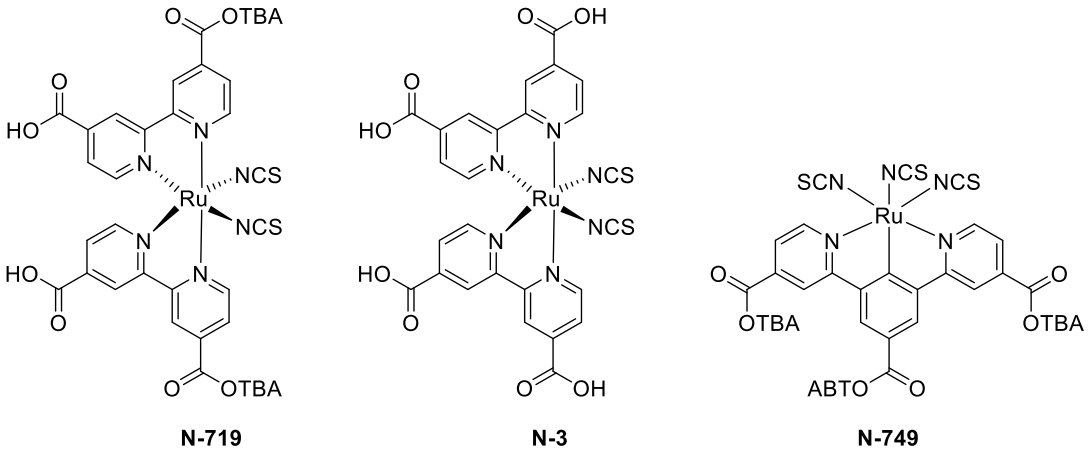


Figure 7. Structures of ruthenium-based dyes N-719, N-3, and N-749.

### 1.4.2 Natural sensitizers

Natural dyes are present in fruits, leaves, roots, and flowers. They can be obtained generally in large amounts by using simple procedures, such as extraction with ethanol, acetone, or water, which turns them into a cheaper and more ecological alternative to synthetic dyes. [59,60]

Some examples of natural dyes applied in DSSCs are anthocyanins[61-63], chlorophylls[64], and betalains[65] (**Figure 8**). These dyes can be used directly as a mixture of compounds (extracts) or in their pure form. Additionally, chemical modifications can be made to improve their efficiencies.

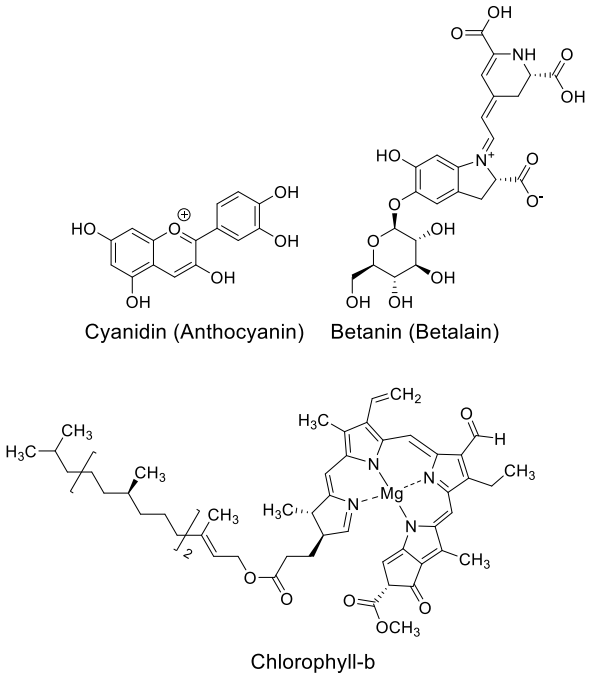


Figure 8. Chemical structures of natural sensitizers.

### 1.4.3 Organic metal-free dyes

Due to the shortage and cost of raw materials or low efficiencies of the two types of dyes mentioned above, the research is now focused on metal-free organic sensitizers. They provide superior long-term chemical stability, high molar extinction coefficients, considerable flexibility in tuning molecular architecture, and easier and less expensive synthesis methods when compared to ruthenium-based dyes.[54]

An efficient metal-free organic dye should accomplish the following requirements:

1) Have a highly conjugated π-system, with a low bandgap between the frontier molecular orbitals.

2) For efficient light harvesting, the absorption spectrum of the dye should cover a wide range of the visible and NIR spectrum; high molar extinction coefficients (ε) are also required.

3) The effective electron transfer process between the excited dye and the semiconductor's conduction band (CB) requires that the LUMO is higher than the CB of the $TiO_2$. Also, to ensure efficient dye regeneration by electron donation from the electrolyte, the HOMO of the dye must be lower than the redox potential of the redox pair (**Figure 3**).

4) Electron lifetime in the excited state must be long enough for the injection of all the excited electrons into the CB of the semiconductor to occur before the dye returns to its fundamental state.

5) The anchoring groups should interact strongly with the semiconductor.

6) The dye must have good heat, electrochemical, chemical, and light stability.[50,51,66,67]

The greatest focus of research in this field is directed towards these organic molecules. In the last few decades, more than half of the published articles have been related to organic dyes (**Figure 6**).

Generally, these metal-free organic dyes have a design based on a D-π-A architecture (**Figure 9**). In the dye structure D corresponds to the donor moiety, π is the π-bridge, and A the acceptor. This push-pull structure can induce intramolecular charge transfer (ICT) from the donor to the acceptor subunits through the π-bridge, when a dye absorbs light. In a D-π-A dye, the HOMO levels are generally localized on the donor and the π-bridge, and the LUMO levels are localized in the acceptor moiety. The energy levels, the photophysical characteristics, and the photovoltaic performance can be modulated by modifying the donor and the π-bridge moieties.[52]

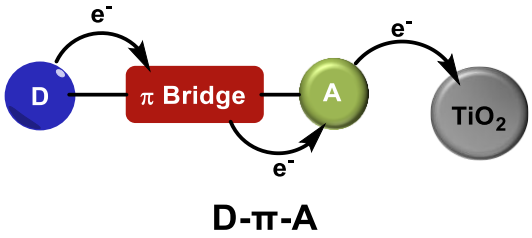


Figure 9. Mono-branched D–π–A architecture of an organic dye sensitizer. Schematic representation of the ICT from the donor to the acceptor and electron injection into the $TiO_2$ nanoparticles.

However, the D-π-A design presents some drawbacks, namely the tendency to aggregate and the existence of only one anchoring group that may lead to reduced electron transfer ability.[68] By taking into account the highly efficient ruthenium dyes that have present in their structure one to four anchoring groups for an efficient electron transfer, di-anchoring and di-branched groups of dyes have emerged (e.g $D\text{-}(\pi\text{-}A)_2$, $D_2\text{-}\pi\text{-}A_2$ and $(D\text{-}\pi)_2\text{-}A$) (Figure 10). This multi-branched architecture presents advantages over the mono branched one, such as a

greater structural variety to achieve panchromatic response, superior optical density conferred by the extended π-conjugated system, and increased binding strength of the dye on $TiO_2$.[69-72]

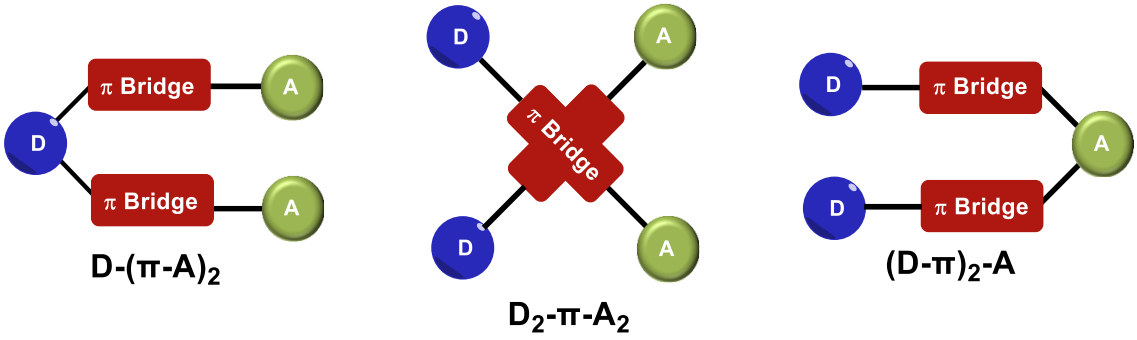


Figure 10. Schematic representation of multi-branched and multi-anchoring design of organic DSSC dyes.

Some examples of di-branched di-anchoring organic dyes are depicted in Figure 11 and its spectroscopic and photovoltaic parameters are presented in Table 1. In all reports, a comparison with a unidimensional dipolar analog is made. In 2009, Abbotto *et al.* introduced the first di-branched di-anchoring dyes, which comprised a donor group, triarylamine, linked to two anchoring groups via a π-spacer, vinylthiophene (1.2). The UV-Vis spectra indicate a bathochromic effect from the mono- (1.1) to the di-branched (1.2) structure, and, also, a superior molar absorptivity (ε) for the latter. The power conversion efficiency of the di-branched structure (1.2) was 5.7 % and the mono-branched (1.1) was 5.5 %. This improvement was due to an increase in photocurrent (from 11.56 to 12.68 $mA/cm^2$) and enhanced stability, conferred by the presence of a di-anchoring system.[72] The effect of mono- and bi-anchors on photovoltaic performance was also studied by Cao's group. Different structures containing the central core di(1-benzothieno)[3,2-*b*:2′,3′-*d*]pyrrole (DBTP), with one or two anchors linked by a thiophene moiety were synthesized (1.3-1.6). The di-anchoring dyes (1.5-1.6), when compared with the mono-anchoring analogues (1.4-1.3), exhibited a red-shift (24-28 nm) and an improvement in molar extinction coefficients. Additionally, concerning the photovoltaic performance, the di-branched achieved higher efficiencies (6.73-7.09%, in contrast to the reported 5.37-5.78% for the mono-anchoring dyes), due to a larger photo-spectral response and a more efficient electron injection.[73] Liu *et al.* synthesized D-D-π-A dyes, in which three different additional units were linked to indoline (carbazole, fluorene, and 4-methylphenyl), and cyanoacrylic acid was used as acceptor linked to the donor via a vinyl thiophene (1.7-1.9). It was possible to observe that by increasing the electron-donating ability of the substituents, the absorption spectra are shifted to a longer wavelength (carbazole – 523 nm > fluorene – 504 nm > 4-methylphenyl -

491 nm). The same behaviour was observed for improved power conversion efficiency and $J_{sc}$, with the carbazole derivative (1.8) being the best-performing dye ( 5.87 %).[74]

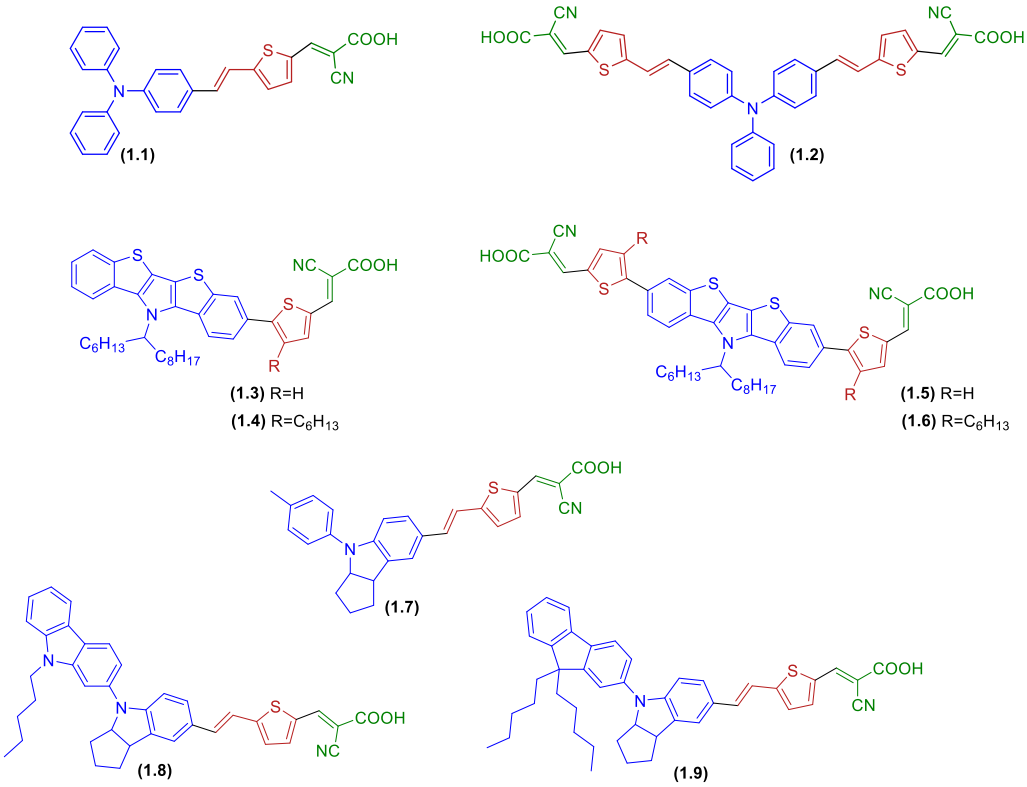


Figure 11. Chemical structures of di-branched di-anchoring sensitizers and respective unidimensional analogues.

Table 1. Spectroscopic and photovoltaic parameters of di-branched di-anchoring sensitizers and respective unidimensional analogues.

| Dye | $\lambda_{max}$ (nm) | ε ($M^{-1}$ $cm^{-1}$) | $J_{sc}$ ($mA/cm^2$) | $V_{oc}$ (V) | FF | η (%) | Ref. |
|---|---|---|---|---|---|---|---|
| **1.1** | 441 | 33 000 | 11.56 | 0.653 | 0.73 | 5.5 | [72] |
| **1.2** | 463 -473 | 44 500 | 12.68 | 0.612 | 0.73 | 5.7 | |
| **1.3** | 457 | 43 516 | 10.66 | 0.702 | 0.72 | 5.37 | [73] |
| **1.4** | 426 | 34 100 | 9.73 | 0.774 | 0.77 | 5.78 | |
| **1.5** | 495 | 81 667 | 15.41 | 0.673 | 0.68 | 7.09 | |
| **1.6** | 450 | 65 280 | 13.19 | 0.741 | 0.69 | 6.73 | |
| **1.7** | 491 | 22 300 | 9.77 | 0.622 | 0.65 | 3.99 | [74] |
| **1.8** | 523 | 27 900 | 14.16 | 0.628 | 0.66 | 5.87 | |
| **1.9** | 504 | 27 200 | 12.28 | 0.614 | 0.68 | 5.09 | |

Following the referred architectures, it is possible to synthesize a vast amount of different promising dyes by combining different donors, acceptors, and π-bridges.

The donor's electron-donating ability will strongly influence the light-harvesting capacity and the energy levels of the molecule. Triarylamines[75] have received prominence as donor groups in the last years. Similarly, donor groups based in phenoxazines[76] and phenothiazines[77] have also been regarded as very promising. These donors have non-planar structures that avoid dye aggregation. Other examples of donors include coumarins[78-80], indolines[81], carbazoles[82], and truxene,[83] which are also widely used for this purpose (**Figure 12**).[84] The existence of a structure containing two distinct donor groups with complementary absorption spectra should confer enhanced optical properties to the final dye. The π-bridge allows the extension of the π-conjugated system of the molecule and works as a passage for charge transfer from the donor to the acceptor. Phenyl or heterocycle rings such as thiophene and their derivatives are frequently used as π-bridges in dye sensitizers, because of their exceptional conjugate structures. Modifying the π-bridge, even if only slightly by changing one atom, will significantly impact the device's performance.[85] Polyaromatic backbones such as thieno[3,4-*b*]thiophene[86] or indenofluorine[87] can be used as a component of the conjugated π-bridge (**Figure 12**). The anchoring group may be the same as the acceptor moiety or be in close proximity to it, and it has the capacity to immobilize the dye in the surface of the $TiO_2$, which is essential for the generation of electrical current flow. The bonding between the dyes and the $TiO_2$ surface is mainly covalent, thus conferring uniform dye distribution, firm coupling, and stability. The cyanoacrylic acid group is the most promising anchoring group to $TiO_2$. Alternatively, catechols, vinylpyrimidines, carboxylic acids, and rhodanine acetic acid can also effectively anchor to $TiO_2$ (**Figure 12**). The carboxylate groups coordinate with the metal ions from the semiconductor surface mainly by monodentate, chelated bidentate, and bridged bidentate modes (**Figure 13**).[84,88-90] Sterically hindered substituents, such as long linear and branched alkyl chains, can also be introduced in the dyes (**Figure 12**). These will help to control the uniform distribution of sensitizers on the metal oxide surface by reducing the π---π interactions, thus having the capacity to suppress dye aggregation and impede charge recombination occurrence (**Figure 12**).[91,92]

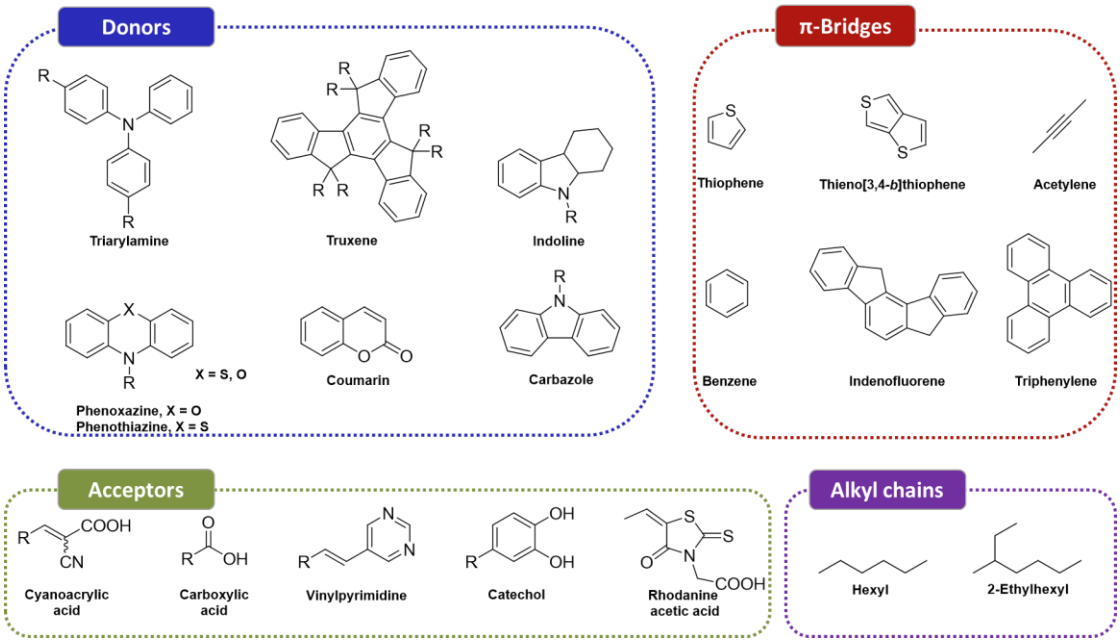


Figure 12. Structures that can be used as donors, π-bridges, acceptors, and substituents alkyl chains in DSSC chromophores.

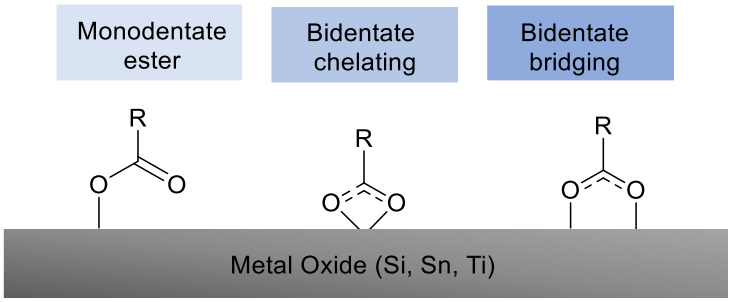


Figure 13. Binding modes of carboxylic acids with metal oxide surface.

### 1.4.3.1 Highly efficient organic dyes

Some examples of highly efficient metal-free organic dyes resulting from an exceptional molecular tailoring approach are dye R6, (blue dye) developed by Grätzel's group[93] and dye ZL003, synthesized and studied by Sun's group.[94] Dye R6 contains an extensive conjugated π-system, containing a benzophenanthrothieno benzophenanthrothiophene as π- bridge, a diarylamine as a donor, and 4-(7-ethynylbenzo[c][1,2,5]-thiadiazol-4-yl)benzoic acid as anchoring group. By using a Co(II/III)tris(bipyridyl)-based redox electrolyte with this dye, the cell achieved

a photovoltaic performance of 12.6 %, with $J_{sc}$, $V_{oc}$, and FF values of 19.69 mA/cm$^2$, 0.850 V and 0.75, respectively.[93] The sensitizer ZL003 is based on a triazatruxene donor core linked to a π-bridge, 4,7-Bis(4-hexylthiophen-2-yl)benzo[c][1,2,5]thiadiazole (BTBT), and 4-ethynylbenzoic acid as the chosen anchoring group. This dye achieved a PCE of 13.6 % when an electrolyte based on Co-bpy was employed (**Figure 14**, **Table 2**).

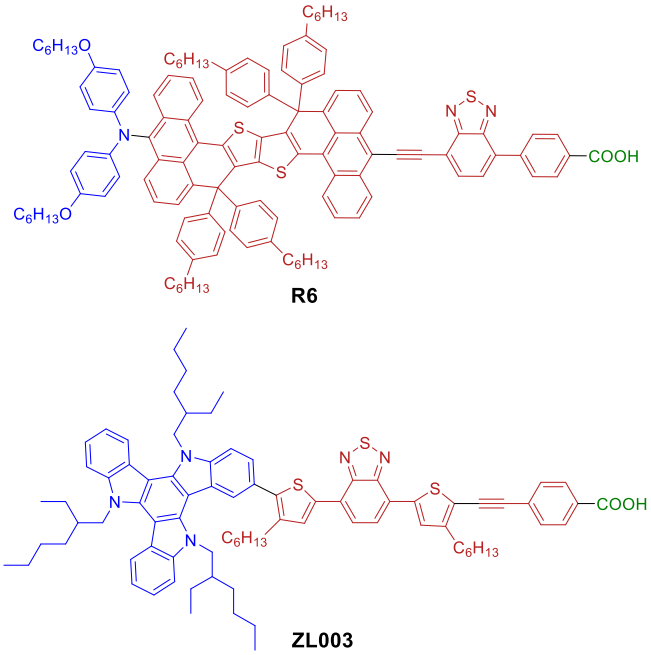


Figure 14. Chemical structures of the highly efficient dyes R6 and ZL003.

In 2023 it was reported a co-sensitization study with two molecules, SL9 and SL10, having complementary absorption spectra (SL9: 330 nm and 557; SL10: 333 nm and 413 nm). A pre-adsorption of 2-(4-butoxyphenyl)-*N*-hydroxyacetamide (BPHA) in $TiO_2$ helped to prevent the desorption of dyes SL9 and SL10 and improved the molecular packing. A remarkable power conversion efficiency of 15.2% was achieved (**Figure 15**, **Table 2**).[95]

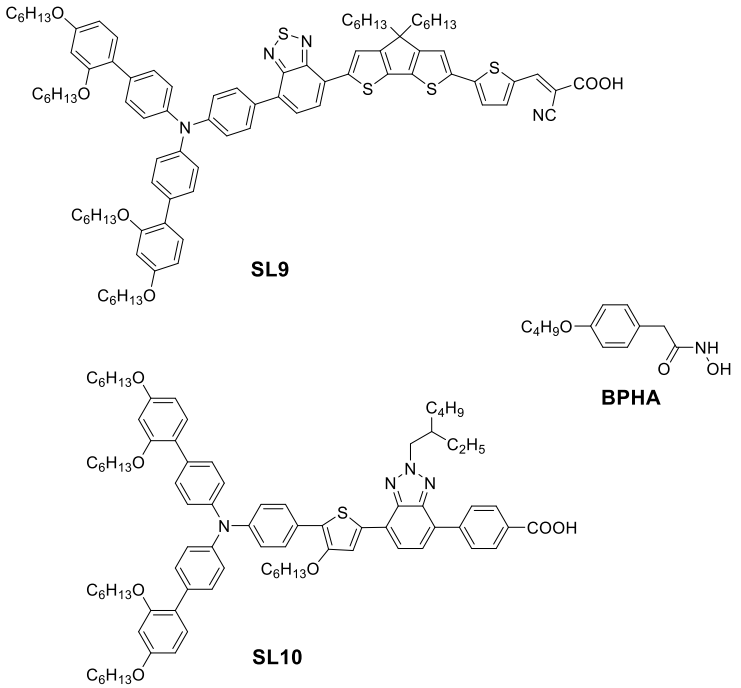


Figure 15. Chemical structures of the highly efficient sensitizers SL9 and SL10

Table 2. Spectroscopic and photovoltaic parameters of highly efficient sensitizers R6, ZL003, SL9, SL10

| Dye | $\lambda_{max}$ (nm) | ε ($M^{-1}$ $cm^{-1}$) | $J_{sc}$ (mA/$cm^2$) | $V_{oc}$ (V) | FF | η (%) | Ref |
|---|---|---|---|---|---|---|---|
| **R6** | 631 | 81 820 | 19.69 | 0.850 | 0.75 | 12.6 | [93] |
| **ZL003** | 519 | 29 042 | 20.73 | 0.956 | 0.69 | 13.6 | [94] |
| **SL9** | 330 | 54 700 | | | | | [95] |
| | 557 | 64 600 | 17.8 | 1.04 | 0.82 | 15.2 | |
| **SL10** | 333 | 41 900 | | | | | |
| | 413 | 33 000 | | | | | |

# 2 COUMARIN DERIVATIVES AS PHOTOSENSITIZERS

*Coumarin derivatives as photosensitizers* chapter is based on the journal article "Sarrato, J.; Pinto, A. L.; Malta, G.; Rock, E. G.; Pina, J.; Lima, J. C.; Parola, A. J.; Branco, P. S. New 3-Ethynylaryl Coumarin-Based Dyes for DSSC Applications: Synthesis, Spectroscopic Properties, and Theoretical Calculations. *Molecules* **2021**, *26*, 2934."

The author contributed to the synthesis and structural characterization of the compounds with the collaboration of João Sarrato (M.Sc.), the DSSCs devices were prepared by Ana Lúcia Pinto (PhD). The absorption and emission spectra and DFT studies were carried out at the University of Coimbra by Professor João Pina and the student Eva Röck (M.Sc.). This chapter only depicts the synthetic methodology performed by its author and several considerations about the photophysical properties and photovoltaic efficiency.

## 2.1 General overview

Coumarins (2*H*-chromen-2-ones) are a class of compounds of natural occurrence that can be found in many plant families. They are secondary metabolites derived from the shikimic acid pathway and were originally extracted from tonka beans by Vogel in 1820.[96,97] They are heterocycle compounds that contain a benzene ring fused with a lactone ring. The double bond present in the latter extends the conjugated π-system across the molecule (**Figure 16**).[98]

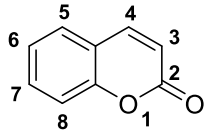


Figure 16. Chemical structure of coumarin.

Coumarins can be synthesized by different methodologies such as Perkin, Pechmann, Knoevenagel, Wittig, Reformatsky, and Kostanecki reactions. The first synthetic methodology to obtain coumarins was developed by Perkin. By reacting salicylaldehyde with acetic anhydride and sodium acetate, the *o*-hydroxycinnamic acid is formed and the coumarin is obtained after an intramolecular cyclization.[99,100] The Pechmann reaction consists of an esterification/transesterification reaction between a β-keto ester and a phenolic derivative in the presence of an acid (e.g. Lewis acid). After ring closure and dehydration the desired coumarin is obtained.[101,102] The Knoevenagel condensation is also applicable for the preparation of this scaffold, by reacting a salicylic aldehyde derivative with a malonate derivative in the presence of amines or ammonia.[103,104] The Wittig reaction can be applied for the synthesis of this heterocycle. In this case, a salicylic aldehyde analog reacts with a phosphonium ylide and, after an intramolecular Wittig cyclization, the coumarin is obtained.[101,105] In the Reformatsky reaction ketones or aldehydes react with a zinc metal to obtain a β-hydroxy ester, affording the desired coumarin after a lactonization.[104] In the Kostanecki reaction, an *o*-acylation occurs by reacting an o-hydroxyaryl ketone with an aliphatic anhydride (eg. acetic anhydride) in the presence of a base. After that, a cyclization occurs via an aldol condensation followed by dehydration (**Figure 17**).[106,107]

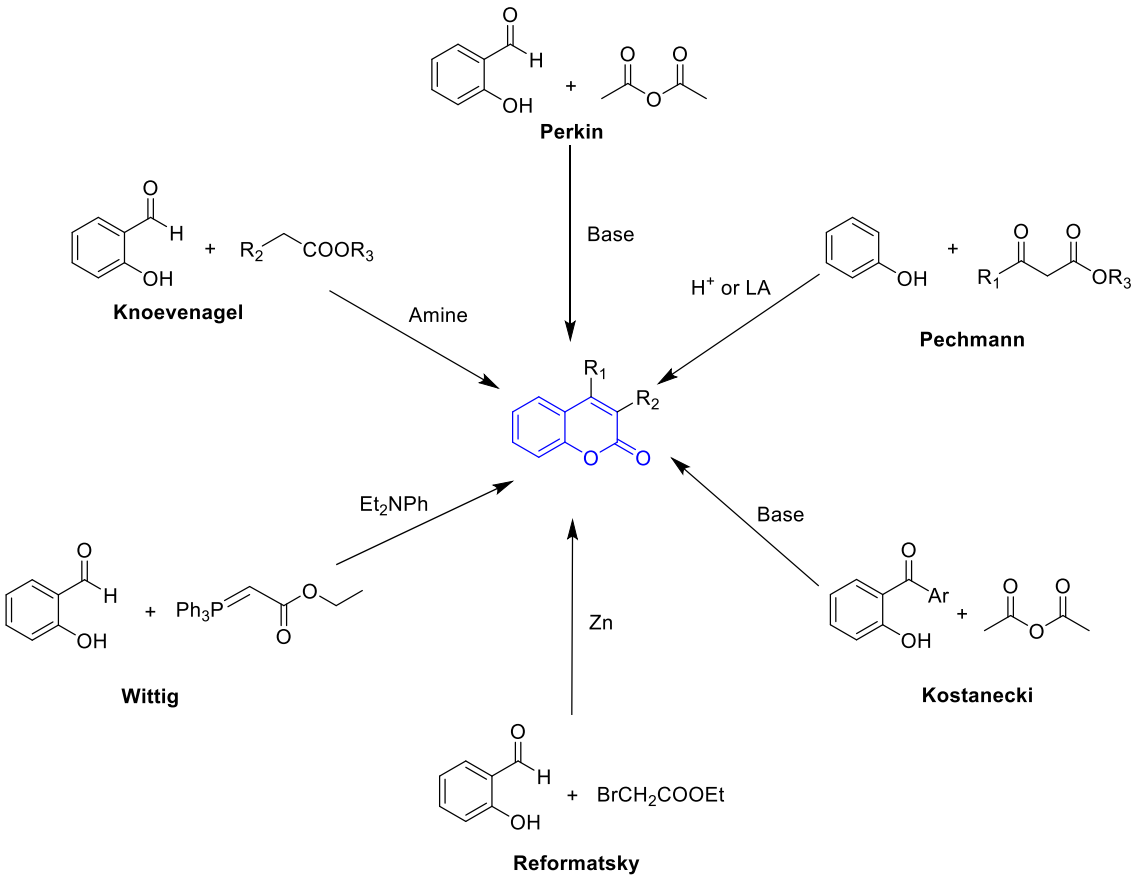


Figure 17. Different synthetic methods for the preparation of coumarins.

This class of compounds is recognized for its biological activity and as so broadly applied in the pharmaceutical industry due to their antiprotozoal[108], anticancer[109], antibacterial[110] activities among others. Additionally, coumarins derivatives present exceptional photochemical and photophysical properties and have been applied in optical brighteners[111], laser dyes[112], non-linear optical chromophores[113], and as fluorescent probes in medicine.[114,115] They have been effectively employed as organic dye photosensitizers in DSSC devices.[79,116-121] Generally, donor groups are introduced in positions 6 and/or 7 (mostly amines) and acceptors in the 3 and/or 4 positions of the coumarin, due to a red shift effect in the absorption and emission spectra. The ICT process, induced by the absorption of photons, is supported by the presence in the molecule of the previously mentioned groups through resonance or inductive effects. Accordingly, this results in the formation of a *para*-quinoidal ring, as depicted in Figure 18.[98,122] Table 3 show some of the developments made in this field over the past decade.

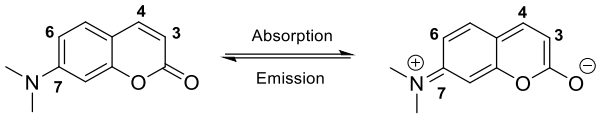


Figure 18. ICT effect in 7-dimethylaminocoumarin via absorption and emission of light.[98]

As mentioned above, coumarins with a dimethylamine in position 7 have recently been the focus of continuous research. Han *et al.* investigated the effects of introducing different π-bridges in the coumarin core and compared cyanoacrylic acid and rhodanine acetic acid as effective anchoring groups. The extension of the π-bridge from phenyl (i-a) to biphenyl (ii-a) did not significantly affect the efficiency (a difference from 2.60% to 2.80%). The biggest improvement occurred when phenylthiophene (ii-c) was employed, an efficiency of 3.60% was achieved due to an increase in $J_{sc}$. Despite the high molar extinction coefficients (ε) and $\lambda_{max}$, the rhodanine acetic acid derivatives (i-b, ii-b, ii-d) have lower IPCE and worse photovoltaic performance than the derivatives containing a cyanoacrylic acid group(i-a, ii-a, ii-c), due to a lower conjugation between the acceptor and the anchoring group.[116] To improve the performance achieved by the phenylthiophene derivatives (ii-c and ii-d), the phenyl moiety was replaced by an electron-withdrawing thiazole (iii-a and iii-b). This improved the electron injection efficiency and induced a red-shift of the maximum absorption band, with the best performing dye achieving an efficiency of 4.78 % (iii-a).[117] To confer rigidity to the molecule and reduce charge recombination, Torres *et al.* introduced as π-spacer in the 7-diethylaminocoumarin, an ethynyl group, resulting in an efficiency of 2.21 % (iv).[119] Jadhav *et al.* studied the effects of introducing different groups in position 4 of the 7-diethylaminocoumarin, namely chlorine, piperidine, and cyano groups (v-a to v-d). The best-performing dye was the one containing the cyano substituent (xiii) with an efficiency of 4.60 %. The presence of this electron withdrawing group in position 4 acts as an electron trap, leading to an improvement of $J_{sc}$, $V_{oc}$ and $P_{max}$ 11.18 mA/cm$^2$, 0.637 V and 4.59 respectively.[121] Based on the promising photophysical results of Pereira's group with 7-(diethylamino)-4-methyl-3-vinylcoumarin-based dyes[80], Sekar's group synthesized two similar coumarins containing cyanoacrylate and cyanoacrylic acid as anchors (vi-a and vi-b). The latter achieved the best performance with an efficiency of 4.31 % (**Figure 19**, **Table 3**).[123]

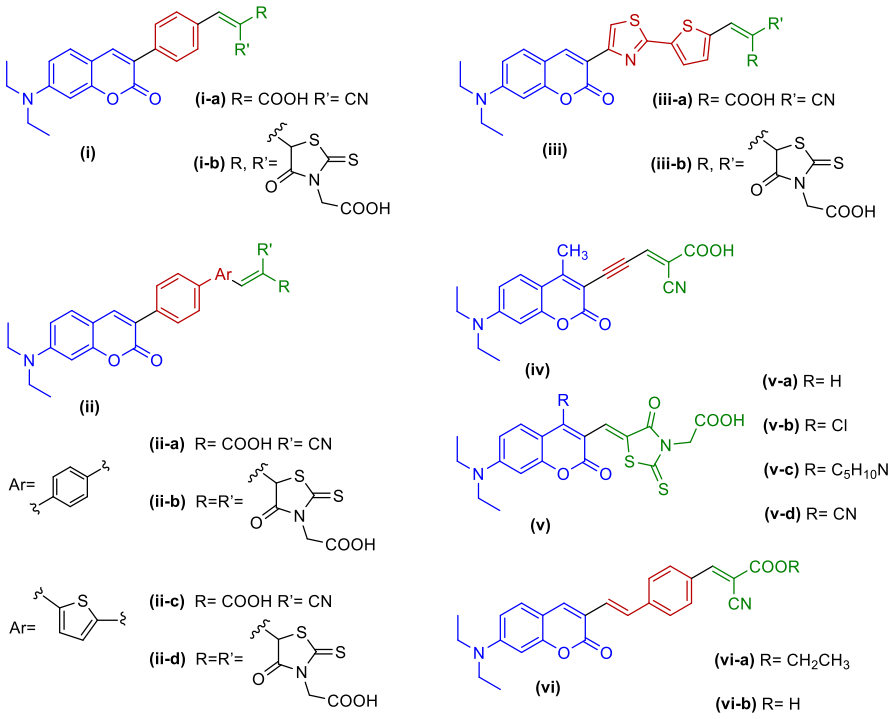


Figure 19. Chemical structures of 7-diethylaminocoumarin dyes for DSSC application.

Table 3. Spectroscopic and photovoltaic parameters of 7-diethylaminocoumarin sensitizers applied in DSSCs in the last decade.

| Dye | $\lambda_{max}$ (nm) | ε ($M^{-1}$ $cm^{-1}$) | $J_{sc}$ ($mA/cm^2$) | $V_{oc}$ (V) | FF | η (%) | Ref |
|---|---|---|---|---|---|---|---|
| **i-a** | 420 | 30 100 | 5.63 | 0.66 | 0.70 | 2.60 | [116] a |
| **i-b** | 449 | 40 300 | 3.33 | 0.58 | 0.73 | 1.41 | |
| **ii-a** | 413 | 49 400 | 5.79 | 0.69 | 0.70 | 2.80 | |
| **ii-b** | 425 | 60 500 | 4.03 | 0.60 | 0.73 | 1.77 | |
| **ii-c** | 438 | 37 300 | 7.72 | 0.66 | 0.71 | 3.62 | |
| **ii-d** | 465 | 44 900 | 3.41 | 0.56 | 0.73 | 1.39 | |
| **iii-a** | 401, 460 | 45 333, 23 433 | 9.79 | 0.69 | 0.71 | 4.78 | [117] b |
| **iii-b** | 413, 489 | 50 800, 34 167 | 0.96 | 0.50 | 0.69 | 0.33 | |
| **iv** | 440 | 14 170 | 6.11 | 0.547 | 0.66 | 2.21 | [119] c |
| **v-a** | 521 | 19 193 | 6.85 | 0.615 | 0.62 | 2.64 | [121] d |
| **v-b** | 491 | 20 366 | 7.79 | 0.636 | 0.64 | 3.19 | |
| **v-c** | 487 | 20 533 | 8.62 | 0.626 | 0.66 | 3.79 | |
| **v-d** | 613 | 16 313 | 11.18 | 0.637 | 0.65 | 4.60 | |
| **vi-a** | 455 | - | 8.70 | 0.52 | 0.61 | 2.85 | [123] e |
| **vi-b** | 464 | - | 12.16 | 0.57 | 0.62 | 4.31 | |

[a] Electrolyte composition: OPV-AN-I containing 0.07 mM/L $I^-$.

[b] Electrolyte composition: solution of 0.3 M 1-methyl-3-propylimidazolium iodide (MPII), 0.03 M $I_2$, 0.07 M LiI, 0.1 M guanidinium thiocyanate and 0.4 M 4-*tert*-butylpyridine (TBP).

[c] Electrolyte composition: 0.5 M lithium iodide (LiI), 0.05 M iodine ($I_2$) and 0.1 M *tert*-butylpyridine (TBP) in $CH_3CN$. [Dye solution]= 0.23 mM in $CH_2Cl_2$. Reference dye: N719 (η= 3.23 %)

[d] Electrolyte composition: 0.5 M lithium iodide (LiI), 0.05 M Iodine ($I_2$), 0.5 M *tert*-butyl pyridine (TBP), and 0.5 M guanidium thiocynate (GSCN) in 3-methoxy propionitrile. [Dye solution] = 3 mM

[e] Electrolyte composition: 0.5 M LiI + 0.05 M $I_2$+ 0.5M guanidinium thiocyanate (GuSCN) + 0.5M tert-butyl pyridine (4-TBP) in 3-methoxy propionitrile (MNP) solvent.

The introduction of π-conjugated donors in position 7 of the coumarin was also explored by Han's group, with the employed donors being diphenylamine, difluorenylamine and triarylamine. The linkage of these donors with the coumarin creates a D-D-π-A system. The presence of an additional donor contributes to the expansion of the conjugated π-system. With this, improvements were expected in the light-harvesting ability, tunability of energy levels of the molecule, and also on the thermostability of the sensitizers. In their studies, three different π-bridges were compared, namely thienyl, bithienyl and thiophene-phenyl (vii-xii).[118,120,124] Regarding the diphenyl coumarin dyes (vii-viii), the extension of the conjugated system increased

the light-harvesting ability and, consequently, the $J_{sc}$, with bithienyl (viii-b) and thiophene-phenyl (viii-a) derivatives having $J_{sc}$ values of 12.91 and 14.33 mA/cm$^2$ and power conversion efficiencies of 4.59 % and 6.24 %, respectively.[120] By taking into account these results, another study was carried out where the diphenylamino core was replaced with a difluorenylamino core (xix-xxi) in order to improve $V_{oc}$ values. This modification resulted in an improvement in the absorption and IPCE spectra and, consequently, all the derivatives presented higher $J_{sc}$ values. The thienyl (ix) and bithienyl (x-a) derivatives had also an improvement concerning $V_{oc}$ values, leading to an improvement of their efficiencies from 3.36 % to 4.70 % and 4.59 % to 5.06 %, respectively.[118] Due to triarylamine's properties, a set of dyes bearing this donor group in position 7 of the coumarin (xi-xii) was synthesized in the same group. Once again the thiophene-phenyl (xii-b) derivative was the best performing dye with an efficiency of 4.99 % (**Figure 20**,

**Table** 4).[124]

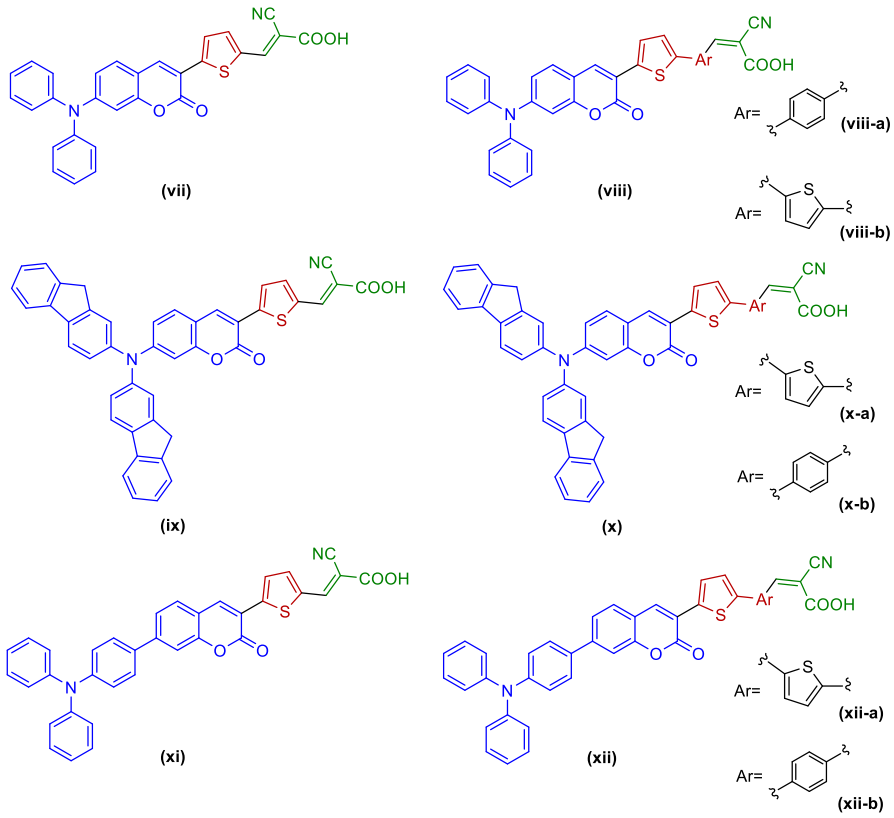


Figure 20. Chemical structures of coumarin dyes containing diphenylamine, difluorenylamine and triarylamine as additional donor groups.

Table 4. Spectroscopic and photovoltaic parameters of coumarin sensitizers containing diphenylamine, difluorenylamine and triarylamine as additional donors applied in DSSCs in the last decade.

| Dye | $\lambda_{max}$ (nm) | ε ($M^{-1}$ $cm^{-1}$) | $J_{sc}$ ($mA/cm^2$) | $V_{oc}$ (V) | FF | η (%) | Ref |
|---|---|---|---|---|---|---|---|
| **vii** | 489 | 45 200 | 9.52 | 0.54 | 0.65 | 3.36 | [120] a |
| **viii-a** | 473 | 61 033 | 14.33 | 0.69 | 0.63 | 6.24 | |
| **viii-b** | 492 | 52 433 | 12.91 | 0.59 | 0.63 | 4.59 | |
| **ix** | 515 | 49 100 | 10.94 | 0.62 | 0.70 | 4.70 | [118] a |
| **x-a** | 497 | 55 733 | 12.97 | 0.61 | 0.64 | 5.06 | |
| **x-b** | 493 | 34 966 | 14.53 | 0.67 | 0.61 | 5.94 | |
| **xi** | 343, 432 | 20 967, 29 667 | 8.20 | 0.65 | 0.85 | 4.52 | [124] a |
| **xii-a** | 350, 467 | 46 533, 33 867 | 9.21 | 0.64 | 0.75 | 4.40 | |
| **xii-b** | 340, 408 | 43 700, 28 933 | 9.17 | 0.70 | 0.78 | 4.99 | |

[a] Electrolyte composition: $CH_3CN$ solution of 0.3 M 1-methyl-3- propylimidazolium iodide (MPII), 0.03 M $I_2$, 0.07 M LiI, 0.1 M guandine thiocyanate and 0.4 M 4-*tert*-butylpyridine (TBP).

Inspired by the work of Hara *et al.* between 2001 and 2007 with coumarins[78,125-128], Liu's group studied two similar coumarins based on a D-π-A-π-A design. The two acceptor groups were benzothiadiazole and a cyanoacrilyc acid, the π-bridges were thienyl ethyne and thienyl or phenylene groups (xiii). The phenylene derivative (xiii-b) obtained an efficiency of 6.29 % with a $J_{sc}$ of 13.31 mA $cm^{-2}$, which is three times higher than the thienyl analog. The efficiency was increased to 8.03% by adding 20 mM of CDCA. [129] Mori et al. also synthesized a coumarin of this family containing an oligothiophene linker, which achieved an efficiency of 6.1% (xiv) (**Figure 21**, **Table 5**).[130]

The performance of 6,7-dihydroxycoumarins derivatives containing styryl and phenylethynyl bridges between the coumarin and the aryl ring (xv-xvi) was evaluated by Martins *et al.*. Efficiencies between 0.99 and 2.0% were obtained, and the study demonstrated that the efficiency increased when a more linear phenylethynyl bridge was used in place of the styryl bridge (**Figure 21**, **Table 5**).[79]

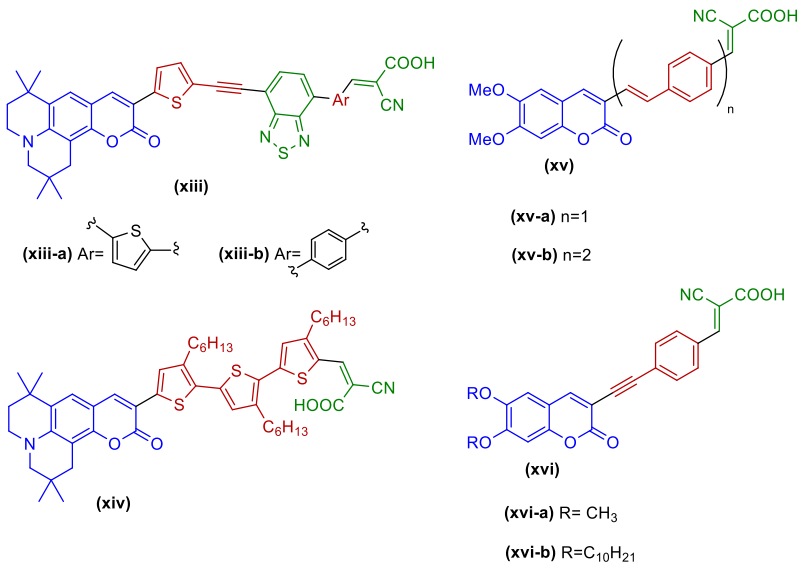


Figure 21. Chemical structures dyes based on NKX coumarins and 6,7-dihydroxycoumarins.

Table 5. Spectroscopic and photovoltaic parameters of dyes based on NKX coumarins and 6,7-dihydroxycoumarins in the last decade.

| Dye | $\lambda_{max}$ (nm) | ε ($M^{-1}$ $cm^{-1}$) | $J_{sc}$ ($mA/cm^2$) | $V_{oc}$ (V) | FF | η (%) | Ref |
|---|---|---|---|---|---|---|---|
| **xiii-a** | 512 | 51 900 | 3.83 | 0.537 | 0.66 | 1.35 | 129 a |
| **xiii-b** | 490 | 22 000 | 13.31 | 0.678 | 0.70 | 6.29 | |
| **xiv** | - | - | 12 | 0.758 | 0.69 | 6.1 | 130 b |
| **xv-a** | 400 | 19 190 | 3.36 | 0.59 | 0.69 | 1.37 | 79 c |
| **xv-b** | 415 | 20 035 | 2.98 | 0.60 | 0.55 | 0.99 | |
| **xvi-a** | 398 | 17 376 | 4.42 | 0.60 | 0.74 | 2.00 | |
| **xvi-b** | 398 | 17 413 | 3.52 | 0.62 | 0.74 | 1.65 | |

[a] Reference dye: coumarin NKX-2677 (η= 5.34%)

[b] Electrolyte composition: 0.22 M cobalt(II) tris-bipyridyl $BCN_4$, 0.02 M cobalt(III) tris-bipyridyl $BCN_4$, 0.1 M $LiClO_4$, and 0.2 M 4-tert-butylpyridine in $CH_3CN$. [Dye solution] = 0.3 mM.

[c] Electrolyte composition: commercial electrolyte from Solaronix with reference Iodolyte AN-50 containing the redox iodide/ triiodide with a concentration of 50 mM. [Dye solution] = 0.5 mM in ethanol. Reference dye: N719 (η=6.36%).

## 2.2 Results and discussion

Considering the previous experience of our group on the derivatization of coumarins[79,131,132], the synthesis of 3-arylethynyl coumarin dyes was proposed. The donor moiety of the molecules consists of a coumarin with methoxy groups linked to the positions 7, and positions 5 or 6. The different π-bridges linked to a cyanoacrylic acid acceptor group were introduced in position 3 of the coumarin since it was observed that this functionalization allowed to decrease the energy gap between HOMO and LUMO levels.[79] Based on previous work[79], the π- bridges consisted of a linear ethynyl group linked to different aryl rings. The effect of the different aryl rings on the photovoltaic and photophysical properties was studied. The applied bridges were the phenylene, thieno[3,2-*b*]thiophene, 2,2'-bithiophene, thiophene units as also a benzotriazole unit containing a long alkyl chain (**Figure 22**). The effect of the methoxy groups in positions 6 and 5 was also compared. The performance of the final coumarin chromophores in DSSC devices was tested and this work was published in the scientific journal Molecules in May 2021.[133]

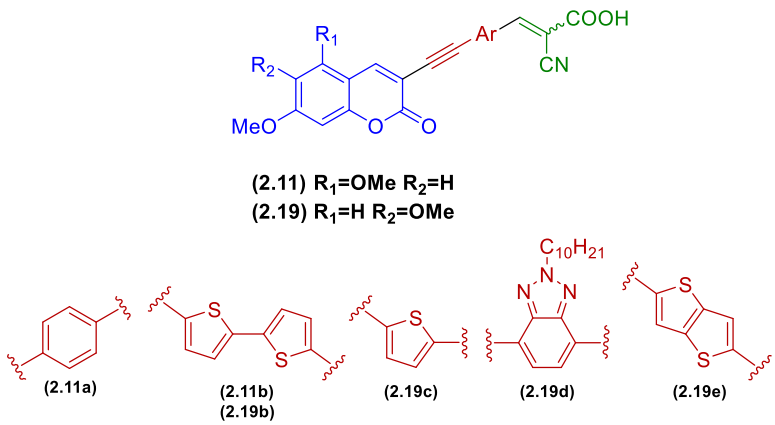


Figure 22. Structures of the synthesized and studied coumarin chromophores in this work.

### 2.2.1 Synthetic methodology

The development of coumarin dyes with a D-π-A architecture involved the derivatization of 5,7-dihydroxycoumarin and 5,6-dihydroxycoumarin.

#### 2.2.1.1 5,7-Dihydroxycoumarin based dyes

Following the Pechmann methodology, phloroglucinol (**2.1**) reacted with ethyl propynoate in the presence of a Lewis acid, $ZnCl_2$, capable of coordinating with both a hydroxyl group of the phenol and the carbonyl group of the ethyl propynoate. Regioselective $ZnCl_2$-catalyzed esterification followed by cyclization occurs, and 5,7-dihydroxycoumarin (**2.2**) can be obtained with a good yield.[134] (**Scheme 1**).

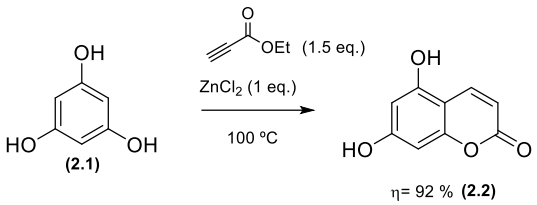


Scheme 1. Synthesis of 5,7-dihydroxycoumarin (**2.2**).

To extend the conjugation length, the coumarin needs to be brominated in position 3. However, position 8 is more reactive than 3 and, so, to deactivate the ring hydroxyl groups, these were acylated by reacting the coumarin with ethyl chloroformate in the presence of piperidine (**2.3**).[135] The bromination reaction was challenging to accomplish since coumarins have an electron-deficient character. The bromination reaction involved two different methods. The first one concerns a reaction with OXONE® ($2KHSO_5 \cdot KHSO_4 \cdot K_2SO_4$) and $HBr^{79}$, where $Br_2$ is formed *in situ.*[136] The reaction was slow and incomplete, and the dibromo compound (bromination at positions 3 and 4 of the coumarin) was also obtained, indicating that elimination did not occur. Alternatively, a pathway in which copper(II) bromide activates NBS was employed. [137] This regioselective 3-halogenation method allowed to obtain the compound (**2.4**) with 51 % yield, which was superior to the OXONE® and HBr method (η= 22 %) (**Scheme 2**).

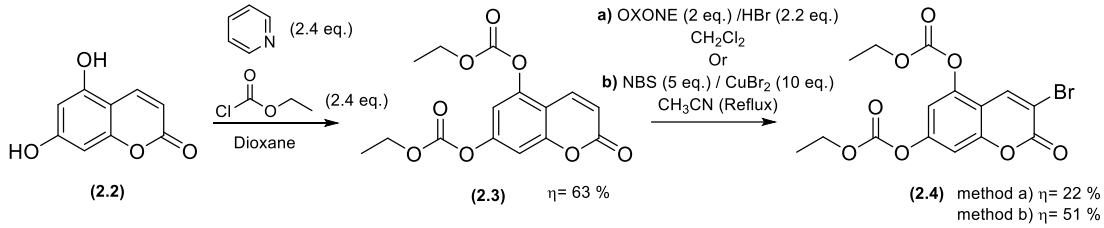


Scheme 2. Synthesis of 5,7-diethylcarbonatecoumarin (**2.3**) and 3-bromo-5,7-diethylcarbonatecoumarin (**2.4**).

The compound was then hydrolyzed to compound **2.5**, and the hydroxyl groups were methylated with iodomethane in basic medium to accomplish compound **2.6** (Scheme 3).

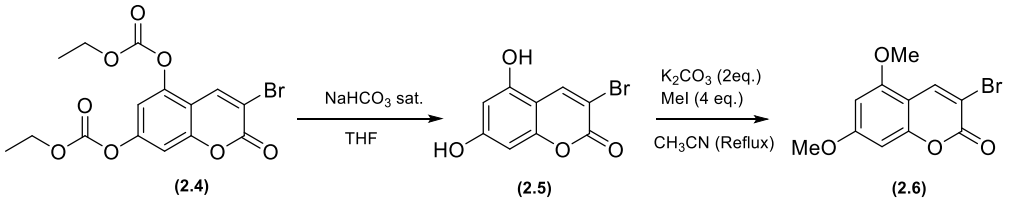


Scheme 3. Synthesis of 3-bromo-5,7-dihydroxycoumarin and 3-bromo-5,7-dimethoxycoumarin.

## Introduction of ethynyl group and aryl-π-bridges

The palladium cross-coupling reactions are crucial for the preparation of metal-free organic dyes. The extension of the π-conjugated system and the coupling between π-bridges and donor involve these types of reactions. In the case of the synthesis of 3-arylethynyl coumarin dyes, the Sonogashira coupling is vital.

The palladium/copper-catalyzed Sonogashira reaction concerns the coupling between a terminal alkyne (sp carbon) and an aryl or vinyl halide ($sp^2$ carbon). In this reaction a palladium source is required (Pd(0) complex), usually CuI is employed as a co-catalyst and the reaction is performed in the presence of amines (**Scheme 4**).

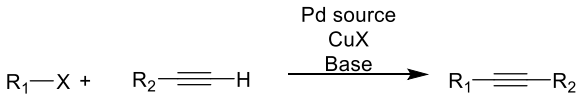


X=I, Br,Cl, OTf
$R_1$=aryl, alkenyl, allyl, benzyl
$R_2$= aryl, alkyl, alkenyl,$SiR_3$

Scheme 4. Copper co-catalyzed Sonogashira reaction.

For this reaction two independent cycles must be considered: the palladium cycle and the copper cycle. The first mentioned cycle starts with an active species, $Pd(0)L_2$, in a catalytic amount, which can be generated by the dissociation of two $PPh_3$ ligands from $Pd(PPh_3)_4$. First, the oxidative addition of the halide to the Pd(0) catalyst occurs, forming a Pd(II) complex. Then, the $[Pd(II)R_1L_2X]$ intermediate suffers a transmetalation reaction with the copper acetylide formed in the parallel copper cycle, giving $[Pd(II)R_1(C{\equiv}R_2)L_2]$. Next, *trans-cis* isomerization occurs, followed by reductive elimination, and the cross-coupling product is obtained. At the end of the cycle, the Pd(0) catalyst is regenerated. It is proposed that, in the copper cycle a π-alkyne copper complex is formed. This complex turns the terminal alkyne more acidic. This makes the acetylenic proton more prone to be removed by an amine, thus favoring the formation of a copper acetylide (**Figure 23**). [138-140]

The use of CuI as a co-catalyst increases the reactivity of the system, however, the use of this co-catalyst brings the disadvantage of the sensibility for oxygen. Due to this sensibility copper acetylide forms easily alkyne homocoupling by-products. As such, coupling approaches that do not include the use of copper have been created by increasing the catalytic system's reactivity ("copper-free" Sonogashira reactions).[141,142]

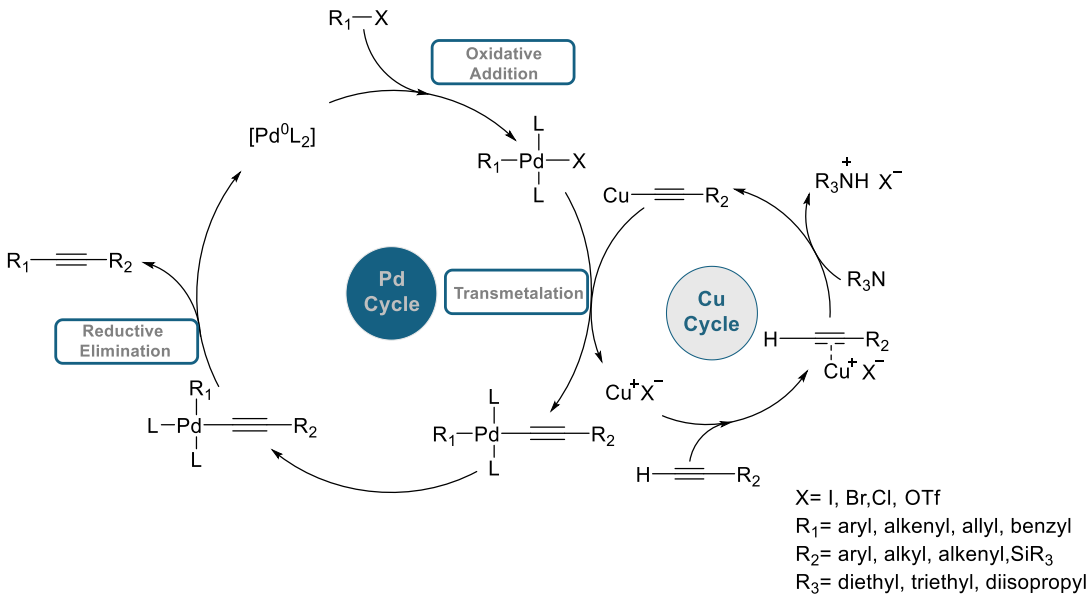


Figure 23. Catalytic cycles of Pd and Cu in Sonogashira coupling.[138,140]

In the Sonogashira couplings, $Pd(PPh_3)_4$ was used as palladium source (Pd(0)), CuI as co-catalyst, and diisopropylamine as a base. A catalytic amount of $PPh_3$ was used to generate Pd(0) *in situ* if undesired Pd(II) is formed in the course of the reaction. Through a Sonogashira

reaction between 3-bromocoumarin (**2.6**) and 4-ethynylbenzaldehyde, compound **2.7** was afforded with 49% yield. For the preparation of dye **2.11b** the 3-bromocoumarin (**2.6**) was reacted with ethynyltrimethylsilane and the compound **2.8** afforded in 73 % yield (**Scheme 5**).

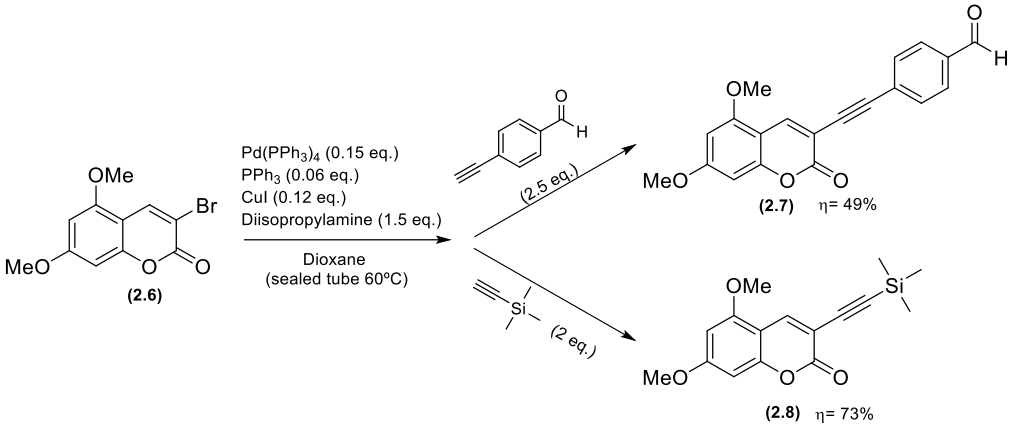


Scheme 5. Synthesis of compounds **2.7** and **2.8** via Sonogashira coupling.

To remove the trimethylsilyl protecting group from compound **2.8**, a catalytic amount of $K_2CO_3$ in methanol was used. In this reaction a nucleophilic attack from the methoxide, formed in basic conditions, at the silicon atom occurs. The free alkyne is then generated in the presence of a proton source. Since this particularly alkyne is prone to polymerization or even cycloaddition reaction, the purification via column chromatography using silica was avoided and the obtained compound **2.9** was directly used in a C-C coupling with 5′-bromo-2,2′-bithiophene-5-carbaldehyde to obtain compound **2.10** with 14.1 % yield (**Scheme 6**).

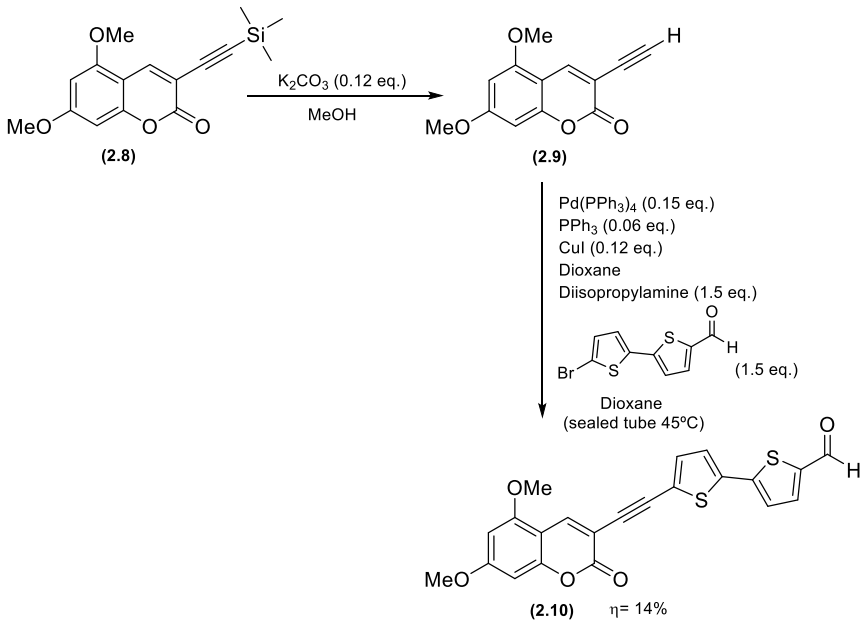


Scheme 6. Preparation of the intermediate compound (**2.9**) and synthesis of compound **2.10** by introduction of the 2,2′-bithiophene π-bridge.

The last step of this synthesis consisted in the introduction of the cyanoacrylic anchoring groups through a Knoevenagel condensation between the aldehydes **2.7** and **2.10**, and the cyanoacetic acid in the presence of piperidine. Dyes **2.11a** and **2.11b** were obtained with 13% (incomplete reaction) and 53% yields, respectively (**Scheme 7**).

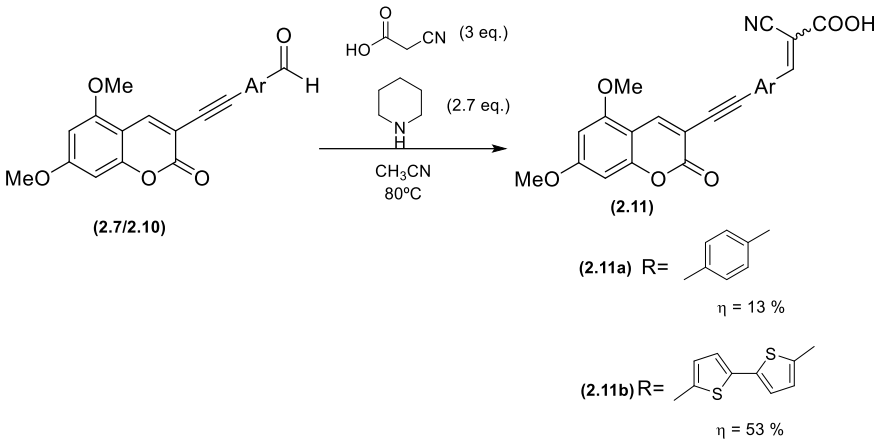


Scheme 7. Synthesis of the final 5,7-dimethoxycoumarin chromophores **2.11a** and **2.11b**.

### 2.2.1.2 6,7-Dihydroxycoumarin based dyes

Similar procedures were used for the synthesis of 5,6-dimethoxycoumarin derivatives but in this particular case it was used the natural compound esculetin (6,7-dihydroxycoumarin). Initially, the hydroxyl groups of the 6,7-dihydroxycoumarin (**2.12**) were methylated to the 6,7-dimethxycoumarin **2.13**, and position 3 of the coumarin ring was brominated with OXONE® and HBr in dichloromethane to attain compound **2.14** (**Scheme 8**).

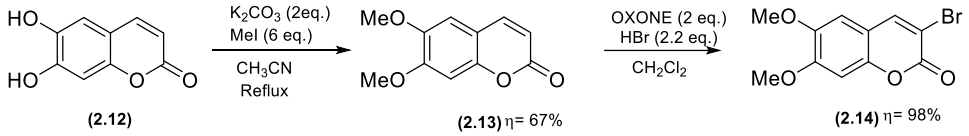


Scheme 8. Synthesis of 6,7-dimethoxycoumarin (**2.13**) and 3-bromo-6,7-dimethoxycoumarin (**2.14**).

The ethynyl group was introduced in the 3-bromo-6,7-dimethoxycoumarin (**2.14**) as previously mentioned. In this synthetic pathway, several attempts have been made to remove the trimethylsilyl protecting group. This step was optimized by using different reagents, solvents, and purification techniques. Originally, TBAF in a THF solution was used as a deprotecting reagent, but it was not possible to remove this reagent without exposing the formed free alkyne to light or silica due to the necessity of purification and removal of TBAF. Given this, the search for more efficient methods led to the use of catalytic amounts of $K_2CO_3$ in the presence of methanol (**Scheme 9**).

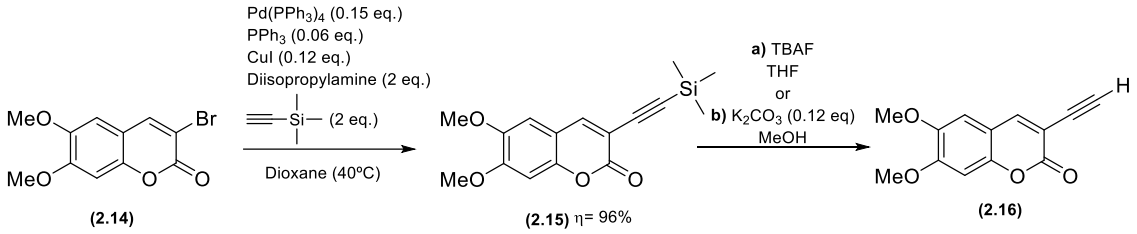


Scheme 9. Synthesis of 3-ethynyl-6,7-dimethoxycoumarin (**2.16**)

After removal of the protecting group, 3-ethynyl-6,7-dimethoxy-2*H*-chromen-2-one (**2.16**) was obtained and used directly in a Sonogashira coupling with different aldehydes. The applied aldehydes were 5-bromothiophene-2-carbaldehyde (**2.17c**) and 7-bromo-2-decyl-2*H*-benzo[1,2,3]triazole-4-carbaldehyde (**2.17d**), with the latter having been prepared in the

laboratory according to what was described in the literature.[143] Compounds **2.18c** and **2.18d** were obtained with 51% and 9% yield respectively (**Scheme 10**).

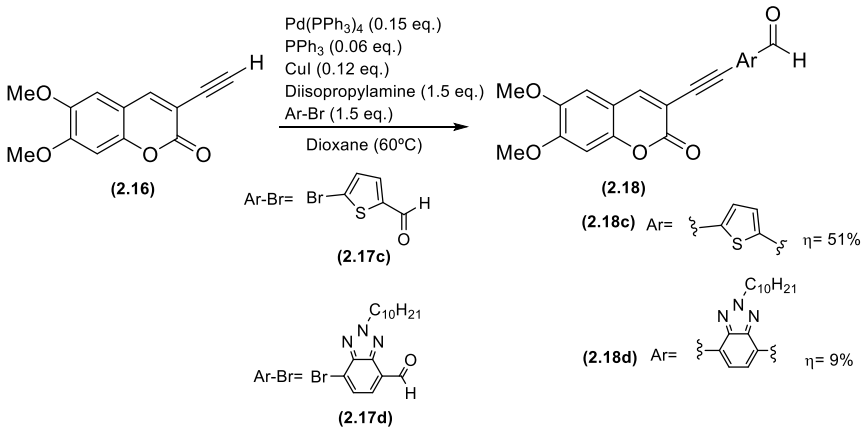


Scheme 10. Introduction of the π-bridges thiophene (**2.17c**) and benzotriazole (**2.17d**) in 3-ethynyl-6,7-dimethoxycoumarin via Sonogashira coupling to obtain compounds **2.18c** and **2.18d** respectively.

The cyanoacrylic anchoring group was introduced in compound **2.18c** to afford **2.19c** with a 53% yield. The same anchoring group was also introduced in **2.18d** and it was possible to obtain compound **2.19d** with a 15% yield. (**Scheme 11**).

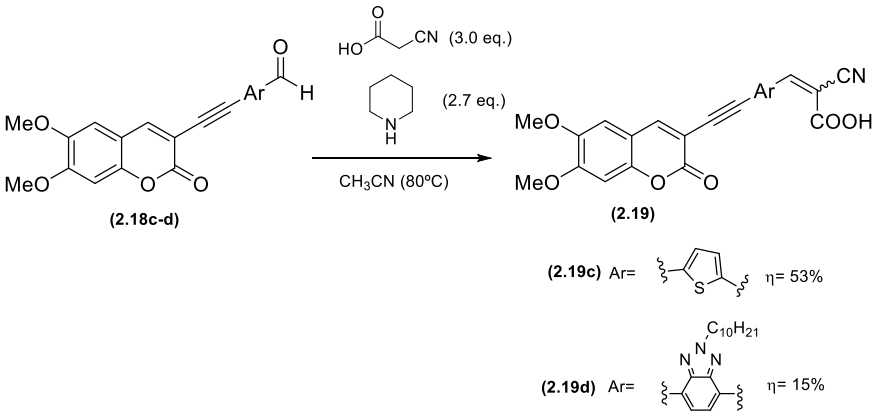


Scheme 11. Synthesis of the 6,7-dimethoxycoumarin final chromophores 2.19c and 2.19d.

The structure of the final chromophores was corroborated by $^{1}$H NMR and HRMS. In contrast with the starting materials (coumarin ethynyl aldehydes **2.7**,**2.10**, **2.18c**), the $^{1}$H NMR spectra of the final chromophores shows the disappearance of the aldehyde proton (10.02-9.87 ppm) and a new singlet at high field 8.53-8.06 ppm emerge corresponding to the β-proton to the cyanoacrylic acid anchoring group (CH). This indicates that the Knoevenagel condensation of the aldehydes and the cyanoacetic acid occurred. The protons of the coumarin moiety

correspond to 3 singlets in the aromatic region. The proton of position 4 appears at 8.53-8.06 ppm. In 6,7-dimethoxy-coumarin, the protons from the positions H6/H8 are less deshielded (6.20-6.65 ppm) than protons H5/H8 (7.11-7.22 ppm). The methoxy groups appear in the form of two singlets around 4 ppm and the remaining signals present in the different spectra are in accordance with the corresponding aryl rings (**Figure 24**). The HRMS showed the expected molecular ion peaks [M+H] 490.0406 for **2.11b**, 408.0529 for **2.19c** and 583.2542 for **2.19d**.

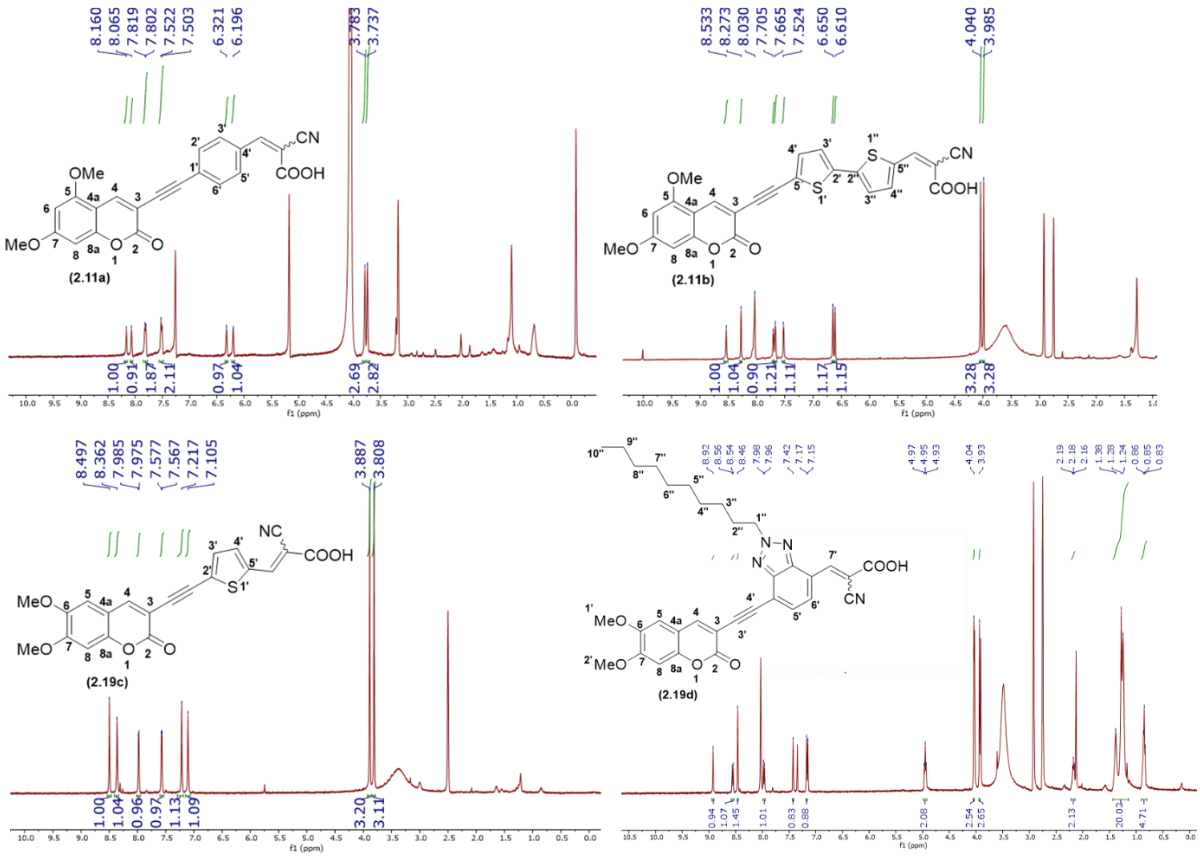


Figure 24. $^{1}$H NMR (400 MHz) spectra of **2.11a-b** and **2.19c-d** final dyes (**2.11a** ($CDCl_3$); **2.11b** (DMF-$d_7$); **2.19c** (DMSO-$d_6$); **2.19d** (DMF-$d_7$)).

## 2.2.2 Absorption and Fluorescence

The optical properties of each coumarin dye were studied by measuring the UV-vis absorption and emission spectra in acetonitrile as solvent at room temperature. The absorption spectra show a band in the region 414-420 nm (12000-64470 $M^{-1}cm^{-1}$). The large Stokes shifts

between the absorption and the emission bands (2201-3998 $cm^{-1}$) point to a charge transfer (CT) character of the fluorescence emission band (**Figure 25**, **Table 6**).

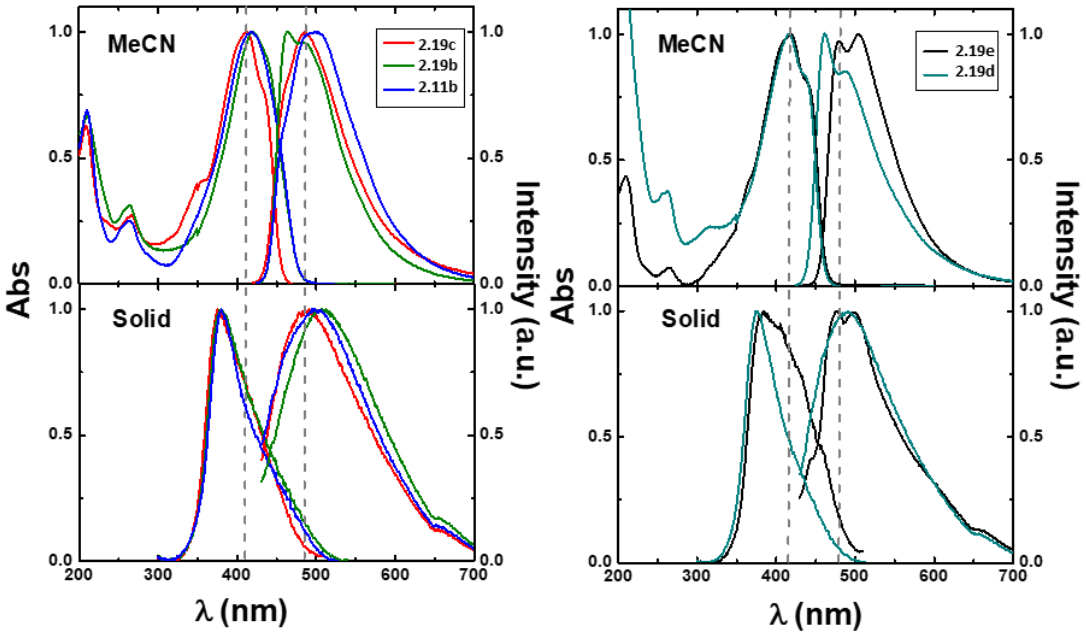


Figure 25. Normalized absorption and fluorescence emission spectra for compounds **2.11b** and **2.19b-e** in acetonitrile solution and in the solid state (adsorbed in $TiO_2$ films) at 293K.

Table 6. Spectroscopic data (absorption and fluorescence emission maxima, molar extinction coefficients, ε, and Stokes shift, $\Delta_{SS}$) for compounds **2.11b** and **2.19b-e** in acetonitrile solution and absorbed in $TiO_2$ films at 293 K.

| Dye | $\lambda_{max}^{Abs}$ (nm) | $\lambda_{max}^{Abs}$ solid (nm) | ε ($cm^{-1}M^{-1}$) | $\lambda_{max}^{Fluo}$ (nm) | $\lambda_{max}^{Fluo}$ solid (nm) | $\Delta_{SS}$ ($cm^{-1}$) |
|---|---|---|---|---|---|---|
| **2.11b** | 418 | 380 | 45480 | 499 | 500 | 3998 |
| **2.19b** | 420 | 380 | 30190 | 464 | 510 | 2201 |
| **2.19c** | 414 | 375 | 15300 | 486 | 488 | 3578 |
| **2.19d** | 416 | 375 | 12060 | 462 | 490 | 2451 |
| **2.19e** | 417 | 386 | 64470 | 489 | 476 | 3589 |

## 2.2.3 Photovoltaic performance

The performance of the final coumarin chromophores (**2.11a-b, 2.19b-e**) in DSSC devices was evaluated by measuring the *I-V* curves (**Figure 26-A**, **Table 7**).[133] Compound **2.19e** presented the best performance, with an efficiency of 2% and the highest values of $V_{oc}$ and $V_{max}$, 0.367 and 0.256 V, respectively. This superior efficiency is related with the superior molar

extinction coefficient of **2.19e** (**Table 6**). The DSSC's performance of dye **2.11b** was 1.78%, while the analog **2.19b** was 0.95%, with the first one having a superior efficiency due to high photocurrent values ($J_{sc}$ = 10.2 and $J_{max}$ = 7.8 mA/cm$^2$). The photophysical, electrochemical computational studies revealed that substitution at the 5- and 7- positions of the coumarin unit is a more suitable choice for the inclusion of electron-donating groups, when compared with substitution at the 6- and 7- positions. Compound **2.11a** was also tested in the cells and obtained the worst efficiency (0.84%) when compared to the other compounds. Despite having the third highest $V_{oc}$ value, it has a low value of $J_{sc}$ when compared with **2.11b**. In the literature, the analog with substituents in position 6 (**Figure 26-C**) has an efficiency of 2.00 % (N-719: 6.36%)[79], however, these efficiencies are not comparable because the cell fabrication conditions and the electrolyte are not equal (the amount of compound **2.11a** obtained was not enough to carry out further studies).

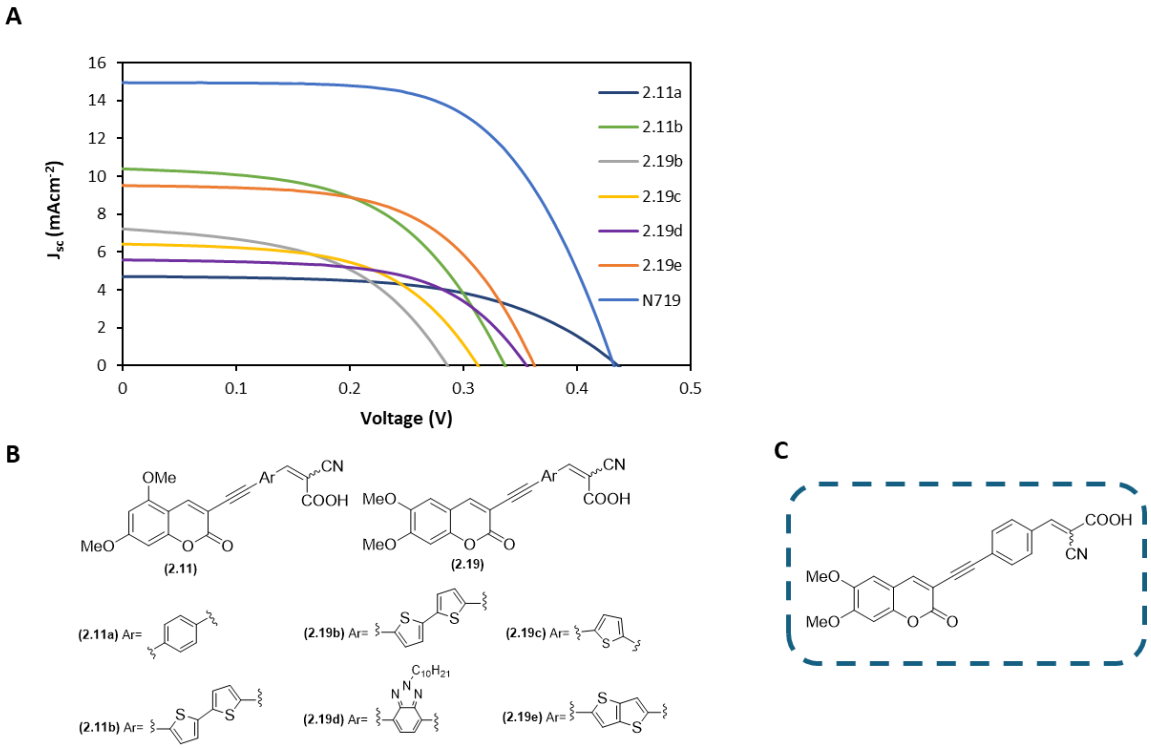


Figure 26. A- *I–V* curves of the test cells based on the synthesized coumarin dyes under 100 mW.cm$^{-2}$ under simulated AM 1.5 illumination; B- Structures of the tested coumarin chromophores; C- structure of the 6,7-dihydroxycoumarin based dye already reported In the literature[79].

Table 7. Performance values of the test cells based on the synthesized dyes and reference dye N719 under 100 mW.cm$^{-2}$ AM 1.5 illumination. The results presented correspond to the average values of at least two cells per dye, each cell measured 5 times. The prepared anodes were soaked for 16 h in an $CH_2Cl_2$/MeOH/$H_2O$ 65:20:2 (% v/v) solution of the dye (0.5 mM), at room temperature in the dark.
Electrolyte composition: 0.8 M LiI and 0.05 M $I_2$ in an acetonitrile/valeronitrile (85:15, % v/v).

| Dye | $V_{oc}$ (V) | $J_{sc}$ (mA/cm$^2$) | $J_{max}$ (mA/cm$^2$) | $V_{max}$ (mV) | FF | η (%) |
|---|---|---|---|---|---|---|
| **2.11a** | 0.362 | 4.5 | 3.5 | 0.243 | 0.51 | 0.84 |
| **2.11b** | 0.339±0.003 | 10.2±0.1 | 7.8±0.2 | 0.227±0.002 | 0.51±0.01 | 1.78±0.06 |
| **2.19b** | 0.289±0.006 | 6.7±0.3 | 4.9±0.3 | 0.193±0.004 | 0.49±0.02 | 0.95±0.07 |
| **2.19c** | 0.311±0.005 | 6.4±0.1 | 4.9±0.3 | 0.214±0.005 | 0.54±0.02 | 1.07±0.05 |
| **2.19d** | 0.359±0.002 | 5.4±0.1 | 4.3±0.2 | 0.258±0.001 | 0.58±0.02 | 1.13±0.04 |
| **2.19e** | 0.367±0.005 | 9.3±0.1 | 7.5±0.2 | 0.256±0.003 | 0.56±0.01 | 2.00±0.06 |
| **N719** | 0.440±0.006 | 15.5±0.4 | 13.1±0.2 | 0.305±0.004 | 0.59±0.02 | 4.06±0.05 |
| **2.19c HPE** | 0.493±0.015 | 2.4±0.1 | 1.8±0.1 | 0.341±0.011 | 0.52±0.02 | 0.63±0.04 |

Compound 2.19c was tested in DSSCs with the commercial electrolyte EL-HPE® (GreatCell Solar) to understand the effect of this electrolyte with ethynyl coumarin dyes. The EL-HPE® electrolyte contains 1-butyl-3-methylimidazolium iodide, 4-butylpyridine (TBP), and guanidinium thiocyanate (GuSCN). TBP acts as a Lewis base and occupies the dye-absent $TiO_2$ surface, reducing the reversed electron transfer from $TiO_2$ CB to triiodide. The $Gu^+$ cations from the GuSCN are adsorbed on the $TiO_2$ surface to slow down electron recombination. The TBP and GuSCN contribute, respectively, to a negative and positive shift of $TiO_2$ CB. This change in the band position influences the charge recombination at the $TiO_2$/electrolyte interface .[144] By being adsorbed these additives block reduction sites, thus preventing their contact with electron acceptor molecules. In this way, the recombination process is suppressed and the open-circuit voltage ($V_{oc}$) increases.[28] Indeed it is observed the positive effect of this electrolyte in $V_{oc}$, due to an increase from 0.311 V to 0.493 V. However, the photocurrent density at short circuit ($J_{sc}$) decreases (from 6.4 mA cm$^{-2}$ to 2.4 mA cm$^{-2}$). This parameter is related to the electron injection efficiency from the photoexcited dyes in the conduction band of the $TiO_2$. The additives can reduce the energy gap between the conduction band of the $TiO_2$ and the LUMO of the dye. As a result, the injection of electrons into the CB of the $TiO_2$ is thermodynamically less favorable, resulting in a decrease in this value. Therefore, it was not possible to improve the cell efficiency because the effect of the increase in $V_{oc}$ was suppressed by the decrease in $J_{sc}$ (Figure 27, Table 7).

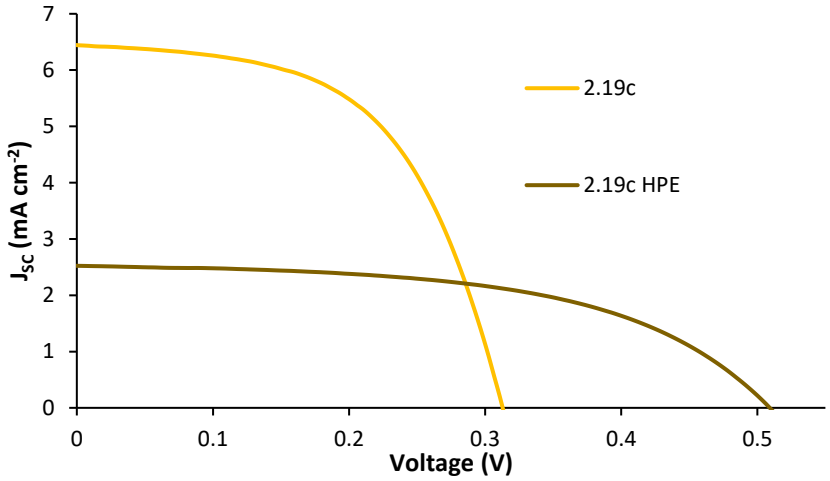


Figure 27. *I–V* curves of the test cells based on the synthesized coumarin dye **2.19c** containing $I^-/I_3^-$ electrolyte and EL-HPE® (GreatCell Solar) electrolyte, under 100 mW.cm$^{-2}$ under simulated AM 1.5 illumination.

## 2.3 Conclusion

It was possible to synthesize successfully a family of 3-arylethynyldimethoxycoumarin-based dyes to explore the effects of different heterocyclic π-bridges and substitution patterns (6,7- *vs.* 5,7-) on their photovoltaic performance. The 6,7-dimethoxycoumarin derivative containing thieno[3,2-*b*]thiophene as π- bridge was the best performing dye (η= 2.00%). The 5,7-Dimethoxycoumarin derivative achieved better efficiency in the cells than the 6,7- equivalent. Theoretical calculations confirmed the stronger electron-donating properties of the 5,7-substituted coumarins.

## 2.4 Experimental section

### General information - synthesis

The solvents and reagents were purchased (Merck KGaA, Darmstadt, Germany) and used without further purification. Solvent drying was performed by using M2A molecular sieves (Merck KGaA), according to the literature.[145] The solution of n-BuLi was always titrated using diphenyl acetic acid as indicator. Zinc chloride, *p*-anisidine and benzoquinone were purified before use as described in the literature.[146]

Cooling baths were prepared by mixing acetone or ethanol and liquid $N_2$.

Thin-layer chromatography (TLC) was performed on aluminum-backed Kieselgel 60 F254 silica gel plates (Merck KGaA). Plates were visualized with UV light (254 and 336 nm) and/or by and by staining with dragendorff and dinitrophenylhydrazine solutions.[147] Preparative-layer chromatography (PLC) was performed on Keiselgel 60 F254 silica gel plates (Merck KGaA). Column chromatography was performed using Kieselgel 60A (Carlo Erba) with particle size 40-63 µm in normal phase.[148]

High-resolution mass spectra (HRMS) were obtained at the University of Salamanca, research support service – NUCLEUS, with a Thermo Vanquish core HPLC coupled to a diode array ultraviolet detector and a mass spectrometer Thermo Orbitrap QExactive Focus.

The $^{1}H$ and $^{13}C$ Nuclear Magnetic Resonance (NMR) spectra were recorded in a Bruker Avance III 400 (Billerica, MA, USA), at 400 and 101 MHz, respectively. The employed solvents were $CDCl_3$, MeOD, $CD_3CN$, DMSO-$d_6$ and DMF-$d_7$. The NMR data is described in the following order: chemical shift (δ, in ppm), signal multiplicity, coupling constant (*J*, in Hz) relative intensity of each signal (nH, number of protons) and corresponding position in the molecule (Hx, position). Trace of deuterated solvents is used as reference signals.

### General information – photovoltaic characterization

The DSSCs detailed fabrication procedure has been described in the literature.[149]

The conductive FTO-glass (TEC7, Greatcell Solar) used for transparent electrodes was first cleaned with soap , followed by rinsing with water and ethanol. To prepare the anodes, the FTO-glass plates were coated with a $TiCl_4$/water solution (40 mM) at 70 °C for 30 min, then washed with water and ethanol before being sintered at 500°C for 30 minutes. This treatment acts as a 'blocking-layer' to prevent charge recombination between electrons in the FTO, and

it also improves the adherence of the subsequently deposited nanocrystalline layers to the glass plates. The transparent $TiO_2$ layers were deposited on the treated plates via the screen-printing method by using a 43.80 mesh per $cm^2$ polyester fiber frame and using a titania paste (18NR-T, Greatcell Solar, Queanbeyan, Australia). After deposition, the plates were heated to 125°C to dry the films, and the coating and drying process was repeated. The $TiO_2$-coated plates were then gradually heated to 325°C and 375°C over 5 minutes, followed by sintering at 500°C for 30 minutes. Once cooled to room temperature, the $TiCl_4$/water treatment (40 mM) was repeated. A reflective titania paste layer (WER2-O, Greatcell Solar) was then deposited via screen-printing, and the plates were sintered at 500°C. This layer, containing 150–200 nm anatase particles, improves photocurrent generation. The plates containing the anodes were divided into rectangles (size: 2 cm × 1.5 cm), containing a spot area of 0.196 $cm^2$ with a thickness of 15 µm. The anodes were immersed for 16 h in a 0.5 mM solution of the dye in $CH_2Cl_2$:MeOH:$H_2O$ (65:35:5, %v/v) or ethanol, at room temperature protected from the light. The photoanodes were rinsed with the same solvent to remove the excess dye.

The cathodes were fabricated using 2 cm × 2 cm FTO-glass plates with a 1.0 mm diameter hole drilled into them. To remove any residual glass powder and organic contaminants, the plates were thoroughly cleaned with water and ethanol. A transparent Pt catalyst (PT1, Greatcell Solar) was applied to the conductive side of the FTO-glass using the doctor blade technique. A strip of adhesive tape (3 M Magic) was placed along 0.5 cm of the edge of the glass in order to control the thickness of the deposited layer and to mask an electrical contact strip. The Pt paste was uniformly distributed across the substrate by sliding a glass rod along the tape spacer. After removing the tape, the cathodes were heated at 550°C for 30 minutes. By using a thermopress, the photoanode and the cathode were assembled into a sandwich-type configuration. Surlyn ionomer (Meltonix 1170-25, Solaronix SA) was used to seal the cells. The redox couple, $I^-/I_3^-$ (0.8 M LiI and 0.05 M $I_2$) was dissolved in a mixture of acetonitrile/valeronitrile (85:15, % v/v) to prepare the electrolyte employed in this work. The electrolyte introduction into the cell was done by filling under vacuum through the hole drilled in the cathode, followed by sealing with adhesive tape. For each compound, at least two cells were assembled under identical conditions, and the efficiencies of each cell were measured five times to ensure accuracy.

Photocurrent voltage measurements were performed using a Keithley SourceMeter multimeter and an Oriel solar simulator (Model LCS-100 Small Area Sol1A, 300 W Xe Arc lamp equipped with AM 1.5G filter, 100 mW $cm^{-2}$) was used to simulate sunlight irradiation.

## 2.4.1 Synthesis of 5,7-dimethoxycoumarin-based dyes

*Synthesis of 5,7-dihydroxycoumarin (**2.2**)*

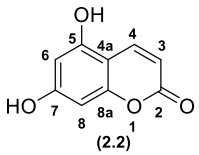


In a round-bottom flask equipped with a magnetic stir bar were added under $N_2$ atmosphere 140 mg of phloroglucinol (**2.1**) (1.11 mmol), 153 mg of zinc chloride (1.11 mmol, 1eq.) and 0.170 mL of ethyl propynoate (2.39 mmol, 1.5eq.). The reactional mixture was heated at 100 ºC and followed by TLC ($CH_2Cl_2$ with 5% of MeOH). After 19 h the reactional mixture was cooled to room temperature and then was added an aqueous solution of HCl (5%). The resultant precipitate was filtered off and washed with water to afford 182 mg of 5,7-dihydroxycoumarin (**2.2**) (η=92%). **$^1$H NMR (400 MHz, DMSO-$d_6$) δ (ppm):** 10.62 (s, 1H, OH), 10.34 (s, 1H, OH), 7.92 (d, *J* = 9.6 Hz, 1H, H4), 6.22 (d, *J* = 2.1 Hz, 1H, H6/H8), 6.14 (d, *J* = 2.1 Hz, 1H, H6/H8), 5.99 (d, *J* = 9.6 Hz, 1H, H3). [134]

*Synthesis of 5,7-diethylcarbonatecoumarin (**2.3**)*

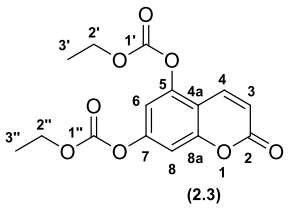


To a solution of 5,7-dihydroxycoumarin (**2.2**) (659 mg, 3.7 mmol) in 5 mL of dry dioxane, were added at 0°C 0.72 mL of pyridine (8.9 mmol, 2.4 eq.) and 0.85 mL of ethyl chloroformate (8.9 mmol, 2.4 eq.). The reaction was stirred at room temperature for 70 h under a nitrogen atmosphere. The solvent was removed, and the product was extracted with dichloromethane. The organic layers were combined, dried with anhydrous $Na_2SO_4$, filtered, and dried under reduced pressure. The crude was purified by flash column chromatography using the eluent hexane/ EtOAc (1/1) to give 749 mg of 5,7-diethylcarbonatecoumarin (**2.3**) (2.32 mmol, η=63 %).[135] **$^1$H NMR (400 MHz, $CDCl_3$) δ (ppm):** 7.84 (d, *J* = 10.0 Hz, 1H, H4), 7.19 (d, *J* = 2.4, 1H, H6/H8), 7.14 (d, *J* = 2.0 Hz, 1H, H6/H8), 6.41 (d, *J* = 9.6 Hz, 1H, H3), 4.36 (m, 4H, H2'/H2''), 1.41 (m, 6H, H3'/H3'')

*Synthesis of 3-bromo-5,7-diethylcarbonatecoumarin (**2.4**)*

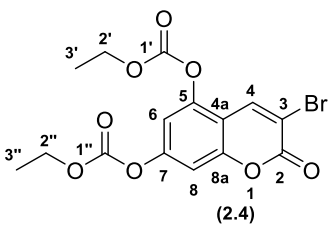


In a round flask containing 144 mg of 5,7-diethylcarbonatecoumarin (**2.3**) (0.45 mmol) were added 398 mg of N-bromosuccinimide (2.23 mmol, 5 eq.), 999 mg of copper(II) bromide (4.47 mmol, 10 eq.) and 20 mL of dry acetonitrile. The mixture was heated to reflux under $N_2$ atmosphere. When the reaction was complete the mixture was cooled to room temperature and the solvent was removed. It was added a 5% aqueous

solution of $NaHSO_3$ and the product was extracted with ethyl acetate. The organic layers were combined, dried with anhydrous $Na_2SO_4$, filtered, and evaporated. The crude was purified by flash column chromatography using the eluent hexane / EtOAc (8/2) to afford 91 mg of 3-bromo-2-oxo-2*H*-chromene-5,7-diyl diethyl bis(carbonate) (**2.4**) (0.228 mmol, η=51%). **$^1$H NMR (400 MHz,$CDCl_3$) δ (ppm):** 8.22 (s, 1H, H4), 7.25 (br s, 1H, H6/H8), 7.15 (br s, 1H, H6/H8), 4.37 (m, 4H, H2′/H2′′), 1.42 (m, 6H, H3′/H3′′).[137]

*Synthesis of 3-bromo-5,7-dihydroxycoumarin (**2.5**)*

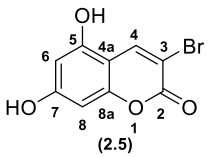

(2.5)

To a solution of 3-bromo-2-oxo-2*H*-chromene-5,7-diyl diethyl bis(carbonate) (**2.4**) (105 mg, 0.26 mmol) in 2.2 mL of THF were added 20 mL of a saturated aqueous solution of $NaHCO_3$. After 20h the reaction was complete, the solvent was removed and the product was extracted once with diethyl ether, then the aqueous phase was acidified with an aqueous solution of HCl 1M and the product was extracted with $CH_2Cl_2$. The combined organic layers were dried with anhydrous $Na_2SO_4$, filtered, and evaporated. The obtained crude containing 3-bromo-5,7-dihydroxycoumarin (**2.5**) (101 mg) was used directly in the next reactional step without further purification.

*Synthesis of 3-bromo-5,7-dimethoxycoumarin (**2.6**)*

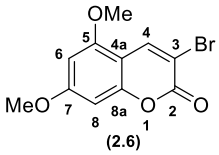

(2.6)

To a solution containing 3-bromo-5,7-dihydroxycoumarin (**2.5**) (0.24 mmol), potassium carbonate (0.48 mmol, 2 eq.) in 3 mL of dry acetonitrile were added 0.18 ml of iodomethane (2.89 mmol, 12 eq.). The reaction was refluxed under $N_2$ atmosphere for 66 h. Then the solvent was removed, water was added, and the product was extracted with $CH_2Cl_2$. The organic phases were dried with anhydrous $Na_2SO_4$, filtered, and evaporated. The crude was purified by column chromatography using hexane/ EtOAc 7/3 as eluent to afford 3-bromo-5,7-dimethoxycoumarin (**2.6**). **$^1$H NMR (400 MHz, $CDCl_3$) δ(ppm):** 8.30 (s, 1H, H4), 6.39 (br s, 1H, H6/H8), 6.28 (br s, 1H, H6/H8), 3.89 (s, 3H, $OCH_3$), 3.85 (s, 3H, $OCH_3$).

## Sonogashira reactions

*Synthesis of 5,7-dimethoxy-3-((trimethylsilyl)ethynyl)coumarin (**2.8**)*

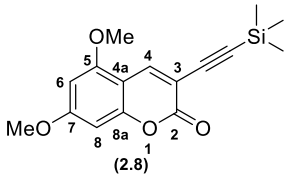

(2.8)

To a sealed tube were added under a $N_2$ atmosphere $PPh_3$ (0.06 eq.), CuI (0.12 eq.), $Pd(PPh_3)_4$ (0.15 eq), 147 mg of 3-bromo-5,7-dimethoxycoumarin (**2.6**) (0.52 mmol, 1 eq.) and 5 mL of dry dioxane. After 15 minutes, were added ethynyltrimethylsilane (2 eq.) and diisopropylamine (2 eq.). The solution was stirred at 45°C for 23 hours. The consumption of the starting materials was monitored by TLC using hexane / EtOAc 6/4 as eluent. The solvent was removed under reduced pressure and the crude was purified by flash chromatography with hexane/ EtOAc 8/2 as eluent, to afford 114 mg of 5,7-dimethoxy-3-((trimethylsilyl)ethynyl)coumarin (**2.8**) (72.9%). **$^1$H NMR (400 MHz, $CDCl_3$) δ (ppm):** 8.14 (s, 1H, H4), 6.37 (s, 1H, H6/H8), 6.25 (d, *J* = 2.4 Hz, 1H, H6/H8), 3.88 (s, 3H, $OCH_3$), 3.84 (s, 3H, $OCH_3$), 0.25 (s, 9H, $Si(CH_3)_3$). **HRMS-ESI(+):** Calculated for $C_{16}H_{19}O_4Si$ $[M+H]^+$ 303.1047; Found 303.1041

*Synthesis of 5,7-dimethoxy-3-ethynylcoumarin (**2.9**)*

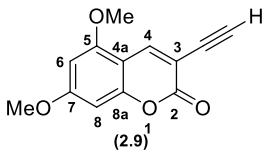

(2.9)

In a round-bottom flask, 114 mg of 5,7-dimethoxy-3-((trimethylsilyl)ethynyl)-coumarin (**2.8**) (0.38 mmol) and 7.5 mg of $K_2CO_3$ (0.054 mmol, 0.14 eq.) were dissolved in 10 mL of methanol. The reaction was monitored by TLC using the eluent hexane/ EtOAc 6/4 and after 6 hours the solvent was removed under reduced pressure. The product was used directly in the following reaction without further purification.

*Synthesis of 4-((5,7-dimethoxy-2-oxo-2H-chromen-3-yl)ethynyl)benzaldehyde (**2.7**)*

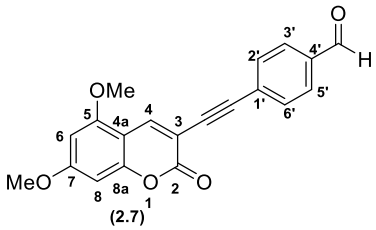

(2.7)

Following the same method of compound **2.7** and starting with 3-bromo-5,7-dimethoxycoumarin (**2.6**) (0.14 mmol) and 4-ethynylbenzaldehyde (0.28 mmol, 2 eq.). After purification by column chromatography using as eluent $CHCl_3$/0.5% MeOH it was possible to afford 23 mg of 4-((5,7-dimethoxy-2-oxo-2*H*-chromen-3-yl)ethynyl)benzaldehyde (**2.7**) ( 0.069 mmol, η= 48.8%). **$^1$H NMR (400 MHz, $CDCl_3$) δ (ppm):** 10.01 (s, 1H, CHO), 8.25 (s, 1H, H4), 7.85 (d, *J* = 8.0 Hz, 2H, H3'/H5'), 7.69 (d, *J* = 8.0 Hz, 2H, H2'/H6'), 6.42 (s, 1H, H6/H8), 6.30 (s, 1H, H6/H8), 3.92 (s, 3H, $OCH_3$), 3.87 (s, 3H, $OCH_3$).

*Synthesis of 5′-((5,7-dimethoxy-2-oxo-2H-chromen-3-yl)ethynyl)-[2,2′-bithiophene]-5-carbaldehyde (**2.10**)*

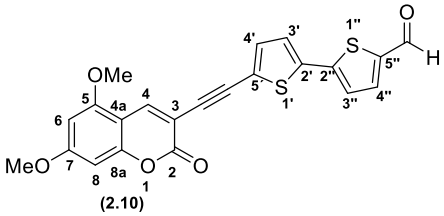


To a sealed tube, $PPh_3$ (0.06 eq), CuI (0.12 eq), $Pd(PPh_3)_4$ (0.15), 154 mg of 5′-Bromo-2,2′-bithiophene-5-carbaldehyde (0.56 mmol, 1.5 eq.) and 5 mL of dry dioxane were added under a $N_2$ atmosphere. After a few minutes, the previously prepared 5,7-dimethoxy-3-ethynylcoumarin (2.9) (1 eq.) and diisopropylamine (2 eq.) were added and the solution was stirred at 45°C for 15 hours. Once the reaction was confirmed to be complete by TLC (hexane/EtOAc (7/3)), the solution was cooled to room temperature, the solvent was removed under reduced pressure, and the solid residue was purified by flash chromatography column with DCM/ 0.2 % MeOH as eluent to afford 22 mg of 5′-((5,7-dimethoxy-2-oxo-2*H*-chromen-3-yl)ethynyl)-[2,2′-bithiophene]-5-carbaldehyde (**2.10**) (0.053 mmol, η= 14.1 %). **$^1$H NMR (400 MHz, DMF-$d_7$) δ (ppm):** 10.02 (s, 1H, CHO), 8.29 (s, 1H, H4), 8.08 (d, *J* = 4.03 Hz, 1H, ArH), 7.69 - 7,67 (m, 2H, ArH), 7,53 (d, *J* = 4.03 Hz, 1H, ArH), 6.67 (s, 1H, H6/H8), 6.63 (s, 1H, H6/H8), 4.04 (s, 3H, $OCH_3$), 3.99 (s, 3H, $OCH_3$). **HRMS-ESI(+):** Calculated for $C_{22}H_{15}O_5S_2$ $[M+H]^+$ 423.0355; Found 423.0349

*Synthesis of 2-cyano-3-(5′-((5,7-dimethoxy-2-oxo-2H-chromen-3-yl)ethynyl)-[2,2′-bithiophen]-5-yl)acrylic acid (**2.11b**)*

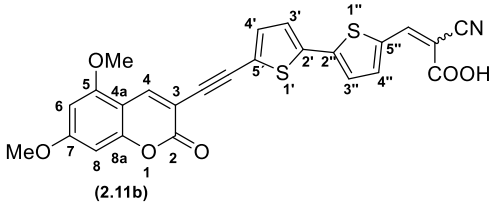


Compound 5′-((5,7-dimethoxy-2-oxo-2H-chromen-3-yl)ethynyl)-[2,2′-bithiophene]-5-carbaldehyde (**2.10**) (23 mg, 0.055mmol) and cyanoacetic acid (14 mg, 0.17 mmol, 3 eq.) were dissolved in 5 mL of dry acetonitrile and 16 µL of piperidine (0.16mmol, 2.9 eq.) were added to the solution. Then the reactional mixture was heated to reflux for 52h (followed by TLC using $CH_2Cl_2$ as eluent). Then the solvent was evaporated under reduced pressure, the solid residue was washed 3 to 5 times with ACN, acidified with HCl (10%) and washed 3 to 5 times with distilled water. After each washing step the solvent used was centrifuged (4500 rpm, 10-30 minutes) to recover any lost product. It was obtained 14 mg of an orange solid corresponding to 2-cyano-3-(5′-((5,7-dimethoxy-2-oxo-2*H*-chromen-3-yl)ethynyl)-[2,2′-bithiophen]-5-yl)acrylic acid (**2.11b**) (0.029 mmol, η=52.5%). **$^1$H NMR (400 MHz, DMF-$d_7$) δ (ppm):** 8.53 (s, 1H, =CH), 8.27 (s, 1H, H4), 8.04 (s, 1H,ArH), 7.70 (br s, 1H, ArH), 7.67 (br s, 1H, ArH), 7.52 (br s, 1H, ArH), 6.65 (s, 1H, H6/H8), 6.61 (s, 1H, H6/H8),

4.04 (s, 3H, $OCH_3$), 3.99 (s, 3H, $OCH_3$). **HRMS-ESI(+):** Calculated for $C_{25}H_{16}NO_6S_2$ $[M+H]^+$ 490.0414; Found 490.0406

*Synthesis of 2-cyano-3-(4-((5,7-dimethoxy-2-oxo-2H-chromen-3-yl)ethynyl)phenyl)acrylic acid (**2.11a**)*

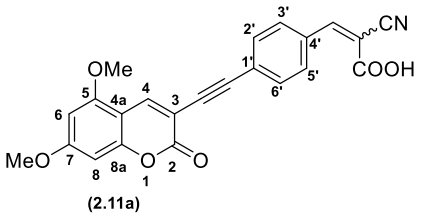

(2.11a)

Following the procedure for compound **2.11b** and starting with 4-((5,7-dimethoxy-2-oxo-2H-chromen-3-yl)ethynyl)benzaldehyde (**2.7**) ( 0.062 mmol) it was possible to afford 2-cyano-3-(4-((5,7-dimethoxy-2-oxo-2*H*-chromen-3-yl)ethynyl)phenyl)acrylic acid (**2.11a**) (0.0082 mmol, η= 13.2 %) (it was not observed the total consumption of the starting material **2.7**). **$^1$H NMR (400 MHz, $CDCl_3$) δ (ppm):** 8.16 (s, 1H, CH), 8.06 (s, 1H, H4), 7.81 (d, *J* = 6.8 Hz, 2H,H3'/H5'), 7.51 (d, *J* = 7.6 Hz, 2H, H2'/H6'), 6.32 (s, 1H, H6/H8), 6.20 (s, 1H, CH, H6/H8), 3.78 (s, 3H, $OCH_3$), 3.74 (s, 3H, $OCH_3$).

## 2.4.2 Synthesis of 6,7-dimethoxycoumarin derivatives

*Synthesis of 6,7-dimethoxycoumarin (**2.13**)*

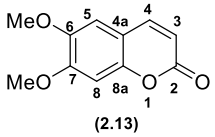

(2.13)

Following the same procedure for compound 2.6 and starting from 250 mg of 6,7-dihydroxycoumarin (**2.12**) (1.40 mmol). After 45h the reaction was completed, then the solvent was evaporated under reduced pressure. Water was added and the compound was extracted with $CH_2Cl_2$. The organic phases were combined, dried with $Na_2SO_4$, filtered and evaporated. It was possible to afford 270 mg of 6,7-dimethoxycoumarin (**2.13**) (η= 66.9 %). **$^1$H NMR (400 MHz, $CDCl_3$) δ (ppm):** 7.60 (d, *J* = 9.2 Hz, 1H, H4), 6.84 (s, 1H, H5), 6.80 (s, 1H, H8), 6.25 (d, *J* = 9.6 Hz, 1H, H3), 3.92 (s, 3H, $OCH_3$), 3.89 (s, 3H, $OCH_3$).

*Synthesis of 3-bromo-6,7-dimethoxycoumarin (**2.14**)*

In a round bottom flask equipped with a magnetic stir bar 6,7-dimethoxycoumarin (**2.13**) (1.31 mmol) was dissolved in 10 mL of $CH_2Cl_2$, then OXONE® (2.62 mmol, 2.0 eq.) and a solution of HBr 2M (2.88 mmol, 2.2 eq.) were added. The reaction was stirred for 20 h at room temperature and it was followed by TLC using as eluent hexane/EtOAc 1/1. After consumption of the starting material water was added and the product was extracted with $CH_2Cl_2$. The organic phases were dried with $Na_2SO_4$, filtered and evaporated under reduced pressure affording 364 mg of 3-bromo-6,7-dimethoxycoumarin (**2.14**) (1.28 mmol, η= 97.9 %). **$^1$H NMR (400 MHz, $CDCl_3$) δ(ppm):** 7.99 (s, 1H, H4), 6.81 (s, 1H, H5), 6.80 (s, 1H, H8), 3.93 (s, 3H, $OCH_3$), 3.90 (s, 3H, $OCH_3$).

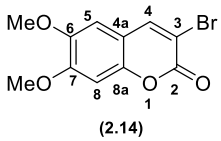

(2.14)

*Synthesis of 6,7-dimethoxy-3-((trimethylsilyl)ethynyl)coumarin (**2.15**)*

Following the experimental procedure for compound 2.8 and starting with 66 mg of 3-bromo-6,7-dimethoxycoumarin (**2.14**) (0.23mmol), after 49 hours the reaction was complete. The crude was purified by flash chromatography with hexane/ EtOAc 7/3 as eluent and it was possible to afford 66.9 mg of 6,7-dimethoxy-3-((trimethylsilyl)ethynyl)coumarin (**2.15**) (0. 22 mmol, η = 95.6%). **$^1$H NMR (400 MHz, $CDCl_3$) δ (ppm):** 7.83 (s, 1H, H4), 6.82 (s, 1H, H5/H8), 6.80 (s, 1H, H5/H8), 3.94 (s, 3H, $OCH_3$), 3.90 (s, 3H, $OCH_3$), 0.26 (s, 9H, $Si(CH_3)_3$). **HRMS-ESI(+):** Calculated for $C_{16}H_{19}O_4Si$ $[M+H]^+$ 303.1047; Found 303.1053

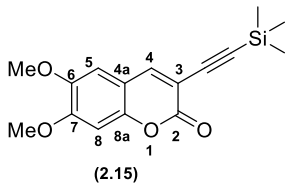

(2.15)

*Synthesis of 3-ethynyl-6,7-dimethoxycoumarin (**2.16**)*

In a round flask equipped with a magnetic stir bar containing 3-ethynyltrimethylsilane-6,7-dimethoxycoumarin (**2.15**) (20 mg, 0.084 mmol) dissolved in dry dioxane (1mL) was added, after cooling to 0 ºC, a solution of TBAF in THF (0.085mL, 1 eq.). The reaction was followed by TLC using as eluent a mixture of n-hexane/EtOAc 6/4. After 30 min. the reaction was complete and the reactional mixture was filtered under silica, then washed with dioxane. The solution of 3-ethynyl-6,7-dimethoxycoumarin (**2.16**) was directly used in Sonogashira couplings with different aldehydes.

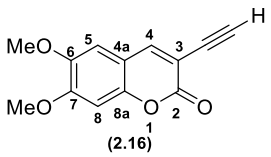

(2.16)

*Synthesis 2-((6,7-dimethoxy-2-oxo-2H-chromen-3-yl)ethynyl)-thiophene-5-carbaldehyde (2.18c)*

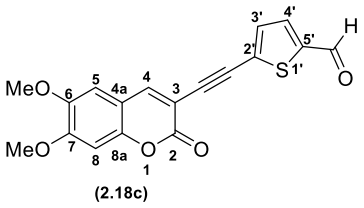

(2.18c)

Following the procedure for compound **2.10** and starting from 42.6 µL(0.34 mmol, 1 eq.) of 5-bromothiophene-2-carbaldehyde (**2.17c**). After purification by column chromatography with $CH_2Cl_2$/ 2% MeOH 58.7mg (50.8%) of 5-((6,7-dimethoxy-2-oxo-2*H*-chromen-3-yl)ethynyl)-thiophene-2-carbaldehyde were obtained (**2.18c**). **$^1$H NMR (400 MHz, $CDCl_3$) δ (ppm):** 9.87 (s, 1H, CHO), 7.92 (s, 1H, H4), 7.67 (d, *J* = 3.8 Hz, 1H, H4'), 7.38 (d, *J* = 3.6 Hz, 1H, H3'), 6.89 (s, 1H, H5/H8), 6.87 (s, 1H, H5/H8), 3.97 (s, 3H, $OCH_3$), 3.93 (s, 3H, $OCH_3$). **HRMS-ESI(+):** Calculated for $C_{18}H_{13}O_5S$ $[M+H]^+$ 341.0478; Found 341.0478

*Synthesis of 2-decyl-2H-benzo[1,2,3]triazole*

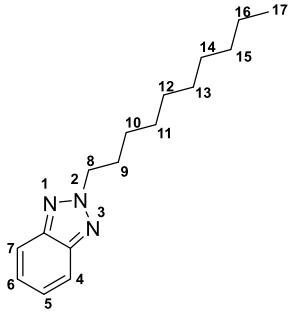


To a round-bottom flask under $N_2$ atmosphere were added 1,2,3-benzotriazole (500 mg, 4.20 mmol), $K_2CO_3$ (1.745g, 12.59 mmol, 3 eq.), 4 mL of DMF and 1 mL of 1-iododecane (4.69 mmol, 1.1 eq.). The reactional mixture was stirred at 40 °C for 1 hour and 30 minutes. Once confirmed to be complete by TLC (hexane/EtOAc (6/4), $H_2O$ was added, and the solution was extracted with $CH_2Cl_2$. The combined organic layers were washed several times with distilled water, then with brine, dried over anhydrous $Na_2SO_4$, filtered and evaporated to dryness. The crude was purified by column chromatography using the eluent hexane/ EtOAc 9/1, to afford 410 mg of an oil corresponding to 2-decyl-2*H*-benzo[1,2,3]triazole (1.67 mmol, η=39.8%). [143] **$^1$H NMR (400 MHz, $CDCl_3$) δ (ppm):** 7.86 (dd, *J* = 6.4, 3.2 Hz, 2H, H4/H7), 7.37 (dd, *J* = 6.4, 3.2 Hz, 2H, H5/H6), 4.72 (t, *J* = 7.0 Hz, 2H,H8), 2.11 (m,2H, H9), 1.24 (s, 14H, H10-H16), 0.86 (t, *J* = 6.6 Hz, 3H, H17). It was also possible to recover the isomer 1-decyl-1H-benzo[*d*][1,2,3]triazole (η=28.5%)

*Synthesis of 4,7-dibromo-2-decyl-2H-benzo[1,2,3]triazole*

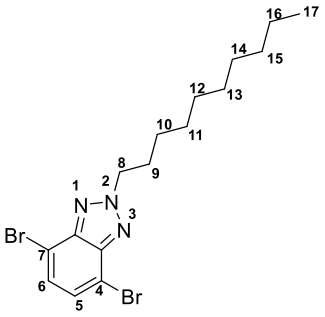

To a two-necked round-bottom flask 642 mg (2.62 mmol) of 2-decyl-2*H*-benzo[1,2,3]triazole and 3.7 mL of HBr (48%) were added, the solution was stirred at 100°C for 1h. Then 0.40 mL of $Br_2$ (7.85mmol, 3 eq.) were added. After stirring at 130°C for 18h, the consumption of the starting material was confirmed by TLC using $CH_2Cl_2$/hexane 8/2, the solution was cooled to room temperature and distilled $H_2O$ was added. The product was extracted with $CH_2Cl_2$, the organic phases were dried over anhydrous $Na_2SO_4$, filtered and evaporated to dryness. The solid residue was purified by flash column chromatography with hexane/$CH_2Cl_2$ 7/3 as eluent, affording 472 mg of 4,7-dibromo-2-decyl-2*H*-benzo[d][1,2,3]triazole as a brown oil (1.13 mmol, 43.1%).[143] **$^1$H NMR (400 MHz, $CDCl_3$) δ (ppm):** 7.44 (s, 2H, H5/H6), 4.77 (t, *J* = 7.4 Hz, 2H, H8), 2.14 (m, 2H, H9), 1.26 (s, 14H, H10-H16), 0.87 (t, *J* = 6.6 Hz, 3H, H17).

*Synthesis of 4-bromo-2-decyl-2H-benzo[d][1,2,3]triazole-7-carbaldehyde (**2.17d**)*

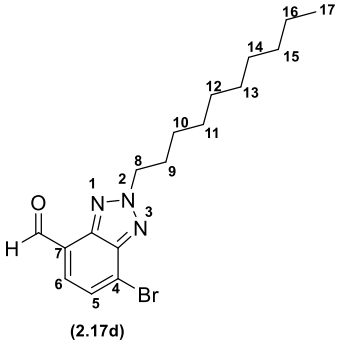


To a round-bottom flask containing 298 mg of 4,7-dibromo-2-decyl-*2H*-benzo[1,2,3]triazole (0.72 mmol) in 5 mL of dry THF was cooled to approximately -78°C and, after a few minutes, 0.5 mL (0. 80 mmol, 1.1 eq.) of a 1,6 M solution of *n*-BuLi in hexanes were added dropwise. After stirring for 15 minutes at -78°C, 56 µL (0.72 mmol, 1 eq.) of dry DMF were added. The temperature was maintained, and the reaction was stirred for more 3h. Once the total consumption of the starting material was confirmed by TLC hexane/ EtOAc 9/1 the solution was slowly warmed to room temperature. The quenching was performed by adding distilled $H_2O$ the organic compound was extracted with $CH_2Cl_2$. The organic phases were combined, dried under anhydrous $Na_2SO_4$, filtered and evaporated to dryness. The solid residue was purified by flash column chromatography with hexane/ EtOAc 9/1 as eluent, affording 120 mg of 7-dibromo-2-decyl-2*H*-benzo[d][1,2,3]triazole-4-carbaldehyde (**2.17d**) as a beige solid ( 0.33 mmol, η= 45.7%). **$^1$H NMR (400 MHz, $CDCl_3$) δ (ppm):** 10.44 (s, 1H, CHO), 7.83 (d, *J* = 7.2 Hz, 1H, H6), 7.76 (d, *J* = 7.6 Hz, 1H, H5), 4.84 (t, *J* = 7.4 Hz, 2H, H8), 2.17 (m, 2H, H9), 1.25 (s, 14H, H10-H16), 0.87 (t, *J* = 6.4 Hz, 3H, H17).

*Synthesis of 2-decyl-7-((6,7-dimethoxy-2-oxo-2H-chromen-3-yl)ethynyl)-2H-benzo[d][1,2,3]triazole-4-carbaldehyde (**2.18d**)*

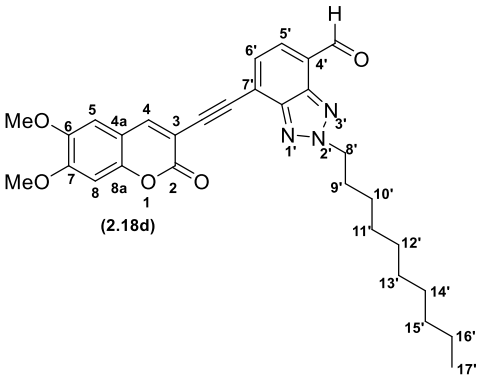


Following the procedure for compound **2.10** and starting with 70.63 mg of 7-dibromo-2-decyl-*2H*benzo[1,2,3]triazole-4-carbaldehyde (**2.17d**) (0.19 mmol) it was possible to obtain 9.2 mg of 2-decyl-7-((6,7- dimethoxy-2-oxo-2*H*-chromen-3-yl)ethynyl)-2*H*-benzo[d][1,2,3]triazole-4-carbaldehyde (**2.18d**) (0.018 mmol, η= 9.2 %). **$^1$H NMR (400 MHz, $CDCl_3$) δ (ppm):** 10.46 (s, 1H, CHO), 8.06 (s, 1H, H4), 7.95 (d, *J* = 7.2 Hz, 1H, H5'), 7.78 (d, *J* = 7.2 Hz, 1H, H6'), 6.87 (s, 1H, H5/H8), 6.87 (s, 1H, H5/H8), 4.85 (t, *J* = 7.2 Hz, 2H, H8'), 3.97 (s, 3H, $OCH_3$), 3.93 (s, 3H, $OCH_3$), 2.17 (m, 2H, H9'), 1.24 (m, 14H, H10'-H16' ), 0.86 (t, *J* = 6.4 Hz, 3H, H17'). **HRMS-ESI(+):** Calculated for $C_{30}H_{34}N_3O_5$ $[M+H]^+$ 516.2493; Found 516.2509

Sy*nthesis of 2-cyano-3-(5-((6,7-dimethoxy-2-oxo-2H-chromen-3-yl)ethynyl)thiophen-2-yl)acrylic acid (**2.19c**)*

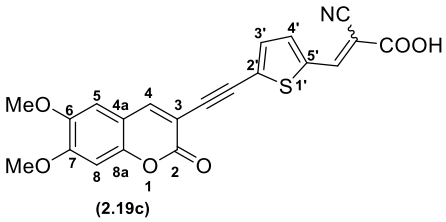


Using the procedure for compound 2.11b and stating with 28.1 mg of 5-((6,7-dimethoxy-2-oxo-2*H*-chromen-3-yl)ethynyl)-thiophene-2-carbaldehyde (**2.18c**) (0.08 mmol) the reaction was stirred under reflux for 17 hours. The consumption of the aldehyde was monitored by TLC using the eluent $CH_2Cl_2$/ 2% MeOH. It was possible to obtain 17.7 mg (52.7 %) of 2-cyano-3-(5-((6,7-dimethoxy-2-oxo-2*H*-chromen-3-yl)ethynyl)-thiophen-2-yl)acrylic acid (**2.19c**). **$^1$H NMR (400 MHz, DMSO-$d_6$) δ (ppm):** 8.50 (s, 1H, H4/CH), 8.36 (s, 1H, H4/CH), 7.98 (d, *J* = 3.8 Hz, 1H, H3'/H4'), 7.57 (d, *J* = 3.9 Hz, 1H, H3'/H4'), 7.22 (s, 1H, H5/H8), 7.11 (s, 1H, H5/H8), 3.89 (s, 3H, $OCH_3$), 3.81 (s, 3H, $OCH_3$). **HRMS-ESI(+):** Calculated for $C_{21}H_{14}NO_6S$ $[M+H]^+$ 408.0536; Found 408.0529

Sy*nthesis of 2-cyano-3-(2-decyl-7-((6,7-dimethoxy-2-oxo-2H-chromen-3-yl)ethynyl)-2H-benzo[d][1,2,3]triazol-4-yl)acrylic acid (**2.19d**)*

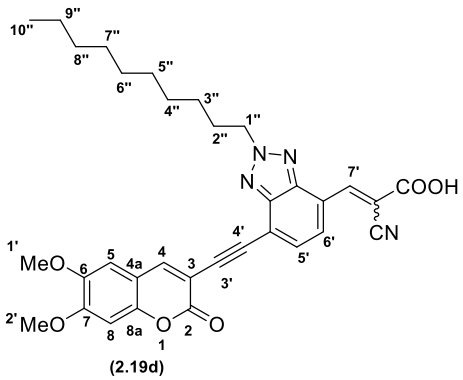


Following the experimental procedure for 2.11b and starting from 51,7 mg of 2-decyl-7-((6,7-dimethoxy-2-oxo-2*H*-chromen-3-yl)ethynyl)-2*H*-benzo[d][1,2,3]triazole-4-carbaldehyde (**2.17d**) (0.10 mmol, 1 eq.), 8.9 mg of 2-cyano-3-(2-decyl-7-((6,7-dimethoxy-2-oxo-*2H*-chromen-3-yl)ethynyl)-*2H*-benzo[*d*][1,2,3]triazol-4-yl)acrylic acid (**2.19d**) (50.8%) were obtained. **$^1$H NMR (400 MHz, DMF-$d_7$) δ (ppm):** 8.92 (s, 1H, H4/H7'), 8.55 (d, *J* = 8.0 Hz, 1H, H5'/H6'), 8.46 (s, 1H, H4/H7'), 7.97 (d, *J* = 7.8 Hz, 1H, H5'/H6'), 7.42 (s, 1H, H5/H8), 7.17 (s, 1H, H5/H8), 4.95 (t, *J* = 7.3 Hz, 2H, H1''), 4.04 (s, 3H, H1'/H2'), 3.93 (s, 3H, H1'/H2'), 2.22 - 2.15 (m, 2H, H2''), 1.44 - 1.14 (m, 20H, H3''-H9''), 0.85 (t, *J* = 6.4 Hz, 5H, H10''). **HRMS-ESI(+):** Calculated for $C_{33}H_{35}N_4O_6$ $[M+H]^+$ 583.2551; Found 583.2542

# 3 ACENAPHTHENE DERIVATIVES AS PHOTOSENSITIZERS

Part of *Acenaphthene derivatives as photosensitizers* chapter is based on the journal article "Malta, G.; Pina, J.; Lima, J. C.; Parola, A. J.; Branco, P. S. Acenaphthylene-Based Chromophores for Dye-Sensitized Solar Cells: Synthesis, Spectroscopic Properties, and Theoretical Calculations. *ACS Omega* **2024**, *9*, 14627-14637."

The author was responsible for all the experiments presented in this chapter. DFT studies were carried out in collaboration with Professor João Pina from the University of Coimbra.

## 3.1 General overview

Acenaphthene is a polycyclic aromatic hydrocarbon (PAH), some examples of acenaphthene derivatives are acenaphthylene, bis(arylimino)acenaphthenes (Ar-BIANs) and 7*H*-acenaphtho[1,2-*d*]imidazoles.

### 3.1.1 Bis(arylimino)acenaphthenes

Bis(arylimino)acenaphthene (Ar-BIAN) compounds are commonly applied as nitrogen bidentate α-diimine ligands for main group elements and transition metals.[150-152] This class of compounds has been quite used as sterically bulky diamine ligands in several reactions, the most remarkable being its use as a catalyst in olefin polymerization.[153,154] Furthermore, these compounds present specific characteristics that are important for their photophysical applications, namely a π-conjugated naphthalene moiety, structural rigidity, and the presence of tunable aryl substituents that allow to vary their steric and electronic capabilities.[150,155] They were tested as active layers in bulk heterojunction devices[156,157] and in the fabrication of graphite electrodes for lithium-ion batteries.[158] The use of Ar-BIAN complexes as dye sensitizers in DSSCs has already been reported, however their energy conversion efficiencies are low. Recently, the synthesis of copper dyes supported by Ar-BIAN ligands containing, as anchoring groups, sulfonates was reported (**Figure 28**). Despite the low conversion efficiencies, the *I–V* curves have shown that these compounds can inject electrons into $TiO_2$.[159]

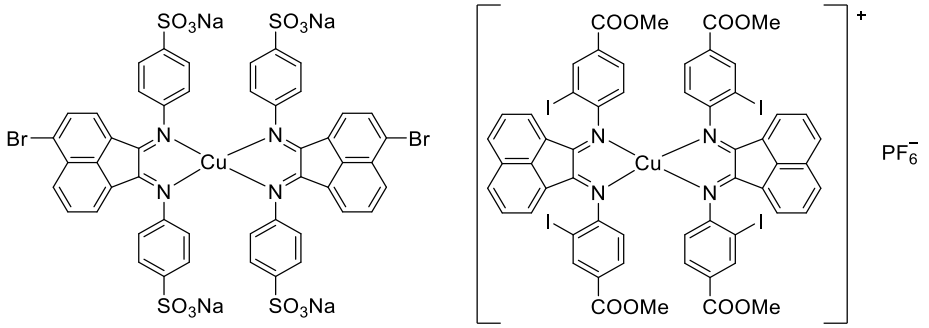


Figure 28. Cu(I) Ar-BIAN complexes applied in DSSCs as sensitizers.

These Ar-BIAN compounds can be easily synthesized via condensation reactions between an aniline and acenaphthoquinone, two cheap and commercially available reagents. As so, their

photophysical and photovoltaic properties can be easily modulated by choosing different anilines. Two stereoisomeric forms are possible for these structures, *anti-anti* and *syn-anti*. The formation of the *syn-syn* isomer is hindered due to steric reasons. (**Figure 29**).[160,161]

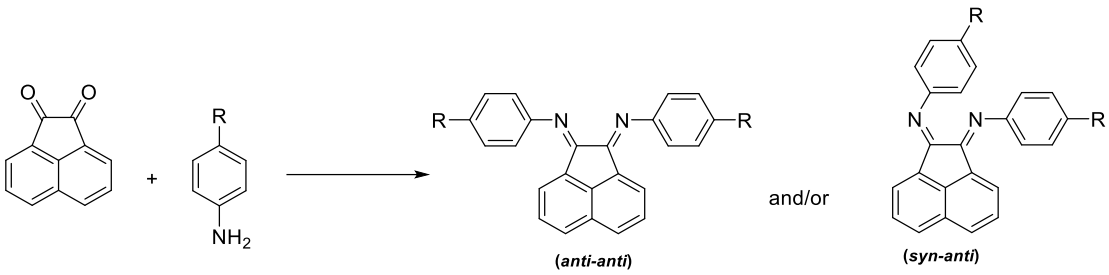


Figure 29. Reaction scheme for the synthesis of Ar-BIAN derivatives.

### 3.1.2 7*H*-acenaphtho[1,2-*d*]imidazoles

Debus-Radziszewski multicomponent reaction is a powerful tool to synthesize imidazole cores. By reacting a 1,2-diketone with an aldehyde in the presence of an ammonia source it is possible to afford a 2,4,5-trisubstituted imidazole, and by adding an aniline to this equation a 1,2,4,5-tetrasubstituted imidazole is obtained.[162] The aforementioned starting material acenaphthenoquinone can be used as 1,2-diketone in these reactions, leading to the formation of 7*H*-acenaphtho[1,2-d]imidazoles derivatives (**Figure 30**). Alternative methods using Lewis acids ($InF_3$, ZnO)[163,164], silver salts ($Ag_2CO_3$)[165], ionic liquids (piperidinium hydrogen sulfate)[166] and other catalysts such as $TiO_2$,[167] $I_2$,[168] $Ph_3CCl$ [169] and L-proline[170] can be also employed to achieve structures of similar types.

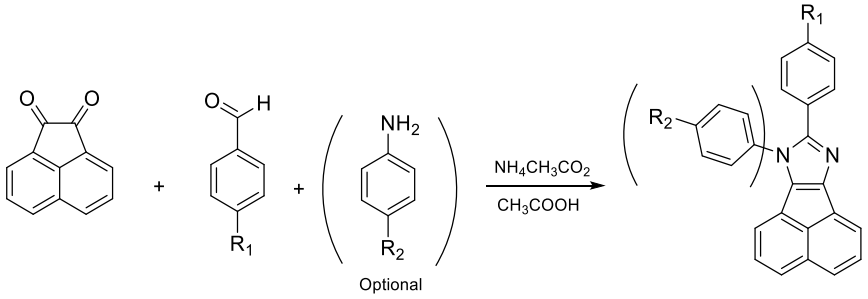


Figure 30. Debus-Radziszewski reaction for the synthesis of 2,4,5-trisubstituted imidazole and 1,2,4,5-tetrasubstituted imidazole.

Recently, Ramanujam *et al.*[171] reported the synthesis of imidazole derivatives with a fused phenanthrene backbone that achieved good overall efficiencies as sensitizers. Structural modifications like the introduction of anisole (ancillary donor) in the pyrrolic nitrogen increased the efficiency from 5.26 % to 6.71% (N719 reference: 7.62%). The compounds were easily prepared by reacting 9,10-phenanthrenequinone, terephthaladehyde, *p*-anisidine, and ammonium acetate in glacial acetic acid under reflux. Then, through a Knoevenagel reaction, the cyanoacrylic anchoring groups were introduced and the final chromophores were obtained (**Figure 31**). [171] This two-step synthesis method allows several units of the molecule to be tuned and the effect on DSSC efficiency to be studied. Taking into account this methodology, if the 9,10-phenanthrenequinone is replaced by an acenaphthoquinone, a family-based on 7*H*-acenaphtho[1,2-d]imidazole can be prepared for the first time.

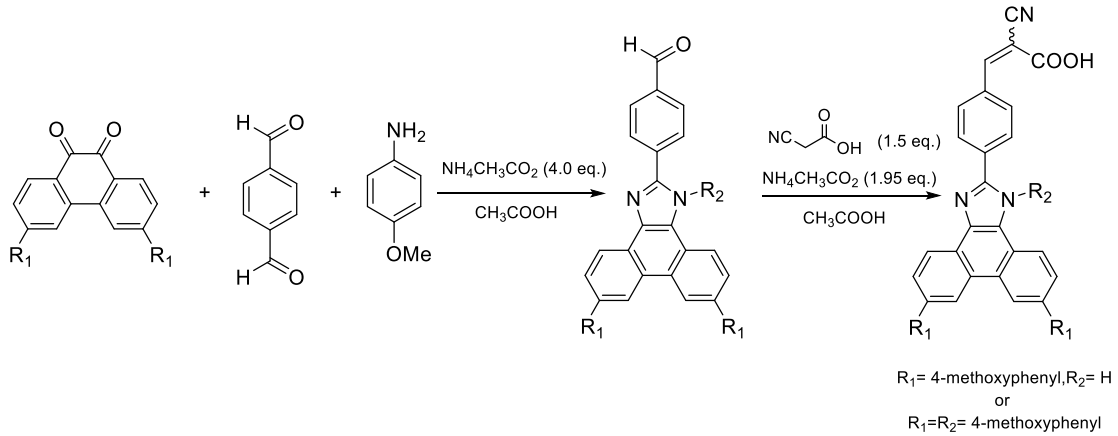


Figure 31. Reactional scheme for the preparation of imidazole derivatives with a fused phenanthrene core embedded in the structure.

### 3.1.3 Acenaphthylene

Acenaphthylene has been widely used as a building block of several π-conjugated functional materials[172] such as bistriphenylamine fluoranthenes[173], acenaphthopyrazines[174] and acenaphthoBODIPYs.[175] Regarding the bistriphenylamine fluoranthenes[173] and acenaphthopyrazines[174] dyes cores, their structures, photovoltaic and photophysical characteristics are depicted on **Figure 32** and **Table 8**. Su's group studied the application of bistriphenylamine fluoranthenes (**i**) in DSSCs with variations in the π-bridge. The thiophene derivative was the best-performing dye (**i-b**) in this study, with an efficiency of 4.57 % due to a more extended conjugated

system.[176] Regarding the acenaphthopyrazines, Sun's group concluded that the absorption spectra of dyes **ii** are red-shifted compared with dyes **iii**, revealing that the former have a more efficient electron push-pull system.[174] The photovoltaic results are in accordance with this. Higher values of $J_{sc}$ were observed for compounds **ii**, thus resulting in better efficiencies. Despite the existence of some reported examples where these cores are applied in DSSCs the use of dyes in this field containing an acenaphthylene as the main core unit is still at an early stage of exploration.

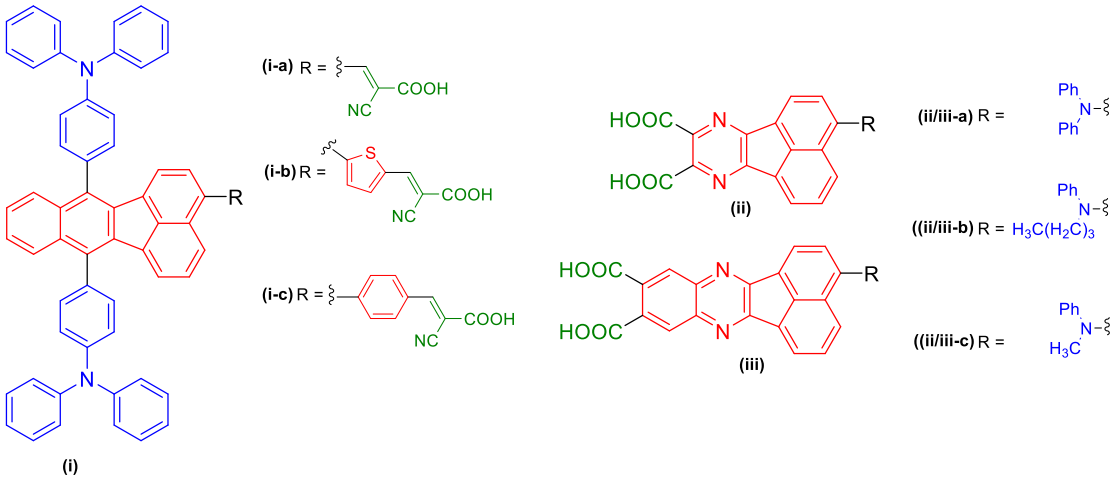


Figure 32. Chemical structures of dyes bearing bistriphenylamine fluoranthenes and acenaphthopyrazines cores.

Table 8. Spectroscopic and photovoltaic parameters of bistriphenylamine fluoranthenes and acenaphthopyrazines based dyes applied in DSSCs.

| Dye | $\lambda_{max}$ (nm) | ε ($M^{-1}$ $cm^{-1}$) | $J_{sc}$ ($mA/cm^2$) | $V_{oc}$ (V) | FF | η (%) [η ref (%)] | Ref |
|---|---|---|---|---|---|---|---|
| **i-a** | 297, 447 | 58 000, 12 000 | 7.59 | 0.73 | 0.72 | 4.00 | 173 a |
| **I-b** | 300, 445 | 54 000, 21 000, | 8.57 | 0.76 | 0.63 | 4.57 | |
| **I-c** | 303, 426 | 51 000, 14 000 | 5.56 | 0.69 | 0.69 | 2.72 | |
| **ii-a** | 461 | 8 000 | 8.11 | 0.693 | 0.72 | 4.04 | 174 b |
| **ii-b** | 457 | 6 300 | 6.43 | 0.662 | 0.63 | 2.68 | |
| **ii-c** | 444 | 3 100 | 4.10 | 0.638 | 0.70 | 1.82 | |
| **iii-a** | 444 | 12 200 | 6.27 | 0.650 | 0.70 | 2.85 | |

| | | | | | | |
|---|---|---|---|---|---|---|
| **iii-b** | 435 | 10 400 | 5.89 | 0.632 | 0.71 | 2.62 |
| **iii-c** | 424 | 11 000 | 3.78 | 0.589 | 0.66 | 1.48 |

[a] Electrolyte composition: 0.1 M LiI, 0.05 M $I_2$, 0.6 M PMII (1-methyl-3-propylimidazolium Iodide), 0.5 M TBP in the mixed solvent of acetonitrile and 3-methoxy-propionitrile (7:3, v/v). Reference dye: N719 (η= 8.00%)

[b]Electrolyte composition: 0.1 M LiI, 0.05 M $I_2$, 0.6 M PMII (1-methyl-3-propylimidazolium Iodide), 0.5 M TBP in the mixed solvent of acetonitrile and 3-methoxy-propionitrile (7:3, v/v). Reference dye: N719 (η= 8.00%)

cohol (v/v, 1:1). Reference dye: N719 (η= 7.05%)

On Figure 33 and Table 9 are depicted some examples of PAH-based dyes widely used in DSSCs such as biphenyl,[177,178] fluorene[179,180] and anthracene[18,181] derivatives. Gao's group reported the use of a biphenyl as a secondary electron donor in a structure with a D-D-π-A design, in which different π-bridges were used, namely phenyl, thiophene and furan (**iv**). The furan derivative (**iv-c**) achieved the best efficiency (5.81 %) with $J_{sc}$ and $V_{oc}$ values of 11.36 mA $cm^{-2}$ and 0.750 V, respectively. This better efficiency is also related to a superior molar extinction coefficient (37 135 and 24 966 $M^{-1}$ $cm^{-1}$) and less charge recombination. Kim's[178] and Lin's[180] groups developed, respectively, structures **v** and **vi** containing a fluorene core, a more rigid and conjugated structure than the biphenyl group, and obtained efficiencies of 9.2 and 6.88 % respectively. Meymian et al.[181] reported a D-π-A dye with a *N,N*-diphenylaniline linked to a diazo moiety, an anthracene core as π-bridge and a carboxylic acid as anchoring group to $TiO_2$ (**vii**). The obtained values of $J_{sc}$, $V_{oc}$ and FF were respectively 14.21 mA $cm^{-2}$, 0.630 V, and 0.56 which resulted in an efficiency of 5.01 %. Yeh's group [18] reported the synthesis of a dye with two anthracene cores linked by ethynyl groups (**viii**) in which a remarkable value of $V_{OC}$ was achieved (1.07 V) and an efficiency of 8.35 % was obtained.

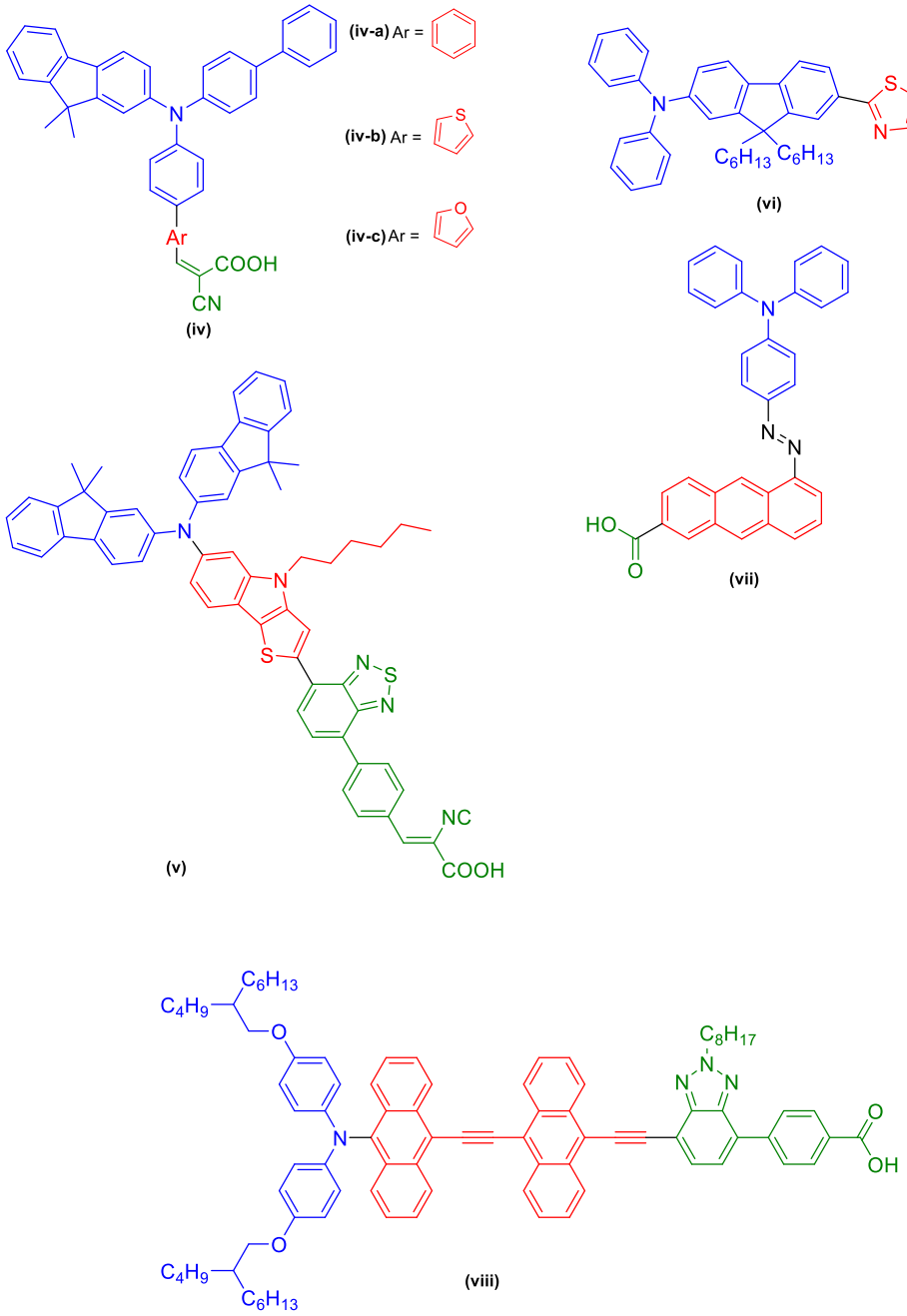


Figure 33. Chemical structures of some PAHs-based dyes used in DSSCs

Table 9. Spectroscopic and photovoltaic parameters of PAHs-based dyes applied in DSSCs.

| Dye | $\lambda_{max}$ (nm) | ε ($M^{-1}$ $cm^{-1}$) | $J_{sc}$ ($mA/cm^2$) | $V_{oc}$ (V) | FF | η (%) [η ref (%)] | Ref |
|---|---|---|---|---|---|---|---|
| **iv-a** | 344<br>408 | 9 944<br>5 685 | 4.96 | 0.640 | 0.72 | 2.28 | 177 a |
| **iv-b** | 349<br>430 | 16 236,<br>10 786 | 9.99 | 0.680 | 0.71 | 4.83 | |
| **iv-c** | 360<br>436 | 37 135<br>24 966 | 11.36 | 0.750 | 0.68 | 5.81 | |
| **v** | 377<br>544 | 38 119<br>16 826 | 18.54 | 0.674 | 0.73 | 9.2 | 178 b |
| **vi** | 448<br>348<br>310 | 51 300<br>30 800<br>31 000 | 14.55 | 0.710 | 0.67 | 6.88 | 179 c |
| **vii** | 541 | 21 740 | 14.21 | 0.630 | 0.56 | 5.01 | 181 d |
| **viii** | 366<br>487<br>535 | 19 000<br>37 000<br>27 000 | 10.82 | 1.07 | 0.72 | 8.35 | 18 e |

[a] Electrolyte composition: OPV-AN-I [$I^-$]= 0.07 mmol $L^{-1}$ (Yingkou Opvtech New Energy Co., Ltd.).

[b] Electrolyte composition: 0.6 M DMPII (1,2-dimethyl-3-propylimidazolium iodide), 0.5 M TBP, 0.05 M $I_2$, and 0.1 M LiI in $CH_3CN$.

[c] Electrolyte composition: LiI, 0.5M, $I_2$, 0.05M, and TBP, 0.5M dissolved in acetonitrile. [Dye solution]= $3x10^{-4}$. Reference dye: N719

[d] Electrolyte composition: LiI ($6.0 \times 10^{-2}$ M), $I_2$ ($4.0 \times 10^{-2}$M), with 0.5 M 4-*tert*-butylpyridine as additive in dry acetonitrile. $4.0 \times 10^{-5}$ M in ethanol.

[e] Electrolyte composition: 0.2 M [$Cu(dmp)_2(TFSI)$], 0.05 M [$Cu(dmp)_2(TFSI)_2$], 0.1 M LiTFSI, 0.6 M 4- *tert*-butylpyridine (TBP) in MeCN. [Dye solution]= 0.15 mM with 0.3 mM chenodeoxycholic acid (CDCA) in *tert*-butanol / ACN / dichloromethane mixture (v/v, 2:2:1).

# 3.2 Results and discussion

## 3.2.1 Synthetic methodology

### 3.2.1.1 Bis(arylimino)acenaphthenes (Ar-BIANs) derivative dyes

In an attempt to enhance the energy conversion efficiencies of bis(arylimino)acenaphthenes (Ar-BIANs), the synthesis of an entirely organic Ar-BIAN dye containing two cyanoacrylic acids as anchoring groups (**3.5**) was proposed (**Figure 34**).

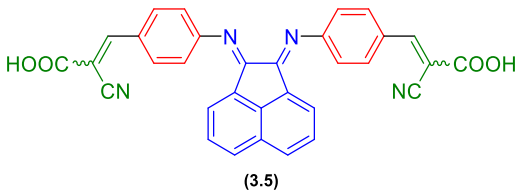


(3.5)

Figure 34. Structure of the target Ar-BIAN-based dye (**3.5**).

The first approach to synthesize the desired compound involved an addition reaction between acenaphthoquinone (**3.1**) and 4-aminobenzoic acid (**3.2**) to obtain compound **3.3**. Two different methods have been employed. The first one uses the Lewis acid $ZnCl_2$ in acidic media. First, a zinc complex is formed which then reacts with $K_2CO_3$ or $C_2K_2O_4$ to obtain the free ligand (Method A).[156] The other method involves acidic catalysis with glacial acetic acid (Method B).[150] However, in both reactions the obtained solids were complex mixtures that were not in agreement with the literature.[150] The following steps would consist of a reduction of the carboxylic acids to aldehydes to obtain **3.4** and, then, to obtain the final chromophore **3.5** a Knoevenagel condensation to introduce the anchoring groups (**Scheme 12**).

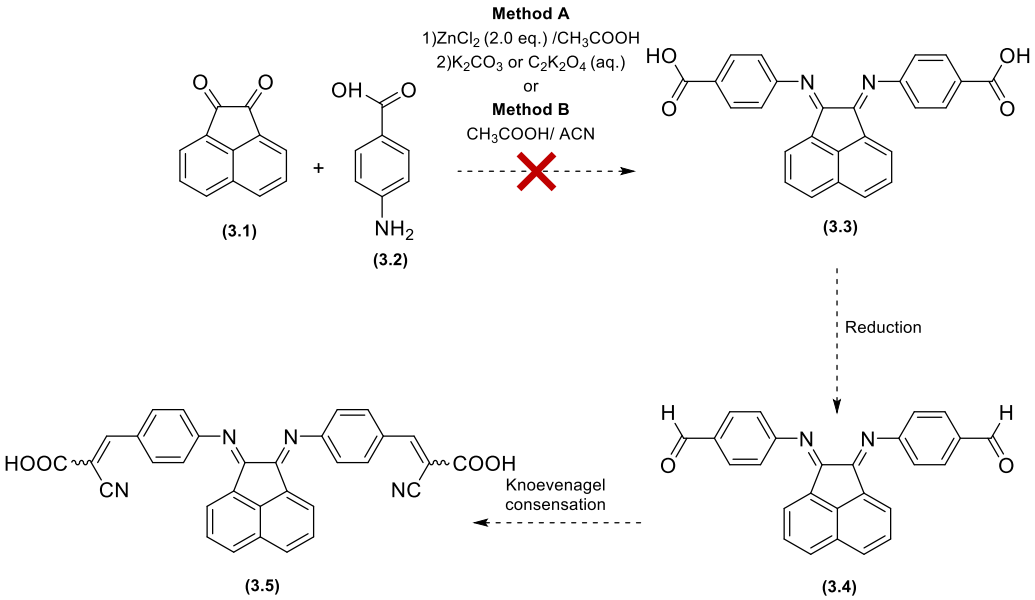


Scheme 12. Synthetic route for the preparation of Ar-BIAN 3.5 starting with 4-aminobenzoic acid (**3.2**).

The second synthetic attempt involved the protection of the aldehyde group of the *p*-nitrobenzaldehyde (**3.6**) with an acetal (**3.7**) by reacting it with ethylene glycol and catalytic *p*-toluenesulfonic acid, employing a dean stark for continuous removal of the water formed during the reaction. Subsequently, the reduction of the nitro group to an amine (**3.8**) was performed through catalytic hydrogenation with a Pt catalyst.[182] These conditions were too harsh and the acetal group hydrolyzed, leading to the formation of 4-aminobenzaldehyde (**3.9**) instead. An intramolecular reaction between the functional groups aldehyde and amine occurred and the compound polymerized (**Scheme 13**).

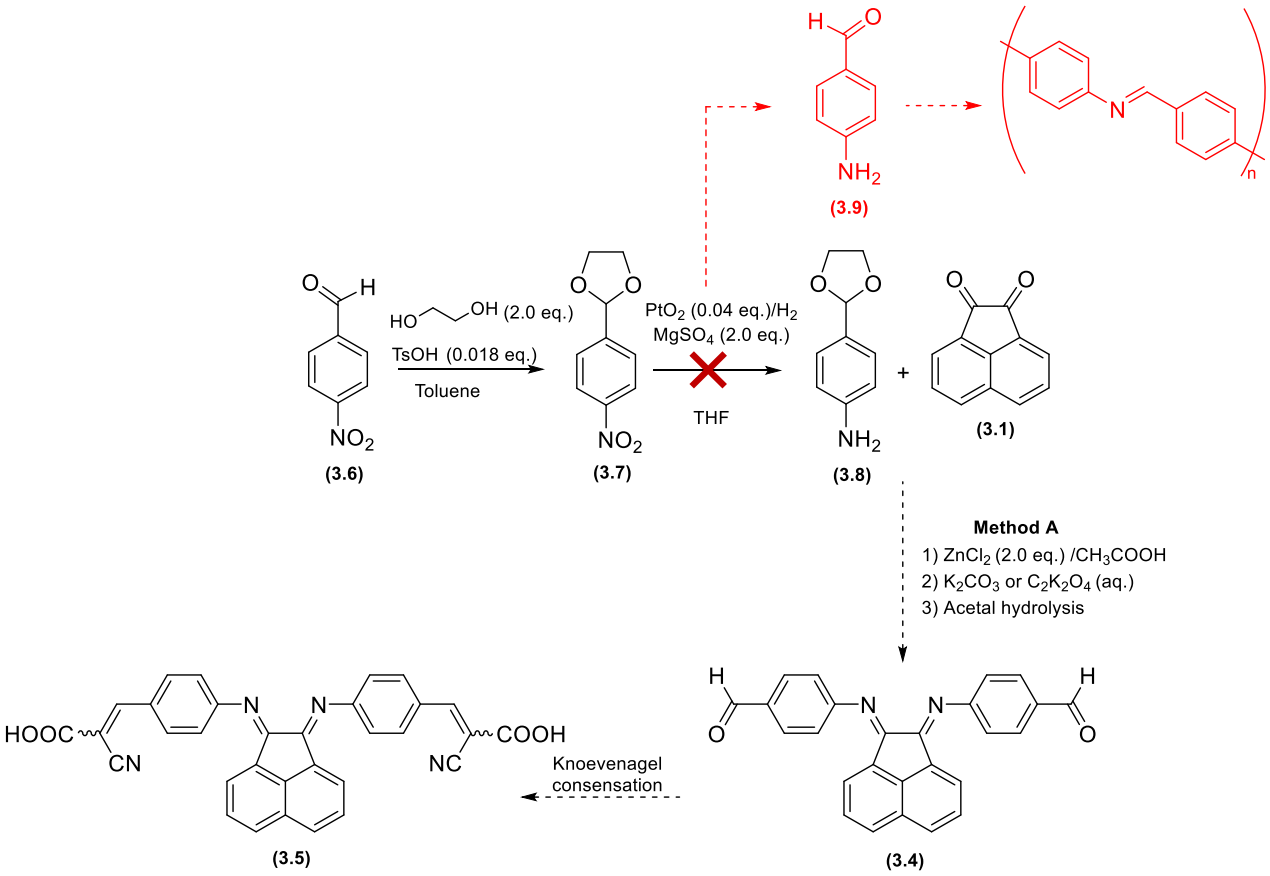


Scheme 13. Synthetic route for the preparation of Ar-BIAN **3.5** using 4-(1,3-dioxolan-2-yl)aniline (**3.8**).

Due to this, the strategy was changed again, and the synthesis of an Ar-BIAN with phenyl methanol substituents (**3.13**) was proposed. Afterwards, the hydroxyl groups would be oxidized to obtain the dialdehyde (**3.4**), and a Knoevenagel condensation would be performed to obtain the desired compound. The previous starting material *p*-nitrobenzaldehyde (**3.6**) was reduced with $NaBH_4$ to a primary alcohol (**3.10**). Several attempts were made to reduce the nitro group to a primary amine (**3.11**). Different conditions for the reduction of (4-nitrophenyl)methanol (**3.11**) are depicted in **Table 10**. The first method used $CuCl_2$ and $KBH_4$. It was expected that the formation of a borohydride-transition metal salt system would be able to reduce the aromatic nitro compound, but monitorization of the reaction by TLC didn't show any significant change.[183] The second attempt consisted of a catalytic hydrogenation. It was observed that, besides the reduction of the nitro group to an amine, the reduction of the alcohol group occurred. Changing the reaction conditions to use atmospheric pressure led to the same result. It was possible to obtain the pure desired compound with a 69 % yield via a method described by Vogel using Pd/C, $NaBH_4$ and NaOH.[184] Then the 4-aminophenylmethanol (**3.11**) reacted

with acenaphthoquinone and $ZnCl_2$ in acetic acid to obtain the Ar-BIAN (**3.13**) (Method A). A complex mixture was obtained, but following analysis of the obtained solid, it was hypothesized that oxidation reactions may have occurred due to characteristic evidence of the functional group aldehyde in $^1H$ NMR (s, 9.56 ppm) and IR (1724 $cm^{-1}$). The method using acidic catalysis with glacial acetic acid (Method B) was also applied but the obtained solid corresponded again to a complex mixture, mainly composed by acenaphthoquinone (**Scheme 14**). Due to these unfruitful reactions, the synthetic pathway was changed again.

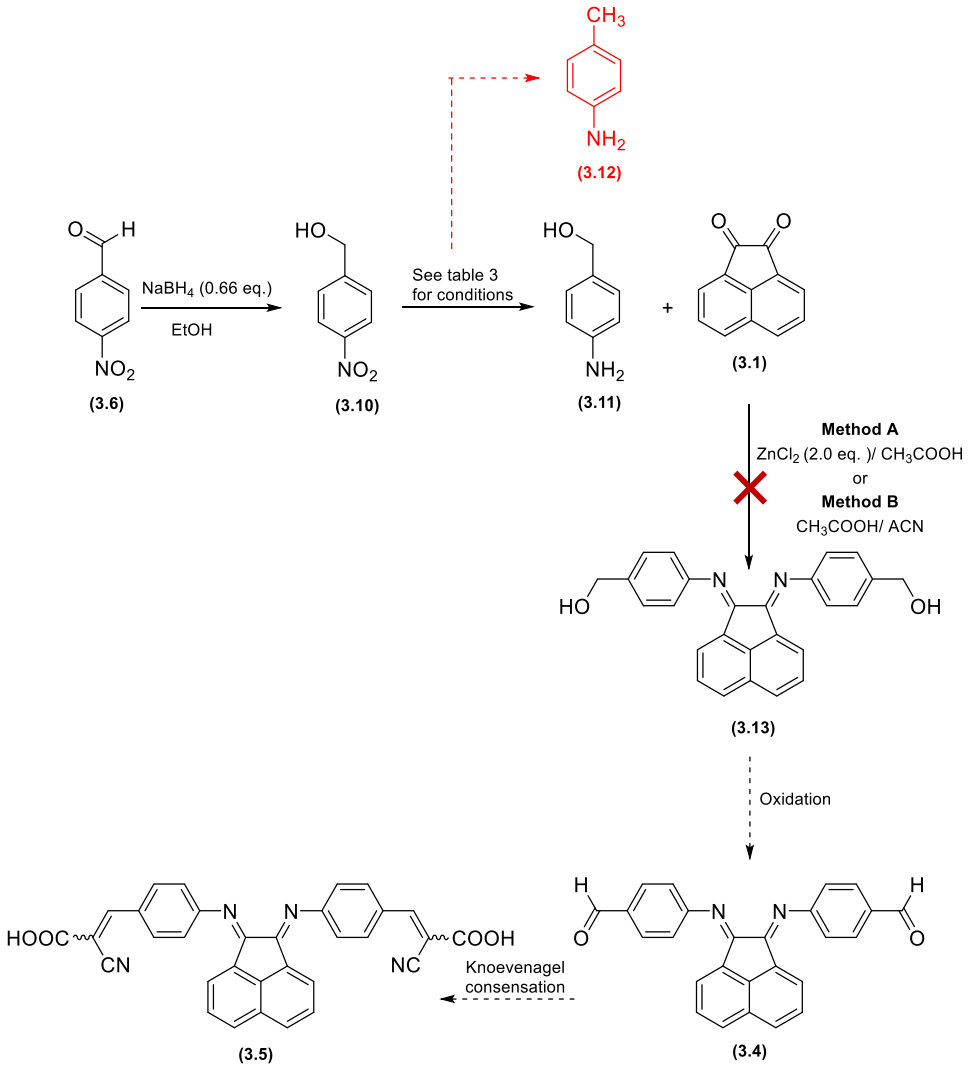


Scheme 14. Synthetic route for the preparation of Ar-BIAN 3.5 using (4-aminophenyl)methanol (**3.11**).

Table 10. Different conditions for the reduction of (4-nitrophenyl)methanol (**3.11**).

| Entry | Reagents | Solvent | Temperature | Time | Observations |
|---|---|---|---|---|---|
| 1 | $CuCl_2$ (3.0 eq.) $KBH_4$ (7.0 eq.) | MeOH | RT | 24 h | No reaction was observed by TLC |
| 2 | Pd/C (10 %)/ $H_2$ (4.6 bar) | MeOH/EtOH (2:1 % v/v) | RT | 5h | 3.11/3.12 ratio (%) 66/34 |
| 3 | Pd/C (10 %)/ $H_2$ (without pressure) | MeOH/EtOH (2:1 % v/v) | RT | 2h | 3.11/3.12 ratio (%) 76/24 |
| 4 | Pd/C 10% (0.009 eq.) $NaBH_4$ (2.0 eq.) NaOH | $H_2O$ | RT | 0.5h | Only compound 3.11 (η= 69 %) |

Another strategy involved the reaction of 3-(4-aminophenyl)-2-cyanoacrylic acid (**3.15**) with acenaphthoquinone (**3.1**). For the preparation of compound **3.15**, the *p*-nitrobenzaldehyde (**3.6**) reacted with cyanoacetic acid through a Knoevenagel condensation. The temperature was crucial in this reaction. It was observed that, at reflux, decarboxylation occurs, due to the presence of four doublets, 7.63 ($J$ = 8.7 Hz) and 6.05 ppm ($J$ = 16.7 Hz) for isomer E and 7.96 ($J$ = 8.6 Hz) and 5.70 ppm ( $J$ = 12.1 Hz) for isomer *Z* (ratio *E*/*Z*: 58/42).[185] The desired compound **3.14** was obtained with the same procedure at room temperature with 89 % yield. Then, the previous method with Pd/C, $NaBH_4$ and NaOH to reduce the nitro group of compound **3.14** was employed, but it was not possible to obtain the desired pure compound **3.15** without purification. As such, a method with $SnCl_2$ in acidic media was used, which allowed to obtain **3.15** in a 86.7% yield. Since the use of high temperatures led to decarboxylation of the cyanoacrylic acid group, the formation of the desired Ar-BIAN (**3.5**) was performed without using high temperatures. Besides the already reported methods A and B, an attempt using *p*-toluenesulfonic acid in toluene was also experimented (Method C). [186] During the attempts to obtain the desired compound, neither the consumption of the starting materials nor the formation of the product was observed (**Scheme 15**).

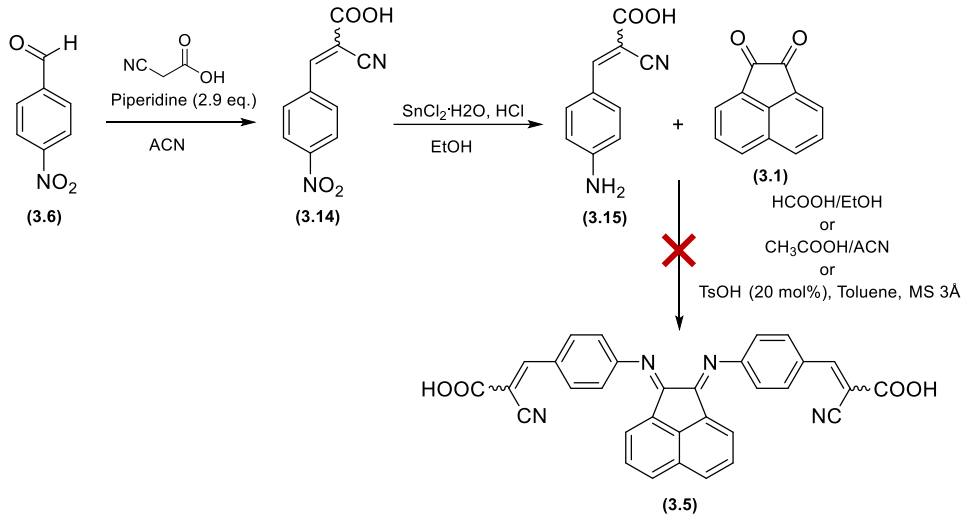


Scheme 15. Synthetic route for the preparation of Ar-BIAN **3.5** using 3-(4-aminophenyl)-2-cyanoacrylic acid (**3.15**).

The synthesis of ester derivative, ethyl-3-(4-aminophenyl)-2-cyanoacrylate (**3.17**) was shown to be the best choice due to its stability in high temperatures and medium polarity. By performing a Knoevenagel condensation between *p*-nitrobenzaldehyde (**3.6**) and ethyl cyanoacetate in the presence of piperidine, the ethyl-2-cyano-3-(4-nitrophenyl)acrylate (**3.16**) was obtained with 88% yield. Next, the nitro group of the afforded compound was reduced to an amine, through a reaction with tin(II) chloride dihydrate in the presence of HCl to obtain the desired aniline (**3.17**). The aniline reacted with acenaphthoquinone (**3.1**) and $ZnCl_2$ in refluxing acetic acid. The Ar-BIAN complex precipitated from the hot solution. The dissociation was made by stirring the precipitate for a few minutes with a solution of potassium oxalate, followed by an extraction of the Ar-BIAN with $CH_2Cl_2$ (Method A). After recrystallization with ethanol, the desired compound **3.18** was obtained with a 22% yield.

The final step involved the hydrolysis of the ethyl ester. Given this, procedures using an aqueous solution of LiOH or NaOH in methanol were used. In the $^1H$ spectra, the presence of the anilines **3.17** and **3.15** was observed, which indicates that the imine groups suffered hydrolysis (**Scheme 16**).

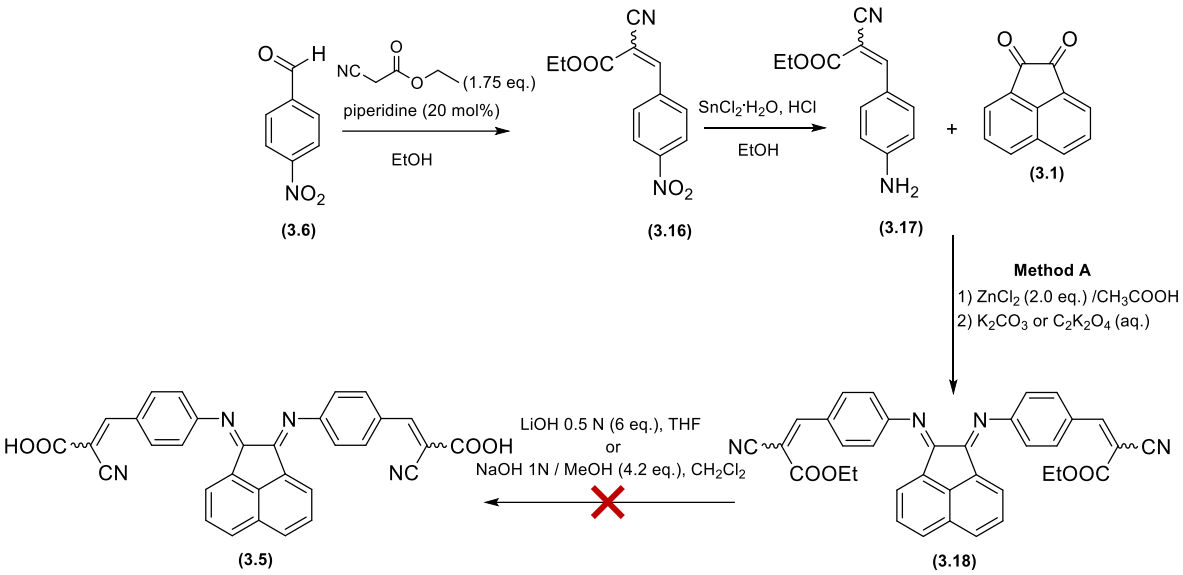


Scheme 16. Synthetic route for the preparation of Ar-BIAN **3.5** using ethyl-3-(4-aminophenyl)-2-cyanoacrylate (**3.17**).

Due to the instability of the Ar-BIAN imine group when the hydrolysis of the esters groups was attempted, the already prepared Ar-BIAN (**3.18**) was reacted with methoxy(methyl) chloride to obtain Ar-BIAN imidazolium chloride (**3.19**) (**Scheme 17**). [187] It was expected that this structure should resist to the hydrolysis step. However, when the reaction with NaOH in methanol was carried out, the cyanoacrylic acid derivative (**3.20**) was not identified in $^{1}$H RMN.

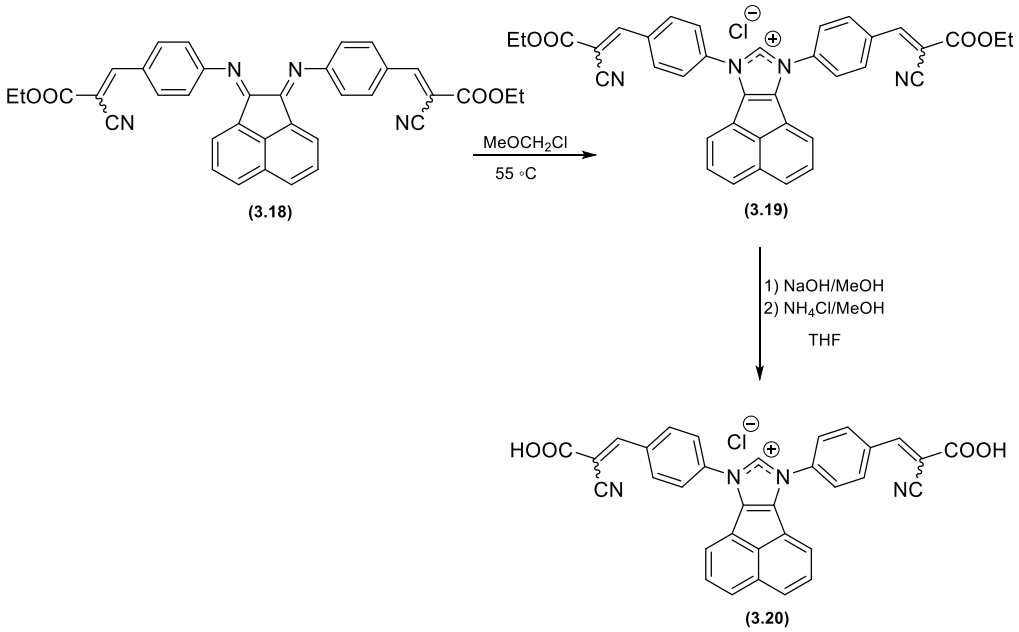


Scheme 17. Reaction scheme for the synthesis of an Ar-BIAN imidazolium chloride derivative (**3.20**).

#### 3.2.1.2 7*H*-acenaphtho[1,2-*d*]imidazole derivative dyes

Since the obtention of Ar-BIANs-based dyes bearing a cyanoacrylic acid as the anchoring group was unfruitful, the synthesis was directed towards the 7*H*-acenaphtho[1,2-d]imidazole dyes. They can be obtained by reacting the previous starting material, the acenaphthoquinone (**3.1**), with an aldehyde, in the presence of an aniline derivative (depending the substrate to obtain) and ammonium acetate in glacial acetic acid under reflux.

By using the method reported by Singh *et. al* [188] with terephthalaldehyde (**3.21a**), it was possible to afford the 7*H*-acenaphtho[1,2-*d*]imidazol-8-yl derivative containing a benzaldehyde group with a 12.9 % yield (**3.22a**). The formation of the oxazole analogue (**3.22b**) was also observed (η=5.1 %) (**Scheme 18**). The difference between the two compounds was observed in the LC-ESI-MS spectra due to the appearance of the molecular ion peaks at *m/z* 297.1 for **3.22a** and at *m/z* 298.1 for **3.22b**. It was also observed that the $^{1}$H NMR spectrum of **3.22b** is more deshielded than **3.22a** due to the presence of the oxygen atom. Both compounds could be isolated by TLC. The formation of these two species is reported in the literature. At low temperatures is only possible to afford the oxazole product, and at high temperatures only the imidazole or a mixture with oxazole is obtained.[189] The cyanoacrylic acid was introduced in the imidazole derivative **3.22b** through a Knoevenagel condensation using cyanoacetic acid, ammonium acetate and glacial acetic acid.[171] The desired chromophore (**3.23**) was obtained with a 70.1 % yield (**Scheme 18**). The structure of the final compound 3.23 was corroborated by $^{1}$H NMR, where it is possible to observe four signals at 8.3–7.6 ppm, integrating for 11 protons and corresponding to the aromatic protons and the CH group from the cyanoacrylic acid moiety. In the IR spectra, it is possible to observe bands corresponding to the carboxylic acid at 3338 and 1634 $cm^{-1}$. The nitrile group from the cyanoacrylic acid appears as a weak band at 2218 $cm^{-1}$, and the bands at 1560 $cm^{-1}$ correspond to the C=N bond from the imidazole ring. In the ESI-HRMS spectra the molecular ion peak appears at *m/z* 364.100078, which is in accordance with the structure **3.23**.

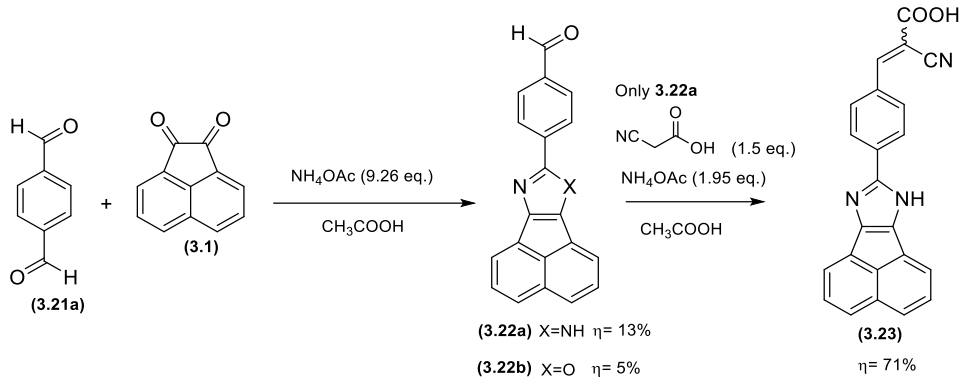


Scheme 18. Reactional scheme for the synthesis of 7H-acenaphtho[1,2-d]imidazol-8-yl derivative (**3.23**).

The next intent was to synthesize the thiophene analogue. For this, the reaction was performed with bromothiophene-2-carbaldehyde (**3.24a**), but only complex mixtures were obtained. Due to this an experiment with thiophene-2,5-dicarbaldehyde (**3.24b**) was performed, but once again the reaction was unfruitful, with emphasis on the appearance in the $^{1}$H NMR of several signals around 10 ppm indicating the formation of other species. 5-(5,5-Dimethyl-1,3-dioxan-2-yl)thiophene-2-carbaldehyde (**3.24c**) was employed in the last attempt to obtain the condensation compound (**3.25**). A complex mixture was obtained. Moreover, it was found that the aldehyde protecting group did not resist under these conditions (**Scheme 19**).

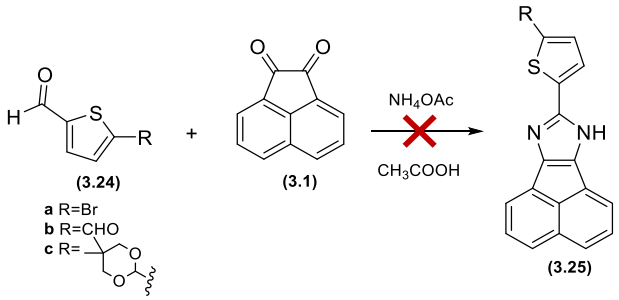


Scheme 19. Reactional scheme for the synthesis of an 7*H*-acenaphtho[1,2-d]imidazol-8-yl derivative with a thiophene moiety (**3.25**).

Another approach to obtain analogues was based on the introduction of an electron-donating group in the pyrrolic nitrogen. Assays with aniline (**3.26a**) and *p*-anisidine (**3.26b**) were done. The presence of the product was not observed in any of the reactions. It was possible to perceive in $^{1}$H NMR spectra the subproducts N-phenylacetamide (**3.28a**) and *N*-(4-methoxyphenyl)acetamide (**3.28b**). These compounds are formed through the reaction of anilines with

acetic acid, with the conversion rate being, in some cases, higher than 50% (entries 4 and 5), which compromises the success of these reactions (**Scheme 20**, **Table 11**).

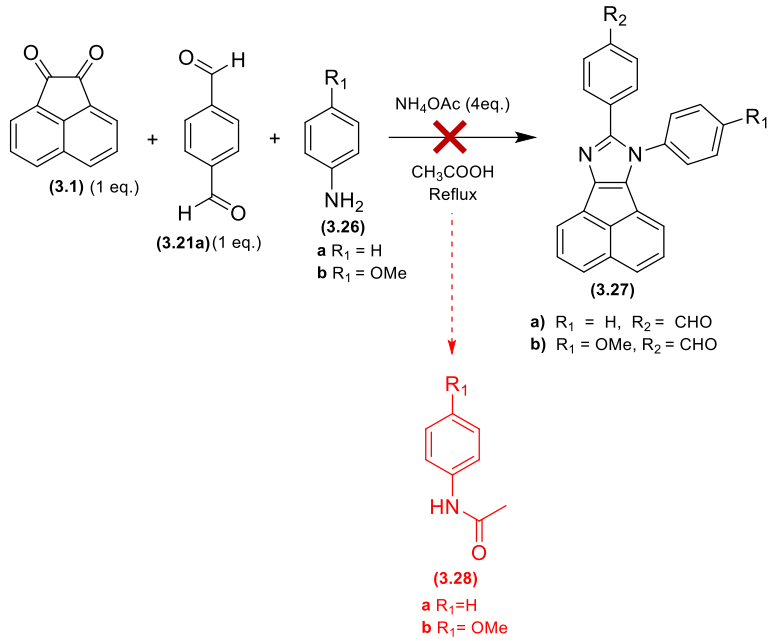


Scheme 20. Attempted synthesis of 7*H*-acenaphtho[1,2-d]imidazole derivatives containing different substituents on the pyrrolic nitrogen (**3.27**).

Table 11. Assays carried out to obtain compound **3.27** and conversion ratio of anilines (**3.26**) into acetamides (**3.28**).

| Entry | Aniline (eq.) | Reaction time (h) | Acetamide (3.28) conversion |
|---|---|---|---|
| **1** | 3.26a (5 eq.) | 28.5 | 20 % |
| **2** | 3.26a (5 eq.) | 14.5 | N.D |
| **3**[a] | 3.26b (4 eq.) | 19 | 15% |
| **4**[b] | 3.26b (1.2 eq.) | 42 | 71 % |
| **5**[c] | 3.26b (1 eq.) | 18 | 52% |

[a] Method A, [b] Method B, [c] Method C in Methods for the synthesis of 7-(4-methoxyphenyl)-8-phenyl-7*H*-acenaphtho[1,2-d]imidazole derivatives (**3.27a** and **3.27b**) experimental section.

Since acetic acid leads to the formation of secondary species, the synthesis efforts were focused on methods that avoid the use of this solvent. Alternatively, was chose a method where L-proline was employed as a catalyst in the presence of 3 Å molecular sieves using acetonitrile as solvent. L-proline reacts with the aldehyde and forms the iminium ion, which facilitates the amination reaction with $NH_3$ forming, consequently, a diamine intermediate.[170] Also a procedure employing ethanol as solvent was tested (**Scheme 21**).[190] Although the consumption of the starting materials was observed by TLC, there was no evidence of the formation of the desired products (**3.27b,c**) in the $^1$H NMR spectra. Instead, intermediates were obtained, namely a derivative of acenaphthoquinone (**3.29**) and also a Schiff base (**3.30**), resulting from nucleophilic addition of the amine group to the carbonyl group of the aldehyde. Even though the following reactions were carried out on a sealed tube with high pressure and temperature to force the reaction between intermediates, it was not possible to obtain the desired products (entries 5 and 6, **Table 12**).

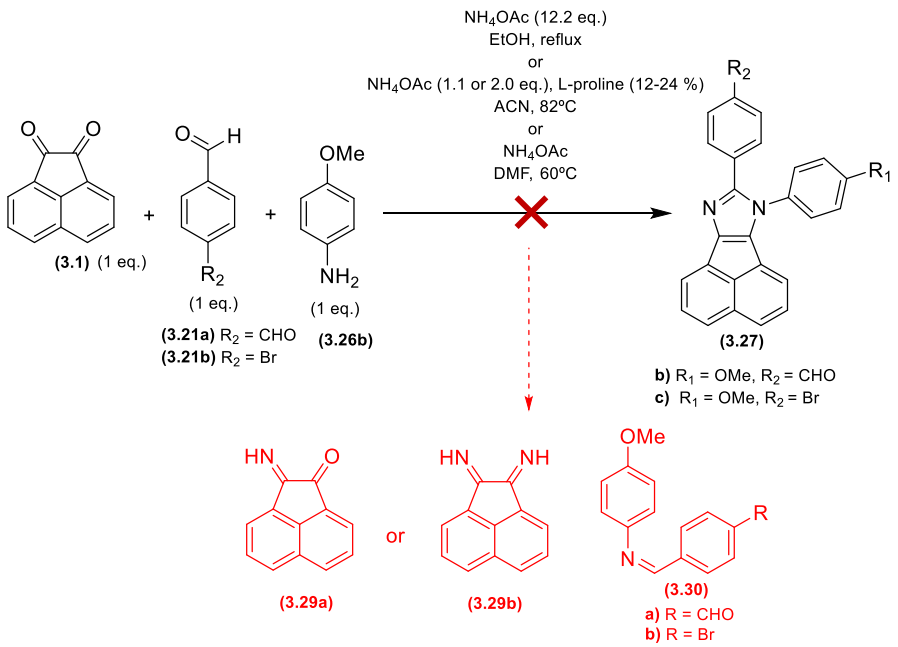


Scheme 21. Alternative approaches for the synthesis of 3.27.

Table 12. Different methods for the synthesis of compound **3.27** without using $CH_3COOH$, recovery of aniline (**3.26b**), conversion rate of the starting materials into compounds **3.29** and **3.30**.

| Entry | Aldehyde | Solvent | Reaction time (h) | Catalyst | Compound 3.29 | Compound 3.30 | Aniline (3.26b) |
|---|---|---|---|---|---|---|---|
| 1[d] | 21a | EtOH | 21 | | - | - | - |
| 2[e] | 21a | Acetonitrile | 5 | L-proline (12 mol %) | 75% | vestigial | - |
| 3[e] | 21a | Acetonitrile | 46 | L-proline (12 mol %) | 15% | - | - |
| 4[e] | 21b | Acetonitrile | 146 | L-proline (24 mol %) | - | 26% | 25% |
| 5[f] | 21b | Acetonitrile /DMF | 57 | L-proline (12 mol %) | 8% | 30% | 16% |
| 6[g] | 21b | DMF | 50 | - | - | 49% | 29% |

d - Method D, e - Method E, f - Method F, g- Method G in Methods for the synthesis of 7-(4-methoxyphenyl)-8-phenyl-7H-acenaphtho[1,2-d]imidazole derivatives (**3.27b** and **3.27c**) experimental section.

With the exception of compound **3.22**, all the attempts to obtain 2,4,5-trisubstituted and 1,2,4,5-tetrasubstituted imidazoles were unsuccessful, either due to the formation of subproducts or the lack of reactivity of the intermediaries. Consequently, only the performance of compound **3.23** was evaluated in DSSCs devices.

#### 3.2.1.3 Diethynylacenaphthylene derivative dyes

After failing to obtain the previous target compounds, the synthesis of 1,2-diethynylacenaphthylene derivatives containing phenyl, thiophene, benzotriazole and thieno-[3,2-*b*]thiophene rings present in their π-bridge(**3.37 a-d**) was proposed (**Figure 35**). In the end, four dyes with a dibranched and dianchoring system were obtained. The dyes were photophysically characterized. Theoretical and electrochemical studies were also performed. The efficiency of the final chromophores in DSSC was evaluated and this work was published in the scientific journal ACS Omega in March 2024.[191]

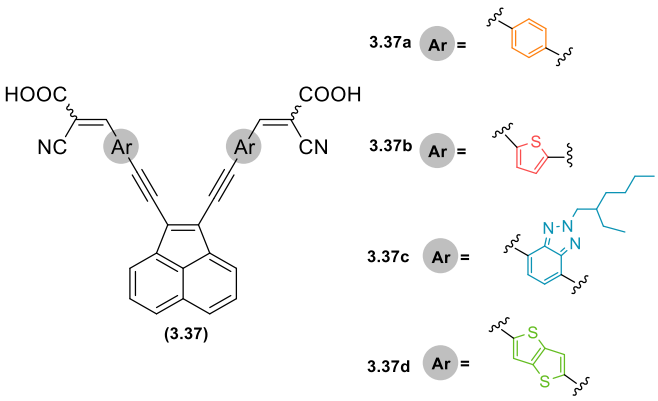


Figure 35. Structure of the final diethynylacenaphthylene dyes **3.37a-d**.

The synthesis of these chromophores starts with a reaction between NBS and acenaphthene (**3.31**) in the presence of catalytic amounts of the radical initiator benzoyl peroxide, where a tribromination followed by elimination occurs and the 1,2-dibromo-acenaphthylene (**3.32**) was obtained (**Scheme 22**).[192]

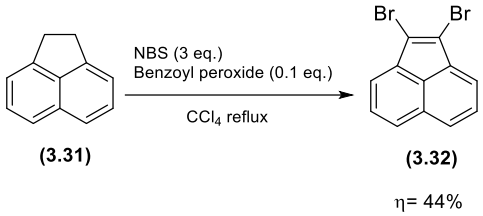


Scheme 22. Synthesis of 1,2-dibromoacenaphthylene (**3.32**).

Through a Sonogashira reaction between the 1,2-dibromoacenaphthylene (**3.32**) and 4-ethynylbenzaldehyde, the phenyl dialdehyde derivative (**3.33a**) was obtained (**Scheme 23**). For the preparation of similar aldehydes (**3.33b-d**), first the trimethylsilylethynyl was introduced in 1,2-dibromoacenaphthylene (**3.32**), then the trimethylsilyl groups were removed with $K_2CO_3$ in the presence of methanol, and the ethynyl intermediate was directly used in a Sonogashira coupling reaction with three different bromoaryl aldehydes (**3.36b-d**) (**Scheme 23**).

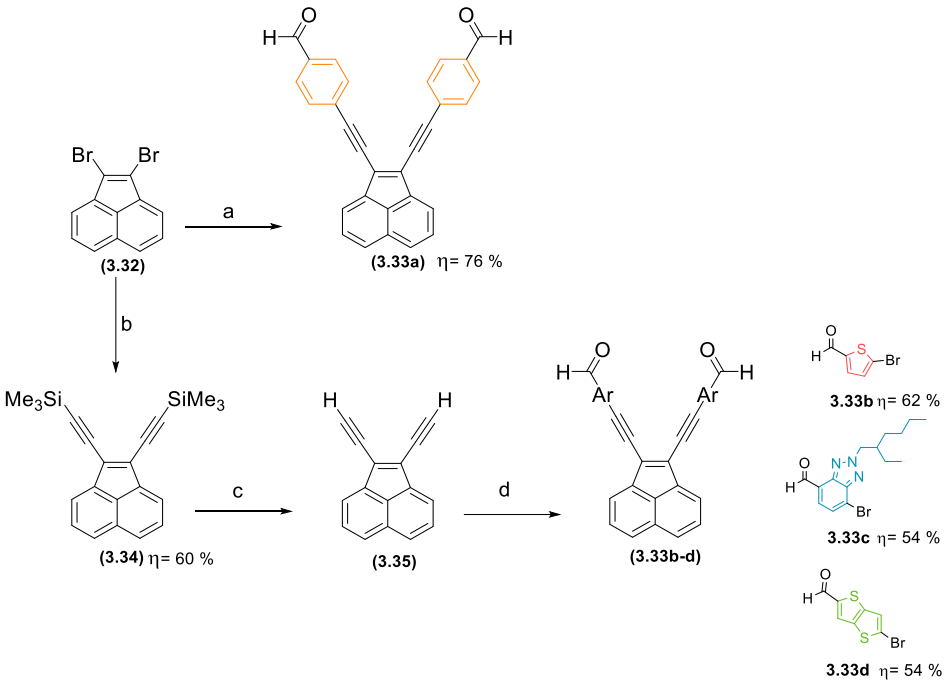


Scheme 23. Synthesis of acenaphthenedialdehydes **3.35a-d**. Reactional conditions: a) **3.32** (1 eq.) $Pd(PPh_3)_4$ (0.30 eq.), $PPh_3$ (0.12 eq.), CuI (0.24 eq.), 4-ethynylbenzaldehyde (3.0 eq.), DIPA (3 eq.), dry dioxane, 40°C in a degassed Schlenk tube; b) **3.32** (1 eq.), $Pd(PPh_3)_4$ (0.30 eq.), $PPh_3$ (0.12 eq.), CuI (0.24 eq.), ethynyltrimethylsilane (3.0 eq.), DIPA (3 eq.), dry dioxane, 40°C in a sealed tube; c) **3.34** (1 eq.), $K_2CO_3$ (2 eq.), Dioxane/MeOH (1:1 v/v), RT; d) $Pd(PPh_3)_4$ (0.20 eq.), $PPh_3$ (0.12 eq.), CuI (0.24 eq.), bromoaryl aldehydes (**3.36b-d**) (2.2 eq.), DIPA (2.0 eq.), dry dioxane, 40°C in a degassed Schlenk tube.

The 4-ethynylbenzaldehyde (**3.36a**) and the 5-bromothiophene-2-carbaldehyde (**3.36b**) were commercially available. The 7-bromo-2-(2-ethylhexyl)-2*H*-benzo[*d*][1,2,3]triazole-4-carbaldehyde[193,194] (**3.36c**) and 5-bromothieno[3,2-*b*]tiophene-2-carbaldehyde (**3.36d**) were prepared in the laboratory.

To synthesize the benzotriazole aldehyde (**3.36c**), 1,2,3-benzotriazole was alkylated with 3-(bromomethyl)heptane. Since benzotriazole exists in tautomeric equilibrium, two isomers were obtained with similar yields. The dibromo compound was then prepared through a reaction with hydrobromic acid and bromine. These harsh conditions were required because when the first bromine atom is introduced the other position becomes less reactive. The final step was the formylation reaction with BuLi and DMF. This reaction procedure was also used in the synthesis of 5-bromothieno[3,2-*b*]tiophene-2-carbaldehyde (**3.36d**), starting from 2,5-dibromothieno[3,2-*b*]thiophene (**Scheme 15**).

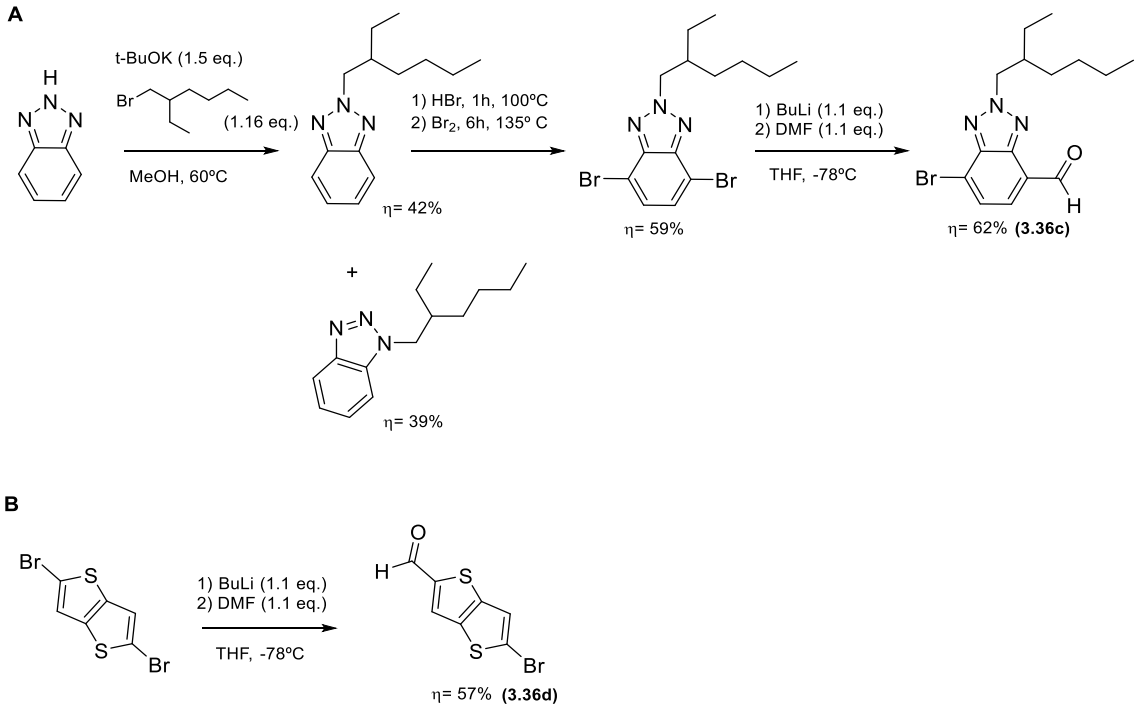


Scheme 24. A. Synthetic procedure for the preparation of 7-bromo-2-(2-ethylhexyl)-2*H*-benzo[d][1,2,3]triazole-4-carbaldehyde (**3.36c**). B. Synthetic procedure for the preparation of 5-bromothieno[3,2-*b*]thiophene-2-carbaldehyde (**3.36d**).

The final chromophores (**3.37a-d**) were obtained through a Knoevenagel condensation between cyanoacetic acid and the four aldehydes (**3.33a-d**) with obtained yields ranging from 50 to 80%.

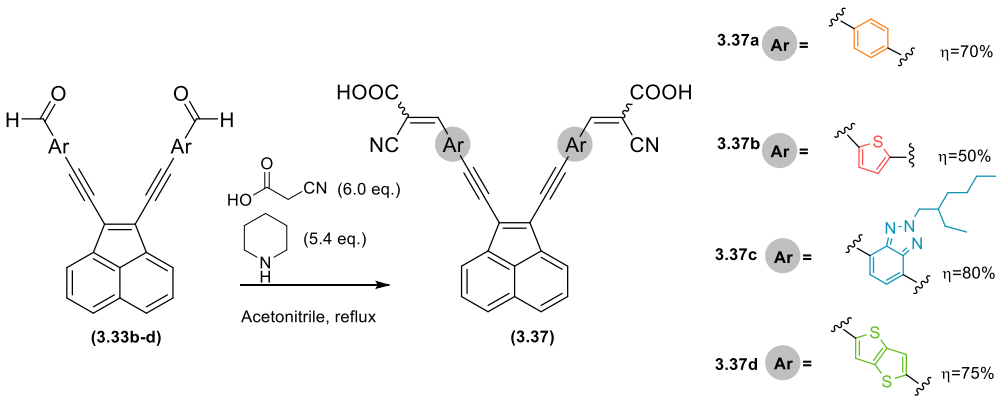


Scheme 25. Synthesis of the final chromophores **3.37a-d**.

The final chromophores were characterized by $^{1}$H NMR (**Figure 36**). However, characterization by $^{13}$C NMR was not possible due to their low solubility. In the spectra of all compounds, a singlet at 8.4–8.5 ppm is observed, integrating for two protons corresponding to the protons of the two cyanoacrylic acid groups (CH). The protons of the acenaphthylene ring appear as two doublets and a triplet in the aromatic region, with each signal integrating for two protons. The remaining signals in the $^{1}$H NMR spectra correspond to the various π-bridges, with their integration and multiplicity consistent with the expected structures. The HRMS showed the expected molecular ion peaks [M-H] at: 541.1202 for **3.37a**, 553.0326 for **3.37b**, 847.3726 for **3.37c** and 664.9767 for **3.37d**.

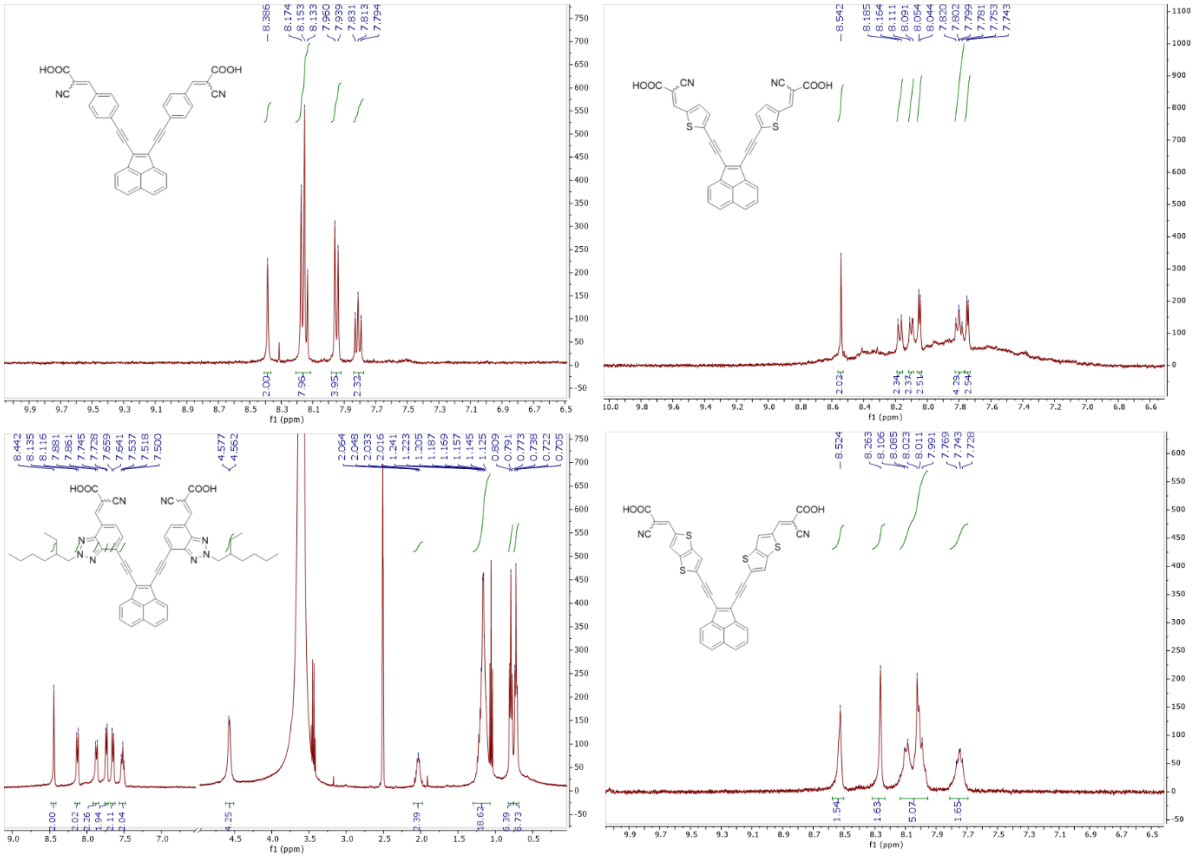

Figure 36. $^{1}$H NMR spectra of the final chromophores 3.37a-d in DMSO-$d_6$ at 400 Hz.

The introduction of a stronger donor group in these acenaphthylene molecules was also explored to increase the ICT (**Figure 37**).

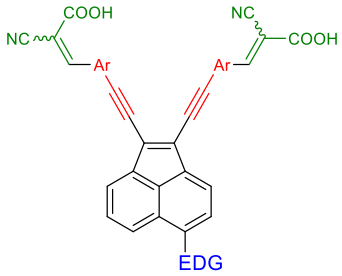


Figure 37. Structure of a diethynylacenaphthylene dye containing an acenaphthylene core with an electron donating group (EDG) in position 5.

In a first attempt triphenylamine was chosen as donor moiety. For this purpose 4-(diphenylamino)phenyl boronic acid was prepared from 4-bromotriphenylamine[195] and immediately reacted with 5-bromo-1,2-dihydroacenaphthylene (**3.38**) through a Suzuki cross-coupling. It was possible to obtain the desired product **3.39** with 31 % yield. Following a reported procedure from literature[196] the bromination of the 1,2-acenaphthene positions was performed with NBS and benzoyl peroxide in $CH_2Cl_2$ (**Scheme 26 - A**). It was observed by TLC the formation of a new compound with fluorescence at 365 nm. In the NMR spectrum the signals of the positions 1 and 2 from acenaphthene still appear around 3.4 ppm. However, the integration of the protons from the aromatic zone indicates that the bromination occurred in the ring of triphenylamine instead.

Alternatively, a diethylamine moiety was introduced in compounds **3.41** and **3.38** through a Buchwald-Hartwig coupling. Different methods were applied but only vestigial traces of compound **3.42** were obtained and high amounts of the starting materials (**3.41** or **3.38**) were recovered (**Scheme 26 - B**).

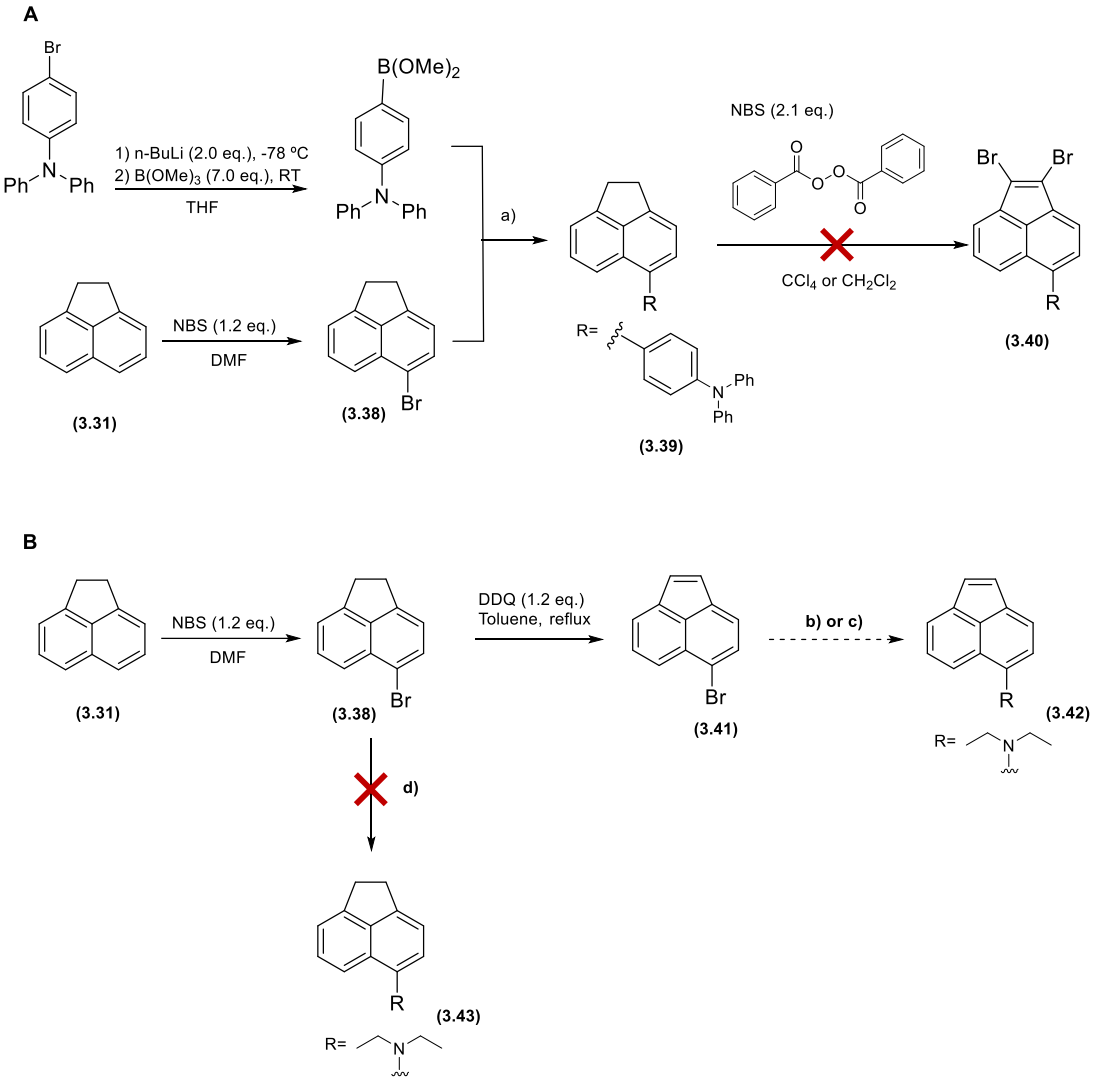


Scheme 26. A- Synthetic procedure for the synthesis of 1,2-dibromoacenaphthylene substituted with a triarylamine on position 5. B - Synthetic procedure for the synthesis of 1,2-dibromoacenaphthylene substituted with a diethylamine on position 5. Reactional conditions: a) Compound **3.38** (1 eq.), $Pd(PPh_3)_4$ (8 mol%), aq. solution $K_2CO_3$ 2.5 M (4.0 eq.), $C_{18}H_{14}B(OH)_2N$ (1.0 eq.), THF reflux (Suzuki coupling). b) Compound **3.41**, diethylamine aq. (excess), $CuSO_4 \cdot 5H_2O$ (0.05 eq.), DMF. c) Compound **3.42** (1eq.), diethylamine (3 eq.), $Pd_2(dba)_3$ (4 mol%), Xantphos (4 mol %), $Cs_2CO_3$ (3 eq.), toluene 80°C. d) Compound **3.38**, diethylamine (6 eq.), $Pd_2(dba)_3$ (8 mol%), Xantphos (8 mol %), $Cs_2CO_3$ (3 eq.), toluene 80°C.

## 3.2.2 Photophysical and photovoltaic studies

### 3.2.2.1 7*H*-acenaphtho[1,2-*d*]imidazole derivative dyes

#### Absorption spectra

The absorption spectrum of compound **3.23** (**Figure 38**, **Figure 39**) was measured at room temperature in methanol. The compound has a maximum absorption at 390 nm and a molar extinction coefficient of 19 562 $cm^{-1}M^{-1}$. By comparison with the work of Sivanadanam *et al.* the similar compound containing a phenanthrene core (depicted on Figure 31) presented two bands at higher wavelengths (426 and 450) but a lower molar extinction coefficient (17 500 $cm^{-1}M^{-1}$). The compound **3.23** has an emission maximum of 570 nm and presents a Stokes shift of 8097 $cm^{-1}$.

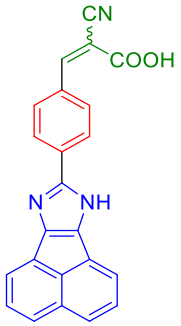


(3.23)

Figure 38. Structure of chromophore **3.23**.

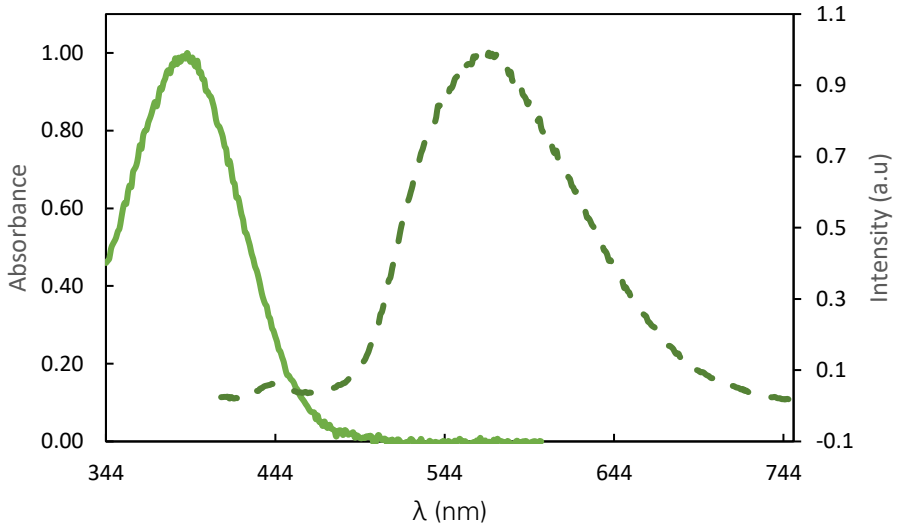


Figure 39. Normalized absorption (solid) and fluorescence emission (dotted; $\lambda_{exc}$=390 nm) of compound **3.23** in methanol at room temperature.

## Photovoltaic characterization

The efficiency of compound **3.23** was tested in DSSC devices, and the current-voltage curve (*I-V*) was measured. The photovoltaic parameters open-circuit voltage ($V_{oc}$), short-circuit current ($J_{sc}$), fill factor (FF) and photovoltaic conversion efficiency (η) and the *I-V* curve are displayed respectively in **Figure 40** and **Table 13**. The compound presented $V_{oc}$, $J_{sc}$ and FF values of 0.450 V, 0.78 mA/cm$^2$ and 0.62, respectively and achieved an efficiency of 0.22 %. Despite the low efficiency due to inefficient electron injection, the $V_{oc}$ and FF values are higher than the reference dye N-719.

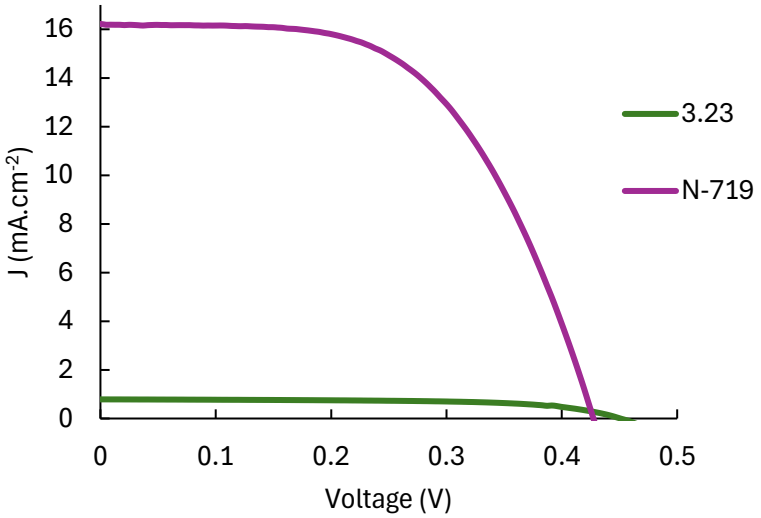


Figure 40. *I–V* curves of the test cells based on the synthesized dye **3.23** and reference N-719 under 100 mW.cm$^{-2}$ simulated AM 1.5 illumination (best performing cell).

Table 13. Performance values of the test cells based on the synthesized dyes and reference dye N-719 under 100 mW.cm$^{-2}$ AM 1.5 illumination. The results presented correspond to the average values of at least two cells per dye, each cell measured 5 times. The prepared anodes were soaked for 16 h in ethanol solution of the dye (0.5 mM), at room temperature in the dark. Electrolyte composition: 0.8 M LiI and 0.05 M $I_2$ in an acetonitrile/valeronitrile (85:15, % v/v).

| Dye | $V_{oc}$ (V) | $J_{sc}$ (mA/cm$^2$) | $J_{max}$ (mA/cm$^2$) | $V_{max}$ (V) | FF | η (%) |
|---|---|---|---|---|---|---|
| **110** | 0.450 | 0.78 | 0.64 | 0.346 | 0.62 | 0.22 |
| **N-719** | 0.422 | 16.33 | 13.51 | 0.277 | 0.54 | 3.75 |

### 3.2.2.2 Diethynyl acenaphthylene derivative dyes

#### Absorption and Fluorescence

The UV-vis absorption and emission spectra were recorded in DMF at room temperature. The UV-vis spectra display two bands: a more intense band (30 000-60 000 M$^{-1}$cm$^{-1}$) in the 351-407 nm range, related with the π–π* transition of the conjugated system, and a weaker band (7 000-17 500 M$^{-1}$cm$^{-1}$) in the region 486-521 nm, attributed to the intramolecular charge transfer (ICT) transition between the donor and the acceptor groups. Compounds **3.37b**, **3.37c**

and **3.37d** exhibit a red-shift relative to **3.37a**. In the case of **3.37a**, the D(π-A)$_2$ system has reduced conjugation efficiency due to the phenyl ring potentially adopting a twisted conformation relative to the acenaphthylene ring. The large Stokes shifts between the absorption and the emission bands (2889 - 3321 cm$^{-1}$) suggest a charge transfer character present on these dyes (**Figure 41, Table 14**).[197]

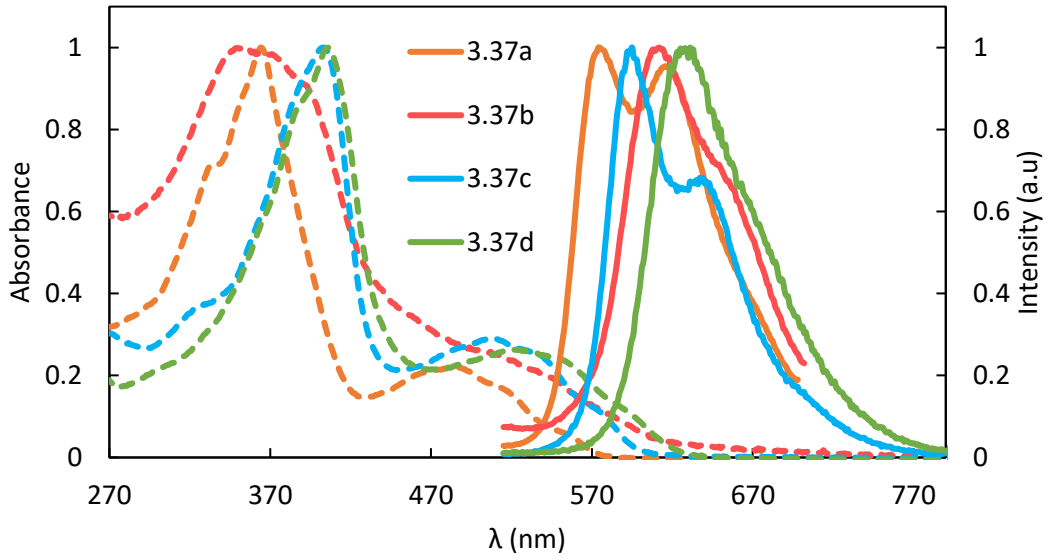


Figure 41. Normalized absorption (dotted) and fluorescence emission (solid; $\lambda_{exc}$(**3.37a**)= 364 nm and 486 nm; $\lambda_{exc}$(**3.37b**)=351 nm; $\lambda_{exc}$(**3.37c**)=402 nm and 507 nm; $\lambda_{exc}$ (**3.37d**)= 407 nm and 521 nm spectra of chromophores **3.37a-d** in DMF solution at room temperature (compounds excited at two different $\lambda_{exc}$ have identical emission spectra).

Table 14. Spectroscopic data for the synthesized compounds (**3.37a-d**) in DMF solution at room temperature (absorption ($\lambda_{abs}$) and emission($\lambda_{em}$) maxima, molar extinction coefficients (ε) and Stokes shift (ΔSS)).

| Dye | $\lambda_{abs\ 1}$ (nm) | $\varepsilon_1$ (cm$^{-1}$M$^{-1}$) | $\lambda_{abs\ 2}$ (nm) | $\varepsilon_2$ (cm$^{-1}$M$^{-1}$) | $\lambda_{em\ 1}$ (nm) | $\lambda_{em2}$ (nm) | ΔSS (cm$^{-1}$) |
|---|---|---|---|---|---|---|---|
| **3.37a** | 364 | 61500 | 486 | 13802 | 575 | 617 | 3185 |
| **3.37b** | 351 | 29495 | 514 sh | 7738 | 612 | - | 3115 |
| **3.37c** | 402 | 59568 | 507 | 17463 | 594 | 640 | 2889 |
| **3.37d** | 407 | 54320 | 521 | 14742 | 630 | - | 3321 |

### Photovoltaic performance

The performance of the final 1,2-diethynylacenaphthylene chromophores (**3.37a-d**) was evaluated in DSSC devices by measuring their current-voltage(*I-V*) curves. The photovoltaic parameters, including open-circuit voltage ($V_{oc}$), short-circuit current ($J_{sc}$), fill factor (FF) and photovoltaic conversion efficiency (η) along with the *I-V* curves are presented in **Figure 42** and **Table 15**. Among the dyes the phenyl-bridged derivative (**3.37a**) exhibited the best performance, achieving an efficiency (η) of 2.51%, with $V_{oc}$, $J_{sc}$ and FF values of 0.365 V, 13.32 mA/cm$^2$ and 0.52, respectively. In contrast, derivatives (**3.37b-d**) exhibited lower efficiencies compared to **3.37a**, with a significant decrease on $J_{sc}$ (3.21 – 5.35 mA/cm$^2$) and also on $V_{oc}$ (0.241 – 0.320 V). Previous studies in our group involving coumarin dyes (Chapter 2),[133] highlighted thieno-[3,2-*b*]thiophene as a highly effective π-bridge due to its extended molecular conjugation, high stability, planar structure and S-S interactions.[198] The lower $J_{sc}$ values of the more planar compounds could result from increased dye aggregation, where excited state quenching could lead to inefficient electron injection into the CB of $TiO_2$ or from a more efficient electron hole recombination in the case of the more planar molecules.[54,199]

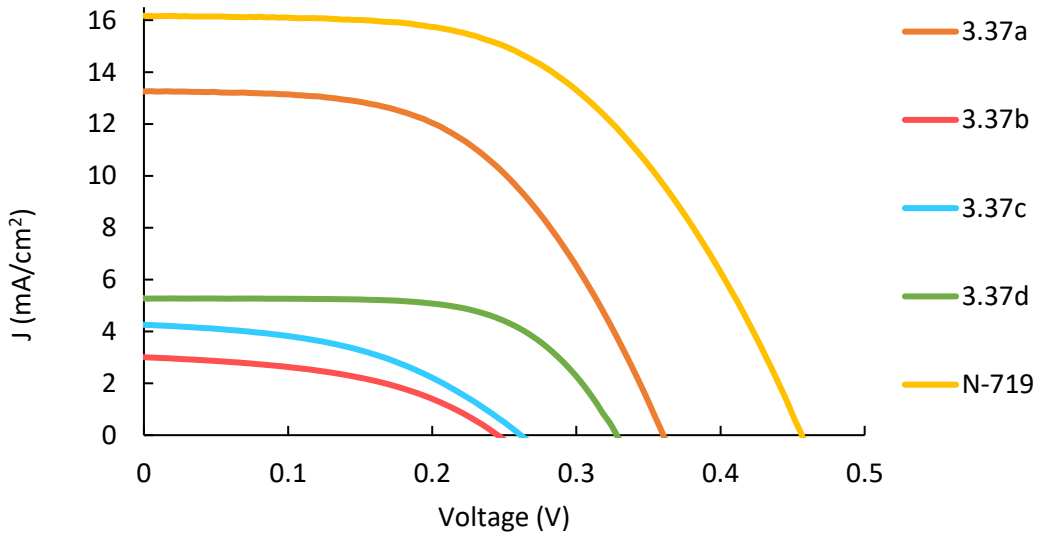


Figure 42. *I–V* curves of the test cells based on the synthesized acenaphthylene dyes and reference N-719 under 100 mW.cm$^{-2}$ simulated AM 1.5 illumination (best performing cell, [CDCA] = 0 mM).

Table 15. Performance values of the test cells based on the synthesized dyes and reference dye N-719 under 100 mW.cm$^{-2}$ AM 1.5 illumination. The results presented correspond to the average values of at least two cells per dye, each cell measured 5 times. Different concentrations of CDCA were applied (0 mM, 10 mM and 50 mM). The prepared anodes were soaked for 16 h in an CH2Cl2/MeOH/H2O 65:35:5 (%v/v) solution of the dye (0.5 mM), at room temperature in the dark. Electrolyte composition: 0.8 M LiI and 0.05 M I2 in an acetonitrile/valeronitrile (85:15, % v/v).

| Dye | [CDCA]/ mM | $V_{oc}$/V | $J_{sc}$/mA cm$^{-2}$ | $V_{max}$/V | $J_{max}$/mA cm$^{-2}$ | FF | η/% |
|---|---|---|---|---|---|---|---|
| 3.37a | 0 | 0.365±0.003 | 13.32±0.07 | 0.234±0.003 | 10.76±0.03 | 0.52±0.01 | 2.51±0.02 |
| | 10 | 0.404±0.008 | 13.62±0.6 | 0.274±0.003 | 11.39±0.5 | 0.57±0.02 | 3.15±0.1 |
| | 50 | 0.371±0.003 | 12.93±0.1 | 0.243±0.005 | 10.33±0.1 | 0.52±0.02 | 2.51±0.07 |
| 3.37b | 0 | 0.241±0.007 | 3.21±0.2 | 0.157±0.004 | 2.24±0.2 | 0.45±0.01 | 0.35±0.02 |
| | 10 | 0.241±0.004 | 4.27±0.3 | 0.152±0.002 | 3.19±0.2 | 0.47±0.004 | 0.49±0.03 |
| | 50 | 0.240±0.007 | 3.39±0.2 | 0.155±0.002 | 2.50±0.1 | 0.48±0.03 | 0.39±0.02 |
| 3.37c | 0 | 0.269±0.006 | 3.75±0.3 | 0.168±0.003 | 2.64±0.2 | 0.44±0.01 | 0.44±0.04 |
| | 10 | 0.287±0.006 | 4.70±0.3 | 0.175±0.003 | 3.66±0.2 | 0.47±0.01 | 0.65±0.04 |
| | 50 | 0.352±0.003 | 10.52±0.3 | 0.226±0.003 | 7.90±0.5 | 0.48±0.02 | 1.78±0.1 |
| 3.37d | 0 | 0.320±0.005 | 5.35±0.1 | 0.225±0.01 | 4.42±0.1 | 0.58±0.06 | 1.00±0.09 |
| | 10 | 0.293±0.01 | 4.52±0.4 | 0.206±0.01 | 3.70±0.4 | 0.57±0.02 | 0.77±0.08 |
| | 50 | 0.291±0.004 | 4.67±0.2 | 0.206±0.005 | 3.90 ±0.1 | 0.59±0.02 | 0.80±0.01 |
| N-719 | 0 | 0.442±0.02 | 16.10±0.07 | 0.294±0.004 | 13.28 ±0.1 | 0.55±0.02 | 3.90±0.07 |
| | 10 | 0.44±0.01 | 16.46±0.1 | 0.298±0.004 | 13.93±0.09 | 0.57±0.07 | 4.19±0.08 |
| | 50 | 0.46±0.01 | 14.59±0.7 | 0.310±0.01 | 12.44±0.4 | 0.58±0.03 | 3.86±0.05 |

Chenodeoxycholic acid (CDCA) was used as co-adsorbing agent, to suppress eventual dye aggregation. The impact of three different concentrations of CDCA (0 mM, 10 mM and 50 mM) was evaluated (**Table 15, Figure 43**). For the benzotriazole derivative (**3.37c**), DSSC performance improved linearly with increasing CDCA concentration, with corresponding enhancements in $J_{sc}$ and $V_{oc}$ values (Appendix **Figure A.29**). The performance of this dye improved notably from 0.44 to 1.78 % (with 0 mM and 50 mM respectively). It was expected that the long and bulky ethylhexyl chains present in benzotriazole would prevent dye aggregation,[47] but apparently this steric hindrance appear insufficient to fully prevent π···π stacking. Indeed, the V shape geometry of the molecule where the alkyl chains extend outwards of the central structure (Appendix **Figure A. 31**) would allow π···π stacking to occur with the ethylhexyl chains occupying the voids. Consequently, co-adsorbents like CDCA remain necessary to enhance cell efficiency. Concerning **3.37a**, a concentration of 10 mM CDCA resulted in an increase in $V_{oc}$, improving the efficiency from 2.51 to 3.15 %, and reaching 75 % of the standard cell based on dye N-719. This marked the best result in this study. No significant effects were observed for **3.37b** and **3.37d**.

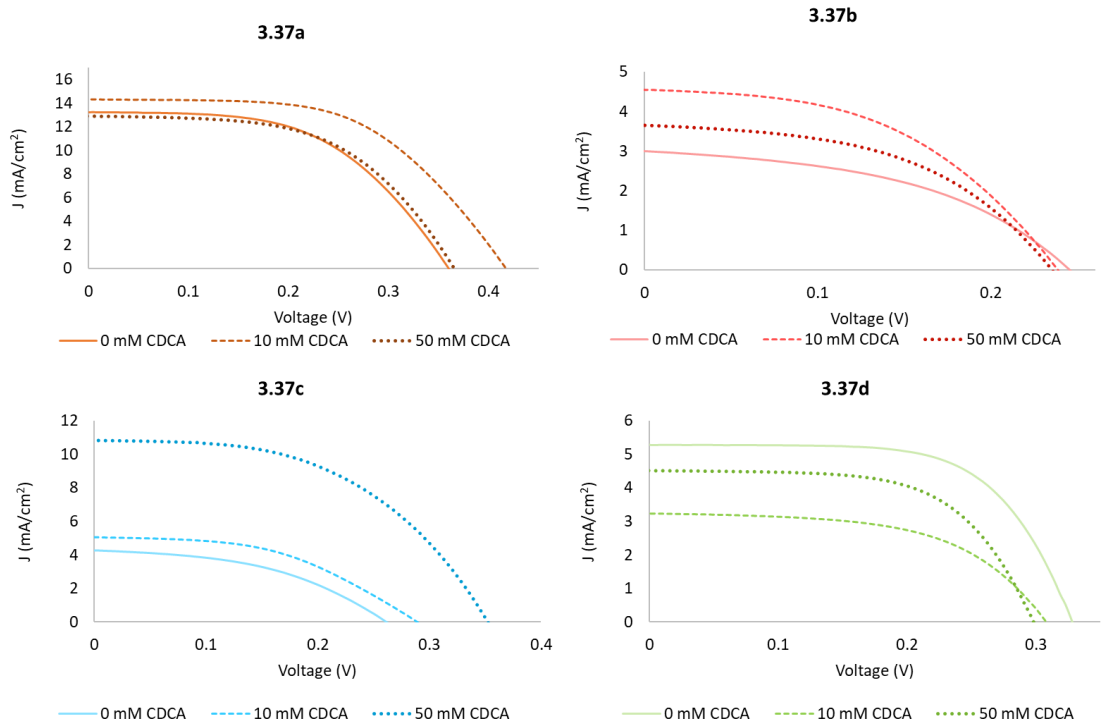


Figure 43. *I–V* curves of the test cells based on the synthesized acenaphthylene dyes (**3.37a-d**) under 100 mW.cm$^{-2}$ simulated AM 1.5 illumination (best performing cell, [CDCA] = 0 mM, 10 mM and 50 mM).

Since **3.37a** had the best efficiency of its family, it was tested with the commercial electrolyte EL-HPE (GreatCell Solar). The $V_{OC}$ increased significantly from 0.365 V to 0.577 V, however the $J_{sc}$ decreased from 13.32 $mAcm^{-2}$ to 5.95 $mAcm^{-2}$. This way the overall efficiency of the cells decreased from 2.51 to 1.90 %, indicating that this commercial electrolyte is not the most suitable for this type of dyes.

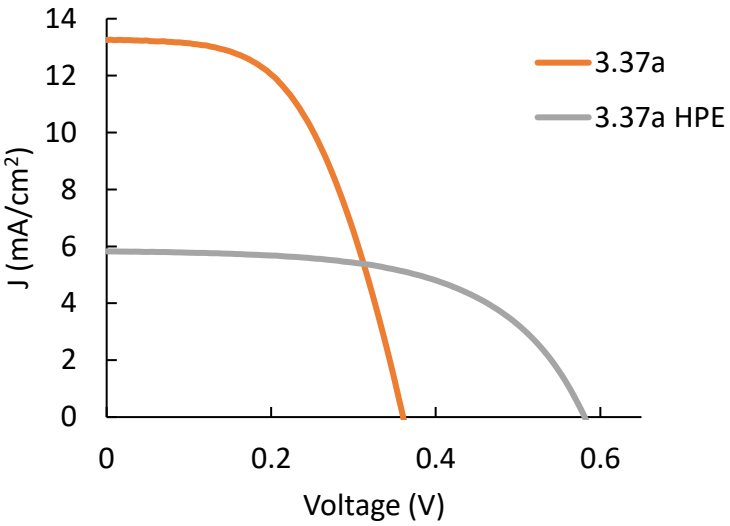


Figure 44. *I–V* curves of the test cells based on the synthesized dye 3.37a using the electrolyte composed by LiI and $I_2$ and the commercial electrolyte EL-HPE (GreatCell Solar) under 100 $mW.cm^{-2}$ simulated AM 1.5 illumination (best performing cell, [CDCA] = 0 mM).

Table 16. Performance values of the test cells based on the dye **3.37a** under 100 $mW.cm^{-2}$ AM 1.5 illumination. The results presented correspond to the average values of at least two cells per dye, each cell measured 5 times. The prepared anodes were soaked for 16 h in an $CH_2Cl_2$/MeOH/$H_2O$ 65:35:5 (%v/v) solution of the dye (0.5 mM), at room temperature in the dark. Electrolytes composition: 0.8 M LiI and 0.05 M $I_2$ in an acetonitrile/valeronitrile (85:15, % v/v); commercial electrolyte EL-HPE(GreatCell Solar) - 1-butyl-3-methylimidazolium iodide, 4-tert-butylpyridin (TBP), and guanidinium thiocyanate (GuSCN).

| Dye | $V_{oc}$/V | $J_{sc}$/mA $cm^{-2}$ | $V_{max}$/V | $J_{max}$/mA $cm^{-2}$ | FF | η/% |
|---|---|---|---|---|---|---|
| **3.37a** | 0.365±0.003 | 13.32±0.07 | 0.234±0.003 | 10.76±0.03 | 0.52±0.01 | 2.51±0.02 |
| **3.37a HPE** | 0.577±0.008 | 5.95±0.06 | 0.407±0.006 | 4.67±0.05 | 0.55±0.01 | 1.90±0.03 |

To investigate the discrepancy in $J_{sc}$ values, the incident photon-to-current efficiency (IPCE) as a function of wavelength was measured. The IPCE determined by the product of three factors: electron injection efficiency from the dye's excited state ($\eta_{inj}$), light-

harvesting efficiency (LHE) and charge collection efficiency ($\eta_{coll}$), as described in equation 1.

$$IPCE = \eta_{inj} \times LHE\ (\lambda) \times \eta_{coll} \quad (1)$$

The IPCE spectra, displayed on Figure 45, align well with the absorption spectra of the dyes (Appendix **Figure A. 30**). The dyes exhibited maximum IPCE values at 400-410 nm, which were 60.8%, 25.8%, 31.9%, 25.3% for **3.37a**, **3.37b**, **3.37c** and **3.37d** respectively. The IPCE spectrum of **3.37a** significantly surpasses those of the other dyes, achieving values of approximately 60% across the 400–550 nm wavelength range.

Given that LHE can be considered 100% for dye-loaded films with thicker than 10 µm[92], and the anodes used in this study have a thickness of 15 µm, the IPCE results are primarily determined by the electron injection efficiency ($\eta_{inj}$). The superior IPCE performance of **3.37a** indicates a higher electron injection efficiency compared to the other dyes.

The lower performance of the more planar dyes, even in the presence of CDCA, suggests that electron-hole recombination is more prominent in these compounds. In contrast, the twisted conformation assumed by the phenyl ring in **3.37a** reduces the recombination thus favoring efficient electron injection.[54]

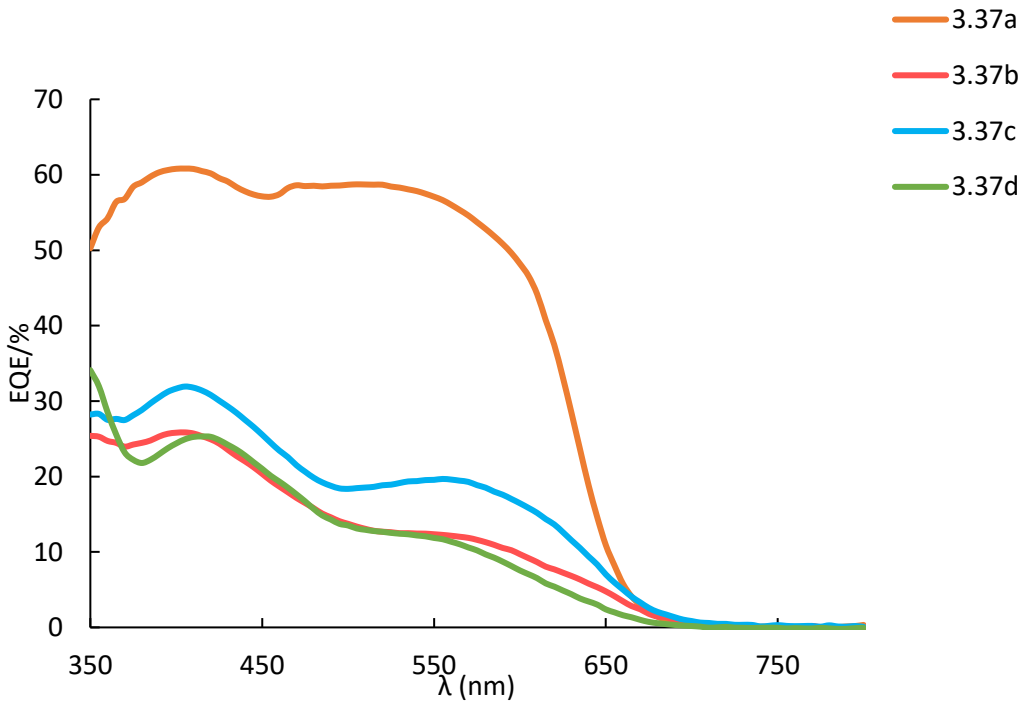


Figure 45. IPCE spectra for the DSSCs based on dyes **3.37a-d** (best performing cell, [CDCA] = 0 mM).

## 3.2.3 Electrochemical characterization

### 3.2.3.1 Diethynyl acenaphthylene derivative dyes

The energy levels of the frontier molecular orbitals were determined using cyclic voltammetry (Appendix **Figure A. 28**). From the obtained onsets of reduction peaks, the values of LUMO energies were calculated following the equation: E [eV] = -($E_{onset}$ (V *vs.* SCE) + 4.44).[200] The highest occupied molecular orbital energy levels, obtained from the LUMO energies and the energy from the optical transition, are located between -6.04 and -5.79 eV, which are lower than the redox potential of the $I^-/I_3^-$ redox couple (-4.60 eV),[201] enabling effective regeneration of the oxidized dye. The lowest unnoccupied molecular orbitals energy levels lie between -3.84 and -3.61 eV, which are higher than the CB of $TiO_2$ (−4.0 eV),[201] indicating that electron injection from the excited molecule to the CB of $TiO_2$ is energetically favorable (**Figure 46**, **Table 17**).

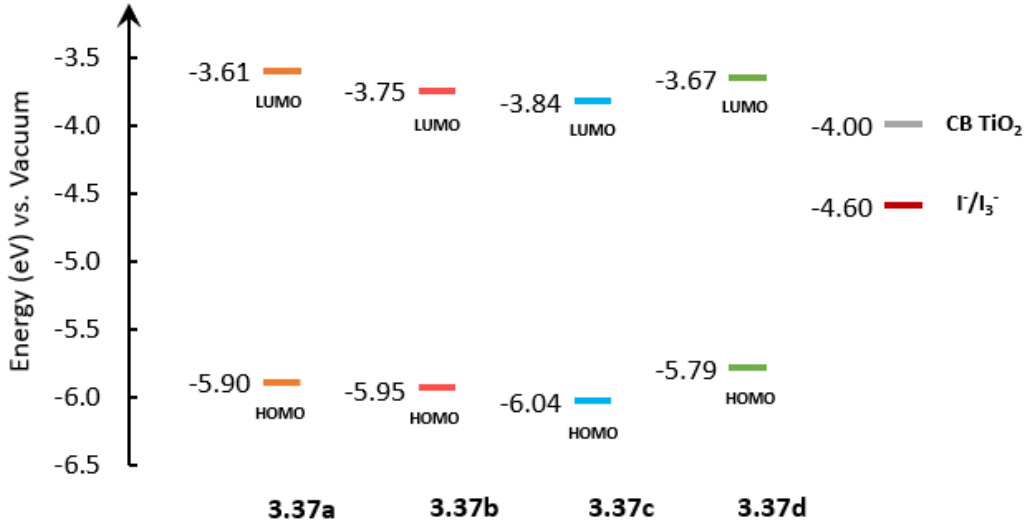


Figure 46. Schematic representation of the HOMO and LUMO energy levels of each chromophore vs. the CB of $TiO_2$ and $I^-/I_3^-$ redox potentials.

Table 17. Electrochemical properties obtained from cyclic voltammetry measurements in dimethylformamide (DMF) solution with a dye (**3.37a-d**) concentration of $1.5X10^{-4}$ M and 0.1 M $TBAPF_6$ at scan rates of 50, 100, 250, 500 mV $s^{-1}$.

| Dye | $E_{red}$ *vs.* SCE (V) | LUMO vs. Vacuum (eV) | HOMO *vs.* Vacuum (eV)[a] | Eg (eV)[b] |
|---|---|---|---|---|
| **3.37a** | -0.83 | -3.61 | -5.90 | 2.29 |
| **3.37b** | -0.69 | -3.75 | -5.95 | 2.21 |
| **3.37c** | -0.60 | -3.84 | -6.04 | 2.21 |
| **3.37d** | -0.77 | -3.67 | -5.79 | 2.13 |

a) HOMO energy level, determined from E(HOMO) = E(LUMO) – Eg; b) Energy gap (Eg) - obtained from the intersection between the normalized absorption and fluorescence emission spectra (Figure 41)

## 3.2.4 Theoretical Calculations

### 3.2.4.1 Diethynyl acenaphthylene derivative dyes

To investigate the geometry and electronic properties of the dyes, a theoretical analysis was conducted at the DFT/CAM-B3LYP/6-311G(d,p) level considering the solvent effects of *N,N*-dimethylformamide using Gaussian 09 (**Figure 47**, **Table 18**). Frequency analyses for each compound were also computed and did not yield any imaginary frequencies, indicating that the optimized structure of each molecule corresponds to at least a local minimum on the potential energy surface. The time-dependent density functional theory (TD-DFT) approach was applied to the previously optimized ground-state molecular geometries to obtain the vertical excitation energies, oscillator strengths (f), dipole moment and excited state compositions in terms of excitations between the occupied and virtual orbitals for the investigated compounds (**Table 18**). Although for aromatic donor-acceptor systems, it is known that the TD-DFT approach overestimates the absorption wavelengths of CT-type transitions (with errors of up to 1 eV)[202] in our case, the predicted transitions (deviations in the 0.07–0.64 eV range, (**Table 14** and **Table 18**) and the calculated frontier molecular orbitals band gaps (see **Table 17** with the cyclic voltammetry data) are found to be in good agreement to the experimental values obtained, thus giving additional support for the calculated molecular geometries. In general, the observed lowest energy absorption bands are associated to the predicted S0→S1 transitions (f values in

the 1.6288 - 2.8073 range) and contributions mainly associated to the HOMO→LUMO orbitals (**Table 18**).

The frontier molecular orbitals' energy levels and their electron distribution surface plots are shown in **Figure 47**. For all the compounds there is an increase in the electronic density in the cyanoacrylic acid moieties upon the transition from HOMO to LUMO. Compound **3.37a** seems to have a slightly more evident intramolecular charge separation than **3.37b**, **3.37c** and **3.37d**, where a larger overlap between HOMO and LUMO densities is observed. This indicates that the HOMO-LUMO excitation moves the electron distribution from the donor to the acceptor, giving support to an efficient photoinduced charge transfer from the dyes to the CB of the semiconductor, more evident in the case of **3.37a**. In the latter compound, a smaller overlap between HOMO and LUMO densities improves the charge separation and is expected to impact both efficiency of the electron injection and the reduction of the charge recombination.

Table 18. Computed absorption properties (predicted vertical excitation energies and associated orbitals transitions major contributions together with oscillator strengths, f, and dipole moments) for the chromophores 3.37a-d obtained by TD-DFT at the CAM-B3LYP/6-311G(d,p) level (using the Polarizable Continuum Model, PCM, to take into account the solvent effects of N,N-dimethylformamide) after ground-state geometry optimization using the same functional and basis set.

| Dye | $\lambda_{max1}$ (nm) | $\lambda_{max2}$ (nm) | Dipole Moment (Debye) | Transition and Orbitals Major Contributions | Oscillator Strength, f $\lambda_{max1}$ | Oscillator Strength, f $\lambda_{max2}$ | HOMO (eV) | LUMO (eV) | $E_g$ (eV) |
|---|---|---|---|---|---|---|---|---|---|
| **3.37a** | 377 | 501 | 9.5146 | $S_0 \rightarrow S_1$, HOMO→LUMO (95 %) | 0.804 | 2.6091 | -5.85 | -3.48 | 2.36 |
| **3.37b** | 413 | 548 | 10.718 | $S_0 \rightarrow S_1$, HOMO→LUMO (98 %) | 0.7273 | 2.1465 | -5.77 | -3.62 | 2.15 |
| **3.37c** | 479 | 685 | 7.9016 | $S_0 \rightarrow S_1$, HOMO→LUMO (97 %) | 1.004 | 1.6288 | -5.81 | -3.63 | 2.18 |
| **3.37d** | 411 | 591 | 5.6747 | $S_0 \rightarrow S_1$, HOMO→LUMO (98 %) | 0.9414 | 2.8073 | -5.63 | -3.53 | 2.10 |

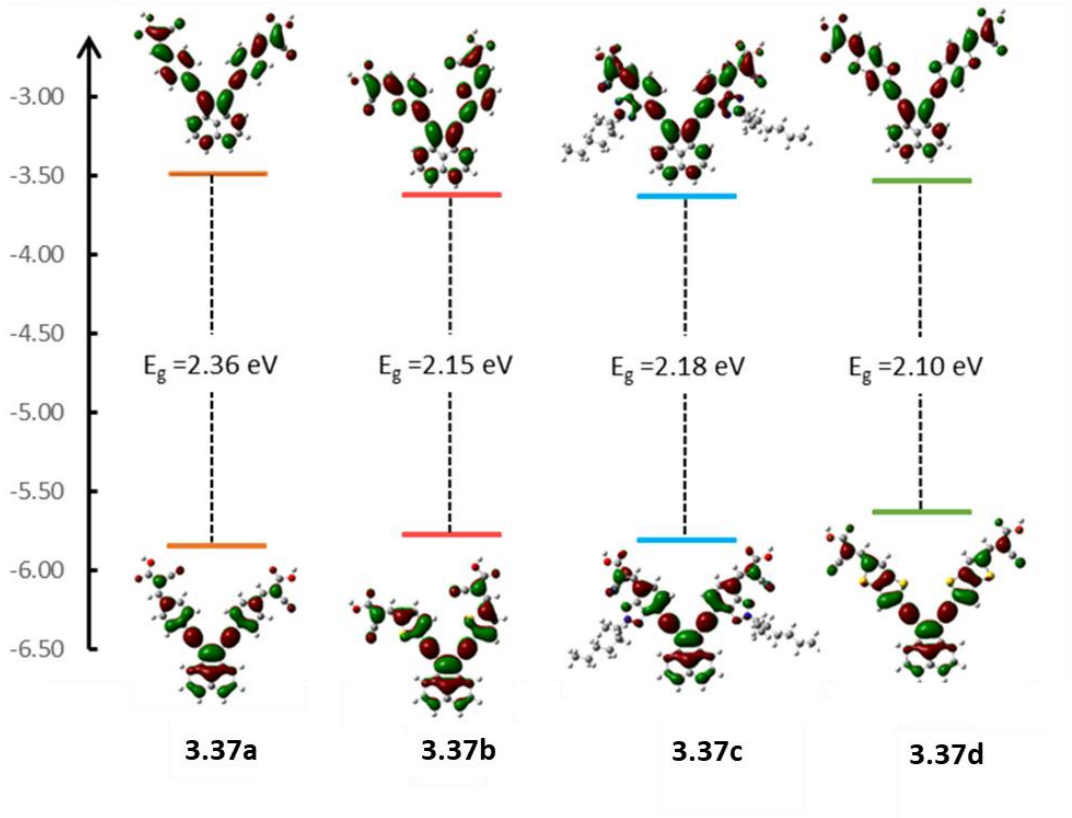


Figure 47. Optimized structures and frontier molecular orbitals (MO) of the HOMO and LUMO calculated with DFT on a B3LYP/6-311G(d,p) level of the dyes. The theoretical optical band gaps (Eg) are also included.

## 3.3 Conclusion

Several attempts to synthesize an organic Ar-BIAN dye were unsuccessful, primarily due to the sensitivity of the cyanoacrylic acid groups to high temperatures and the susceptibility of the imine groups to hydrolysis.

Regarding the 7*H*-acenaphtho[1,2-*d*]imidazoles, It was possible to synthesize a derivative with a phenyl moiety and cyanoacrylic acid as the anchoring group. The photovoltaic performance of this dye was tested and despite the low efficiency (η= 0.22 %) the $V_{oc}$ and FF values were higher than those of reference dye N-719. Attempts to obtain the thiophene analogue were unsuccessful. It was also not possible to synthesize the compound with a substituent on the pyrrolic nitrogen due to the formation of secondary products and the lack of reactivity of the intermediates.

Four diethynylacenaphthylene dyes with varying aryl π-bridges were successfully synthesized and tested as sensitizers in dye-sensitized solar cells (DSSCs). Spectroscopic analysis showed that all dyes were red-shifted compared to the phenyl-bridged parent compound, consistent with TD-DFT calculations. Spectroscopic and electrochemical data allowed to prove that the HOMO and LUMO energies of the four dyes are adequately located above the CB of $TiO_2$, and below the $I^-/I_3^-$ redox potential, respectively. The phenylethynyl derivative (**3.37a**) outperformed the other aryl derivatives, achieving a 2.51% efficiency, which increased to 3.15% with CDCA. This dye was also tested in DSSCs with the commercial electrolyte EL-HPE, however it was not possible to improve its efficiency because $J_{sc}$ decreased significantly.

## 3.4 Experimental section

The synthetic methods and the fabrication of the photovoltaic devices were performed as described in Chapter 2, Section 2.4.

### General information – Photophysical and photovoltaic characterization

Absorption spectra were recorded on a VWR M4 spectrometer (Ismaning, Germany). Fluorescence spectra were acquired on a SPEX Fluorolog 1681 0.22 m spectrofluorimeter (Metuchen, NJ, USA) equipped with a 150 W Xe−Hg lamp, which were then corrected for the system's wavelength response.

The incident photon to current conversion efficiency (IPCE) of the photovoltaic devices was measured as a function of wavelength from 350 nm to 800 nm, and it was performed in a Newport QuantX-300 system containing a 100 W Xe lamp (Montana, USA).

### General information – Cyclic voltammetry

Cyclic voltammetry (CV) measurements were conducted using a μAutolab Type III potentiostat/galvanostat (Metrohm Autolab B. V., Utrecht, The Netherlands), monitored by GPES (General Purpose Electrochemical System) software version 4.9 (Eco-Chemie, B. V. Software, Utrecht, The Netherlands). A cylindrical three-electrode cell with a 5 mL capacity was used for the experiments. Saturated calomel electrode (SCE, saturated KCl) reference electrode (Metrohm, Utrecht, The Netherlands) was used as the standard for all the measurements. A

glassy carbon electrode (MF-2013, f = 1.6 mm, BAS inc., West Lafayette, IN, USA) was employed as the working electrode and as counter-electrode a Pt wire. Prior to each measurement, the working electrode was polished with 1.0 and 0.3 μm alumina aqueous suspensions (Buehler, Esslingen, Germany) on 2–7 μm micro-cloth polishing pads (Buehler), followed by rinsing with water and ethanol. This cleaning procedure was consistently applied before all electrochemical measurements. The electrolyte contained a solution of 0.1 M tetrabutylammonium hexafluorophosphate ($TBAPF_6$) in dry DMF, with a dye concentration of $1.5 \times 10^{-4}$ M. Measurements were performed with scan rates of 50, 100, 250 and 500 mV $s^{-1}$. Before and throughout the electrochemical measurements the solutions were de-aerated by purging with $N_2$. The onset values were considered the crossing points between the tangent lines of the rising current and the baseline current.

### 3.4.1 Synthetic procedure for the preparation of bis(phenylimino)acenaphthene derivatives

*Reactions between acenaphthoquinone (**3.1**) and 4-aminobenzoic acid (**3.2**) with the aim of synthesizing 4,4'-((acenaphthylene-1,2-diylidene)bis(azaneylylidene))dibenzoic acid (**3.3**)*

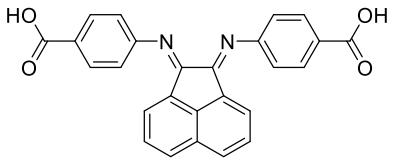


**(3.3)**

**Procedure A:**

Following the literature procedure of Mak[156], in a round bottom flask containing 75 mg of $ZnCl_2$ (0.55 mmol, 2.0 eq.), 96 mg of 4-aminobenzoic acid (**3.2**) (0.70 mmol, 2.6 eq.), and 50 mg of acenaphthoquinone (**3.1**) (0.27 mmol, 1.0 eq.) were added 1.5 mL of glacial acetic acid. The reactional mixture was heated under reflux for 1 hour and 45 minutes, it was monitored by TLC (hexane/ AcOEt 6/4). The reactional mixture was cooled to room temperature, the supernatant was removed and the formed solid was centrifuged and washed with acetic acid (2x) and diethyl ether (3x). An aqueous solution of $K_2CO_3$ (1.2g in 1.2 mL $H_2O$ (optional: solution of $C_2K_2O_4$)) was added to the solid and it was heated under reflux for 2 hours. The mixture was cooled to room temperature and the supernatant was removed, and the solid was washed 3x with water.

It was possible to obtain 43.3 mg of a brown-red solid. The solid corresponds to a complex mixture.

**Procedure B:**

Following the literature procedure of Quintal[150], to a round bottom flask were added 100 mg of acenaphthoquinone (**3.1**) (0.55 mmol), 5 mL of acetonitrile, and then 0.88 mL of glacial acetic acid. After 30 minutes a solution containing 174 mg of 4-nitrobenzoic acid (**3.2**) (1.27 mmol, 2.3 eq.) in 2.6 mL of acetonitrile was added. The mixture was heated under reflux for 48h. Then it was cooled to room temperature, the supernatant was removed by centrifugation, and reduced under vacuum until the formation of a precipitate. This precipitate was washed with diethyl ether. The obtained solid was very insoluble and corresponds to a complex mixture.

*Synthesis of 2-(4-nitrophenyl)-1,3-dioxolane (**3.7**)*

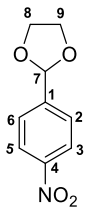

(3.7)

To a solution of 150 mg of *p*-nitrobenzaldehyde (**3.6**) (0.99 mmol) and 3.8 mg of *p*-toluenesulfonic acid monohydrate (0.02 mmol, 0.02 eq.) in toluene (4 mL), 120 µL of ethylene glycol (1.77 mmol, 1.8 eq.) were added. The mixture was stirred at reflux with a dean-stark for 16 hours. Then the solvent was removed, and ethyl acetate was added. The organic phase was washed twice with a $NaHCO_3$ saturated solution and then with brine. It was possible to afford 198.1 mg of 2-(4-nitrophenyl)-1,3-dioxolane (**3.7**) in quantitative yield. **$^1$H NMR (400 MHz, $CDCl_3$) δ (ppm):** 8.24 (d, *J* = 7.6 Hz, 2H, H3/H5), 7.66 (d, *J* = 7.6 Hz, 2H, H2/H6), 5.90 (s, 1H, H7), 4.14-4.06 (m, 4H, H8/H9).

*Reduction of 2-(4-nitrophenyl)-1,3-dioxolane (3.7) – synthesis of 4-aminobenzaldehyde (**3.9**)*

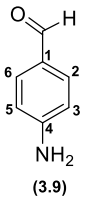

(3.9)

Following the procedure reported by Riddle[182], a vessel containing 2-(4-nitrophenyl)-1,3-dioxolane (**3.7**) (0.99mmol), $PtO_2$ (9.3mg,0.04 mmol, 0.04 eq.), $MgSO_4$ (239.4 mg, 1.99 mmol, 2.0 eq.), and THF (3 mL) was purged with $N_2$ and subsequently charged with $H_2$ (55 psi). The reaction was monitored by TLC using the eluent hexane/ ethyl acetate 7/3 and after 19 hours the reaction was stopped. The reactional mixture was filtrated and the remaining solid was washed with acetone. The filtrates were evaporated and it was possible to afford 151 mg of 4-aminobenzaldehyde (**3.9**) instead of 4-(1,3-dioxolan-2-yl)aniline (**3.8**). **$^1$H NMR (400 MHz,$CDCl_3$) δ(ppm):** 9.74 (s, 1H,CHO), 7.68 (d, *J* = 7.6 Hz, 2H,H2/H6), 6.69 (d, *J* = 7.8 Hz, 2H,H3/H5).

*Synthesis of (4-nitrophenyl)methanol (**3.10**)*

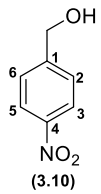

(3.10)

Following the literature procedure described by Desroches[203], to a solution of 4-nitrobenzadehyde (100 g, 0.66 mmol) in 0.9 mL of ethanol was added a suspension of $NaBH_4$ (17 mg, 0.46 mmol, 0.69 equiv.) in 1.5 mL of ethanol. The reaction mixture was stirred for 1 hour at room temperature. Then the reaction mixture was quenched with an aqueous solution of NaOH 10%. Water was added and the solvent was removed under reduced pressure. The product was extracted with $CH_2Cl_2$. The organic layers were washed with an aqueous solution of $NaHCO_3$ 5% and water, then dried over $Na_2SO_4$, filtered, and evaporated to dryness. It was possible to afford 95 mg of (4-nitrophenyl)methanol (**3.10**) (0.62 mmol, η= 93.7%). **$^1$H NMR (400 MHz, $CDCl_3$) δ (ppm):** 8.21 (d, *J* = 7.2 Hz, 2H, H3/H5), 7.53 (d, *J* = 7.2 Hz, 2H, H2/H6), 4.83 (d, *J* = 4.4 Hz, 2H, $CH_2OH$).

*Synthesis of (4-aminophenyl)methanol (**3.11**)*

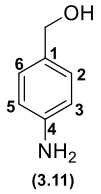

(3.11)

Following the methodology describes in the literature by Vogel[184], a suspension of 3.4 mg of Pd-C (10%) (0.0032 mmol, 0.009eq.) in 0.34 mL of $H_2O$ was placed in a round bottom flask and 24.5 mg of $NaBH_4$ (0.64 mmol, 2.0 eq.) and 0.49 mL of $H_2O$ were added. $N_2$ was purged into the mixture and then a solution containing 50.1 mg of (4-nitrophenyl)methanol (**3.10**) (0.327 mmol) in 1.6 mL of NaOH 2M and 0.4 mL of MeOH was added dropwise. The reactional mixture was stirred for 30 minutes (until the yellow color disappeared), it was monitored by TLC using as eluent a mixture of hexane and ethyl acetate 6/4. The mixture was filtered and acidified with HCl 2M to destroy the excess of $NaBH_4$. Then it was neutralized by adding diluted NaOH. The product was extracted with ethyl ether, the combined organic layers were dried over anhydrous $Na_2SO_4$, filtered and evaporated to dryness. It was possible to afford 28 mg of (4-aminophenyl)methanol (**3.11**) (0.22 mmol, η= 68.5 %). **$^1$H NMR (400 MHz, MeOD) δ (ppm):** 7.09 (d, *J* = 8.0 Hz, 2H, H6/H2), 6.69 (d, *J* = 7.6 Hz, 2H, H5/H3), 4.44 (s, 2H, $CH_2OH$).

*Reaction between acenaphthoquinone (**3.1**) and (4-aminophenyl)methanol (**3.11**) with the aim of synthesizing ((((1E,2E)-acenaphthylene-1,2-diylidene)bis(azaneylylidene))bis(4,1-phenylene))dimethanol (**3.13**)*

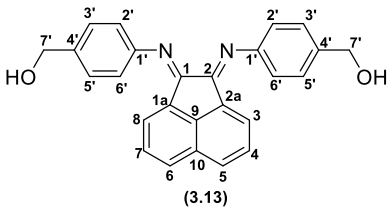

(3.13)

**Procedure A:**

Following procedure A for compound **3.3** and starting with 32 mg of acenaphthoquinone (**3.1**) (0.18 mmol), 48 mg of $ZnCl_2$ (0.35 mmol, 2.0 eq.), 50 mg of (4-aminophenyl)methanol (**3.11**) (0.41 mmol, 2.25 eq.) and 1 mL of glacial acetic acid were refluxed under $N_2$ atmosphere for 4 hours. It was possible to afford 44 mg of a brown solid corresponding to a complex mixture.

**Procedure B:**

Following procedure B for compound **3.3** and starting with 32.1 mg of acenaphthoquinone (**3.1**) (0.18 mmol) dissolved in 1.6 mL of acetonitrile 0.28 mL of acetic acid were added. After 30 minutes a solution containing 50 mg of (4-aminophenyl)methanol (**3.11**) 0.41mmol, 2.25 eq.) in 0.5 mL of acetonitrile was added. The mixture was heated under reflux for 46h. It was possible to obtain 54.5 mg of a brown solid. The solid corresponded to a mixture composed mainly of acenaphthoquinone (**3.1**).

*Synthesis of 2-cyano-3-(4-nitrophenyl)acrylic acid (**3.14**)*

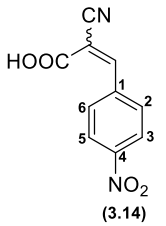

(3.14)

To a mixture of *p*-nitrobenzaldehyde (**3.6**) (299.9 mg, 1.98 mmol), cyanoacetic acid (507.3 mg, 6.0 mmol, 3.0 eq.) in 10 mL of acetonitrile were added 0.57 mL of piperidine (5.77 mmol, 2.9 eq.). The mixture was stirred at room temperature under $N_2$ atmosphere for 4 hours. The consumption of aldehyde was monitored by TLC using the eluent hexane / ethyl acetate 6/4. The solvent was removed and HCl 1M was added, the product was extracted with ethyl acetate. The combined organic phases were washed with $H_2O$, then dried with $Na_2SO_4$, filtered and evaporated. It was possible to afford 387.3 mg of a solid corresponding to 2-cyano-3-(4-nitrophenyl)acrylic acid (**3.14**) (1.76 mmol, η=89.2%). **$^1$H NMR (400 MHz, MeOD) δ(ppm):** 8.41 (s, 1H, CH), 8.36 (d, *J* = 8.0 Hz, 2H, H3/H5), 8.19 (d, *J* = 8.0 Hz, 2H, H2/H6).

*Synthesis of 3-(4-aminophenyl)-2-cyanoacrylic acid (**3.15**)*

To a mixture of 2-cyano-3-(4-nitrophenyl)acrylic acid (**3.14**) (380.9 mg, 1.75 mmol) in 10 mL of ethanol was added a suspension of $SnCl_2$. $H_2O$ (1.184 g, 5.25 mmol, 3.0 eq) in 7 mL of HCl 1M. The reaction was stirred to room temperature for 2 hours. The formation of the amine and the consumption of the starting material was detected by TLC using the eluent $CH_2Cl_2$/ MeOH/$H_2O$ 65/20/2 and staining with Dragendorff reagent. A solution of $NaHCO_3$ was added until pH ≈ 3, the product was extracted with ethyl acetate, the combined organic layers were washed with brine and water, then dried over $Na_2SO_4$, filtered and evaporated. Affording 285.6 mg of 3-(4-aminophenyl)-2-cyanoacrylic acid (**3.15**) (1.52 mmol, η=86.7 %). **$^1$H NMR (500 MHz, DMSO) δ(ppm):** 13.13 (s, 1H, OH), 7.99 (s, 1H, CH), 7.81 (d, *J* = 9.0 Hz, 2H, H6/H2), 6.65 (d, *J* = 9.0 Hz, 2H, H3/H5).

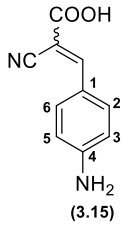

(3.15)

*Reaction between 3-(4-aminophenyl)-2-cyanoacrylic acid (**3.15**) and acenaphthoquinone (**3.1**) with the aim of synthesizing 3,3'-((((1E,2E)-acenaphthylene-1,2-diylidene)bis(azaneylylidene))bis(4,1-phenylene))bis(2-cyanoacrylic acid) (**3.5**)*

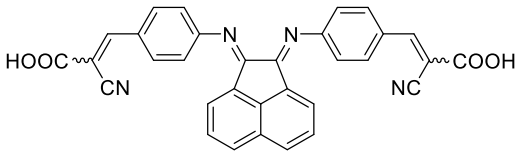

(3.5)

**Procedure A:**

Following the procedure reported by Zou[154], a solution containing 3-(4-aminophenyl)-2-cyanoacrylic acid (**3.15**) (57 mg, 0.30 mmol, 2.1 eq.) acenaphthoquinone (**3.1**) (25.1 mg, 0.14 mmol, 1 eq.) and formic acid (0.1 mL) in ethanol (3 mL) was stirred at room temperature for 31 hours. Then the reaction was warmed to 40°C. Since the starting material wasn't consumed after 24 hours the reactional mixture was refluxed for more 20 hours. After this time the solvent was removed, $ZnCl_2$ (2.0 eq.) and 1.5 mL of glacial acetic acid were added. After stirring at room temperature for 3 hours and 30 minutes, the reactional mixture was cooled to room temperature. Then the supernatant was removed and the formed solid was centrifuged and washed with acetic acid (2x) and diethyl ether (3x). An aqueous solution of $K_2CO_3$ (1.2g in 1.2 mL $H_2O$ was added to the solid and it was heated under reflux for 2 hours. The mixture was cooled to room temperature and the supernatant was removed, and the solid was washed 3x with water. It was obtained 17.8 mg of a solid corresponding to a complex mixture.

**Procedure B:**

A solution containing 3-(4-aminophenyl)-2-cyanoacrylic acid (**3.15**) (57 mg, 0.30 mmol, 2.1 eq.) acenaphthoquinone (**3.1**) (25.0 mg, 0.14 mmol, 1 eq.) and acetic acid (1mL) was stirred at room temperature for 28 hours and 30 minutes, and then warmed to 50°C. After 19h the reaction was transferred to a sealed tube, the reaction was stirred for more 75 hours under pressure.

**Procedure C:**

Following the methodology of Liu in the literature[186], a mixture containing 3-(4-aminophenyl)-2-cyanoacrylic acid (**3.15**) (57.3 mg, 0.30 mmol, 2.1 eq.), acenaphthoquinone (**3.1**) (25.2 mg, 0.14 mmol and *p*-toluenesulfonic acid (5.3 mg, 0.028 mmol, 20 mol %) in 3 mL of toluene was stirred at 50°C for 5 days. After this time the solvent was removed and the solid was washed with MeOH. Only starting materials were recovered.

*Synthesis of ethyl-2-cyano-3-(4-nitrophenyl)acrylate (**3.16**)*

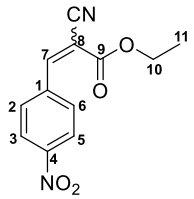

(3.16)

Following the procedure in the literature described by Suzuki[204], to a solution of *p*-nitrobenzaldehyde (**3.6**) (500 mg, 3.3 mmol) and ethyl cyanoacetate (62 µL, 5.8 mmol, 1.75 eq.) in EtOH (1.5 mL) was added piperidine (32 µL). The mixture was stirred under nitrogen atmosphere at room temperature. The reaction was followed by TLC using the eluent hexane / Ethyl acetate 6/4. After 4 hours and 30 minutes the reaction was complete. The solid was centrifuged and washed 3x with ethanol. It was possible to afford 715 mg of ethyl-2-cyano-3-(4-nitrophenyl)acrylate (**3.16**) (2.90 mmol, η= 88 %). **$^1$H NMR (500 MHz, $CDCl_3$) δ (ppm):** 8.35 (d, *J* = 9.0 Hz, 2H, H3/H5), 8.30 (s, 1H, H7), 8.13 (d, *J* = 9.0 Hz, 2H, H2/H6), 4.42 (q, *J* = 7.2 Hz, 2H, $CH_2$), 1.42 (t, *J* = 7.3 Hz, 3H, $CH_3$). **$^{13}$C NMR (126 MHz, $CDCl_3$) δ (ppm):** 161.55 (C9), 151.87 (C7), 149.86 (C4), 137.04 (C1), 131.65 (C6/C2), 124.46 (C3/C5), 114.66 (C≡N), 107.52 (C8), 63.49 (C12), 14.24 (C11).

*Synthesis of ethyl-3-(4-aminophenyl)-2-cyanoacrylate (**3.17**)*

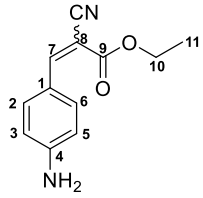

(3.17)

Following the methodology of Lu[205] and Cui[206], to a solution of ethyl-2-cyano-3-(4-nitrophenyl)acrylate (**3.6**) (400 mg, 1.62 mmol) in EtOH (6.6 mL) was added $SnCl_2{\cdot}2H_2O$ (1.833 g, 8.12 mmol, 5.0 eq.) in HCl 6M (6.6 mL). The mixture was heated to reflux for 1 h and 30 minutes. It was followed by TLC using the eluent hexane / ethyl acetate 6/4. The mixture was cooled

to room temperature and a solution of NaOH 2M (50 mL) was added. The product was extracted with ethyl acetate. The organic layers were washed with brine, dried over anhydrous $Na_2SO_4$, filtered and evaporated to dryness. It was possible to afford 307.7 mg of ethyl-3-(4-aminophenyl)-2-cyanoacrylate (**3.17**) (1.42 mmol, η= 88%, yellow solid). **$^1$H NMR (400 MHz, MeOD) δ (ppm):** 8.07 (s, 1H, H7), 7.84 (d, J = 8.4 Hz, 2H, H2/H6), 6.70 (d, J = 8.4 Hz, 2H, H5/H3), 4.32 (q, J = 7.1 Hz, 2H, H10), 1.36 (t, J = 7.1 Hz, 3H,H11). **$^{13}$C RMN (126 MHz, MeOD) δ (ppm):** 164.87 (C9), 155.36 (C7), 134.86 (C4), 129.71 (C2/C6), 120.14 (C1), 117.67 (C≡N), 114.08 (C3/C5), 92.99 (C8), 62.12 (C11), 13.77 (C12).

*Synthesis of diethyl 3,3'-((((1E,2E)-acenaphthylene-1,2-diylidene)bis(azaneylylidene))bis(4,1-phenylene))(2E,2'E)-bis(2-cyanoacrylate) (**3.18**)*

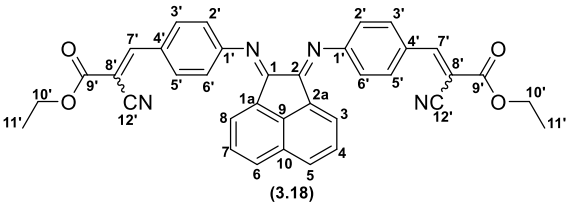


A mixture of acenaphthoquinone (**3.1**) (164.5 mg, 0.90 mmol), $ZnCl_2$ (244.6 mg, 1.79 mmol, 2.0 eq.) and acetic acid (2 mL) was heated to 60°C. Then ethyl-3-(4-aminophenyl)-2-cyanoacrylate (**3.17**) (495.15 mg, 2.29 mmol, 1.0 eq.) was added to the mixture, it was stirred under reflux and $N_2$ atmosphere. The consumption of the acenaphthoquinone was monitored by TLC using the eluent hexane/ EtOAc 6/4. The supernatant was removed and the obtained solid was washed with hot acetic acid and diethyl ether. The complex was dissolved in $CH_2Cl_2$ and an aqueous solution of potassium oxalate 1.5M was added. The mixture was stirred for 5 minutes and then was added to a separatory funnel. The product was extracted with $CH_2Cl_2$ and the combined organic phases were washed with water, dried over anhydrous $Na_2SO_4$, filtered and evaporated to dryness. The product was recrystallized with ethanol to afford 290.2 mg of an orange solid corresponding to diethyl 3,3'-((((1E,2E)-acenaphthylene-1,2-diylidene)bis(azaneylylidene))bis(4,1-phenylene))(2E,2'E)-bis(2-cyanoacrylate) (**3.18**) (0.50 mmol, η= 21.9 %).[156,207] **$^1$H NMR (400 MHz,$CDCl_3$) δ (ppm):** 8.31 (s, 2H, H7'), 8.18 (d, *J* = 8.0 Hz, 4H,H3'/H5'), 7.98 (d, *J* = 8.4 Hz, 2H,H5/H6), 7.45 (t, *J* = 7.8 Hz, 2H,H4/H7), 7.27 (br s, 4H,H2'/H6'), 6.96 (d, *J* = 7.2 Hz, 2H,H3/H8), 4.42 (q, *J* = 7.2 Hz, 4H,H10'), 1.42 (t, *J* = 7.2 Hz, 6H,H11'). **$^{13}$C NMR (101 MHz, $CDCl_3$) δ (ppm):** 162.99 (C9'), 161.12 (C1/C2), 156.26 (C1'), 154.44 (C7'), 142.28 (C1a/C2a), 133.31 (C3'/C5'), 131.52 (C9/C10), 130.05 (C5/C6), 128.17 (C4/C7), 128.01 (C4'), 124.43 (C3/C8), 119.26 (C2'/C6'), 116.18 (C12'), 101.31 (C8'), 62.81 (C10'), 14.36 (C11').

*Hydrolysis reactions of compound 3.18 to obtain (2E,2'E)-3,3'-((((1E,2E)-acenaphthylene-1,2-diylidene)bis(azaneylylidene))bis(4,1-phenylene))bis(2-cyanoacrylic acid) (**3.5**)*

**Procedure A**

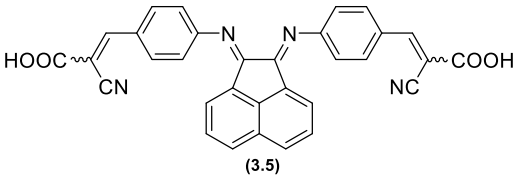

(3.5)

Diethyl 3,3'-((((1E,2E)-acenaphthylene-1,2-diylidene)bis(azaneylylidene))bis(4,1-phenylene))(2E,2'E)-bis(2-cyanoacrylate) (**3.18**) (21.2 mg, 0.037 mmol) was dissolved in 1 mL of THF and an aqueous solution of lithium hydroxide 0.5 N ( 0.44 mL,0.22 mmol, 6 eq.) was added. The reaction was stirred at room temperature for 2h and it was followed by TLC using the eluent hexane/ ethyl acetate 6/4. The reactional mixture was taken to dryness and then a solution of $NH_4Cl$ was added until pH 6, the mixture was evaporated once again. The resulting crude was washed with water to remove LiCl and $NH_4Cl$.[208]

**Procedure B**

Ar-BIAN **3.18** (15.0 mg, 0.026 mmol) was dissolved in 0.94 mL of $CH_2Cl_2$ and a solution of NaOH 1M in methanol was added (0.11 mL, 0.11 mmol, 4.2 eq.) The reaction was stirred at room temperature for 45 minutes. After this time the solvent was removed, the compound was dissolved in water and a saturated solution of $NH_4Cl$ was added until pH≈6. The compound was taken to dryness again and the solid was washed with acetonitrile and methanol.[209]

*Synthesis of 7,9-bis(4-(2-cyano-3-ethoxy-3-oxoprop-1-en-1-yl)phenyl)-7H-acenaphtho[1,2-d]imidazol-9-ium chloride (3.19)*

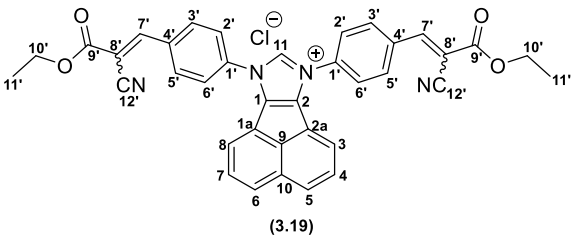
(3.19)

Ar(BIAN) (**3.18**) (50.5 mg, 0.086 mmol) and methoxy(methyl)chloride (0.14mL, 1.73 mol, 20 eq.) were added to a round bottom flask. The reaction mixture was stirred at 55°C for 2 hours, after this time the reaction mixture was cooled to ambient temperature. The obtained solid was washed with diethyl ether, hot toluene and ethanol. It was possible to afford 10.4 mg of a solid corresponding to compound **3.19** (0.017 mmol, η=19.2%).[187] **$^1$H NMR (400 MHz, DMSO-$d_6$) δ (ppm):** 10.42 (s, 1H, H11), 8.64 (s, 2H, H7'), 8.51 (d, *J* = 8.4 Hz, 4H, ArH), 8.37 (d, *J* = 8.4 Hz, 4H, ArH), 8.27 (d, *J* = 8.4 Hz, 2H,H3/H8/H6/H5), 8.03 (d, *J* = 7.2 Hz, 2H, H3/H8/H6/H5), 7.83 (t, *J*= 7.8 Hz, 2H, H4/H7), 4.40 (q, *J* = 7.1 Hz, 4H, H10'), 1.36 (t, *J* = 7.0 Hz, 6H, H11').

*Hydrolysis reaction of compound 3.19 to obtain 7,9-bis(4-(2-carboxy-2-cyanovinyl)phenyl)-7H-acenaphtho[1,2-d]imidazol-9-ium chloride (**3.20**)*

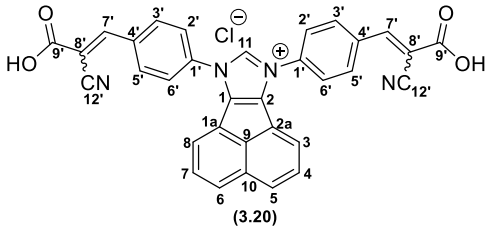


Following the procedure B for the hydrolysis of compound **3.18** and starting with 8.9 mg of compound **3.19** (0.015 mmol) in 0.55 mL of THF and 0.06 mL of NaOH 1 M in MeOH (0.06 mmol, 4 eq.). After 1h a solution of $NH_4Cl$ in MeOH was added and the solvent was removed. The solid was washed with ethanol and distilled water. A complex mixture was obtained.

## 3.4.2 Synthesis of 7H-acenaphtho[1,2-d]imidazole derivatives

*Synthesis of 4-(7H-acenaphtho[1,2-d]imidazol-8-yl)benzaldehyde (**3.22a**)*

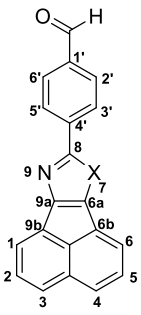


A mixture of terephthalaldehyde (**3.21a**) (100.6 mg, 0.75 mmol, 1 eq.), acenaphthoquinone (**3.1**) (134.45 mg, 0.74 mmol), ammonium acetate (544.1 mg, 7.1 mmol, 9.5 eq.) in glacial acetic acid (3.4 mL) was refluxed for 1 hour. The reaction was followed by TLC using the eluent hexane/ EtOAc 6/4. Then it was cooled to room temperature and the quenching was performed by adding $H_2O$. The formed solid was filtered and washed with $H_2O$ via centrifugation. The resulting solid was purified by flash column chromatography using as eluent $CH_2Cl_2$ to $CH_2Cl_2$/ 5 % MeOH. It was possible to isolate a red solid corresponding to the secondary product 4-(acenaphtho[1,2-*d*]oxazol-8-yl)benzaldehyde (**51b**) (11.4 mg, 0.038 mmol, η=5.1 % ). The fraction containing the desired product was purified a second time by preparative chromatography using the eluent $CH_2Cl_2$/2.5% MeOH, it was possible to obtain 28.3 mg of an orange solid corresponding to 4-(7H-acenaphtho[1,2-d]imidazol-8-yl)benzaldehyde (**3.22a**) (0.096 mmol, η=12.9%). [188] 4-(7*H*-Acenaphtho[1,2-*d*]imidazol-8-yl)benzaldehyde (**3.22a**): **$^1$H NMR (500 MHz, $CDCl_3$) δ (ppm):** 9.66 (s, 1H,CHO), 7.88 (d, *J* = 8.0 Hz, 2H, ArH), 7.62 (d, *J* = 8.0 Hz, 4H, ArH), 7.59 (d, *J* = 8.0 Hz, 2H, ArH), 7.43 (t, *J* = 7.8 Hz, 2H, H5/H2). **LC-ESI-MS**, RT: 8.12 min, *m/z*: 297.1 $[M]^+$ 4-(Acenaphtho[1,2-d]oxazol-8-yl)benzaldehyde (**3.22b**): **$^1$H NMR (500 MHz,$CDCl_3$) δ (ppm):** 10.08 (s, 1H, CHO), 8.34 (d, *J* = 8.5 Hz, 2H,ArH), 8.01 (d, *J* = 8.5 Hz, 2H, ArH), 7.95 (d, *J* = 6.5 Hz, 1H, ArH), 7.87 – 7.81 (m, 3H, ArH), 7.61 (ddd, *J* = 8.3, 7.0, 2.5 Hz, 2H, H5/H2). **LC-ESI-MS**, RT: 20.16 min, *m/z*: 298.1 $[M]^+$

*Synthesis of 3-(4-(7H-acenaphtho[1,2-d]imidazol-8-yl)phenyl)-2-cyanoacrylic acid (**3.23**)*

A mixture of 4-(7*H*-acenaphtho[1,2-*d*]imidazol-8-yl)benzaldehyde (**3.22a**) (21.3 mg, 0.07 mmol), cyanoacetic acid (9.1 mg, 0.11mmol,1.5 eq.), ammonium acetatate ( 10.7 mg, 0.14 mmol, 1-9.5 eq.) in 3.6 mL of glacial acid acetic was stirred at 85°C under $N_2$ atmosphere for 20 hours. The consumption of aldehyde was monitored by TCL using the eluent $CH_2Cl_2$ / MeOH 2.5 %. Then the reactional mixture was cooled to room temperature and the quenching was performed by adding cold water. An aqueous solution of $NaHCO_3$ solution was added and the solid was centrifuged and washed with water. It was possible to afford 18.3 mg of an orange solid corresponding to 3-(4-(7*H*-acenaphtho[1,2-*d*]imidazol-8-yl)phenyl)-2-cyanoacrylic acid (**3.23**) (0.05 mmol, η=70.1 %).[171] **ATR (ν (cm$^{-1}$)):** 3388 (m, O-H), 3054 (w, C-Har), 2218 (w, C≡N), 1624 (m, C=O), 1560 (s, C=N).**$^1$H NMR (500 MHz, DMSO-$d_6$) δ (ppm):** 13.58 (br s, 1H), 8.30 (br s, 1H, $CH_2$), 8.23 – 8.09 (m, 4H, ArH), 7.79 (br s, 4H, ArH), 7.59 (br s, 2H, ArH). **ESI-MS (+)** *m/z*: 364.1 $[M+H]^+$ **ESI-HRMS** calculated for $C_{23}H_{13}N_3O_2$ 363.10078; Found: 364.1074 $[M+H]^+$

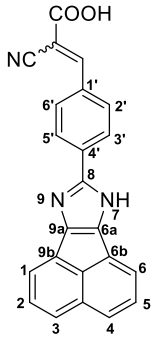

(3.23)

*Reactions to obtain 8-(thiophen-2-yl)-7H-acenaphtho[1,2-d]imidazole derivative (**3.25**)*

*Reaction with acenaphthoquinone (**3.1**) and 5-bromothiophene-2-carbaldehyde (**3.24a**)*

To a boiling solution of acenaphthoquinone (**3.1**) (50 mg, 0.27 mmol) in 1.7 mL of acetic acid was rapidly added a solution of ammonium acetate (423,2 mg, 0.24 mmol, 20 eq.) and 46 µL of 5-bromothiophene-2-carbaldehyde (**3.24a**) (0.27 mmol, 1.4 eq.) in 0.6 mL of acetic acid. The mixture was stirred under reflux for 1 hour and 30 minutes and allowed to stand at room temperature for 2 hours and 30 minutes. Water was added to the reactional mixture and the precipitate was centrifuged. Then a mixture of water and ammonia 25% (1:1) was added and the solid was centrifuged again. The obtained solid was dried and purified by chromatography in column.[189,210]

*Reaction with acenaphthoquinone (**3.1**) and thiophene-2,5-dicarbaldehyde (**3.24b**)*

Following procedure for **3.22a** and starting from 57.7 mg of acenaphthoquinone (**3.1**) (0.32 mmol), 48.7 mg of (0.35 mmol, 1.1 eq.) of thiophene-2,5-dicarbaldehyde (**3.24b**), 228.7 mg of ammonium acetate (2.97 mmol, 9.3 eq.) and 1.5 mL of acetic acid. After 18 hours the reaction was complete, the crude was purified with $CH_2Cl_2$ to $CH_2Cl_2$/ 5% MeOH.

*Reaction with acenaphthoquinone (**3.1**) and 5-(5,5-dimethyl-1,3-dioxan-2-yl)thiophene-2-carbaldehyde (**3.24c**)*

Following procedure for compound **3.22a** and starting from 45.7 mg of acenaphthoquinone (**3.1**) (0.25 mmol), 62.6 mg of 5-(5,5-dimethyl-1,3-dioxan-2-yl)thiophene-2-carbaldehyde (**3.24c**) (0.28 mmol, 1.1 eq.), 177.9 mg of ammonium acetate (2.3 mmol, 9.2 eq.) and 1.12 mL of acetic acid. After 1 hour and 30 minutes the reaction was complete, the crude was purified with $CH_2Cl_2$ to $CH_2Cl_2$/ 5% MeOH.

*General procedure for the synthesis of 4-(7-phenyl-7H-acenaphtho[1,2-d]imidazol-8-yl)benzaldehyde derivatives (**3.27a-c**)*

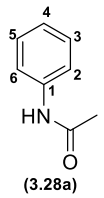

(3.28a)

In a round bottom flask containing a magnetic stir bar were added acenaphthenequinone (**3.1**) (1 eq.), terephthalaldehyde (**3.21a**) (1 eq.), ammonium acetate (4 eq.) acetic acid and aniline (**3.26a** or **3.26b**) (1 to 5 eq.). The reaction was stirred under reflux and nitrogen atmosphere until consumption of the limiting reagents, it was monitored by TLC using as eluent hexane: ethyl acetate 6:4. Water was added to the reactional mixture and a precipitate was formed, it was centrifuged for 20 minutes, and the supernatant removed. The solid was washed with water, dried and purified by column chromatography using as eluent hexane/ EtOAc 6/4 to EtOAc/ MeOH 10/1.[211] It was possible to identify the formation of a secondary product in these reactions corresponding to N-phenylacetamide (**3.28a**). **$^1$H NMR (400 MHz, $CDCl_3$) δ (ppm):** 7.71 (s, 1H, NH), 7.52 (d, *J* = 7.8 Hz, 2H, H2/H6), 7.32 (t, *J* = 7.4 Hz, 2H, H5/H3), 7.11 (t, *J* = 7.2 Hz, 1H, H4), 2.18 (s, 3H, $CH_3$).

*Other methods for the synthesis of 7-(4-methoxyphenyl)-8-phenyl-7H-acenaphtho[1,2-d]imidazole derivatives (**3.27b** and **3.27c**)*

Method A

A mixture of acenaphthoquinone (**3.1**) (1 eq.), terephthalaldehyde (**3.21a**) (1 eq.), 4-methoxyaniline (**3.26b**) (1.2 to 4 eq.), ammonium acetate (4 eq.) and 8 mL of $CH_3COOH$ was refluxed under nitrogen atmosphere until consumption of the limiting reagents. After cooling to room temperature quenching with ice water was preformed. The obtained solid was centrifuged and washed with water and then purified trough column chromatography.[171]

### Method B

Acenaphthoquinone (**3.1**) (1 eq.) reacted with ammonium acetate (4 eq.) and 4-methoxyaniline (**3.26b**) (1.2 eq.) in acetic acid at 110°C for 1h. After observing the consumption of the starting materials and the formation of a new specie the terephthalaldehyde (**3.21a**) (1 eq.) was added to the reactional mixture. It was stirred util consumption of the starting materials. Cold water was added to the mixture and the obtained solid was centrifuged and then purified through column chromatography with petroleum ether/EtOAc. Is was possible to observe the formation of a subproduct corresponding to N-(4-methoxyphenyl)acetamide (**3.28b**) **$^1$H NMR (400 MHz,$CDCl_3$) δ (ppm):** 7.37 (d, *J* = 8.0 Hz, 2H, H2/H6), 6.84 (d, *J* = 8.4 Hz, 2H,H3/H5), 3.78 (s, 3H,$OCH_3$), 2.14 (s, 3H, $CH_3$).

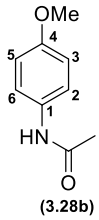

(3.28b)

### Method C

Acenaphthoquinone (**3.1**) (1 eq.) reacted with ammonium acetate (4 eq.) in acetic acid under reflux. Simultaneously terephthalaldehyde (**3.21a**) (1 eq.) reacted with 4-methoxyaniline (**3.26b**) (1.0 eq.) in $CH_3COOH$ at 60°C. After 1 hour and 30 minutes the latter solution was added to the first one and it was refluxed under nitrogen atmosphere until consumption of the limiting reagents. After cooling to room temperature quenching with ice water was performed. The obtained solid was centrifuged and washed with water and then purified trough column chromatography using DCM/ 1% MeOH .[171]

### Method D

Acenaphthoquinone (**3.1**) (0.44 mmol, 1 eq.) was refluxed with terephthalaldehyde (**3.21a**) (1 eq.), 4-methoxyaniline (**3.26b**) (1.2 eq.) and ammonium acetate (12.2 eq.) in ethanol under $N_2$ atmosphere for 21 hours. After cooling to room temperature the solid was centrifuged and washed with ethanol.[190]

### Method E

A mixture containing acenaphthoquinone (**3.1**) (0.44 mmol, 1 eq.), terephthalaldehyde (**3.21a**) or *p*-bromobenzaldehyde (**3.21b**) (1 eq.), 4-methoxyaniline (**3.26b**) (1 eq.), ammonium acetate (1.1 to 2.2 eq.) and L-Proline (12 mol % to 24 mol%) and 2 mL of acetonitrile was refluxed at 82 °C in the presence of molecular sieves 3Å. After consumption of the starting materials dichloromethane was added and the mixture was washed twice with brine. The combined organic phases were dried with $Na_2SO_4$, filtered and evaporated. The crude was adsorbed in celite

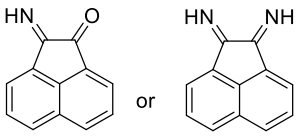

(3.29)

and purified by flash column chromatography using the eluent petroleum ether/EtOAc. It was possible to identify the intermediate products (**3.29**) derived from acenaphthoquinone and also compound **3.30**. For compound **3.29**: **$^1$H NMR (500 MHz, $CDCl_3$) δ (ppm):** 8.29 (d, *J* = 8.5 Hz, 2H), 8.13 (d, *J* = 7.0 Hz, 2H), 7.87 (t, *J* = 7.8Hz, 2H). For compound **3.30b**: **$^1$H NMR (400 MHz, $CDCl_3$) δ (ppm):** 8.46 (s, 1H, $CH_2$), 7.78 (d, *J* = 8.0 Hz, 2H, ArH ), 7.62 (d, *J* = 8.0 Hz, 2H, ArH), 7.28 (d, *J* = 4.8 Hz, 2H, ArH), 6.96 (d, J = 8.0 Hz, 2H, ArH), 3.86 (s, 3H, $OCH_3$).

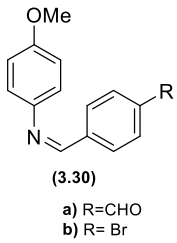

(3.30)
**a)** R=CHO
**b)** R= Br

### Method F

Following the same procedure as method E and using *p*-bromobenzaldehyde (**3.21b**), the reaction was performed in a sealed tube in acetonitrile at 82°C for 24h. Then the solvent was removed and replaced by DMF, the temperature has been raised to 110 °C. After 32 hours the solvent was removed, and the crude was purified by column chromatography using petroleum ether/EtOAc as eluent.

### Method G

*p*-Bromobenzaldehyde (**3.21b**) (1 eq.) and 4-methoxyaniline (**3.26b**) (1 eq.) reacted in DMF at room temperature. At the same time acenaphthoquinone (**3.1**) reacted with ammonium acetate at 60 °C in DMF. After consumption of the starting materials and observing the formation of intermediary species (6 hours), the two mixtures were combined in a sealed tube. After 44 hours the solvent was removed. The crude was purified by column chromatography using mixtures of petroleum ether/EtOAc.

## 3.4.3 Synthesis of diethynylacenaphthylene derivatives

*Synthesis of 1,2-Dibromoacenaphthylene (**3.32**)*

The compound 1,2-dibromoacenaphthylene (**3.32**) was synthesized according to the literature procedures.[192] A solution containing 499.3 mg of acenaphthene (**1**) (3.24 mmol), 79.1 mg of benzoyl peroxide (0.33 mmol, 0.1 mmol) and 1.7318 g of N-Bromosuccinimide (9.73 mmol, 3.00 eq.) in $CCl_4$ was refluxed under nitrogen atmosphere for 4 hours. The reaction was monitored by TLC using the eluent hexane/EtOAc 9:1. The reactional mixture was filtered to remove the solid. An aqueous solution of $Na_2S_2O_5$ 1 M was added to the filtrate and it was extracted with $CH_2Cl_2$. The organic phases were washed

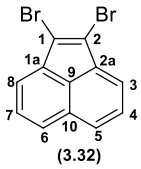

(3.32)

with water and brine, then dried with anhydrous $Na_2SO_4$, filtered and evaporated. The crude was absorbed in celite and purified by flash column chromatography using the eluent petroleum ether. It was possible to afford 439.1 mg of a crystalline yellow solid, corresponding to the 1,2-dibromoacenaphthylene (**3.32**) ($\eta$ = 44 %). **$^1$H NMR (400 MHz,$CDCl_3$) δ (ppm):** 7.84 (d, *J* = 8.4 Hz, 2H, H8/H3), 7.66 (d, *J* = 6.8 Hz, 2H, H6/H5), 7.57 (t, *J* = 7.6 Hz, 2H,H7/H4).

*Synthesis of 1,2-Bis((trimethylsilyl)ethynyl)acenaphthylene (**3.34**)*

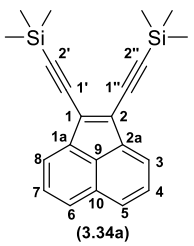

(3.34a)

To a sealed tube, 345.6 mg of 1,2-dibromoacenaphthylene (**3.32**) (1.12 mmol, 1 eq.), $Pd(PPh_3)_4$ (0.30 eq.), CuI (0.24 eq.), $PPh_3$ (0.12 eq.), diisopropylamine (3 eq.) and 6 mL of dioxane were added under $N_2$ atmosphere. The mixture was stirred at 40 °C for 7 hours and then 3 eq. of ethynyltrimethylsilane were added. The consumption of the starting material was monitored by TLC using petroleum ether as eluent. After 20 h the reaction was complete, and the solvent was removed under reduced pressure. The crude was washed with water and extracted with dichloromethane. The combined organic layers were dried over $Na_2SO_4$, filtered and evaporated to dryness. The crude was purified via column chromatography using the eluent $CH_2Cl_2$/petroleum ether 9.5/0.5. It was possible to afford an orange oil corresponding to 1,2-bis((trimethylsilyl)ethynyl)acenaphthylene (**3.34**) (229.5 mg, $\eta$ = 60 %). **$^1$H NMR (400 MHz, $CDCl_3$) δ (ppm):** 7.86 (d, *J* = 8.0 Hz, 2H, H3/H8), 7.81 (d, *J* = 7.2 Hz, 2H,H5/H6), 7.59 (dd, *J* = 8.2, 7.0 Hz, 2H,H4/H7), 0.34 (s, 18H, Si($CH_3$)$_3$). **$^{13}$C NMR (101 MHz, $CDCl_3$) δ (ppm):** 138.28, 128.70, 128.31, 128.23, 127.93, 127.31, 124.10, 106.59 (C1'/C1''), 99.31(C2'/C2''), 0.27 Si($CH_3$)$_3$. **HRMS-ESI(+)** calculated for $C_{22}H_{24}{}^{28}Si_2$ [M+H] 345.14893; Found: 345.1486

*Synthesis of 7-bromo-2-(2-ethylhexyl)-2H-benzo[d][1,2,3]triazole-4-carbaldehyde (**3.36c**)*

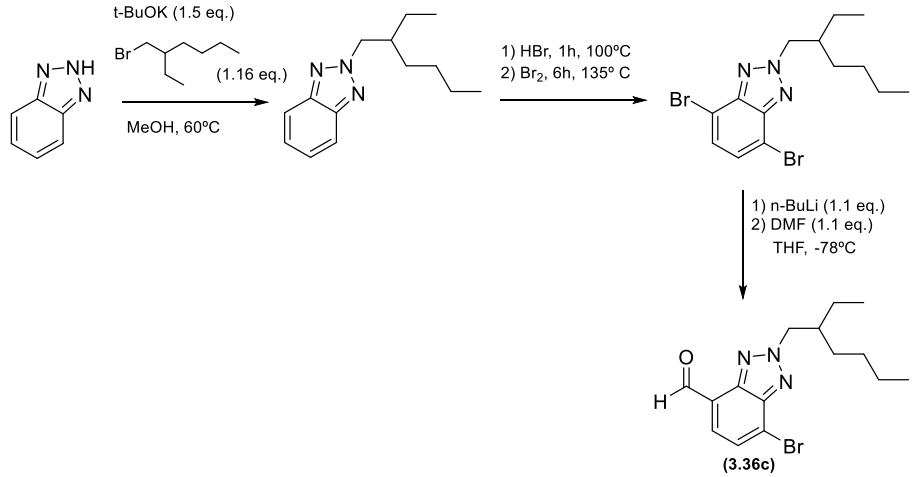


Scheme 27. Synthetic route for the preparation of 7-bromo-2-(2-ethylhexyl)-2H-benzo[d][1,2,3]triazole-4-carbaldehyde (**3.36c**) using as starting material 1,2,3-benzotriazole.

*Synthesis of 2-(2-ethylhexyl)-2H-benzotriazole*

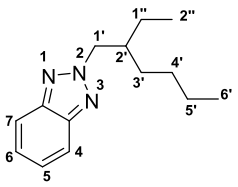

To a round-bottom flask under $N_2$ atmosphere were added methanol (9 mL), 1,2,3-benzotriazole (0.599 mg, 5.03 mmol, 1 eq.), potassium butoxide (848 mg, 7.55 mmol, 1.5 eq.) and 3-(bromomethyl)heptane (1.04 mL, 5.84 mmol, 1.16 eq.). The reactional mixture was stirred at reflux for 118 hours. After cooling the solvent was removed and the crude dissolved in chloroform, washed with water, and then dried with anhydrous $Na_2SO_4$, filtered and evaporated. The residue was purified by flash column chromatography using the eluent petroleum ether/EtOAc 9:1 [193,194] . It was possible to afford two isomers. 2-(2-ethylhexyl)-2*H*-benzotriazole (colorless oil) ($\eta$ = 42 %) **$^1$H NMR (400 MHz,$CDCl_3$) δ (ppm):** 7.86 (dd, *J* = 6.6, 3.0 Hz, 2H, H7/H4), 7.37 (dd, *J* = 6.6, 3.0 Hz, 2H,H5/H6), 4.63 (d, *J* = 7.2 Hz, 2H,H1'), 2.23 (m, 1H,H2'), 1.37 – 1.24 (m, 8H,H1''/H3'/H4'/H5'), 0.92 (t, *J* = 7.6 Hz, 3H,H2,H2''/H6'), 0.87 (t, *J* = 7.0 Hz, 3H, H2''/H6') and also 2-(2-ethylhexyl)-1*H*-benzotriazole (η=38.5 %) **$^1$H NMR (400 MHz, $CDCl_3$) δ (ppm):** 8.06 (d, *J* = 8.4 Hz, 1H), 7.49 (m, 2H), 7.35 (ddd, J = 8.0, 6.4, 1.4 Hz, 1H), 4.52 (d, *J* = 7.2 Hz, 2H), 2.09 (m, 1H), 1.36 – 1.24 (m, 8H), 0.93 (d, *J* = 7.4 Hz, 3H), 0.86 (t, J = 7.0 Hz, 3H).

*Synthesis of 4,7-dibromo-2-(2-ethylhexyl)benzotriazole*

To a round-bottom flask containing 2-(2-ethylhexyl)-2H-benzotriazole (484.8 mg, 2.1 mmol) were added 3.43 mL of and aqueous HBr solution (5.8 M). The reactional mixture was stirred for 1h at 100 °C. Then 0.35 mL of $Br_2$ (6.64 mmol, 3.2 eq.) was added and the mixture was stirred for 24 hours and 30 minutes. After cooling to room temperature, the mixture was dissolved in $CH_2Cl_2$ and washed with a solution of $NaHCO_3$. The combined organic layers were dried with $Na_2SO_4$, filtered and evaporated. The crude was purified by flash column chromatography (eluent: petroleum ether/$CH_2Cl_2$ 6:4), it was possible to afford 481.6 mg of a yellow oil corresponding to 4,7-dibromo-2-(2-ethylhexyl)benzotriazole ($\eta$ = 59 %). **$^1$H NMR (400 MHz, $CDCl_3$) δ(ppm):** 7.44 (s, 2H, H5/H6), 4.68 (d, $J$ = 7.2 Hz, 2H,H1'), 2.30 (m, 1H,H2'), 1.33 (m, 8H,H1'',H3'/H4'/H5'), 0.92 (t, $J$ = 7.6 Hz, 3H, H2''/H6'), 0.87 (t, $J$ = 6.8 Hz, 3H, H2''/H6') [194].

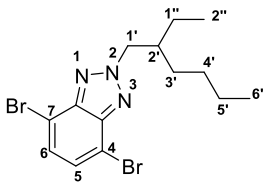

*Synthesis of 7-bromo-2-(2-ethylhexyl)-2H-benzo[d][1,2,3]triazole-4-carbaldehyde (**3.36c**)*

To a round-bottom flask containing 257 mg of 4,7-dibromo-2-(2-ethylhexyl)benzotriazole (0.66 mmol) were added 3.8 mL of dry THF and the mixture was cooled to -78°C in an acetone/liquid $N_2$ bath. Then 0.62 mL of a 1.17M solution of n-BuLi in Hexanes (0.73mmol, 1.1 eq.) were added dropwise. After 15 minutes 51 µL of dry DMF (1 eq.) were added and the reaction was stirred for more 3h at -78°C. The consumption of the starting material was confirmed by TLC using the eluent petroleum ether/EtOAc 9:1. Then the reaction was warmed to room temperature and $H_2O$ was added, the organic product was extracted with $CH_2Cl_2$. The combined organic layers were dried over $Na_2SO_4$, filtered and evaporated. The resulting crude was subjected to a by flash column chromatography (eluent: petroleum ether / ethyl acetate 9:1) to afford 139.4 mg of a colourless oil corresponding to 7-bromo-2-(2-ethylhexyl)-2H-benzo[d][1,2,3]triazole-4-carbaldehyde (**3.36c**) (0.41mmol, $\eta$ = 62 %). **$^1$H NMR (400 MHz, $CDCl_3$) δ (ppm):** 10.47 (s, 1H, C**H**O), 7.83 (d, $J$ = 7.6 Hz, 1H, H6), 7.75 (d, $J$ = 7.6 Hz, 1H, H5), 4.74 (d, $J$ = 7.3 Hz, 2H, H1'), 2.39 – 2.28 (m, 1H, H2'), 1.40 – 1.23 (m, 9H; H1'',H3',H4',H5'), 0.93 (t, $J$ = 7.6 Hz, 3H, H2''/H6'), 0.87 (t, $J$ = 7.0 Hz, 3H, H2''/H6'). $^{13}$C NMR (101 MHz, $CDCl_3$) δ (ppm): 188.99, 144.95, 141.70, 131.15, 128.83, 125.72, 118.99, 61.05, 40.47, 30.43, 28.40, 23.88, 22.98, 14.08, 10.49. **HRMS-ESI(+)** calculated for $C_{15}H_{20}BrN_3O$ [M+H] 338.08625. Found: 338.0856.

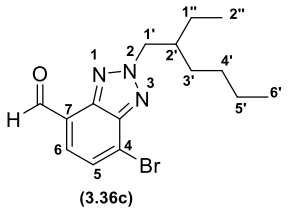

*Synthesis of 5-bromothieno[3,2-b]thiophene-2-carbaldehyde (**3.36d**)*

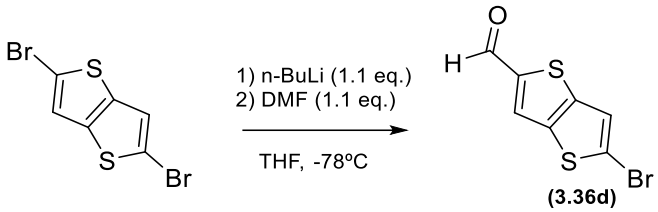


Scheme 28 Synthetic pathway for the preparation of 5-bromothieno[3,2-*b*]tiophene-2-carbaldehyde (3.36d) using as starting material 2,5-dibromothieno[3,2-*b*]thiophene.

Starting from 150 mg of 2, 5-dibromothieno[3,2-*b*]thiophene (0.5 mmol) and following the same procedure for **5c**. The crude was purified by flash chromatography column using the eluent petroleum ether: dichloromethane 8:2 and it was obtained 70 mg of a white/yellow solid corresponding to 5-bromothieno[3,2-*b*]thiophene-2-carbaldehyde (**3.36d**) (0.28 mmol, $\eta$ = 57%). **$^1$H NMR (400 MHz, $CDCl_3$) δ (ppm):** 9.97 (s, 1H, C**H**O), 7.84 (s, 1H,H3), 7.36 (s, 1H,H6).[212]

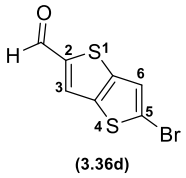


*Synthesis of compound 3.33a*

1,2-dibromoacenaphthylene (**3.32**) (50.17 mg, mmol, 0.16 mmol), $PPh_3$ (5.33 mg, 0.02 mmol, 0.12 eq.), CuI (7.76 mg, 0.04 mmol, 0.25 eq.), 4-ethynylbenzaldehyde (63.56 mg, 0.49 mmol, 3.05 eq.) and $Pd(PPh_3)_4$ (59.3 mg, 0.05mmol, 0.32 eq.) were added to a Schlenk tube under $N_2$ atmosphere. Then 4 mL of dry dioxane and 68 µL of diisopropylamine (0.49 mmol, 3.03 eq.) were added and the reactional mixture was degassed under vaccum. The reactional mixture was stirred for 19 hours and 30 minutes at 60 °C, it was followed by TLC using the eluent hexane/EtOAc 7:3. The solvent was removed, $H_2O$ was added and the organic product was extracted with $CH_2Cl_2$. The combined organic layers were dried over $Na_2SO_4$, filtered and evaporated to dryness. The crude was purified via column chromatography using $CH_2Cl_2$ as eluent to afford 49.9 mg of a red solid corresponding to 4,4'-(acenaphthylene-1,2-diylbis(ethyne-2,1-diyl))dibenzaldehyde (**3.33a**) ($\eta$ = 76 %). **$^1$H NMR (400 MHz, $CDCl_3$) δ (ppm):** 10.06 (s, 2H, 2xC**H**O), 7.95 (m, 8H, ArH), 7.82 (d, $J$ = 7.6 Hz, 4H, ArH), 7.69 (t, $J$ = 7.6 Hz, 2H, ArH). **$^{13}$C NMR (126 MHz, DMSO) δ (ppm):** 192.06, 136.77, 135.84, 131.21, 129.55, 128.68, 128.51, 127.92, 127.60, 126.49, 125.83, 124.62, 100.04, 87.34. **HRMS-ESI(+)** calculated for $C_{30}H_{16}O_2$ $[M+H]^+$ 409.12231; Found: 409.1216

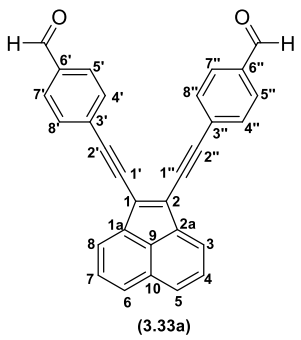

## General procedure for the synthesis of aldehydes (3b-d)

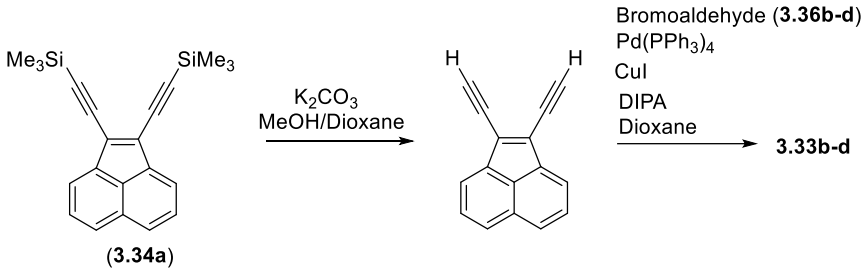


Scheme 29. Synthetic pathway for *the synthesis of aldehydes (**3.33b-d**).*

*Synthesis of 1,2-diethynylacenaphthylene*

To a solution of 1,2-bis((trimethylsilyl)ethynyl)acenaphthylene (**3.34**) (1 eq.) in methanol and dioxane (1:1) was added $K_2CO_3$ (2eq.). The reaction was monitored by TLC using the eluent petroleum ether/EtOAc 6:4. After the consumption of the starting material the reactional mixture containing 1,2-diethynylacenaphthylene was directly transferred to the next reactional step.

In a Schlenk tube were added under $N_2$ atmosphere the bromoaldehyde (2.2 eq.), $(PdPPh_3)_4$ (0.20 eq.), CuI (0.24 eq.), $PPh_3$ (0.12 eq.), diisopropylamine (3 eq.) and 4 mL of dioxane. The reaction was degassed and then it was stirred for 3 hours at 40 °C. Then the reactional mixture containing 1,2-diethynylacenaphthylene (1 eq.) was added and the solution was degassed again under vaccum. The reaction was monitored by TLC. After consumption of the starting material the solvent was removed and water was added, the organic compound was extracted with dichloromethane. The combined organic layers were dried over anhydrous $Na_2SO_4$, filtered and evaporated to dryness. The crude was purified via column chromatography.

*Compound **3.33b***

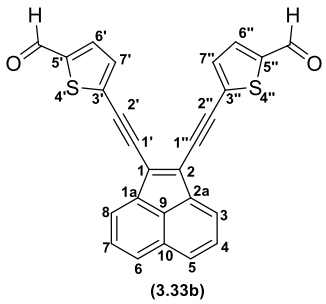


Starting from 5-bromothiophene-2-carbaldehyde (0.37 mmol, 2.2 eq) and 1,2 bis((trimethylsilyl)ethynyl)-acenaphthylene (0.17 mmol, 1 eq.). The reaction was monitored by TLC using the eluent petroleum ether: EtOAc 6:4 and after 24 hours the reaction was complete. The crude was purified via column chromatography using as eluent $CH_2Cl_2$/petroleum ether 9.5: 0.5 and then one of the collected fractions was subjected to preparative layer plate chromatography (PLC) to afford 44.2 mg of a red solid corresponding to 5,5'-(acenaphthylene-

1,2-diylbis(ethyne-2,1-diyl))bis(thiophene-2-carbaldehyde) (**3.33b**) ($\eta$ = 62%). **$^1$H NMR (400 MHz, $CDCl_3$) δ (ppm):** 9.91 (s, 2H, 2xC**H**O), 7.94 (d, *J* = 8.0 Hz, 2H, ArH), 7.90 (d, *J* = 6.8 Hz, 2H, ArH), 7.72 (d, *J* = 4.0 Hz, 2H, ArH), 7.66 (t, 2H, ArH), 7.44 (d, *J* = 4.0 Hz, 2H, ArH). **$^{13}$C NMR (101 MHz, $CDCl_3$) δ (ppm):** 182.47, 144.73, 137.56, 136.26, 133.29, 132.45, 129.56, 128.63, 128.55, 127.73, 126.83, 124.73, 93.71, 93.23. **HRMS-ESI(+)** calculated for $C_{26}H_{12}O_2{}^{32}S_2$ $[M+H]^+$ 421.03515; Found: 421.0344.

*Compound **3.33c***

Starting from 7-bromo-2-(2-ethylhexyl)-2H-benzo[d][1,2,3]triazole-4-carbaldehyde (**3.36c**) (0.38 mmol, 2.2 eq.) and 1,2-bis((trimethylsilyl)ethynyl)acenaphthylene (0.17 mmol, 1 eq.).The reaction was monitored by TLC using the eluent petroleum ether: EtOAc 8:2 and after 21 hours and 30 minutes the reaction was complete. The crude was purified via column chromatography using $CH_2Cl_2$ as eluent. One of the collected fractions was subjected to a preparative layer plate chromatography (PLC) using a mixture of $CH_2Cl_2$ with 0.5% of MeOH to afford 67.7 mg of a dark red solid corresponding to 7,7'-(acenaphthylene-1,2-diylbis(ethyne-2,1-diyl))bis(2-(2-ethylhexyl)-2H-benzo[d][1,2,3]triazole-4-carbaldehyde) (**3.33c**) (0.095 mmol, $\eta$ = 54%). **$^1$H NMR (400 MHz, $CDCl_3$) δ (ppm):** 10.52 (s, 2H, 2xCHO), 8.12 (d, *J* = 6.9 Hz, 2H, ArH), 7.98 (d, *J* = 8.5 Hz, 4H, ArH), 7.87 (d, *J* = 7.4 Hz, 2H, ArH), 7.74 – 7.68 (m, 2H, ArH), 4.78 (d, *J* = 7.1 Hz, 4H,H1'' ), 2.36 (dt, *J* = 12.3, 6.3 Hz, 2H,H2''), 1.44 – 1.24 (m, 19H, H1''',H3'',H4'',H5''), 0.95 (t, *J* = 7.4 Hz, 6H, 2x$CH_3$), 0.86 (t, *J* = 7.0 Hz, 6H, 2x$CH_3$). **$^{13}$C NMR (101 MHz, $CDCl_3$) δ (ppm):** 189.01, 145.51, 141.86, 138.26, 130.06, 129.55, 129.44, 128.64, 128.49, 127.99, 127.35, 126.08, 124.97, 120.42, 97.10, 94.10, 60.68, 40.50, 30.54, 28.49, 23.94, 22.99, 14.11, 10.54. **HRMS-ESI(+)** calculated for $C_{47}H_{46}N_6O_2$ $[M+H]^+$ 715.37549; Found 715.3748.

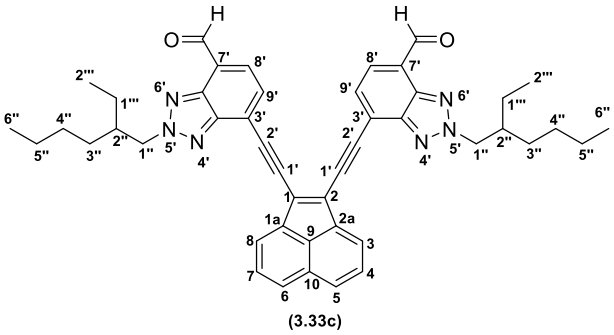
(3.33c)

*Compound **3.33d***

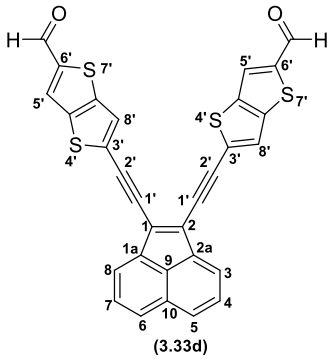
(3.33d)

Starting from 5-bromothieno-[3,2-*b*]-tiophene-2-carbaldehyde (**3.36d**) (0.28 mmol, 2.2 eq.) and 1,2 bis((trimethylsilyl)ethynyl)acenaphthylene (0.13 mmol, 1 eq.). The reaction was monitored by TLC using the eluent petroleum ether: EtOAc 8:2, after 20 hours is was observed the consumption of the starting material. The crude was purified by column chromatography using the eluent $CH_2Cl_2$/petroleum ether to $CH_2Cl_2$/MeOH 5%. The fraction containing the product was washed with ethanol to remove some impurities. It was obtained 37.3 mg of a dark red solid corresponding to 5,5'-(acenaphthylene-1,2-diylbis(ethyne-2,1-diyl))bis(thieno[3,2-*b*]thiophene-2-carbaldehyde) (**3.33d**) (0.07 mmol, $\eta$ = 54 %). **$^1$H NMR (400 MHz,$CDCl_3$) δ (ppm):** 10.01 (s, 2H, 2xCHO), 7.99 – 7.92 (m, 6H, ArH), 7.72 – 7.67 (m, 3H, ArH), 7.63 (s, 2H, ArH). **HRMS-ESI(+)** calculated for $C_{30}H_{12}O_2S_4$ $[M+Na]^+$ 554.96123; Found: 554.9603.

## Synthesis of final chromophores

*Compound **3.37a***

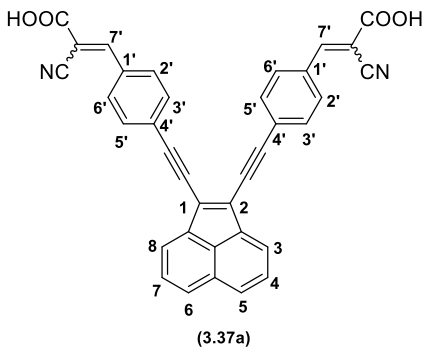
(3.37a)

A mixture of 4,4'-(acenaphthylene-1,2-diylbis(ethyne-2,1-diyl))dibenzaldehyde (**3.33a**) (25.1 mg, 0.061 mmol), cyanoacetic acid (33.5 mg, 0.39 mmol, 6.5 eq.), 34 µL of piperidine (0.34 mmol, 5.6 eq.) and 3 mL of acetonitrile was refluxed under $N_2$ atmosphere for 16 hours. The consumption of the start material was monitored by TLC using the eluent hexane: EtOAc 6:4. The solvent was removed under reduced pressure, and the crude was washed with hexane to remove non polar impurities. The resulting solid was dissolved in methanol and HCl 1 M was added. The mixture was taken to dryness and the solid was washed with $H_2O$ to remove salts and then with ethanol. It was obtained a dark red/purple solid corresponding to 3,3'-((acenaphthylene-1,2-diylbis(ethyne-2,1-diyl))bis(4,1-phenylene))bis(2-cyanoacrylic acid) (**3.37a**) (23.4 mg, $\eta$ = 70%) **$^1$H NMR (400 MHz, DMSO-$d_6$) δ (ppm):** 8.39 (s, 2H, H7'), 8.15 (m, 8H, ArH), 7.95 (d, $J$ = 8.4 Hz, 4H, ArH), 7.81 (t, $J$ = 7.4 Hz, 2H, ArH). **HRMS-ESI(-)** calculated for $C_{36}H_{17}O_4N_2$ [M-H] 541.11938; Found: 541.1202.

*Compound **3.37b***

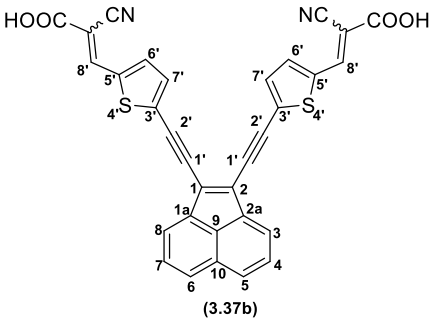


Following the same procedure for **3.37a** and starting from 31,7 mg of 5,5'-(acenaphthylene-1,2-diylbis(ethyne-2,1-diyl))bis(thiophene-2-carbaldehyde) (**3.33b**) ( 0.075 mmol) the reaction was monitored by TLC using the eluent $CH_2Cl_2$. The solvent was removed under reduced pressure, and the solid was washed with acetonitrile. Then the resulting solid was dissolved in a mixture of $CH_2Cl_2$/MeOH/$H_2O$ (65/35/5, %v/v) and HCl 1 M was added. The mixture was taken to dryness and the solid was washed with $H_2O$ to remove salts. To remove the less polar impurities the solid was washed with hexane, ethyl acetate and ethanol. It was possible to obtain a dark red/ brown solid corresponding to 3,3'-((acenaphthylene-1,2-diylbis(ethyne-2,1-diyl))bis(thiophene-5,2-diyl))bis(2-cyanoacrylic acid) (**3.37b**) (20.7 mg, $\eta$ = 50%). **$^1$H NMR (400 MHz, DMSO-$d_6$) δ (ppm):** 8.54 (s, 2H, H8'), 8.17 (d, $J$ = 8.3 Hz, 2H, ArH), 8.10 (d, $J$ = 8.0 Hz, 2H, ArH), 8.05 (d, $J$ = 4.1 Hz, 2H, ArH), 7.80 (t, $J$ = 7.8 Hz, 4H, ArH), 7.75 (d, $J$ = 3.9 Hz, 2H, ArH). **HRMS-ESI(-)** calculated for $C_{32}H_{14}N_2O_4S_2$ [M-H] 553.03222; Found: 553.0326.

*Compound **3.37c***

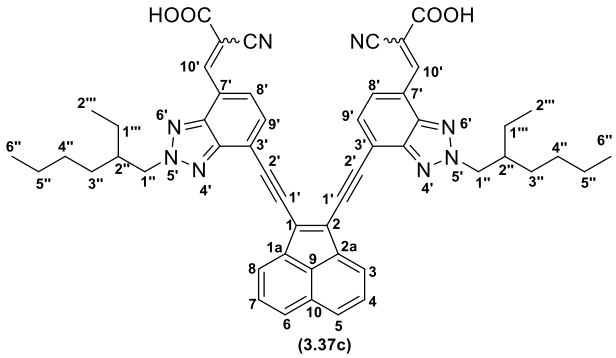


Following the procedure for compound **3.37a** and starting with 7,7'-(acenaphthylene-1,2-diylbis(ethyne-2,1-diyl))bis(2-(2-ethylhexyl)-2H-benzo[d][1,2,3]triazole-4-carbaldehyde) (**3.33c**) (40.1 mg, 0.063mmol, 1 eq.), the reaction was followed by TLC using the eluents $CH_2Cl_2$/MeOH/$H_2O$ (65/10/1, %v/v) and petroleum ether/EtOAc 8:2, and after 25 hours was complete. The solvent was removed and the solid was washed with acetonitrile. Then the resulting solid was dissolved in a mixture of $CH_2Cl_2$/MeOH/$H_2O$ (65/35/5, %v/v) and HCl 1 M was added. The mixture was taken to dryness and the solid was washed with $H_2O$ to remove salts to afford 3,3'-((acenaphthylene-1,2-diylbis(ethyne-2,1-diyl))bis(2-(2-ethylhexyl)-2H-benzo[d][1,2,3]triazole-7,4-diyl))bis(2-cyanoacrylic acid) (**3.37c**) (44.2 mg, 0.052mmol, $\eta$ = 83 %). **$^1$H NMR (400 MHz, DMSO-$d_6$) δ (ppm):** 8.44 (s, 2H, H10'), 8.13 (d, $J$ = 7.6 Hz, 2H, ArH), 7.87 (d, $J$ = 8.2 Hz, 2H, ArH), 7.74 (d, $J$ = 6.6 Hz, 2H, ArH), 7.65 (d, $J$ = 7.4 Hz, 2H, ArH), 7.52 (t, $J$ = 7.3 Hz, 2H, ArH), 4.57 (d, $J$ = 6.0 Hz, 4H, H1''),

2.10 – 1.98 (m, 2H, H2''), 1.18 (m, 7.7 Hz, 19H,H1'''/H3'',H4'',H5''), 0.79 (t, *J* = 7.4 Hz, 6H, 2x$CH_3$), 0.75 – 0.68 (m, 7H, 2x$CH_3$). **HRMS-ESI(-)** calculated for $C_{52}H_{48}N_8O_4$ [M-H] 847.37257; Found: 847.3726

*Compound **3.37d***

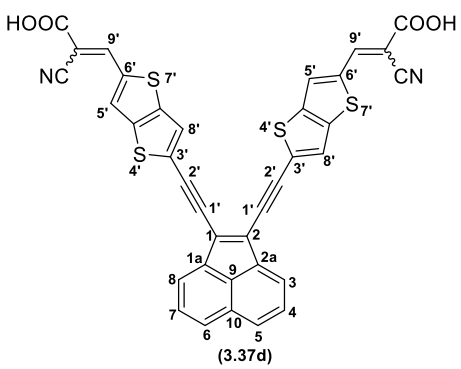


Following the procedure for compound **3.37a** and starting with 5,5'-(acenaphthylene-1,2-diylbis(ethyne-2,1-diyl))bis(thieno[3,2-b]thiophene-2-carbaldehyde) (**3.33d**) (35.3 mg, 0.066 mmol, 1 eq.) the reaction was firstly stirred at room temperature and after 40 hours was warmed to 80 °C, it was stirred for more 33 hours. The reaction was monitored by TLC using the eluents $CH_2Cl_2$/MeOH/$H_2O$ (65/10/1, %v/v and petroleum ethe/EtOAc 8:2. When it was completed the solvent was removed and the solid was dissolved in a mixture of $CH_2Cl_2$/MeOH/$H_2O$ (65/35/5, %v/v) and HCl 1 M was added. The mixture was taken to dryness and the solid was washed with $H_2O$, to remove salts, and then with acetonitrile and $CH_2Cl_2$ to afford 33 mg of 3,3'-((acenaphthylene-1,2-diylbis(ethyne-2,1-diyl))bis(thieno[3,2-*b*]thiophene-5,2-diyl))bis(2-cyanoacrylic acid) (**3.37d**) (0.049 mmol, $\eta$ = 75%). **$^1$H NMR (400 MHz, DMSO-$d_6$) δ (ppm):** 8.52 (s, 2H, H9'), 8.26 (s, 2H, ArH), 8.16 – 7.96 (m, 6H, ArH), 7.82 – 7.70 (m, 2H, ArH). **HRMS-ESI(-)** calculated for: $C_{36}H_{14}N_2O_4S_4$ [M-H] 664.97636; Found: 664.9767.

*Synthesis of 5-bromo-1,2-dihydroacenaphthylene (**3.38**)*

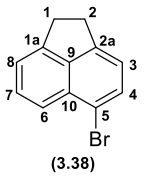


To a suspension of acenaphthene (**3.31**) (302mg, 1.95 mmol) in 3 mL of DMF were added slowly at room temperature a solution of NBS (415 mg, 2.31 mmol, 1.2 eq.) in 3 mL of DMF. The reaction was stirred for 3h and monitored by TLC using the eluent hexane/ ethyl acetate 8:2. Then water was added to the reactional mixture and a formation of a solid was observed. The solid was filtered and recrystallized from ethanol. The compound 5-bromo-1,2-dihydroacenaphthylene (**3.38**) was obtained.[196] **$^1$H NMR (400 MHz, $CDCl_3$) δ (ppm):** 7.78 (d, *J* = 8.4 Hz, 1H, H6), 7.66 (d, *J* = 7.6 Hz, 1H, H4), 7.55 (t, *J* = 7.8 Hz, 1H, H7), 7.33 (d, *J* = 6.8 Hz, 1H, H8), 7.13 (d, *J* = 7.2 Hz, 1H, H3), 3.45 – 3.38 (m, 2H, H1/H2), 3.37 – 3.31 (m, 2H, H1/H2).

*Synthesis of 4-bromo-N,N-diphenylaniline*

To a round bottom flask were added 300 mg of triphenylamine (1.22 mmol) and 3.6 mL of DMF, after dissolution a mixture of NBS (218mg, 1.22 mmol, 1 eq.) in 1.2 mL of DMF was added dropwise. The mixture was stirred in the dark for 24h, then cold water was added, and the organic compound was extracted with $CH_2Cl_2$. The combined organic phases were dried with $Na_2SO_4$, filtered and evaporated to dryness. The compound was recrystallized with ethanol and it was possible to obtain *4-bromo-N,N-diphenylaniline*.[195] **$^1$H NMR (400 MHz,$CDCl_3$) δ (ppm):** 7.33 (d, J = 8.4 Hz, 2H, ArH), 7.26 (t, J = 7.6 Hz, 4H, ArH), 7.09 – 7.02 (m, 6H, ArH), 6.95 (d, J = 8.4 Hz, 2H, ArH).

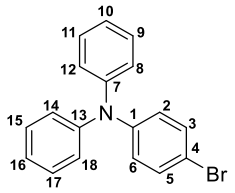


*Synthesis of dimethyl (4-(diphenylamino)phenyl)boronate*

In a round bottom flask were added 130 mg of *4-bromo-N,N-diphenylaniline* (0.4 mmol) and 3 mL of THF. Then the mixture was cooled to -78 °C and 0.82 mL of n-BuLi (0.98 M in hexanes, 0.8 mmol, 2.0 eq.) was added dropwise. The reaction was stirred for 30 minutes at -78 °C and then 0.32 mL of trimethyl borate (2.8 mmol, 7 eq.) were added. The mixture was stirred for 2h and 30 min at room temperature and this reactional mixture containing the formed dimethyl (4-(diphenylamino)phenyl)boronate was directly transferred for the following Suzuki coupling reaction.

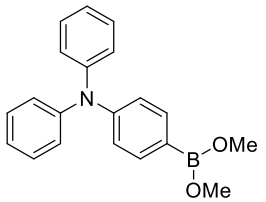


*Synthesis of 4-(1,2-dihydroacenaphthylen-5-yl)-N,N-diphenylaniline (**3.39**)*

To a degassed double neck round bottom flask were added $Pd(PPh_3)_4$ (0.08 eq.) and a solution containing 102.8 mg of 5-bromo-1,2-dihydroacenaphthylene (**3.38**) (0.44 mmol, 1.1 eq.) dissolved in degassed THF. The reactional mixture was refluxed for 20 minutes, after this an aqueous solution of $NaHCO_3$ (2.5 M, degassed, 10 eq.) was added. The reactional mixture containing the dimethyl (4-(diphenylamino)phenyl)boronate dissolved in degassed THF was added 20 minutes later. The reaction was stirred and after 18 h the consumption of the starting material was observed by TLC using the eluent hexane/ AcOEt 6/4. The solvent was removed, and water was added. Then the compound was extracted with $CH_2Cl_2$, dried with $Na_2SO_4$ and taken to dryness. The crude was purified via chromatography in column (silica flash) using the eluent petroleum ether / diethyl ether 99/1. It was possible to afford 49 mg of 4-(1,2-dihydroacenaphthylen-5-yl)-N,N-

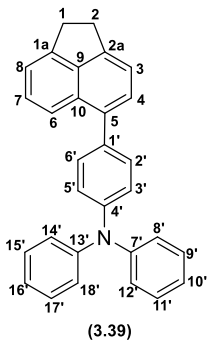

(3.39)

diphenylaniline (0.12 mmol, η=31 %).**$^1$H NMR (400 MHz, $CDCl_3$) δ(ppm):** 7.78 (d, *J* = 8.4 Hz, 1H, ArH), 7.46 – 7.43 (m, 4H, ArH), 7.35 – 7.27 (m, 6H, ArH), 7.19 (d, *J* = 8.4 Hz, 6H, ArH), 7.04 (t, *J* = 7.2 Hz, 2H, ArH), 3.44 (s, 4H, H1/H2).

*Synthesis of 5-bromoacenaphthylene (**3.41**)*

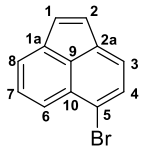

(3.41)

To a solution containing 233 mg of 5-bromo-1,2-dihydroacenaphthylene (**3.38**) (0.97 mmol) in toluene (5 mL) were added 272 mg of DDQ (1.16 mmol, 1.2 eq.). The reaction was refluxed for 48 h, after this time $H_2O$ was added and the organic compound was extracted with $CH_2Cl_2$. The organic phase was washed with $H_2O$, and dried over anhydrous $Na_2SO_4$ and filtered. The crude was purified by flash column chromatography (silica flash) using the petroleum ether as eluent to afford 88.8 mg of 5-bromoacenaphthylene (**3.41**) ( η= 41 %).[133]

*Synthesis of N,N-diethylacenaphthylen-5-amine (**3.42**)*

**Method A**

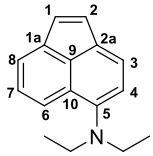

(3.42)

To a suspension of 5-bromoacenaphthylene (**3.41**) (73 mg, 0.34) in DMF (0.57 mL) were added diethylamine (0.57 mL, 40 % aqueous solution) and $CuSO_4 \cdot 5H_2O$ (4.83 mg, 0.017 mmol, 0.05eq.). The mixture was refluxed under N2 atmosphere. The reaction was monitored by TLC using the eluent hexane: ethyl acetate 6:4 and after 92 h water was added and a precipitate was formed. The mixture was centrifuged, the supernatant was removed and the solid was dissolved in $CHCl_3$ and filtered through a Celite pad. Then the solvent was removed and the crude was purified via column chromatography (silica flash) using the eluent hexane/ AcOEt 6/4. It was not observed the formation of the desired compound.[213]

**Method B**

To a solution of 5-bromoacenaphthylene (**3.41**) (91 mg, 0.40 mmol) in toluene (7.8 mL) were added sequentially $Pd_2(dba)_3$ (17 mg, 4 mol%), Xanthphos (10mg, 4 mol %), diethylamine (0.12 mL, 3.0 eq.) and $Cs_2CO_3$ (386 mg, 3.0 eq.). The mixture was stirred at 80 °C for 24 hours, it was monitored by TCL using petroleum ether as eluent. The mixture was filtered through a pad of Celite and washed with $CH_2Cl_2$. The solvent was removed and then the crude was purified by column chromatography using petroleum ether as eluent until petroleum ether: ethyl acetate 8:2. It was possible to recover 43 % of starting material and to isolate a fraction containing the desired product impure (8.7 mg). **$^1$H NMR (400 MHz,$CDCl_3$) δ (ppm):** 8.03 (d, *J* = 8.4 Hz, 1H,

ArH), 7.63 (d, *J* = 6.8 Hz, 1H, ArH), 7.53 (d, *J* = 7.6 Hz, 2H, ArH), 7.46 (dd, *J* = 8.2, 7.0 Hz, 1H, ArH), 7.15 (m, 1H, ArH), 6.99 (d, *J* = 5.2 Hz, 1H, ArH), 6.95 – 6.90 (m, 2H, ArH), 3.42 (q, *J* = 7.1 Hz, 4H, 2x$CH_2$), 1.17 (t, *J* = 7.1 Hz, 6H, 2x$CH_3$).

*Synthesis of N,N-diethyl-1,2-dihydroacenaphthylen-5-amine (**3.43**)*

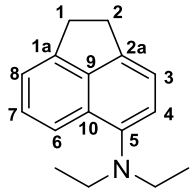


**(3.43)**

Following the same procedure for *N,N*-diethylacenaphthylen-5-amine and starting from 5-bromo-1,2-dihydroacenaphthylene (**3.38**) (0.21 mmol), $Pd_2(dba)_3$ ( 8 mol%), Xanthphos (8 mol %), diethylamine (6.0 eq.) and $Cs_2CO_3$ (3.0 eq.). The crude was purified via PLC using the eluent petroleum ether ethyl acetate 9.5:0.5. Only 72 % of the starting material was recovered.

# 4 OLIGOTHIOPHENES DERIVATIVES AS PHOTOSENSITIZERS

## 4.1 General overview

### 4.1.1 The π-spacer

Thiophene-based π-conjugated systems possess efficient electron transfer, moderate band gap, and structural versatility. Fused thiophenes represent a promising class of π-bridge due to their extended molecular conjugation, high stability, ring planarity and S-S interactions.[198] Due to these properties, fused thiophenes have aroused much interest in the fields of organic photovoltaic cells (OPVs),[214,215] organic field-effect transistors (OFETs)[216] and DSSCs[198,217]. Thienothiophenes are one example of fused thiophenes formed by two thiophene rings and featuring a completely planar system. Their incorporation into a molecular structure has the potential to dramatically improve or alter the characteristics of the compounds. There are four possible isomeric forms of thienothiophenes (**Figure 48**).[218,219] The thieno[3,2-*b*]thiophene-based dyes have been widely explored in the DSSC field.[220-226] In contrast, thieno[3,4-*b*]thiophenes are less stable than the [3,2-*b*] derivatives,[218] despite this there are some examples of their application in this type of dyes.[86,227]

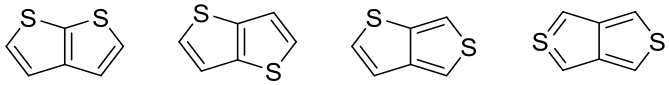


Figure 48. Possible isomeric forms of thienothiophenes.

In **Figure 49** and **Table 19** are depicted some examples of sensitizers containing fused thiophenes in their structures which were applied in DSSCs.

Wang's laboratory[220] synthesized a family of dyes containing a thieno[3,2-*b*]thiophene unit and cyanoacrylic acid as anchoring group, the employed donors were triarylamines containing different substituents (**i**). The overall energy conversion efficiency of these dyes in DSSCs devices ranged from 5.93% to 7.05 %, with the dye containing the triarylamine bearing the longest alkoxy aliphatic chain presenting the best performing (**i-d**). Dyes containing as π-bridge thieno[3,2-*b*]thiophenes and as donor triarylamines were also developed by Eom *et al.*[221] and Fernandes et al.[222] (**ii**), with the ones bearing cyanoacrylic acid as anchoring group having better efficiencies than the one using rhodanine-3-acetic acid due to higher molar extinction

coefficients, lower recombination and more efficient electron injection into the CB of $TiO_2$. The elongation of the π-bridge by adding aryl substituents between a triarylamine containing *p,o*-butoxy groups and the thieno[3,4-*b*]thiophene moiety was studied by Brogdon and co-workers.[227] It was observed that the addition of thiophene and furan π-spacers results in a red-shift in the absorption spectra due to an extended conjugation. The efficiency in DSSCs decreased with the addition of these moieties due to a substantial increment of the recombination rate (dyes **iii-b** and **iii-c**). The same group[86] developed also a set of dyes with different donors linked to alkyl thieno[3,4-*b*]thiophene-2-carboxylate moiety. The employed donors included dihexlyoxytriphenylamine and indoline-based donors, and the alkyl groups present on the thieno[3,4-*b*]thiophene ester were also varied (**iv**). The use of an indoline donor resulted in a red shift in the absorption spectra compared to dihexlyoxytriphenylamine. Additionally, the introduction of long alkyl chains on thieno[3,4-*b*]thiophene ester led to an increment in the molar extinction coefficient when compared to dyes containing ethyl chains. Regarding the performance of the dyes in DSSCs, the best $J_{sc}$ value was observed with **iv-d** (13.7 mA $cm^{-2}$), this was the best performing dye of the set, achieving an efficiency of 7.41 % and values on IPCE spectrum of 81 %.

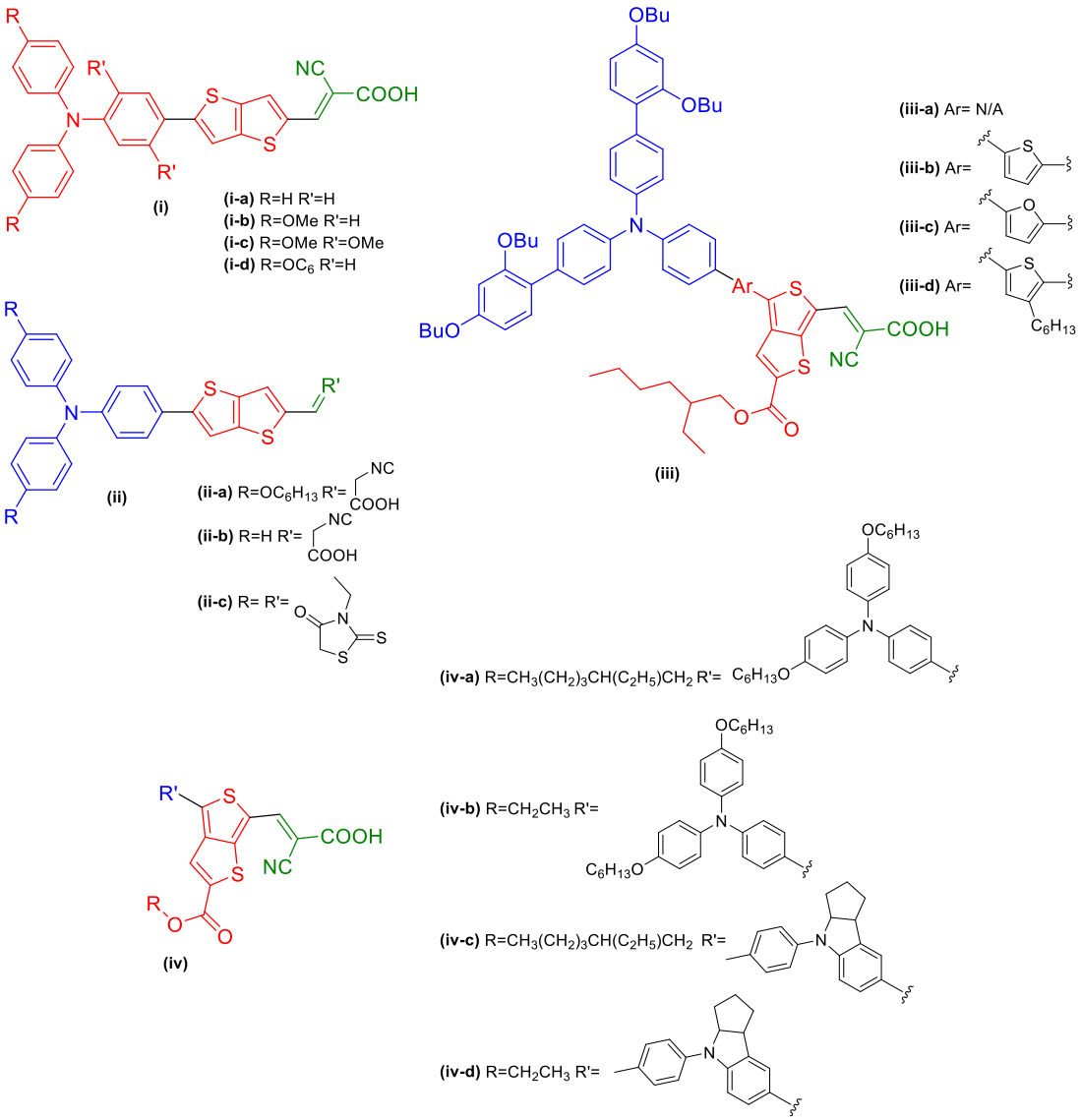


Figure 49. Chemical structures of dyes containing fused thiophenes and arylamines for DSSC application.

Table 19. Spectroscopic and photovoltaic parameters of sensitizers applied in DSSCs containing fused thiophenes and arylamines.

| Dye | $\lambda_{max}$ (nm) | ε ($M^{-1}$ $cm^{-1}$) | $J_{sc}$ ($mA/cm^2$) | $V_{oc}$ (mV) | FF | η (%) | Ref |
|---|---|---|---|---|---|---|---|
| **i-a** | 493 | 36 600 | 11.74 | 0.661 | 0.76 | 5.93 | 220 a |
| **i-b** | 512 | 40 500 | 13.38 | 0.664 | 0.74 | 6.54 | |
| **i-c** | 517 | 33 700 | 13.56 | 0.673 | 0.75 | 6.80 | |
| **i-d** | 516 | 41 900 | 14.49 | 0.693 | 0.70 | 7.05 | |
| **ii-a** | 451 | 28 690 | 14.38 | 0.694 | 0.74 | 7.40 | 221 b |
| **ii-b** | 422 | 22 079 | 9.52 | 0.600 | 0.63 | 3.68 | 222 c |

| | | | | | | | |
|---|---|---|---|---|---|---|---|
| **ii-c** | 476 | 13 627 | 0.97 | 0.517 | 0.69 | 0.35 | |
| **iii-a** | 535 | 27 000 | 12.9 | 0.658 | 0.71 | 6.3 | 227 d |
| **iii-b** | 585 | 21 000 | 14.4 | 0.552 | 0.72 | 5.9[7] | |
| **iii-c** | 605 | 16 000 | 10.6 | 0.530 | 0.68 | 3.9[7] | |
| **iii-d** | 570 | 24 000 | 13.9 | 0.622 | 0.69 | 6.2[7] | |
| **iv-a** | 560 | 26 000 | 12.1 | 0.704 | 0.75 | 6.50 | 86 e |
| **iv-b** | 558 | 22 000 | 10.9 | 0.680 | 0.75 | 5.61[4] | |
| **iv-c** | 584 | 30 000 | 12.7 | 0.648 | 0.75 | 6.24[4] | |
| **iv-d** | 591 | 20 000 | 13.7 | 0.697 | 0.76 | 7.41[4] | |

[a] Electrolyte composition: DMII/EMII/EMITCB/$I_2$/NBB/GNCS (molar ratio: 12/12/16/1.67/3.33/0.67). [Dye solution] = 300 μM and 2 mM of CDCA in the mixture of acetonitrile and tert-butanol (volume ratio: 1/1).

[b] Electrolyte composition: 0.6 M 1,2-dimethyl-3-propylimidazole iodide (DMPII), 0.5M 4-*tert*-butylpyridine (TBP), 0.05 M $I_2$ and 0.1 M LiI in acetonitrile. [Dye solution]= 0.3 mM (EtOH/THF ¼ 2:1) with 20 mM CDCA.

[c] Electrolyte composition: iodide/triiodide redox couple Iodolyte AN-50, Solaronix, Switzerland [Dye solution] = 0.5 mM in ethanol. Reference dye: N-719 (ɳ=8.42 %)

[d] Electrolyte composition: 0.1M guanidinium thiocyanate, 1.0M dimethylimidazolium iodide (DMII), 0.03M $I_2$, 0.5M *tert*-butylpyridine, and 1.0M LiI in 85:15 MeCN/valeronitrile. [Dye solution]= 0.3 mM in THF/EtOH (1:4) with 40x CDCA.

[e] Electrolyte composition: 1.0M 1,3-dimethylimidazolium iodide (DMII), 100 mM LiI, 30 mM $I_2$, 0.5M *tert*-butylpyridine,0.1M guanidinium thiocyanate (GNCS) in acetonitrile.

Paek et al.[223] synthesized organic dyes containing 3,4-ethylenedioxythiophene and thienothiophene as π-spacers and studied the effect of introducing long alkyl groups on it (**v**). Efficiencies between 5.34 and 8.70 % were obtained, with the best efficiencies being predominant for hexyl and hexyloxy substituents. Choi and co-workers[224] synthesized two thienothiophene-vinylene-thienothiophene dyes, the introduction of two aryl groups, a phenyl ring (**vi-a**) and a benzothiophene ring (**vi-b**), to extend the conjugation length was compared. The applications of these dyes in DSSCs achieved efficiencies of 8.0 % and 9.1 % for phenyl (**vi-a**) and benzothiophene (**vi-b**) derivatives respectively. The introduction of ethynyl-thienothiophene as π-spacer was introduced by Hong's group (**vii-a** and **vii-b**).[225] According to their experiments, adding a second thienothiophene moiety to the molecule (**vii-b**) narrows the bandgap and improves the light-harvesting in the visible region. However, the structural planarity and HOMO level of the dye are badly impacted by the extended conjugation which results in lower $V_{oc}$ and FF values. Marco *et al.*[226] presented the synthesis of four dyes bearing a 4*H*-pyranylidene donor, a thienothiophene unit as π-bridge and cyanoacrylic acid as anchoring group, with the best performing dye in this study achieving an efficiency of 6.41 % (**viii-d**) (**Figure 50**, **Table 20**).

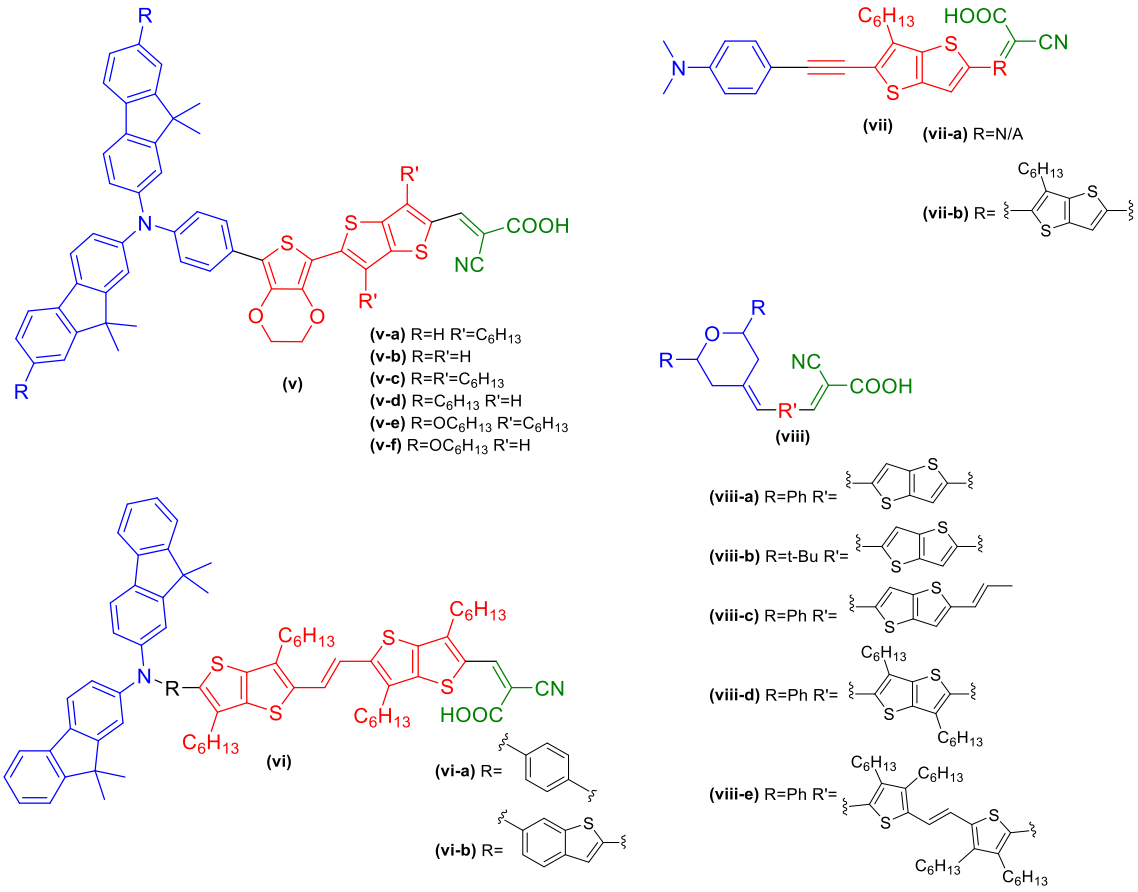


Figure 50. Chemical structures of dyes containing thienothiophenes for DSSC application.

Table 20. Spectroscopic and photovoltaic parameters of sensitizers applied in DSSCs thienothiophenes.

| Dye | λmax (nm) | ε ($M^{-1}$ $cm^{-1}$) | $J_{sc}$ ($mA/cm^2$) | $V_{oc}$ (mV) | FF | η (%) | Ref |
|---|---|---|---|---|---|---|---|
| **v-a** | 368 / 450 | 38 100 / 23 100 | 13. 02 | 0.57 | 0.72 | 5.34 | 223 a |
| **v-b** | 371 / 481 | 25 700 / 25 000 | 13.81 | 0.59 | 0.68 | 5.65 | |
| **v-c** | 371 / 455 | 44 900 / 32 100 | 16.34 | 0.64 | 0.74 | 7.83 | |
| **v-d** | 370 / 476 | 38 300 / 38 400 | 15.22 | 0.58 | 0.70 | 6.21 | |
| **v-e** | 370 / 466 | 69 600 / 45 1000 | 17.49 | 0.70 | 0.70 | 8.70 | |
| **v-f** | 369 / 484 | 46 300 / 47 800 | 15.94 | 0.66 | 0.67 | 7.04 | |
| **vi-a** | 365 / 480 | 51 800 / 73 800 | 15.7 | 0.690 | 0.74 | 8.0 | 224 b |

| | | | | | | | |
|---|---|---|---|---|---|---|---|
| **vi-b** | 365 / 490 | 50 400 / 85 000 | 17.6 | 0.710 | 0.72 | 9.1 | |
| **vii-a** | 419 | 46 700 | 12.55 | 0.627 | 0.69 | 5.46 | 225 [c] |
| **vii-b** | 455 | 50 400 | 14.85 | 0.587 | 0.58 | 5.07 | |
| **viii-a** | 551 | 21 380 | 13.51 | 0.519 | 0.59 | 4.13 | 226 [d] |
| **viii-b** | 562 | 28 106 | 16.94 | 0.569 | 0.63 | 6.06 | |
| **viii-c** | 583 | 39 811 | 10.05 | 0.475 | 0.56 | 2.68 | |
| **viii-d** | 574 | 44 668 | 16.82 | 0.592 | 0.64 | 6.41 | |
| **viii-e** | 626 | 25 119 | 12.30 | 0.571 | 0.64 | 4.45 | |

[a] Electrolyte composition: 0.6 M DMPImI, 0.05 $I_2$, and 0.1 M LiI in acetonitrile. [Dye solution]= 0.3 mM in EtOH/THF (2/1) containing 10 mM of CDCA.

[b] Electrolyte composition: 0.6m DMPImI, 0.05m $I_2$, 0.1m LiI, and 0.5M tert-butylpyridine in acetonitrile. [Dye solution]= 0.3 mM in THF.

[c] Electrolyte solution: Iodolyte AN-50, Solaronix. [Dye solution]= 0.5 mM in ethanol. Reference dye: N-719 (η= 5.57 %).

[d] [Dye solution]= 0.3 mM $CH_2Cl_2$ containing 0.3mM of CDCA.

### 4.1.2 The donors

#### Phenoxazine and phenothiazine

Phenoxazine (POZ) and phenothiazine (PTZ) are two structural analogs of acridine with notable donor properties (**Figure 51**). Phenoxazine is a heterocyclic compound containing electron-rich oxygen and nitrogen heteroatoms, whereas phenothiazine contains a sulfur heteroatom instead of oxygen. Their non-planar rings with a bent conformation (butterfly-like geometry) in the ground state help to avoid molecular aggregation and the formation of excimers. These structures exhibit superior ability to harvest light in the visible region, and good thermal and electrochemical stability. It is possible to carry out selective halogenation reactions, and by adjusting the reaction conditions large yields of mono- or di-halogenated phenothiazine can be obtained. This facilitates the use of metal-catalyzed coupling reactions to extend the π-system of the molecules.[76,228-230] Various structural modifications can be made, such as introducing different alkyl or aryl groups in the nitrogen atom and functionalizing the C7 and C3 positions. It has been observed that branched alkyl chains, such as ethylhexyl, present in the nitrogen atom allow to achieve better results in DSSC application.[76,231,232]

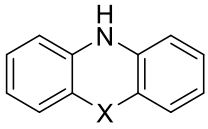


X = O 10*H*-phenoxazine
X = S 10*H*-phenothiazine

Figure 51. Chemical structure of phenothiazine and phenoxazine.

### Carbazole

Carbazole is a heterocyclic compound with a planar tricyclic skeleton, consisting of two fused benzene rings on either side of a central pyrrole ring (**Figure 52**). This molecular system has been used in several applications, such as conductive materials, liquid crystals, and in the optical and thermoelectric fields. Although carbazole has been studied in DSSCs, it has not been explored as extensively as other donors.[233,234] Komura et al. investigated carbazole dyes linked to linear oligothiophenes. DSSC devices containing these molecules achieved efficiencies of around 7 %.[235]

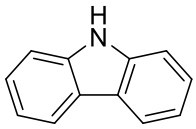


Figure 52. Chemical structure of carbazole.

## 4.2 Results and discussion

Considering the promising properties of the dyes containing the thienothiophene nucleus, a family of compounds containing this moiety in their π-bridge has been proposed. The design features a D-π-$(A)_2$ structure (**Figure 53**), where the π-spacer can be extended by attaching a phenyl or thiophene group. Phenothiazine and carbazole will be tested as donor groups in these molecules.

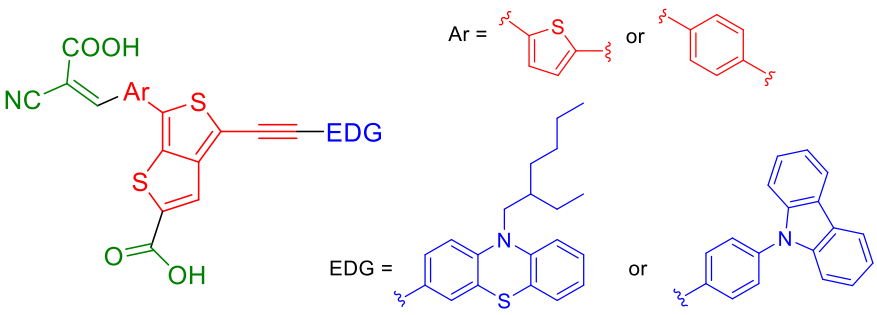


Figure 53. Delineated chromophores with a D-π-$(A)_2$ architecture containing a thieno[3, 4-*b*]thiophene in their π-bridge.

## 4.2.1 Synthetic methodology

### 4.2.1.1 Development of the π-spacer

The most challenging part of this synthetic pathway is the development of the π-spacer. The starting material is 3,4-dibromothiophene, from this compound a thieno[3,4-*b*] core is formed. Then phenyl or thiophene rings are linked into it. The presence of an aldehyde and an ester group in the molecule at this stage is vital to form the anchoring groups in the final steps of the synthesis (**Figure 54**).

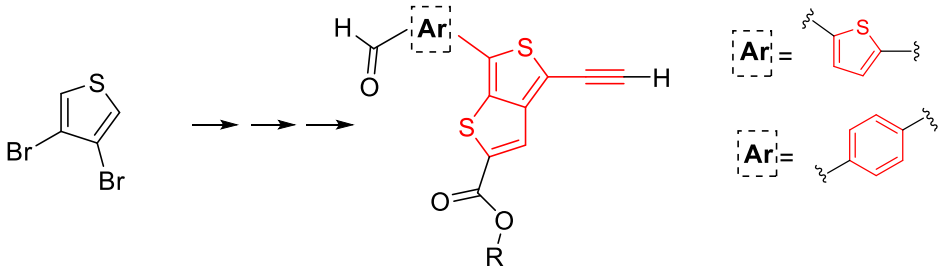


Figure 54. Chemical structure of π-spacer.

Following the methodology developed by Keller[236], the synthesis of these dyes starts with the formylation of 3,4-dibromothiophene (**4.1**), the compound reacts with *n*-BuLi and a lithium halogen exchange occurs. After quenching with DMF, the 4-bromothiophene-3-carbaldehyde (**4.2**) was obtained with 48 % yield. Then, through a copper-catalysed thiol cross-

coupling/condensation reaction between the bromoaldehyde and methyl/ethyl sulfanylacetate the ethy/methyl thieno[3,4-*b*]thiophene-2-carboxylate (**4.3**) was afforded (**Scheme 30**).

To extend the conjugated system, a bromine is introduced in position 6 by reacting the previous compound **4.3** with NBS. A mixture of the 6-bromo- (**4.4a**) and the 4-bromothieno[3,4-b]thiophene-2-carboxylate (**4.4b**) (76:24) was obtained.[86,236] The isomers were identified based on the $^{1}$H NMR signals for protons 6 and 4, observed at 7.52 ppm and 7.24 ppm, respectively. It was not possible to separate the two isomers, as so in the next reaction steps, the presence of the two isomeric reaction products was identified. Despite that, at the end of the synthesis, it was possible to afford the final chromophores in their pure form. The obtained mixture of **4.4a** and **4.4b** changed its colour from pink to black and became insoluble in only a few hours, even protected from light and in a cold environment. Its degradation was evident, and, in fact, the next reactional step was several times unfruitful or low yields were achieved. In the literature it is referred that this C-Br bond can suffer photocleavage, followed by bromine initiated cationic polymerization. [237] To overcome this issue, a solution containing benzoquinone was introduced in each test tube during the chromatographic purification step to avoid C-Br bond cleavage (**Scheme 30**).

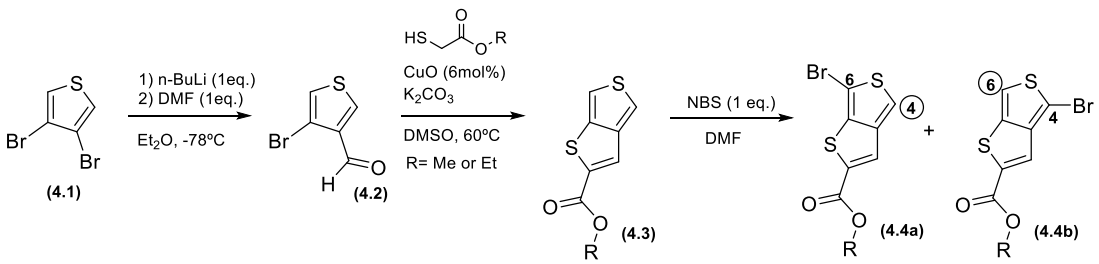


Scheme 30. Synthesis of compounds **4.4a** and **4.4b** starting from 3,4-dibromothiophene (**4.1**)

## The C-C bond formation dilemma

Keller et al.[236]report the formation of a C-C ($sp^2$-$sp^2$) bond between position 6 of the 4-bromothieno[3,4-*b*]thiophene-2-carboxylate and thiophene-2-carbaldehyde to obtain compound **4.5** through a Stille coupling (**Scheme 31**). We did not choose this method due to the toxicity of organotin derivatives. Direct arylation between **4.3** and 5-bromothiophene-2-carbaldehyde (**4.7**) to avoid the synthesis of the sensitive bromine compound was attempted. However, it seems that the C-C bond formation occurred at a different position of the molecule. Hiyama coupling was also considered to avoid the sensitive bromination reaction.

Nevertheless, this method requires the introduction of the silyl group followed by the formation of silanol, which increases the number of reaction steps. It seemed that the most adequate method for the achievement of **4.5** was the Suzuki-Miyaura cross-coupling (**Scheme 31**).

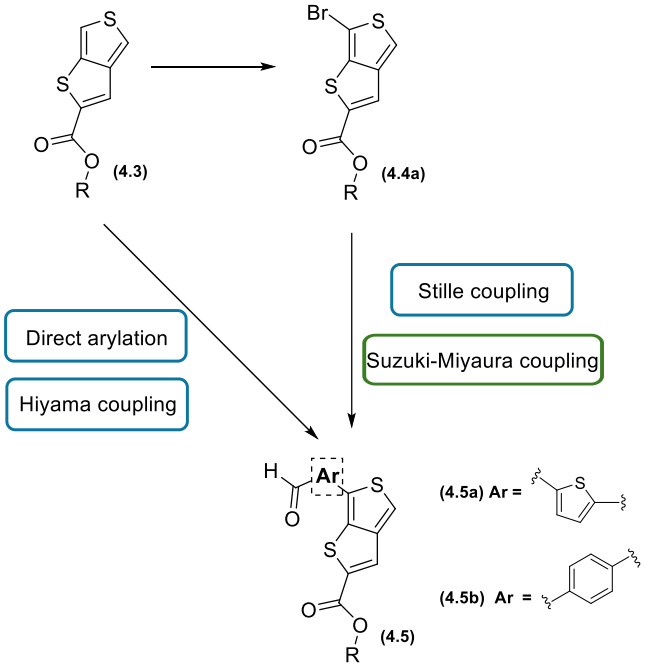


Scheme 31. Possible pathways to achieve compounds **4.5a** and **4.5b**.

In chapter 2 an overview of the Sonogashira palladium cross-coupling is reported. Here, a brief description of the Suzuki-Miyaura coupling reaction is given, which is vital for this synthetic pathway. The Suzuki cross-coupling reaction enables the formation of C-C ($sp^2$-$sp^2$) bonds formation between boronic acids or esters and vinyl halides, aryl halides or triflates in the presence of a Pd(0) catalyst and a base (usually in aqueous solution). The use of organoboron compounds offers the advantage of using an easily available reagent that is low in toxicity and highly stable with water and various functional groups (**Figure 55**).

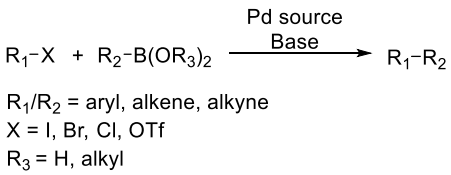


Figure 55. Suzuki-Miyaura cross-coupling reaction.

The catalytic cycle of Suzuki-Miyaura reaction begins with the oxidative addition of Pd(0) to the $R_1$-X bond of the organohalide, resulting in the formation of the $R_1$-Pd(II)-X complex. Subsequently, transmetalation between the aforementioned complex and the boronate $R_2$-$B(OH)_3$ occurs forming $R_1$-Pd(II)-$R_2$. The aqueous base plays a crucial role in this step by increasing the electronegativity of the organoborane. Additionally, the base's hydroxyl groups help to form a bridge with the R1-Pd(II)-X complex, making it a more reactive species. In the end, reductive elimination occurs, resulting in the formation of the C-C coupling product $R_1$-$R_2$ (**Figure 56**).[238,239]

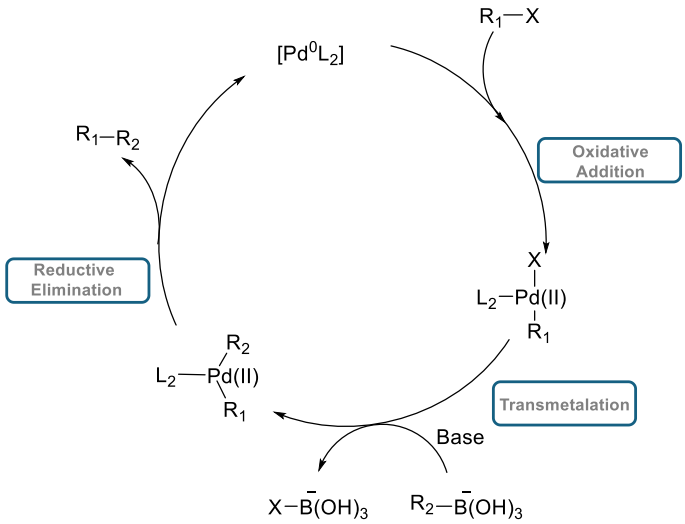


Figure 56. Catalytic cycle of Pd in Suzuki-Miyaura coupling.

The mixture **4.4a** and **4.4b** was used in a Suzuki cross-coupling with the respective boronic ester (**4.9** or **4.11**; the synthesis of the boronic ester is illustrated below in **Scheme 33**) to afford compound **4.5a** and **4.5b**. In the case of using compound **4.9**, after Suzuki- coupling the acetal protecting group was hydrolyzed with HCl to obtain **4.5a**. Then, bromination in position 4 of the thienothiophene was performed in the dark at room temperature with NBS in $CHCl_3$ to afford **4.6** (**Scheme 32**).

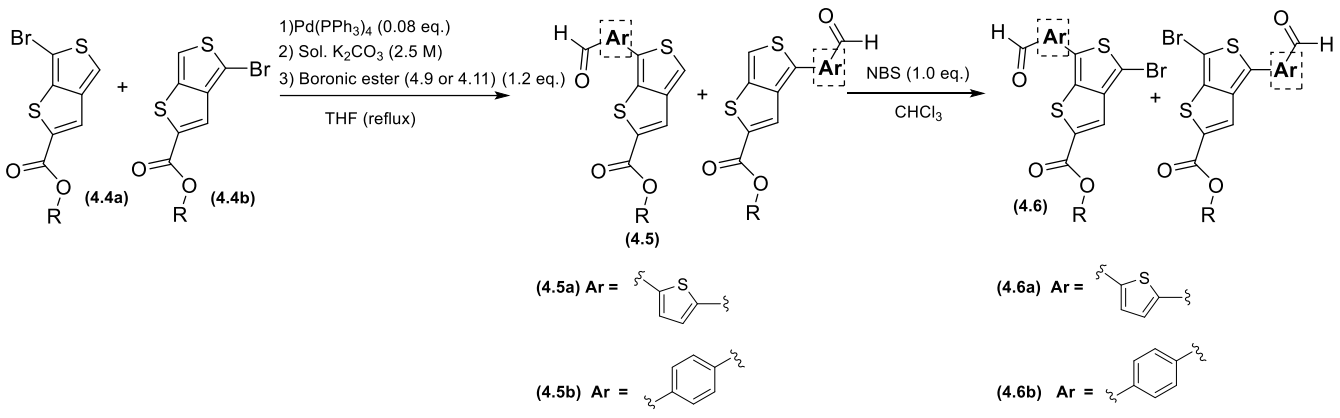


Scheme 32. Suzuki coupling to obtain **4.5a** and **4.5b** and bromination reaction to obtain **4.6**.

## Synthesis of boronic esters

The Suzuki coupling reaction requires the synthesis of boronates. In the case of the thiophene ring the synthesis started from 5-bromothiophene-2-carbaldehyde (**4.7**). The aldehyde group was protected with an acetal to avoid hydroboration in the next reactional step. Then lithiation-borylation occurs and the boronic ester **4.9** is obtained (**Scheme 33**).

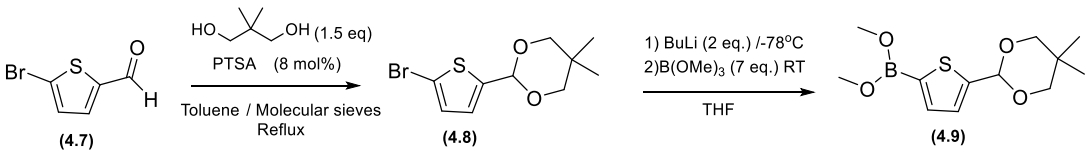


Scheme 33. Synthesis of boronic ester **4.9**.

For the synthesis of **4.11** the starting material was 4-bromobenzaldehyde (**4.10**). The previous procedure was unfruitful for this molecule. This way, a Miyaura borylation reaction was performed via a palladium-catalyzed cross-coupling reaction of bis(pinacolato)diboron with 4-bromobenzaldehyde (**4.10**) (**Scheme 34**).[240]

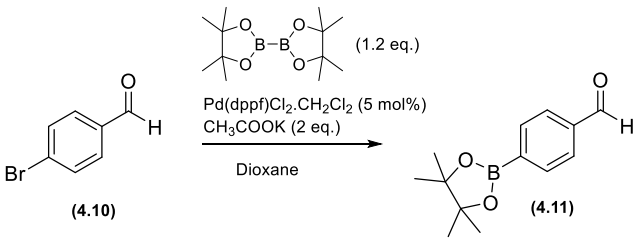


Scheme 34. Miyaura borylation reaction for the preparation of compound **4.11**.

#### 4.2.1.2 Development and introduction of donors

The chosen donors to be introduced into 4.6 were a phenothiazine with an etylhexyl chain in the nitrogen and 9-phenyl-9*H*-carbazole (**Figure 57**)

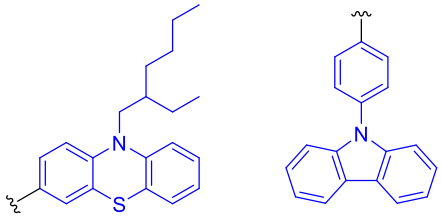

Figure 57. Chemical structures of donors 10-(2-ethylhexyl)-10*H*-phenothiazine and 9-phenyl-9*H*-carbazole.

The functionalization of the phenothiazine (**4.12**) starts with the alkylation of the nitrogen atom with 3-(bromomethyl)heptane, to afford the alkylated product (**4.13**). Then the compound is brominated selectively in position 7 with NBS to afford **4.14**. After this, the ethynyl group is introduced via Sonogashira coupling to obtain **4.15** (**Scheme 35**). Hydrolysis of the trimethylsilyl group to attain **4.16** was achieved in a one-pot reaction immediately previously to the use of the intermediate in the following Sonogashira coupling reaction.

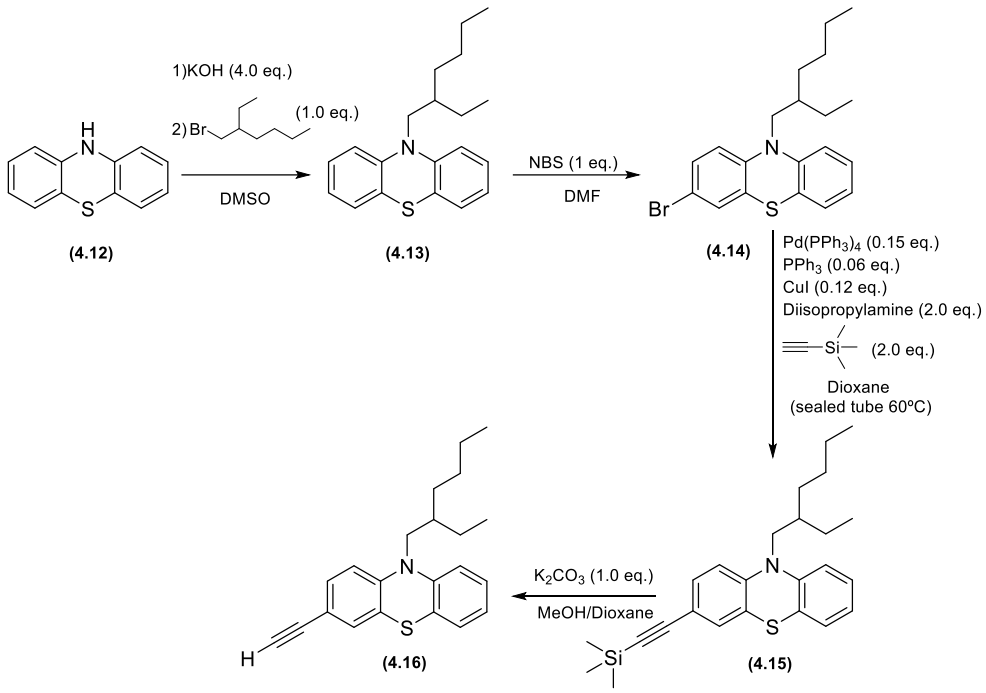


Scheme 35. Derivatization of phenothiazine.

Carbazole (**4.17**) was treated with base and then reacted with 1-fluoro-4-iodobenzene to obtain 9-(4-iodophenyl)-9*H*-carbazole (**4.18**). Afterwards the ethynyl group was introduced to obtain **4.19** (**Scheme 36**). Again, hydrolysis of the trimethylsilyl group to attain **4.20** was achieved in a one-pot reaction immediately previously to the use of the intermediate in the following Sonogashira coupling reaction.

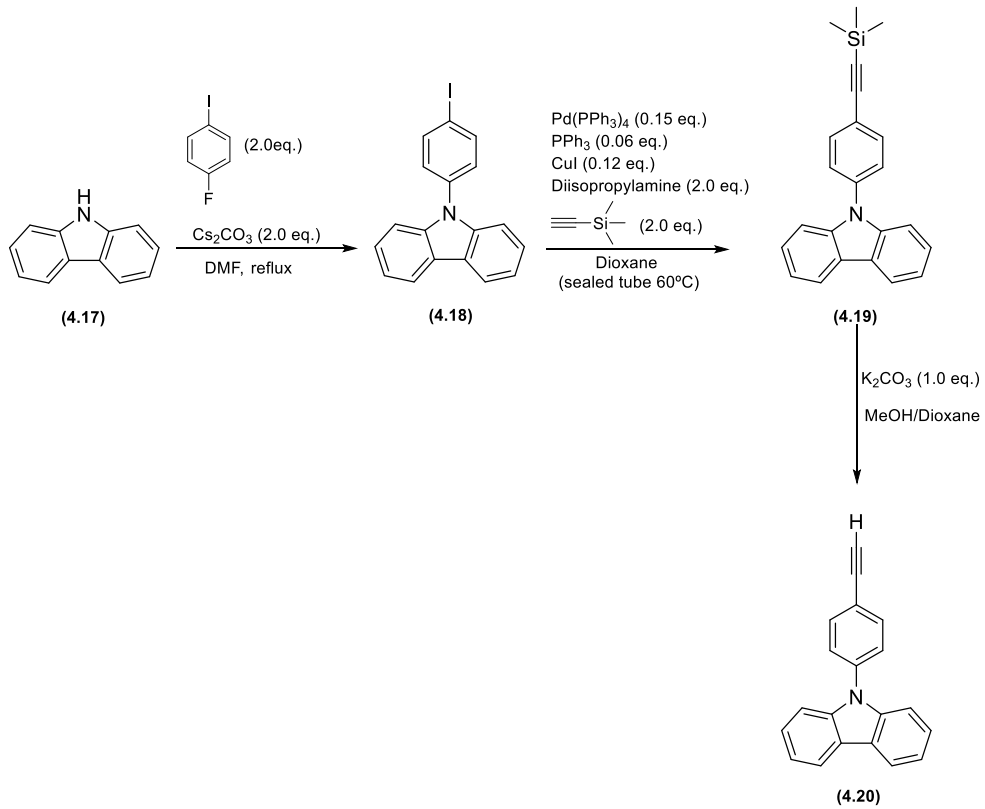


Scheme 36. Derivatization of carbazole.

The next synthetic steps involved the Sonogashira coupling between compound **4.6** and the donnor units **4.16** and **4.20** to obtain compounds **4.21a-d** (**Scheme 37**).

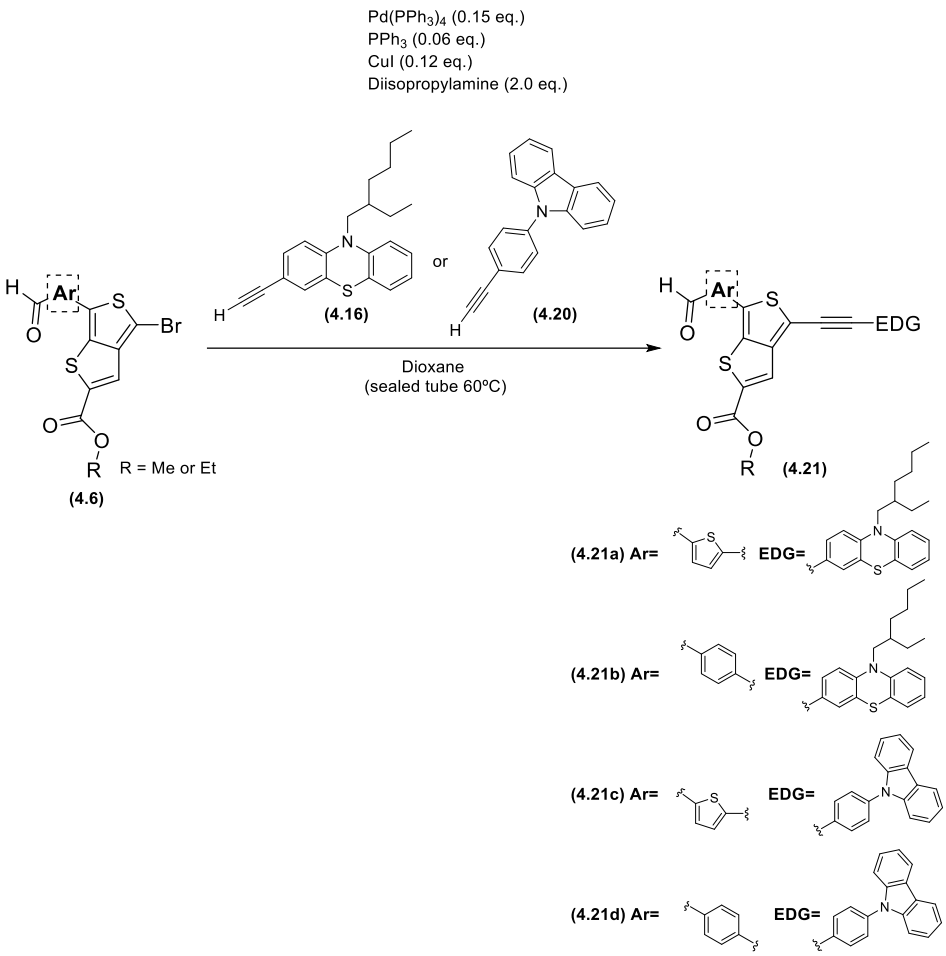


Scheme 37. Synthesis of compounds **21a-d** via Sonogashira coupling.

#### 4.2.1.3 Introduction of anchoring groups

The ester group was hydrolysed with NaOH to form the carboxylic acid anchoring group. Afterwards, the introduction of the cyaonoacrylic acid was achieved by a Knoevenagel condensation between the aldehyde moiety and the cyanoacetic acid. Thus, four final chromophores **4.23 a-d** were obtained to be studied in DSSCs devices (**Scheme 38**).

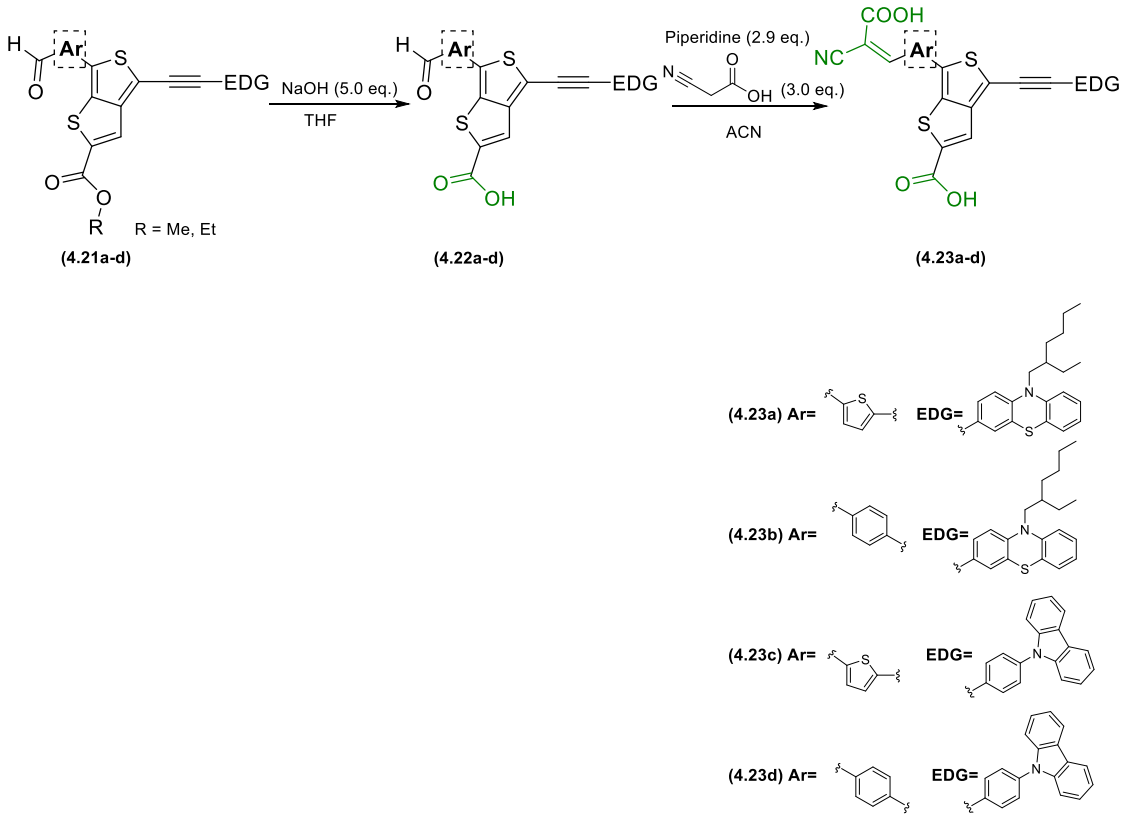


Scheme 38. Synthesis of the final chromophores **4.23a-d**.

The final structures were confirmed using $^{1}$H NMR. When the compounds exhibited sufficient solubility to prepare a more concentrated solution, characterization by $^{13}$C NMR was also possible. Additionally, HRMS analysis confirmed the identification of the final product.

### 4.2.1 Photophysical and photovoltaic studies

The performance of the final chromophores (**3.23a-d**) was evaluated in DSSC devices by measuring their current-voltage(*I-V*) curves. The photovoltaic parameters, including open-circuit voltage ($V_{oc}$), short-circuit current ($J_{sc}$), fill factor (FF) and photovoltaic conversion efficiency (η) along with the *I-V* curves are presented in **Figure 58** and **Table 21**. The best performing dye was the derivative containing a phenyl ring linked to the π–bridge and a phenothiazine as the donor unit (**4.23b**) (η = 1.96%). The compound achieved also the best $V_{oc}$ value, 0.376 V. In compounds containing a thiophene ring (**4.23a** and **4.23c**) the best results were achieved when the donor was a carbazole. For compounds containing a phenyl ring (**4.23b** and **4.23d**), better results were achieved with a phenothiazine moiety present in the molecule.

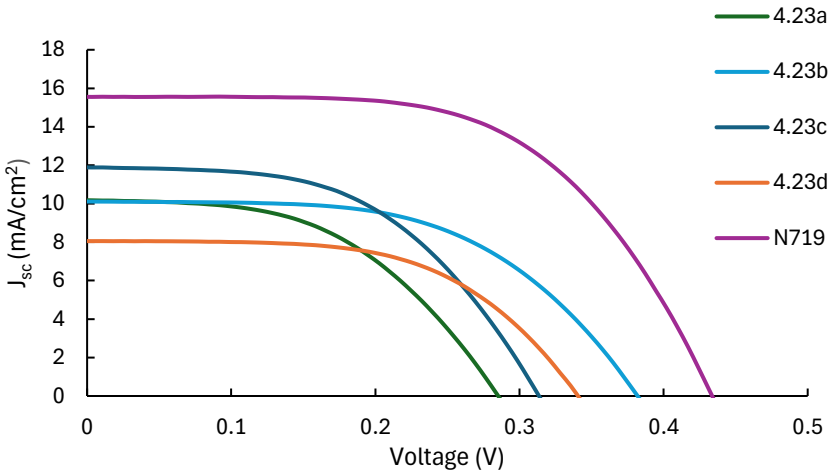


Figure 58. *I–V* curves of the test cells based on the synthesized thieno[3,4-*b*]thiophene based dyes and reference N-719 under 100 mW.cm$^{-2}$ simulated AM 1.5 illumination (best performing cell).

Table 21. Performance values of the test cells based on the dyes **4.23a-d** under 100 mW.cm$^{-2}$ AM 1.5 illumination. The results presented correspond to the average values of at least two cells per dye, each cell measured 5 times. The prepared anodes were soaked for 16 h in an $CH_2Cl_2$/MeOH/$H_2O$ 65:35:5 (%v/v) solution of the dye (0.5 mM), at room temperature in the dark. Electrolyte composition: 0.8 M LiI and 0.05 M $I_2$ in an acetonitrile/valeronitrile (85:15, % v/v).

| Dye | $V_{oc}$/V | $J_{sc}$/mA cm$^{-2}$ | $V_{max}$/V | $J_{max}$/mA cm$^{-2}$ | FF | η/% |
|---|---|---|---|---|---|---|
| **4.23a** | 0.283±0.004 | 10.69±0.45 | 0.173±0.01 | 8.00±0.07 | 0.46±0.04 | 1.39±0.05 |
| **4.23b** | 0.376±0.004 | 9.40±0.57 | 0.252±0.01 | 7.77±0.43 | 0.55±0.01 | 1.96±0.13 |
| **4.23c** | 0.323±0.02 | 11.21±1.76 | 0.213±0.03 | 8.86±0.99 | 0.52±0.07 | 1.86±0.09 |
| **4.23d** | 0.327±0.01 | 8.06±0.12 | 0.220±0.01 | 6.65±0.08 | 0.56±0.01 | 1.47±0.05 |
| **N719** | 0.427±0.02 | 14.28±1.23 | 0.289±0.02 | 12.01±1.01 | 0.57±0.02 | 3.46±0.33 |

The IPCE spectra of the thieno[3,4-*b*]thiophene derivatives are displayed on **Figure 59**. The dyes bearing a thiophene ring **4.23a** and **4.23c** showed maximum IPCE values at 510 nm, which were 29 % and 33% respectively. The dyes containing a phenyl ring **4.23b** and **4.23d** showed maximum IPCE values at 480 nm, which were 13% and 26 % respectively.

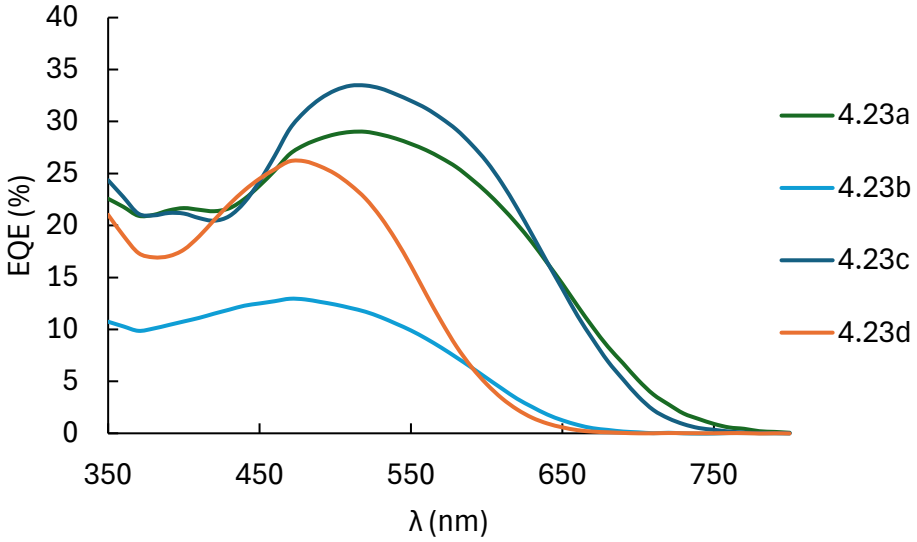


Figure 59. IPCE spectra for the DSSCs based on dyes **4.23a-d** (best performing cell).

## 4.3 Conclusion

It was successfully synthesized, for the first time, dianchoring dyes based on thieno[3,4-*b*]thiophene core. The synthesis was highly demanding, involving multiple steps and the potential formation of isomeric structures, which made the purification process somewhat challenging. Variations were made to the π-bridge (phenyl or thiophene) and the donor unit (phenoxazine or carbazole) to evaluate their impact when applied in DSSC devices. The derivative containing phenyl ring and a phenothiazine as donor (**4.23b**) was the best performing dye with $V_{oc}$ $J_{sc}$ and FF values of 0.376 V, 9.40 mA/cm$^2$ and 0.55, respectively. Which resulted in an efficiency of 1.96 %.

## 4.4 Experimental section

The synthetic methods and the fabrication of the photovoltaic devices were performed as described in Chapter 2 - Section 2.4.

*Synthesis of 4-bromothiophene-3-carbaldehyde (**4.2**)*

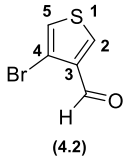

(4.2)

Following the methodology of Keller[236], in a round bottom flask equipped with a magnetic stir bar were added 3 mL of dry diethyl ether and 0.46 mL of 3,4-dibromothiophene (**4.1**) (4.13 mmol). The mixture was cooled to -78 °C and then 2.58 mL of n-BuLi (1.6 M in hexanes) was added dropwise (4.13 mmol, 1 eq.). The reaction was stirred for 15 minutes and 0.32 mL of DMF (4.13 mmol, 1 eq.) were added to the reactional mixture. The reaction was stirred for 3h at -78 °C and then was slowly warmed to room temperature. Then $H_2O$ was added to perform the quenching of the reaction. The product was extracted with dichloromethane, the combined organic layers were dried over $Na_2SO_4$, filtered and evaporated to dryness. The crude was purified by column chromatography (flash) using the eluent hexane/ethyl acetate 9/1, affording 381 mg of 4-bromothiophene-3-carbaldehyde (**4.2**) (1.20 mmol, η=48.3 %). Spectroscopic data in accordance with the literature. [236] **ATR (ν ($cm^{-1}$)):** 3103 (w, C-$H_{aryl}$), 2856 (w, C-$H_{aldehyde}$) 1680 (s, C=$O_{aldehyde}$), 1490-1409 (C=C). $^1$H **NMR (400 MHz, $CDCl_3$) δ (ppm):** 9.95 (s, 1H, CHO), 8.16 (d, *J* = 3.4 Hz, 1H, H2), 7.36 (d, *J* = 3.4 Hz, 1H, H5). **$^{13}$C NMR (101 MHz, $CDCl_3$) δ (ppm):** 184.9 (CHO), 137.6 (C3), 134.7 (C2) , 125.2 (C5), 111.4 (C4).

*Synthesis of methyl thieno[3,4-b]thiophene-2-carboxylate (**4.3**)*

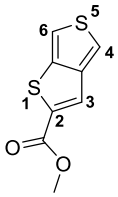

(4.3)

Following the methodology developed by Keller[236], to a solution of 4-bromothiophene-3-carbaldehyde (**4.2**) (748.9 mg, 3.92 mmol), $K_2CO_3$ (812 mg, 5.88 mmol, 1.5 eq.), CuO (19.0 mg, 0.24 mmol, 6 mol %) in 7.8 mL of DMSO at 60 °C was added methyl 2-sulfanylacetate (0.40 mL, 4.31 mmol, 1.1 eq.). The reaction was followed by TLC using the eluent hexane / ethyl acetate 9/1, after 32 hours the reaction was complete, cold $H_2O$ and brine were added to the solution and the product was extracted with $CH_2Cl_2$. The organic layers were washed with brine, dried over $Na_2SO_4$, filtered and evaporated to dryness. The crude was purified by column chromatography (flash) using the eluent hexane/ethyl acetate 95/5. It was possible to afford of 526 mg of methyl thieno[3,4-*b*]thiophene-2-carboxylate (**4.3**) (2.65 mmol, η= 68%). %). Spectroscopic data in accordance with literature. [236]

**$^1$H NMR (400 MHz, $CDCl_3$) δ (ppm):** 7.71 (s, 1H, H3), 7.60 (d, *J* = 2.8 Hz, 1H, H4), 7.29 (d, *J* = 3.6 Hz, 1H, H6), 3.92 (s, 3H, $CH_3$).

*Synthesis of methyl 6-bromothieno[3,4-b]thiophene-2-carboxylate (**4.4a**) and methyl 4-bromothieno[3,4-b]thiophene-2-carboxylate (**4.4b**)*

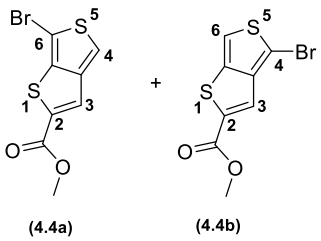

(4.4a) (4.4b)

Following the methodology developed by Keller[236], in a round bottom flask, methyl thieno[3,4-*b*]thiophene-2-carboxylate (**4.3**) (536 mg, 2.71 mmol) was dissolved in 19 mL of $CHCl_3$ and stirred in the dark at 0 °C. Then was added dropwise a solution of N-bromosuccinimide (506 mg, 2.84 mmol, 1.05 eq.) in a mixture of $CHCl_3$ and DMF (19 mL/2 mL). The reaction was stirred at room temperature during 21 h and it was followed by TLC using the eluent petroleum ether/ $CH_2Cl_2$ 8/2. The solvent was removed and the crude was purified via column chromatography using the aforementioned eluent. Due to the instability of the brominated compound it was necessary to add 0.5 mL of a solution containing benzoquinone (0,1M) in each test tube to avoid possible photoinduced polymerization. It was possible to isolate a fraction containing methyl 6-bromo- and the 4-bromothieno[3,4-*b*]thiophene-2-carboxylate (**4.4a** and **4.4b**) (83:17, 239mg, 0.863 mmol, η≈ 32 %)[c] and benzoquinone. This mixture was directly used in the next reaction step. Methyl 4,6-dibromothieno[3,4-*b*]thiophene-2-carboxylate was also isolated (137 mg, 0.39 mmol, η= 14%).

**General procedure for the Suzuki coupling between the compounds 4.4a and 4.4b with borates 4.9 and 4.11.**

To a degassed double neck round bottom flask were added $Pd(PPh_3)_4$ (0.16 eq.) and a mixture of the 6-bromo- and the 4-bromothieno[3,4-*b*]thiophene-2-carboxylate (**4.4a** and **4.4b**) (1 eq.) dissolved in degassed THF. The reactional mixture was refluxed for 20 minutes, after this a 2.5M aqueous solution of $NaHCO_3$ (degassed, 10 eq.) was added. The boron derivative (**4.9** or **4.11**, 1.2 eq.) dissolved in degassed THF was added 20 minutes later. The reaction was stirred at reflux until total consumption of the starting material.

[c] Due to the high volatility of benzoquinone, it is not possible to quantify the precise amount of different species, so the yield of 4.4a and 4.4b can only be approximated.

*Synthesis of ethyl 6-(5-formylthiophen-2-yl)thieno[3,4-b]thiophene-2-carboxylate (**4.5a**)*

**Step1**

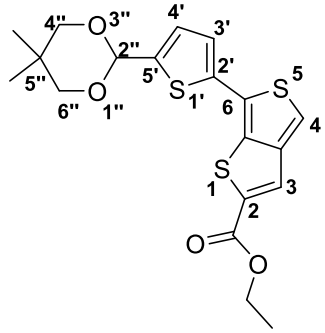

To a round bottom flask containing a mixture (130.1 mg) of the 6-bromo- and the 4-bromothieno[3,4-*b*]thiophene-2-carboxylate (**4.4**) (110.1mg, 0.38mmol, 1.0 eq.) were added 72.74 mg of $Pd(PPh_3)_4$ (0.06 mmol, 16 mol %) and 2 mL of THF. The solution was degassed under vacuum. The reactional mixture was refluxed for 20 minutes, after this 0.60 mL of a 2.5 M aqueous solution of $K_2CO_3$ (1.512 mmol, 4.0 eq.) was added. After 20 minutes was added the reactional mixture containing (5-(5,5-dimethyl-1,3-dioxan-2-yl)thiophen-2-yl)boronic acid (**4.9**) (1.2 eq.). The reaction was stirred under reflux for 21 hours, and it was followed by TLC using as eluent a mixture of hexane/EtOAc 7/3. The solvent was removed under vacuum and water was added, the product was extracted with $CH_2Cl_2$. The organic layers were combined and dried over $Na_2SO_4$, filtered and evaporated to dryness. The crude was purified via column chromatography using as eluent a mixture of hexane/ ethyl acetate 8/2, to afford 82 mg of ethyl 6-(5-(5,5-dimethyl-1,3-dioxan-2-yl)thiophen-2-yl)thieno[3,4-*b*]thiophene-2-carboxylate (0.20 mmol, η=52.6 %).**$^1$H NMR (400 MHz, $CDCl_3$) δ (ppm):** 7.96 (s, 1H,H3), 7.17 (d, *J* = 4.0 Hz, 1H,H4), 7.13 (s, 1H,H3'), 7.10 (d, *J* = 4.0 Hz, 1H,H4'), 5.65 (s, 1H, H2''), 4.39 (q, *J* = 7.2 Hz, 2H,$CH_2$), 3.79 (d, *J* = 10.8 Hz, 2H), 3.66 (d, *J* = 10.8 Hz, 2H), 1.40 (t, *J* = 7.2 Hz, 3H, $CH_3$), 1.31 (s, 3H), 0.82 (s, 3H). **HRMS-ESI(+)** calculated for $C_{18}H_{18}O_4S_3$ $[M+H]^+$ 395.04400; Found 395.0436

**Step 2**

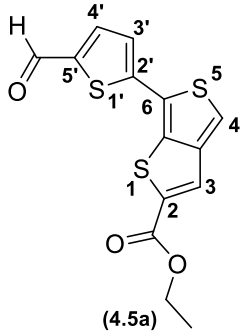

(4.5a)

Ethyl 6-(5-(5,5-dimethyl-1,3-dioxan-2-yl)thiophen-2-yl)thieno[3,4-*b*]thiophene-2-carboxylate (**4.5a**) (149.6 mg, 0.37 mmol) was dissolved in 10 mL of THF and 1.5 mL of a 1M HCl aqueous solution was added. The reaction was stirred under $N_2$ atmosphere for 70 hours. The solvent was removed under vacuum and water was added. The product was extracted with $CH_2Cl_2$, the combined organic layers were dried over $Na_2SO_4$, filtered and evaporated to dryness. The resulting crude was purified by column chromatography using the eluent $CH_2Cl_2$ / hexane 7/3 to afford 76 mg of compound **4.5a** (0.24 mmol, η= 64.0 %). Spectroscopic data in accordance with literature[236]. **$^1$H NMR (400 MHz, $CDCl_3$) δ (ppm):** 9.91 (s, 1H, CHO), 8.00 (s, 1H, H3), 7.73 (d, *J* = 4.0 Hz, 1H, H4'), 7.37 (d, *J* = 4.0

Hz, 1H, H3'), 7.34 (s, 1H, H4), 4.42 (q, *J* = 7.1 Hz, 2H, $CH_2$), 1.43 (t, *J* = 7.2 Hz, 4H, $CH_3$). **HRMS-ESI(+)** calculated for $C_{13}H_8O_3S_3$ $[M+H]^+$ 308.97083; Found 308.9711

*Synthesis of methyl 6-(4-formylphenyl)thieno[3,4-b]thiophene-2-carboxylate (**4.5b**)*

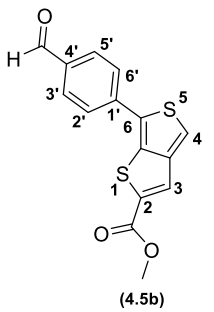


Starting from a mixture containing 6-bromo- and the 4-bromothieno[3,4-*b*]thiophene-2-carboxylate (**4.4**) (0.86 mmol, 1 eq.) and 4-(4,4,5,5-tetramethyl-1,3,2-dioxaborolan-2-yl)benzaldehyde (**4.11**) ( 1.30 mmol, 1.5 eq.). The reaction was monitored by TLC using the eluent petroleum ether/ ethyl acetate 9/1 and after 20h the reaction was complete. The solvent was removed, water was added and the compound was extracted to the organic phase with $CH_2Cl_2$. The organic phases were washed with brine, dried over $Na_2SO_4$, filtered and evaporated to dryness. The crude was purified by column chromatography using as eluent $CH_2Cl_2$/petroleum ether 8/2 to $CH_2Cl_2$/MeOH 98/2. It was possible to afford a yellow solid corresponding to methyl 6-(4-formylphenyl)thieno[3,4-*b*]thiophene-2-carboxylate (**4.5b**) (262 mg, 0.87 mmol). **$^1$H NMR (400 MHz,$CDCl_3$) δ (ppm):** 10.05 (s, 1H, CHO), 8.01 (d, *J* = 0.4 Hz, 1H, H3), 7.97 (d, *J* = 8.4 Hz, 2H, ArH ), 7.84 (d, *J* = 8.4 Hz, 2H, ArH), 7.40 (s, 1H, H4), 3.95 (s, 3H, $CH_3$). **HRMS-ESI(+)** calculated for $C_{15}H_{10}O_3S$ [M+H] 303.01441 ; Found 303.0145.

**General procedure for the bromination of 4.5a and 4.5b**

Following the methodology developed by Keller[236], to a solution of **4.5a** or **4.5b** (1 eq.) in dry $CHCl_3$ was added dropwise a solution of N-bromosuccinimide (1.2 eq) in $CHCl_3$ at 0° C. The reaction was stirred in the dark under $N_2$ until consumption of the starting material by TLC. Then water was added and the product was extracted with $CH_2Cl_2$. The organic phases were washed with brine, dried over $Na_2SO_4$, filtered and evaporated to dryness.

*Synthesis of methyl 4-bromo-6-(5-formylthiophen-2-yl)thieno[3,4-b]thiophene-2-carboxylate (**4.6a**)*

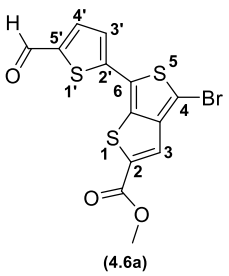


Starting from 68 mg of methyl 6-(5-formylthiophen-2-yl)thieno[3,4-*b*]thiophene-2-carboxylate (**4.5a**) (0.22 mmol) dissolved in 5.5 mL of $CHCl_3$ and 46.2 mg of N-bromosuccinimide (0.26 mmol, 1.2 eq.) in 4.5 mL of $CHCl_3$. The crude was purified by column chromatography using a mixture of $CH_2Cl_2$/ petroleum ether 8/2. It was possible to afford 70 mg of 4-bromo-6-(5-formylthiophen-2-yl)thieno[3,4-*b*]thiophene-2-carboxylate (**4.6a**) (η= 79 %).

Spectroscopic data in accordance with the literature[236]. **$^1$H NMR (400 MHz, $CDCl_3$) δ (ppm):** 9.91 (s, 1H, CHO), 7.99 (s, 1H, H3), 7.71 (d, *J* = 4.0 Hz, 1H, H4'), 7.29 (d, *J* = 4.0 Hz, 1H, H3'), 3.96 (s, 3H, $CH_3$). **$^{13}$C NMR (101 MHz, $CDCl_3$) δ (ppm):** 182.82, 163.16, 142.47, 142.14, 137.69, 137.49, 125.17, 124.81, 124.65, 124.01, 100.06. **HRMS-ESI(+)** calculated for $C_{13}H_7BrO_3S_3$ $[M+Na]^+$ 408.86329; Found 408.8628

*Synthesis of methyl 4-bromo-6-(4-formylphenyl)thieno[3,4-b]thiophene-2-carboxylate (**4.6b**)*

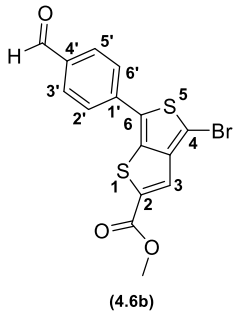

(4.6b)

Starting from 238 mg of methyl 6-(4-formylphenyl)thieno[3,4-*b*]thiophene-2-carboxylate (**4.5b**) (0.79 mmol) dissolved in 8 mL of $CHCl_3$ and 169 mg N-bromosuccinimide (0.95 mmol) dissolved in 8 mL of $CHCl_3$. The reaction was monitored by TLC using the eluent $CH_2Cl_2$/ petroleum ether 8/2. The crude was purified by column chromatography using a mixture of $CH_2Cl_2$/ petroleum ether 8/2 to only $CH_2Cl_2$. It was possible to afford 216 mg of a dark yellow compound corresponding to methyl 4-bromo-6-(4-formylphenyl)thieno[3,4-*b*]thiophene-2-carboxylate (**4.6b**) (0.57 mmol, 72%). **$^1$H NMR (400 MHz,$CDCl_3$) δ (ppm):** 10.03 (s, 1H, CHO), 7.95 (d, *J* = 8.5 Hz, 3H), 7.73 (d, *J* = 8.4 Hz, 2H), 3.95 (s, 3H, $CH_3$). **HRMS-ESI(+)** calculated for $C_{15}H_9BrO_3S_2$ $[M+H]^+$ 380.92492 ; Found 380.9250

## Synthesis of boronic esters for Suzuki coupling

*Synthesis of 2-(5-bromothiophen-2-yl)-5,5-dimethyl-1,3-dioxane (**4.8**)*

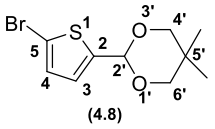

(4.8)

Following the procedure of Capodilupo[241], in a round flask containing 156 mg of neopentylglycol (1.5 mmol, 1.5 eq.) and molecular sieves were added 15 mg of *p*-toluenesulfonic acid (0.08 mmol, 8 mol %), 3 mL of dry toluene and 120 µL of 5-bromothiophene-2-carbaldehyde (1.0 mmol, 1 eq.). The reaction was refluxed for 18 h, then the solvent was removed. The crude was dissolved in ethyl acetate and washed with brine. Then combined organic layers were dried over $Na_2SO_4$, filtered and evaporated to dryness. The crude was subjected to column chromatography separation to afford 225.3 mg of 2-(5-bromothiophen-2-yl)-5,5-dimethyl-1,3-dioxane (**4.8**) (0.81 mmol, η= 81 %). **$^1$H NMR (400 MHz, $CDCl_3$) δ (ppm):** 6.93 (d, *J* = 4.0 Hz, 1H, H3), 6.87 (d, *J* = 4.0 Hz, 1H, H4), 5.54 (s, 1H, H2'), 3.73 (d, *J* = 11.6 Hz, 2H, H4'/H6'), 3.60 (d, *J* = 11.2 Hz, 2H, H4'/H6'), 1.25 (s, 3H, $CH_3$), 0.79 (s, 3H, $CH_3$).

*Synthesis of dimethyl (5-(5,5-dimethyl-1,3-dioxan-2-yl)thiophen-2-yl)boronate (**4.9**)*

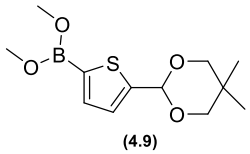
(4.9)

In a round bottom flask containing 2-(5-bromothiophen-2-yl)-5,5-dimethyl-1,3-dioxane (**4.8**) (1 eq.) and THF was added at -78 °C n-BuLi (1.6 M in hexanes, 2.0eq.). The reaction was stirred during 30 minutes at -78 °C and then trimethyl borate (7 eq.) was added. The mixture was stirred for 2h and 30 min at room temperature, then this reactional mixture was directly transferred for the Suzuki coupling reaction.

*Synthesis of 4-(4,4,5,5-tetramethyl-1,3,2-dioxaborolan-2-yl)benzaldehyde (**4.11**)*

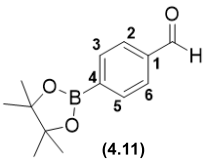
(4.11)

Following the methodology of Gao[240], in a round bottom flask were added 500 mg of 4-bromobenzaldehyde (2.70 mmol), 7.5 mL of dioxane, 443 mg potassium acetate (5.40 mmol, 2.0 eq.), 824 mg of bis(pinacolato)diboron (3.24 mmol, 1.2 eq.) and 110 mg $Pd(dppf)Cl_2\,CHCl_3$ (0.14 mmol 5 mol%). The mixture was purged with $N_2$ and warmed to 85°C. After 45 hours the consumption of the starting material was observed. The mixture was filtered, water was added and the product was extracted with ethyl acetate. The organic phases were washed with brine, dried over $Na_2SO_4$, filtered and evaporated to dryness. The crude was purified by flash column chromatography with petroleum ether to petroleum ether/ ethyl acetate 8/2 to afford a white solid corresponding to 4-(4,4,5,5-tetramethyl-1,3,2-dioxaborolan-2-yl)benzaldehyde (**4.11**) (η=89.2 %). **$^1$H NMR (400 MHz, $CDCl_3$) δ (ppm):** 10.01 (s, 1H, CHO), 7.93 (d, *J* = 8.0 Hz, 2H, H2/H6), 7.83 (d, *J* = 8.4 Hz, 2H, H3/H5), 1.33 (s, 13H, 4x$CH_3$).

## Synthesis of donor groups

*Synthesis 10-(2-ethylhexyl)-10H-phenothiazine (**4.13**)*

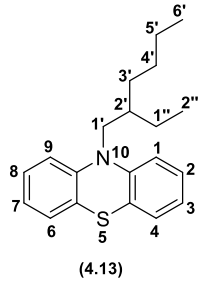
(4.13)

To a round bottom flask equipped with a magnetic stir bar were added 500 mg of phenothiazine (**4.12**) (2.51 mmol) 596 mg of KOH (10.0 mmol, 4.0 eq.) and 2.5 mL of DMSO. The reactional mixture was stirred for 30 minutes. Then 0.90 mL of 3-(bromomethyl)heptane (3.02 mmol, 2.0 eq.) was added dropwise. The reaction was stirred at room temperature and monitored with petroleum ether/ ethyl acetate 99/1. After 48 h the reaction was complete, and the reactional mixture was poured into water. The organic compound was extracted with $CH_2Cl_2$, then it was washed with brine. The organic phase was dried over $Na_2SO_4$, filtered and

evaporated to dryness. The crude was purified by flash column chromatography, it was possible to afford 541 mg of 10-(2-ethylhexyl)-10H-phenothiazine (**4.13**) (1.74 mmol, η = 69 %). Spectroscopic data in accordance with literature.[242] **$^1$H NMR (400 MHz, $CDCl_3$) δ (ppm):** 7.16 – 7.13 (m, 4H, H2/H4/H6/H8), 6.94 – 6.84 (m, 4H, H1/H3/H7/H9), 3.72 (d, *J* = 7.1 Hz, 2H, H1'), 1.93 (hept, *J* = 6.4 Hz, 1H,H2'), 1.48 – 1.32 (m, 4H, H1''/H3'), 1.28 – 1.25 (m, 4H, H4'/H5'), 0.89 – 0.83 (m, 7H, H6'/H2'').

*Synthesis of 3-bromo-10-(2-ethylhexyl)-10H-phenothiazine (**4.14**)*

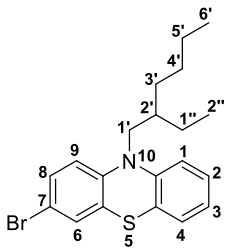
(4.14)

A solution of NBS (304 mg, 1.71 mmol, 1.0 eq.) in DMF (20 mL) was added to a solution of 10-(2-ethylhexyl)-10H-phenothiazine (**4.13**) (533 mg, 1.71 mmol) in DMF 20 mL. The reaction was monitored by TLC using hexane as eluent and after 12 hours at room temperature. Water was added to the reactional mixture and it was extracted with ether. The organic phase was washed several times with an aqueous solution $NH_4Cl$, dried over $Na_2SO_4$, filtered and evaporated to dryness. The crude was purified via column chromatography (silica flash) using hexane as eluent. It was possible to afford 517 mg of 3-bromo-10-(2-ethylhexyl)-10H-phenothiazine (**4.14**) (1.32 mmol, η = 77 %). Spectroscopic data in accordance with literature.[232] **$^1$H NMR (400 MHz,$CDCl_3$) δ (ppm):** 7.26 – 7.22 (m, 2H, H8/H2), 7.18 – 7.12 (m, 2H, H6/H4), 6.93 (t, *J* = 7.4 Hz, 1H, H1), 6.87 (d, *J* = 8.2 Hz, 1H, H3), 6.71 (d, *J* = 8.5 Hz, 1H, H9), 3.68 (d, *J* = 7.1 Hz, 2H, H1'), 1.89 (hept, *J* = 6.0 Hz, 1H, H2'), 1.47–1.21 (m, 4H, H1''/H3'), 1.31 – 1.19 (m, 4H, H4'/H5'), 0.86 (t, *J* = 7.3 Hz, 6H,H6'/H2'').

*Synthesis of 10-(2-ethylhexyl)-3-((trimethylsilyl)ethynyl)-10H-phenothiazine (**4.15**)*

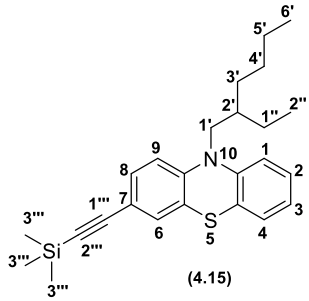
(4.15)

In a Schlenk flask were added CuI (0.034 mmol, 0.12 eq.) $PPh_3$ (0.017 mmol, 0.06 eq.), $Pd(PPh_3)_4$ (0.042 mmol, 0.15eq.), 6 mL of dry dioxane, 3-bromo-10-(2-ethylhexyl)-10H-phenothiazine (**4.14**) (0.28 mmol, 1 eq.), diisopropylamine (0.56 mmol, 2.0 eq.), ethynyl trimethylsilane (0.56 mmol, 2.0 eq.). The reactional mixture was degassed under vacuum. The reaction was stirred at 40° C for 72h and it was monitored by TLC with hexane. The solvent was removed and the crude dissolved with $CH_2Cl_2$, the organic compound was extracted with $CH_2Cl_2$ dried over $Na_2SO_4$, filtered and evaporated to dryness. Then the crude was purified via PLC using hexane as eluent to afford 48.5 mg 10-(2-ethylhexyl)-3-((trimethylsilyl)ethynyl)-10H-phenothiazine (**4.15**) (0.12 mmol, η= 42.3 %). **$^1$H NMR (400 MHz, $CDCl_3$) δ (ppm):** 7.25 – 7.23 (m, 2H, H8/H2),

7.17 – 7.10 (m, 2H, H6/H4), 6.92 (t, *J* = 7.2 Hz, 1H, H1), 6.86 (d, *J* = 8.0 Hz, 1H, H3), 6.75 (d, *J* = 8.8 Hz, 1H, H9), 3.70 (d, *J* = 7.1 Hz, 2H, H1'), 1.89 (hept, *J* = 6.0 Hz, 1H, H2'), 1.48 – 1.31 (m, 4H, H1''/H3'), 1.30 – 1.20 (m, 4H, H4'/H5'), 0.85 (t, *J* = 7.4 Hz, 6H, H6'/H2''), 0.23 (s, 9H, H3'''). **HRMS-ESI(+)** calculated for $C_{25}H_{33}NSSi$ [M+H] 408.21757; Found 408.2174

*Synthesis of 10-(2-ethylhexyl)-3-ethynyl-10H-phenothiazine (**4.16**)*

To a solution of compound 4.15 in MeOH/Dioxane 1/1 was added $K_2CO_3$ (1 eq.). After the total consumption of the starting material the solvent was removed under reduced pressure at room temperature. The crude was directly transferred to the next reactional step.

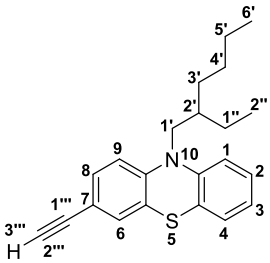

(4.16)

*Synthesis of 9-(4-iodophenyl)-9H-carbazole (**4.18**)*

To a round bottom flask were added 1954 mg of $Cs_2CO_3$ (6.0 mmol, 2eq.), 500 mg of carbazole (3.0 mmol, 1 eq.), 69 µL 1-fluoro-4-iodobenzene (6.0 mmol, 2eq.) and 10 mL of DMF. The reaction was stirred under $N_2$ atmosphere at 150°C for 19 hours. The reaction was monitored by TLC using petroleum ether/DCM 9/1 and after the consumption of the staring material, $CH_2Cl_2$ and cold water were added and the compound was extracted to the organic phase. The combined organic layers were washed with brine, dried over $Na_2SO_4$, filtered and evaporated to dryness. The resulting crude was purified via chromatography column using the aforementioned eluent. It was possible to obtain a white solid (961 mg, 2.60 mmol, η= 87%) corresponding to 9-(4-iodophenyl)-9*H*-carbazole (**4.18**). **$^1$H NMR (400 MHz, $CDCl_3$) δ(ppm):** 8.14 (d, *J* = 7.6 Hz, 2H, H5/H4), 7.93 (d, *J* = 8.4 Hz, 2H, H5'/H3'), 7.45 – 7.36 (m, 4H, H8/H1/H6'/H2'), 7.37 – 7.27 (m, 4H, H6/H3/H2/H7).

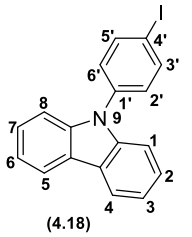

(4.18)

*Synthesis of 9-(4-((trimethylsilyl)ethynyl)phenyl)-9H-carbazole (**4.19**)*

To a Schlenk flask were added CuI (0.101 mmol, 0.12 eq.) $PPh_3$ (0.051 mmol, 0.06 eq.), $Pd(PPh_3)_4$ (0.126 mmol, 0.15eq.), 6 mL of dry dioxane, 9-(4-iodophenyl)-9*H*-carbazole (**4.18**) (0.84mmol, 1 eq.), diisopropylamine (1.68 mmol,2 eq.), ethynyl trimethylsilane (2.50 mmol, 3.0 eq.). The reactional mixture was degassed under vacuum. The reaction was stirred at 40° C for 48h and it was monitored with petroleum ether /DCM 9/1. The solvent was removed, then DCM and water were added and the organic

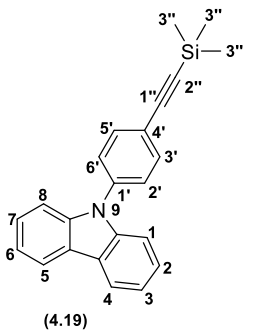

(4.19)

compound was extracted. The combined organic layers were washed with brine, dried over $Na_2SO_4$, filtered and evaporated to dryness. The crude was purified via column chromatography using as eluent a mixture of petroleum ether/DCM 9/1. It was possible to afford 265 mg of a pale yellow solid corresponding to 9-(4-((trimethylsilyl)ethynyl)phenyl)-9*H*-carbazole (**4.19**) ( 0.78 mmol η = 92.7 %). **$^1$H NMR (400 MHz, $CDCl_3$) δ (ppm):** 8.14 (d, *J* = 7.6 Hz, 2H, H5/H4), 7.70 (d, *J* = 8.4 Hz, 2H, H5′/H3′), 7.53 (d, *J* = 8.4 Hz, 2H, H8/H1), 7.46 – 7.38 (m, 4H, H6′/H2′H6/H3), 7.30 – 7.28 (m, 2H, H2/H7), 0.30 (s, 9H, H3′′). **$^{13}$C NMR (101 MHz, $CDCl_3$) δ (ppm):** 140.65, 137.89, 133.63, 126.83, 126.19, 123.68, 122.24, 120.50, 120.35, 109.83, 104.41, 95.52, 0.12.

*Synthesis of 9-(4-ethynylphenyl)-9H-carbazole (**4.20**)*

To a solution of compound **4.19** in MeOH/Dioxane 1/1 was added $K_2CO_3$ (1 eq.). After the total consumption of the starting material the solvent was removed under reduced pressure at room temperature. The crude was directly transferred to the next reactional step (Sonogahsira coupling with formylarylthieno[3,4-*b*]thiophene π-bridge).

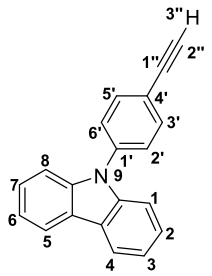

(4.20)

**Introduction of donor groups in formylarylthieno[3,4-*b*]thiophene π-bridge**

**General procedure:**

As previously described to a solution of compound **4.15** or **4.19** in MeOH/Dioxane 1/1 was added $K_2CO_3$ (1 eq.). After the total consumption of the starting material the solvent was removed under reduced pressure at room temperature. The crude was directly transferred to the next reactional step.

In a Schlenk tube were added under $N_2$ atmosphere **4.6a** or **4.6b** (1.2 eq.), $Pd(PPh_3)_4$ (0.15 eq.), CuI (0.12 eq.), $PPh_3$ (0.06 eq.), dry dioxane and diisopropylamine (2 eq.). The reaction was degassed and then it was stirred at 40° C. Then the donor moiety containing the deprotected ethynyl group **4.16** or **4.20** was dissolved in dioxane and added to the reactional mixture. Degass was preformed again and the reaction was stirred under $N_2$ atmosphere at 40°C. After consumption of the limiting reagent the solvent was removed, water was added and extractions with $CH_2Cl_2$ were performed. The organic phases were washed with brine, dried over $Na_2SO_4$, filtered and evaporated to dryness. The crude was purified via column chromatography.

*Synthesis of compound* ***4.21a***

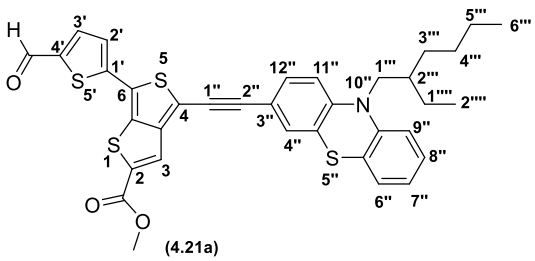


Starting from 10-(2-ethylhexyl)-3-((trimethylsilyl)ethynyl)-10*H*-phenothiazine (**4.15**) (0.14 mmol) and methyl 4-bromo-6-(5-formylthiophen-2-yl)thieno[3,4-*b*]thiophene-2-carboxylate (**4.6a**) (0.14 mmol). The reaction was monitored by TLC using the eluent $CHCl_2$/ petroleum ether 1/1, and after 20 hours the reaction was complete. The crude was purified by column chromatography using as eluent $CH_2Cl_2$ / petroleum ether 1/1 to only $CH_2Cl_2$, it was possible to afford 71.1 mg of methyl 4-((10-(2-ethylhexyl)-10*H*-phenothiazin-3-yl)ethynyl)-6-(5-formylthiophen-2-yl)thieno[3,4-*b*]thiophene-2-carboxylate (**4.21a**) (0.11 mmol, η ≈ 78 %) with some traces of isomer presence. **$^1$H NMR (400 MHz,$CDCl_3$) δ(ppm):** 9.87 (s, 1H, CHO), 7.96 (s, 1H, ArH), 7.71 – 7.68 (m, 1H, ArH), 7.37 – 7.28 (m, 3H, ArH), 7.22 – 7.12 (m, 2H, ArH), 6.95 (t, *J* = 7.1 Hz, 1H, ArH), 6.89 (d, *J* = 8.1 Hz, 1H, ArH), 6.84 (dd, *J* = 8.4, 4.4 Hz, 1H, ArH), 3.95 (s, 3H, $OCH_3$), 3.74 (d, J = 7.1 Hz, 2H,H1‴), 1.92 (hept, *J* = 6.0 Hz, 1H, H2‴), 1.42 – 1.36 (m, 4H,H1⁗/H3‴), 1.27 – 1.25 (d, 4H,H4‴/H5‴), 0.90 – 0.82 (m, 6H, H6‴/H2⁗). **$^{13}$C NMR (101 MHz, $CDCl_3$) δ(ppm):** 182.42, 162.87, 146.82, 145.01, 144.94, 144.81, 144.52, 142.60, 142.16, 142.03, 137.19, 130.82, 130.22, 127.81, 127.48, 127.19, 126.17, 125.21, 125.10, 123.71, 123.12, 116.34, 115.80, 115.75, 111.94, 100.37, 80.28, 52.96, 51.28, 36.02, 30.76, 28.66, 24.08, 23.16, 14.14, 10.61. **HRMS-ESI(+)** calculated for $C_{35}H_{31}NO_3S_4$ [M+H] 642.12595; Found 642.1255

*Synthesis of compound* ***4.21b***

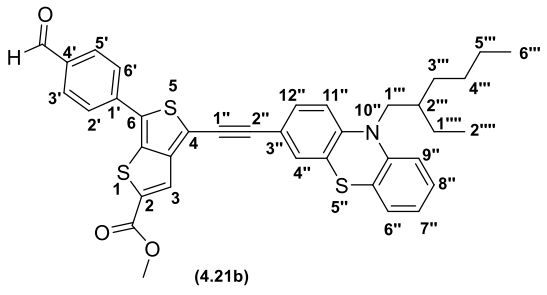


Starting from 10-(2-ethylhexyl)-3-((trimethylsilyl)ethynyl)-10*H*-phenothiazine (**4.15**) (0.13 mmol) and methyl 4-bromo-6-(4-formylphenyl)thieno[3,4-*b*]thiophene-2-carboxylate (**4.6b**) (0.13 mmol). The reaction was monitored by TLC using the eluent petroleum ether/EtOAc 9/1, and after 17 hours the reaction was complete. The crude was purified by column chromatography using as eluent $CH_2Cl_2$ / petroleum ether 1/1 to 7/3, it was possible to afford 71 mg of 4-((10-(2-ethylhexyl)-10*H*-phenothiazin-3-yl)ethynyl)-6-(4-formylphenyl)thieno[3,4-*b*]thiophene-2-carboxylate as an dark orange solid (**4.21b**) (0.11 mmol, η= 86.0%). **$^1$H NMR (400 MHz,$CDCl_3$) δ (ppm):** 10.00 (s, 1H, CHO), 7.94 (s, 1H, ArH), 7.92

(d, *J* = 8.4 Hz, 2H, ArH), 7.76 (d, *J* = 8.0 Hz, 2H, ArH), 7.35 – 7.27 (m, 2H, ArH), 7.21 – 7.12 (m, 2H, ArH), 6.95 (t, *J* = 7.4 Hz, 1H, ArH), 6.88 (d, *J* = 8.0 Hz, 1H, ArH), 6.82 (d, *J* = 8.4 Hz, 1H, ArH), 3.94 (s, 3H, $OCH_3$), 3.74 (d, *J* = 7.2 Hz, 2H, H1‴), 1.93 (hept, *J* = 6.0 Hz, 1H, H2‴), 1.50 – 1.35 (m, 4H, H1⁗/H3‴), 1.30 – 1.24 (m, 6H, H4‴/H5‴), 0.92 – 0.82 (m, 7H, H6‴/H2⁗). **$^{13}$C NMR (101 MHz, $CDCl_3$) δ (ppm):** 191.26, 163.09, 146.67, 145.19, 145.05, 141.87, 141.31, 138.89, 135.48, 134.10, 130.74, 130.46, 130.20, 128.12, 127.79, 127.45, 127.33, 126.14, 125.12, 123.88, 123.07, 116.30, 115.94, 115.77, 111.91, 99.52, 80.36, 52.89, 51.27, 36.01, 30.76, 28.66, 24.08, 23.15, 14.13, 10.60. **HRMS-ESI(+)** calculated for $C_{37}H_{33}NO_3S_3$ [M+H] 636.16953 ; Found 636.1686

*Synthesis of compound* ***4.21c***

Starting from 9-(4-((trimethylsilyl)ethynyl)phenyl)-9*H*-carbazole (**4.19**) (0.20 mmol) and ethyl 4-bromo-6-(5-formylthiophen-2-yl)thieno[3,4-*b*]thiophene-2-carboxylate (0.20 mmol). The reaction was monitored by TLC using the eluent petroleum ether /AcOEt 9/1, and after 19 hours the reaction was complete. The crude was purified by column chromatography using as eluent $CH_2Cl_2$ / petroleum ether 1/1 to only $CH_2Cl_2$, it was possible to afford 85 mg of ethyl 4-((4-(9*H*-carbazol-9-yl)phenyl)ethynyl)-6-(5-formylthiophen-2-yl)thieno[3,4-*b*]thiophene-2-carboxylate (**4.21c**) as an orange solid (0.15 mmol, η= 73.2%). **$^1$H NMR (400 MHz,$CDCl_3$) δ(ppm):** 9.92 (s, 1H, CHO), 8.15 (d, *J* = 7.7 Hz, 2H, ArH), 8.00 (s, 1H, ArH), 7.79 (d, *J* = 8.5 Hz, 2H, ArH), 7.74 (d, *J* = 4.0 Hz, 1H, ArH), 7.63 (d, *J* = 8.5 Hz, 2H, ArH), 7.52 – 7.43 (m, 3H, ArH), 7.43 – 7.37 (m, 2H, ArH), 7.37 – 7.29 (m, 2H, ArH), 4.44 (q, *J* = 7.1 Hz, 2H, $CH_2$), 1.45 (t, *J* = 7.1 Hz, 3H, $OCH_3$). **$^{13}$C NMR (101 MHz, $CDCl_3$) δ (ppm):** 182.52, 162.47, 145.64, 144.40, 142.97, 142.82, 142.40, 140.55, 138.53, 137.22, 133.13, 127.92, 127.05, 126.28, 125.56, 123.82, 123.47, 121.09, 120.57, 120.54, 111.15, 109.86, 99.69, 81.29. **HRMS-ESI(+)** calculated for $C_{34}H_{21}NO_3S_3$ [M+H] 588.07563 ; Found 588.0760

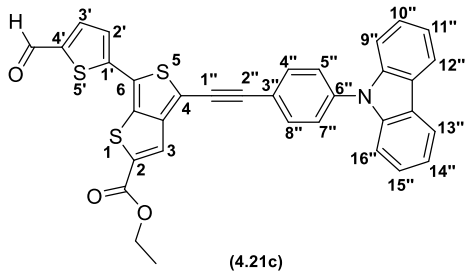

(4.21c)

*Synthesis of compound* ***4.21d***

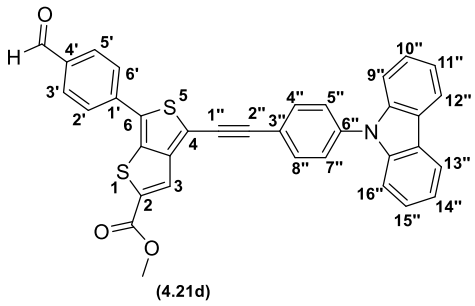
(4.21d)

Starting from 9-(4-((trimethylsilyl)ethynyl)phenyl)-9*H*-carbazole (**4.19**) (0.22 mmol) and of methyl 4-bromo-6-(4-formylphenyl)thieno[3,4-*b*]thiophene-2-carboxylate (**4.6b**) (0.26 mmol). The reaction was monitored by TLC using the eluent petroleum ether /AcOEt 9/1, and after 22 hours the reaction was complete. The crude was purified by column chromatography (silica flash) using as eluent $CH_2Cl_2$, it was possible to afford 52 mg of methyl 4-(4-(9*H*-carbazol-9-yl)phenyl)-6-(4-formylphenyl)thieno[3,4-*b*]thiophene-2-carboxylate **(4.21d)** as an orange solid (0.091 mmol, η =43 %). **$^1$H NMR (400 MHz, $CDCl_3$) δ (ppm):** 10.06 (s, 1H,CHO), 8.16 (d, *J* = 7.7 Hz, 2H, ArH ), 8.02 (s, 1H,H3), 7.99 (d, *J* = 8.3 Hz, 2H, ArH), 7.85 (d, *J* = 8.2 Hz, 2H, ArH), 7.81 (d, *J* = 8.5 Hz, 2H, ArH), 7.63 (d, *J* = 8.5 Hz, 2H, ArH), 7.49 – 7.41 (m, 4H, ArH), 7.32 (ddd, *J* = 8.0, 6.7, 1.5 Hz, 3H, ArH), 3.98 (s, 3H, $OCH_3$). **$^{13}$C NMR (101 MHz, $CDCl_3$) δ (ppm):** 191.30, 163.10, 142.04, 141.49, 140.57, 138.82, 138.39, 135.73, 135.00, 133.09, 130.84, 127.04, 126.27, 123.93, 123.80, 121.26, 120.56, 120.51, 109.86, 98.99, 81.41, 52.99.

## Introduction of anchoring groups

### General procedure for the ester hydrolysis

To a solution containing **4.21b-d** or **4.22a** dissolved in THF was added NaOH (5eq.). After consumption of the starting material, the solvent was removed, $CH_2Cl_2$ and water were added, the solution was acidified with the HCl (1M) until pH≈1. The organic compound was extracted with $CH_2Cl_2$, the organic phases were dried over $Na_2SO_4$, filtered and evaporated to dryness.

*Synthesis of compound* ***4.22b***

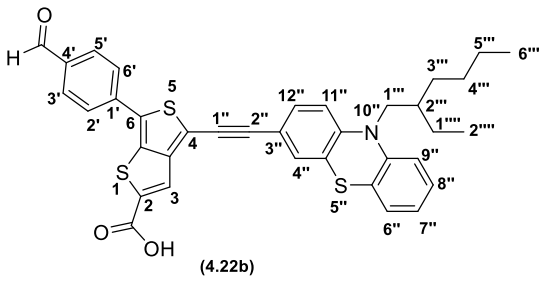
(4.22b)

Starting from 47 mg of compound **4.21b** (0.074 mmol). The reaction was monitored by TLC using $CH_2Cl_2$/ petroleum ether 1/1 and after 24h it was complete. The crude was purified by PLC using as eluent $CH_2Cl_2$/MeOH 9/1 it was possible to afford 20 mg of compound **4.22b** (0.033 mmol, η= 44 %). **$^1$H NMR (400 MHz, DMSO-$d_6$) δ (ppm):** 10.00 (s, 1H), 7.97 (d, *J* = 8.3 Hz, 2H), 7.89 (d, *J* = 8.3 Hz, 2H), 7.59 (s, 1H), 7.43 – 7.40 (m, 1H), 7.37 (d,

*J* = 1.6 Hz, 1H), 7.26 – 7.17 (m, 3H), 7.08 (d, *J* = 7.6 Hz, 2H), 6.99 (t, *J* = 7.7 Hz, 1H), 3.84 – 3.78 (m, 2H), 1.86 – 1.77 (m, 2H), 1.38 (dd, *J* = 14.3, 7.2 Hz, 4H), 1.28 – 1.15 (m, 7H), 0.83 (dd, *J* = 9.4, 6.1 Hz, 8H). **$^{13}$C NMR (126 MHz, DMSO-$d_6$) δ (ppm):** 192.63, 164.65, 146.61, 146.55, 145.59, 144.85, 144.04, 138.73, 138.11, 135.24, 131.39, 131.00, 129.84, 128.25, 127.86, 127.16, 125.94, 125.39, 124.13, 123.58, 117.18, 116.91, 115.61, 109.43, 98.47, 81.41, 50.76, 35.89, 30.18, 28.25, 23.67, 22.93, 14.27, 10.78. **HRMS-ESI(-)** calculated for $C_{36}H_{31}NO_3S_3$ [M-H] 620.13933; Found 620.1394

*Synthesis of compound **4.22c***

Starting from 40 mg of compound **4.21c** (0.068 mmol). The reaction was monitored by TLC using petroleum ether/ ethyl acetate 1/1 and after 144h it was complete. The crude was purified by chromatography in column (silica flash) using as eluent $CH_2Cl_2$ it was possible to afford 36 mg of compound **4.22c** (0.064 mmol, η= 94 %).

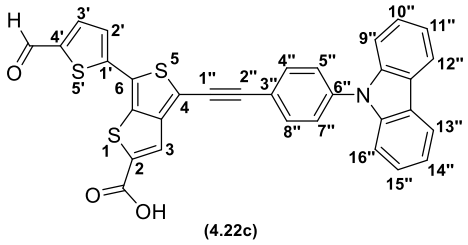

(4.22c)

**$^{1}$H NMR (400 MHz, DMSO-$d_6$) δ (ppm):** 9.90 (s, 1H, CHO), 8.24 (d, *J* = 7.7 Hz, 2H, ArH), 8.02 (d, *J* = 3.9 Hz, 1H, ArH), 7.86 (d, *J* = 8.4 Hz, 2H, ArH), 7.76 (s, 1H, ArH), 7.71 (d, *J* = 8.5 Hz, 2H, ArH), 7.65 (d, *J* = 4.0 Hz, 1H, ArH), 7.45 (d, *J* = 5.7 Hz, 4H, ArH), 7.33 – 7.27 (m, 2H, ArH). **$^{13}$C NMR (101 MHz, DMSO-$d_6$) δ (ppm):** 183.87, 163.72, 145.48, 142.73, 142.26, 139.71, 139.03, 137.72, 133.15, 126.86, 126.71, 126.49, 126.29, 123.56, 123.09, 120.72, 120.67, 120.57, 120.07, 109.78, 109.07, 99.02, 81.21. **HRMS-ESI(+)** calculated for $C_{32}H_{17}NO_3S_3$ [M+H] 560.04433; Found 560.0447

*Synthesis of compound **4.22d***

Starting from 32 mg of compound **4.21d** (0.056 mmol). The reaction was monitored by TLC using petroleum ether/ ethyl acetate 8/2 and after 24h it was complete. The crude was purified by PLC using as eluent $CH_2Cl_2$/MeOH 9/1 it was possible to afford 18 mg of compound **4.22d** (0.33 mmol, η=58 %).

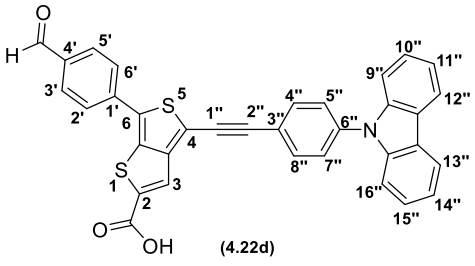

(4.22d)

**$^{1}$H NMR (400 MHz, DMSO-$d_6$) δ (ppm):** 9.97 (s, 1H, CHO), 8.24 (d, *J* = 7.7 Hz, 2H, ArH), 7.94 (d, *J* = 8.2 Hz, 2H, ArH), 7.86 (d, *J* = 7.6 Hz, 2H, ArH), 7.82 (d, *J* = 8.2 Hz, 2H, ArH), 7.71 – 7.64 (m, 3H, ArH), 7.47 – 7.43 (m, 5H, ArH), 7.30 (ddd, *J* = 7.9, 5.4, 2.6 Hz, 2H, ArH). **$^{13}$C NMR (126 MHz, DMSO-$d_6$) δ (ppm):** 192.26, 164.42, 146.76, 143.57,

139.79, 139.76, 138.19, 137.50, 134.99, 133.03, 131.45, 130.60, 126.90, 126.51, 123.08, 120.69, 120.56, 120.42, 109.80, 108.48, 99.66, 97.89, 81.87. **HRMS-ESI(-)** calculated for $C_{34}H_{19}NO_3S_2$ [M-H] 552.07336; Found 552.0732

*Synthesis of compound **4.23a***

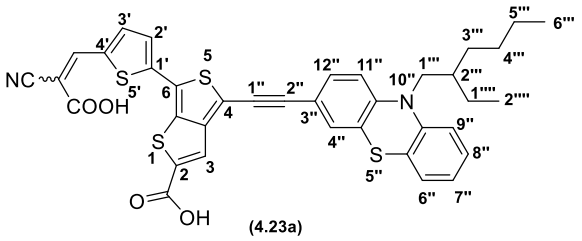

(4.23a)

Starting from 16 mg of compound **4.22a**. The reaction was monitored by TLC using $CH_2Cl_2$/ MeOH/$H_2O$ 65/10/1 and after 48h it was complete. The solvent was removed, then the solid was dissolved in a mixture of $CH_2Cl_2$/ MeOH/$H_2O$ 65/35/5. It was acidified by adding HCL 1M, and then washed with $H_2O$ to remove salts. The residue was also washed with toluene to remove less polar impurities. It was possible to afford 15 mg of the final chromophore **4.23a** (0.021 mmol, η= 98 %). **$^1$H NMR (400 MHz, DMSO-$d_6$) δ(ppm)**: 8.52 (s, 1H, CH), 8.03 (d, *J* = 4.4 Hz, 1H, ArH), 7.93 (s, 1H, ArH), 7.77 (d, *J* = 4.2 Hz, 1H, ArH), 7.47 – 7.41 (m, 1H, ArH), 7.39 (d, *J* = 2.7 Hz, 2H, ArH), 7.26 – 7.20 (m, 1H, ArH), 7.18 (d, *J* = 7.4 Hz, 1H, ArH), 7.08 (d, *J* = 6.4 Hz, 2H, ArH), 6.99 (t, *J* = 8.0 Hz, 1H, ArH), 3.82 (d, *J* = 6.9 Hz, 4H,H1‴), 1.85 – 1.76 (s, 2H,H2‴), 1.41– 1.32 (m, 4H, H1‴‴/H3‴), 1.24 – 1.17 (m, 6H, H4‴/H5‴), 0.84 – 0.78 (m, 8H, H6‴/H2‴‴). **HRMS-ESI(-)** calculated for $C_{37}H_{30}N_2O_4S_4$ [M-H] 693.10156; Found 693.1014

**Introduction of the cyanoacrylic acid**

**General procedure:**

Compound 4.21a or 4.22b-d and cyanoacetic acid (3.0 eq.) were dissolved in acetonitrile, then piperidine was added (2.9 eq.). The mixture was refluxed under $N_2$ atmosphere, after consumption of the starting material the solvent was removed. The crude was washed with several solvents to remove impurities, then it was acidified with HCl 1M and washed with water to remove salts.

*Synthesis of compound **4.22a***

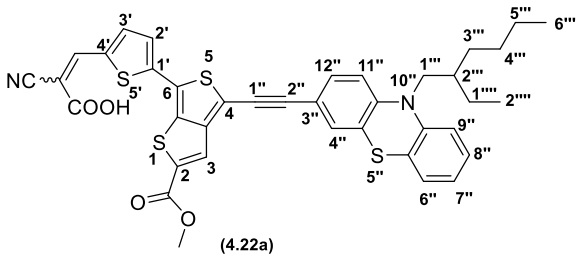


Starting from 27 mg of compound **4.21a** (0.042 mmol). The reaction was monitored by TLC using $CH_2Cl_2$/ MeOH/$H_2O$ 65/10/1 and after 17h it was complete. The crude was washed with petroleum ether to remove impurities. It was possible to afford 20 mg of a purple solid corresponding to compound **4.22a** (0.028 mmol, η= 67%). **$^1$H NMR (400 MHz, DMSO-$d_6$) δ (ppm):** 8.17 (s, 1H), 7.99 (s, 1H), 7.79 (d, *J* = 2.1 Hz, 1H, ArH), 7.71 (d, *J* = 4.0 Hz, 1H, ArH), 7.47 – 7.41 (m, 1H, ArH), 7.41 – 7.38 (m, 1H, ArH), 7.26 – 7.16 (m, 2H, ArH), 7.08 (d, *J* = 8.3 Hz, 2H, ArH), 7.00 (q, *J* = 8.0, 1H), 3.90 (s, 3H, $OCH_3$), 3.85 – 3.78 (m, 2H, H1‴), 1.84 – 1.78 (s, 1H, H2‴), 1.41 – 1.28 (m, 5H, H1⁗/H3‴), 1.26 – 1.17 (m, 5H, H4‴/H5‴), 0.81 (q, J = 7.6 Hz, 6H, H6‴/H2⁗). **HRMS-ESI(-)** calculated for $C_{38}H_{32}N_2O_4S_4$ [M-H] 707.11721; Found 707.1174.

*Synthesis of compound **4.23b***

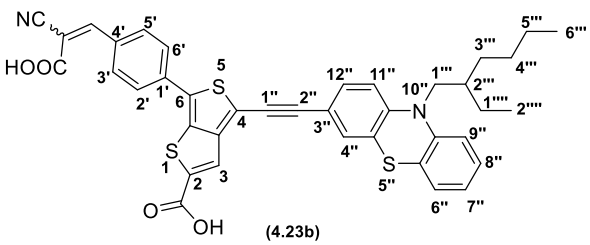


Starting from 10 mg of compound **4.22b** (0.017 mmol). The reaction was monitored by TLC using $CH_2Cl_2$/ MeOH/$H_2O$ 65/10/1 and after 48h it was complete. The crude was washed with toluene/petroleum ether 1/1 to remove impurities. It was possible to afford 10 mg of a dark purple solid corresponding to compound **4.23b** (0.014 mmol, η= 85 %). **$^1$H NMR (400 MHz, DMSO-$d_6$) δ (ppm):** 8.30 (s, 1H, CH), 8.15 (d, *J* = 8.3 Hz, 1H, ArH), 8.11 (s, 1H, ArH), 7.99 (d, *J* = 7.8 Hz, 2H, ArH), 7.48 – 7.41 (m, 2H, ArH), 7.27 – 7.17 (m, 3H, ArH), 7.11 – 7.08 (m, 2H, ArH), 6.99 (t, *J* = 7.2 Hz, 2H, ArH), 3.83 (d, *J* = 7.2 Hz, 2H, H1‴), 1.86 – 1.77 (m, 2H, H2‴), 1.41 – 1.34 (m, 4H, H1⁗/H3‴), 1.26 – 1.18 (m, 6H, H4‴/H5‴), 0.82 (q, *J* = 7.5 Hz, 7H, H6‴/H2⁗). **HRMS-ESI(-)** calculated for $C_{39}H_{32}N_2O_4S_3$ [M-H] 687.14514; Found 687.1454

*Synthesis of compound **4.23c***

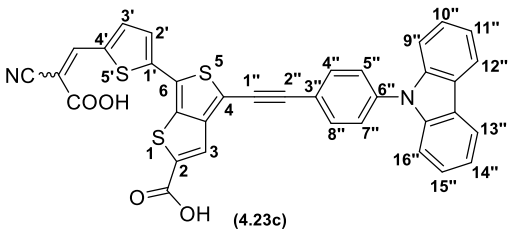

(4.23c)

Starting from 28 mg of compound **4.22c** (0.050 mmol). The reaction was monitored by TLC using $CH_2Cl_2$/ MeOH/$H_2O$ 65/10/1 and after 144h it was complete. The crude was washed with diethyl ether to remove impurities. It was possible to afford 29 mg of a purple solid corresponding to compound **4.23c** (0.046 mmol, η= 93%). **$^1$H NMR (400 MHz, DMSO-$d_6$) δ (ppm):** 8.54 (s, 1H,CH), 8.26 (d, *J* = 7.8 Hz, 2H, ArH), 8.06 (d, *J* = 4.2 Hz, 1H, ArH), 7.97 (s, 1H, ArH), 7.91 (d, *J* = 8.4 Hz, 2H, ArH), 7.82 (d, *J* = 4.0 Hz, 1H, ArH), 7.75 (d, *J* = 8.5 Hz, 2H, ArH), 7.50 – 7.44 (m, 4H, ArH), 7.35 – 7.29 (m, 2H, ArH). **$^{13}$C NMR (126 MHz, DMSO-$d_6$) δ (ppm):** 163.45, 163.03, 145.89, 144.88, 143.95, 142.18, 141.56, 141.03, 139.67, 137.81, 135.61, 133.16, 127.82, 126.96, 126.81, 126.46, 123.07, 122.97, 120.64, 120.54, 119.88, 116.54, 109.77, 109.68, 99.70, 99.14, 80.81. **HRMS-ESI(-)** calculated for $C_{35}H_{18}N_2O_4S_3$ [M-H] 625.03559; Found 625.0359

*Synthesis of compound **4.23d***

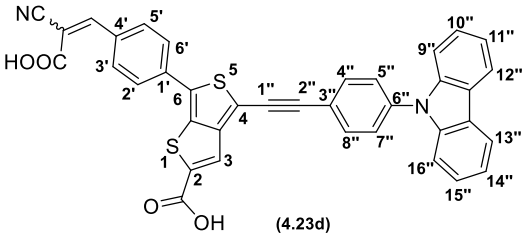

(4.23d)

Starting from 15 mg of compound **4.22d** (0.027 mmol). The reaction was monitored by TLC using $CH_2Cl_2$/ MeOH/$H_2O$ 65/10/1 and after 48h it was complete. The crude was washed with toluene to remove impurities. It was possible to afford 14 mg of a dark red solid corresponding to compound **4.23d** (0.022 mmol, η= 81%). **$^1$H NMR (500 MHz, DMSO-$d_6$) δ (ppm):** 8.26 (d, *J* = 7.8 Hz, 2H), 8.18 – 8.14 (m, 1H), 8.01 (d, *J* = 8.5 Hz, 1H), 7.91 (d, *J* = 8.4 Hz, 2H), 7.74 (d, *J* = 8.4 Hz, 2H), 7.47 (q, *J* = 7.9 Hz, 4H), 7.34 – 7.29 (m, 2H). **$^{13}$C NMR (126 MHz, DMSO-$d_6$) δ (ppm):** 165.69, 163.35, 163.27, 152.66, 145.29, 141.67, 139.69, 137.69, 135.88, 135.03, 133.14, 131.82, 131.52, 127.37, 126.95, 126.87, 126.44, 123.04, 120.64, 120.51, 120.06, 116.42, 115.65, 109.75, 109.16, 98.75, 81.04. **HRMS-ESI(-)** calculated for $C_{37}H_{20}N_2O_4S_2$ [M-H] 619.07972; Found 619.0793

# GENERAL CONCLUSIONS

In this study, three distinct families of chromophores were successfully synthesized, aiming to advance knowledge in the fields of dye sensitized solar cells and renewable energy.

Regarding the coumarin dyes, six new 3-ethynylaryldimethoxycoumarin-based dyes were successfully synthesized. The effects of different heterocyclic π-bridges (mono and bithiophenes, phenyl and benzotriazole) and substitution patterns (6,7- *vs.* 5,7-) on their photovoltaic performance were explored. The 5,6-dimethoxycoumarin bearing thieno[3,2-*b*]thiophene moiety was the best performing dye of the study, achieving an efficiency of 2.00%.

Concerning the diethynylacenaphthylene dyes, it was possible to synthesize four novel dianchoring dyes employing as π-bridges phenyl, thiophene, benzotriazole and thieno-[3,2-*b*]thiophene rings. The one bearing a phenyl ring was shown to be a particular case with an efficiency superior to that of the other derivatives. This dye achieved an efficiency of 2.51%, with $V_{oc}$, $J_{sc}$ and FF values 0.365 V, 13.32 mA/cm$^2$ and 0.52, respectively. The other dyes exhibited a significant decrease in $J_{sc}$ (3.21 – 5.35 mA/cm$^2$) and, also, on $V_{oc}$ (0.241 – 0.320 V). This difference was also observed in the IPCE spectra, where the phenyl derivative presented superior maximum IPCE value (60.8%). This improved electron injection is likely related to the fact that the phenyl ring has a twisted conformation with respect to the acenaphthylene ring. The efficiency of this compound improved to 3.15% with the addition of CDCA (10 mM), representing the best efficiency result in this study.

In this work it was also possible to synthesize four new thieno[3,4-*b*]thiophene based dyes with a D-π-$(A)_2$. Variations were made to the π-bridge (phenyl or thiophene) and the donor unit (phenoxazine or carbazole). The best performing dye in this study was the derivative containing phenyl ring and a phenothiazine as donor achieving an efficiency of 1.96 %, with $V_{oc}$ $J_{sc}$ and FF values of 0.376 V, 9.40 mA/cm$^2$ and 0.55, respectively.

The photovoltaic performance of the compounds contributes to the understanding of the impact of specific groups present in the molecules. The photophysical data are also an indicator for future experiments, such as co-sensitization.

# WORK DISSEMINATION

**Journal articles:**

Malta, G.; Pina, J.; Lima, J. C.; Parola, A. J.; Branco, P. S. Acenaphthylene-Based Chromophores for Dye-Sensitized Solar Cells: Synthesis, Spectroscopic Properties, and Theoretical Calculations. *ACS Omega* **2024**, 9, 14627-14637. DOI: https://doi.org/10.1021/acsomega.4c01201

Sarrato, J.; Pinto, A. L.; Malta, G.; Rock, E. G.; Pina, J.; Lima, J. C.; Parola, A. J.; Branco, P. S. New 3-Ethynylaryl Coumarin-Based Dyes for DSSC Applications: Synthesis, Spectroscopic Properties, and Theoretical Calculations. *Molecules* **2021**, 26, 2934. DOI: https://doi.org/10.3390/molecules26102934

**Oral presentations:**

*New acenaphthylene-based sensitizers for DSSC applications.* In 14th National Organic Chemistry Meeting & 7th National Medicinal Chemistry Meeting (Caparica, Portugal, 21/04/22) Authors: Gabriela Malta; A. Jorge Parola; Paula S. Branco.

*Acenaphthylene-based chromophores for dye–sensitized solar cells: synthesis, spectroscopic properties, and theoretical calculations*. In Synthesis&Catalysis Workshop (Caparica, Portugal, 07/11/23). Authors: Gabriela Malta; João Pina; J. Carlos Lima; A. Jorge Parola; Paula S. Branco.

**Poster presentations:**

*Thienothiophene-based dyes for DSSC applications*. In XXVIII ENCONTRO GALEGO-PORTUGUÉS DE QUÍMICA (Vigo, Spain, 13/11/24-15/11/24). Authors: Gabriela Malta, A. Jorge Parola, Paula S. Branco.

*New acenaphthylene-based sensitizers for DSSC applications: synthesis, photovoltaic performance, and spectroscopic properties.* In 23rd Tetrahedron Symposium (Gothenburg, Sweden, 27/06/23-30/06/23). Authors: Gabriela Malta, J. Carlos Lima, A. Jorge Parola, Paula S. Branco.

*New acenaphthylene-based dyes for DSSC applications.* In 8th EuChemS Chemistry Congress (Lisboa, Portugal 28/08/22- 1/09/22). Authors: Gabriela Malta, J. Carlos Lima, A. Jorge Parola, Paula S. Branco.

# BIBLIOGRAPHY


(1) Olabi, A. G.; Abdelkareem, M. A. Renewable energy and climate change. *Renew. sustain. energy rev.* **2022**, *158*, 112111. DOI: https://doi.org/10.1016/j.rser.2022.112111.

(2) Wang, F. *et al.* Technologies and perspectives for achieving carbon neutrality. *Innovation (Camb)* **2021**, *2*, 100180. DOI: https://doi.org/10.1016/j.xinn.2021.100180.

(3) Sustainable Development Goals. https://www.undp.org/sustainable-development-goals (accessed 24/04/2023 2023).

(4) Sustainable Development Goals Icons. https://www.un.org/sustainabledevelopment (accessed 27-12-2023.

(5) Li, G.; Li, M.; Taylor, R.; Hao, Y.; Besagni, G.; Markides, C. N. Solar energy utilisation: Current status and roll-out potential. *Appl. Therm. Eng.* **2022**, *209*. DOI: https://doi.org/10.1016/j.applthermaleng.2022.118285.

(6) Kabir, E.; Kumar, P.; Kumar, S.; Adelodun, A. A.; Kim, K.-H. Solar energy: Potential and future prospects. *Renew. sustain. energy rev.* **2018**, *82*, 894-900. DOI: https://doi.org/10.1016/j.rser.2017.09.094.

(7) Hayat, M. B.; Ali, D.; Monyake, K. C.; Alagha, L.; Ahmed, N. Solar energy-A look into power generation, challenges, and a solar-powered future. *Int. J. Energy Res.* **2019**, *43*, 1049-1067. DOI: https://doi.org/10.1002/er.4252.

(8) Crabtree, G. W.; Lewis, N. S. Solar energy conversion. *Phys. Today* **2007**, *60*, 37-42. DOI: https://doi.org/10.1063/1.2718755.

(9) Pastuszak, J.; Wegierek, P. Photovoltaic Cell Generations and Current Research Directions for Their Development. *Materials* **2022**, *15*, 5542. DOI: https://doi.org/10.3390/ma15165542.

(10) Obaideen, K.; Olabi, A. G.; Al Swailmeen, Y.; Shehata, N.; Abdelkareem, M. A.; Alami, A. H.; Rodriguez, C.; Sayed, E. T. Solar Energy: Applications, Trends Analysis, Bibliometric Analysis and Research Contribution to Sustainable Development Goals (SDGs). *Sustainability* **2023**, *15*, 1418. DOI: https://doi.org/10.3390/su15021418.

(11) Grätzel, M. Photovoltaic and photoelectrochemical conversion of solar energy. *Philos Trans A Math Phys Eng Sci* **2007**, *365*, 993-1005. DOI: https://doi.org/10.1098/rsta.2006.1963.

(12) O'Regan, B.; Grätzel, M. A low-cost, high-efficiency solar cell based on dye-sensitized colloidal TiO2 films. *Nature* **1991**, *353*, 737-740. DOI: https://doi.org/10.1038/353737a0.

(13) Munoz-Garcia, A. B. *et al.* Dye-sensitized solar cells strike back. *Chem Soc Rev* **2021**, *50*, 12450-12550. DOI: https://doi.org/10.1039/d0cs01336f.

(14) Carballo, M. S.; Urbani, M.; Chandiran, A. K.; Rodriguez, D. G.-.; Vazquez, P.; Gratzel, M.; Nazeeruddin, M. K.; Torres, T. Branched and bulky substituted ruthenium sensitizers for dye-sensitized solar cells. *Dalton Trans* **2014**, *43*, 15085-15091. DOI: https://doi.org/10.1039/c4dt01357c.

(15) *Mineral commodity summaries 2023: U.S. Geological Survey.*2023.

(16) Bartolotta, A.; Calogero, G.: Dye-sensitized solar cells: from synthetic dyes to natural pigments. In *Solar Cells and Light Management*; 1st ed.; Francesco Enrichi, G. R., Ed.; Elsevier, 2020; pp 107-161.

(17) Balasingam, S. K.; Lee, M.; Kang, M. G.; Jun, Y. Improvement of dye-sensitized solar cells toward the broader light harvesting of the solar spectrum. *Chem Commun (Camb)* **2013**, *49*, 1471-1487. DOI: https://doi.org/10.1039/c2cc37616d.

(18) Chen, C. C.; Nguyen, V. S.; Chiu, H. C.; Chen, Y. D.; Wei, T. C.; Yeh, C. Y. Anthracene-Bridged Sensitizers for Dye-Sensitized Solar Cells with 37% Efficiency under Dim Light. *Advanced Energy Materials* **2022**, *12*, 2104051. DOI: https://doi.org/10.1002/aenm.202104051.

(19) Chapin, D. M.; Fuller, C. S.; Pearson, G. L. A new silicon p-n junction photocell for converting solar radiation into electrical power. *J. Appl. Phys.* **1954**, *25*, 676-677. DOI: http://dx.doi.org/10.1063/1.1721711

(20) Pearson, G. L.; Chapin, D. M.; Fuller, C. S. Solar Energy Converting Apparatus US2780765.

(21) Theerthagiri, J.; Senthil, R. A.; Madhavan, J.: Design and Fabrication of Carbon-based Nanostructured Counter Electrode Materials for Dye-sensitized Solar Cells. In *Rational Design of Solar Cells for Efficient Solar Energy Conversion*; Pandikumar, A., Ramaraj, R., Eds.; Wiley, 2018; pp 193-217.

(22) Singh, B. P.; Goyal, S. K.; Kumar, P. Solar PV cell materials and technologies: Analyzing the recent developments. *Mater. Today: Proc.* **2021**, *43*, 2843-2849. DOI: https://doi.org/10.1016/j.matpr.2021.01.003.

(23) Moser, J. Notiz über Verstärkung photoelektrischer Ströme durch optische Sensibilisirung. *Monatsh. Chem. Verw. Teile Anderer Wiss. [ZDB]* **1887**, *8*, 373-373. DOI: https://doi.org/10.1007/BF01510059.

(24) Yahya, M.; Bouziani, A.; Ocak, C.; Seferoğlu, Z.; Sillanpää, M. Organic/metal-organic photosensitizers for dye-sensitized solar cells (DSSC): Recent developments, new trends, and future perceptions. *Dyes Pigm.* **2021**, *192*, 109227. DOI: https://doi.org/10.1016/j.dyepig.2021.109227.

(25) Namba, S.; Hishiki, Y. Color sensitization of zinc oxide with cyanine dyes. *The Journal of Physical Chemistry* **1965**, *69*, 774-779. DOI: https://doi.org/10.1021/j100887a010.

(26) Gerischer, H.; Michel-Beyerle, M.; Rebentrost, F.; Tributsch, H. Sensitization of charge injection into semiconductors with large band gap. *Electrochim. Acta* **1968**, *13*, 1509-1515. DOI: https://doi.org/10.1016/0013-4686(68)80076-3.

(27) Spitler, M. T.; Calvin, M. Electron transfer at sensitized TiO2 electrodes. *J. Chem. Phys.* **1977**, *66*, 4294-4305. DOI: https://doi.org/10.1063/1.433739.

(28) Gong, J.; Liang, J.; Sumathy, K. Review on dye-sensitized solar cells (DSSCs): Fundamental concepts and novel materials. *Renew. sustain. energy rev.* **2012**, *16*, 5848-5860. DOI: https://doi.org/10.1016/j.rser.2012.04.044.

(29) Chen, Y. C.; Lin, J. T. Multi-anchored sensitizers for dye-sensitized solar cells. *Sustain. Energy Fuels* **2017**, *1*, 969-985. DOI: https://doi.org/10.1039/c7se00141j.

(30) Mariotti, N.; Bonomo, M.; Fagiolari, L.; Barbero, N.; Gerbaldi, C.; Bella, F.; Barolo, C. Recent advances in eco-friendly and cost-effective materials towards sustainable dye-sensitized solar cells. *Green Chem.* **2020**, *22*, 7168-7218. DOI: https://doi.org/10.1039/D0GC01148G.

(31) Grätzel, M. Recent advances in sensitized mesoscopic solar cells. *Acc Chem Res* **2009**, *42*, 1788-1798. DOI: https://doi.org/10.1021/ar900141y.

(32) Grätzel, M. Molecular photovoltaics that mimic photosynthesis. *Pure Appl. Chem.* **2001**, *73*, 459-467. DOI: https://doi.org/10.1351/pac200173030459.

(33) Muthukumar, A.; Rey, G.; Giusti, G.; Consonni, V.; Appert, E.; Roussel, H.; Dakshnamoorthy, A.; Bellet, D.: Fluorine doped tin oxide (FTO) thin film as transparent conductive oxide (TCO) for photovoltaic applications. In *AIP Conference Proceedings*: American Institute of Physics, 2013; pp 710-711.

(34) Cavallo, C.; Di Pascasio, F.; Latini, A.; Bonomo, M.; Dini, D. Nanostructured Semiconductor Materials for Dye-Sensitized Solar Cells. *J. Nanomater.* **2017**, *2017*, 5323164. DOI: https://doi.org/10.1155/2017/5323164.

(35) Bai, Y.; Mora-Sero, I.; De Angelis, F.; Bisquert, J.; Wang, P. Titanium dioxide nanomaterials for photovoltaic applications. *Chem Rev* **2014**, *114*, 10095-10130. DOI: https://doi.org/10.1021/cr400606n.

(36) Yeoh, M.-E.; Chan, K.-Y. Recent advances in photo-anode for dye-sensitized solar cells: a review. *Int. J. Energy Res.* **2017**, *41*, 2446-2467. DOI: https://doi.org/10.1002/er.3764.

(37) Wu, J.; Lan, Z.; Lin, J.; Huang, M.; Huang, Y.; Fan, L.; Luo, G. Electrolytes in dye-sensitized solar cells. *Chem Rev* **2015**, *115*, 2136-2173. DOI: https://doi.org/10.1021/cr400675m.

(38) Carella, A.; Borbone, F.; Centore, R. Research Progress on Photosensitizers for DSSC. *Front Chem* **2018**, *6*, 481. DOI: https://doi.org/10.3389/fchem.2018.00481.

(39) Hao, Y.; Yang, W. X.; Zhang, L.; Jiang, R.; Mijangos, E.; Saygili, Y.; Hammarstrom, L.; Hagfeldt, A.; Boschloo, G. A small electron donor in cobalt complex electrolyte significantly improves efficiency in dye-sensitized solar cells. *Nat. Commun.* **2016**, *7*. DOI: https://doi.org/10.1038/ncomms13934.

(40) Zhang, D. *et al.* A molecular photosensitizer achieves a Voc of 1.24V enabling highly efficient and stable dye-sensitized solar cells with copper(II/I)-based electrolyte. *Nature Communications* **2021**, *12*. DOI: https://doi.org/10.1038/s41467-021-21945-3

(41) Abu Talip, R. A.; Yahya, W. Z. N.; Bustam, M. A. Ionic Liquids Roles and Perspectives in Electrolyte for Dye-Sensitized Solar Cells. *Sustainability* **2020**, *12*. DOI: https://doi.org/10.3390/su12187598.

(42) Ye, M.; Wen, X.; Wang, M.; Locozzia, J.; Zhang, N.; Lin, C.; Lin, Z. Recent advances in dye-sensitized solar cells: from photoanodes, sensitizers and electrolytes to counter electrodes. *Mater. Today* **2015**, *18*, 155-162. DOI: https://doi.org/10.1016/j.mattod.2014.09.001.

(43) Ooyama, Y.; Harima, Y. Photophysical and electrochemical properties, and molecular structures of organic dyes for dye-sensitized solar cells. *ChemPhysChem* **2012**, *13*, 4032-4080. DOI: https://doi.org/10.1002/cphc.201200218.

(44) Murakami, T. N.; Koumura, N. Development of Next-Generation Organic-Based Solar Cells: Studies on Dye-Sensitized and Perovskite Solar Cells. *Adv. Energy Mater.* **2018**, *9*, 1802967. DOI: https://doi.org/10.1002/aenm.201802967.

(45) Iftikhar, H.; Sonai, G. G.; Hashmi, S. G.; Nogueira, A. F.; Lund, P. D. Progress on Electrolytes Development in Dye-Sensitized Solar Cells. *Mater.* **2019**, *12*, 1998. DOI: https://doi.org/10.3390/ma12121998

(46) Ning, Z.; Fu, Y.; Tian, H. Improvement of dye-sensitized solar cells: what we know and what we need to know. *Energy Environ. Sci.* **2010**, *3*, 1170-1181. DOI: https://doi.org/10.1039/c003841e.

(47) Zhang, L.; Cole, J. M. Dye aggregation in dye-sensitized solar cells. *J. Mater. Chem. A* **2017**, *5*, 19541-19559. DOI: https://doi.org/10.1039/c7ta05632j.

(48) Bisquert, J.: *The Physics of Solar Cells Perovskites, Organics, and Photovoltaic Fundamentals* CRC Press, 2018. pp. 16-21.

(49) Reference Air Mass 1.5 Spectra. https://www.nrel.gov/grid/solar-resource/spectra-am1.5.html
(accessed 05-01-2024 2024).

(50) Hagfeldt, A.; Boschloo, G.; Sun, L.; Kloo, L.; Pettersson, H. Dye-sensitized solar cells. *J. Chem. Rev.* **2010**, *110*, 6595-6663. DOI: https://doi.org/10.1021/cr900356p.

(51) Nam, S.-H.; Lee, K. H.; Yu, J.-H.; Boo, J.-H. Review of the Development of Dyes for Dye-Sensitized Solar Cells. *Appl. Sci. Converg. Technol.* **2019**, *28*, 194-206. DOI: https://doi.org/10.5757/asct.2019.28.6.194.

(52) Qu, S.; Hua, J.; Tian, H. New D-π-A dyes for efficient dye-sensitized solar cells. *Sci. China Chem.* **2012**, *55*, 677-697. DOI: https://doi.org/10.1007/s11426-012-4517-x.

(53) Chen, Z. *et al.*: Incident photon-to-current efficiency and photocurrent spectroscopy. In *Photoelectrochemical Water Splitting: Standards, Experimental Methods*; Springer New York, NY, 2013; pp 87-97.

(54) Ji, J.-M.; Zhou, H.; Kim, H. K. J. J. o. M. C. A. Rational design criteria for D–π–A structured organic and porphyrin sensitizers for highly efficient dye-sensitized solar cells. **2018**, *6*, 14518-14545. DOI: https://doi.org/10.1039/C8TA02281J.

(55) Shalini, S.; Balasundaraprabhu, R.; Kumar, T. S.; Prabavathy, N.; Senthilarasu, S.; Prasanna, S. Status and outlook of sensitizers/dyes used in dye sensitized solar cells (DSSC): a review. *Int. J. Energy Res.* **2016**, *40*, 1303-1320. DOI: https://doi.org/10.1002/er.3538.

(56) Vougioukalakis, G. C.; Philippopoulos, A. I.; Stergiopoulos, T.; Falaras, P. Contributions to the development of ruthenium-based sensitizers for dye-sensitized solar cells. *Coord. Chem. Rev.* **2011**, *255*, 2602-2621. DOI: https://doi.org/10.1016/j.ccr.2010.11.006.

(57) Qin, Y. C.; Peng, Q. Ruthenium Sensitizers and Their Applications in Dye-Sensitized Solar Cells. *Int. J. Photoenergy* **2012**, *2012*, 291579. DOI: https://doi.org/10.1155/2012/291579.

(58) Wu, Y.; Zhu, W. H.; Zakeeruddin, S. M.; Gratzel, M. Insight into D-A-pi-A Structured Sensitizers: A Promising Route to Highly Efficient and Stable Dye-Sensitized Solar Cells. *ACS Appl. Mater. Interfaces* **2015**, *7*, 9307-9318. DOI: https://doi.org/10.1021/acsami.5b02475.

(59) Richhariya, G.; Kumar, A.; Tekasakul, P.; Gupta, B. Natural dyes for dye sensitized solar cell: A review. *Renew. Sust. Energ. Rev.* **2017**, *69*, 705-718. DOI: http://dx.doi.org/10.1016/j.rser.2016.11.198.

(60) Zhou, H.; Wu, L.; Gao, Y.; Ma, T. Dye-sensitized solar cells using 20 natural dyes as sensitizers. *J. Photochem. Photobiol., A* **2011**, *219*, 188-194. DOI: https://doi.org/10.1016/j.jphotochem.2011.02.008.

(61) Amogne, N. Y.; Ayele, D. W.; Tsigie, Y. A. Recent advances in anthocyanin dyes extracted from plants for dye sensitized solar cell. *Mater. Renew. Sustain. Energy.* **2020**, *9*, 23. DOI: https://doi.org/10.1007/s40243-020-00183-5.

(62) Calogero, G.; Sinopoli, A.; Citro, I.; Di Marco, G.; Petrov, V.; Diniz, A. M.; Parola, A. J.; Pina, F. Synthetic analogues of anthocyanins as sensitizers for dye-sensitized solar cells. *Photochem. Photobiol. Sci.* **2013**, *12*, 883-894. DOI: https://doi.org/10.1039/C3PP25347C.

(63) Pinto, A. L.; Máximo, P.; Pina, J.; Calogero, G.; Laia, C. A. T.; Parola, A. J.; Lima, J. C. Exploring the impact of structural rigidification of amino-substituted bio-inspired flavylium dyes in DSSCs. *Dyes Pigm.* **2023**, *218*. DOI: https://doi.org/10.1016/j.dyepig.2023.111495.

(64) Syafinar, R.; Gomesh, N.; Irwanto, M.; Fareq, M.; Irwan, Y. J. Chlorophyll pigments as nature based dye for dye-sensitized solar cell (DSSC). *Energy Procedia* **2015**, *79*, 896-902. DOI: https://doi.org/10.1016/j.egypro.2015.11.584.

(65) Zhang, D.; Lanier, S. M.; Downing, J. A.; Avent, J. L.; Lum, J.; McHale, J. L. Betalain pigments for dye-sensitized solar cells. *J. Photochem. Photobiol., A* **2008**, *195*, 72-80. DOI: https://doi.org/10.1016/j.jphotochem.2007.07.038.

(66) Chen, Z.; Li, F.; Huang, C. Organic D-π-A dyes for dye-sensitized solar cell. *Curr. Org. Chem.* **2007**, *11*, 1241-1258. DOI: https://doi.org/10.2174/138527207781696008.

(67) Yanagida, S. Recent research progress of dye-sensitized solar cells in Japan. *C. R. Chim.* **2006**, *9*, 597-604. DOI: https://doi.org/10.1016/j.crci.2005.05.021.

(68) Pecnikaj, I.; Minudri, D.; Otero, L.; Fungo, F.; Cavazzini, M.; Orlandi, S.; Pozzi, G. Fluorous molecules for dye-sensitized solar cells: synthesis and properties of di-branched, di-

anchoring organic sensitizers containing fluorene subunits. *New J Chem* **2017**, *41*, 7729-7738. DOI: https://doi.org/10.1039/C7NJ01516J.

(69) Sirohi, R.; Kim, D. H.; Yu, S.-C.; Lee, S. H. Novel di-anchoring dye for DSSC by bridging of two mono anchoring dye molecules: A conformational approach to reduce aggregation. *Dyes Pigm.* **2012**, *92*, 1132-1137. DOI: https://doi.org/10.1016/j.dyepig.2011.09.003.

(70) Dai, X.-X.; Feng, H.-L.; Chen, W.-J.; Yang, Y.; Nie, L.-B.; Wang, L.; Kuang, D.-B.; Meier, H.; Cao, D. Synthesis and photovoltaic performance of asymmetric di-anchoring organic dyes. *Dyes Pigm.* **2015**, *122*, 13-21. DOI: https://doi.org/10.1016/j.dyepig.2015.06.004.

(71) Manfredi, N.; Cecconi, B.; Abbotto, A. Multi-Branched Multi-Anchoring Metal-Free Dyes for Dye-Sensitized Solar Cells. *Eur. J. Org. Chem.* **2014**, *2014*, 7069-7086. DOI: https://doi.org/10.1002/ejoc.201402422.

(72) Abbotto, A.; Manfredi, N.; Marinzi, C.; De Angelis, F.; Mosconi, E.; Yum, J.-H.; Xianxi, Z.; Nazeeruddin, M. K.; Grätzel, M. Di-branched di-anchoring organic dyes for dye-sensitized solar cells. *Energy Environ. Sci.* **2009**, *2*, 1094-1101. DOI: https://doi.org/10.1039/b910654e.

(73) Wu, H. L.; Huang, Z. S.; Hua, T.; Liao, C. Q.; Meier, H.; Tang, H.; Wang, L. Y.; Cao, D. R. Metal-free organic dyes with di(1-benzothieno)[3,2-b:2′,3′-d] pyrrole as a donor for efficient dye-sensitized solar cells: Effect of mono- and bi-anchors on photovoltaic performance. *Dyes Pigm.* **2019**, *165*, 103-111. DOI: https://doi.org/10.1016/j.dyepig.2019.02.003.

(74) Liu, B.; Liu, Q. B.; You, D.; Li, X. Y.; Naruta, Y.; Zhu, W. H. Molecular engineering of indoline based organic sensitizers for highly efficient dye-sensitized solar cells. *J. Mater. Chem.* **2012**, *22*, 13348-13356. DOI: https://doi.org/10.1039/c2jm31704d.

(75) Liang, M.; Chen, J. Arylamine organic dyes for dye-sensitized solar cells. *Chem Soc Rev* **2013**, *42*, 3453-3488. DOI: https://doi.org/10.1039/c3cs35372a.

(76) Tan, H.; Pan, C.; Wang, G.; Wu, Y.; Zhang, Y.; Zou, Y.; Yu, G.; Zhang, M. Phenoxazine-based organic dyes with different chromophores for dye-sensitized solar cells. *Org. Electron.* **2013**, *14*, 2795-2801. DOI: https://doi.org/10.1016/j.orgel.2013.07.008.

(77) Hung, W. I.; Liao, Y. Y.; Hsu, C. Y.; Chou, H. H.; Lee, T. H.; Kao, W. S.; Lin, J. T. High-performance dye-sensitized solar cells based on phenothiazine dyes containing double anchors and thiophene spacers. *Chem Asian J* **2014**, *9*, 357-366. DOI: https://doi.org/10.1002/asia.201301228.

(78) Wang, Z. S.; Cui, Y.; Dan-Oh, Y.; Kasada, C.; Shinpo, A.; Hara, K. Thiophene-functionalized coumarin dye for efficient dye-sensitized solar cells: Electron lifetime improved by coadsorption of deoxycholic acid. *J. Phys. Chem. C* **2007**, *111*, 7224-7230. DOI: https://doi.org/10.1021/jp067872t.

(79) Martins, S.; Avó, J.; Lima, J.; Nogueira, J.; Andrade, L.; Mendes, A.; Pereira, A.; Branco, P. S. Styryl and phenylethynyl based coumarin chromophores for dye sensitized solar cells. *J. Photochem. Photobiol., A* **2018**, *353*, 564-569. DOI: https://doi.org/10.1016/j.jphotochem.2017.12.018.

(80) Martins, S.; Candeias, A.; Caldeira, A. T.; Pereira, A. 7-(diethylamino)-4-methyl-3-vinylcoumarin as a new important intermediate to the synthesis of photosensitizers for DSSCs and fluorescent labels for biomolecules. *Dyes Pigm.* **2020**, *174*, 108026. DOI: https://doi.org/10.1016/j.dyepig.2019.108026.

(81) Ito, S.; Miura, H.; Uchida, S.; Takata, M.; Sumioka, K.; Liska, P.; Comte, P.; Péchy, P.; Gräetzel, M. High-conversion-efficiency organic dye-sensitized solar cells with a novel indoline dye. *Chem. Commun.* **2008**, 5194-5196. DOI: https://doi.org/10.1039/B809093A.

(82) Thomas, K. R. J.; Venkateswararao, A.; Lee, C. P.; Ho, K. C. Organic dyes containing fluoreneamine donor and carbazole π-linker for dye-sensitized solar cells. *Dyes Pigm.* **2015**, *123*, 154-165. DOI: https://doi.org/10.1016/j.dyepig.2015.07.034.

(83) Tang, J.; Hua, J.; Wu, W.; Li, J.; Jin, Z.; Long, Y.; Tian, H. New starburst sensitizer with carbazole antennas for efficient and stable dye-sensitized solar cells. *Energy & Environmental Science* **2010**, *3*. DOI: https://doi.org/10.1039/C0EE00008F.

(84) Zhang, X.; Grätzel, M.; Hua, J. Donor design and modification strategies of metal-free sensitizers for highly-efficient n-type dye-sensitized solar cells. *Front. Optoelectron.* **2016**, *9*, 3-37. DOI: https://doi.org/10.1007/s12200-016-0563-x.

(85) Jia, H. L.; Ju, X. H.; Zhang, M. D.; Ju, Z. M.; Zheng, H. G. Effects of heterocycles containing different atoms as π-bridges on the performance of dye-sensitized solar cells. *Physical Chemistry Chemical Physics* **2015**, *17*, 16334-16340. DOI: https://doi.org/10.1039/C5CP02194D.

(86) Brogdon, P.; Giordano, F.; Puneky, G. A.; Dass, A.; Zakeeruddin, S. M.; Nazeeruddin, M. K.; Gratzel, M.; Tschumper, G. S.; Delcamp, J. H. A Computational and Experimental Study of Thieno[3,4-b]thiophene as a Proaromatic pi-Bridge in Dye-Sensitized Solar Cells. *Chem. Eur. J.* **2016**, *22*, 694-703. DOI: https://doi.org/10.1002/chem.201503187.

(87) Chaurasia, S.; Chen, Y. C.; Chou, H. H.; Wen, Y. S.; Lin, J. T. Coplanar indenofluorene-based organic dyes for dye-sensitized solar cells. *Tetrahedron* **2012**, *68*, 7755-7762. DOI: https://doi.org/10.1016/j.tet.2012.07.045.

(88) Duerto, I.; Sarasa, S.; Barrios, D.; Orduna, J.; Villacampa, B.; Blesa, M.-J. Enhancing the temporal stability of DSSCs with novel vinylpyrimidine anchoring and accepting group. *Dyes Pigm.* **2022**, *203*, 110310. DOI: https://doi.org/10.1016/j.dyepig.2022.110310.

(89) Zhang, L.; Cole, J. M. Anchoring groups for dye-sensitized solar cells. *ACS Appl. Mater. Interfaces* **2015**, *7*, 3427-3455. DOI: https://doi.org/10.1021/am507334m.

(90) Anselmi, C.; Mosconi, E.; Pastore, M.; Ronca, E.; De Angelis, F. Adsorption of organic dyes on TiO2 surfaces in dye-sensitized solar cells: interplay of theory and experiment. *Phys. Chem. Chem. Phys.* **2012**, *14*, 15963-15974. DOI: https://doi.org/10.1039/C2CP43006A.

(91) Singh, A. K.; Kavungathodi, M. F. M.; Nithyanandhan, J. Alkyl-Group-Wrapped Unsymmetrical Squaraine Dyes for Dye-Sensitized Solar Cells: Branched Alkyl Chains Modulate the Aggregation of Dyes and Charge Recombination Processes. *ACS Appl. Mater. Interfaces* **2020**, *12*, 2555-2565. DOI: https://doi.org/10.1021/acsami.9b19809.

(92) Feng, Q. Y.; Zhou, G.; Wang, Z. S. Varied alkyl chain functionalized organic dyes for efficient dye-sensitized solar cells: Influence of alkyl substituent type on photovoltaic properties. *Journal of Power Sources* **2013**, *239*, 16-23. DOI: https://doi.org/10.1016/j.jpowsour.2013.03.091.

(93) Ren, Y. M.; Sun, D. Y.; Cao, Y. M.; Tsao, H. N.; Yuan, Y.; Zakeeruddin, S. M.; Wang, P.; Grätzel, M. A Stable Blue Photosensitizer for Color Palette of Dye-Sensitized Solar Cells Reaching 12.6% Efficiency. *J. Am. Chem. Soc.* **2018**, *140*, 2405-2408. DOI: https://doi.org/10.1021/jacs.7b12348.

(94) Zhang, L. *et al.* 13.6% Efficient Organic Dye-Sensitized Solar Cells by Minimizing Energy Losses of the Excited State. *ACS Energy Lett.* **2019**, *4*, 943-951. DOI: https://doi.org/10.1021/acsenergylett.9b00141.

(95) Ren, Y. M.; Zhang, D.; Suo, J. J.; Cao, Y. M.; Eickemeyer, F. T.; Vlachopoulos, N.; Zakeeruddin, S. M.; Hagfeldt, A.; Grätzel, M. Hydroxamic acid pre-adsorption raises the efficiency of cosensitized solar cells. *Nature* **2023**, *613*, 60-65. DOI: https://doi.org/10.1038/s41586-022-05460-z.

(96) Loncaric, M.; Gaso-Sokac, D.; Jokic, S.; Molnar, M. Recent Advances in the Synthesis of Coumarin Derivatives from Different Starting Materials. *Biomolecules* **2020**, *10*, 151. DOI: https://doi.org/10.3390/biom10010151.

(97) Vogel, A. J. A. d. P. Darstellung von Benzoesäure aus der Tonka-Bohne und aus den Meliloten-oder Steinklee-Blumen. **1820**, *64*, 161-166.

(98) Liu, X.; Cole, J. M.; Waddell, P. G.; Lin, T. C.; Radia, J.; Zeidler, A. Molecular origins of optoelectronic properties in coumarin dyes: toward designer solar cell and laser applications. *J Phys Chem A* **2012**, *116*, 727-737. DOI: https://doi.org/10.1021/jp209925y.

(99) Perkin, W. H. On the artificial production of coumarin and formation of its homologues. *J. Chem. Soc.* **1868**, *21*, 53-63. DOI: https://doi.org/10.1039/JS8682100053.

(100) Tian, G.; Zhang, Z. X.; Li, H. D.; Li, D. S.; Wang, X. R.; Qin, C. G. Design, Synthesis and Application in Analytical Chemistry of Photo-Sensitive Probes Based on Coumarin. *Crit. Rev. Anal. Chem.* **2021**, *51*, 565-581. DOI: https://doi.org/10.1080/10408347.2020.1753163.

(101) Ansary, I.; Taher, A.: One-pot synthesis of coumarin derivatives. In *Phytochemicals in Human Health*; Rao, A. V., Ed.; IntechOpen, 2019; pp 1-34.

(102) Heravi, M. M.; Khaghaninejad, S.; Mostofi, M.: Pechmann Reaction in the Synthesis of Coumarin Derivatives. In *Advances in Hetercyclic Chemistry*; Katritzky, A. R., Ed.; Advances in Heterocyclic Chemistry, 2014; Vol. 112; pp 1-50.

(103) Vekariya, R. H.; Patel, H. D. Recent Advances in the Synthesis of Coumarin Derivatives via Knoevenagel Condensation: A Review. *Synth. Commun.* **2014**, *44*, 2756-2788. DOI: https://doi.org/10.1080/00397911.2014.926374.

(104) Borges, F.; Roleira, F.; Milhazes, N.; Santana, L.; Uriarte, E. Simple coumarins and analogues in medicinal chemistry: Occurrence, synthesis and biological activity. *Curr. Med. Chem.* **2005**, *12*, 887-916. DOI: https://doi.org/10.2174/0929867053507315.

(105) Desai, V. G.; Shet, J. B.; Tilve, S. G.; Mali, R. S. Intramolecular Wittig reactions. A new synthesis of coumarins and 2-quinolones. *J. Chem. Res.* **2003**, 628-629. DOI: https://doi.org/10.3184/0308234033226558.

(106) Hwang, I. T.; Lee, S. A.; Hwang, J. S.; Lee, K. I. A Facile Synthesis of Highly Functionalized 4-Arylcoumarins via Kostanecki Reactions Mediated by DBU. *Molecules* **2011**, *16*, 6313-6321. DOI: https://doi.org/10.3390/molecules16086313.

(107) Parikh, A.; Parikh, H.; Parikh, K.: Kostanecki-Robinson Reaction. In *Name reactions in organic synthesis*; Foundation Books, 2006; pp 562 - 565.

(108) Pierson, J. T.; Dumètre, A.; Hutter, S.; Delmas, F.; Laget, M.; Finet, J. P.; Azas, N.; Combes, S. Synthesis and antiprotozoal activity of 4-arylcoumarins. *Eur. J. Med. Chem.* **2010**, *45*, 864-869. DOI: https://doi.org/10.1016/j.ejmech.2009.10.022.

(109) Combes, S. *et al.* Synthesis and Biological Evaluation of 4-Arylcoumarin Analogues of Combretastatins. Part 2. *J. Med. Chem.* **2011**, *54*, 3153-3162. DOI: https://doi.org/10.1021/jm901826e.

(110) Chin, Y. P.; Huang, W. J.; Hsu, F. L.; Lin, Y. L.; Lin, M. H. Synthesis and Evaluation of Antibacterial Activities of 5,7-Dihydroxycoumarin Derivatives. *Arch. Pharm.* **2011**, *344*, 386-393. DOI: https://doi.org/10.1002/ardp.201000233.

(111) Zhang, G. H.; Zheng, H.; Guo, M. Y.; Du, L.; Liu, G. J.; Wang, P. Synthesis of polymeric fluorescent brightener based on coumarin and its performances on paper as light stabilizer, fluorescent brightener and surface sizing agent. *Appl. Surf. Sci.* **2016**, *367*, 167-173. DOI: http://dx.doi.org/10.1016/j.apsusc.2016.01.110.

(112) Keskin, S. S.; Aslan, N.; Bayrakçeken, N. Optical properties and chemical behavior of Laser-dye Coumarin-500 and the influence of atmospheric corona discharges. *Spectrochim Acta A Mol Biomol Spectrosc.* **2009**, *72*, 254-259. DOI: https://doi.org/10.1016/j.saa.2008.09.024.

(113) Pramod, A. G.; Nadaf, Y. F.; Renuka, C. G. Synthesis, photophysical, quantum chemical investigation, linear and non-linear optical properties of coumarin derivative: Optoelectronic and optical limiting application. *Spectrochim Acta A Mol Biomol Spectrosc.* **2019**, *223*. DOI: https://doi.org/10.1016/j.saa.2019.117288.

(114) Sun, Y.-F.; Xu, S.-H.; Wu, R.-T.; Wang, Z.-Y.; Zheng, Z.-B.; Li, J.-K.; Cui, Y.-P. The synthesis, structure and photoluminescence of coumarin-based chromophores. *Dyes Pigm.* **2010**, *87*, 109-118. DOI: https://doi.org/10.1016/j.dyepig.2010.03.003.

(115) Jung, Y.; Jung, J.; Huh, Y.; Kim, D. Benzo[*g*]coumarin-Based Fluorescent Probes for Bioimaging Applications. *J. Anal. Methods Chem.* **2018**, *2018*, 5249765. DOI: https://doi.org/10.1155/2018/5249765.

(116) Han, L.; Wu, H. B.; Cui, Y. H.; Zu, X. Y.; Ye, Q.; Gao, J. R. Synthesis and density functional theory study of novel coumarin-type dyes for dye sensitized solar cells. *J. Photochem. Photobiol. A* **2014**, *290*, 54-62. DOI: https://doi.org/10.1016/j.jphotochem.2014.06.001.

(117) Han, L.; Kang, R.; Zu, X. Y.; Cui, Y. H.; Gao, J. R. Novel coumarin sensitizers based on 2-(thiophen-2-yl)thiazole π-bridge for dye-sensitized solar cells. *Photochem. Photobiol. Sci.* **2015**, *14*, 2046-2053. DOI: https://doi.org/10.1039/C5PP00216H.

(118) Han, L.; He, J.; Zhao, J. G.; Jiang, S. L. New difluorenylaminocoumarin photosensitizers for dye-sensitized solar cells. *Rev. Chem. Intermed.* **2017**, *43*, 5779-5794. DOI: https://doi.org/10.1007/s11164-017-2962-z.

(119) Torres, É.; Sequeira, S.; Parreira, P.; Mendes, P.; Silva, T.; Lobato, K.; Brites, M. J. Coumarin dye with ethynyl group as π-spacer unit for dye sensitized solar cells. *J. Photochem. Photobiol., A* **2015**, *310*, 1-8. DOI: https://doi.org/10.1016/j.jphotochem.2015.05.017.

(120) Zhong, C. J.; Gao, J. R.; Cui, Y. H.; Li, T.; Han, L. Coumarin-bearing triarylamine sensitizers with high molar extinction coefficient for dye-sensitized solar cells. *J. Power Sources* **2015**, *273*, 831-838. DOI: https://doi.org/10.1016/j.jpowsour.2014.09.163.

(121) Jadhav, M. M.; Vaghasiya, J. V.; Patil, D. S.; Soni, S. S.; Sekar, N. Structure-efficiency relationship of newly synthesized 4-substituted donor-π-acceptor coumarins for dye-sensitized solar cells. *New J. Chem.* **2018**, *42*, 5267-5275. DOI: https://doi.org/10.1039/C7NJ04954D.

(122) Gupta, P. O.; Sharma, S. J.; Sekar, N. Theoretical investigation of substitution effect on the sixth and seventh positions of coumarin derivatives. *Spectrochim Acta A Mol Biomol Spectrosc.* **2024**, *304*. DOI: https://doi.org/10.1016/j.saa.2023.123373.

(123) Sharma, S. J.; Prasad, J.; Soni, S. S.; Sekar, N. The impact of anchoring groups on the efficiency of dye-sensitized solar cells: 2-Cyanoacrylic acid vs. ethyl 2-cyanoacrylate. *J. Photochem. Photobiol., A.* **2023**, *444*, 114915. DOI: https://doi.org/10.1016/j.jphotochem.2023.114915.

(124) He, J.; Liu, Y.; Gao, J. R.; Han, L. New D-D-π-A triphenylamine-coumarin sensitizers for dye-sensitized solar cells. *Photochem. Photobiol. Sci.* **2017**, *16*, 1049-1056. DOI: https://doi.org/10.1039/c6pp00410e.

(125) Hara, K.; Sayama, K.; Ohga, Y.; Shinpo, A.; Suga, S.; Arakawa, H. A coumarin-derivative dye sensitized nanocrystalline TiO2 solar cell having a high solar-energy conversion efficiency up to 5.6%. *Chem. Comm.* **2001**, 569-570. DOI: https://doi.org/10.1039/B010058G.

(126) Hara, K.; Dan-Oh, Y.; Kasada, C.; Ohga, Y.; Shinpo, A.; Suga, S.; Sayama, K.; Arakawa, H. Effect of additives on the photovoltaic performance of coumarin-dye-sensitized nanocrystalline TiO2 solar cells. *Langmuir* **2004**, *20*, 4205-4210. DOI: https://doi.org/10.1021/la0357615.

(127) Hara, K.; Miyamoto, K.; Abe, Y.; Yanagida, M. Electron transport in coumarin-dye-sensitized nanocrystalline TiO2 electrodes. *J. Phys. Chem. B* **2005**, *109*, 23776-23778. DOI: https://doi.org/10.1021/jp055572q.

(128) Hara, K. *et al.* Molecular design of coumarin dyes for efficient dye-sensitized solar cells. *J. Phys. Chem. B* **2003**, *107*, 597-606. DOI: https://doi.org/10.1021/jp026963x.

(129) Feng, H. J.; Li, R. R.; Song, Y. C.; Li, X. Y.; Liu, B. Novel D-π-A-π-A coumarin dyes for highly efficient dye-sensitized solar cells: Effect of π-bridge on optical, electrochemical, and photovoltaic performance. *J. Power Sources* **2017**, *345*, 59-66. DOI: https://doi.org/10.1016/j.jpowsour.2017.01.115.

(130) Murakami, T. N.; Koumura, N.; Kimura, M.; Mori, S. Structural Effect of Donor in Organic Dye on Recombination in Dye-Sensitized Solar Cells with Cobalt Complex Electrolyte. *Langmuir* **2014**, *30*, 2274-2279. DOI: https://doi.org/10.1021/la4047808.

(131) Martins, S. M. A.; Branco, P. C. S.; Pereira, A. M. D. R. L. An Efficient Methodology for the Synthesis of 3-Styryl Coumarins. *Chem. Soc.* **2012**, *23*, 688-693. DOI: https://doi.org/10.1590/S0103-50532012000400014

(132) Gordo, J.; Avó, J.; Parola, A. J.; Lima, J. C.; Pereira, A.; Branco, P. S. Convenient Synthesis of 3-Vinyl and 3-Styryl Coumarins. *Org. Lett.* **2011**, *13*, 5112-5115. DOI: https://doi.org/10.1021/ol201983u.

(133) Sarrato, J.; Pinto, A. L.; Malta, G.; Rock, E. G.; Pina, J.; Lima, J. C.; Parola, A. J.; Branco, P. S. New 3-Ethynylaryl Coumarin-Based Dyes for DSSC Applications: Synthesis, Spectroscopic Properties, and Theoretical Calculations. *Molecules* **2021**, *26*, 2934. DOI: https://doi.org/10.3390/molecules26102934.

(134) Costa, P.; Leão, R.; de F. de Moraes, P.; Pedro, M. Synthesis of Coumarins and Neoflavones through Zinc Chloride Catalyzed Hydroarylation of Acetylenic Esters with Phenols. *Synth.* **2011**, *2011*, 3692-3696. DOI: https://doi.org/10.1055/s-0031-1289576.

(135) Chang, C.-F.; Yang, L.-Y.; Chang, S.-W.; Fang, Y.-T.; Lee, Y.-J. Total synthesis of demethylwedelolactone and wedelolactone by Cu-mediated/Pd(0)-catalysis and oxidative-cyclization. *Tetrahedron* **2008**, *64*, 3661-3666. DOI: https://doi.org/10.1016/j.tet.2008.02.031.

(136) Lente, G.; Kalmár, J.; Baranyai, Z.; Kun, A.; Kék, I.; Bajusz, D.; Takács, M.; Veres, L.; Fábián, I. One- Versus Two-Electron Oxidation with Peroxomonosulfate Ion: Reactions with Iron(II), Vanadium(IV), Halide Ions, and Photoreaction with Cerium(III). *Inorg. Chem.* **2009**, *48*, 1763-1773. DOI: https://doi.org/10.1021/ic801569k.

(137) Zhang, M.; Su, J.; Zhang, Y.; Chen, M.; Li, W.; Qin, X.; Xie, Y.; Qin, L.; Huang, S. A Copper Halide Promoted Regioselective Halogenation of Coumarins Using N-Halosuccinimide as Halide Source. *Synlett* **2019**, *30*, 630-634. DOI: https://doi.org/10.1055/s-0037-1612080.

(138) Chinchilla, R.; Nájera, C. Recent advances in Sonogashira reactions. *Chem. Soc. Rev.* **2011**, *40*, 5084-5121. DOI: https://doi.org/10.1039/C1CS15071E.

(139) Clayden, J.; Greeves, N.; Warren, S.: Cross-coupling of organometalic halides. In *Organic Chemistry*, 2nd, Ed.; Oxford: Oxford, 2001; pp 1087-1088.

(140) Kivala, T. A. S. a. M.: Cross-Coupling Reactions to sp Carbon Atoms. In *Metal-Catalyzed Cross-Coupling Reactions and More*; Armin de Meijere, S. B., Martin Oestreich, Ed.; Wiley-VCH, 2013; pp 665-671.

(141) Mohajer, F.; Heravi, M. M.; Zadsirjan, V.; Poormohammad, N. Copper-free Sonogashira cross-coupling reactions: an overview. *Rsc Adv.* **2021**, *11*, 6885-6925. DOI: https://doi.org/10.1039/D0RA10575A.

(142) Luo, Y.; Wu, J. Copper-free Sonogashira reactions of 4-hydroxycoumarins with alkynes. *Tetrahedron* **2009**, *65*, 6810-6814. DOI: https://doi.org/10.1016/j.tet.2009.06.089.

(143) Irie, S. *et al.* Rapid Synthesis of D-A'-pi-A Dyes through a One-Pot Three-Component Suzuki-Miyaura Coupling and an Evaluation of their Photovoltaic Properties for Use in Dye-Sensitized Solar Cells. *Chemistry* **2016**, *22*, 2507-2514. DOI: https://doi.org/10.1002/chem.201504277.

(144) Wang, Y. *et al.* Influence of 4-tert-butylpyridine/guanidinium thiocyanate co-additives on band edge shift and recombination of dye-sensitized solar cells: experimental and theoretical aspects. *Electrochim. Acta* **2015**, *185*, 69-75. DOI: https://doi.org/10.1016/j.electacta.2015.10.103.

(145) Bradley, D.; Williams, G.; Lawton, M. Drying of Organic Solvents: Quantitative Evaluation of the Efficiency of Several Desiccants. *J. Org. Chem.* **2010**, *75*, 8351-8354. DOI: https://doi.org/10.1021/jo101589h.

(146) Perrin, D. D.; Armarego, W. L. F.; Perrin, D. R.: *Purification of laboratory chemicals perrin amarego*; Pergamon Press, 1980.

(147) Stahl, E.: *Thin-Layer Chromatography*; Springer, 1967.

(148) Still, W. C.; Kahn, M.; Mitra, A. Rapid chromatographic technique for preparative separations with moderate resolution. *J. Org. Chem.* **1978**, *43*, 2923-2925. DOI: https://doi.org/10.1021/jo00408a041.

(149) Pinto, A. L.; Cruz, L.; Gomes, V.; Cruz, H.; Calogero, G.; de Freitas, V.; Pina, F.; Parola, A. J.; Lima, J. C. Catechol versus carboxyl linkage impact on DSSC performance of synthetic pyranoflavylium salts. *Dyes Pigm.* **2019**, *170*. DOI: https://doi.org/10.1016/j.dyepig.2019.107577.

(150) Quintal, S. *et al.* Molybdenum(ii) complexes with p-substituted BIAN ligands: synthesis, characterization, biological activity and computational study. *Dalton Trans.* **2019**, *48*, 8449-8463. DOI: https://doi.org/10.1039/C9DT00469F.

(151) Hill, N. J.; Vargas-Baca, I.; Cowley, A. H. Recent developments in the coordination chemistry of bis(imino)acenaphthene (BIAN) ligands with s- and p-block elements. *Dalton Trans.* **2009**, 240-253. DOI: https://doi.org/10.1039/B815079F.

(152) Wang, J. Y.; Soo, H. S.; Garcia, F. Synthesis, properties, and catalysis of p-block complexes supported by bis(arylimino)acenaphthene ligands. *Commun. Chem.* **2020**, *3*, 1-13. DOI: https://doi.org/10.1038/s42004-020-00359-0.

(153) Wang, F. Z.; Yuan, J. C.; Li, Q. S.; Tanaka, R.; Nakayama, Y.; Shiono, T. New nickel(II) diimine complexes bearing phenyl and sec-phenethyl groups: synthesis, characterization and ethylene polymerization behaviour. *Appl. Organomet. Chem.* **2014**, *28*, 477-483. DOI: https://doi.org/10.1002/aoc.3151.

(154) Zou, W. P.; Chen, C. L. Influence of Backbone Substituents on the Ethylene (Co)polymerization Properties of α-diimine Pd(II) and Ni(II) Catalysts. *Organometallics* **2016**, *35*, 1794-1801. DOI: https://doi.org/10.1021/acs.organomet.6b00202.

(155) Evans, D. A.; Lee, L. M.; Vargas-Baca, I.; Cowley, A. H. Aggregation-Induced Emission of Bis(imino)acenaphthene Zinc Complexes: Photophysical Tuning via Methylation of the Flanking Aryl Substituents. *Organometallics* **2015**, *34*, 2422-2428. DOI: https://doi.org/10.1021/om501191c.

(156) Mak, C. S. K.; Wong, H. L.; Leung, Q. Y.; Tam, W. Y.; Chan, W. K.; Djurišić, A. B. The use of sublimable chlorotricarbonyl bis(phenylimino)acenaphthene rhenium(I) complexes as photosensitizers in bulk-heterojunction photovoltaic devices. *J. Organomet. Chem.* **2009**, *694*, 2770-2776. DOI: https://doi.org/10.1016/j.jorganchem.2009.04.037.

(157) Wong, H. L.; Lam, L. S. M.; Cheng, K. W.; Man, K. Y. K.; Chan, W. K.; Kwong, C. Y.; Djurisic, A. B. Low-band-gap, sublimable rhenium(I) diimine complex for efficient bulk heterojunction photovoltaic devices. *Appl. Phys. Lett.* **2004**, *84*, 2557-2559. DOI: https://doi.org/10.1063/1.1682676.

(158) Patnaik, S. G.; Vedarajan, R.; Matsumi, N. BIAN based functional diimine polymer binder for high performance Li ion batteries. *J. Mater. Chem. A.* **2017**, *5*, 17909-17919. DOI: https://doi.org/10.1039/C7TA03843G.

(159) Kee, J. W.; Ng, Y. Y.; Kulkarni, S. A.; Muduli, S. K.; Xu, K.; Ganguly, R.; Lu, Y.; Hirao, H.; Soo, H. S. Development of bis(arylimino)acenaphthene (BIAN) copper complexes as visible light harvesters for potential photovoltaic applications. *Inorg. Chem. Front.* **2016**, *3*, 651-662. DOI: https://doi.org/10.1039/C5QI00221D.

(160) Gasperini, M.; Ragaini, F.; Gazzola, E.; Caselli, A.; Macchi, P. Synthesis of mixed Ar,Ar'-BIAN ligands (Ar,Ar'-BIAN = bis(aryl)acenaphthenequinonediimine). Measurement of

the coordination strength of hemilabile ligands with respect to their symmetric counterparts. *Dalton Trans.* **2004**, 3376-3382. DOI: https://doi.org/10.1039/B406582D.

(161) Vanasselt, R.; Elsevier, C. J.; Smeets, W. J. J.; Spek, A. L.; Benedix, R. Synthesis and characterization of rigid bidentate nitrogen ligands and some examples of coordination to divalent palladium. X-ray crystal structures of bis (p-tolylimino) acenaphthene and methylchloro [bis(o,o′-diisopropylphenyl-imino) acenaphthene] palladium (II). *Recueil Des Travaux Chimiques Des Pays-Bas-Journal of the Royal Netherlands Chemical Society* **1994**, *113*, 88-98. DOI: https://doi.org/10.1002/recl.19941130204.

(162) Saxer, S.; Marestin, C.; Mercier, R.; Dupuy, J. The multicomponent Debus-Radziszewski reaction in macromolecular chemistry. *Polym. Chem.* **2018**, *9*, 1927-1933. DOI: https://doi.org/10.1039/C8PY00173A.

(163) Jayabharathi, J.; Thanikachalam, V.; Ramanathan, P.; Arunpandiyan, A. Intramolecular excited proton transfer of 1-(1-phenyl-1H-phenanthro[9,10-d]imidazol-2-yl)naphthalen-2-ol--a combined experimental and quantum chemical studies. *Spectrochim. Acta A Mol. Biomol. Spectrosc.* **2014**, *121*, 551-558. DOI: https://doi.org/10.1016/j.saa.2013.10.097

(164) Bahrami, K.; Khodaei, M. M.; Nejati, A. One-pot synthesis of 1,2,4,5-tetrasubstituted and 2,4,5-trisubstituted imidazoles by zinc oxide as efficient and reusable catalyst. *Monatsh. Chem.* **2010**, *142*, 159-162. DOI: https://doi.org/10.1007/s00706-010-0428-8.

(165) Sarkar, R.; Mukhopadhyay, C. Silver-Mediated Cα(sp3)-H Functionalization of Primary Amines: An Oxidative C-N Coupling Strategy for the Synthesis of Two Different Types of 1,2,4,5-Tetrasubstituted Imidazoles. *EurJOC* **2015**, *2015*, 1246-1256. DOI: https://doi.org/10.1002/ejoc.201403465.

(166) Albayati, M. R.; Marzouk, A. A.; Abdelhamid, A. A. Piperidinium Hydrogen Sulfate (PHS) as an Efficient Ionic Liquid Catalyst for the Synthesis of Imidazole Derivative under Solvent-Free Condition. *J. Heterocycl. Chem.* **2019**, *56*, 1514-1519. DOI: https://doi.org/10.1002/jhet.3525.

(167) Jayabharathi, J.; Ramanathan, P.; Thanikachalam, V. Synthesis and optical properties of phenanthromidazole derivatives for organic electroluminescent devices. *New J. Chem.* **2015**, *39*, 142-154. DOI: https://doi.org/10.1039/C4NJ01515K.

(168) Okda, H. E.; El Sayed, S.; Otri, I.; Ferreira, R. C. M.; Costa, S. P. G.; Raposo, M. M. M.; Martínez-Máñez, R.; Sancenón, F. A simple and easy-to-prepare imidazole-based probe for

the selective chromo-fluorogenic recognition of biothiols and Cu(II) in aqueous environments. *Dyes Pigm.* **2019**, *162*, 303-308. DOI: https://doi.org/10.1016/j.dyepig.2018.10.017.

(169) Moosavi-Zare, A. R.; Asgari, Z.; Zare, A.; Zolfigol, M. A.; Shekouhy, M. One pot synthesis of 1,2,4,5-tetrasubstituted-imidazoles catalyzed by trityl chloride in neutral media. *RSC Adv.* **2014**, *4*, 60636-60639. DOI: https://doi.org/10.1039/C4RA10589C.

(170) Sarkar, R.; Chaudhuri, T.; Karmakar, A.; Mukhopadhyay, C. Synthesis and photophysics of selective functionalized pi-conjugated, blue light emitting, highly fluorescent C7-imidazo indolizine derivatives. *Org. Biomol. Chem.* **2015**, *13*, 11674-11686. DOI: https://doi.org/10.1039/C5OB01646K.

(171) Sivanadanam, J.; Aidhen, I. S.; Ramanujam, K. New cyclic and acyclic imidazole-based sensitizers for achieving highly efficient photoanodes for dye-sensitized solar cells by a potential-assisted method. *New J. Chem.* **2020**, *44*, 10207-10219. DOI: https://doi.org/10.1039/D0NJ00137F.

(172) Liu, Y.-H.; Perepichka, D. F. Acenaphthylene as a building block for π-electron functional materials. *J. Mater. Chem. C* **2021**, *9*, 12448-12461. DOI: https://doi.org/10.1039/D1TC02826J.

(173) Wang, T.; Han, J.; Zhang, Z.; Xu, B.; Huang, J.; Su, J. Bistriphenylamine-substituted fluoranthene derivatives as electroluminescent emitters and dye-sensitized solar cells. *Tetrahedron* **2012**, *68*, 10372-10377. DOI: https://doi.org/10.1016/j.tet.2012.09.013.

(174) Kong, Z.; Zhou, H.; Cui, J.; Ma, T.; Yang, X.; Sun, L. A new class of organic dyes based on acenaphthopyrazine for dye-sensitized solar cells. *J. Photochem. Photobiol., A* **2010**, *213*, 152-157. DOI: https://doi.org/10.1016/j.jphotochem.2010.05.017.

(175) Okujima, T.; Shida, Y.; Ohara, K.; Tomimori, Y.; Nishioka, M.; Mori, S.; Nakae, T.; Uno, H. Synthesis of NIR-emitting O-chelated BODIPYs fused with benzene and acenaphthylene. *J. Porphyr. Phthalocyanines* **2014**, *18*, 752-761. DOI: https://doi.org/10.1142/S1088424614500503.

(176) Wang, T. H.; Han, J. L.; Zhang, Z. Y.; Xu, B.; Huang, J. H.; Su, J. H. Bistriphenylamine-substituted fluoranthene derivatives as electroluminescent emitters and dye-sensitized solar cells. *Tetrahedron* **2012**, *68*, 10372-10377. DOI: https://doi.org/10.1016/j.tet.2012.09.013.

(177) Xie, Y.; Han, L.; Ge, C.-S.; Cui, Y.-H.; Gao, J.-R. Novel organic dye sensitizers containing fluorenyl and biphenyl moieties for solar cells. *Chinese Chem. Lett.* **2017**, *28*, 285-292. DOI: https://doi.org/10.1016/j.cclet.2016.06.042.

(178) Ji, J. M.; Zhou, H.; Eom, Y. K.; Kim, C. H.; Kim, H. K. 14.2% Efficiency Dye-Sensitized Solar Cells by Co-sensitizing Novel Thieno[3,2-b]indole-Based Organic Dyes with a Promising Porphyrin Sensitizer. *Adv. Energy Mat.* **2020**, *10*, 2000124. DOI: https://doi.org/10.1002/aenm.202000124.

(179) Chen, C. H.; Hsu, Y. C.; Chou, H. H.; Thomas, K. R.; Lin, J. T.; Hsu, C. P. Dipolar compounds containing fluorene and a heteroaromatic ring as the conjugating bridge for high-performance dye-sensitized solar cells. *Chem. Eur. J.* **2010**, *16*, 3184-3193. DOI: https://doi.org/10.1002/chem.200903151.

(180) Baheti, A.; Tyagi, P.; Thomas, K. R. J.; Hsu, Y. C.; Lin, J. T. Simple Triarylamine-Based Dyes Containing Fluorene and Biphenyl Linkers for Efficient Dye-Sensitized Solar Cells. *Journal of Physical Chemistry C* **2009**, *113*, 8541-8547. DOI: https://doi.org/10.1021/jp902206g.

(181) Chenab, K. K.; Meymian, M. R. Z. Replacing naphthalene with anthracene pi-bridge improves efficiency of D-pi-A triphenylamine dyes-based dye-sensitized solar cells. *Solar Energy* **2022**, *234*, 9-20. DOI: https://doi.org/10.1016/j.solener.2022.01.062.

(182) Riddle, J. A.; Jiang, X.; Huffman, J.; Lee, D. Signal-amplifying resonance energy transfer: a dynamic multichromophore array for allosteric switching. *Angew. Chem. Int. Ed. Engl.* **2007**, *46*, 7019-7022. DOI: https://doi.org/10.1002/anie.200701410.

(183) He, Y.; Zhao, H.; Pan, X.; Wang, S. Reduction with Metal Borohydride-Transition Metal Salt System. I. Reduction of Aromatic Nitro Compounds with Potassium Borohydride-Copper(I) Chloride. *Synth. Commun.* **1989**, *19*, 3047-3050. DOI: https://doi.org/10.1080/00397918908052699.

(184) Vogel, A. I.; Tatchell, A. R.; Furnis, B. S.; Hannaford, A. J.; Smith, P. W. G.: *Vogel's Textbook of Practical Organic Chemistry*, 5th ed.; Longman Scientific & Tecnhical, 1989.

(185) Valle-González, O. A.; Salazar-Bello, A. I.; Luján-Montelongo, J. A. Stereoselective synthesis of vinyl nitriles through a Ramberg-Backlund approach. *Org. Biomol. Chem.* **2023**, *21*, 2894-2898. DOI: https://doi.org/10.1039/D3OB00214D.

(186) Liu, H.; Zhao, W.; Hao, X.; Redshaw, C.; Huang, W.; Sun, W.-H. 2,6-Dibenzhydryl-N-(2-phenyliminoacenaphthylenylidene)-4-methylbenzenamine Nickel Dibromides: Synthesis, Characterization, and Ethylene Polymerization. *Organometallics* **2011**, *30*, 2418-2424. DOI: https://doi.org/10.1021/om200154a.

(187) Vasudevan, K. V.; Butorac, R. R.; Abernethy, C. D.; Cowley, A. H. Synthesis and coordination compounds of a bis(imino)acenaphthene (BIAN)-supported N-heterocyclic carbene. *Dalton Trans.* **2010**, *39*, 7401-7408. DOI: https://doi.org/10.1039/C0DT00278J.

(188) Singh, I.; Rani, R.; Luxami, V.; Paul, K. Synthesis of 5-(4-(1H-phenanthro[9,10-d]imidazol-2-yl)benzylidene)thiazolidine-2,4-dione as promising DNA and serum albumin-binding agents and evaluation of antitumor activity. *Eur. J. Med. Chem.* **2019**, *166*, 267-280. DOI: https://doi.org/10.1016/j.ejmech.2019.01.053.

(189) El'chaninov, M. M.; Achkasova, A. A.; El'chaninov, I. M. Synthesis and some transformations of 2-(2-thienyl)-1H-acenaphtho[1,2-d]imidazole. *Russ J Gen Chem* **2014**, *84*, 1697-1700. DOI: https://doi.org/10.1134/S1070363214090096.

(190) Thanikachalam, V.; Sarojpurani, E.; Jayabharathi, J.; Jeeva, P. Efficient phenanthroimidazole-styryl-triphenylamine derivatives for blue OLEDs: a combined experimental and theoretical study. *New J. Chem.* **2017**, *41*, 2443-2457. DOI: https://doi.org/10.1039/C6NJ03801H.

(191) Malta, G.; Pina, J.; Lima, J. C.; Parola, A. J.; Branco, P. S. Acenaphthylene-Based Chromophores for Dye-Sensitized Solar Cells: Synthesis, Spectroscopic Properties, and Theoretical Calculations. *ACS Omega* **2024**, *9*, 14627-14637. DOI: https://doi.org/10.1021/acsomega.4c01201.

(192) Trost, B. M.; Brittelli, D. R. The Halogenation of Acenaphthene Derivatives. *J. Org. Chem.* **1967**, *32*, 2620–2621.

(193) Majumdar, P.; Mack, J.; Nyokong, T. Synthesis, characterization and photophysical properties of an acenaphthalene fused-ring-expanded NIR absorbing aza-BODIPY dye. *RSC Advances*
**2015**, *5*, 78253-78258. DOI: https://doi.org/10.1039/C5RA14916A.

(194) Murugesan, V.; de Bettignies, R.; Mercier, R.; Guillerez, S.; Perrin, L. Synthesis and characterizations of benzotriazole based donor-acceptor copolymers for organic photovoltaic applications. *Synth. Met.* **2012**, *162*, 1037-1045. DOI: 10.1016/j.synthmet.2012.04.006.

(195) Arslan, B. S.; Arkan, B.; Gezgin, M.; Derin, Y.; Avci, D.; Tutar, A.; Nebioglu, M.; Sisman, I. The improvement of photovoltaic performance of quinoline-based dye-sensitized solar cells by modification of the auxiliary acceptors. *J Photochem Photobiol A Chem* **2021**, *404*, 112936. DOI: https://doi.org/10.1016/j.jphotochem.2020.112936.

(196) Rani, S.; Luxami, V.; Paul, K. Synthesis of Triphenylethylene-Naphthalimide Conjugates as topoisomerase-II$\alpha$ inhibitor and HSA binder. *ChemMedChem* **2021**, *16*, 1821-1831. DOI: https://doi.org/10.1002/cmdc.202100034.

(197) Lin, J. T.; Chen, P. C.; Yen, Y. S.; Hsu, Y. C.; Chou, H. H.; Yeh, M. C. P. Organic Dyes Containing Furan Moiety for High-Performance Dye-Sensitized Solar Cells. *Organic Letters* **2009**, *11*, 97-100. DOI: https://doi.org/10.1021/ol8025236.

(198) Kumaresan, P.; Vegiraju, S.; Ezhumalai, Y.; Yau, S.; Kim, C.; Lee, W.-H.; Chen, M.-C. Fused-Thiophene Based Materials for Organic Photovoltaics and Dye-Sensitized Solar Cells. *Polymers* **2014**, *6*, 2645-2669. DOI: https://doi.org/10.3390/polym6102645.

(199) Zhang, H.; Fan, J.; Iqbal, Z.; Kuang, D.-B.; Wang, L.; Cao, D.; Meier, H. J. D.; Pigments. Anti-recombination organic dyes containing dendritic triphenylamine moieties for high open-circuit voltage of DSSCs. **2013**, *99*, 74-81. DOI: https://doi.org/10.1016/j.dyepig.2013.04.023.

(200) Cardona, C. M.; Li, W.; Kaifer, A. E.; Stockdale, D.; Bazan, G. C. Electrochemical considerations for determining absolute frontier orbital energy levels of conjugated polymers for solar cell applications. **2011**, *23* 2367–2371. DOI: https://doi.org/10.1002/adma.201004554.

(201) Fernandes, S. S.; Castro, M. C. l. R.; Pereira, A. I.; Mendes, A. l.; Serpa, C.; Pina, J. o.; Justino, L. L.; Burrows, H. D.; Raposo, M. M. M. J. A. o. Optical and Photovoltaic Properties of Thieno[3, 2-b]thiophene-based Push–Pull Organic Dyes with Different Anchoring Groups for Dye-Sensitized Solar Cells. **2017**, *2*, 9268-9279. DOI: https://doi.org/10.1021/acsomega.7b01195.

(202) Fabian, J. Electronic excitation of sulfur-organic compounds–performance of time-dependent density functional theory. *J Theoretical Chemistry Accounts* **2001**, *106*, 199-217. DOI: https://doi.org/10.1007/s002140100250.

(203) Desroches, J.; Champagne, P. A.; Benhassinea, Y.; Paquin, J.-F. In situ activation of benzyl alcohols with XtalFluor-E: formation of 1,1-diarylmethanes and 1,1,1-triarylmethanes through Friedel–Crafts benzylation. *Org. Biomol. Chem.* **2015**, *13*, 2243-2246. DOI: https://doi.org/10.1039/C4OB02655A.

(204) Suzuki, I.; Shimazu, J.-y.; Tsunoi, S.; Shibata, I. Diastereoselective Synthesis of Spiro[2.3]hexanes from Methylenecyclopropane and Cyanoalkenes Catalyzed by a Tin-Ate Complex. *EurJOC* **2019**, *2019*, 3658-3661. DOI: https://doi.org/10.1002/ejoc.201900518.

(205) Lu, C.; Tang, K.; Li, Y.; Li, P.; Lin, Z.; Yin, D.; Chen, X.; Huang, H. Design, synthesis and evaluation of novel diaryl urea derivatives as potential antitumor agents. *Eur. J. Med. Chem.* **2014**, *77*, 351-360. DOI: https://doi.org/10.1016/j.ejmech.2014.03.020.

(206) Cui, M.; Ono, M.; Kimura, H.; Liu, B.; Saji, H. Synthesis and structure-affinity relationships of novel dibenzylideneacetone derivatives as probes for beta-amyloid plaques. *J Med Chem* **2011**, *54*, 2225-2240. DOI: https://pubs.acs.org/doi/10.1021/jm101404k.

(207) Gasperini, M.; Ragaini, F.; Cenini, S. Synthesis of Ar-BIAN Ligands (Ar-BIAN ) Bis(aryl acenaphthenequinonediimine) Having Strong Electron-Withdrawing Substituents on

the Aryl Rings and Their Relative Coordination Strength toward Palladium(0) and -(II) Complexes. *Organometallics* **2002**, *21*, 2950-2957. DOI: https://doi.org/10.1021/om020147u.

(208) Liu, X.; Flores, A. A.; Situ, L.; Gu, W.; Ding, H.; Christofk, H. R.; Lowry, W. E.; Jung, M. E. Development of Novel Mitochondrial Pyruvate Carrier Inhibitors to Treat Hair Loss. *J. Med. Chem.* **2021**, *64*, 2046-2063. DOI: https://doi.org/10.1021/acs.jmedchem.0c01570.

(209) Theodorou, V.; Skobridis, K.; Tzakos, A. G.; Ragoussis, V. A simple method for the alkaline hydrolysis of esters. *Tetrahedron Lett.* **2007**, *48*, 8230-8233. DOI: https://doi.org/10.1016/j.tetlet.2007.09.074.

(210) Achkasova, A. A.; El'chaninov, M. M. Synthesis and properties of 2-(2-furyl)-1-methyl-1h-acenaphtho[9,10-d]imidazole. *Chem. Heterocycl. Compd.* **2006**, *Vol. 42*, 166–171. DOI: https://doi.org/10.1007/s10593-006-0065-7.

(211) Kula, S.; Szlapa-Kula, A.; Kotowicz, S.; Filapek, M.; Bujak, K.; Siwy, M.; Janeczek, H.; Maćkowski, S.; Schab-Balcerzak, E. Phenanthro[9,10-d]imidazole with thiophene rings toward OLEDs application. *Dyes Pigm.* **2018**, *159*, 646-654. DOI: https://doi.org/10.1016/j.dyepig.2018.07.014.

(212) Sarrato, J.; Pinto, A. L.; Cruz, H.; Jordao, N.; Malta, G.; Branco, P. S.; Lima, J. C.; Branco, L. C. Effect of Iodide-Based Organic Salts and Ionic Liquid Additives in Dye-Sensitized Solar Cell Performance. *Nanomaterials* **2022**, *12*, 2988. DOI: https://doi.org/10.3390/nano12172988.

(213) Al-Aqar, R.; Atahan, A.; Benniston, A. C.; Perks, T.; Waddell, P. G.; Harriman, A. Exciton Migration and Surface Trapping for a Photonic Crystal Displaying Charge-Recombination Fluorescence. *Chem. Eur. J.* **2016**, *22*, 15420-15429. DOI: https://doi.org/10.1002/chem.201602155.

(214) Pearson, A. J. *et al.* Impact of dithienyl or thienothiophene units on the optoelectronic and photovoltaic properties of benzo 1,2,5 thiadiazole based donor-acceptor copolymers for organic solar cell devices. *Rsc Advances* **2014**, *4*, 43142-43149. DOI: https://doi.org/10.1039/C4RA07186G.

(215) Karaman, C. Z. *et al.* Effect of thiophene, 3-hexylthiophene, selenophene, and Thieno 3,2-b thiophene spacers on OPV device performance of novel 2,1,3-benzothiadiazole based alternating copolymers. *J. Electroanal. Chem.* **2021**, *895*. DOI: https://doi.org/10.1016/j.jelechem.2021.115483.

(216) Liu, Y.; Di, C. A.; Du, C. Y.; Liu, Y. Q.; Lu, K.; Qiu, W. F.; Yu, G. Synthesis, Structures, and Properties of Fused Thiophenes for Organic Field-Effect Transistors. *Chem. Eur. J.* **2010**, *16*, 2231-2239. DOI: https://doi.org/10.1002/chem.200902755.

(217) Kurumisawa, Y.; Higashino, T.; Nimura, S.; Tsuji, Y.; Iiyama, H.; Imahori, H. Renaissance of Fused Porphyrins: Substituted Methylene-Bridged Thiophene-Fused Strategy for High-Performance Dye-Sensitized Solar Cells. *J. Am. Chem. Soc.* **2019**, *141*, 9910-9919. DOI: https://doi.org/10.1021/jacs.9b03302.

(218) Podlesny, J.; Bures, F. Thienothiophene Scaffolds as Building Blocks for (Opto)Electronics. *Organics* **2022**, *3*, 446-469. DOI: https://doi.org/10.3390/org3040029.

(219) Cinar, M. E.; Ozturk, T. Thienothiophenes, Dithienothiophenes, and Thienoacenes: Syntheses, Oligomers, Polymers, and Properties. *Chem. Rev.* **2015**, *115*, 3036-3140. DOI: https://doi.org/10.1021/cr500271a.

(220) Xu, M. F.; Li, R. Z.; Pootrakulchote, N.; Shi, D.; Guo, J.; Yi, Z. H.; Zakeeruddin, S. M.; Grätzel, M.; Wang, P. Energy-Level and Molecular Engineering of Organic D-π-A Sensitizers in Dye-Sensitized Solar Cells. *J. Phys. Chem. C* **2008**, *112*, 19770-19776. DOI: https://doi.org/10.1021/jp808275z.

(221) Eom, Y. K.; Hong, J. Y.; Kim, J.; Kim, H. K. Triphenylamine-based organic sensitizers with π-spacer structural engineering for dye -sensitized solar cells: Synthesis, theoretical calculations, molecular spectroscopy and structure-property-performance relationships. *Dyes Pigm.* **2017**, *136*, 496-504. DOI: https://doi.org/10.1016/j.dyepig.2016.09.007.

(222) Fernandes, S. S. M.; Castro, M. C. R.; Pereira, A. I.; Mendes, A.; Serpa, C.; Pina, J.; Justino, L. L. G.; Burrows, H. D.; Raposo, M. M. M. Optical and Photovoltaic Properties of Thieno[3,2-b]thiophene-Based Push-Pull Organic Dyes with Different Anchoring Groups for Dye-Sensitized Solar Cells. *ACS Omega* **2017**, *2*, 9268-9279. DOI: https://doi.org/10.1021/acsomega.7b01195.

(223) Paek, S.; Choi, H.; Choi, H.; Lee, C. W.; Kang, M. S.; Song, K.; Nazeeruddin, M. K.; Ko, J. Molecular Engineering of Efficient Organic Sensitizers Incorporating a Binary π-Conjugated Linker Unit for Dye-Sensitized Solar Cells. *J. Phys. Chem. C* **2010**, *114*, 14646-14653. DOI: https://doi.org/10.1021/jp104310r.

(224) Choi, H. *et al.* High Molar Extinction Coefficient Organic Sensitizers for Efficient Dye-Sensitized Solar Cells. *Chem. Eur. J.* **2010**, *16*, 1193-1201. DOI: https://doi.org/10.1002/chem.200902197.

(225) Lim, D. S.; Park, K. W.; Wiles, A. A.; Hong, J. Metal-Free Organic Chromophores Featuring an Ethynyl-Thienothiophene Linker with an n-Hexyl Chain for Translucent Dye-Sensitized Solar Cells. *Materials* **2019**, *12*, 1741. DOI: https://doi.org/10.3390/ma12111741.

(226) Marco, A. B.; de Baroja, N. M.; Andrés-Castán, J. M.; Franco, S.; Andreu, R.; Villacampa, B.; Orduna, J.; Garín, J. Pyranylidene/thienothiophene-based organic sensitizers for dye-sensitized solar cells. *Dyes Pigm.* **2019**, *161*, 205-213. DOI: https://doi.org/10.1016/j.dyepig.2018.09.035.

(227) Brogdon, P.; Cheema, H.; Delcamp, J. H. Low-Recombination Thieno 3,4-b thiophene-Based Photosensitizers for Dye-Sensitized Solar Cells with Panchromatic Photoresponses. *ChemSusChem* **2017**, *10*, 3624-3631. DOI: https://doi.org/10.1002/cssc.201701259.

(228) Li, P.; Cui, Y.; Song, C.; Zhang, H. A systematic study of phenoxazine-based organic sensitizers for solar
cells. *Dyes Pigm.* **2017**, *137*, 12-23. DOI: https://doi.org/10.1016/j.dyepig.2016.09.060.

(229) Al-Ghamdi, S. N.; Al-Ghamdi, H. A.; El-Shishtawy, R. M.; Asiri, A. M. Advances in phenothiazine and phenoxazine-based electron donors for organic dye-sensitized solar cells. *Dyes Pigm.* **2021**, *194*, 109638. DOI: https://doi.org/10.1016/j.dyepig.2021.109638.

(230) Buene, A. F.; Almenningen, D. M. Phenothiazine and phenoxazine sensitizers for dye-sensitized solar cells - an investigative review of two complete dye classes. *J. Mater. Chem. C* **2021**, *9*, 11974-11994. DOI: https://doi.org/10.1039/D1TC03207K.

(231) Tan, H. J.; Pan, C. Y.; Wang, G.; Wu, Y. Y.; Zhang, Y. P.; Yu, G. P.; Zhang, M. A comparative study on properties of two phenoxazine-based dyes for dye-sensitized solar cells. *Dyes Pigm.* **2014**, *101*, 67-73. DOI: https://doi.org/10.1016/j.dyepig.2013.09.039.

(232) Hung, W. I.; Liao, Y. Y.; Hsu, C. Y.; Chou, H. H.; Lee, T. H.; Kao, W. S.; Lin, J. T. High-Performance Dye-Sensitized Solar Cells Based on Phenothiazine Dyes Containing Double Anchors and Thiophene Spacers. *Chem. Asian J.* **2014**, *9*, 357-366. DOI: https://doi.org/10.1002/asia.201301228.

(233) Duvva, N.; Kanaparthi, R. K.; Kandhadi, J.; Marotta, G.; Salvatori, P.; De Angelis, F.; Giribabu, L. Carbazole-based sensitizers for potential application to dye sensitized solar cells. *J. Chem. Sci.* **2015**, *127*, 383-394. DOI: https://doi.org/10.1007/s12039-015-0794-1.

(234) Georgiades, S. N.; Nicolaou, P. G.: Recent advances in carbazole syntheses. In *Adv. Heterocycl. Chem.*; Scriven, E. F. V., Ramsden, C. A., Eds.; Advances in Heterocyclic Chemistry, 2019; Vol. 129; pp 1-88.

(235) Koumura, N.; Wang, Z. S.; Mori, S.; Miyashita, M.; Suzuki, E.; Hara, K. Alkyl-functionalized organic dyes for efficient molecular photovoltaics. *J. Am. Chem. Soc.* **2006**, *128*, 14256-14257. DOI: https://doi.org/10.1021/ja0645640.

(236) Keller, N.; Bessinger, D.; Reuter, S.; Calik, M.; Ascherl, L.; Hanusch, F. C.; Auras, F.; Bein, T. Oligothiophene-Bridged Conjugated Covalent Organic Frameworks. *J. Am. Chem. Soc.* **2017**, *139*, 8194-8199. DOI: https://doi.org/10.1021/jacs.7b01631

(237) Liu, X.; Sharapov, V.; Zhang, Z.; Wiser, F.; Awais, M. A.; Yu, L. Photoinduced cationic polycondensation in solid state towards ultralow band gap conjugated polymers. *J. Mater. Chem. C* **2020**, *8*, 7026-7033. DOI: https://doi.org/10.1039/D0TC01257B.

(238) D'Alterio, M. C.; Casals-Cruañas, E.; Tzouras, N. V.; Talarico, G.; Nolan, S. P.; Poater, A. Mechanistic Aspects of the Palladium-Catalyzed Suzuki-Miyaura Cross-Coupling Reaction. *Chem. Eur. J.* **2021**, *27*, 13481-13493. DOI: https://doi.org/10.1002/chem.202101880.

(239) Blakemore, D.: Suzuki–Miyaura coupling. In *Synthetic Methods in Drug Discovery*, David Blakemore, Paul Doyle, Fobian, Y., Eds.; Royal Society of Chemistry, 2016; Vol. 1; pp 1-69.

(240) Gao, C.; Li, J.; Yin, S.; Lin, G. Q.; Ma, T. Q.; Meng, Y.; Sun, J. L.; Wang, C. Isostructural Three-Dimensional Covalent Organic Frameworks. *Angew. Chem. Int. Ed.* **2019**, *58*, 9770-9775. DOI: https://doi.org/10.1002/anie.201905591.

(241) Capodilupo, A. L.; De Marco, L.; Corrente, G. A.; Giannuzzi, R.; Fabiano, E.; Cardone, A.; Gigli, G.; Ciccarella, G. Synthesis and characterization of a new series of dibenzofulvene based organic dyes for DSSCs. *Dyes Pigm.* **2016**, *130*, 79-89. DOI: https://doi.org/10.1016/j.dyepig.2016.02.030.

(242) Dong, Y.; Chen, Z.; Hou, M.; Qi, L.; Yan, C.; Lu, X.; Liu, R.; Xu, Y. Mitochondria-targeted aggregation-induced emission active near infrared fluorescent probe for real-time imaging. *Spectrochim. Acta A Mol. Biomol. Spectrosc.* **2020**, *224*, 117456. DOI: https://doi.org/10.1016/j.saa.2019.117456.

# A | Appendix

## Chapter 2

### Compound characterization

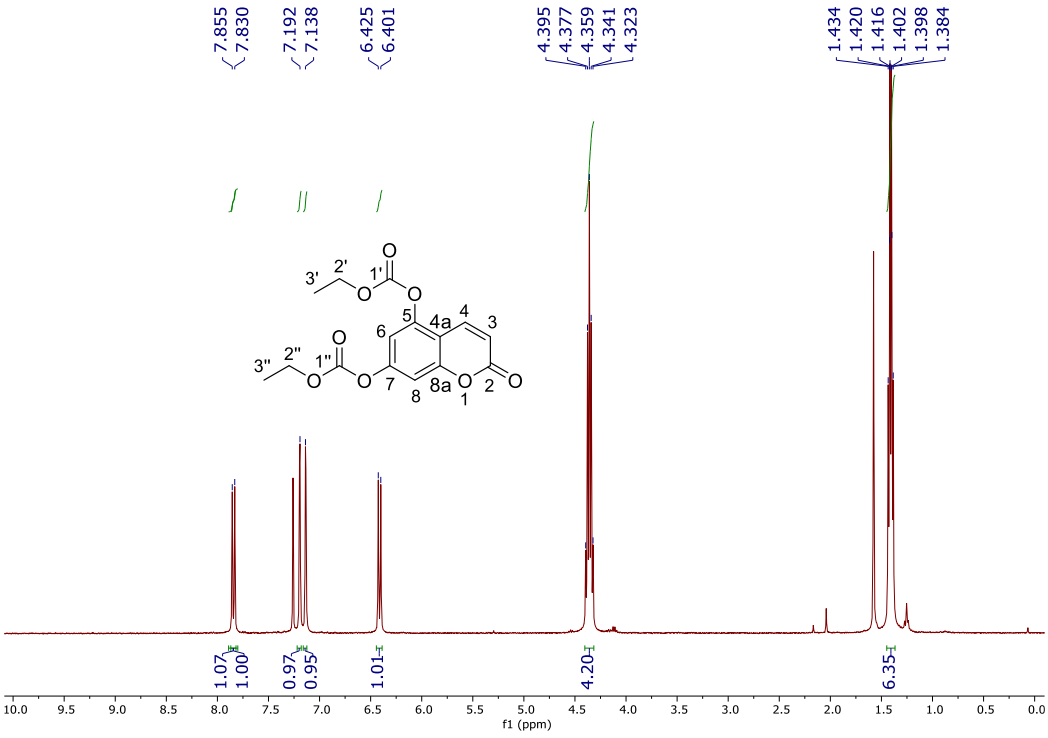


Figure A. 1. $^{1}$H-NMR (400 MHz, $CDCl_3$) spectrum of 3-bromo-5,7-dihydroxycoumarin (2.3)

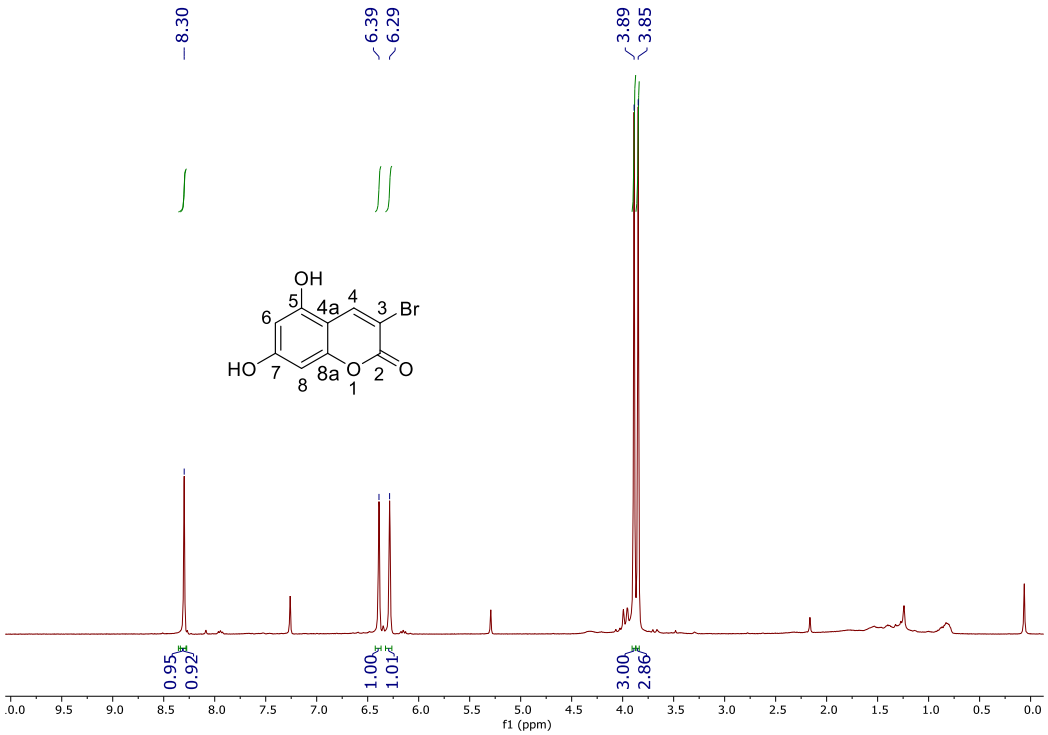


Figure A. 2. $^{1}H$ NMR (400 MHz, $CDCl_3$) spectrum of diethyl (2-oxo-2H-chromene-5,7-diyl) bis(carbonate) (2.5)

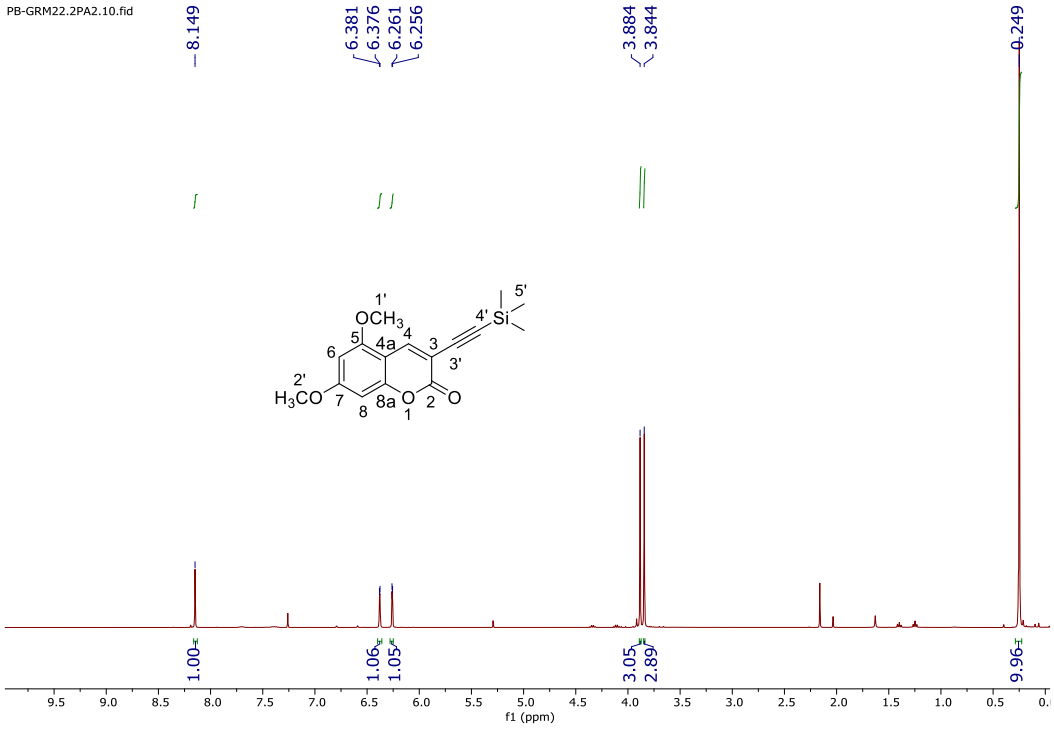


Figure A. 3. $^{1}H$ NMR (400 MHz, $CDCl_3$) spectrum of 5,7-dimethoxy-3-((trimethylsilyl)ethynyl)coumarin (2.8)

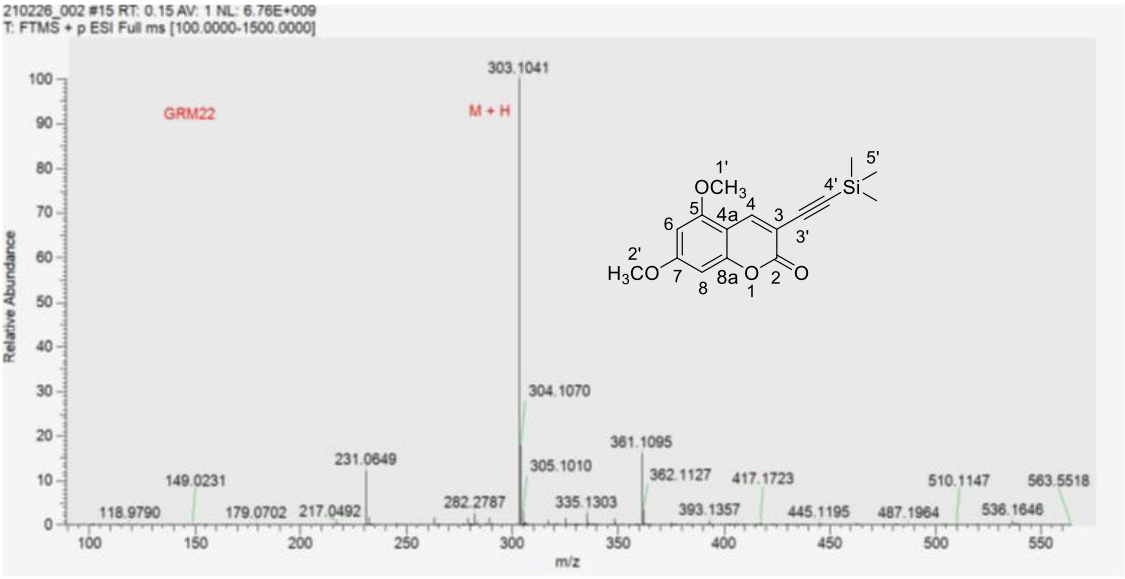


Figure A. 4. HRMS-ESI spectrum of 5,7-dimethoxy-3-((trimethylsilyl)ethynyl)coumarin (2.8)

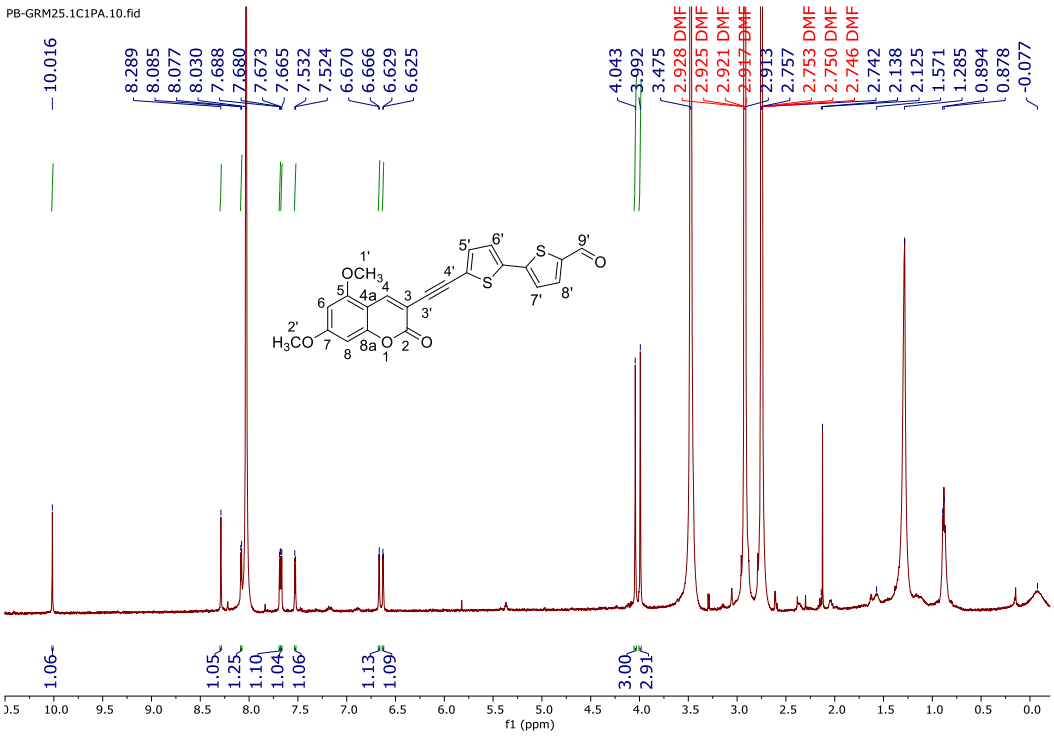


Figure A. 5. $^{1}$H NMR (400 MHz, DMF-$d_7$) spectrum of 5′-((5,7-dimethoxi-2-oxo-2H-chromen-3-yl)ethynyl)-[2,2′-bithiophene]-5-carbaldehyde (2.10)

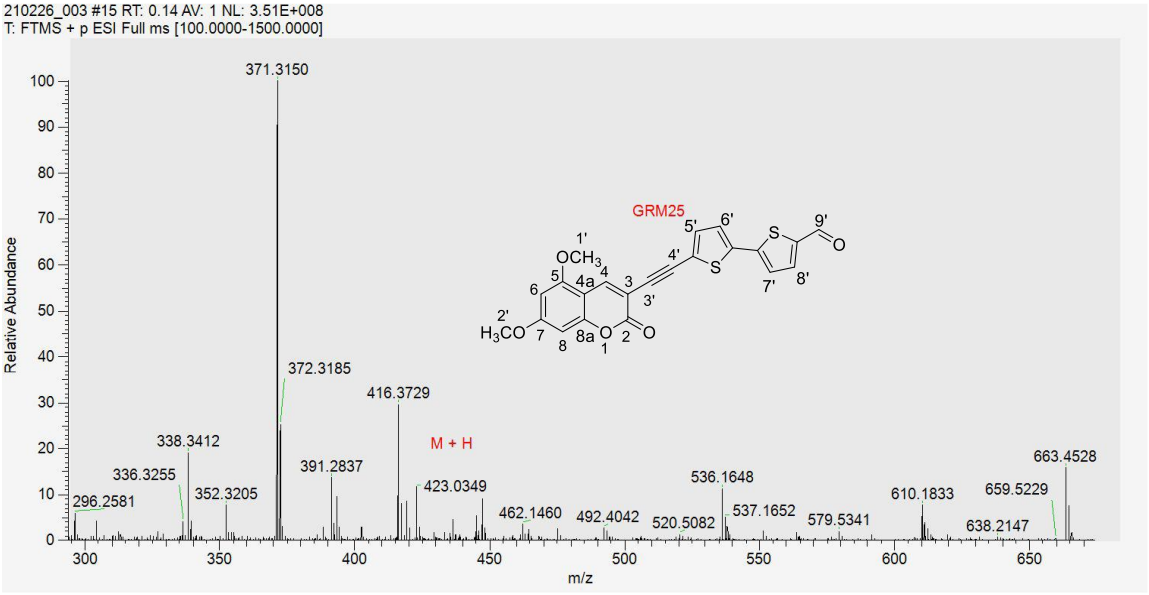


Figure A. 6. HRMS-ESI spectrum of 5′-((5,7-dimethoxi-2-oxo-2H-chromen-3-yl)ethynyl)-[2,2′-bithiophene]-5-carbaldehyde (2.10)

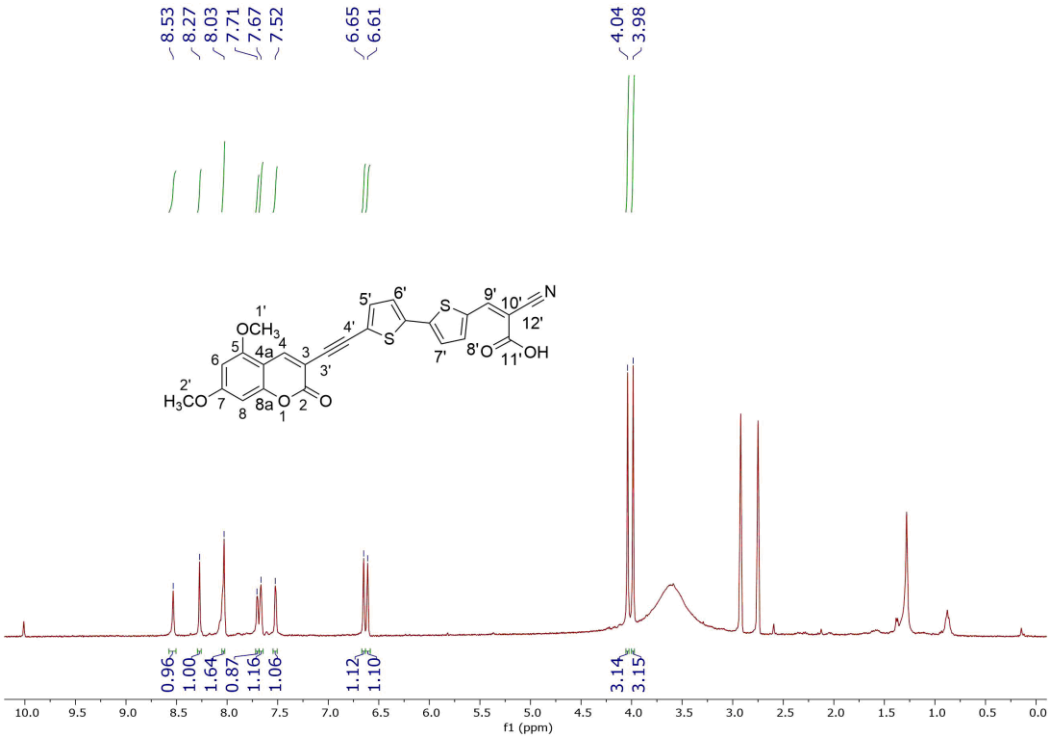


Figure A. 7. $^{1}$H NMR (400 MHz, DMF-$d_7$) spectrum of 2-cyano-3-(5′-((5,7-dimethoxy-2-oxo-2H-chromen-3-yl)ethynyl)-[2,2′-bithiophen]-5-yl)acrylic acid (2.11b)

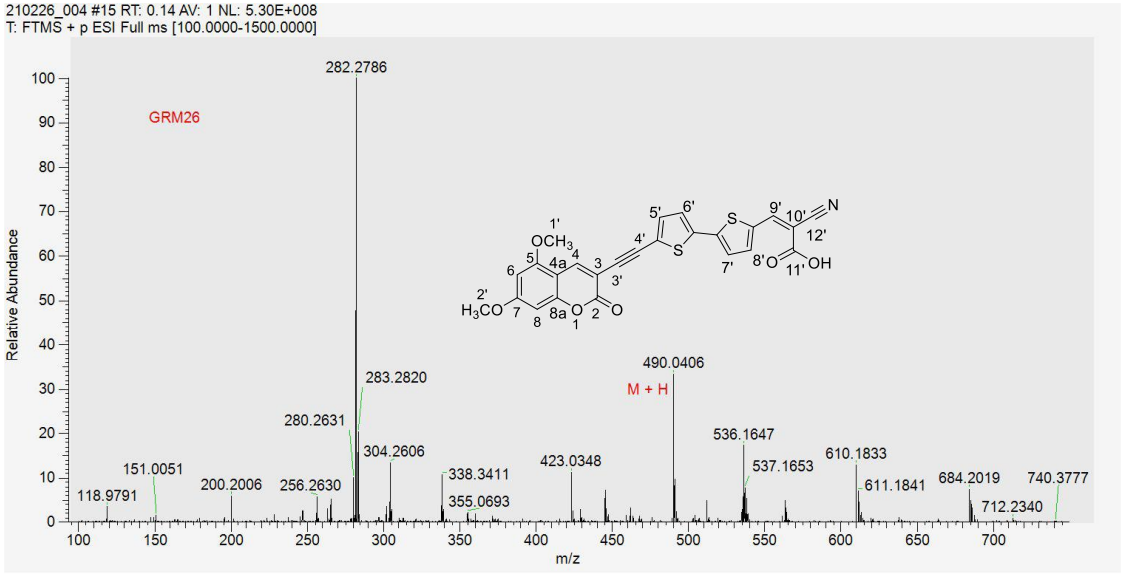


Figure A. 8. HRMS-ESI spectrum of 2-cyano-3-(5′-((5,7-dimethoxy-2-oxo-2H-chromen-3-yl)ethynyl)-[2,2′-bithiophen]-5-yl)acrylic acid (2.11b)

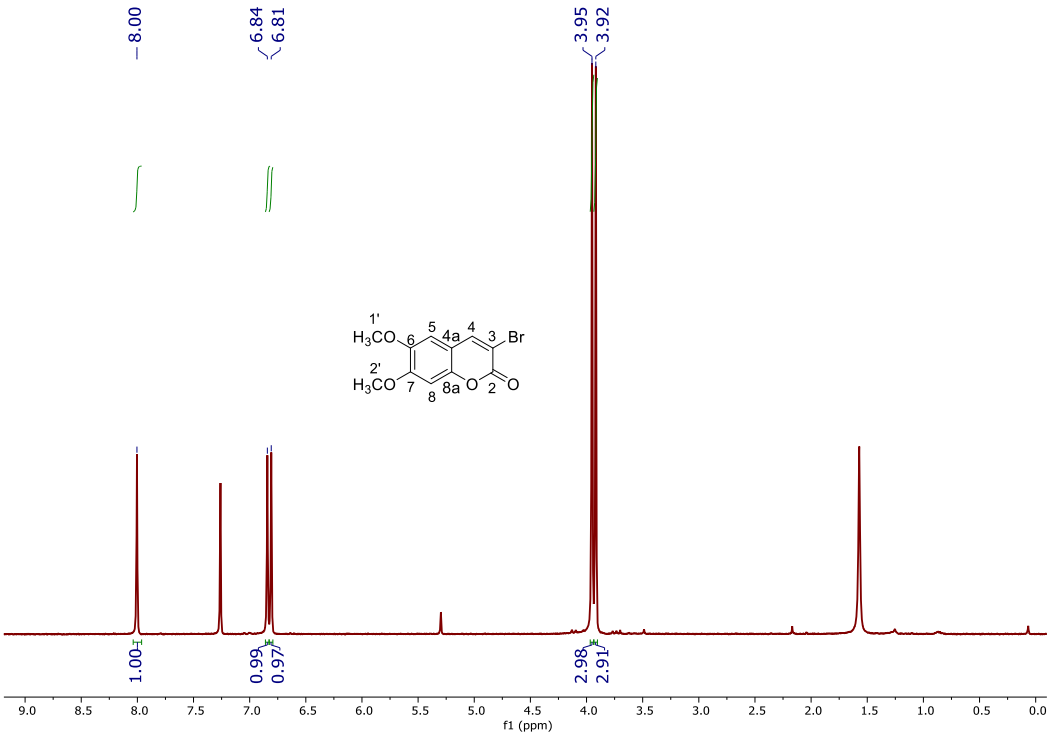


Figure A. 9. $^{1}$H-NMR (400 MHz, $CDCl_3$) spectrum of 3-bromo-6,7-dihydroxycoumarin (2.14).

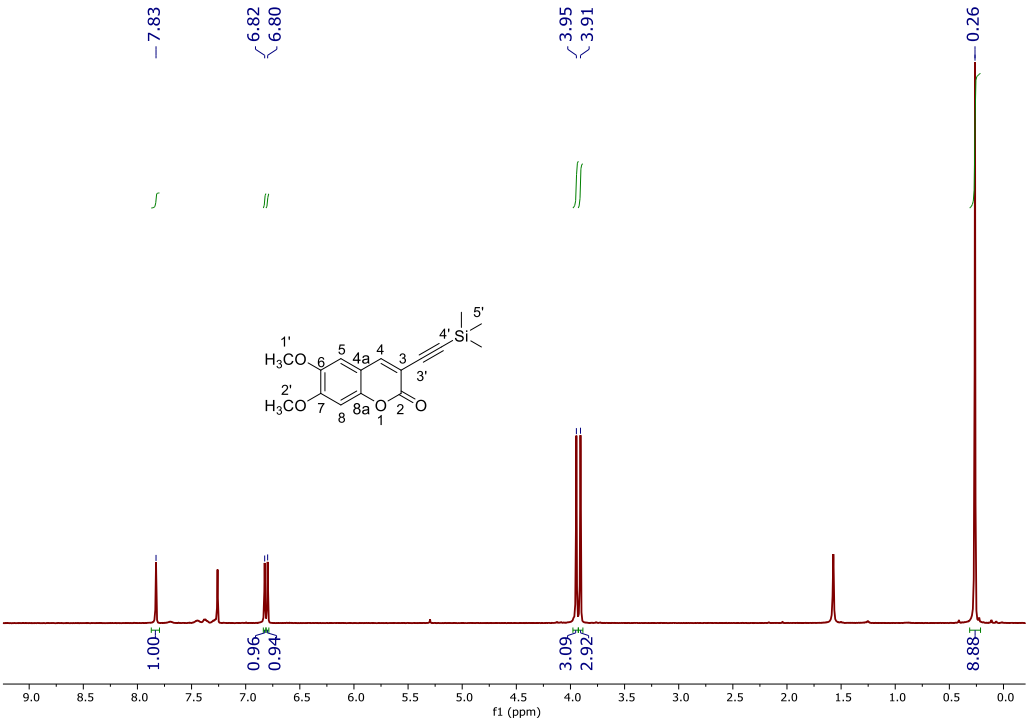


Figure A. 10. $^{1}$H-NMR (400 MHz, $CDCl_3$) spectrum of 6,7-dimethoxy-3-((trimethylsilyl)ethynyl)coumarin (2.15)

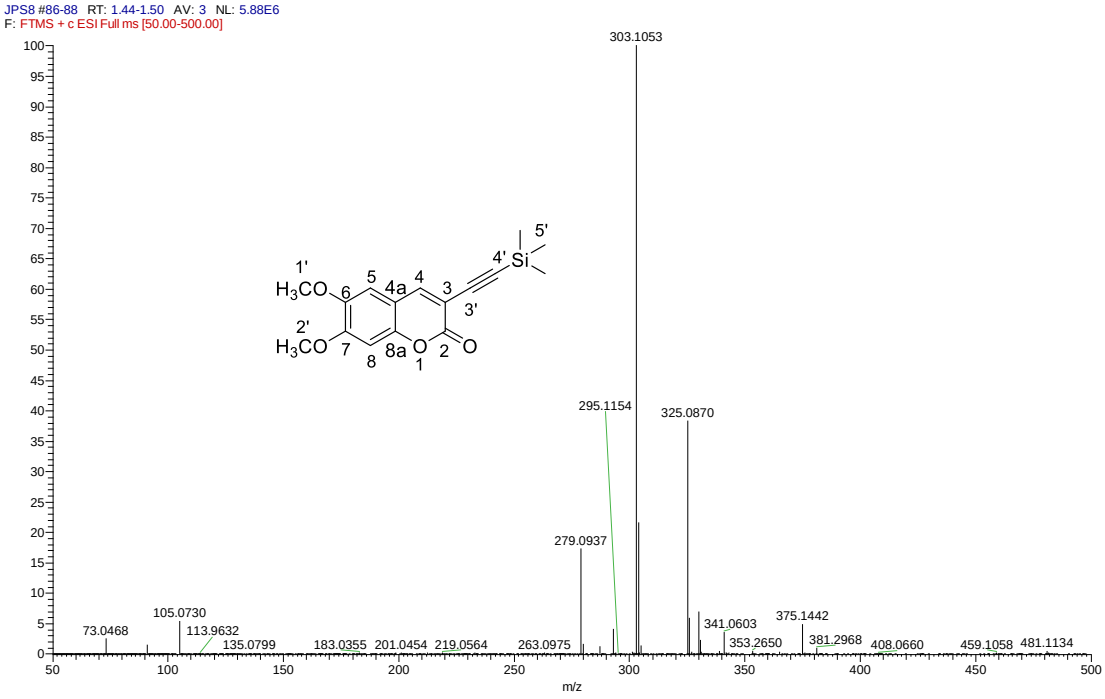


Figure A. 11. HRMS-ESI spectrum of 6,7-dimethoxy-3-((trimethylsilyl)ethynyl)coumarin (2.15)

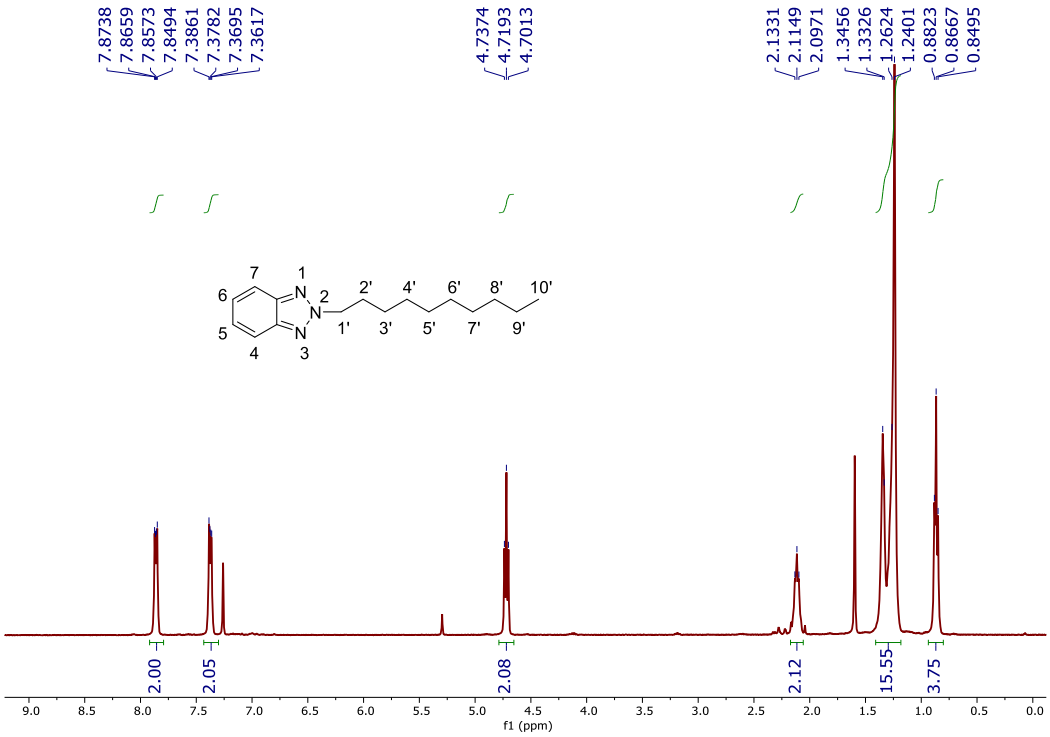


Figure A. 12. $^{1}$H-NMR (400 MHz, $CDCl_3$) spectrum of 2-decyl-*2H*-benzo[*d*][1,2,3]triazole

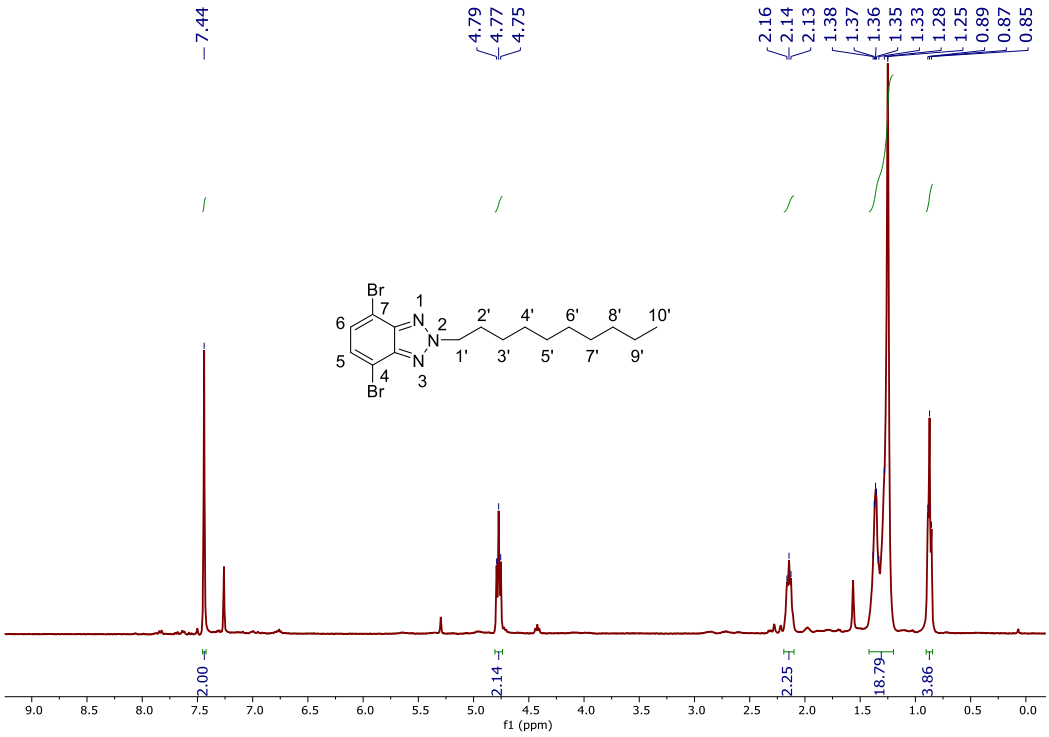


Figure A. 13. $^{1}$H-NMR (400 MHz, $CDCl_3$) spectrum of 4,7-dibromo-2-decyl-*2H*-benzo[*d*][1,2,3]triazole

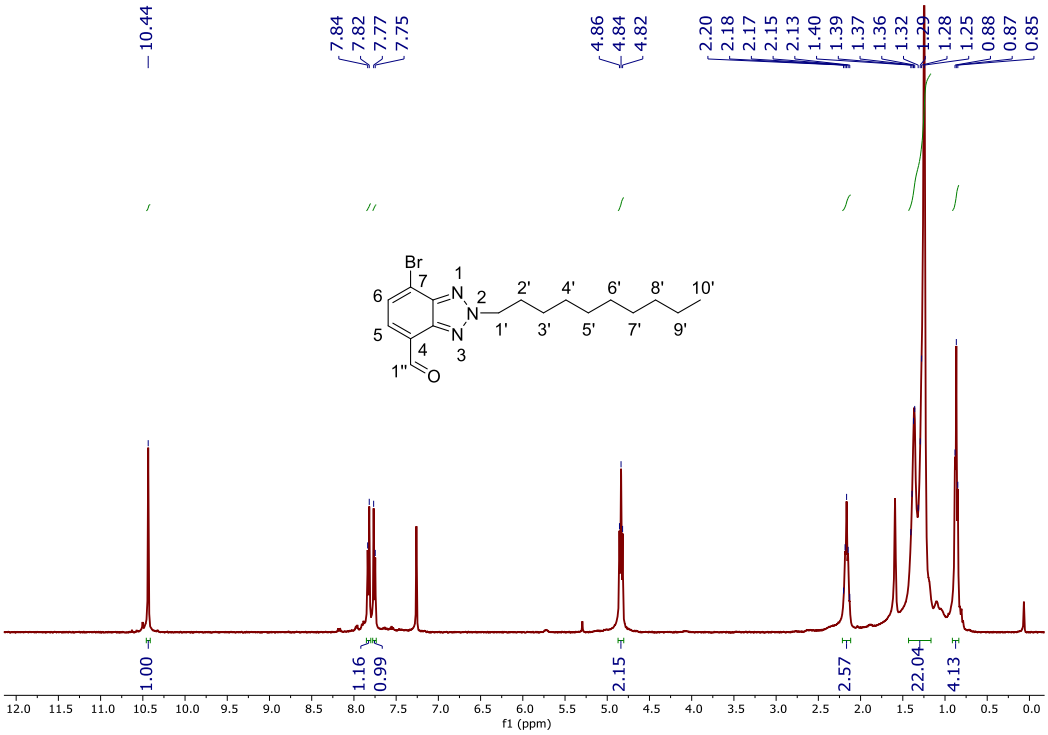


Figure A. 14. $^{1}$H-NMR (400 MHz, $CDCl_3$) spectrum of 7-dibromo-2-decyl-2H-benzo[d][1,2,3]triazole-4-carbaldehyde (2.17d)

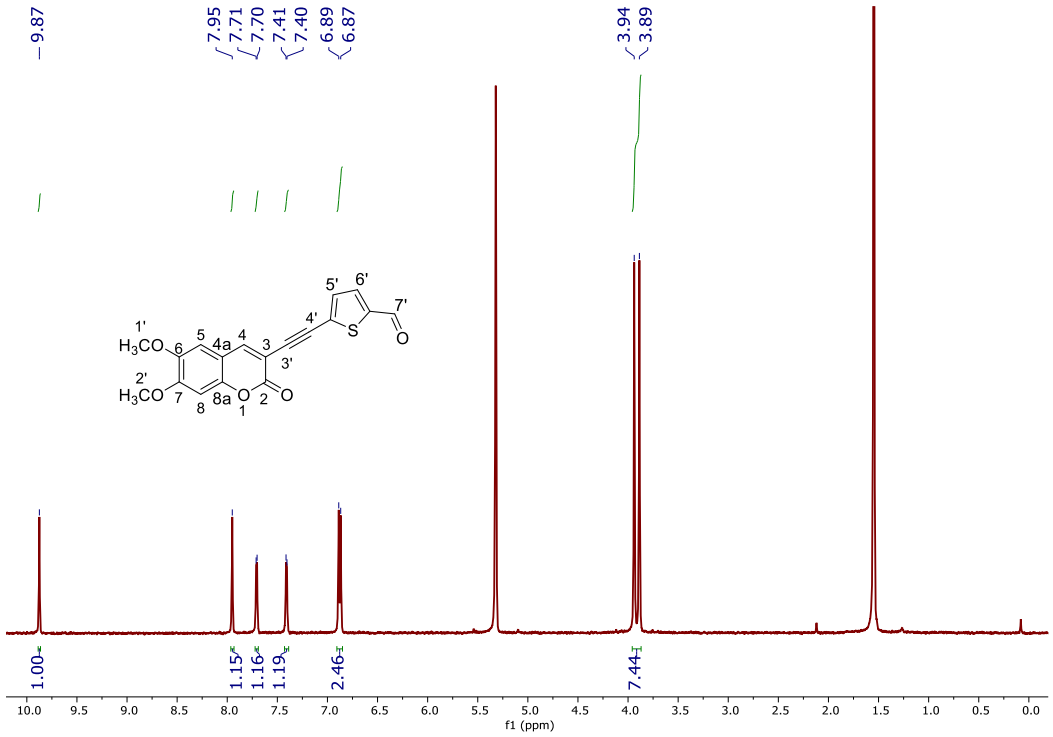


Figure A. 15. $^{1}$H-NMR (400 MHz, $CD_2Cl_2$) spectrum of 5-((6,7-dimethoxi-2-oxo-2H-chromen-3-yl)ethynyl)-thiophene-5-carbaldehyde (2.18c)

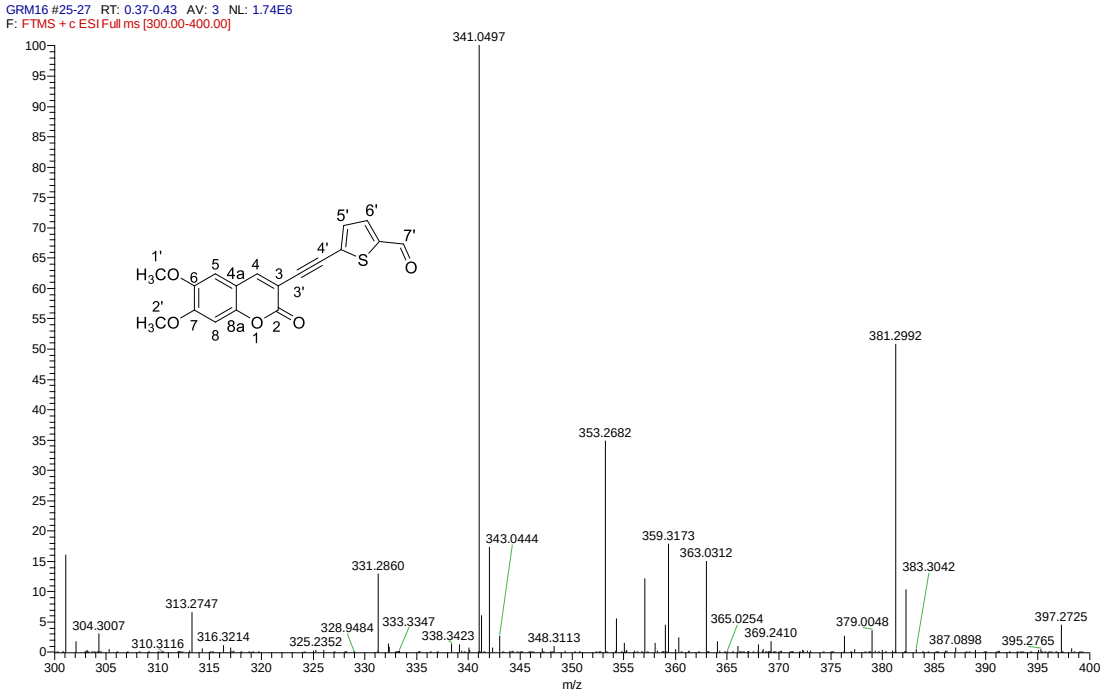


Figure A. 16. HRMS-ESI spectrum of 5-((6,7-dimethoxi-2-oxo-2H-chromen-3-yl)ethynyl)-thiophene-5-carbaldehyde (2.18c)

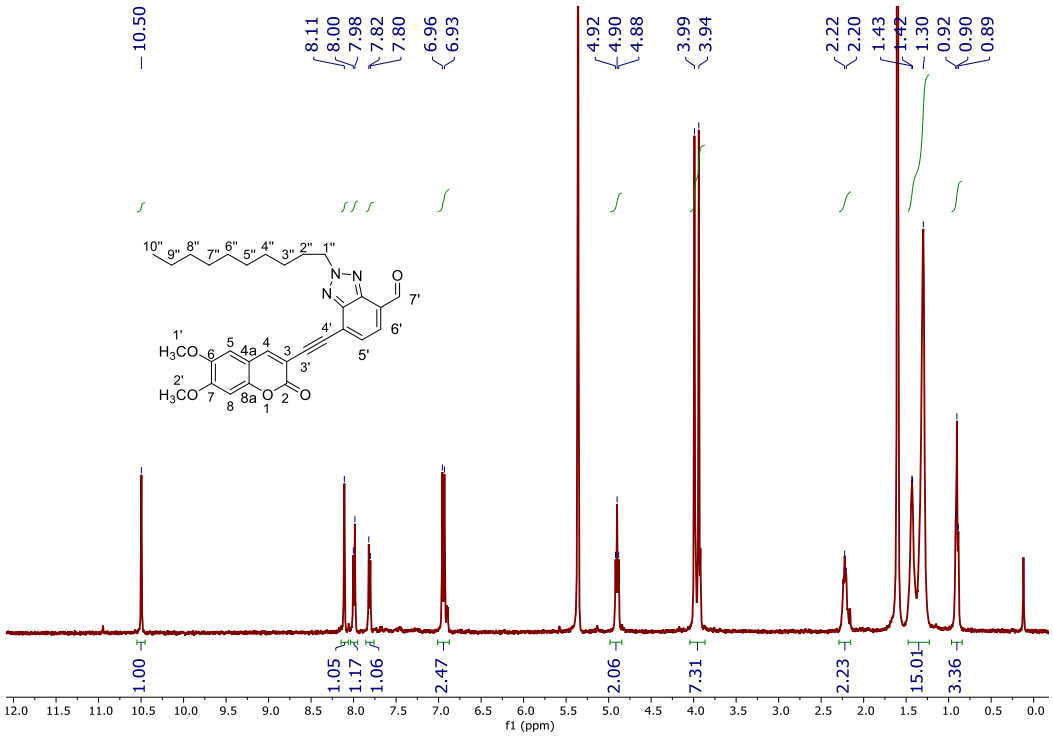


Figure A. 17. $^{1}$H-NMR (400 MHz, $CD_2Cl_2$) spectrum of 2-decyl-7-((6,7-dimethoxy-2-oxo-2H-chromen-3-yl)ethynyl)-2H-benzo[d][1,2,3]triazole-4-carbaldehyde (2.18d)

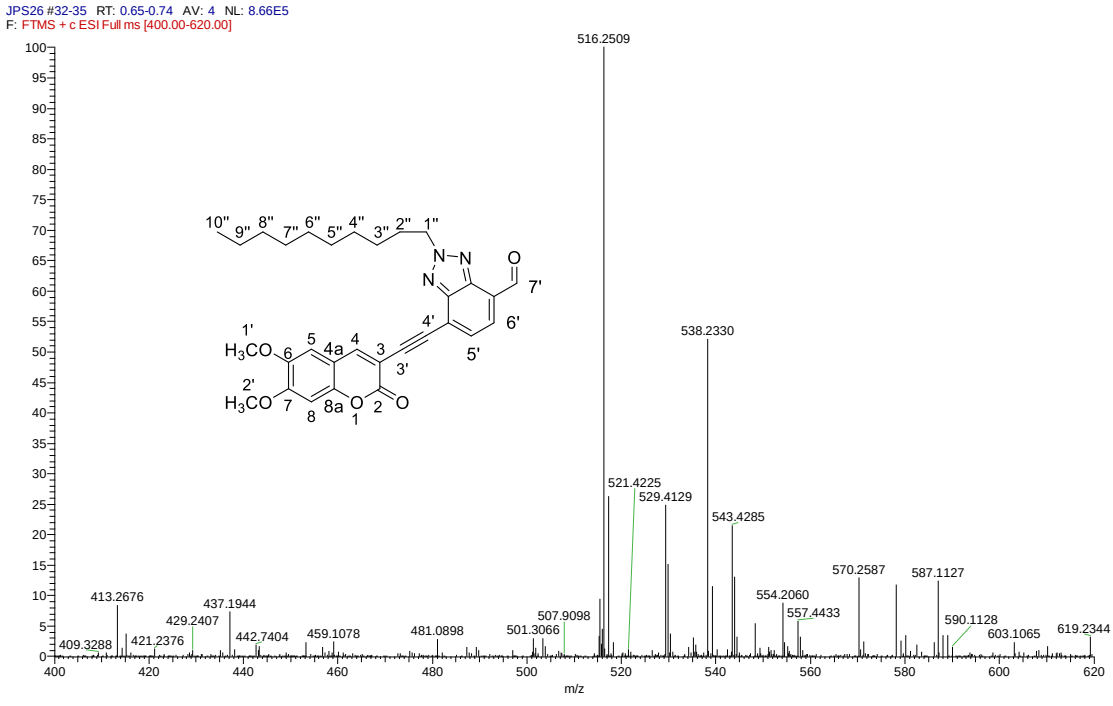


Figure A. 18. HRMS-ESI spectrum of 2-decyl-7-((6,7-dimethoxy-2-oxo-2H-chromen-3-yl)ethynyl)-2H-benzo[d][1,2,3]triazole-4-carbaldehyde (2.18d

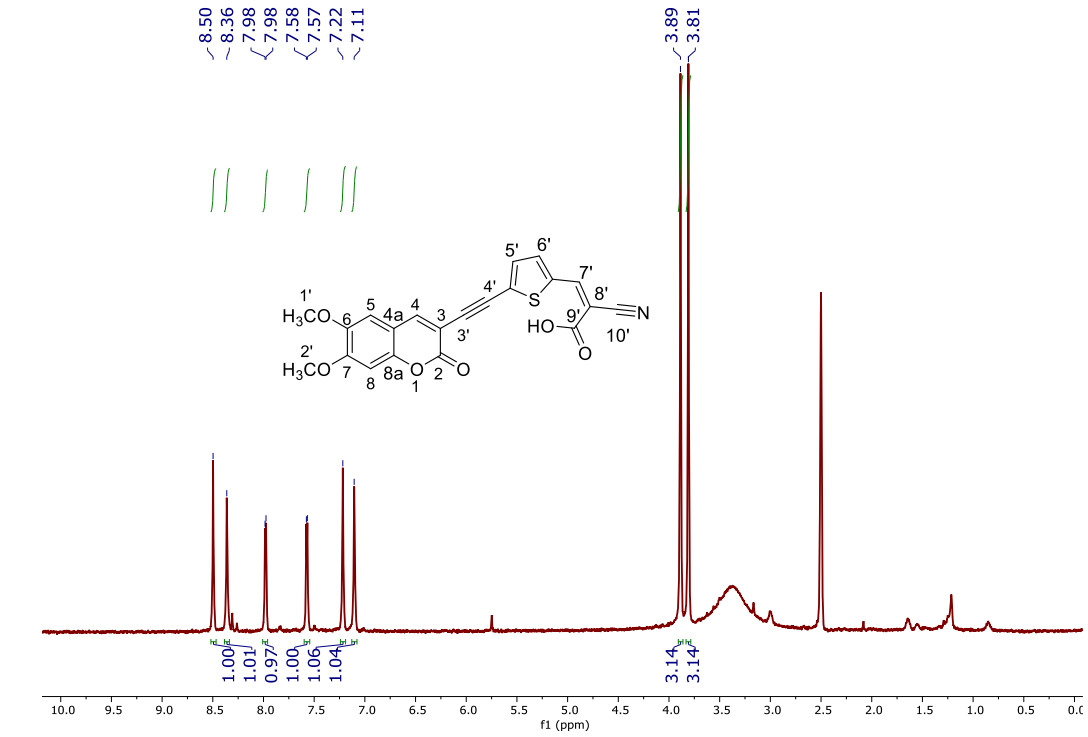


Figure A. 19. $^{1}$H-NMR (400 MHz, DMSO-$d_6$) spectrum of 2-cyano-3-(5-((6,7-dimethoxy-2-oxo-2H-chromen-3-yl)ethynyl)-thiophen-2-yl)acrylic acid (2.19c)

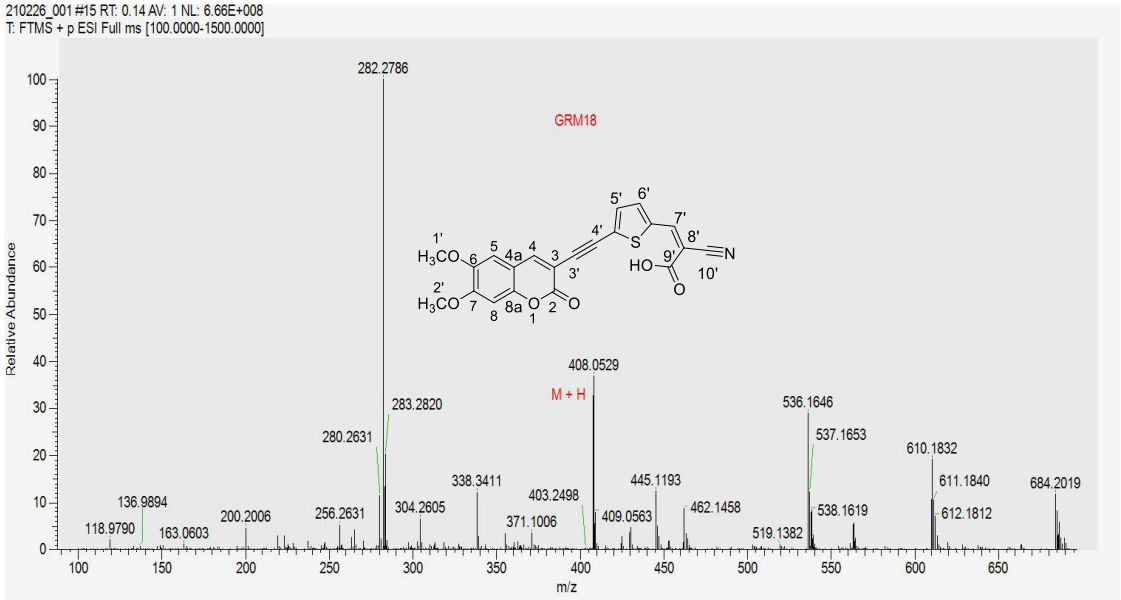


Figure A. 20. HRMS-ESI spectrum of 2-cyano-3-(5-((6,7-dimethoxy-2-oxo-2H-chromen-3-yl)ethynyl)-thiophen-2-yl)acrylic acid (2.19c)

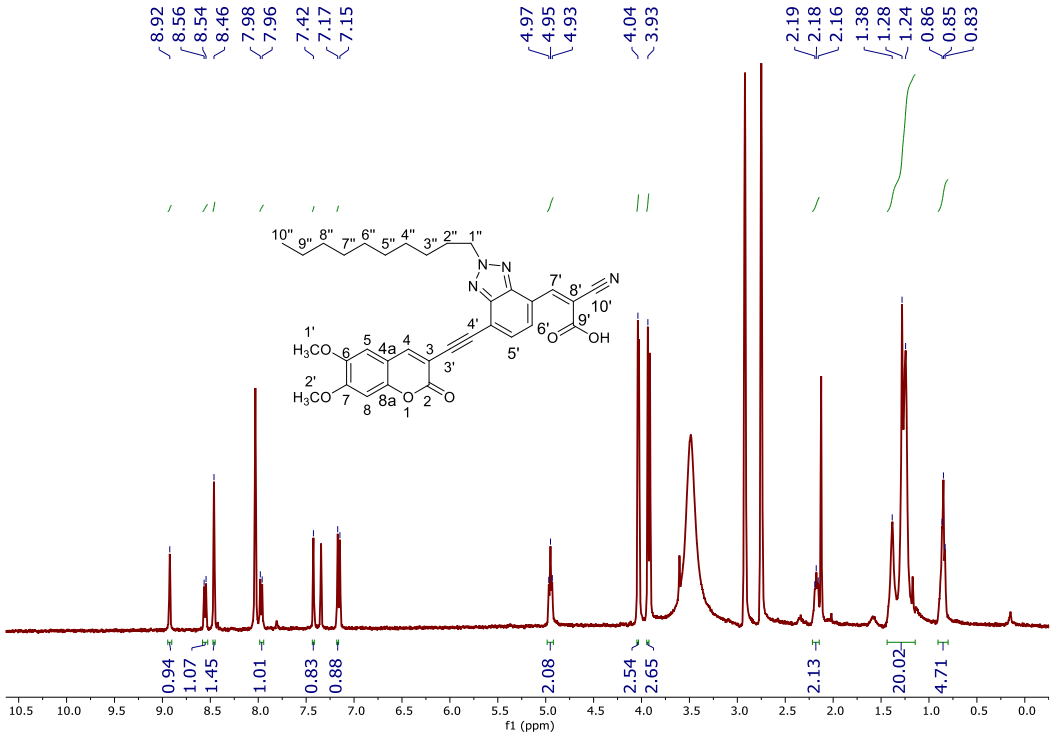


Figure A. 21. 1H-NMR (400 MHz, DMF-d7) spectrum of 2-cyano-3-(2-decyl-7-((6,7-dimethoxy-2-oxo-2H-chromen-3-yl)ethynyl)-2H-benzo[d][1,2,3]triazol-4-yl)acrylic acid (2.19d)

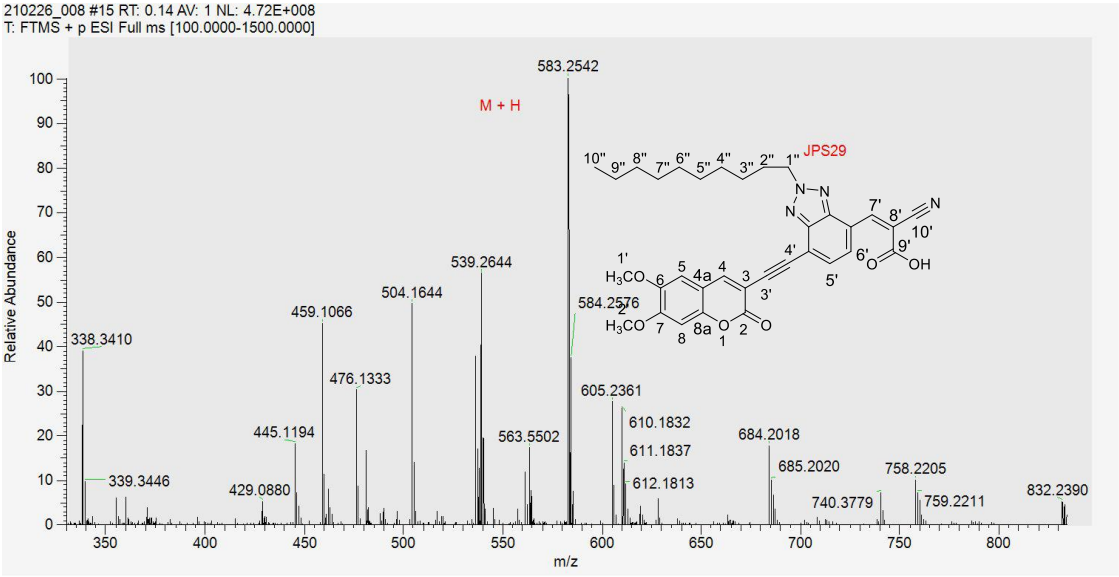


Figure A. 22. HRMS-ESI spectrum of 2-cyano-3-(2-decyl-7-((6,7-dimethoxy-2-oxo-2H-chromen-3-yl)ethynyl)-2H-benzo[d][1,2,3]triazol-4-yl)acrylic acid (2.19d)

# Chapter 3

## Absorption spectra

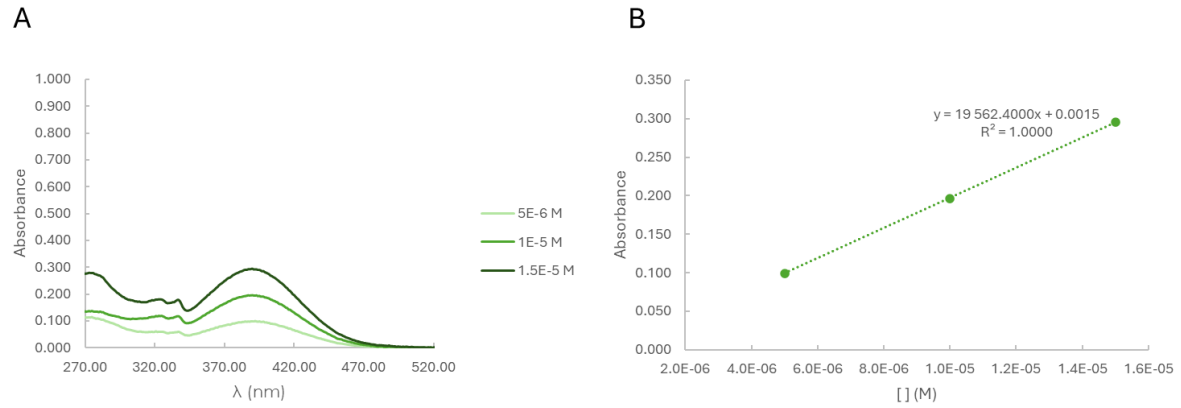


Figure A. 23. A- UV-Vis spectrum of compound **3.23** at different concentrations. B- Linear correlation between the absorbance at $\lambda_{max}$ and the concentration of dye in solution.

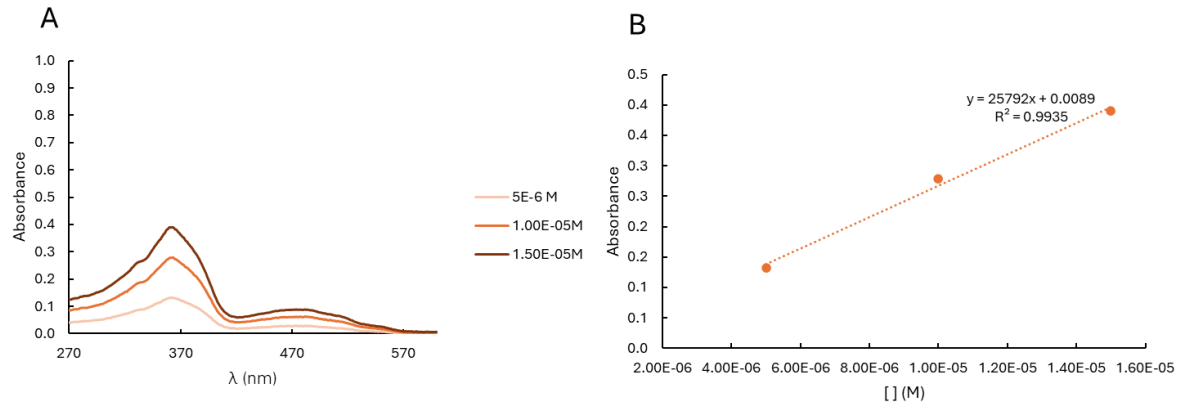


Figure A. 24. A- UV-Vis spectrum of compound **3.37a** at different concentrations. B- Linear correlation between the absorbance at $\lambda_{max}$ and the concentration of dye in solution.

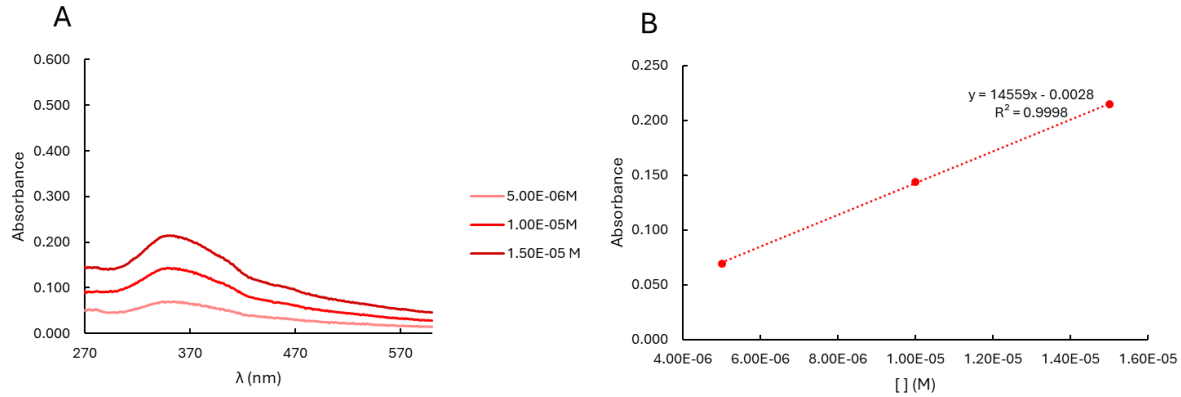


Figure A. 25. A- UV-Vis spectrum of compound **3.37b** at different concentrations. B- Linear correlation between the absorbance at $\lambda_{max}$ and the concentration of dye in solution.

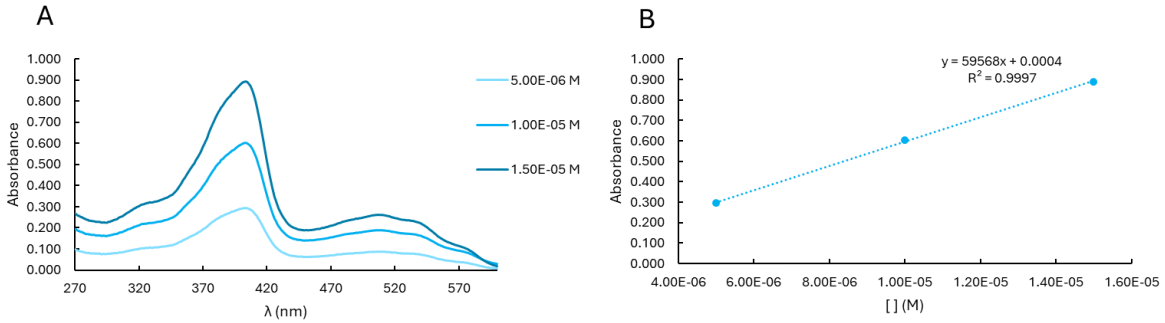


Figure A. 26. A- UV-Vis spectrum of compound **3.37c** at different concentrations. B- Linear correlation between the absorbance at $\lambda_{max}$ and the concentration of dye in solution.

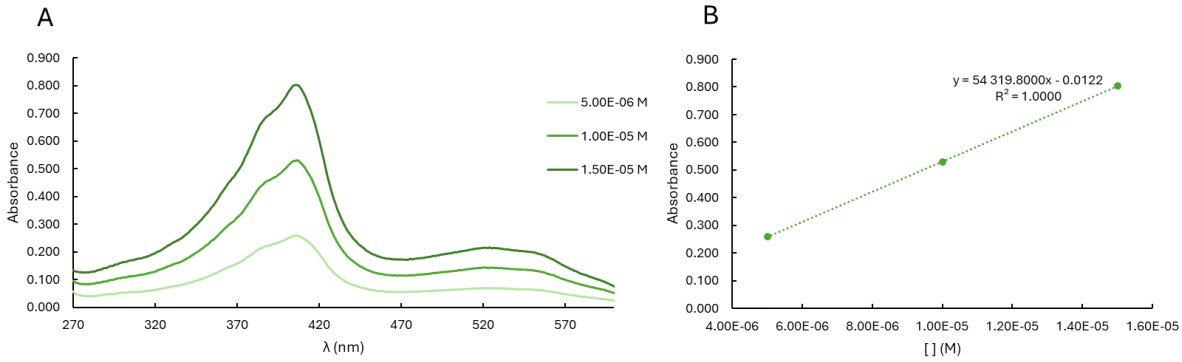


Figure A. 27. A- UV-Vis spectrum of compound **3.37c** at different concentrations. B- Linear correlation between the absorbance at $\lambda_{max}$ and the concentration of dye in solution.

## Cyclic voltammetry

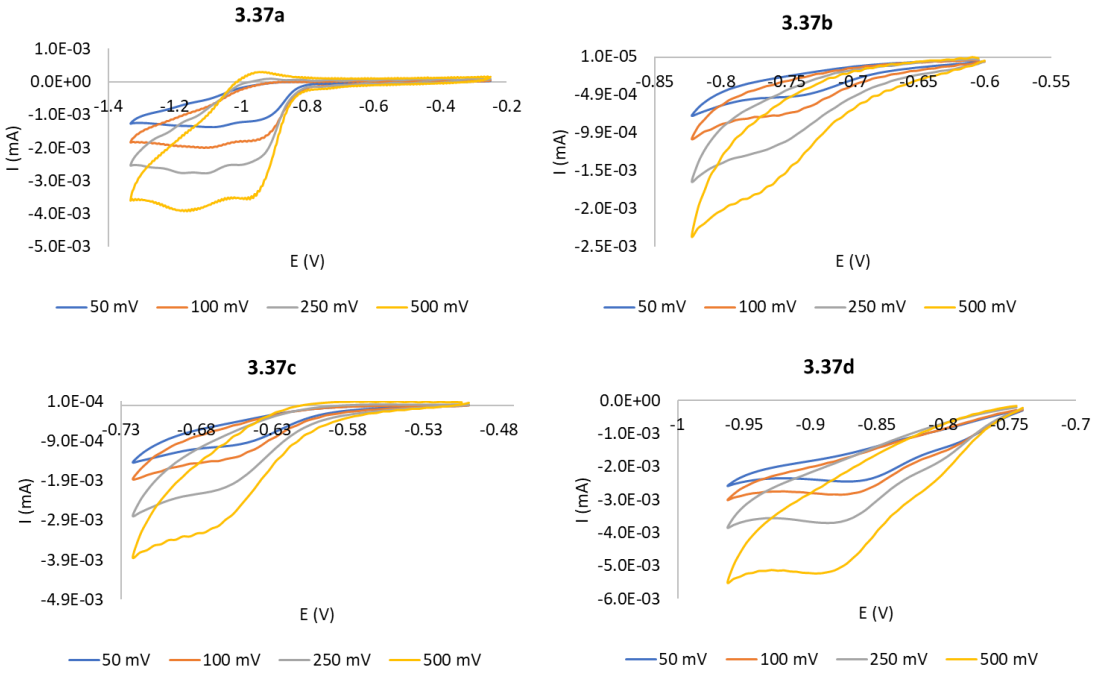


Figure A. 28. Cyclic voltammograms of compounds 3.37a-d in dimethylformamide (DMF) (dye concentration of $1.5X10^{-4}$ M and 0.1 M $TBAPF_6$ ) at scan rates of 50, 100, 250, 500 mV $s^{-1}$.

## Photovoltaic Performance

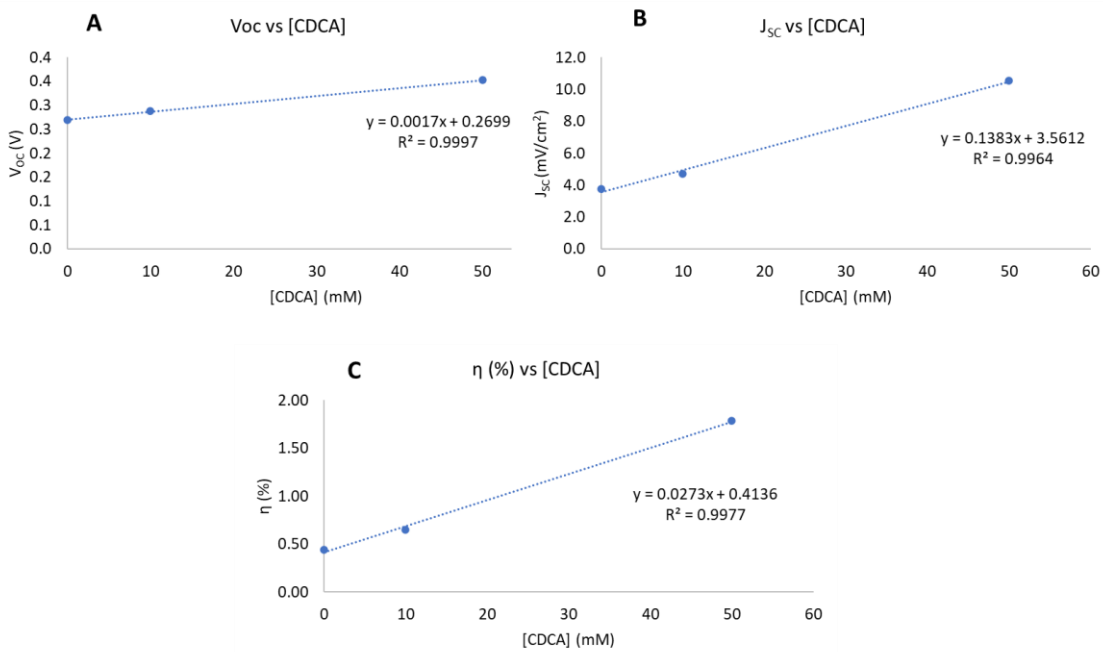


Figure A. 29. Linear correlations between the concentration of CDCA and the photovoltaic parameters obtained for DSSCs devices based on dye 3.37c. A- open-circuit voltage ($V_{OC}$

## IPCE spectra

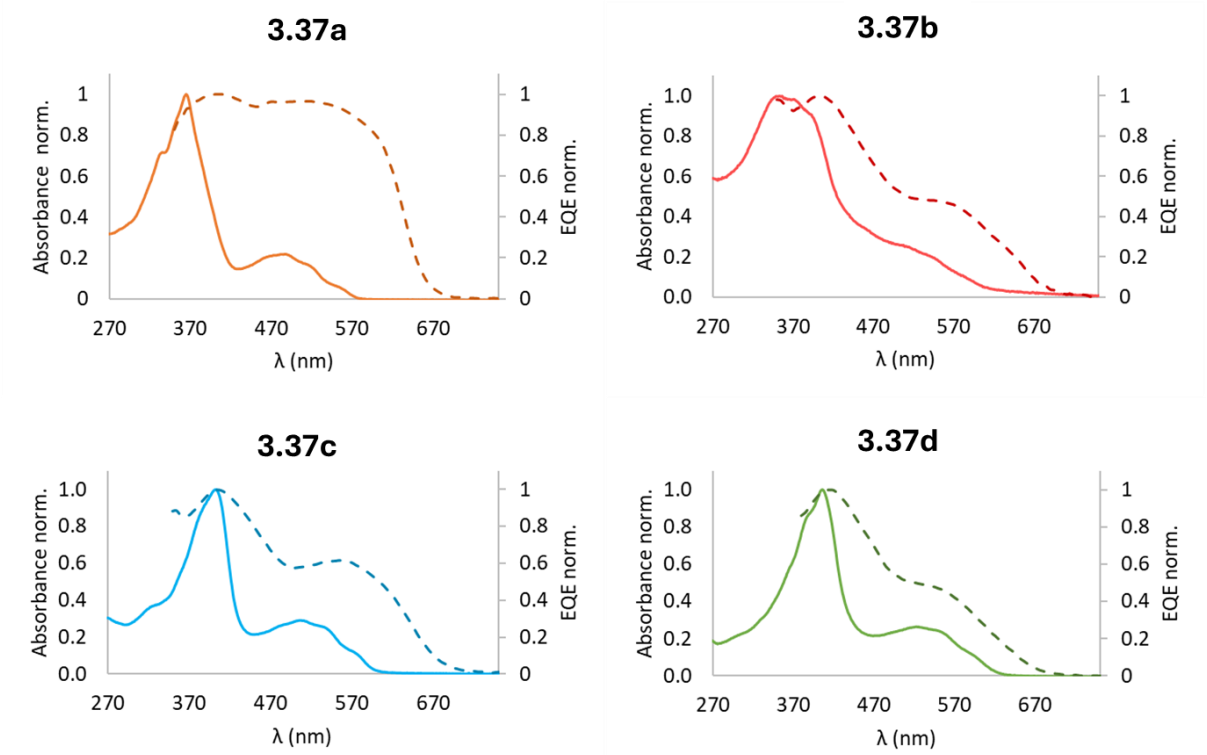


Figure A. 30. IPCE spectra DSSCs based on dyes 3.37a-d (best performing cell, [CDCA] = 0 mM, dotted) and UV-Vis spectra in DMF solution (solid).

## Theoretical Calculations

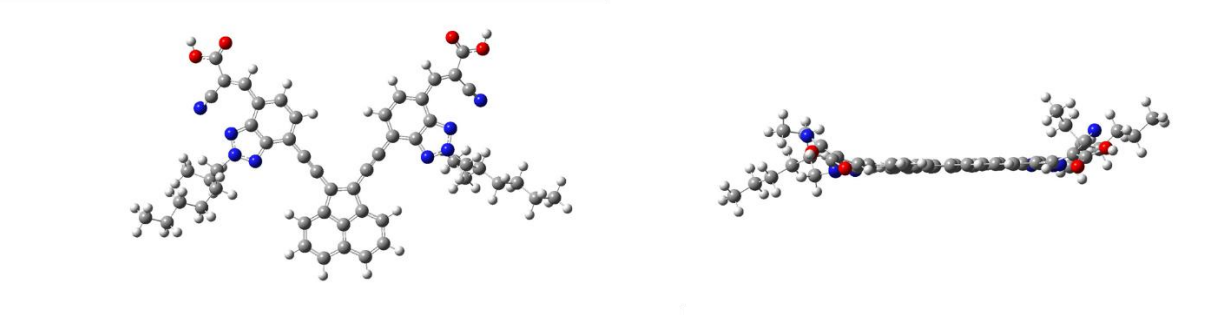

Figure A. 31. DFT B3LYP/6-31G(d,p) optimized geometry of compound 3.37c.

## Compound characterization

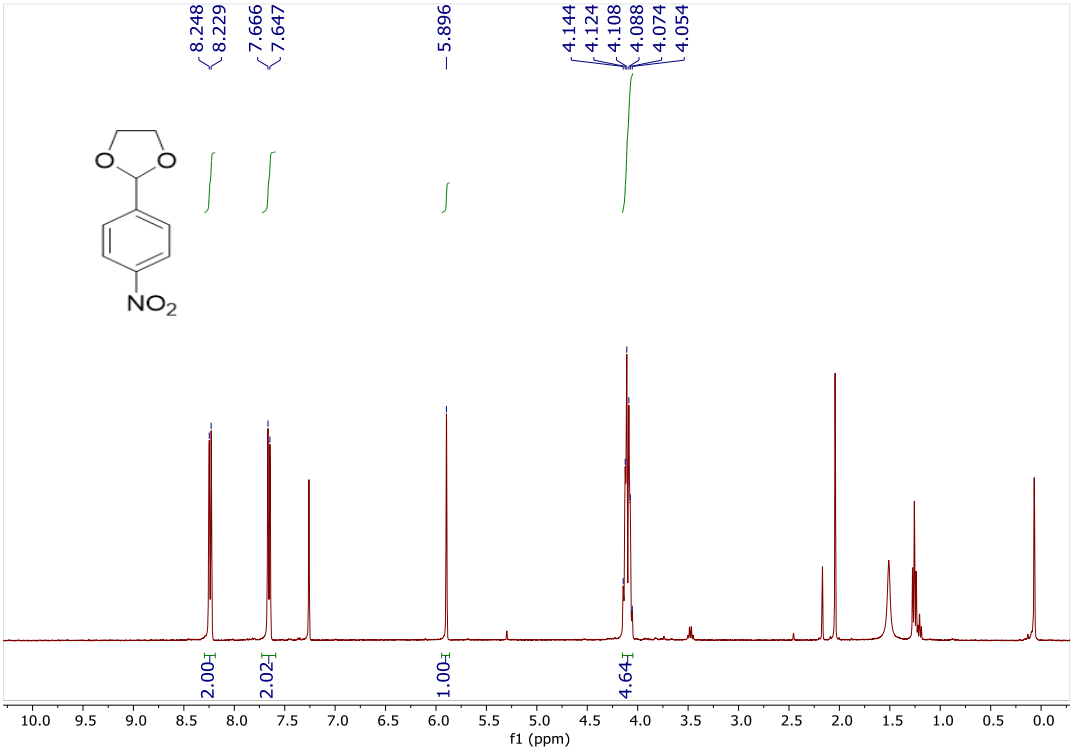


Figure A. 32. $^{1}$H NMR ($CDCl_3$, 400 MHz) spectrum of 2-(4-nitrophenyl)-1,3-dioxolane (**3.7**)

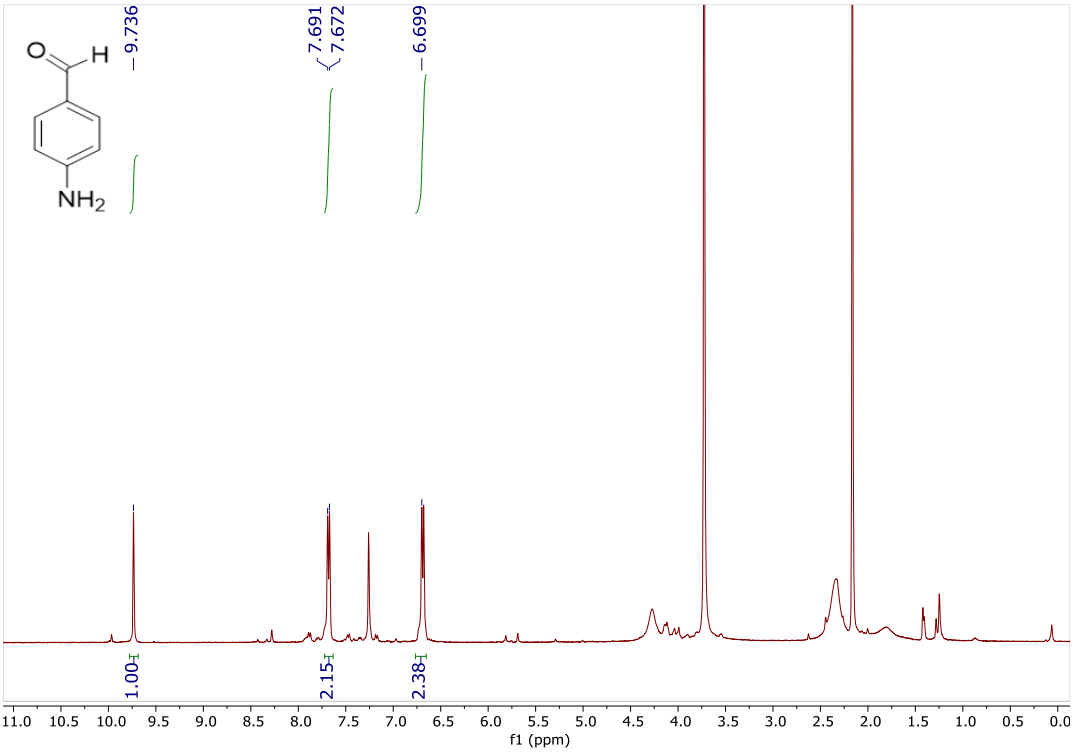


Figure A. 33. $^{1}$H NMR ($CDCl_3$, 400 MHz) spectrum of 4-aminobenzaldehyde (**3.9**).

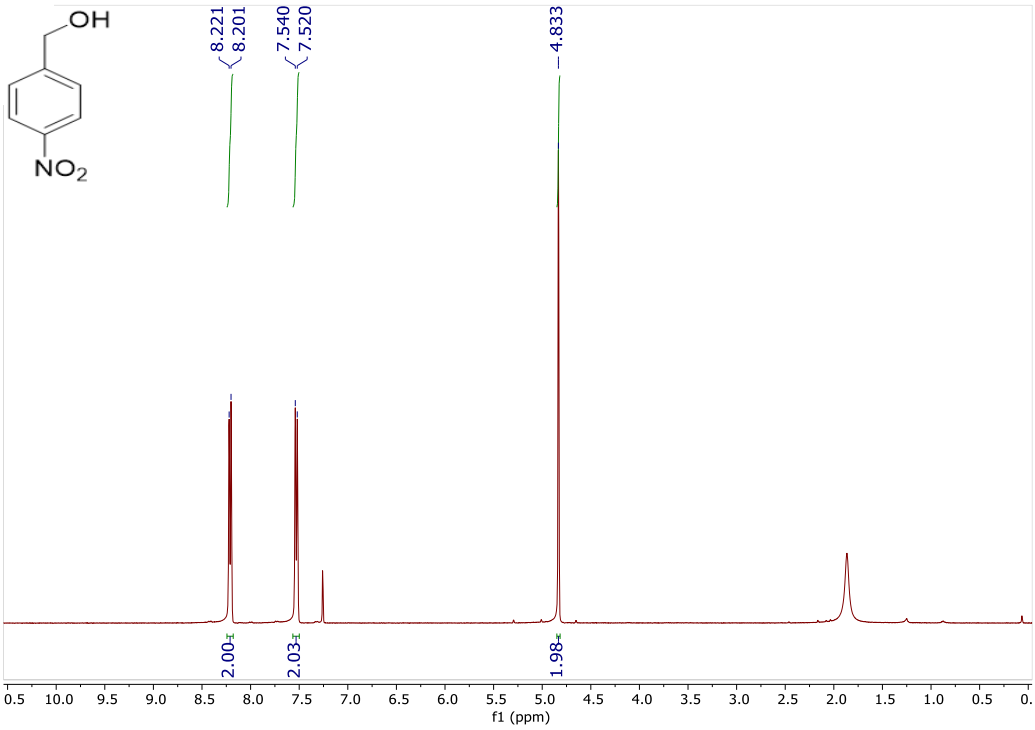


Figure A. 34. $^{1}$H NMR ($CDCl_3$, 400 MHz) spectrum of (4-nitrophenyl)methanol (**3.10**)

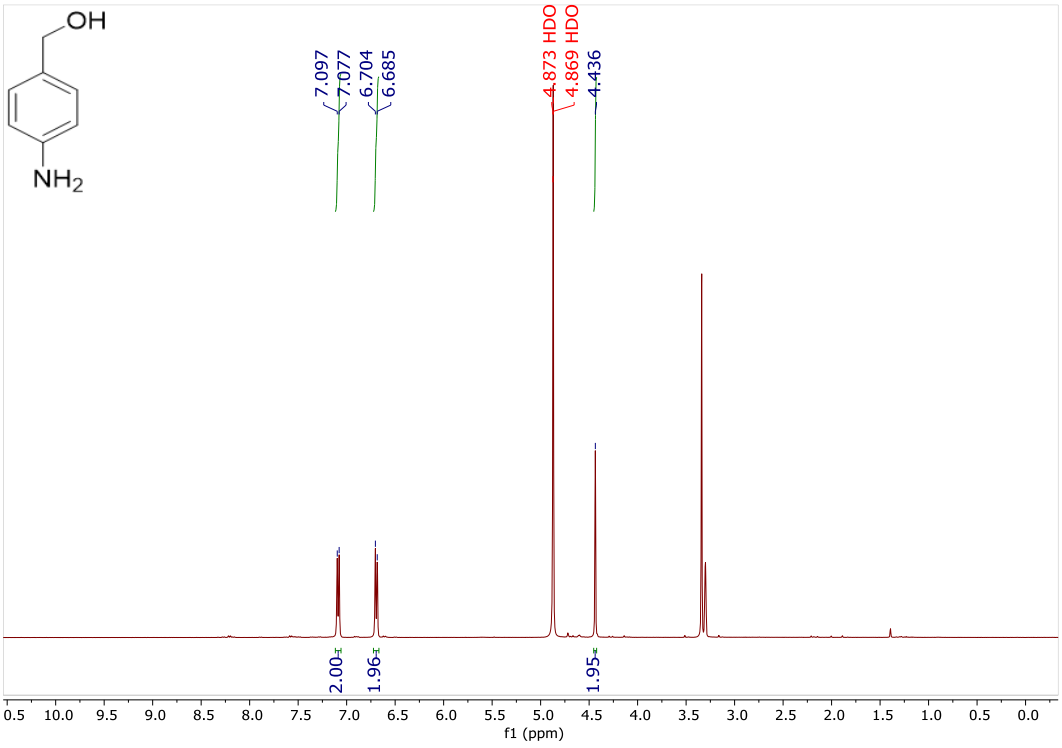


Figure A. 35. $^{1}$H NMR (MeOD, 500 MHz) spectrum of (4-aminophenyl)methanol (**3.11**).

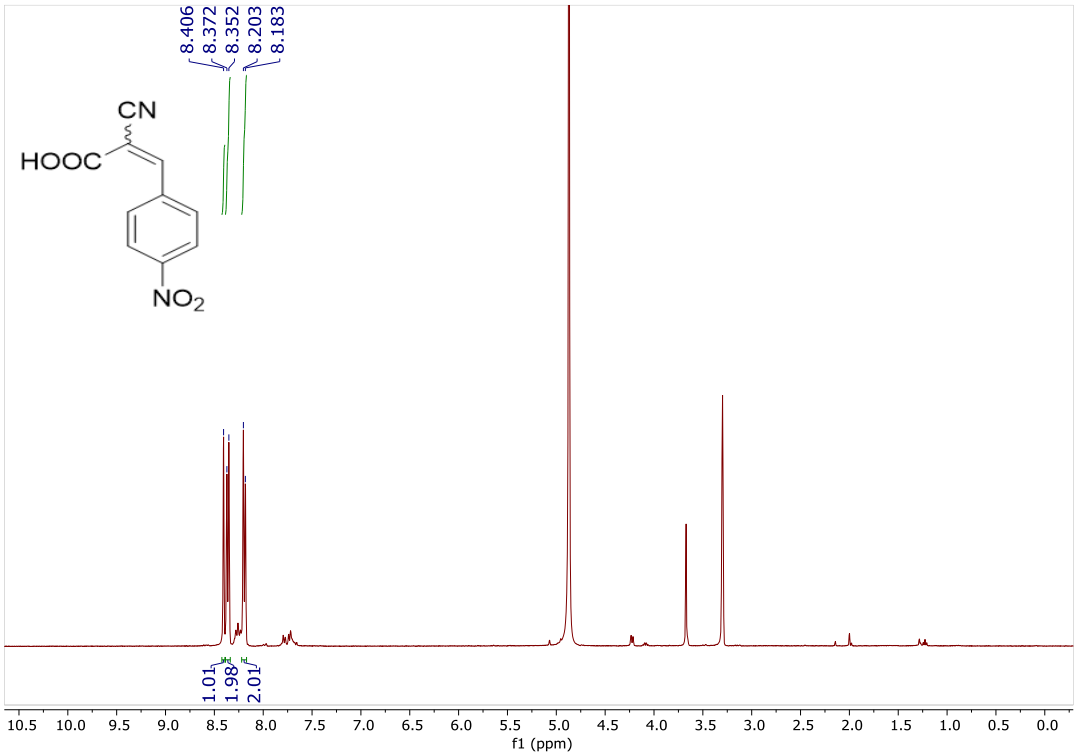


Figure A. 36. $^{1}$H NMR (MeOD, 500 MHz) spectrum of 2-cyano-3-(4-nitrophenyl)acrylic acid (**3.14**).

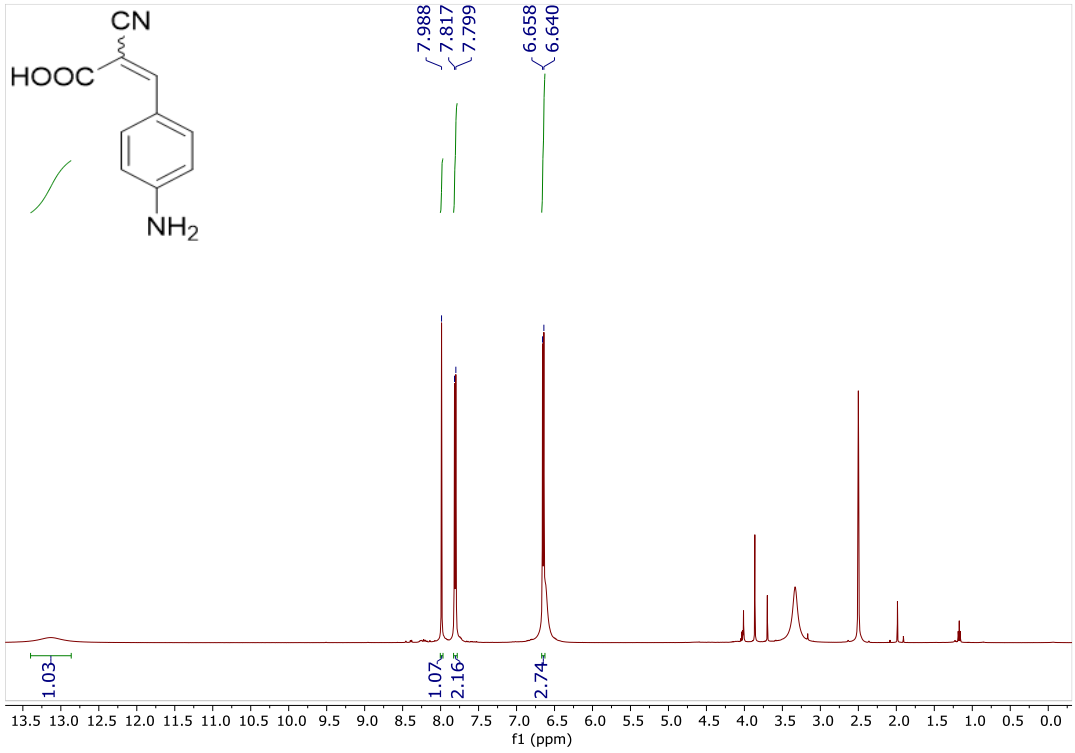


Figure A. 37. $^{1}$H NMR (DMSO, 500 MHz) spectrum of 3-(4-aminophenyl)-2-cyanoacrylic acid (**3.15**).

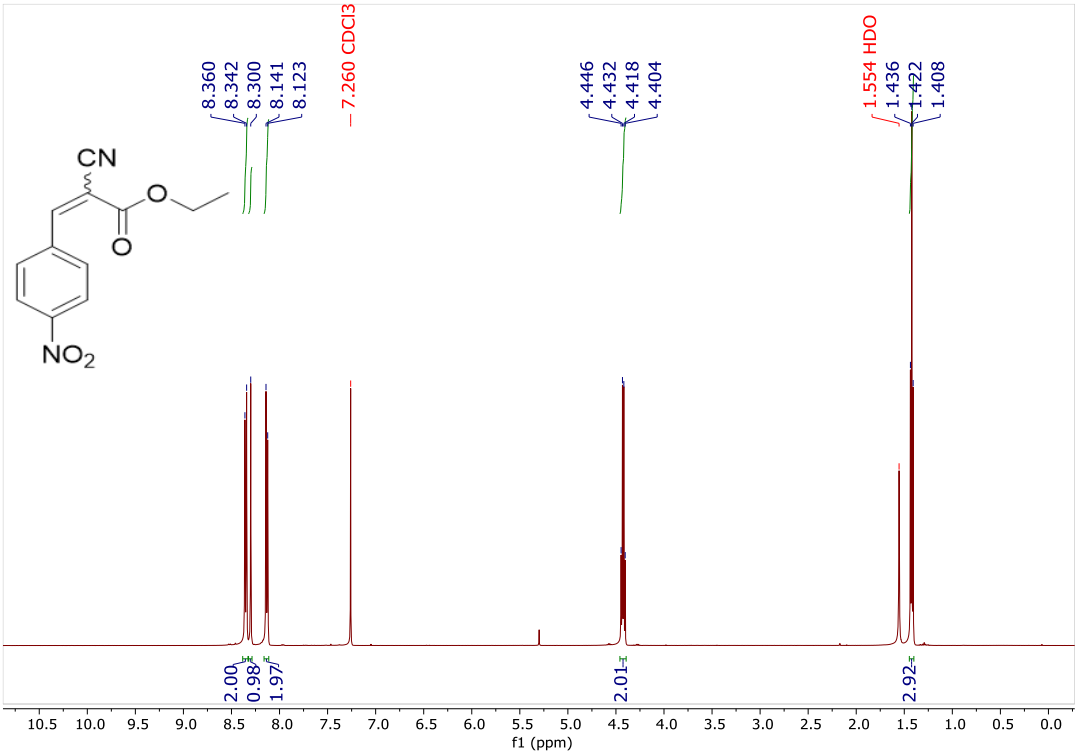


Figure A. 38. $^{1}$H NMR ($CDCl_3$, 500 MHz) spectrum of ethyl-2-cyano-3-(4-nitrophenyl)acrylate (**3.16**)

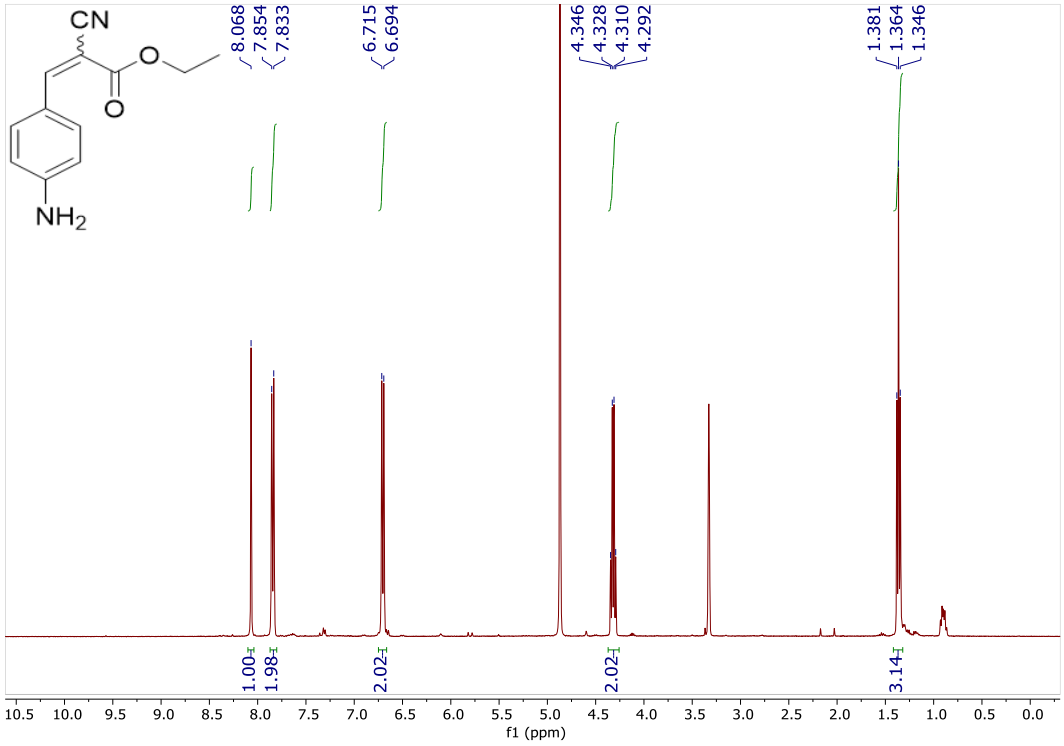


Figure A. 39. $^{1}$H NMR (MeOD, 500 MHz) spectrum of ethyl-3-(4-aminophenyl)-2-cyanoacrylate (**3.17**)

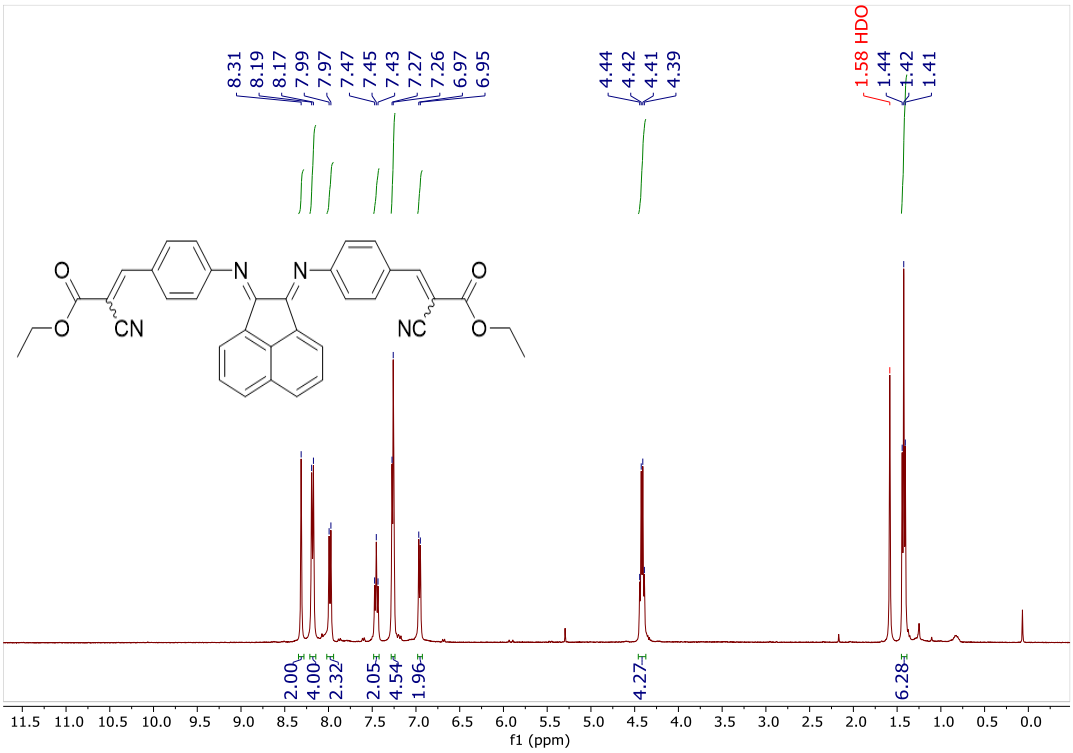


Figure A. 40. $^{1}H$ NMR ($CDCl_3$, 400 MHz) spectrum of compound 3.18

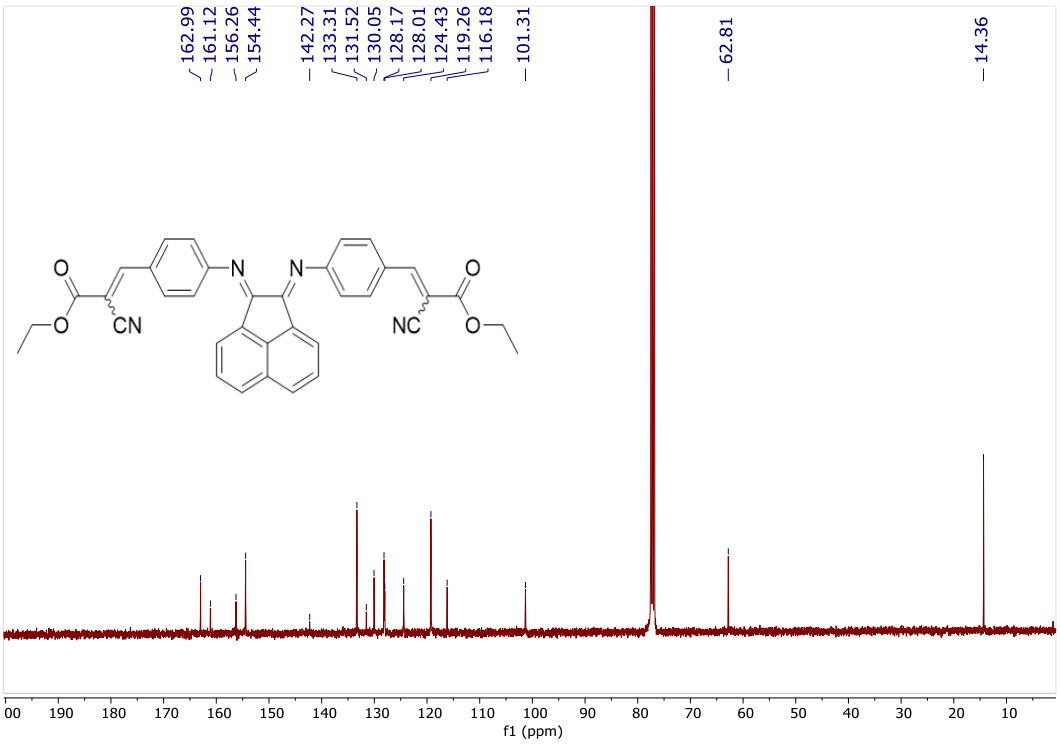


Figure A. 41. $^{13}C$ NMR ($CDCl_3$, 101 MHz) spectrum of compound 3.18.

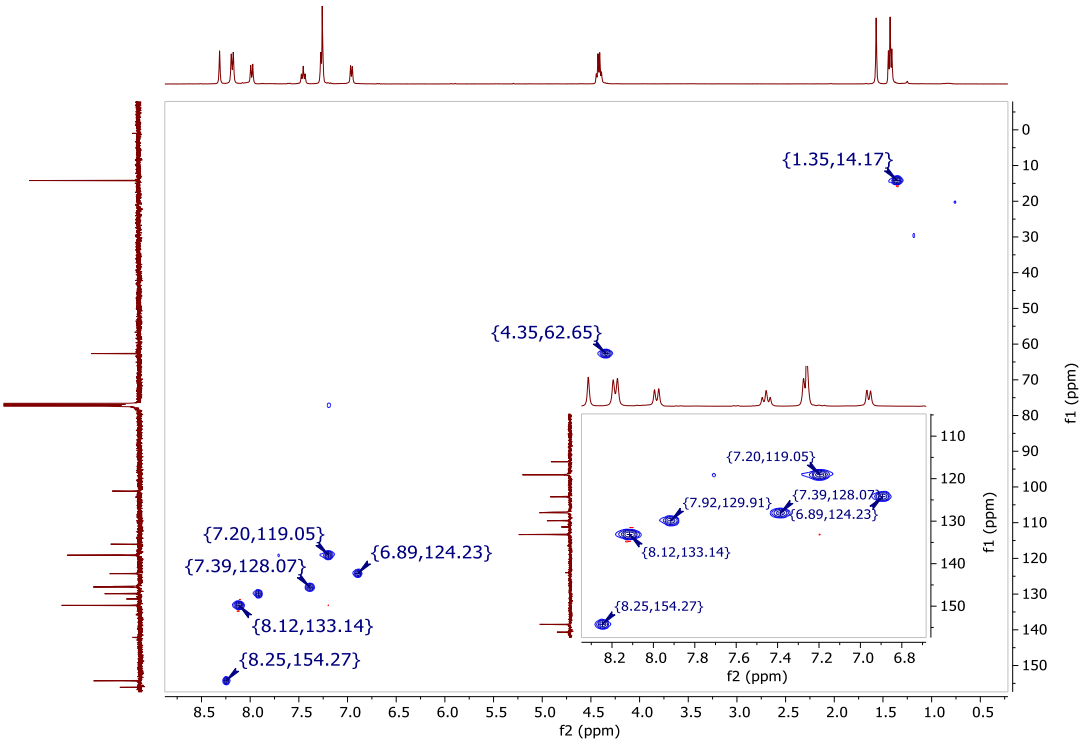


Figure A. 42. HSQC spectrum of compound 3.18.

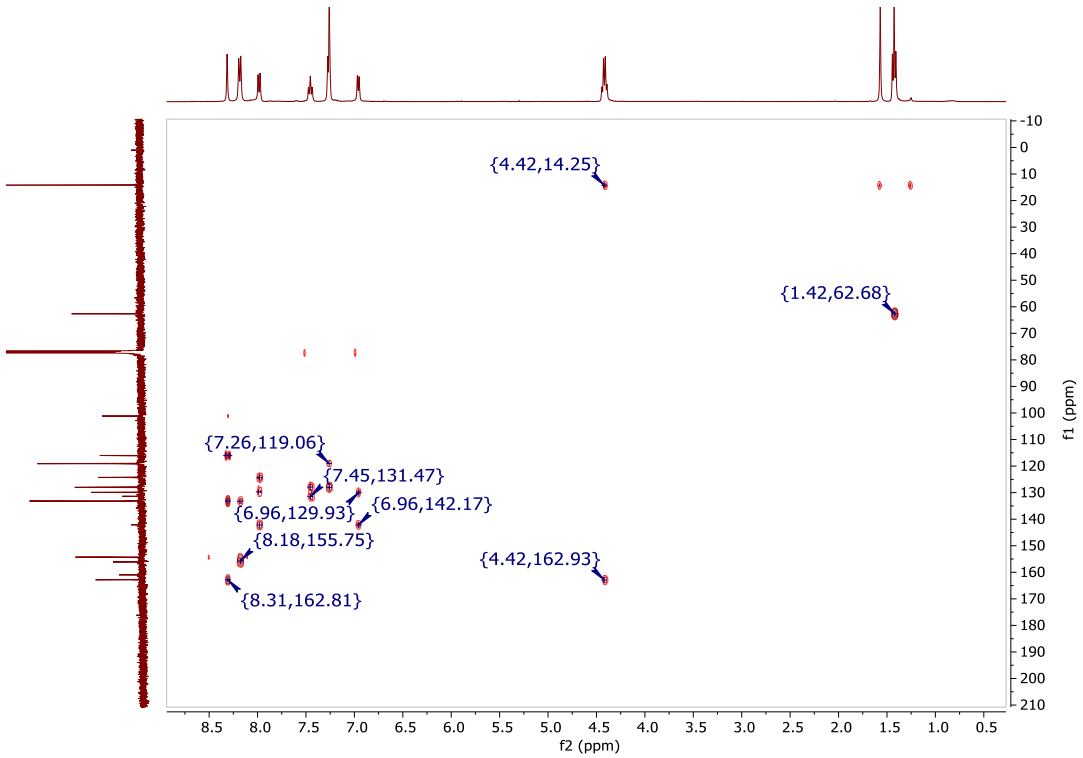


Figure A. 43. HMBC spectrum of compound 3.18.

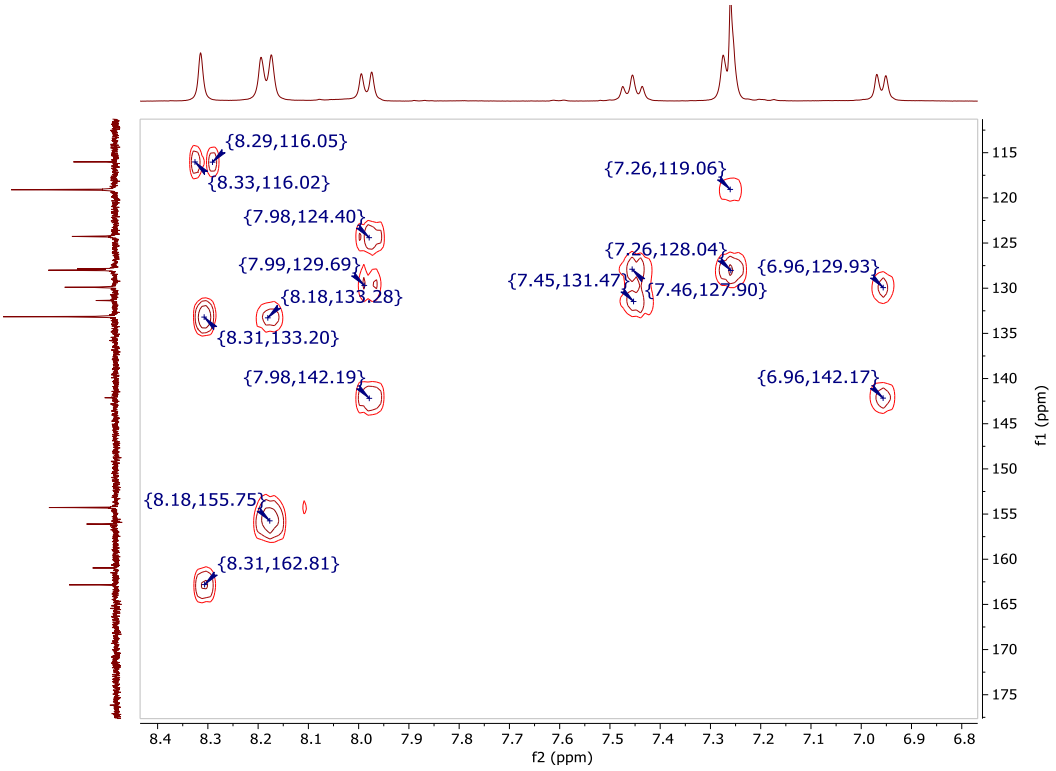


Figure A. 44. Expansion of HMBC spectrum of compound 3.18.

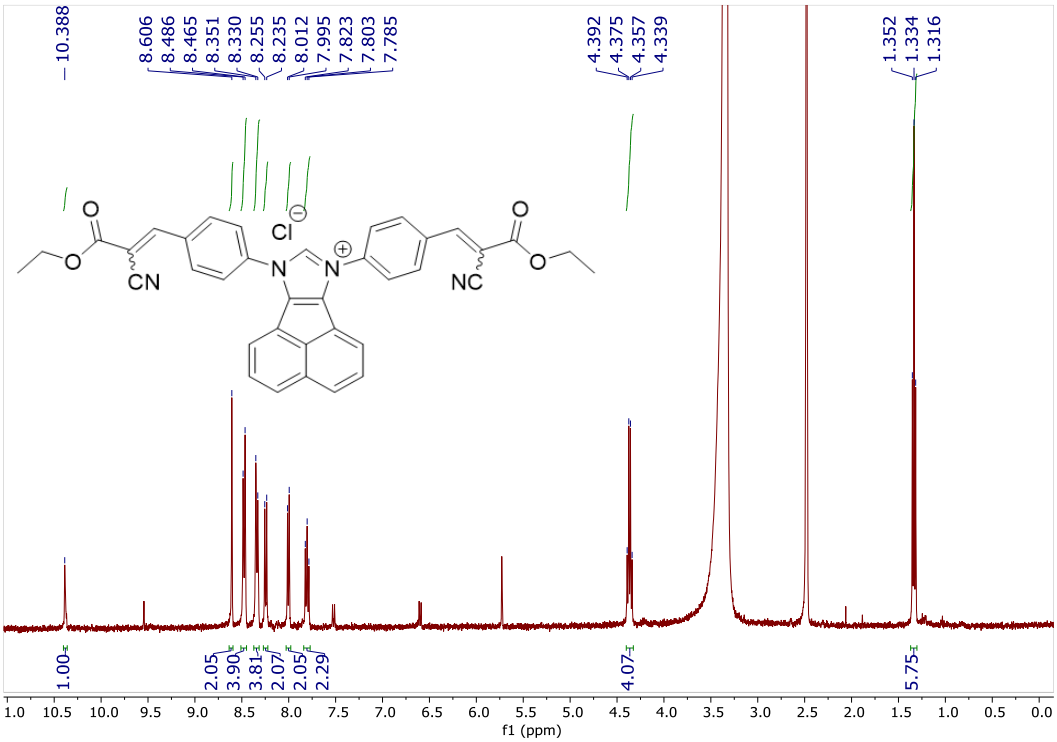


Figure A. 45. $^{1}$H NMR (DMSO-d6, 400 MHz) spectrum of 7,9-bis(4-(2-cyano-3-ethoxy-3-oxoprop-1-en-1-yl)phenyl)-7H-acenaphtho[1,2-d]imidazol-9-ium chloride (**3.19**)

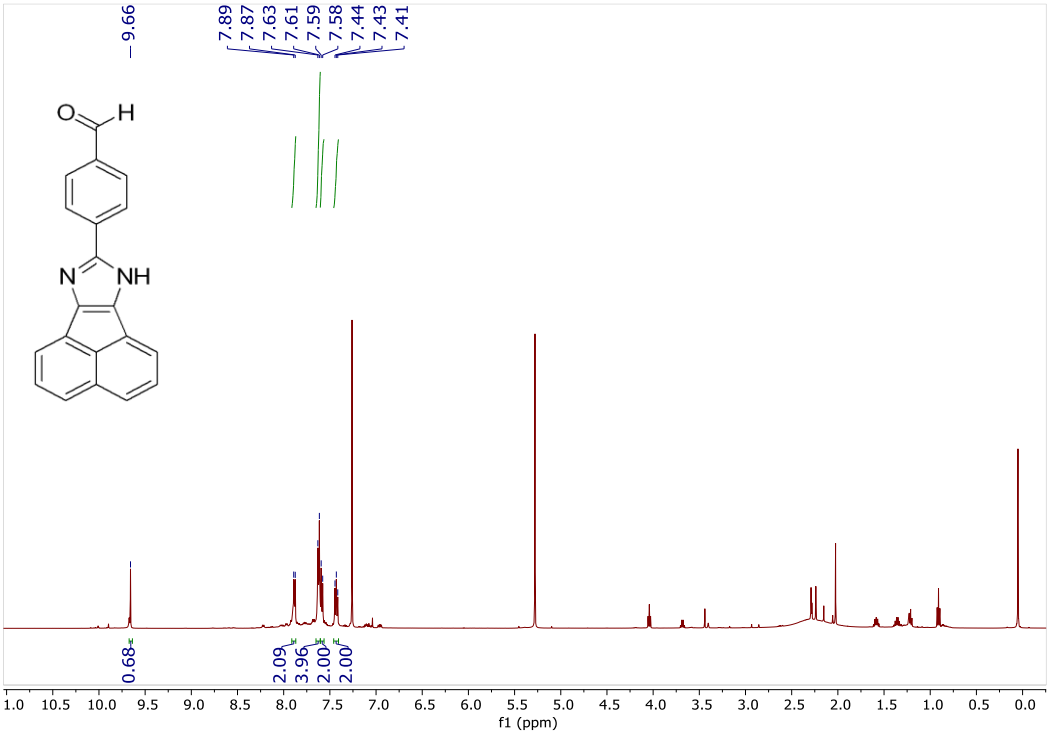


Figure A. 46. $^{1}$H NMR ($CDCl_3$, 500 MHz) spectrum of 4-(7H-acenaphtho[1,2-d]imidazol-8-yl)benzaldehyde (**3.22a**)

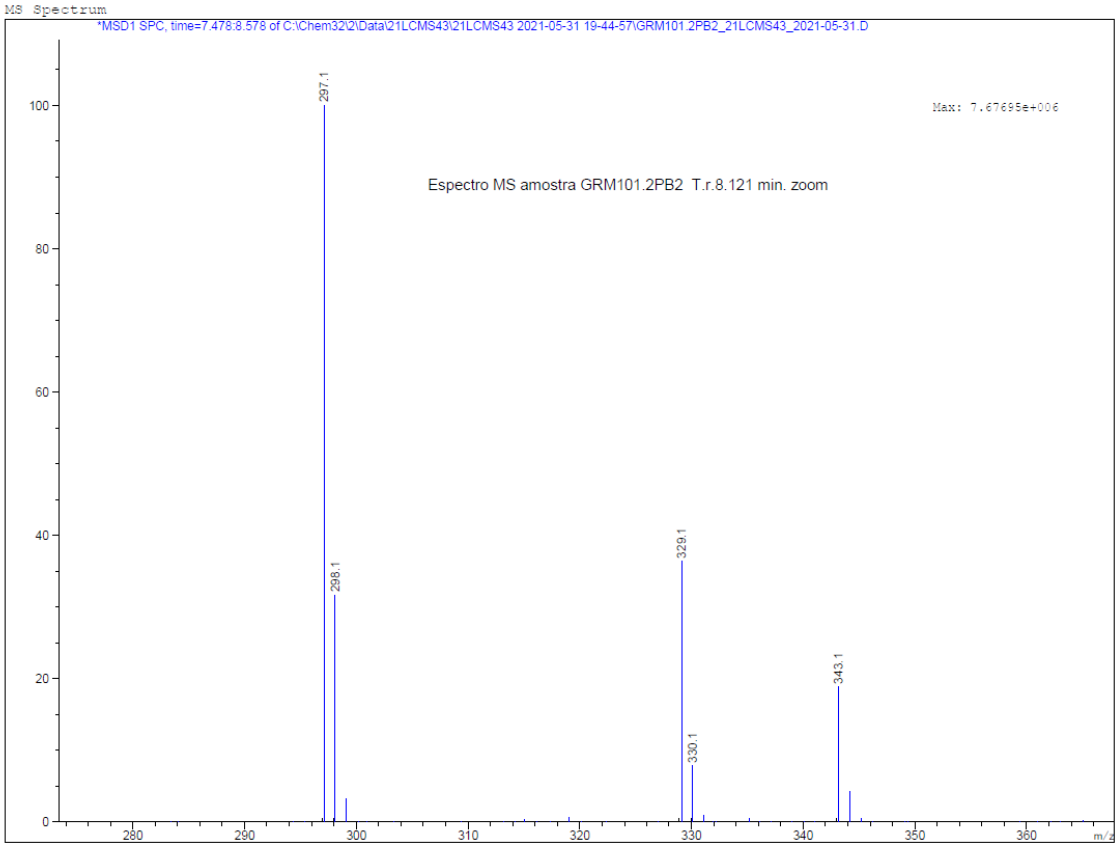


Figure A. 47. LC-ESI-MS spectrum of 4-(7H-acenaphtho[1,2-d]imidazol-8-yl)benzaldehyde (**3.22a**) at RT 8.12 min.

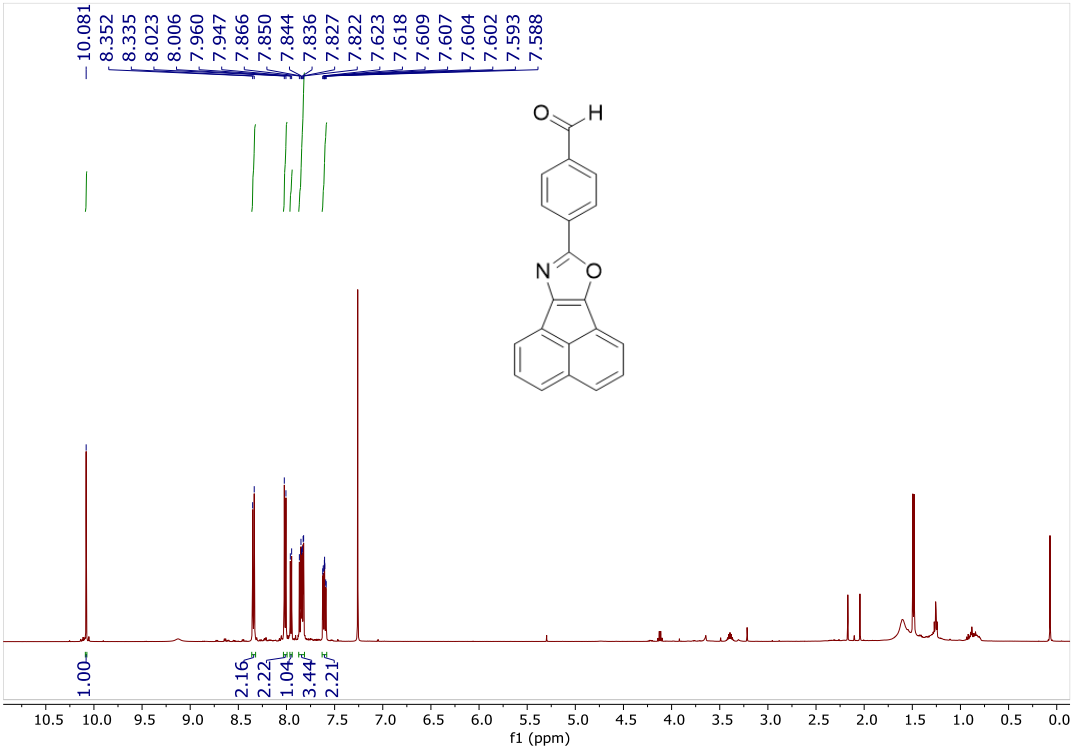


Figure A. 48. $^{1}H$ NMR ($CDCl_3$, 500 MHz) spectrum of 4-(Acenaphtho[1,2-d]oxazol-8-yl)benzaldehyde (**3.22b**).

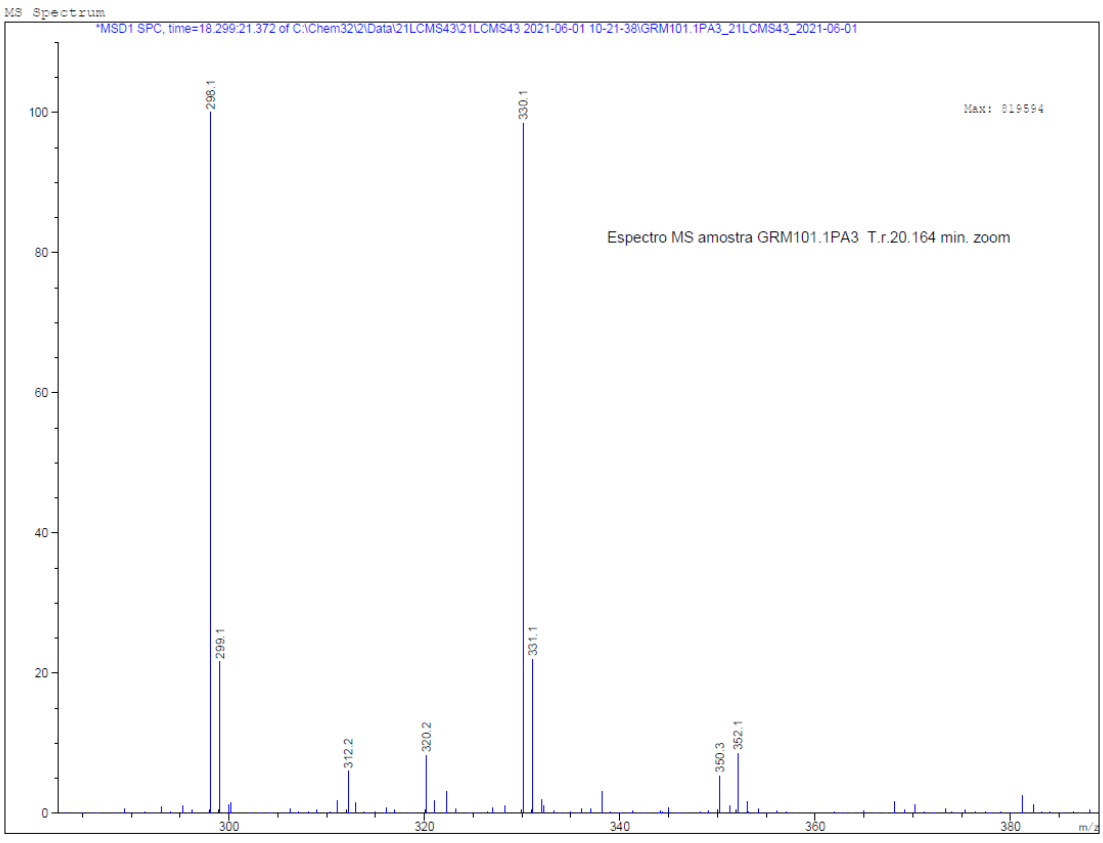


Figure A. 49. LC-ESI-MS spectrum of 4-(Acenaphtho[1,2-d]oxazol-8-yl)benzaldehyde (**3.22b**) at RT 20.16 min.

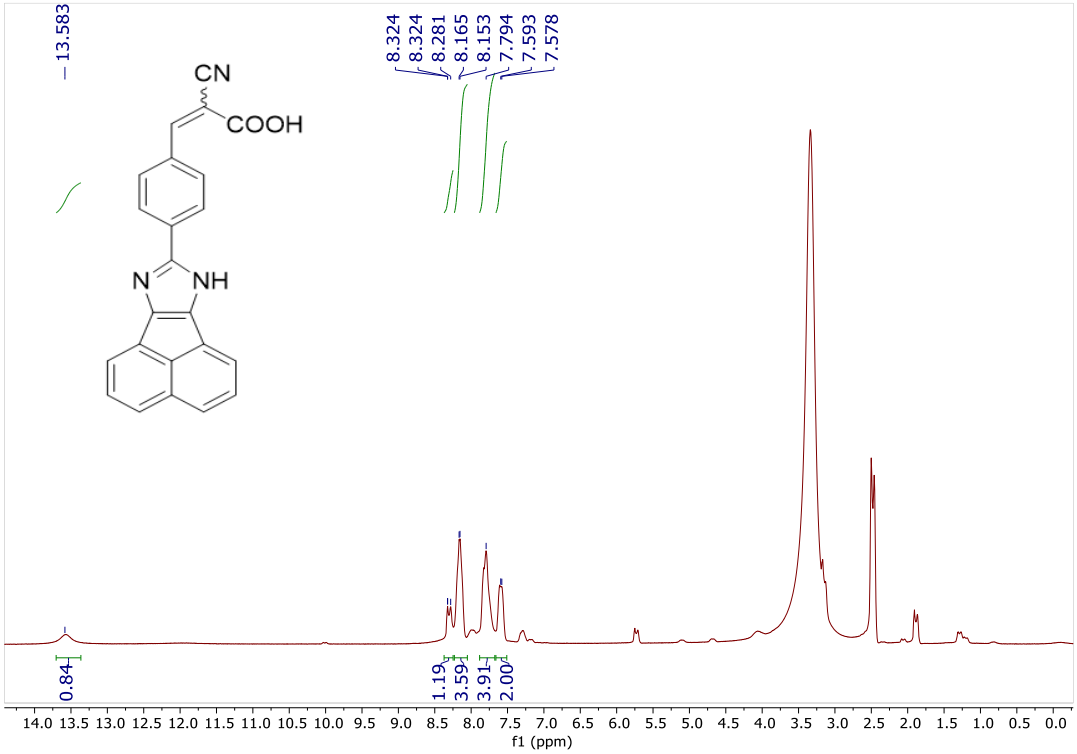


Figure A. 50. $^{1}$H NMR (DMSO-d6, 500 MHz) spectrum of 3-(4-(7H-acenaphtho[1,2-d]imidazol-8-yl)phenyl)-2-cyanoacrylic acid (**3.23**).

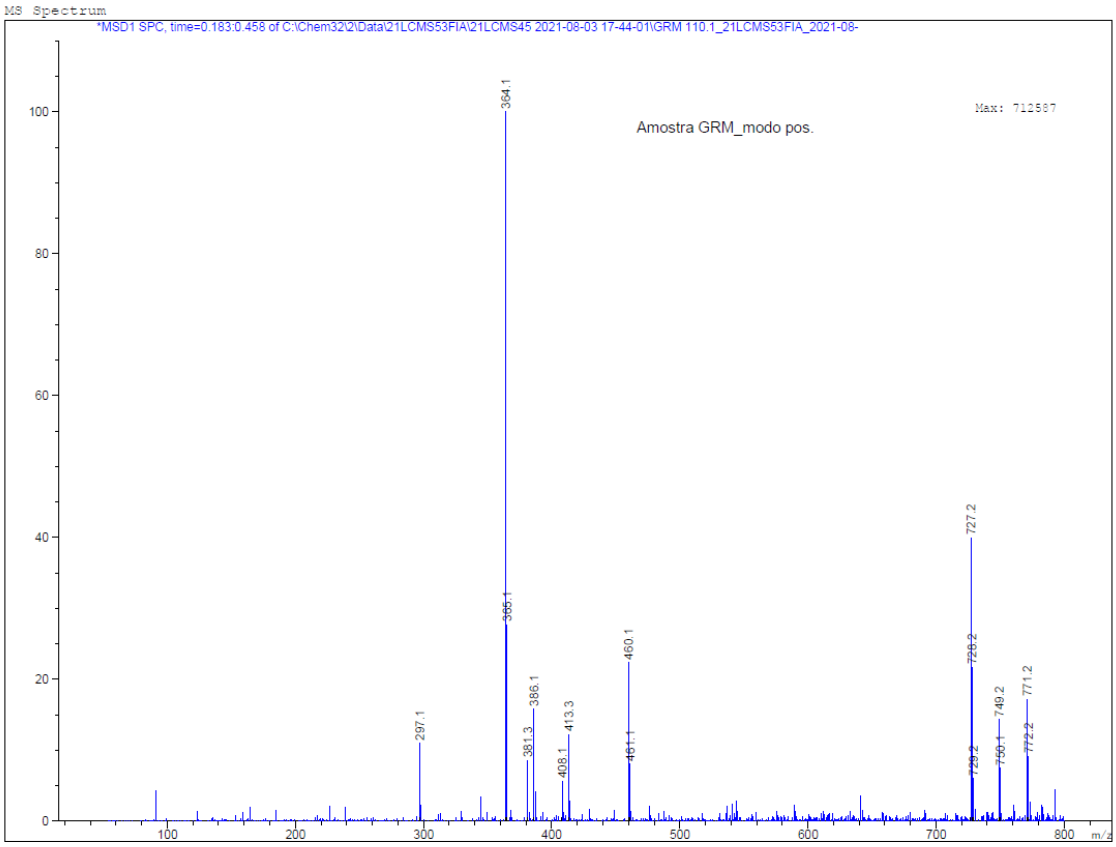


Figure A. 51. ESI-MS spectrum of 3-(4-(7H-acenaphtho[1,2-d]imidazol-8-yl)phenyl)-2-cyanoacrylic acid (**3.23**), positive mode.

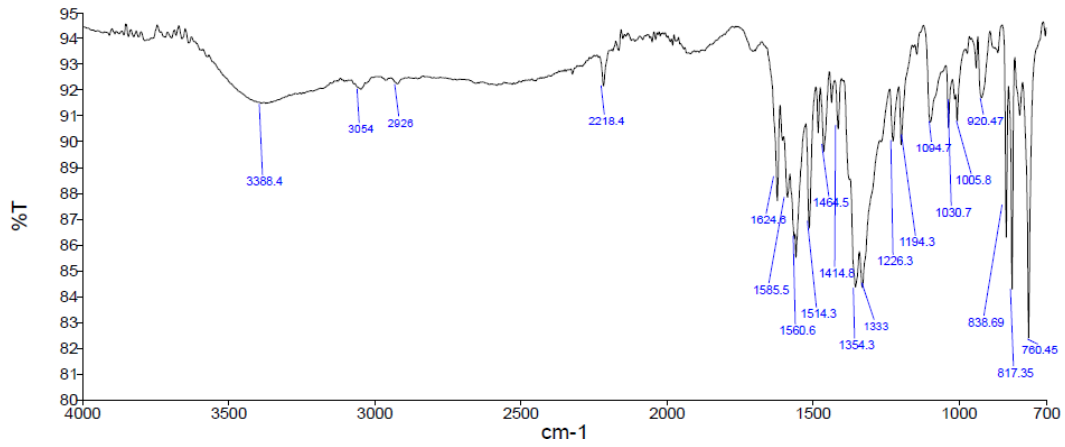


Figure A. 52. IR spectrum of compound 3.23.

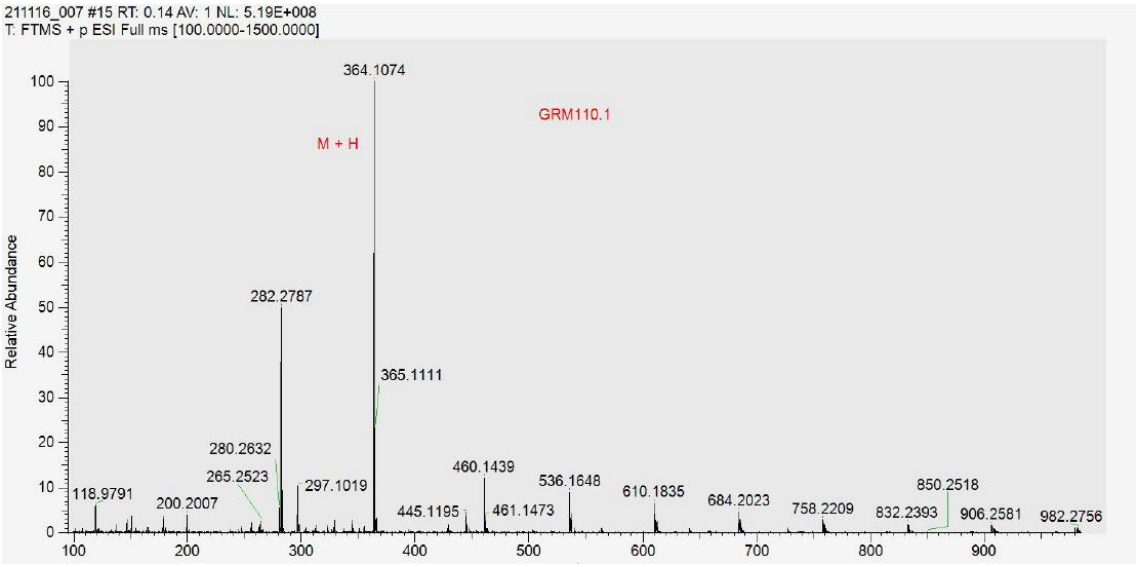


Figure A. 53. HRMS-ESI spectrum of 3-(4-(7H-acenaphtho[1,2-d]imidazol-8-yl)phenyl)-2-cyanoacrylic acid (**3.23**)

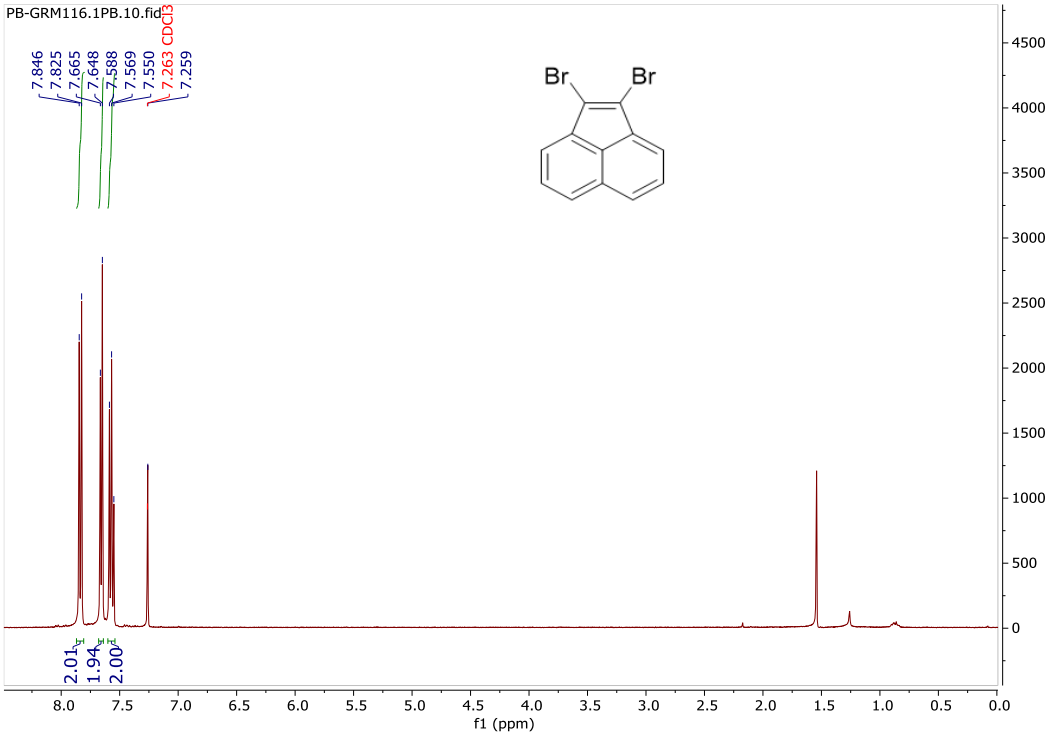


Figure A. 54. $^{1}H$ NMR ($CDCl_3$, 400 MHz) spectrum of 1,2-Dibromoacenaphthylene (**3.32**).

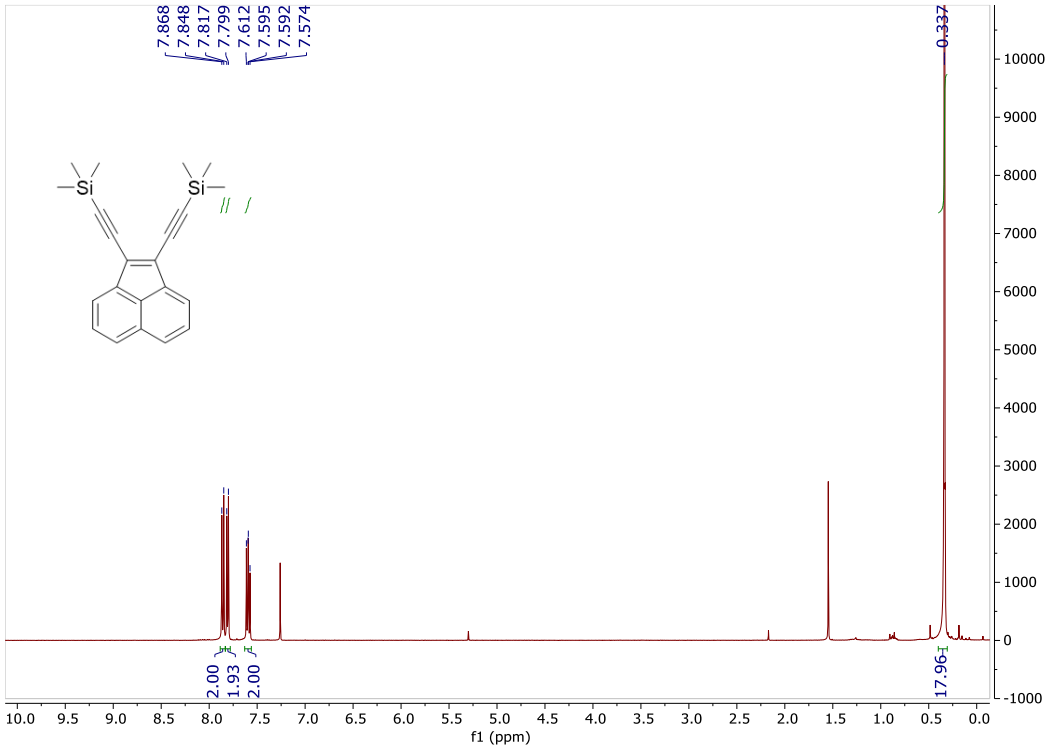


Figure A. 55. $^{1}H$ NMR ($CDCl_3$, 400 MHz) spectrum of 1,2-bis((trimethylsilyl)ethynyl) acenaphthylene (**3.34**).

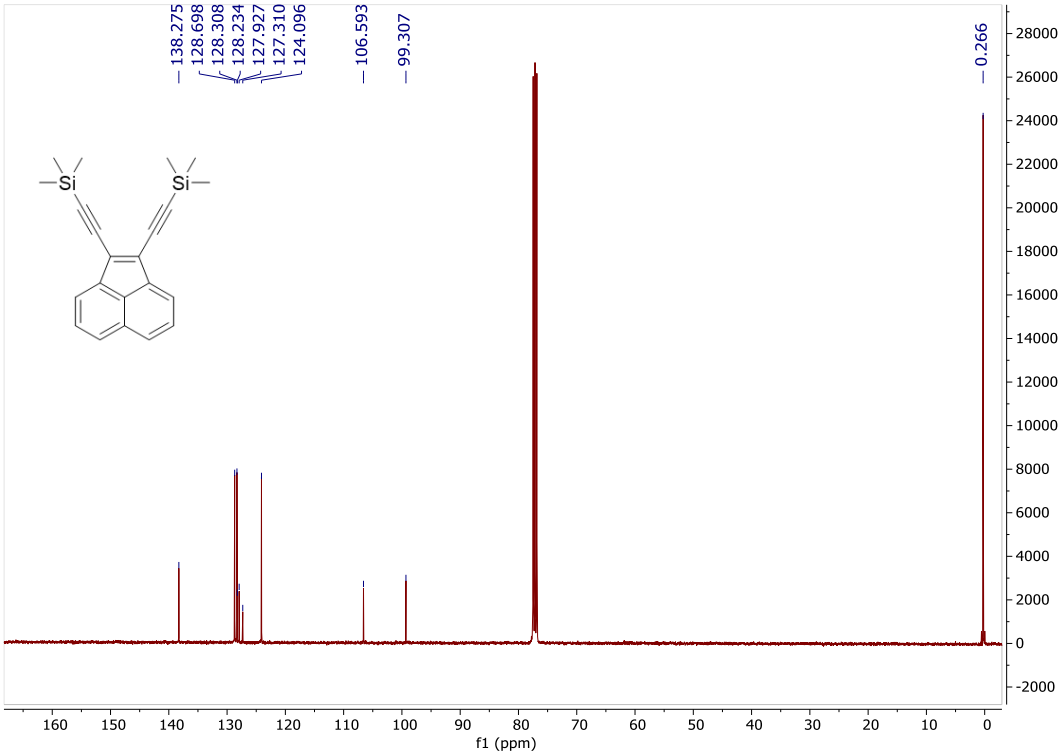


Figure A. 56. $^{13}C$ NMR ($CDCl_3$, 101 MHz) spectrum of 1,2-bis((trimethylsilyl)ethynyl) acenaphthylene (**3.34**).

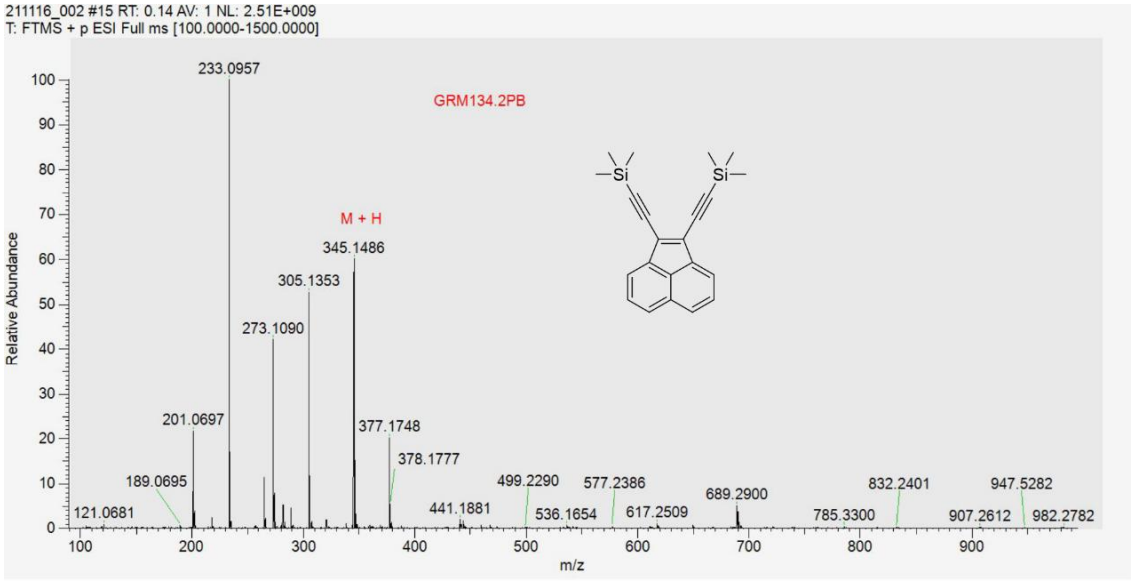


Figure A. 57. HRMS-ESI spectrum of 1,2-bis((trimethylsilyl)ethynyl)acenaphthylene (**3.34**).

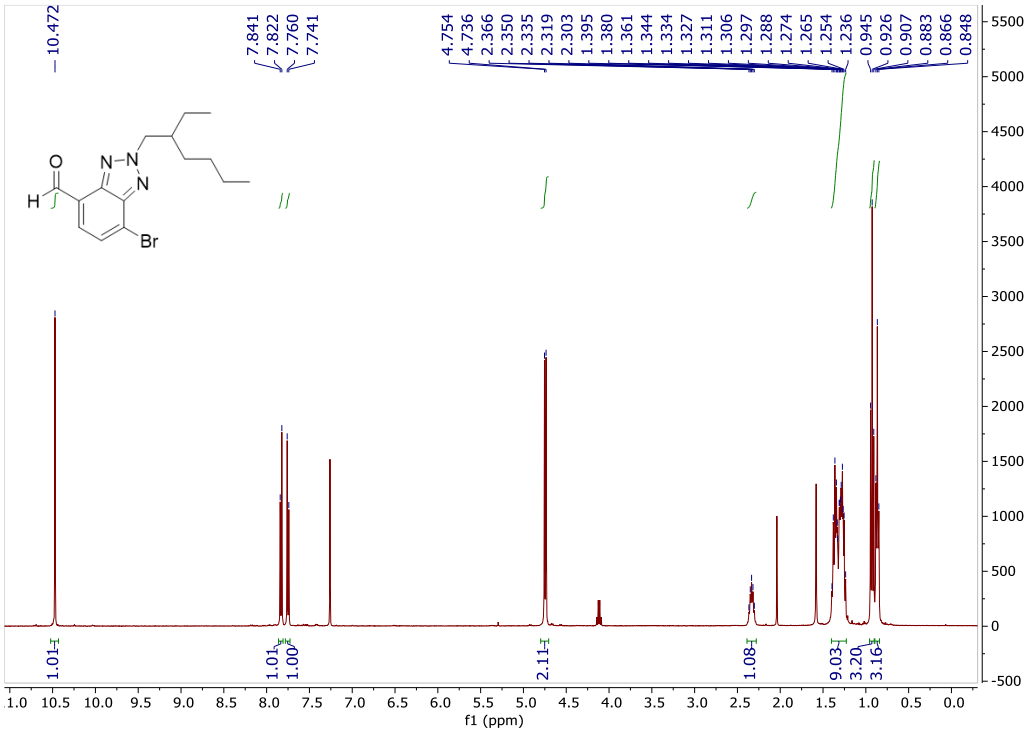


Figure A. 58. $^{1}H$ NMR ($CDCl_3$, 400 MHz) spectrum of 7-bromo-2-(2-ethylhexyl)-2H-benzo[d][1,2,3]triazole-4-carbaldehyde (**3.36c**).

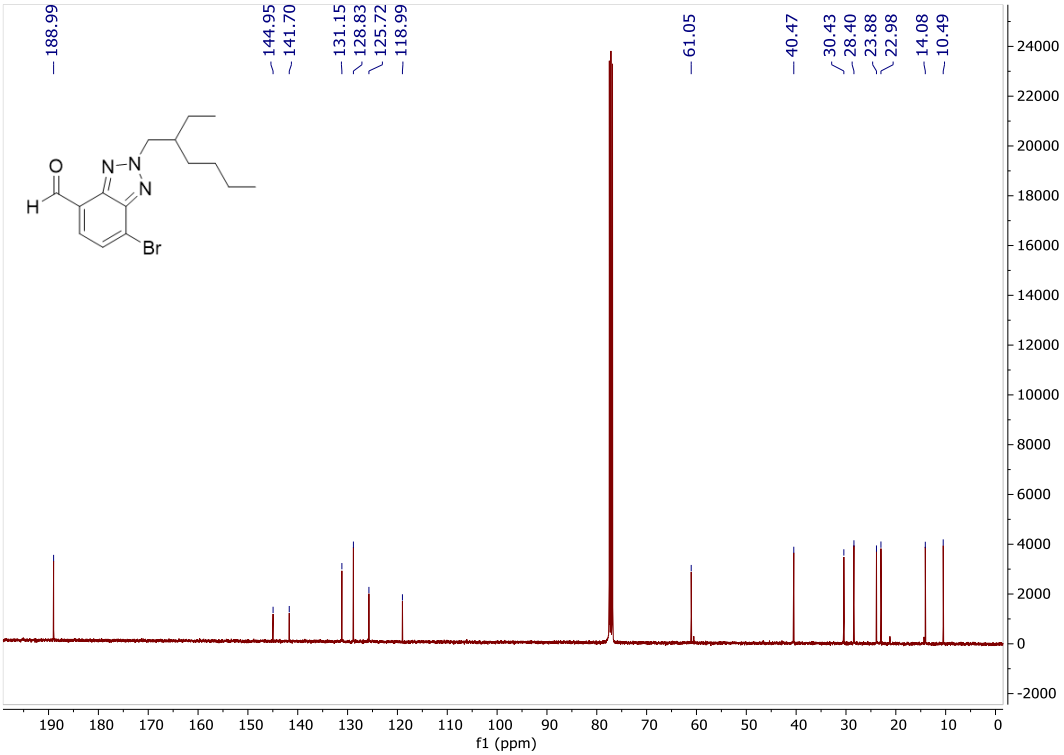


Figure A. 59. $^{13}C$ NMR ($CDCl_3$, 101 MHz) spectrum of 7-bromo-2-(2-ethylhexyl)-2H-benzo[d][1,2,3]triazole-4-carbaldehyde (**3.36c**).

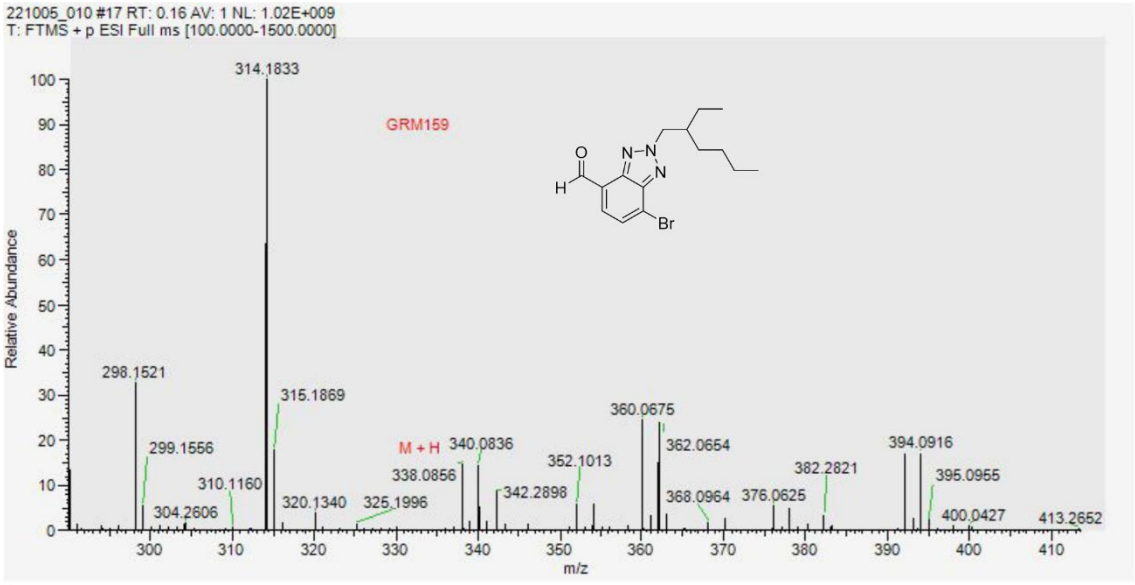


Figure A. 60. HRMS-ESI spectrum of 7-bromo-2-(2-ethylhexyl)-2H-benzo[d][1,2,3]triazole-4-carbaldehyde (**3.36c**).

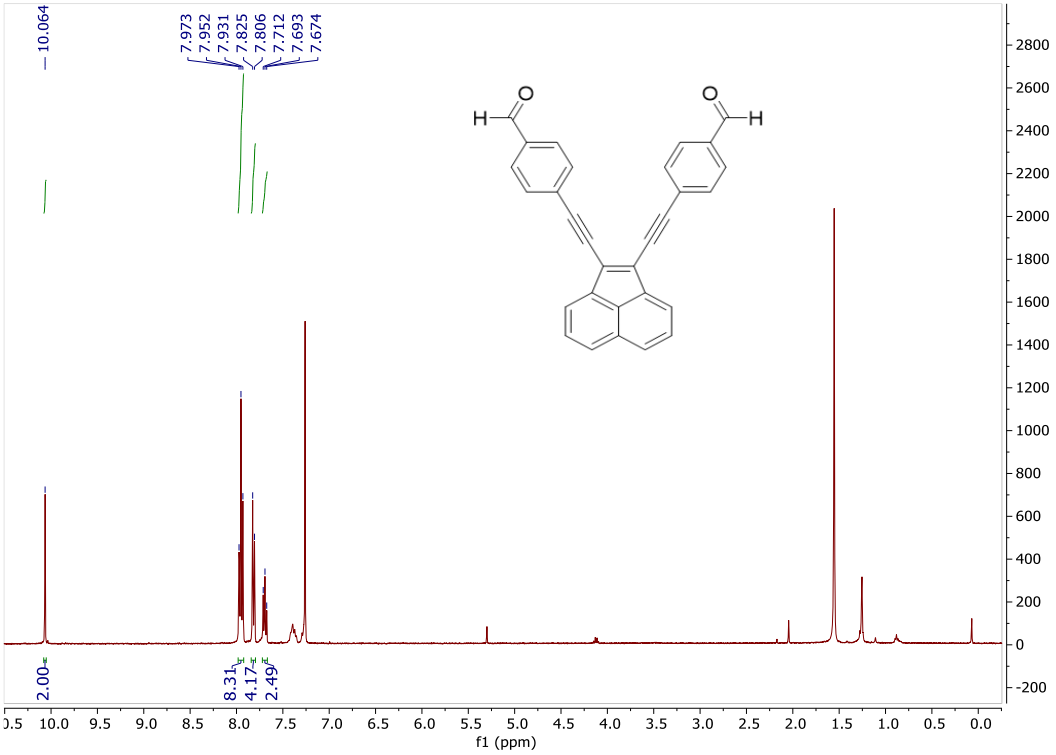


Figure A. 61. $^{1}H$ NMR ($CDCl_3$, 400 MHz) spectrum of compound 3.33a.

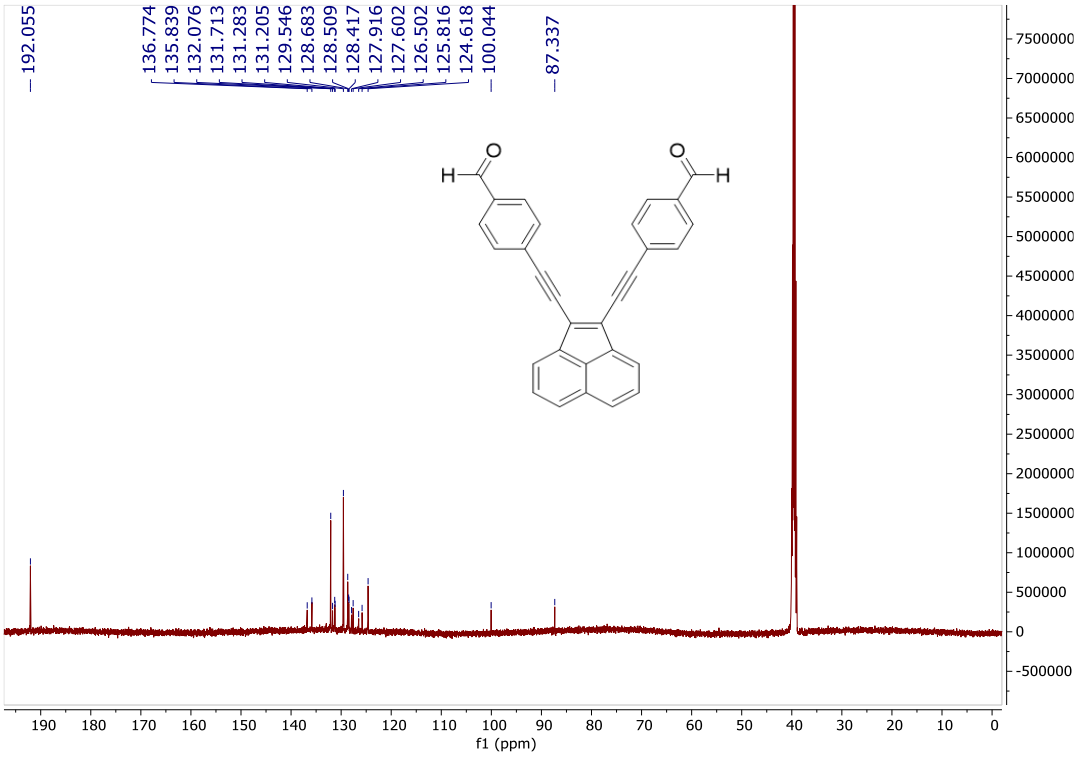


Figure A. 62. $^{13}C$ NMR (DMSO, 101 MHz) spectrum of compound 3.33a.

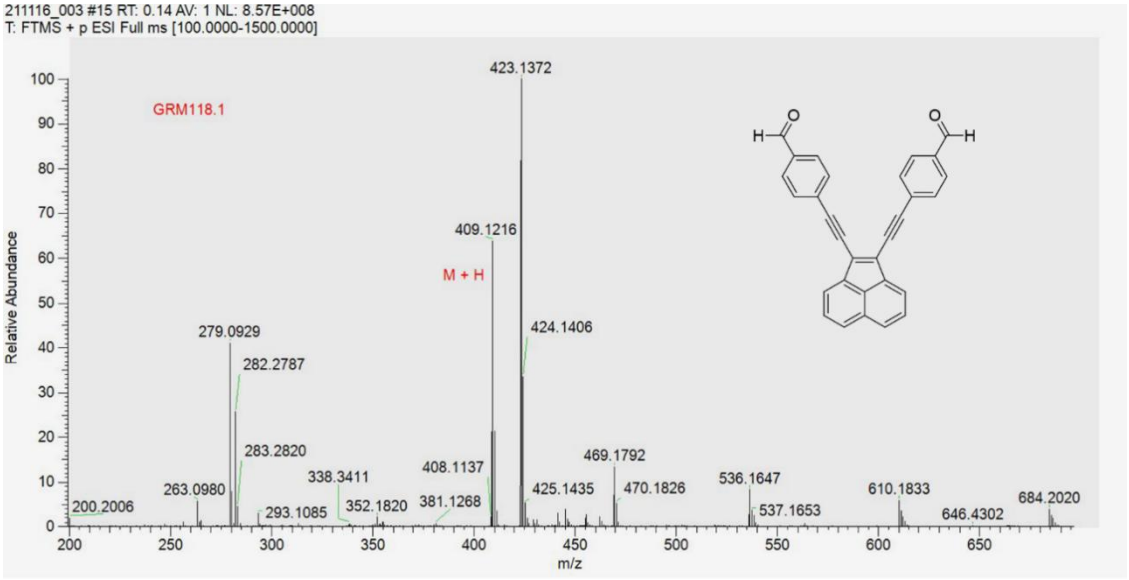


Figure A. 63. HRMS-ESI spectrum of compound 3.33a.

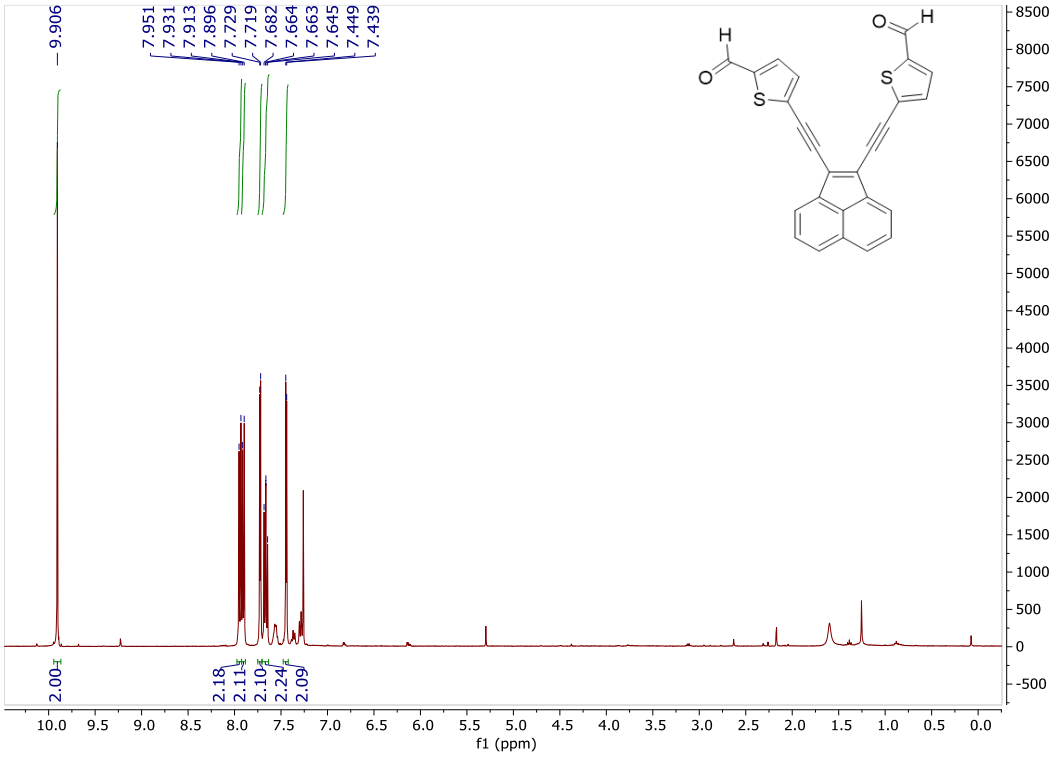


Figure A. 64. $^{1}H$ NMR ($CDCl_3$, 400 MHz) spectrum of compound 3.33b.

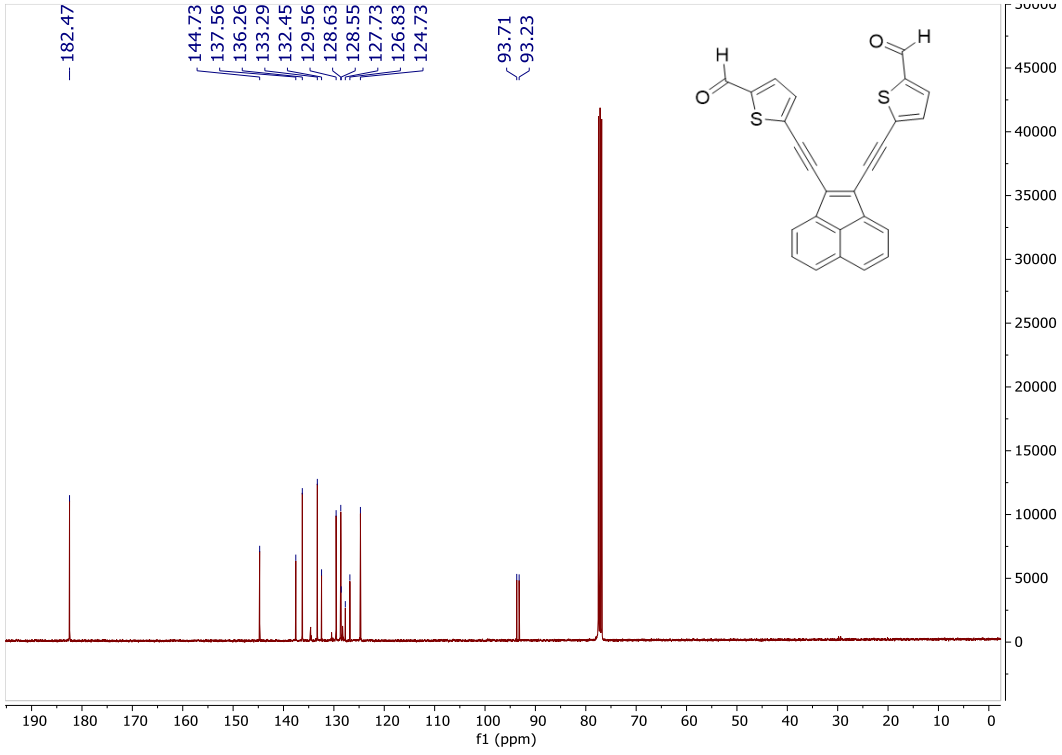


Figure A. 65. $^{13}C$ NMR ($CDCl_3$, 101 MHz) spectrum of compound 3.33b.

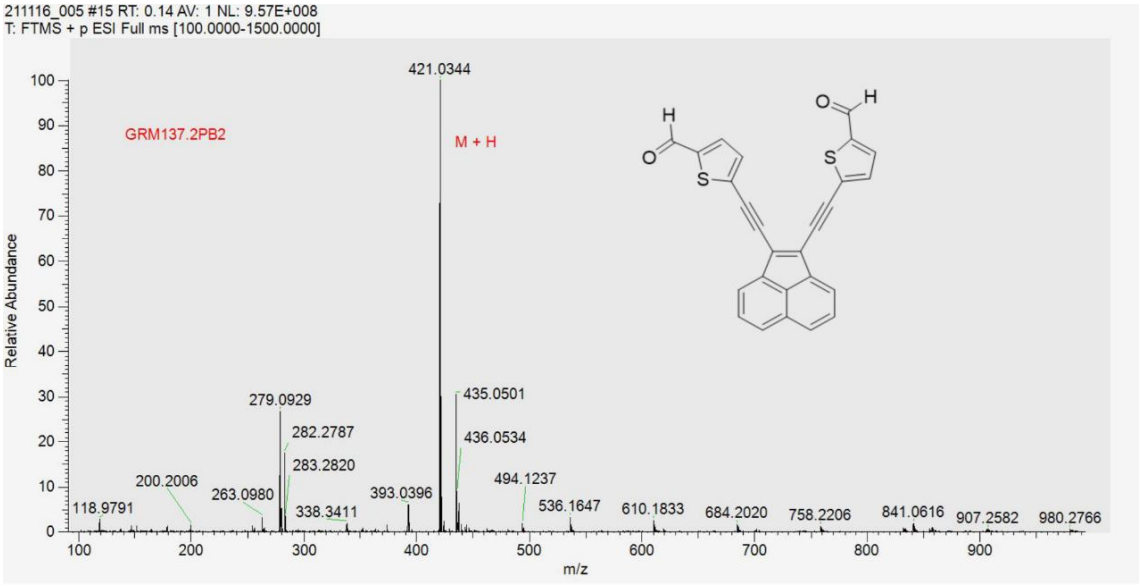


Figure A. 66. HRMS-ESI spectrum of compound 3.33b.

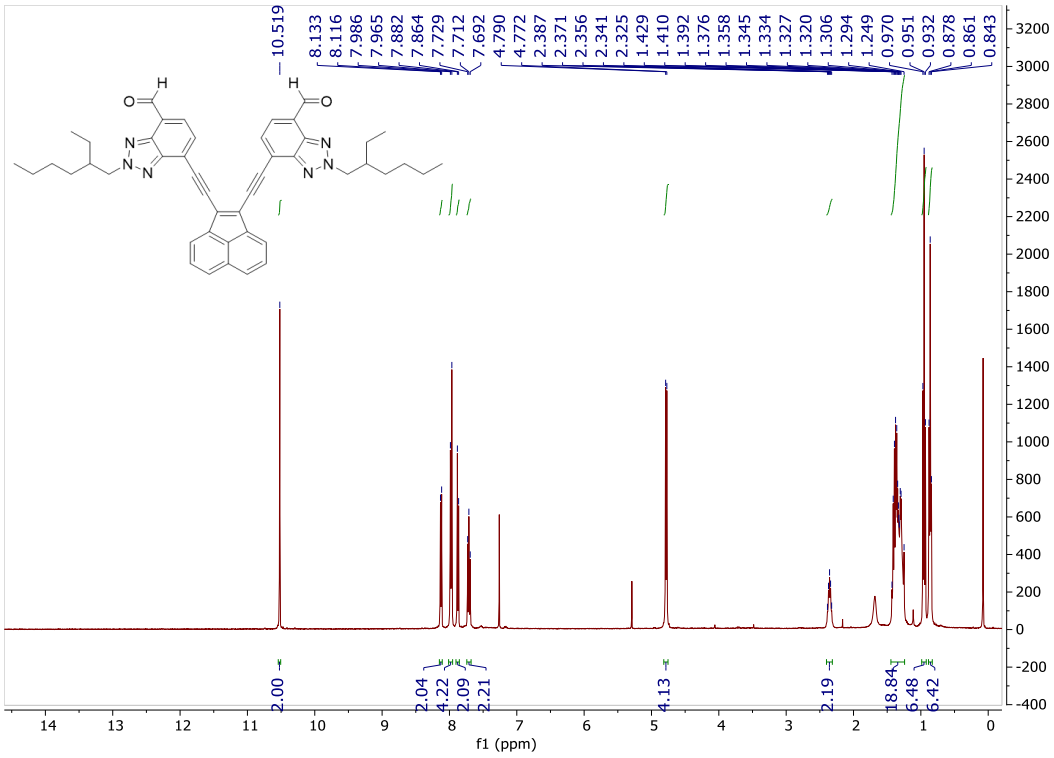


Figure A. 67. $^{1}$H NMR ($CDCl_3$, 400 MHz) spectrum of compound 3.33c.

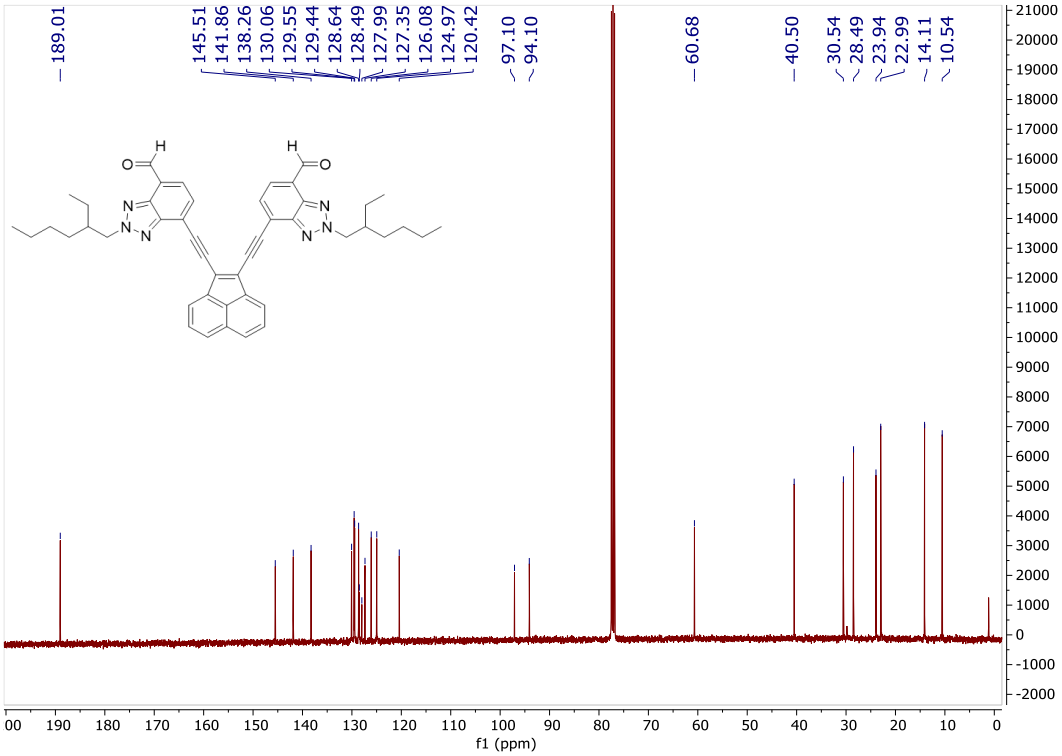


Figure A. 68. $^{13}C$ NMR ($CDCl_3$, 101 MHz) spectrum of compound 3.33c.

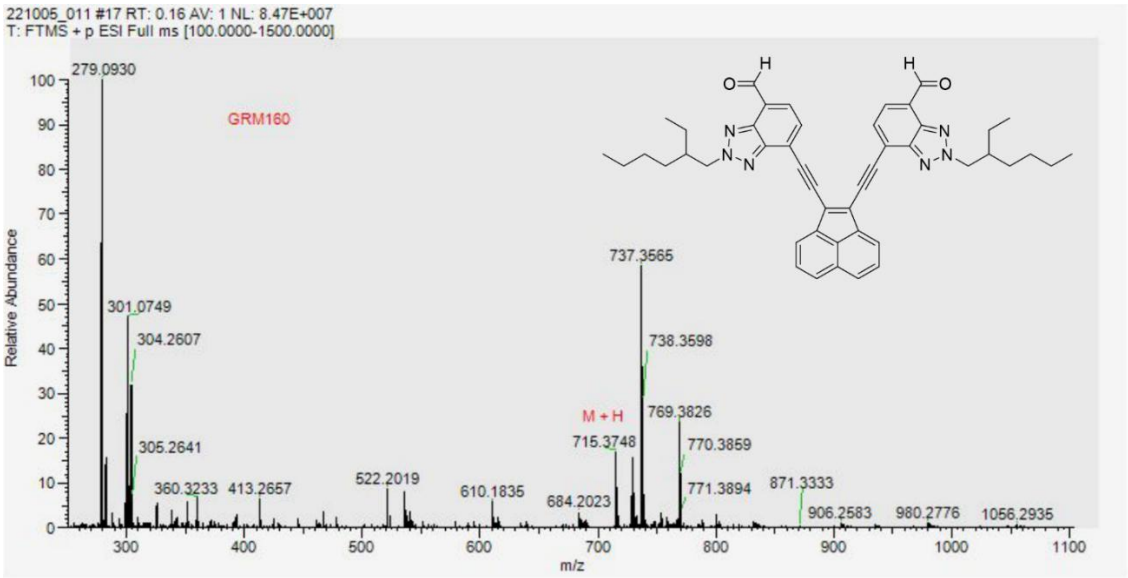


Figure A. 69. HRMS-ESI spectrum of compound 3.33c.

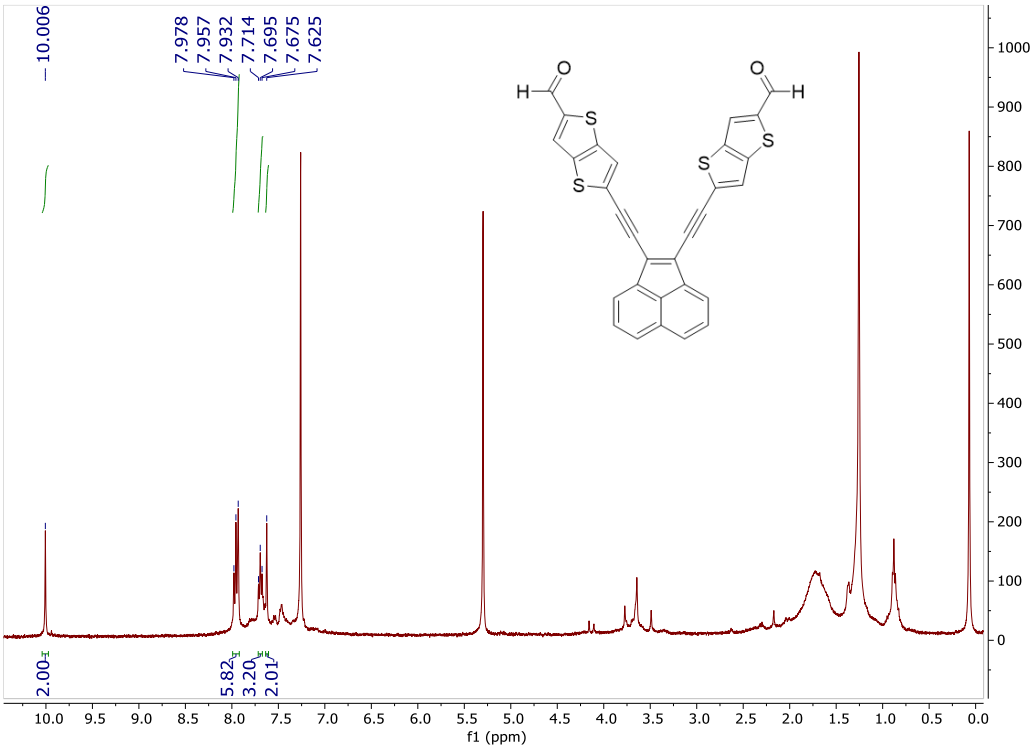


Figure A. 70. $^{1}H$ NMR ($CDCl_3$, 400 MHz) spectrum of compound 3.33d.

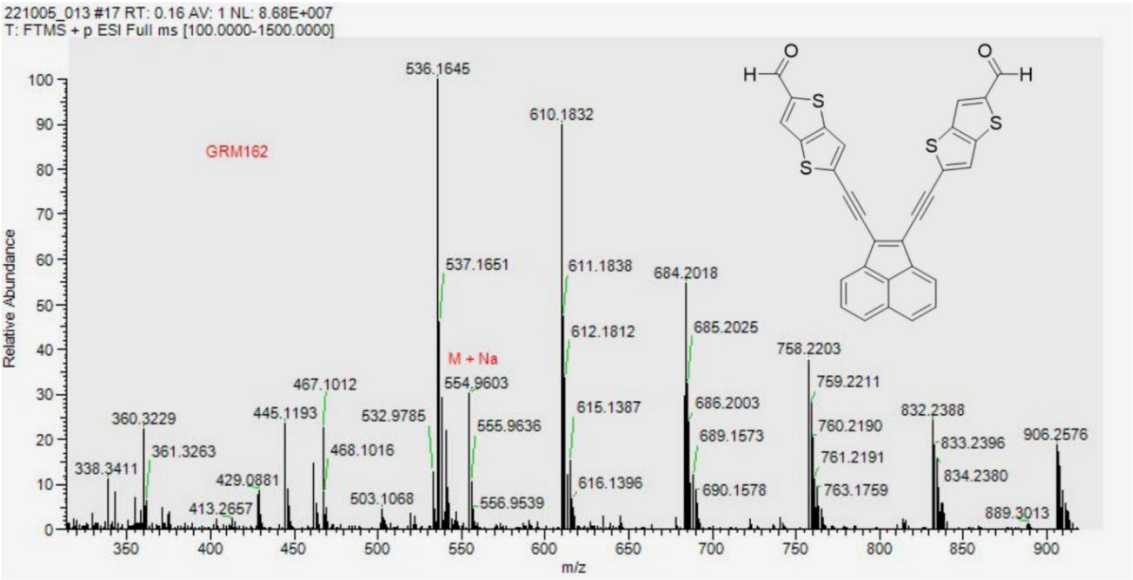


Figure A. 71. HRMS-ESI spectrum of compound 3.33d.

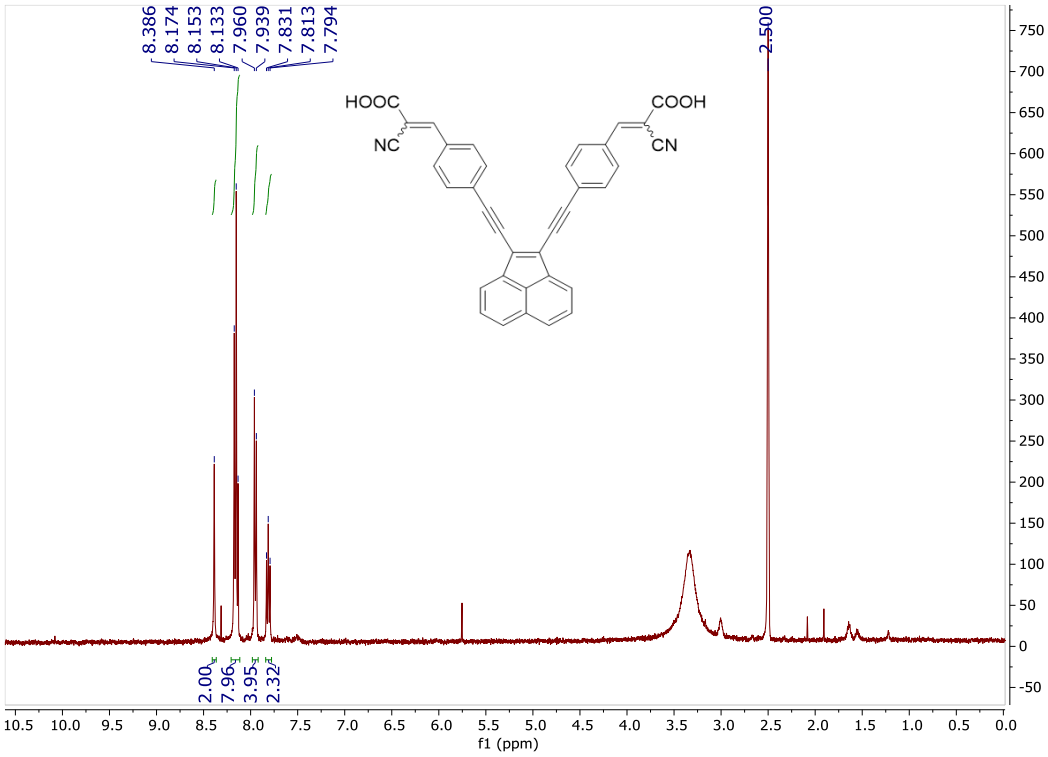


Figure A. 72. $^{1}$H NMR (DMSO-$d_6$, 400 MHz) spectrum of compound 3.37a.

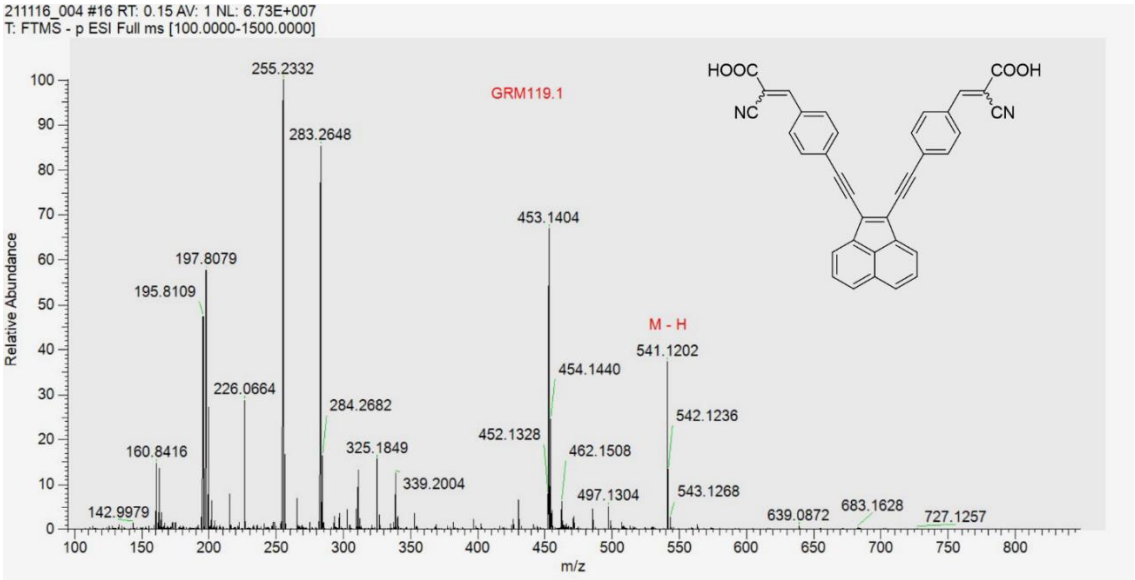


Figure A. 73. HRMS-ESI spectrum of compound 3.37a.

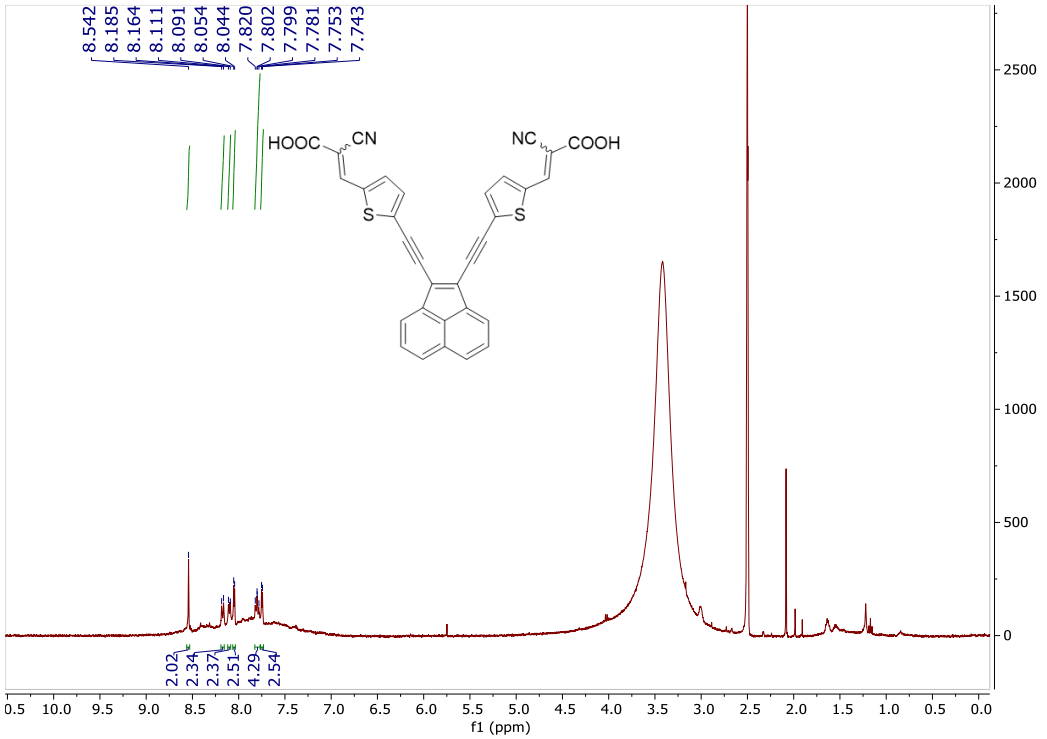


Figure A. 74. $^{1}$H NMR (DMSO-$d_6$, 400 MHz) spectrum of compound 3.37b.

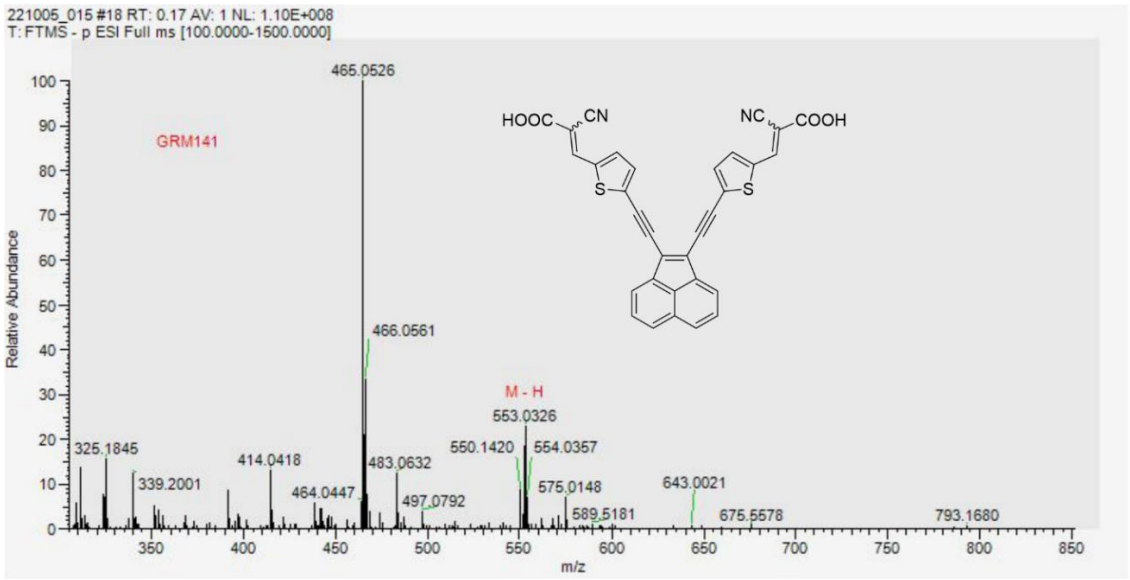


Figure A. 75. HRMS-ESI spectrum of compound 3.37b.

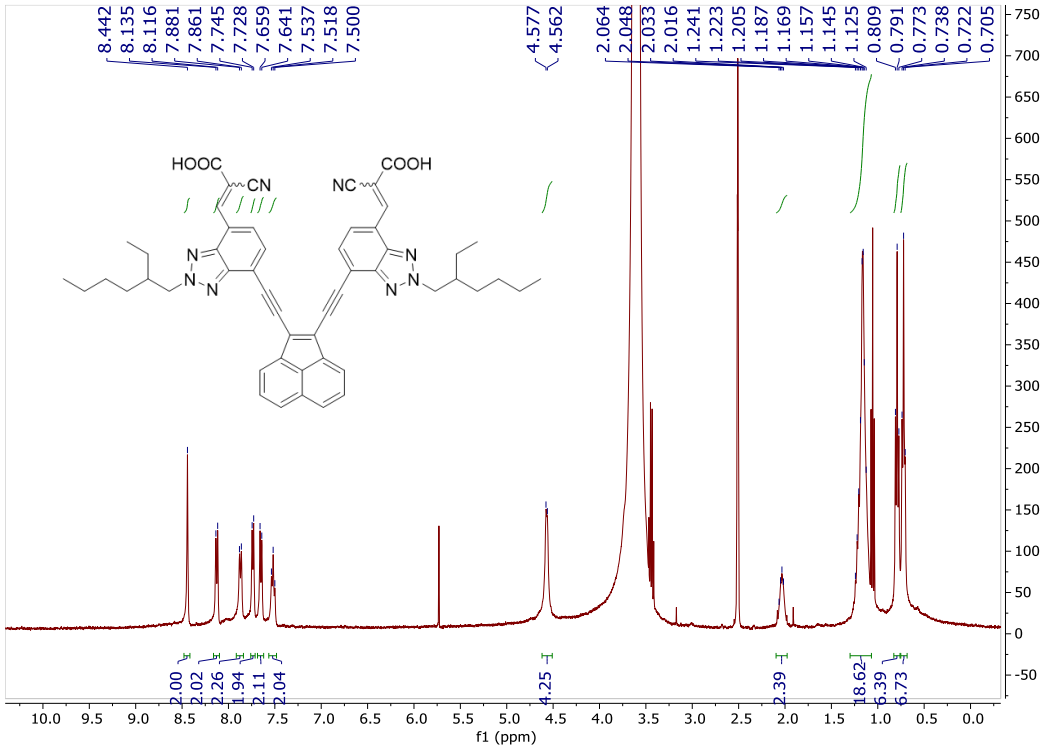


Figure A. 76. $^{1}$H NMR (DMSO-$d_6$, 400 MHz) spectrum of compound 3.37c.

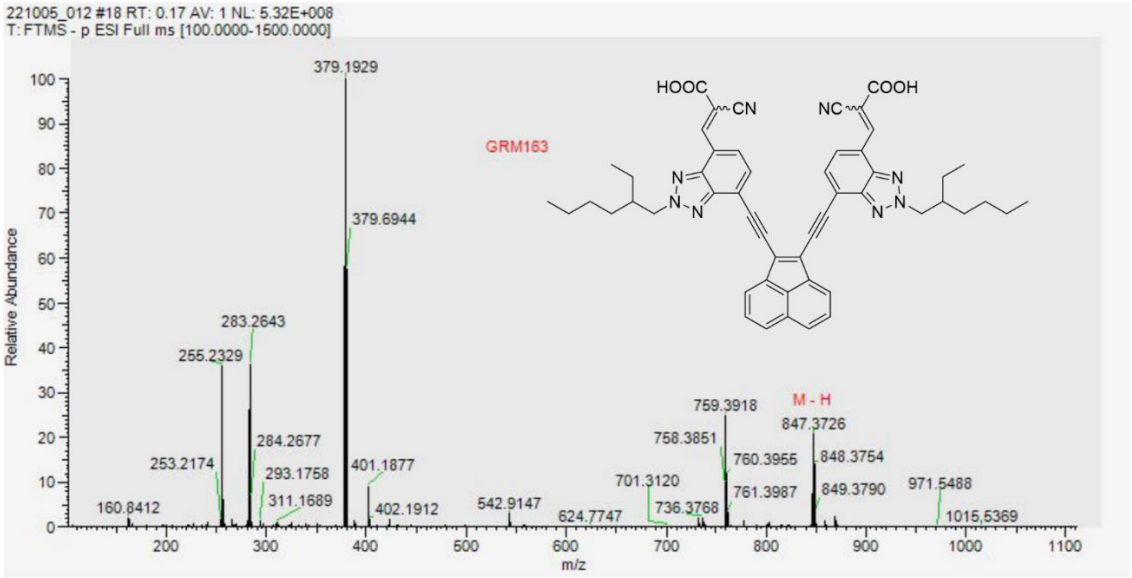


Figure A. 77. HRMS-ESI spectrum of compound 3.37c.

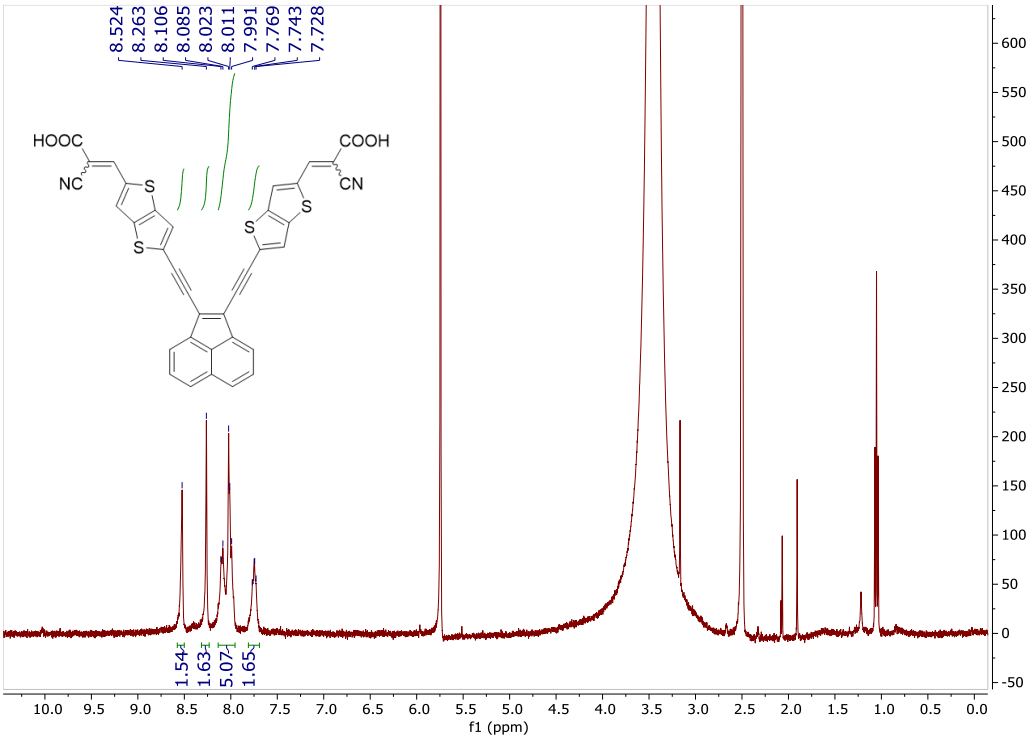


Figure A. 78. $^{1}$H NMR (DMSO-$d_6$, 400 MHz) spectrum of compound 3.37d.

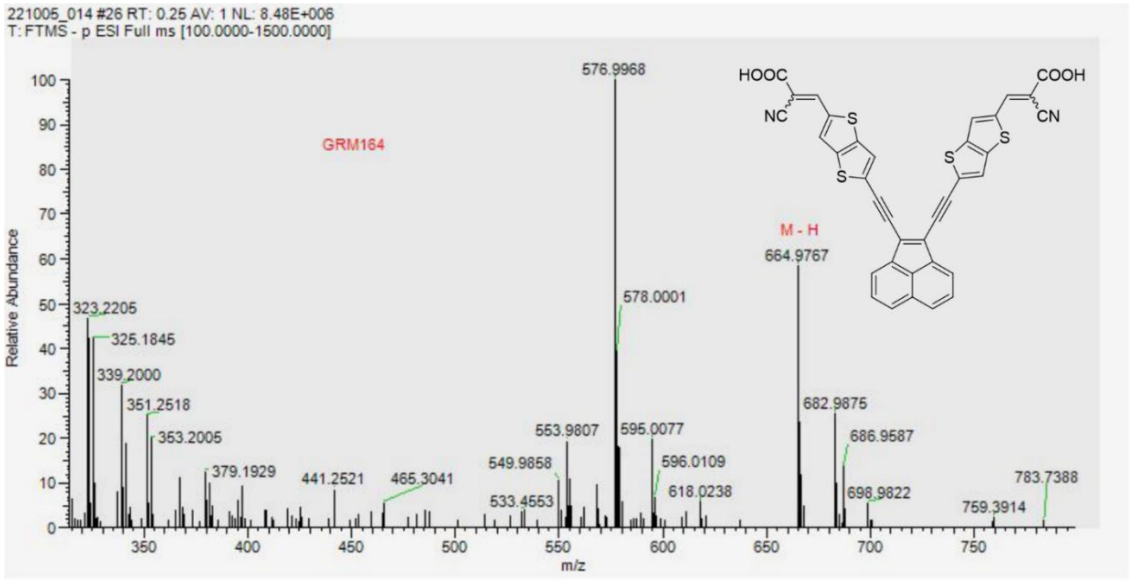


Figure A. 79. HRMS-ESI spectrum of compound 3.37d.

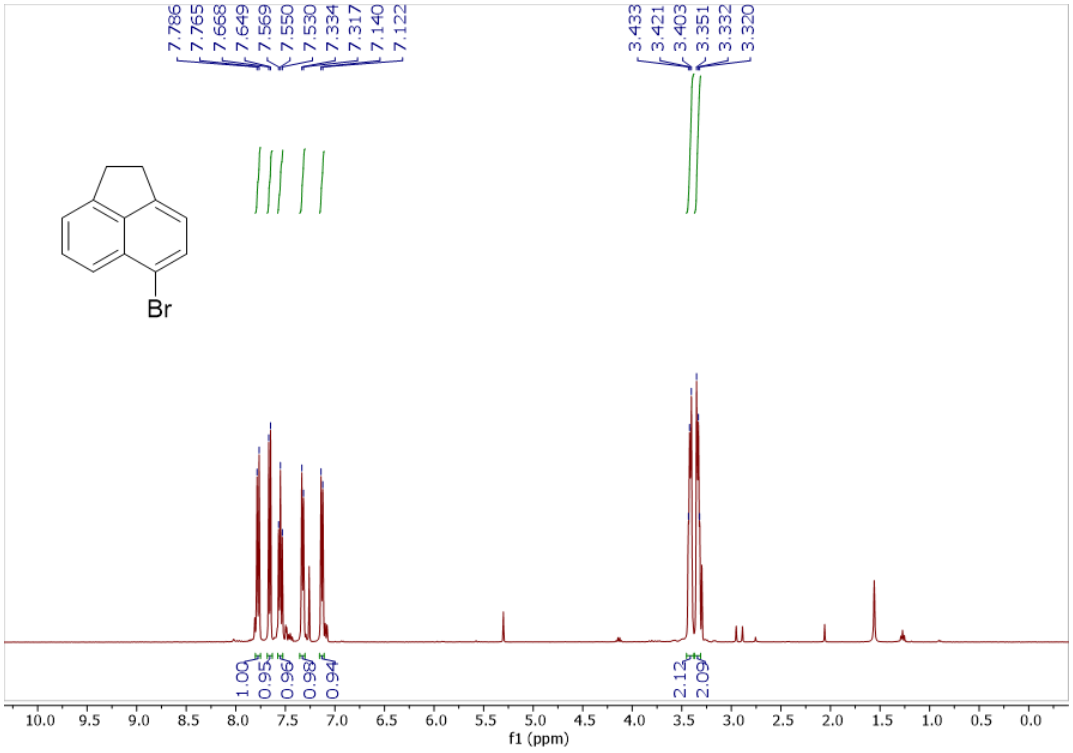


Figure A. 80. $^{1}H$ NMR ($CDCl_3$, 400 MHz) spectrum of compound 3.38

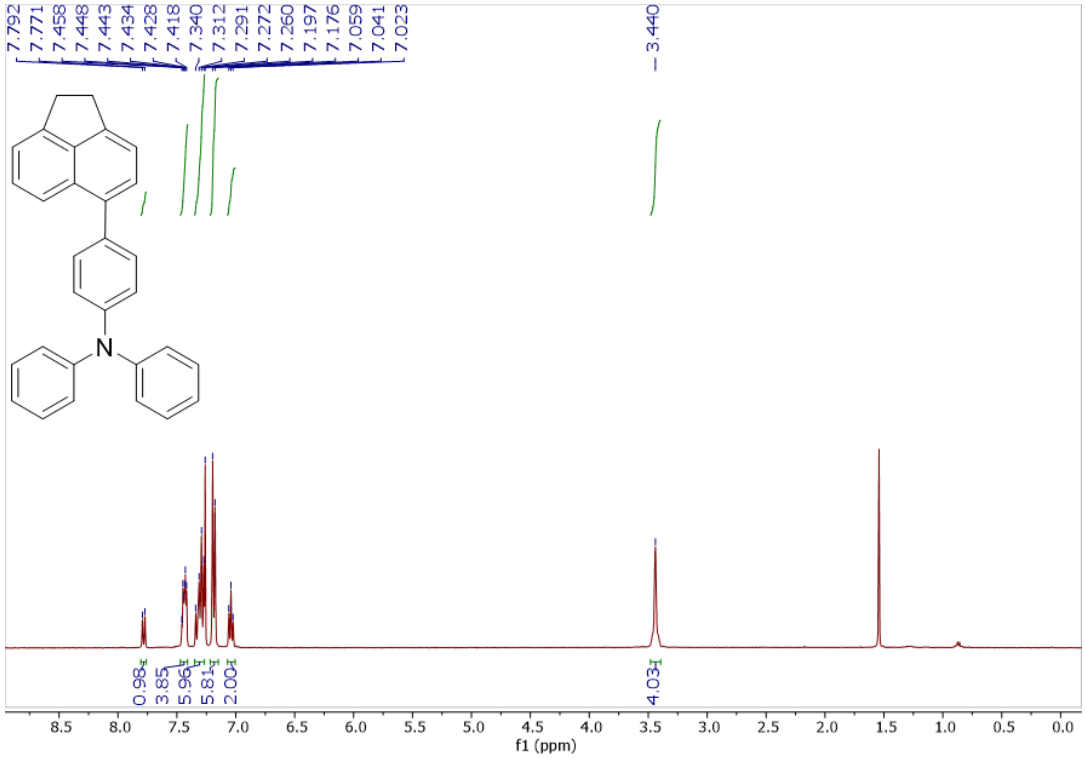


Figure A. 81. $^{1}H$ NMR ($CDCl_3$, 400 MHz) spectrum of compound 3.39

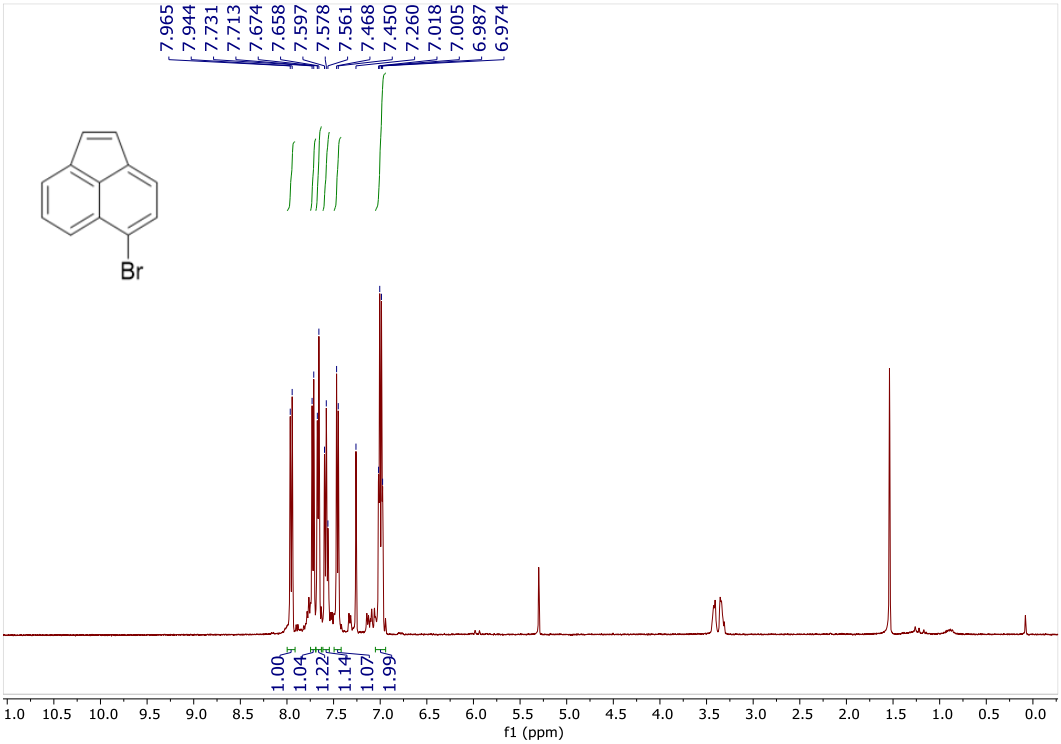


Figure A. 82. $^{1}H$ NMR ($CDCl_3$, 400 MHz) spectrum of compound 3.41

# Chapter 4

## Compound characterization

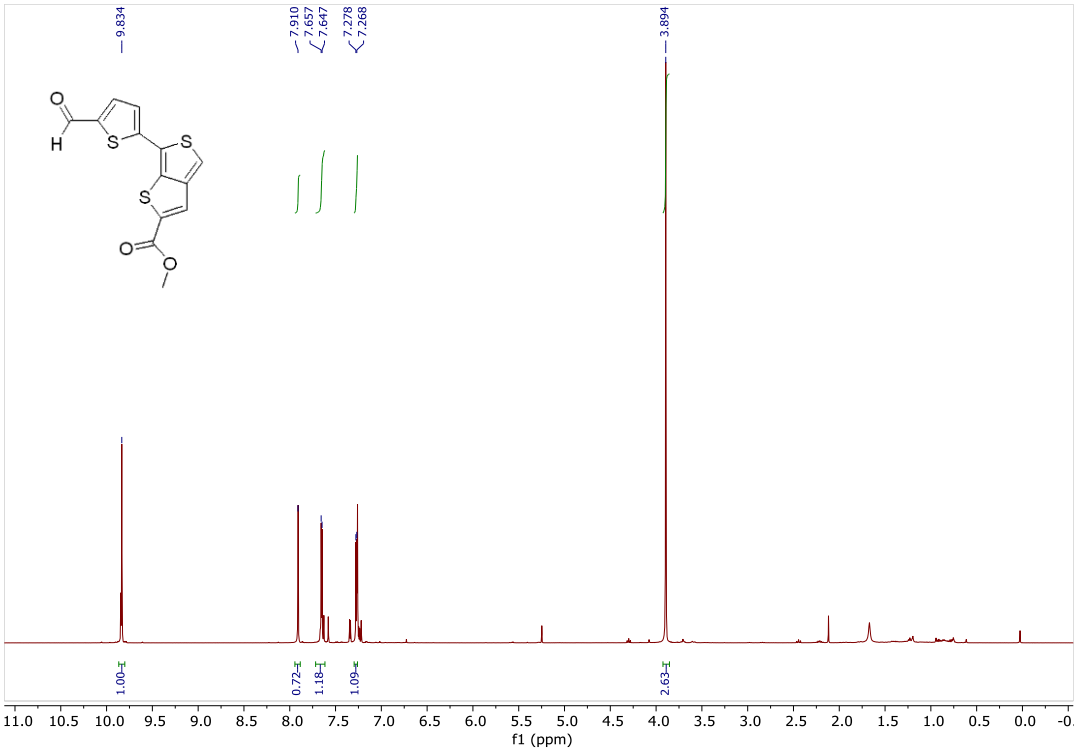


Figure A. 83. $^{1}$H NMR ($CDCl_3$, 400 MHz) spectrum of compound 4.5a

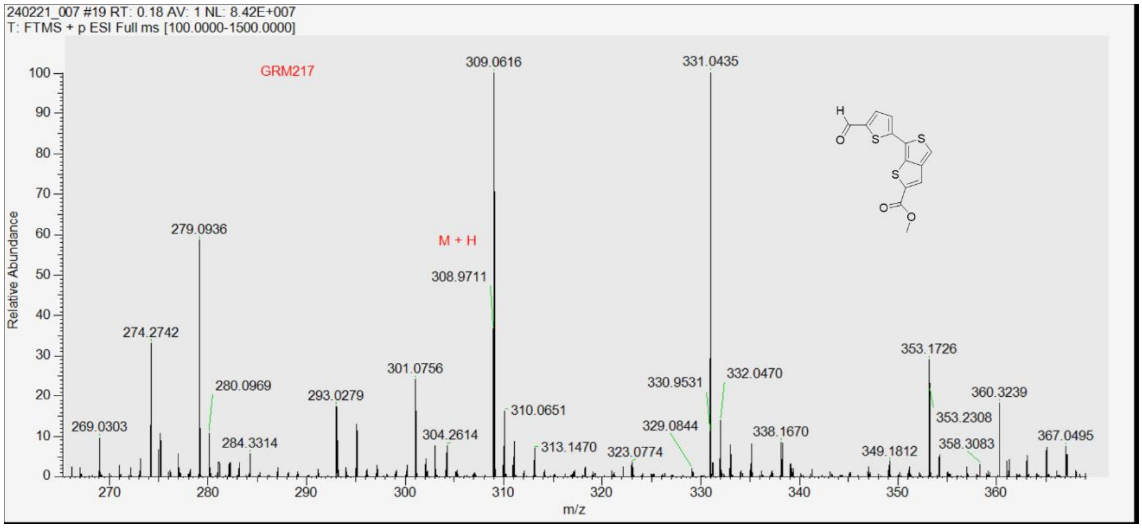


Figure A. 84. HRMS-ESI spectrum of compound 4.5a

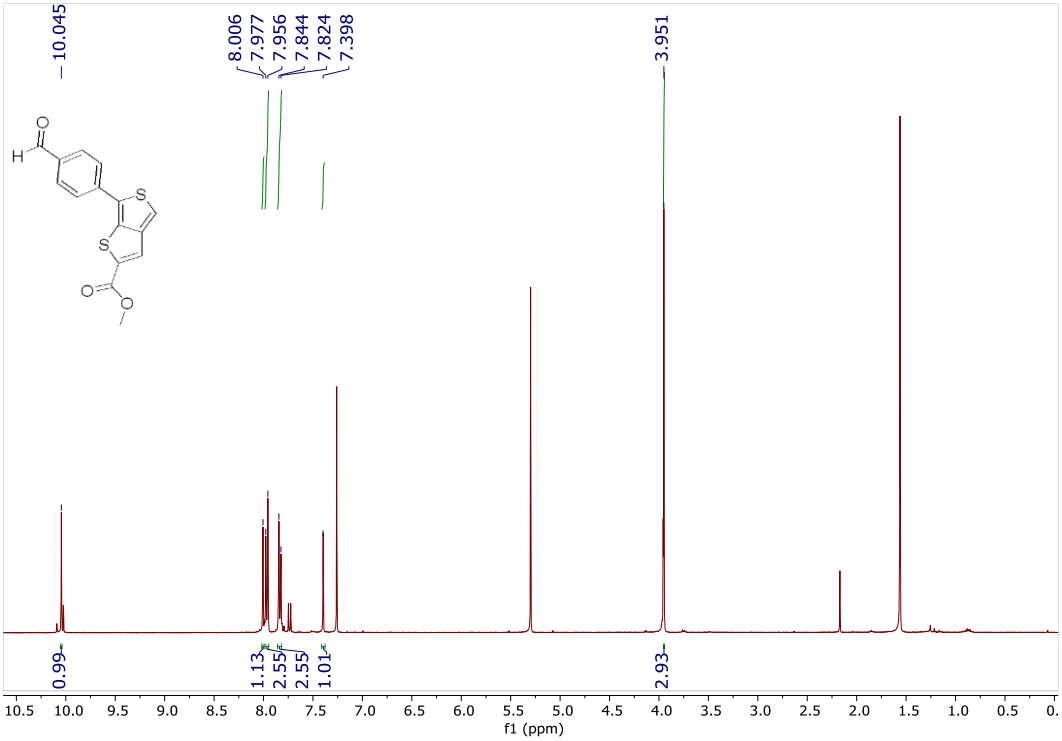


Figure A. 85.[1] H NMR ($CDCl_3$, 400 MHz) spectrum of compound 4.5b.

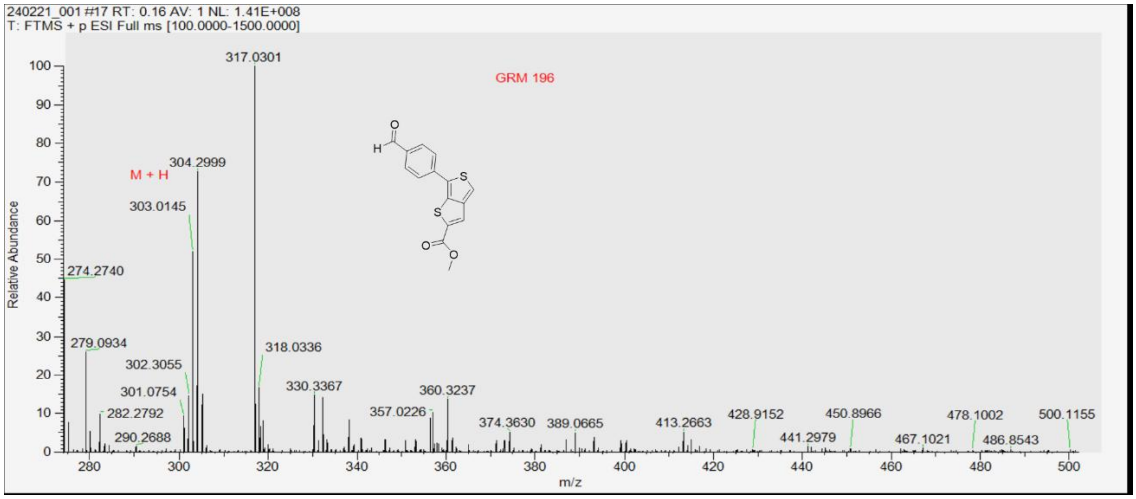


Figure A. 86. HRMS-ESI spectrum of compound 4.5b.

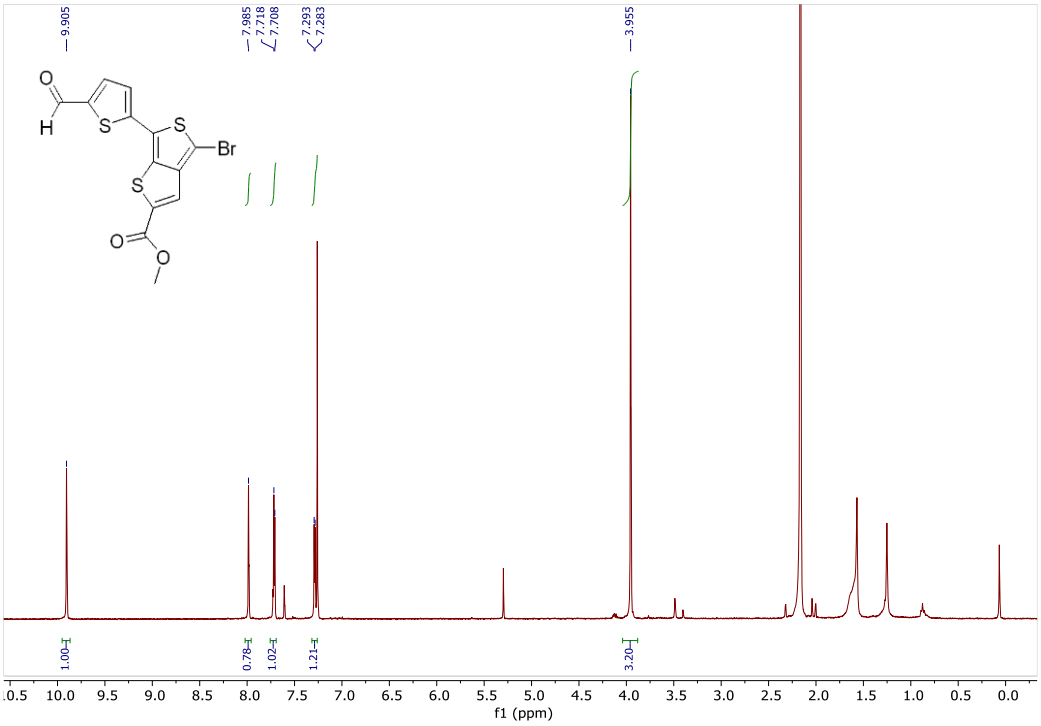


Figure A. 87. $^{1}$H NMR ($CDCl_3$, 400 MHz) spectrum of compound 4.6a.

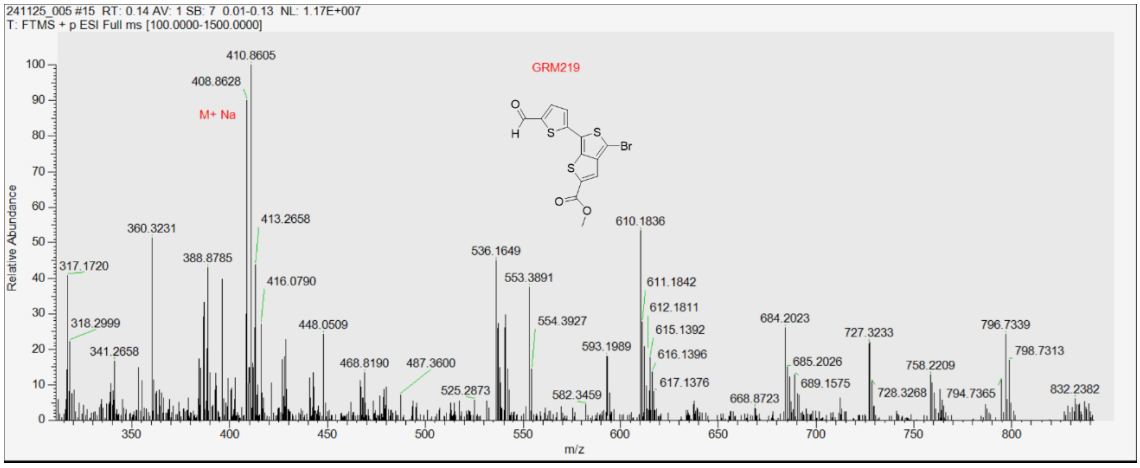


Figure A. 88. HRMS-ESI spectrum of compound 4.6a.

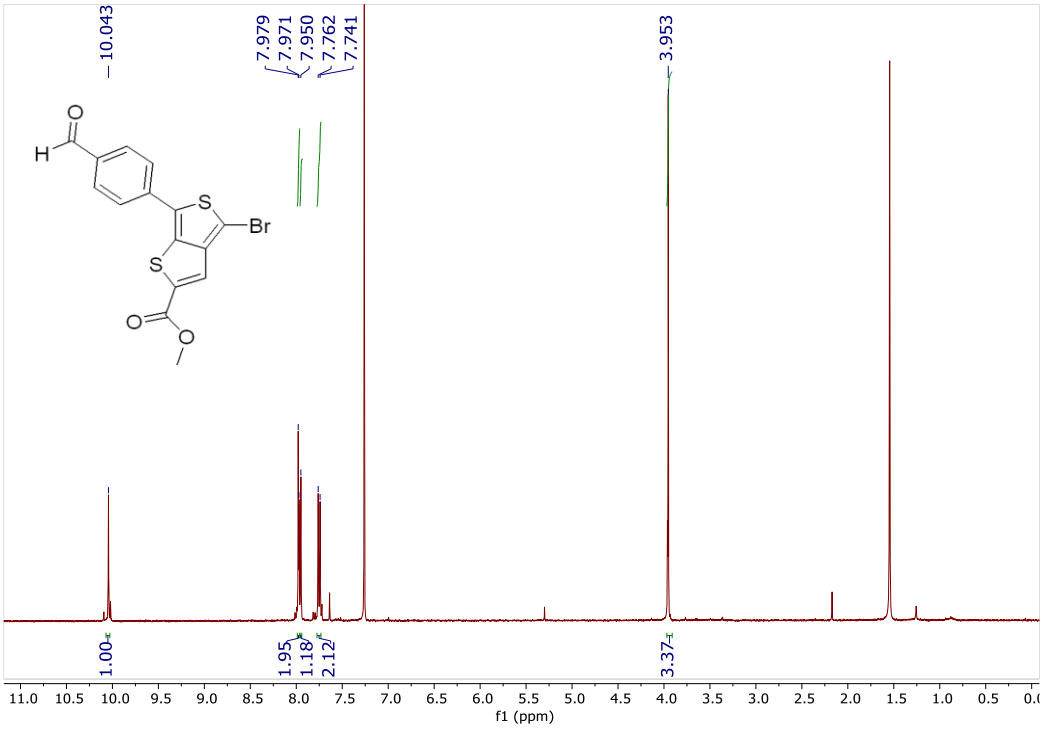


Figure A. 89. $^{1}$H NMR ($CDCl_3$, 400 MHz) spectrum of compound 4.6b.

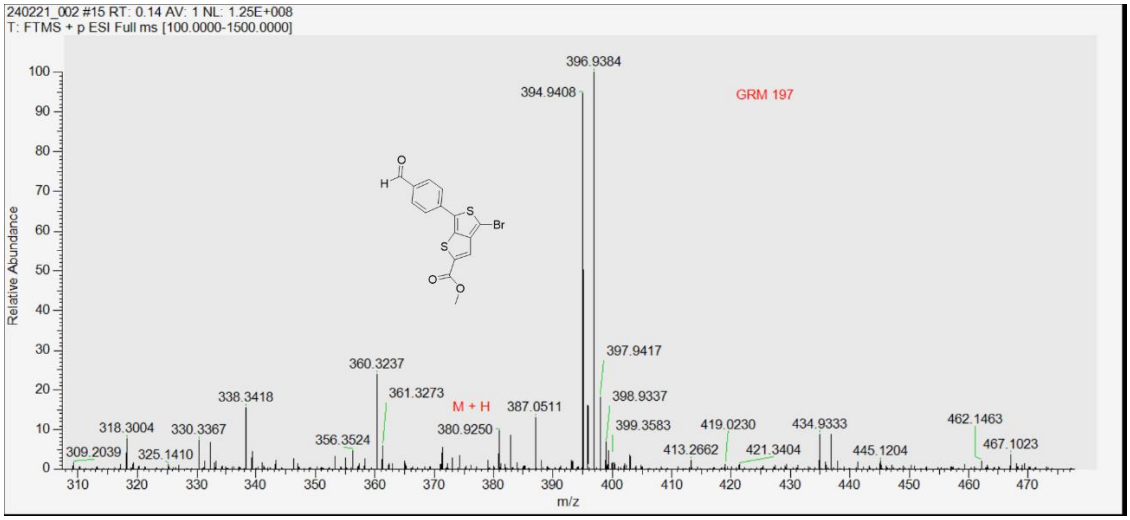


Figure A. 90. HRMS-ESI spectrum of compound 4.6b.

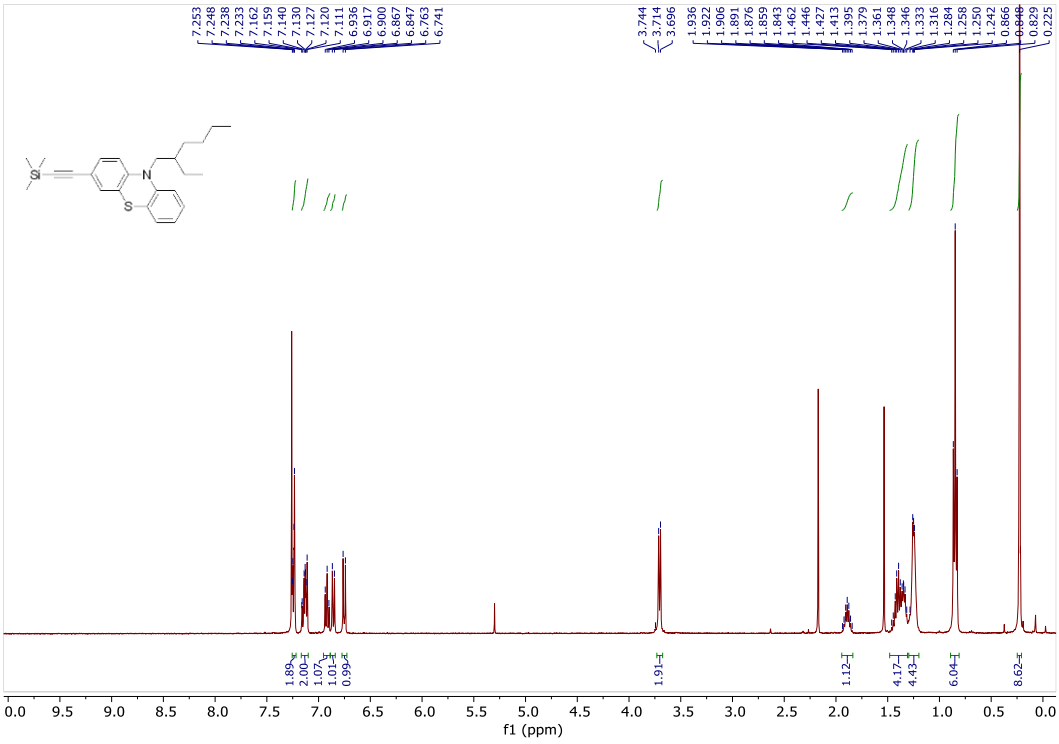


Figure A. 91. $^{1}$H NMR ($CDCl_3$, 400 MHz) spectrum of compound 4.15

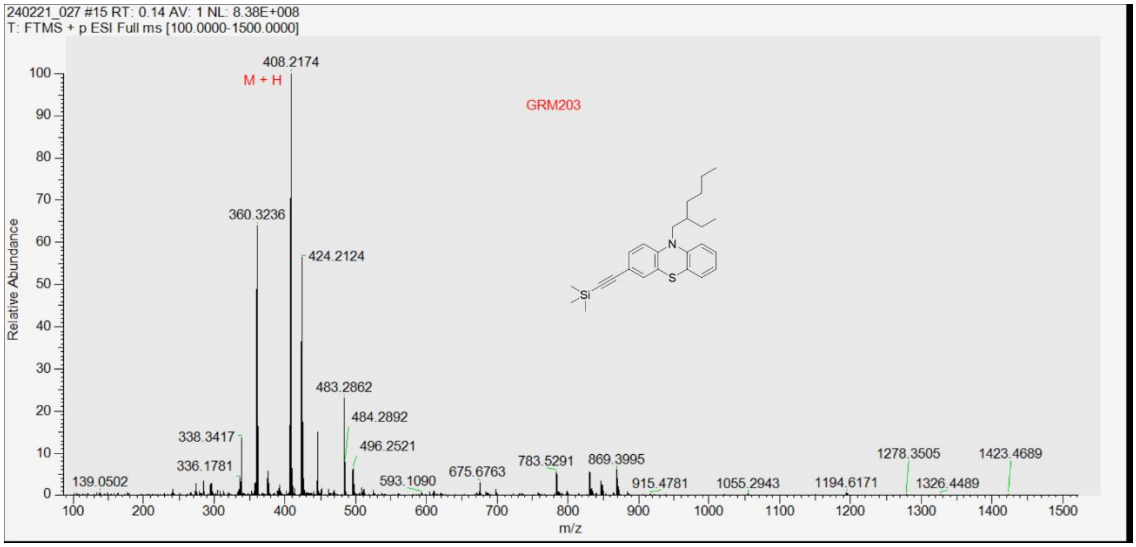


Figure A. 92. HRMS-ESI spectrum of compound 4.15.

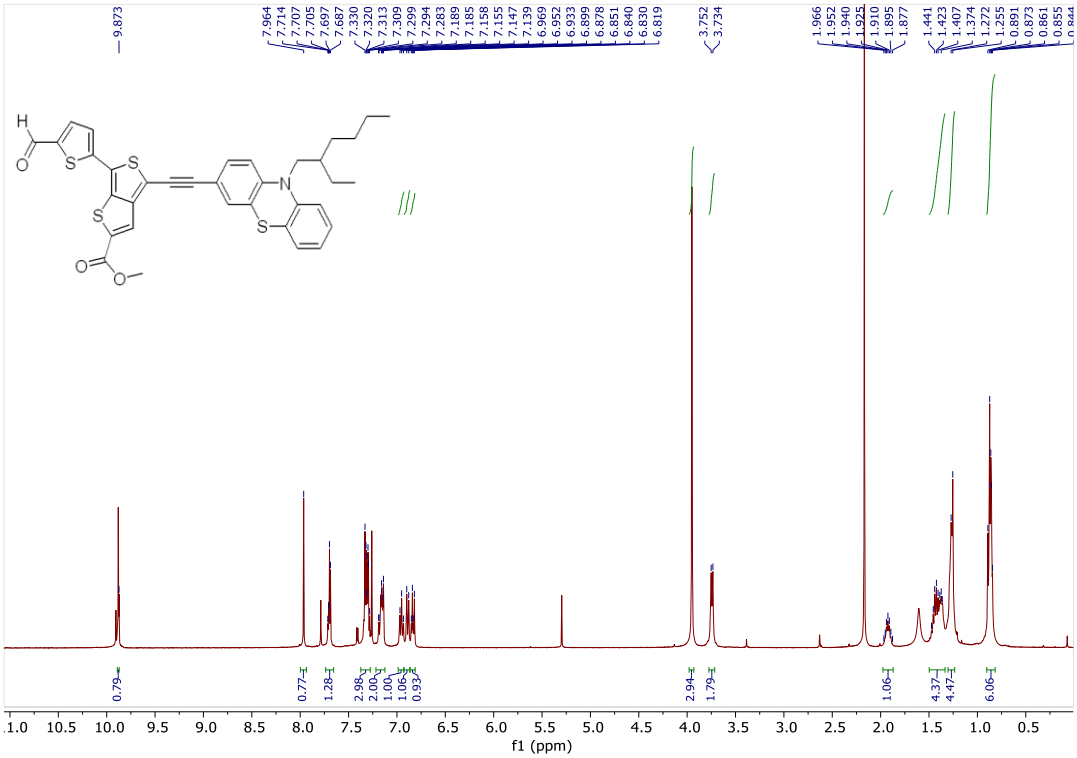


Figure A. 93. $^{1}$H NMR ($CDCl_3$, 400 MHz) spectrum of compound 4.21a.

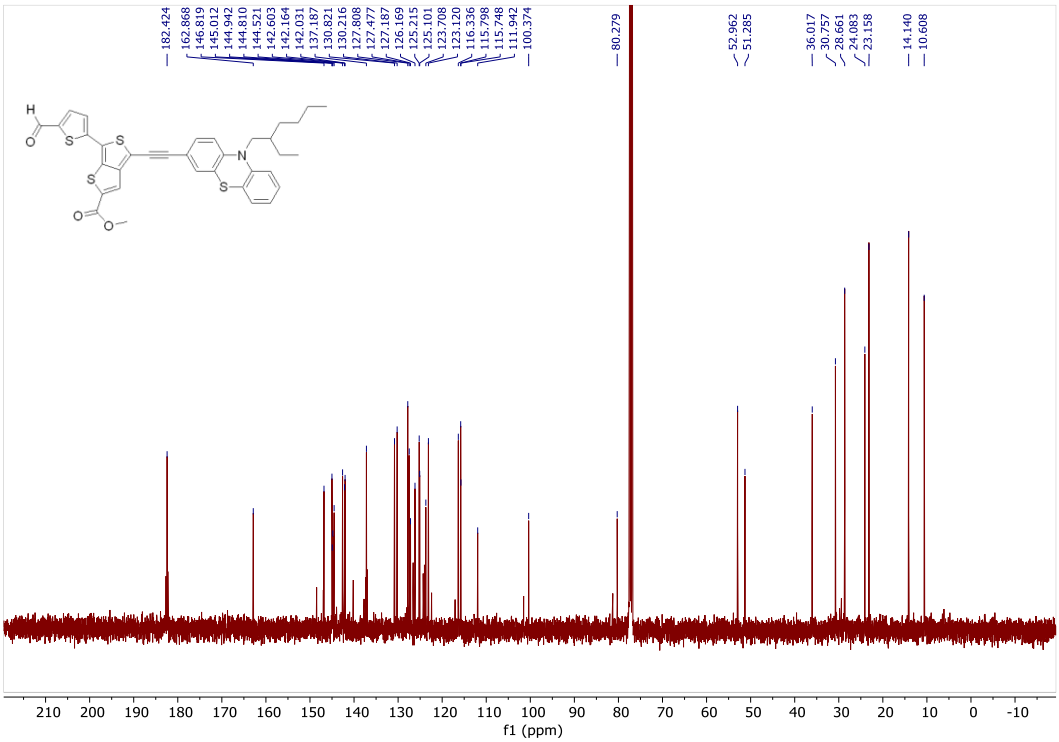


Figure A. 94. $^{13}C$ NMR ($CDCl_3$, 101 MHz) spectrum of compound 4.21a.

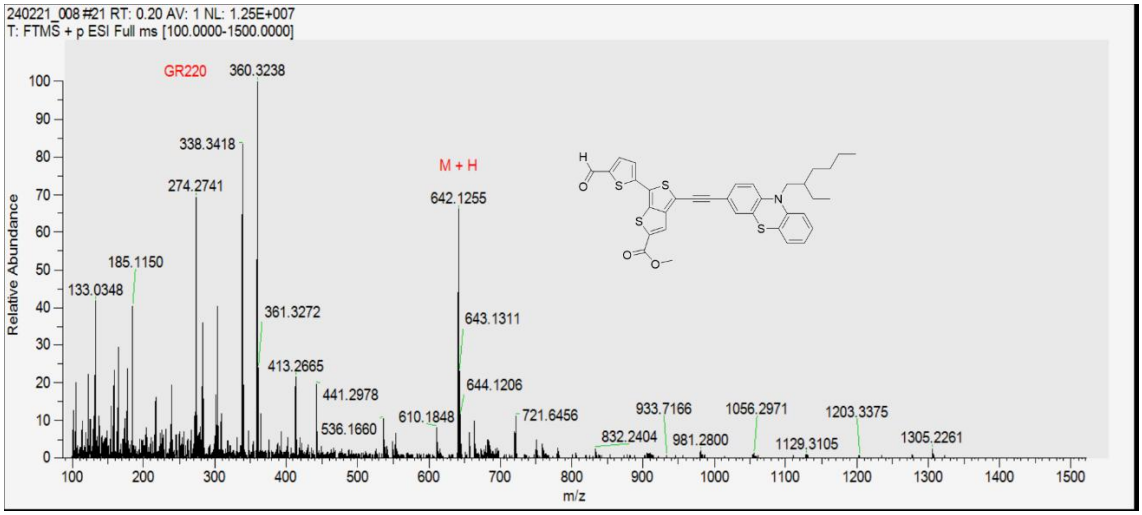


Figure A. 95. HRMS-ESI spectrum of compound 4.21a

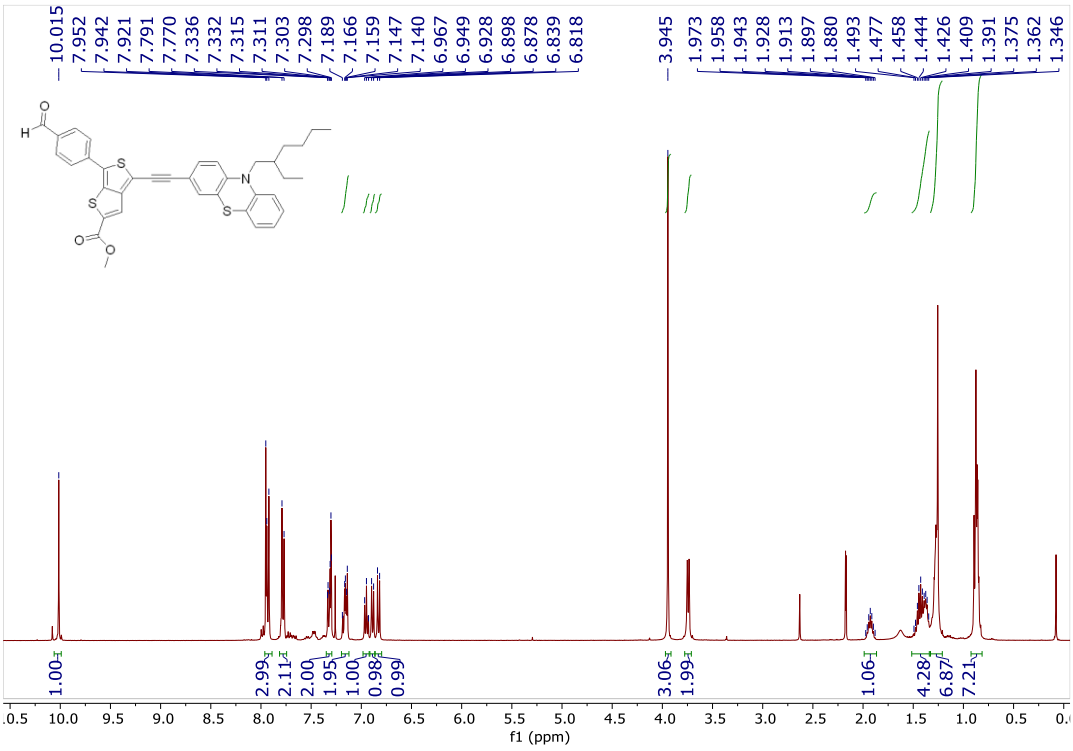


Figure A. 96. . [1] H NMR ($CDCl_3$, 400 MHz) spectrum of compound 4.21b.

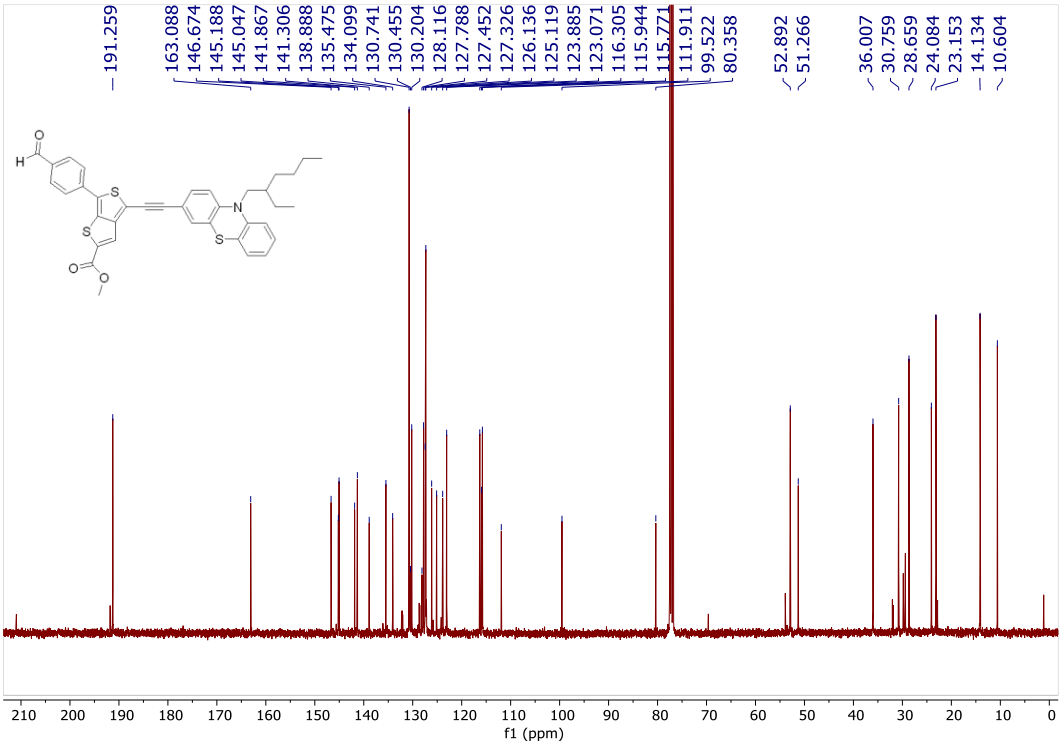


Figure A. 97. [13]C NMR (CDCl3, 101 MHz) spectrum of compound 4.21b.

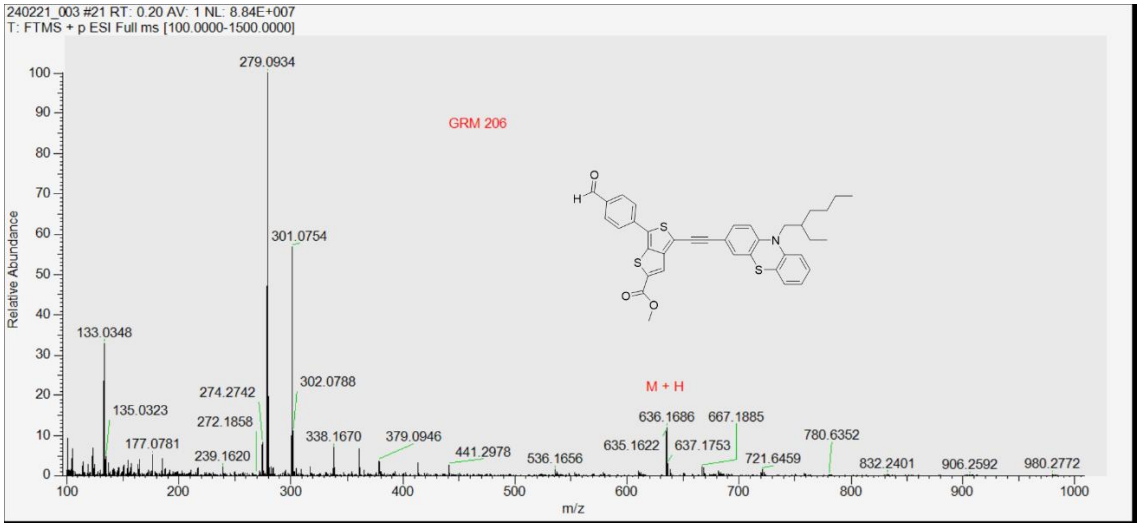


Figure A. 98. HRMS-ESI spectrum of compound 4.21b.

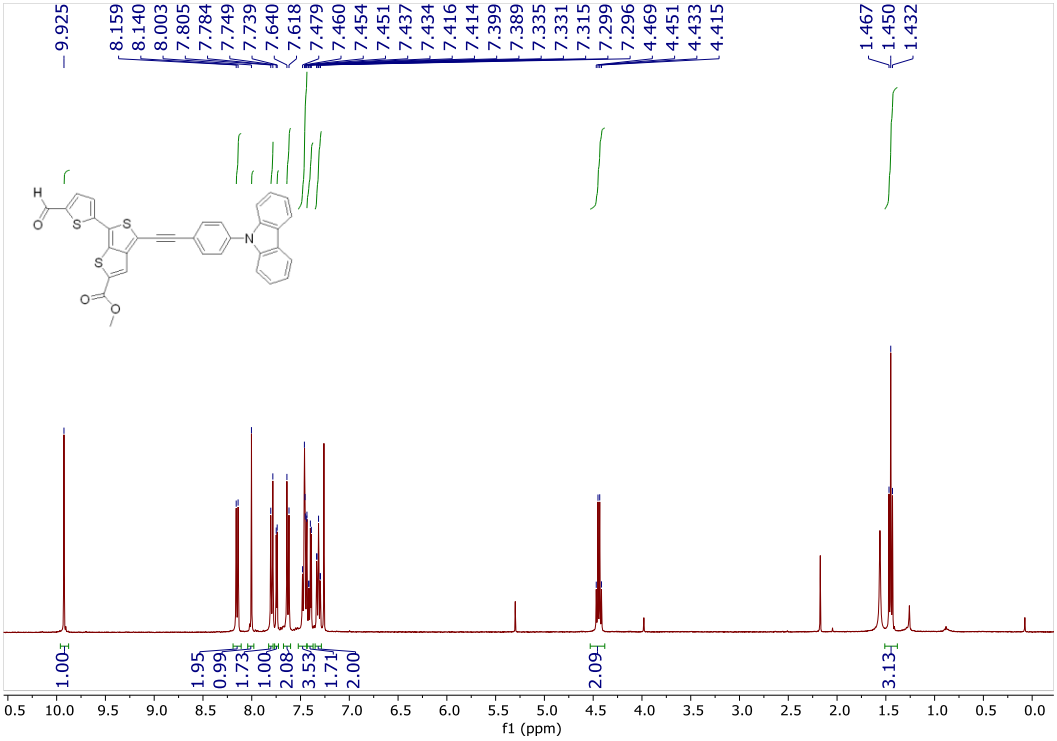


Figure A. 99. $^{1}$H NMR ($CDCl_3$, 400 MHz) spectrum of compound 4.21c.

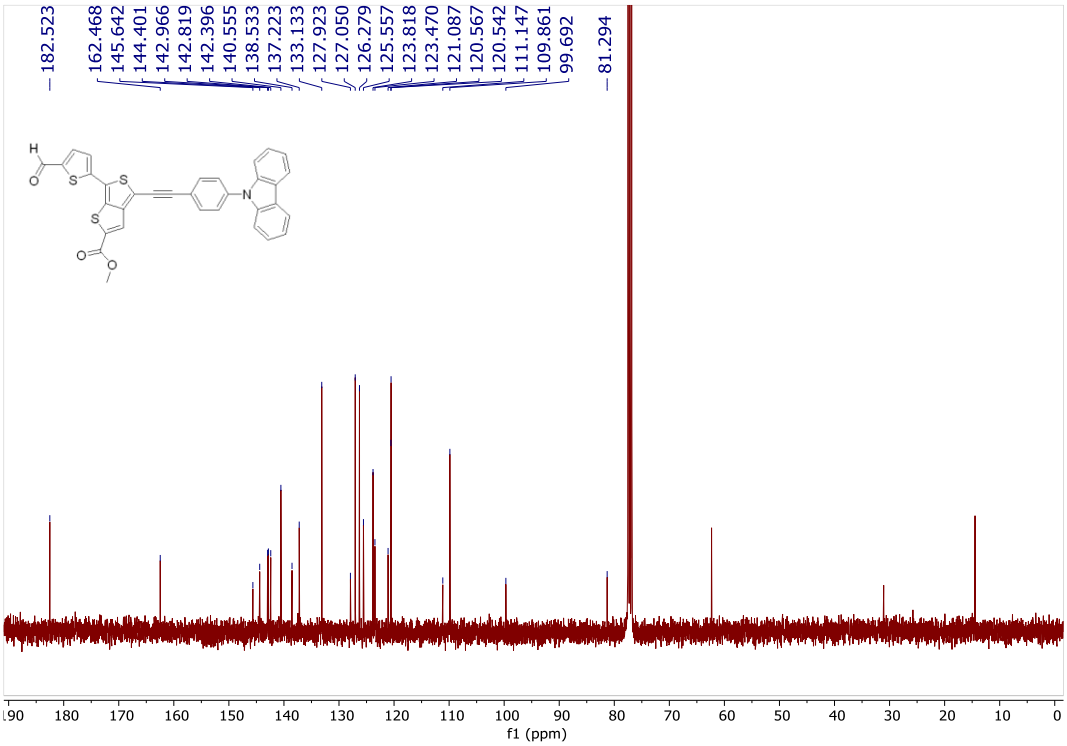


Figure A. 100. $^{13}C$ NMR (CDCl3, 101 MHz) spectrum of compound 4.21c.

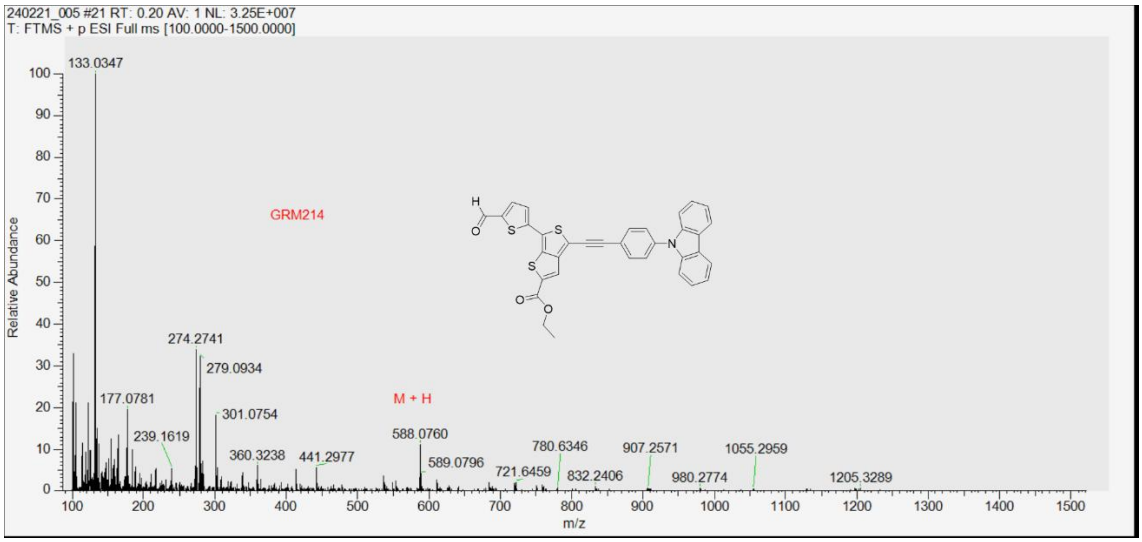


Figure A. 101. HRMS-ESI spectrum of compound 4.21c.

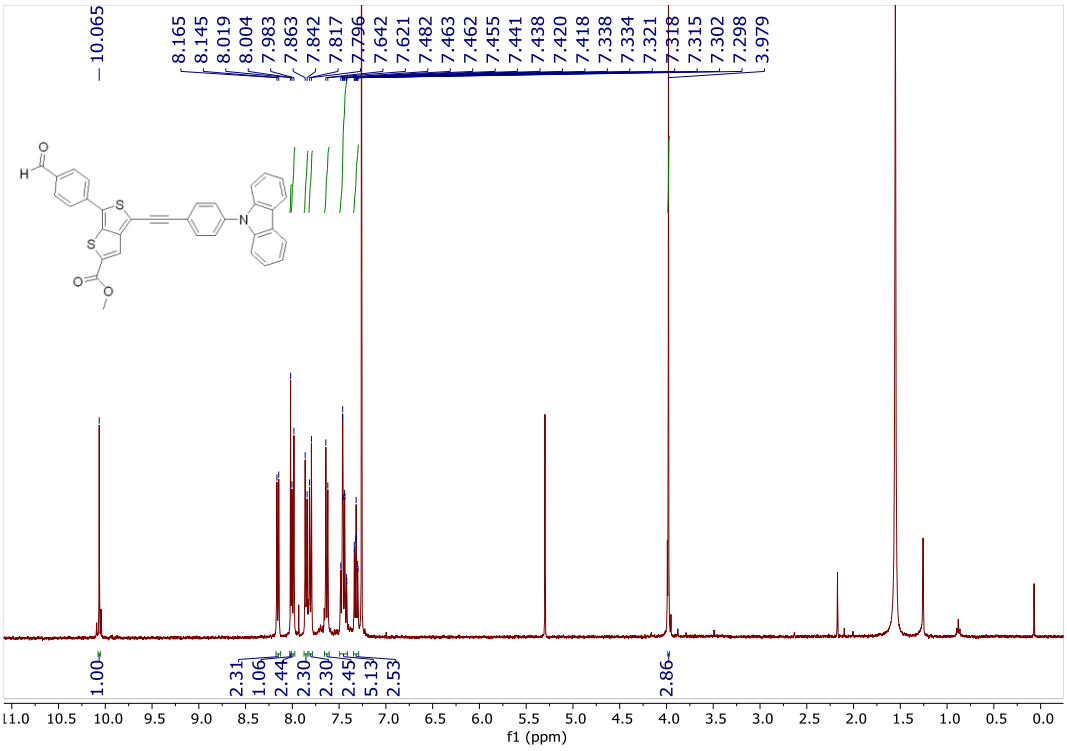


Figure A. 102. $^{1}$H NMR ($CDCl_3$, 400 MHz) spectrum of compound 4.21d.

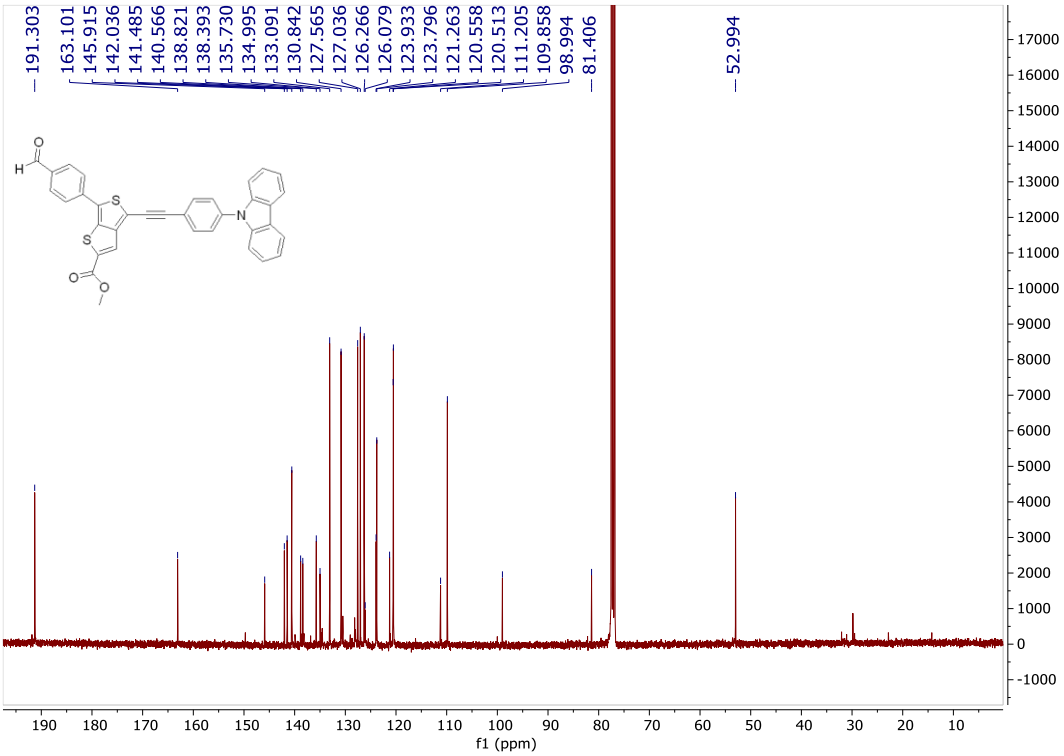


Figure A. 103. $^{13}$C NMR (CDCl3, 101 MHz) spectrum of compound 4.21d

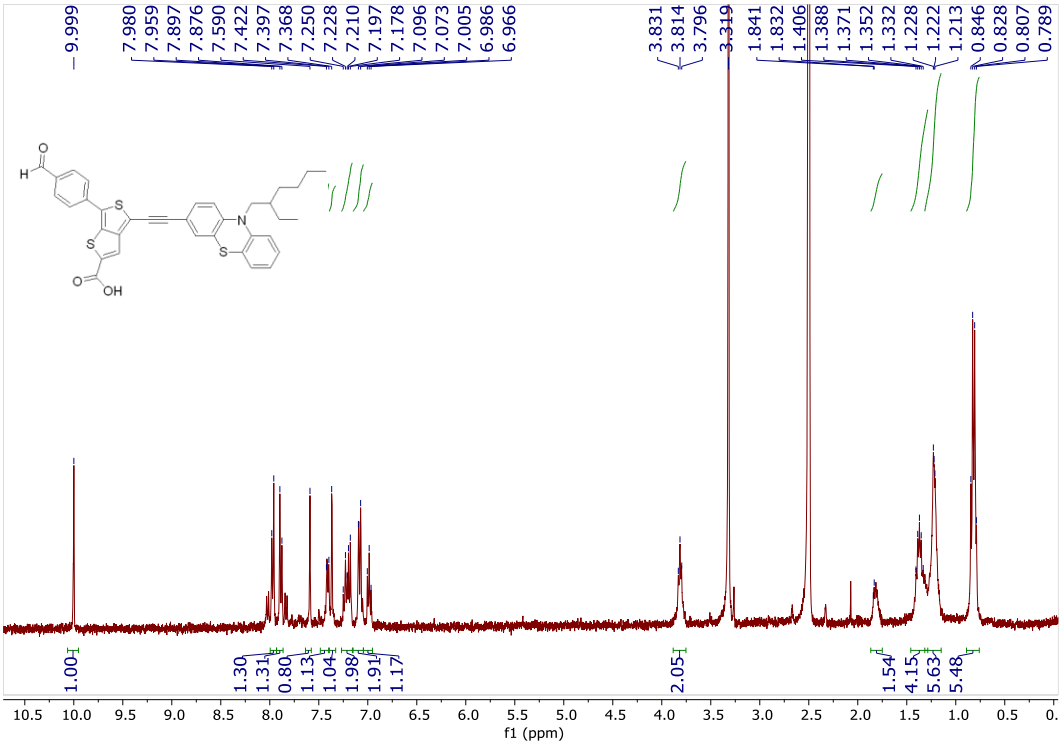


Figure A. 104. $^{1}$H NMR (DMSO-$d_6$, 400 MHz) spectrum of compound 4.22b.

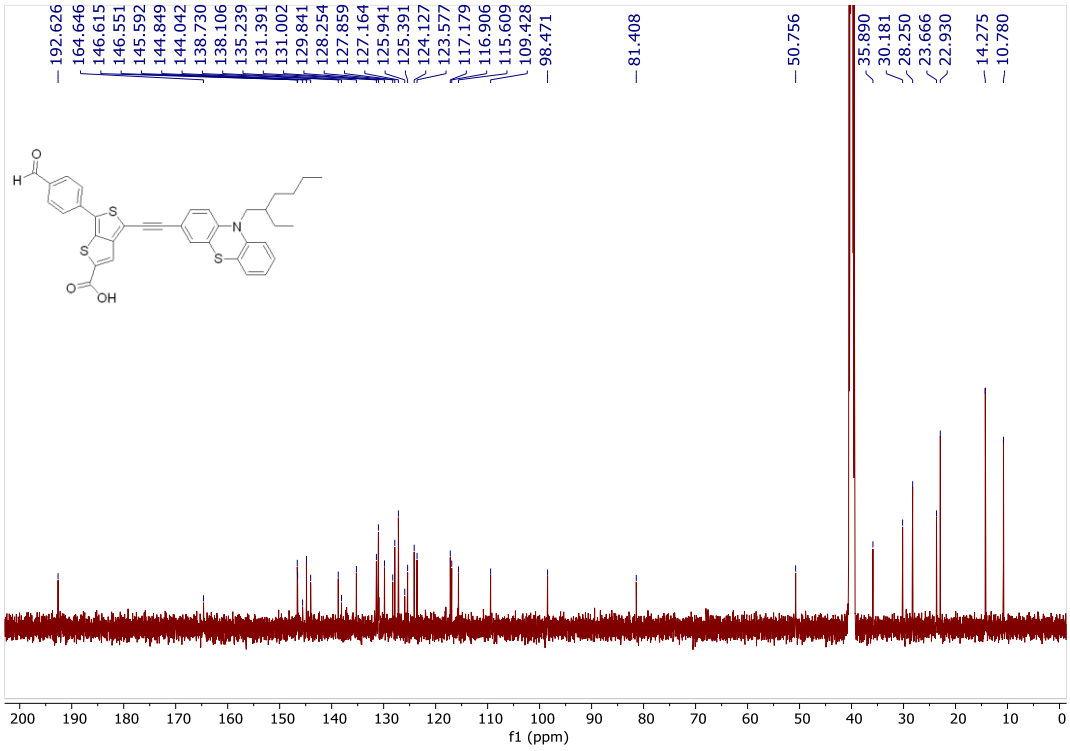


Figure A. 105. $^{13}$C NMR (DMSO-$d_6$, 126 MHz) spectrum of compound 4.22b.

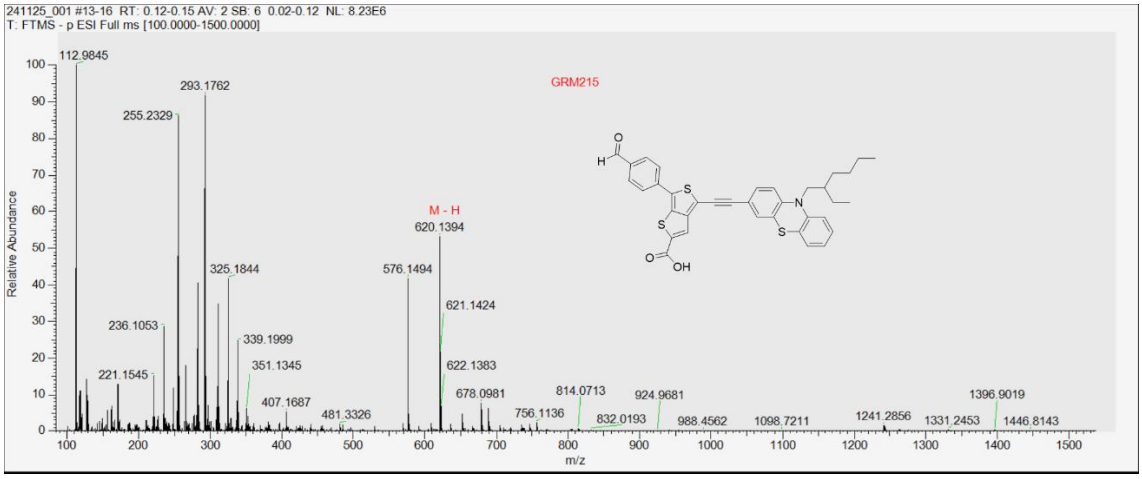


Figure A. 106. HRMS-ESI spectrum of compound 4.22b.

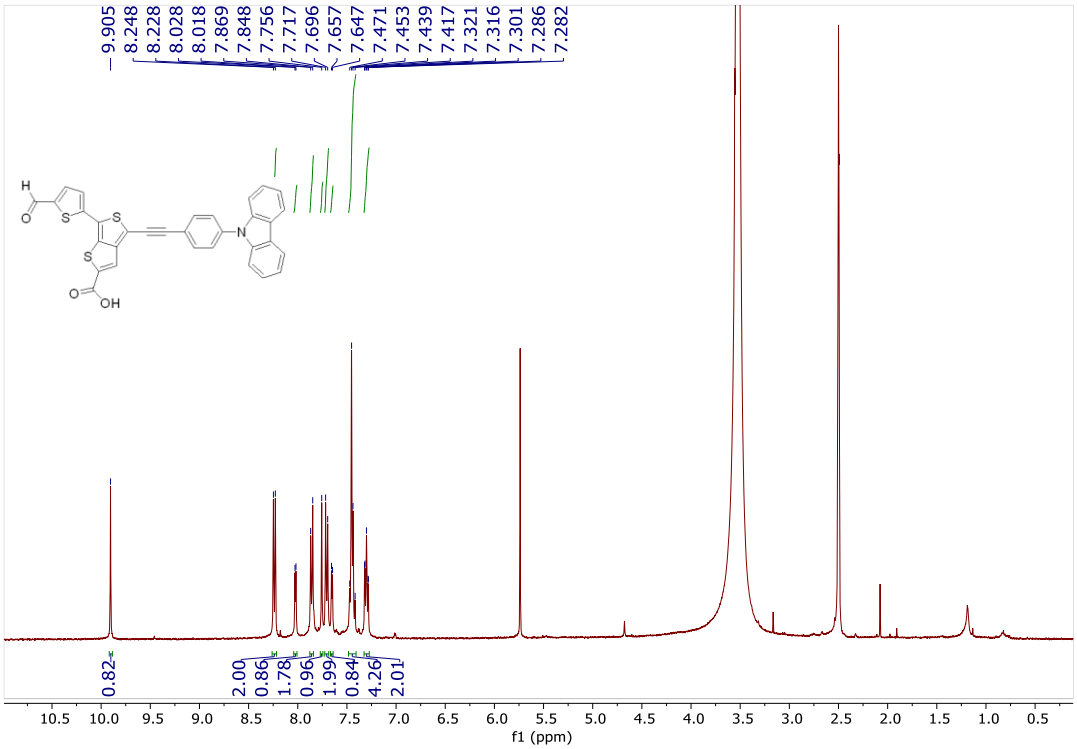


Figure A. 107. [1] H NMR (DMSO-$d_6$, 400 MHz) spectrum of compound 4.22c.

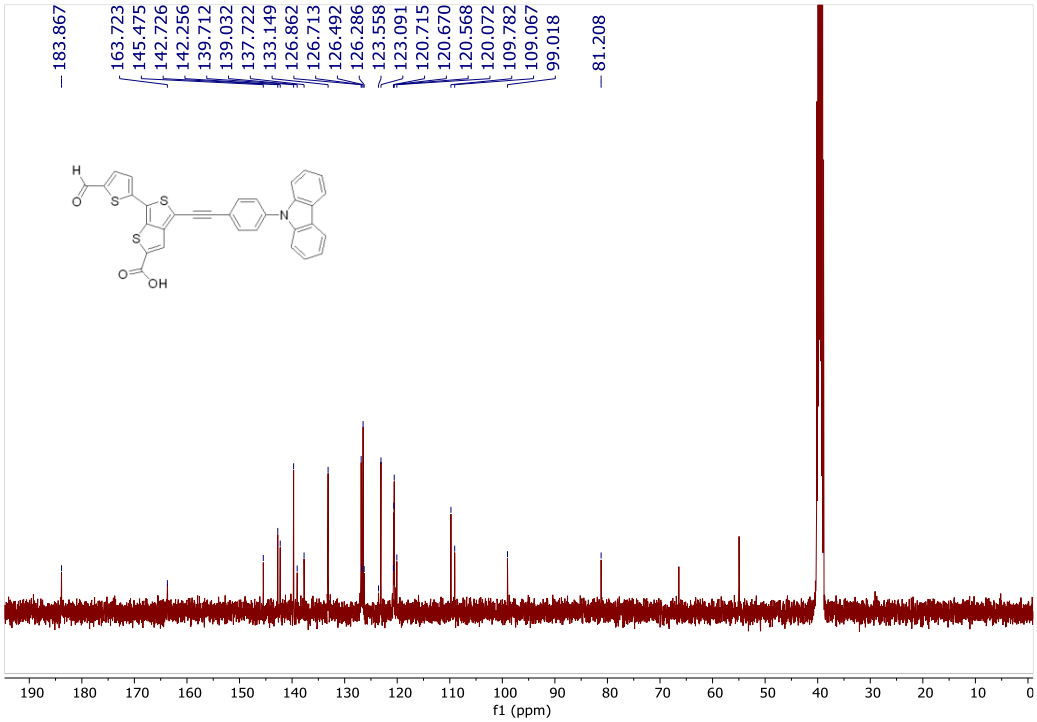


Figure A. 108. [13]C NMR (DMSO-$d_6$, 101 MHz) spectrum of compound 4.22c.

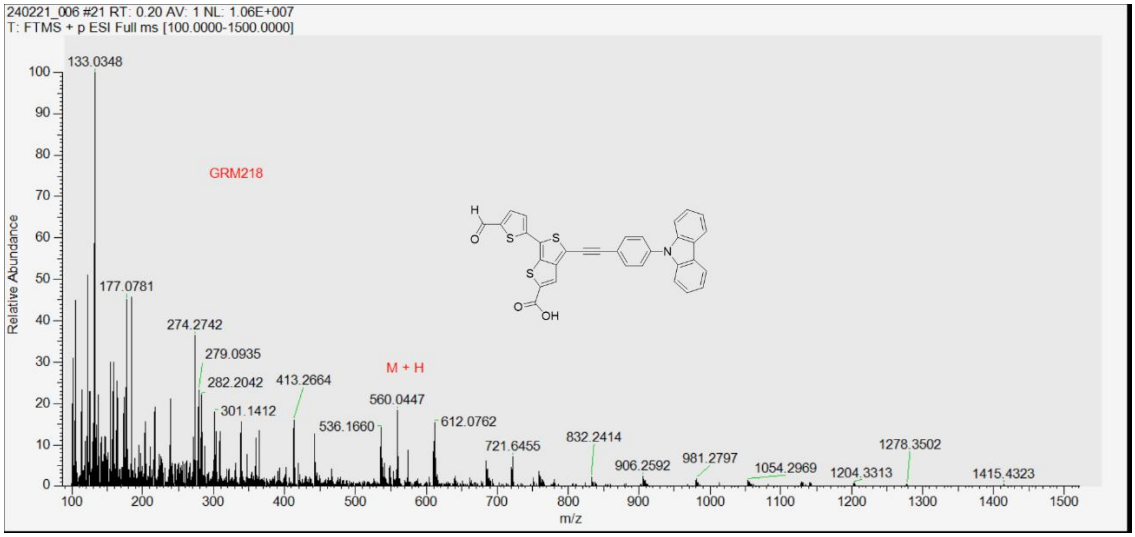


Figure A. 109. HRMS-ESI spectrum of compound 4.22c.

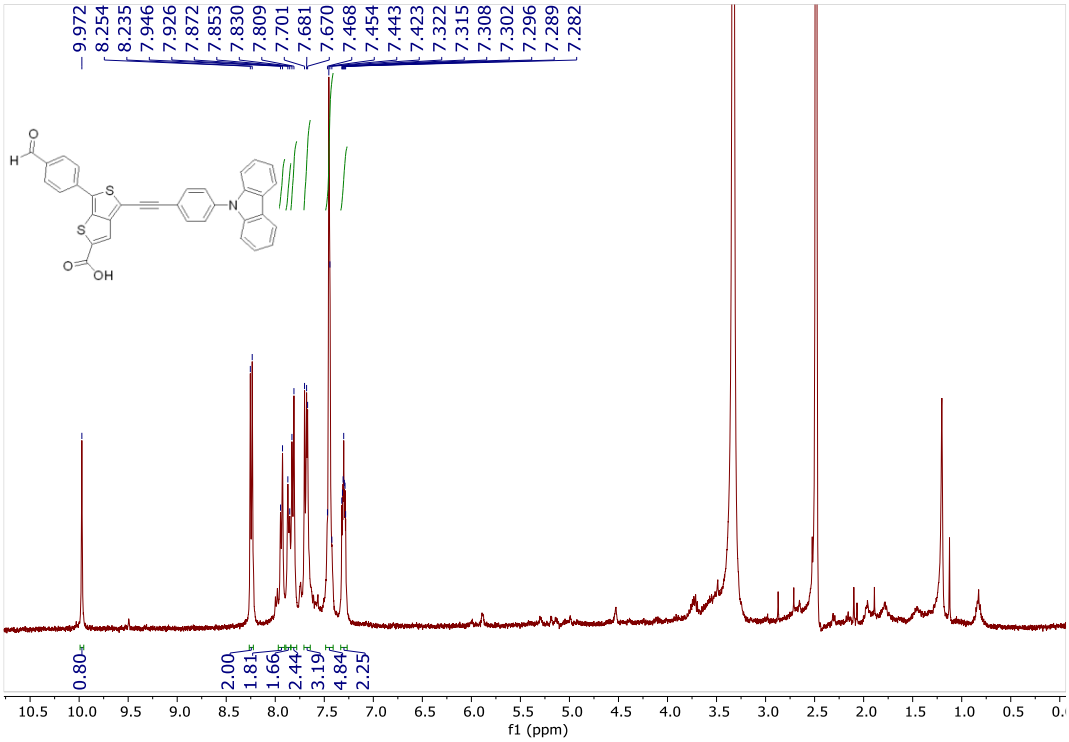


Figure A. 110. $^{1}$H NMR (DMSO-$d_6$, 400 MHz) spectrum of compound 4.22d.

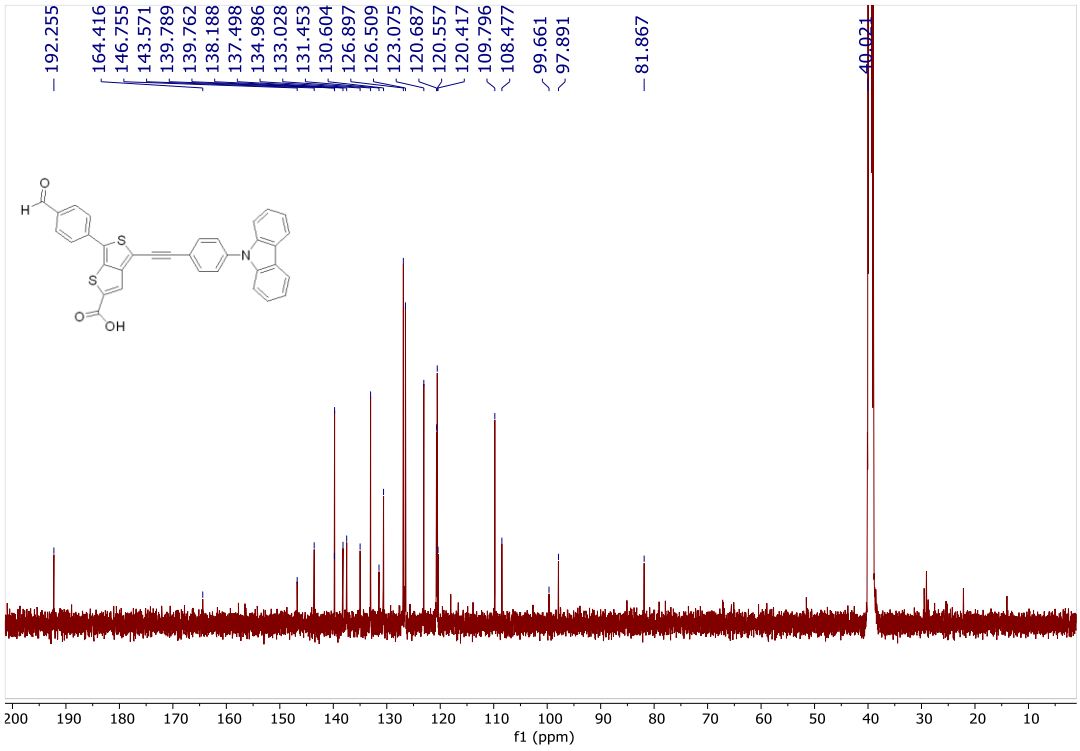


Figure A. 111. $^{13}$C NMR (DMSO-$d_6$, 126 MHz) spectrum of compound 4.22d

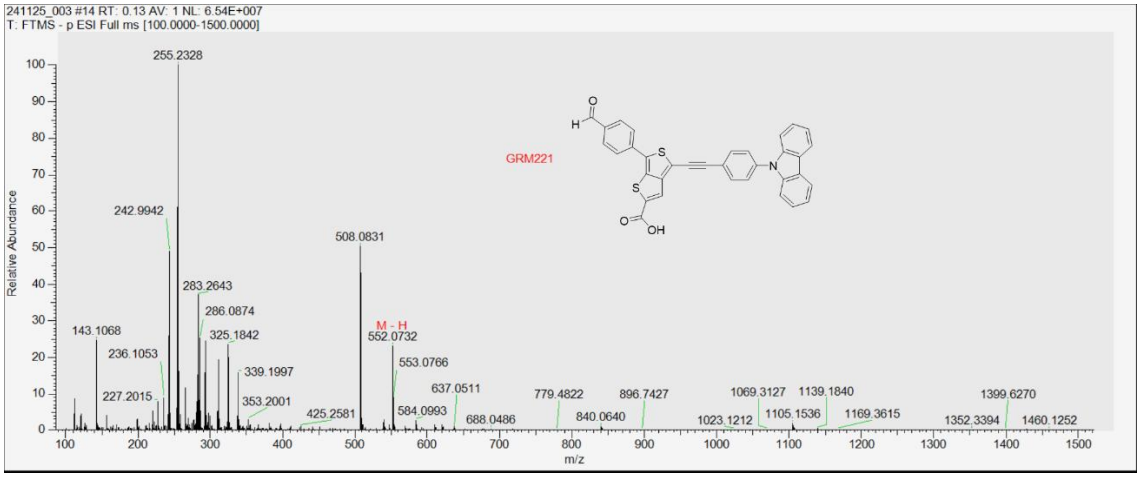


Figure A. 112. HRMS-ESI spectrum of compound 4.22d.

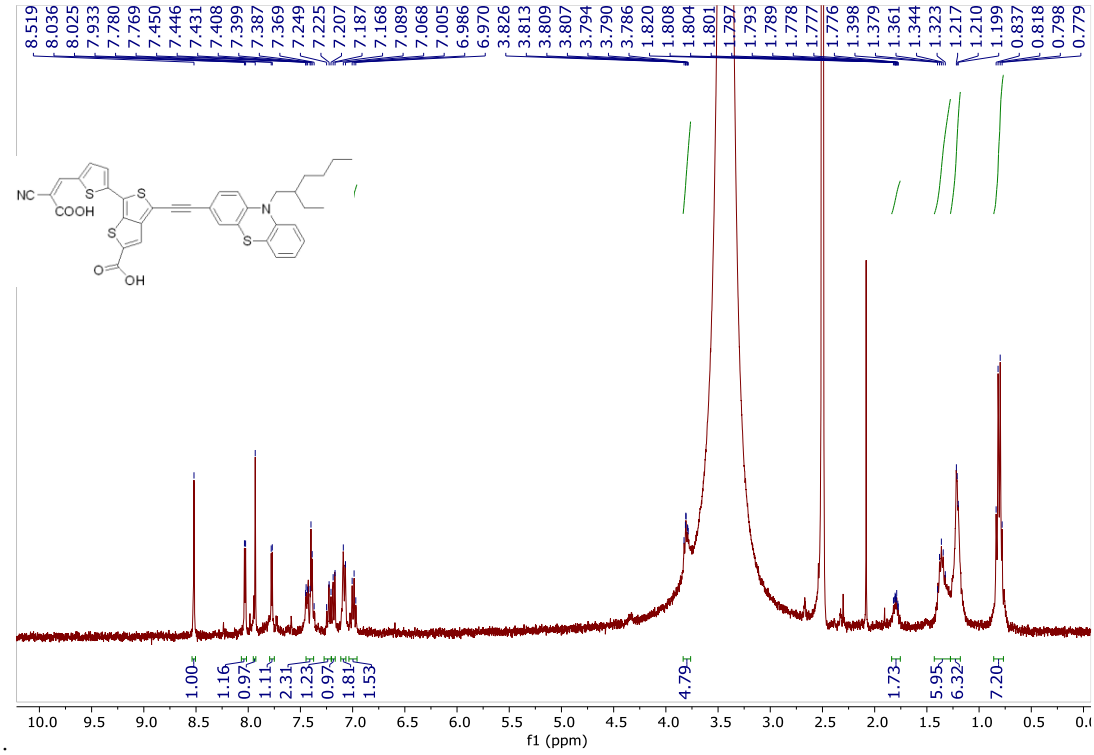


Figure A. 113. $^{1}$H NMR (DMSO-$d_6$, 400 MHz) spectrum of compound 4.23a.

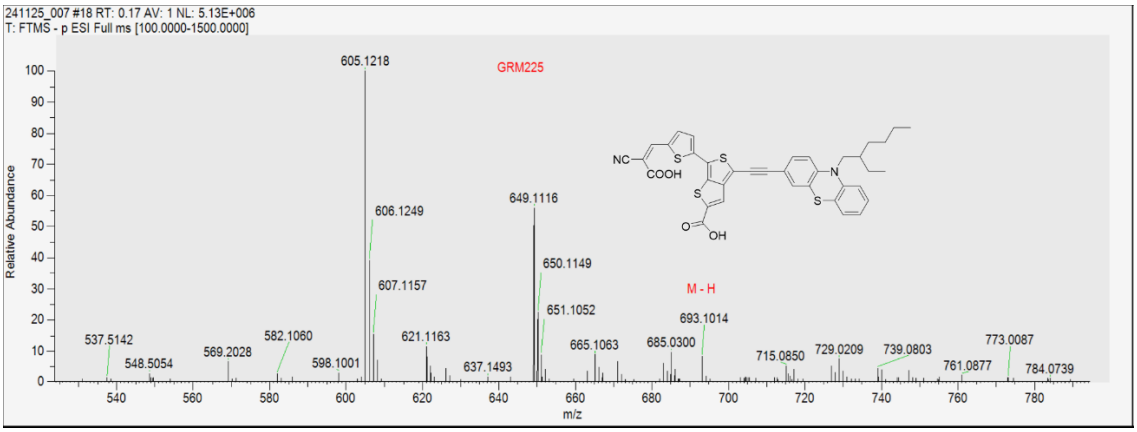


Figure A. 114. HRMS-ESI spectrum of compound 4.23a.

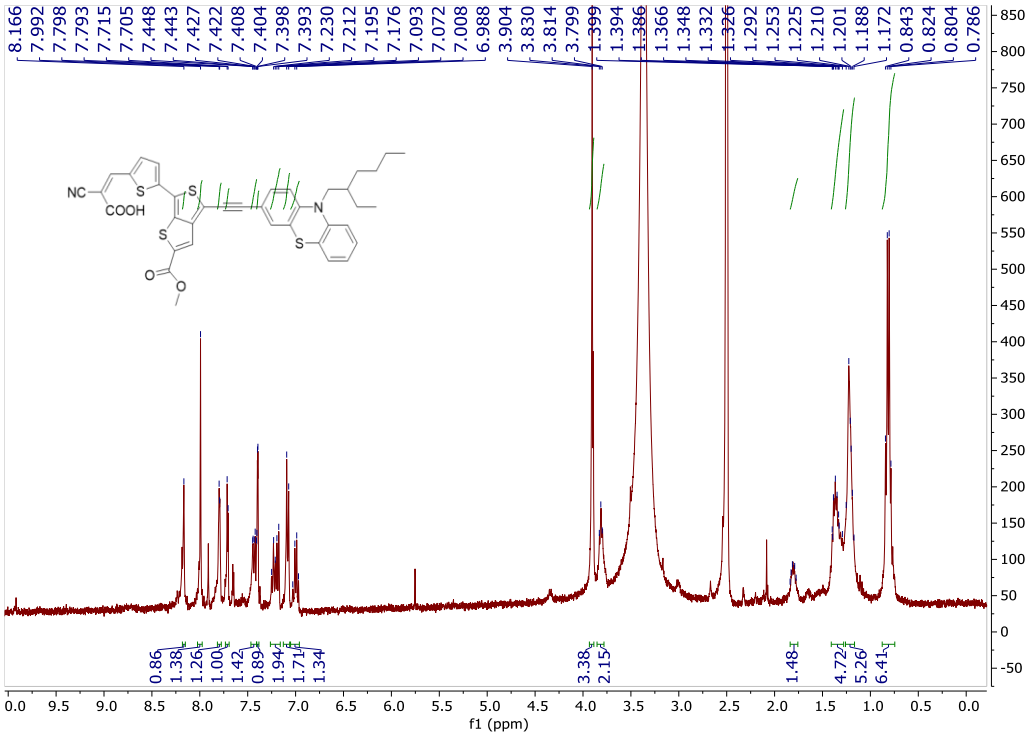


Figure A. 115. $^{1}$H NMR (DMSO-$d_6$, 400 MHz) spectrum of compound 4.22a.

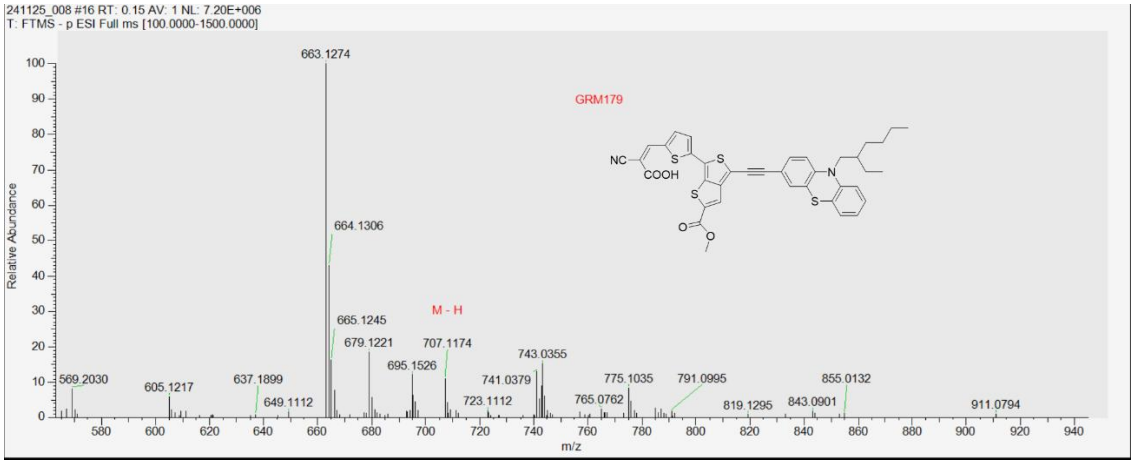


Figure A. 116. HRMS-ESI spectrum of compound 4.22a.

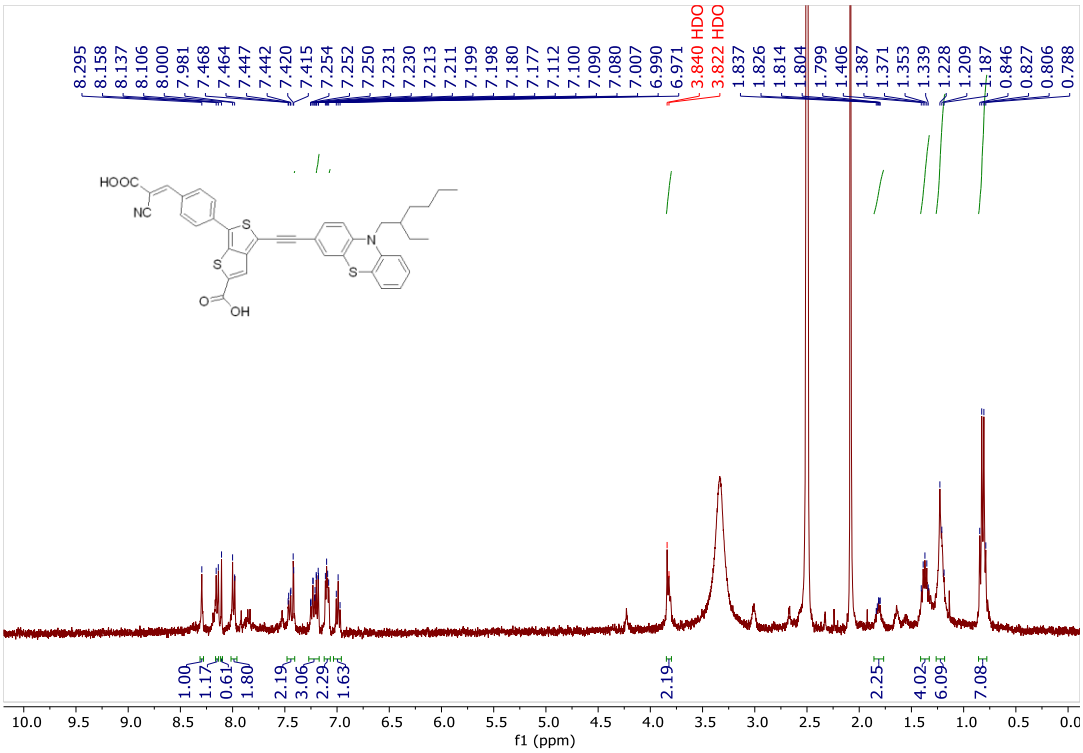


Figure A. 117. $^{1}$H NMR (DMSO-$d_6$, 400 MHz) spectrum of compound 4.23b.

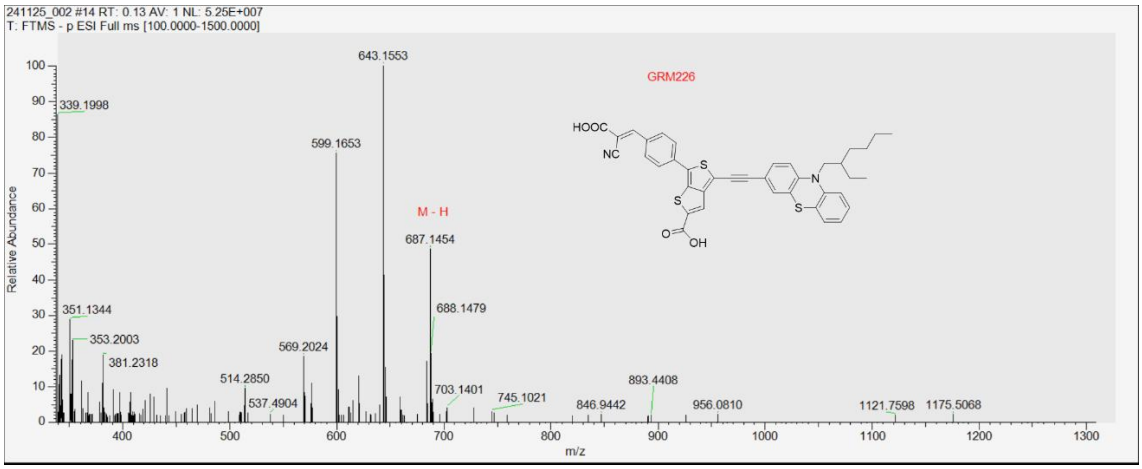


Figure A. 118. HRMS-ESI spectrum of compound 4.23b.

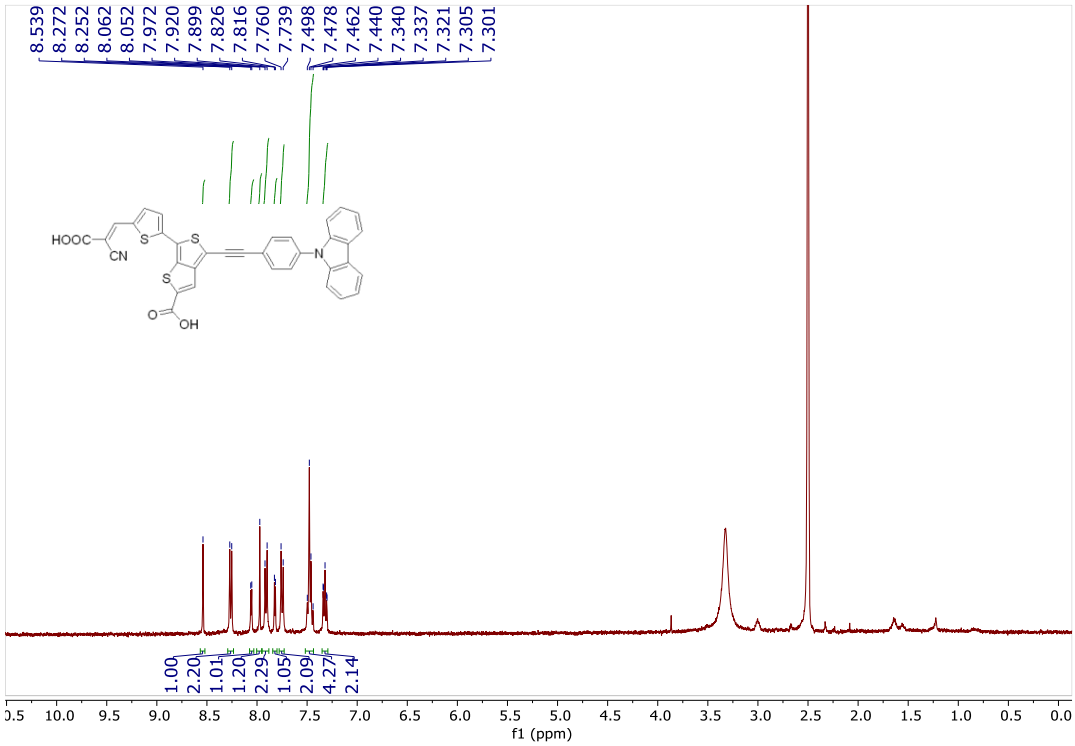


Figure A. 119. $^{1}$H NMR (DMSO-$d_6$, 400 MHz) spectrum of compound 4.23c

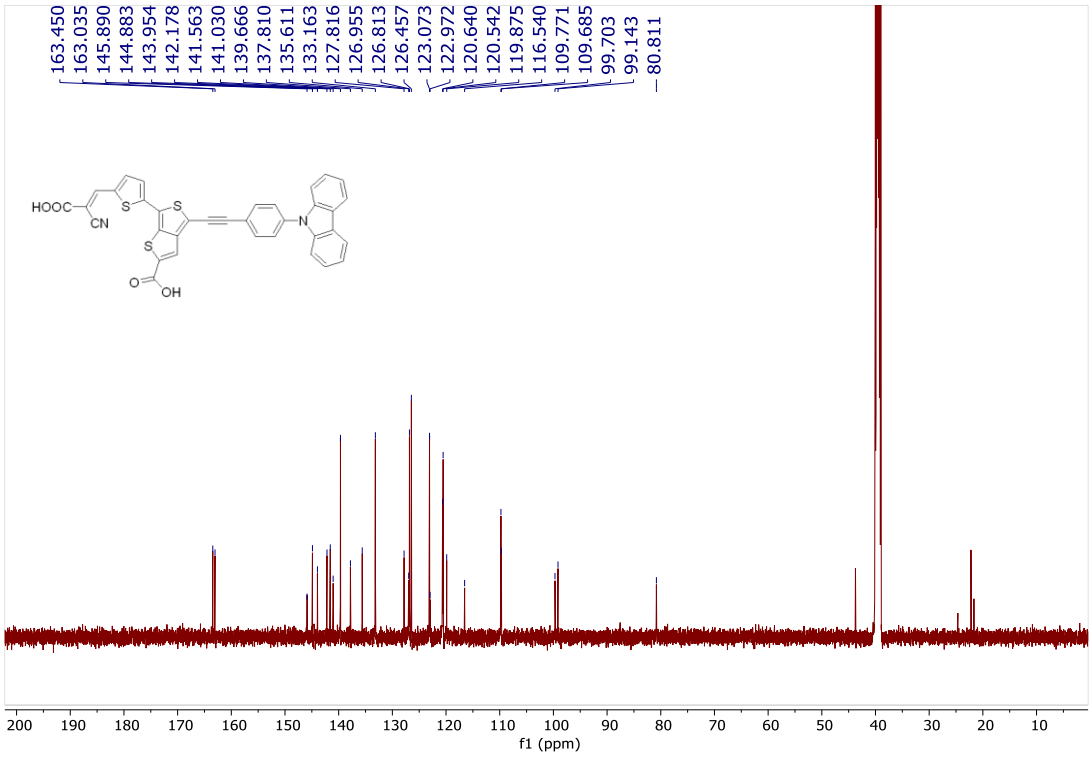


Figure A. 120. $^{13}$C NMR (DMSO-$d_6$, 126 MHz) spectrum of compound 4.23c.

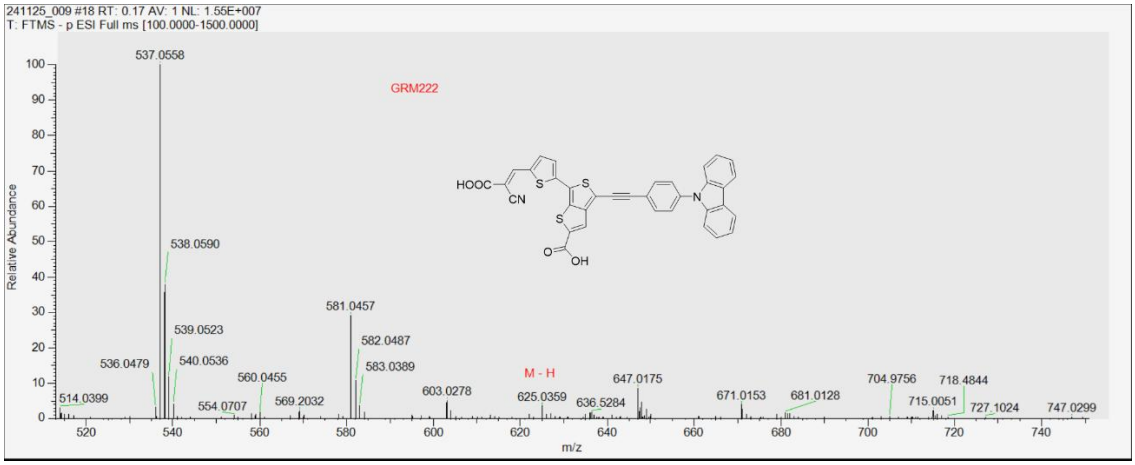


Figure A. 121. HRMS-ESI spectrum of compound 4.23c.

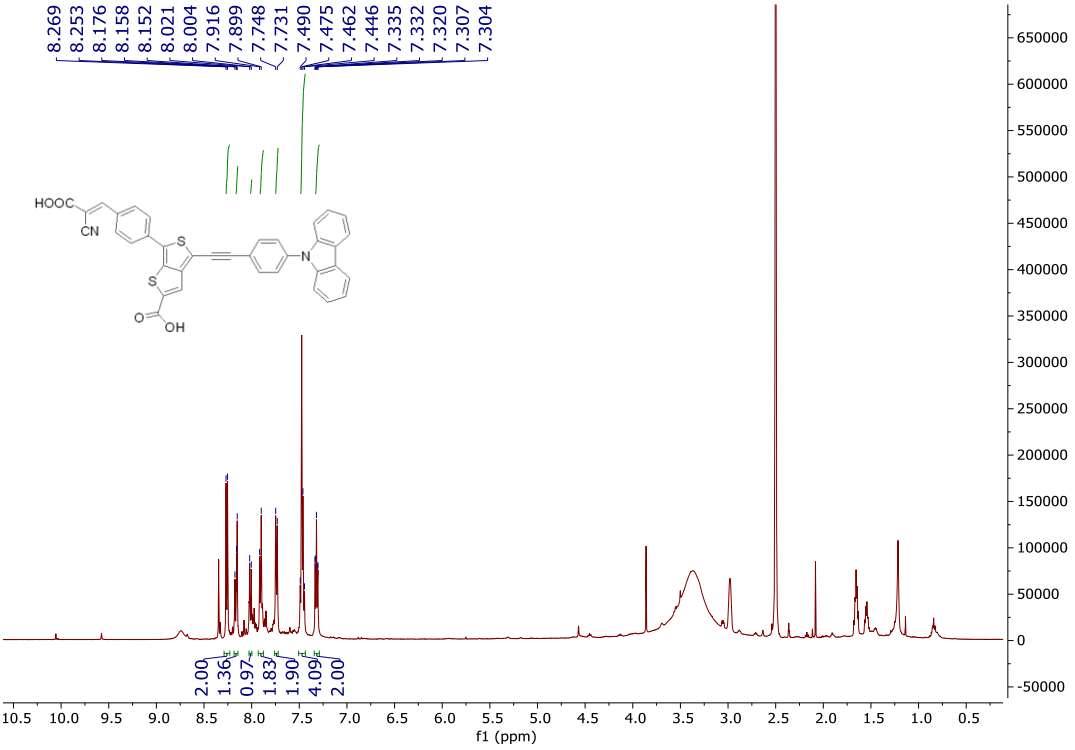


Figure A. 122. $^{1}$H NMR (DMSO-$d_6$, 500 MHz) spectrum of compound 4.23d

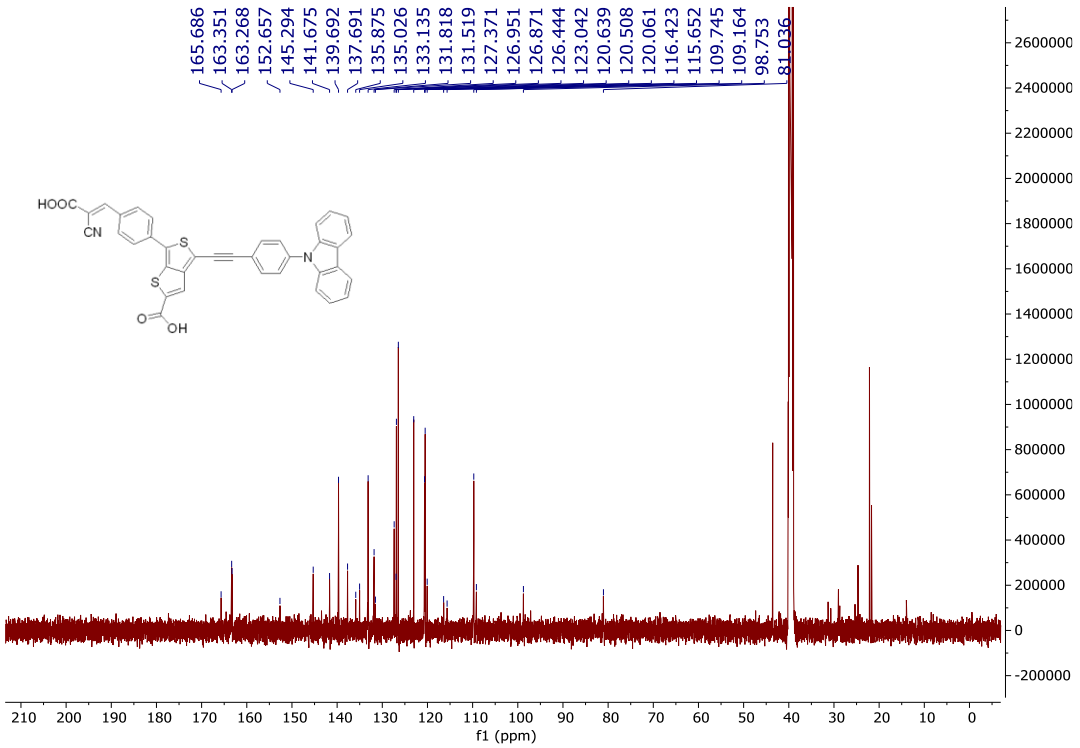


Figure A. 123. $^{13}$C NMR (DMSO-$d_6$, 126 MHz) spectrum of compound 4.23d.

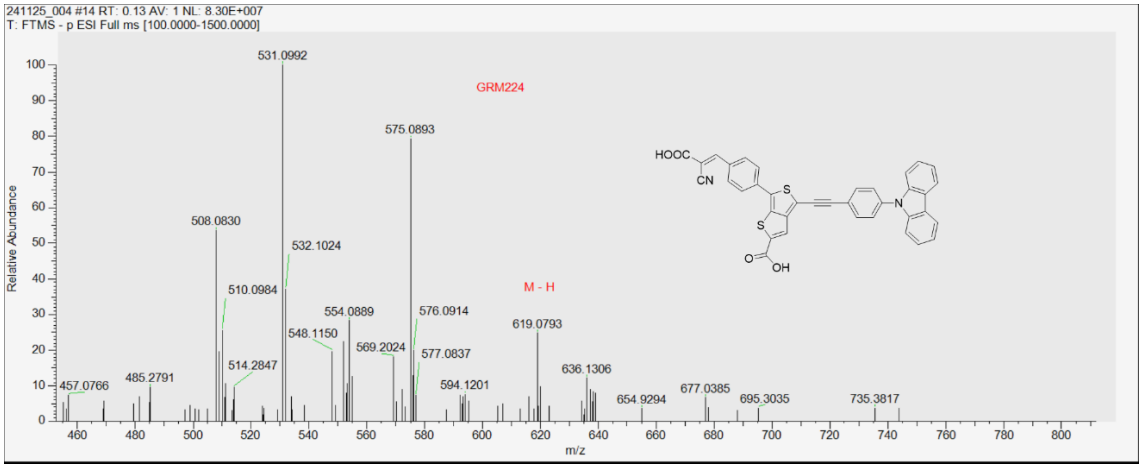


Figure A. 124. HRMS-ESI spectrum of compound 4.23d.

2024

GABRIELA RODRIGUES MALTA

# NEW MONO- AND HETERO-BRANCHED SENSITIZERS FOR DSSC